

# JOURNAL OF MINING AND GEOLOGICAL SCIENCES

Volume 63

Sofia 2020



UNIVERSITY OF  
MINING AND GEOLOGY  
"ST. IVAN RILSKI"



UNIVERSITY OF MINING AND GEOLOGY  
"ST. IVAN RILSKI"

**JOURNAL**  
**OF**  
**MINING AND GEOLOGICAL**  
**SCIENCES**

Volume 63



Sofia 2020

## Editorial Board

Assoc. Prof. Dr. Elena Vlasseva (Editor-in-Chief), Prof. Dr. Ognyan Petrov, Prof. DSc Petur Stavrev, Assoc. Prof. Dr. Yassen Gorbunov, Assoc. Prof. Dr. Nikolay Yanev, Prof. Dr. Hao Chen, Prof. Dr. Georg Unland, Prof. Dr. Dragan Antić, Assoc. Prof. Dr. Kazem Kashyzadeh, Assist. Prof. Monika Hristova, Kalina Marinova (Secretary)

## Contributing Editors

Prof. Dr. Jordan Kortenski, Prof. Dr. Nikolay Stoyanov, Prof. Dr. Stefan Dimovski, Prof. Dr. Marinela Panayotova, Prof. Dr. Efrosima Zaneva-Dobranova, Assoc. Prof. Dr. Anatoly Angelov, Prof. Dr. Michail Vulkov, Assoc. Prof. Dr. Evgeniya Aleksandrova, Prof. Dr. Stefcho Stoynev, Assoc. Prof. Dr. Kiril Dzhustrov, Assoc. Prof. Dr. Iliyan Iliev

University of Mining and Geology “St. Ivan Rilski”  
1, Prof. Boyan Kamenov Str., 1700 Sofia, Bulgaria  
<http://www.mgu.bg>

ISSN 2682-9525 (print)

ISSN 2683-0027 (online)  
[www.mgu.bg/new/journal](http://www.mgu.bg/new/journal)

© Publishing House “St. Ivan Rilski”, Sofia, 2020

## CONTENTS

### SECTION MINING AND MINERAL PROCESSING

<i>Aleksandrova, E., I. Koprev.</i> Complex solutions for the construction of integrated facilities in stoped-out open-pit mining facilities	9
<i>Asenov, R., P. Nedkov, P. Karamihov.</i> Drilling and blasting to form the wall of the non-operational benches of Ellatzite mine	13
<i>Bozhko, L.L., I.D. Turgel, R.K. Sapanova.</i> Comparative analysis of state support programmes for clusters: experience of the Republic of Kazakhstan and the Russian Federation	17
<i>Chepushtanova, T.A., M. Yessirkegenov, K.K. Mamyrbayeva, A. Nikoloski, V.A. Luganov.</i> Interphase formations in copper extraction systems	25
<i>Chepushtanova, T.A., I.Y. Motovilov, Y.S. Merkitabayev, M.S. Sarsenova, G. Sumedh.</i> Technology of sulfidizing-pyrrhotizing roasting of lead flotation tailings	31
<i>Debelyashki, K., M. Nicolova.</i> Waste management in Kostinbrod area	37
<i>Gicheva, G., N. Mintcheva, L. Djerahov.</i> ZnO-based nanomaterials for organic pollutants removal from wastewater	41
<i>Hristov, M.</i> Study of the physico-mechanical properties of the rock massif in the <i>Shumachevski dol</i> deposit, the <i>Androw</i> section	47
<i>Ivanov, N., P. Shishkov.</i> Application of non-detonating charges for cautious blasting of concretes	53
<i>Ivanova, M.</i> Tooth wear on a two-shaft shredder	59
<i>Kaykov, D., D. Georgiev.</i> Identifying the dig lines for ore extraction in the case of open-pit mining	63
<i>Luganov, V.A., T.A. Chepushtanova, G.D. Guseynova, B. Mishra.</i> Biotechnologies application at arsenic-bearing materials processing	69
<i>Nachev, S., G. Georgiev, I. Vasilev, M. Takeva.</i> Geotechnical assessment of the benches in the Elatzite open pit mine after blasting	75
<i>Nicolova, M., I. Spasova, P. Georgiev, S. Groudev.</i> Electricity generation by different microbial strains	81
<i>Penev, V., Z. Mollova.</i> Design optimization of drilling and blasting operations: A case study on copper ore mining in Asarel	84
<i>Plochev, S., S. Zeinelov.</i> Pollution of groundwater and surface water from the mining industry	89
<i>Stoyanchev, G., K. Dermendjiev, G. Dachev.</i> Types passports for roofbolting for crosses on broad roads with hydraulic tilting friction anchors in the condition of the Koshava mine, „Gypsum“ JSC	95
<i>Stoycheva, N.K.</i> Combined methods for extraction of large dimension stone blocks for decorative purposes	99

<i>Toshev, S., A. Loukanov.</i> Ultrasound-propelled biomimetic nanorobot for targeting and isolation of pathogenic bacteria from diverse environmental media	105
<i>Toshkov, N., I. Vasilev, L. Svilenov.</i> Transient, three-dimensional, hydrogeological numerical model of Ellatzite open pit mine	108
<i>Vatzkitcheva, M., K. Velichkova, N. Kolev, P. Savov.</i> A study of horizontal distribution pattern of particulate pollutants near a highway	113
<i>Vucheva, R., V. Trifonova–Genova.</i> Stress and strain state around elliptic opening in transversally isotropic rock mass-2	118
<i>Vucheva, R., M. Ivanova.</i> On the determination of the function for stress in transversally isotropic rock mass with elliptic opening	122
<i>Yalamov, Z., N. Hadzhieva.</i> Adopted approaches and practices during the structural-geological investigation of the rock mass in Ellatsite open pit mine, for the purpose of numerical modelling and mine design	125

## SECTION MECHANISATION, ELECTRIFICATION AND AUTOMATION OF MINES

<i>Boyadjiev, M.</i> Analysis of the hydrogen concentration on networks for gas supply	133
<i>Chetyov, S., K. Dzhustrov.</i> Ore load influence on ball mills specific electricity consumption	138
<i>Dzhustrov, K., N. Haralambiev.</i> Electrical losses in the electricity distribution networks when connecting new generator power	142
<i>Gorbounov, Y., R. Alexandrov.</i> Platform for experimental study of a switched reluctance motor	146
<i>Jordanov, J.M.</i> Aspects of origin mechanism for continuous (in situ) hydrocarbon accumulations	152
<i>Nedyalkov, P.</i> Reliability function improved fitting using goodness-of-fit procedures	161
<i>Petrov, P., R. Istalianov, S. Manev.</i> Electricity efficiency of a semi-autogenous mill investigation	167
<i>Pulev, S.</i> Tighting the pieces of material in centrifugal roller mills	172
<i>Pulev, S.</i> Storage of the goods under the operation of the mining dumper truck	175
<i>Stoyanov, A., J. Javorova.</i> Determination of kinematic characteristics of the complex motion of a particle by MATHCAD	178
<i>Slavkov, T., V. Mitkov.</i> Technical diagnostics and service of gas distribution networks	183
<i>Velinova, S.</i> Research of growth and development of plants under artificial light	186
<i>Velinova, S., V. Ilieva, K. Velinov.</i> Lighting conditions in photovoltaic greenhouses	193
<i>Yanakiev, V.</i> Implementation of remote monitoring systems and commercial measurement	196

## SECTION GEOLOGY AND PROSPECTING OF MINERAL AND ENERGY RESOURCES

<i>Apostolova, D., A. Bechtel, I. Kostova, M. Stefanova.</i> Biomarkers assemblage of unburned coal particles in fly ashes from Bulgarian thermoelectric power plants	203
<i>Chanachev, A.</i> Synthesis, biofunctionalization and application of gold nanoparticles	207
<i>Georgieva, B., B. Rangelov, D. Solakov, S. Dimovsky, A. KisyoV.</i> Methodology of mapping and digitalization of $V_{s_{30}}$ for the seismic hazard assessment in big cities	210
<i>Gerdjikov, I., Y. Dinev, D. Vangelov.</i> Structural geology of the central part of Kamenitsa-Rakovitsa fault zone	214
<i>Lakov, A., S. Stoynev, A. Hristov.</i> Strength and deformation properties of the intact gneiss rock from Zheleznitsa tunnel of Struma highway (Bulgaria)	220
<i>Marinov, I., K. Ruskov, K. Popov, N. Temelakiev.</i> 3D implicit modelling of alteration rocks and lithological units in the Milin kamak Au-Ag deposit: results and applications	226
<i>Nikolova, V., A. Kamburov, R. Rizova.</i> Modelling and assessment of debris flow erosion and deposition using geoinformation technologies	232
<i>Sabeva, R., S. Velev, H. Georgieva, T. Stanimirova.</i> Hydrothermal alteration and ore mineralization of the Nunatak de Castillo, Livingston Island, Antarctica	238
<i>Sinnyovsky, D.</i> Holocene transgressions in the area of the Burgas lakes complex – manifestation of global climatic fluctuations	243
<i>Sinnyovsky, D.</i> Holocene deposits of the Varna lake	249
<i>Stoyanov, N., S. Dimovski.</i> Prognostication of groundwater contamination caused by old sanitary landfills – part I. Models of the mass transport of pollutants through the unsaturated zone	255
<i>Stoyanov, N., S. Dimovski.</i> Prognostication of groundwater contamination caused by old sanitary landfills – part II. Models of the mass transport of pollutants in the saturated zone	261
<i>Tzankova, N., D. Stavrakeva.</i> Mineralogical study of archaeological copper slags found in the area of the Boyadzhik village, Yambol region, Southeast Bulgaria	267
<i>Velev, S., C. Trevisan, D. Dochev, J. Gerdjikov, K. Bonev.</i> New data about volcano-sedimentary successions on Byers peninsula and Hannah point, Livingston island, Antarctica	272

## SECTION SUSTAINABLE DEVELOPMENT OF THE MINERAL RESOURCES INDUSTRY

<i>Buyukliev, E.</i> Regional conflicts for natural resources	279
<i>Deliyska, D., N. Yanev, M. Trifonova-Draganova.</i> A model for building a mobile application for indoor navigation	283
<i>Dimov, E., R. Bakyr djieva, N. Stratiev.</i> The mining industry and the recycling of raw materials as an important element of the Bulgarian economy	289
<i>Dimov, G.D.</i> Decision making process in peace time with real risks and threats for security	293

<i>Dobreva, H.N.</i> Hybrid distance learning during Covid-19 in Bulgaria	297
<i>Dotseva, Z., I. Gerdjikov.</i> Assessment of debris flows-prone watersheds in the southern slopes of Stara planina mountain by combined raster and morphometric analysis	302
<i>Ilieva-Obretenova, M.</i> Blockchain node management in smart grid	308
<i>Kuzmin, S., A. Turbit, O. Salko.</i> Substantiation of the efficiency of container technologies application for the transportation of rock in deep pits	315
<i>Mindova, I.</i> Public-private partnership in declared state of emergency – a comparative study of the USA federal defense priorities and allocations system	320
<i>Purvanova, M., V. Panichkova, B. Dimitrova.</i> Practical work with the language of mathematics in the module in English for special purposes at the University of Mining and Geology “St. Ivan Rilski”	323
<i>Sereenen, S.</i> Possibilities and resolutions of the Mongolian energy sector	329
<i>Spasov, S.I., G.M. Marinov.</i> Challenges in the blackboard platform usage for knowledge verification in master training	335
<i>Stavreva, I., Y. Ivanov, V. Tsoleva, S. Stavrev, N. Kostova, E. Yordanov, M. Purvanova.</i> Study of students' attitudes in applying innovative forms of training in physical education and sports at the University of Mining and Geology “St. Ivan Rilski”	339
<i>Trifonova, B.</i> Committed employees - innovative competitive advantage of mining companies	344
<i>Tsakova, Ts. Ts.</i> The new generation of managers in a global aspect	348

**SECTION**

**MINING AND MINERAL PROCESSING**

## COMPLEX SOLUTIONS FOR THE CONSTRUCTION OF INTEGRATED FACILITIES IN STOPPED-OUT OPEN-PIT MINING FACILITIES

*Evgenia Aleksandrova<sup>1</sup>, Ivailo Koprev<sup>2</sup>*

<sup>1</sup>University of Mining and Geology "St. Ivan Rilski", 1700 Sofia; jogeni72@gmail.com

<sup>2</sup>University of Mining and Geology "St. Ivan Rilski", 1700 Sofia; ivokoprev@gmail.com

**ABSTRACT.** An analysis of the generated solid household and mining non-hazardous waste in Bulgaria has been performed. A quantitative-territorial assessment of the exhaust space in open pit mines and quarries in the country has been made. The possibilities for construction of integrated facilities (landfills) for solid household and industrial waste in the waste areas (ditches) and subsequent environmentally friendly reclamation are considered.

**Keywords:** open pit mining facilities, integrated facilities, land reclamation

### КОМПЛЕКСНИ РЕШЕНИЯ ЗА ИЗГРАЖДАНЕ НА ИНТЕГРИРАНИ СЪОРЪЖЕНИЯ В ОТРАБОТЕНИ ОТКРИТИ МИННИ ИЗРАБОТКИ

*Евгения Александрова<sup>1</sup>, Ивайло Копрев<sup>2</sup>*

<sup>1,2</sup>Минно-геоложки университет „Св. Иван Рилски“, 1700 София

**РЕЗЮМЕ.** Извършен е анализ на генерираните твърди битови и минни неопасни отпадъци в България. Направена е количествено-териториална оценка на отработените пространства в открити рудници и кариери в страната. Разгледани са възможностите за изграждане на интегрирани съоръжения (депа) за твърди битови и промишлени отпадъци в отработените пространства (котловани) и последваща екологосъобразна рекултивация.

**Ключови думи:** открити минни изработки, интегрирани съоръжения, рекултивация

### Introduction

Mineral resources exploitation is undoubtedly related to the excavation of considerable volumes of rock unusable mass along with the ore. On a world-wide scale over 120 billion tons of ores, coal, oil, gas and construction materials are extracted annually (approximately a total of 20 t for all type of mineral resources per world capita). In terms of scale, the mining and processing industries exceed volcanic activity (10 million tons per year) and the erosive processes of the rivers worldwide (25 billion tons per year). At the same time only 5-10% (according to some authors 1-2%) from the extracted mineral resources are utilized. The remaining volumes include ores below the cut-off grade, overburden, processing waste (tailing waste, slags, coal ash, etc.), which form technogenic dumps. The magnitude of the utilization of these technogenic facilities as a source of mineral resources still remains very low.

### Quantitative analysis of the generated solid waste

Data from the National Statistics Institute show that for the 2014 – 2018 period the total volume of the generated waste in Bulgaria is 663 million tons (which corresponds to 132,8 million tons annually) (nsi.bg, figure.1). The relative part of non-

hazardous waste for the period remains in the interval 88,5 – 92,5%, according to the list of waste types from Regulation (EC) № 2150/2002, the remaining waste types are considered as hazardous (Regulation № 2 from 27.07.2014 by the Ministry of Environment and Water).

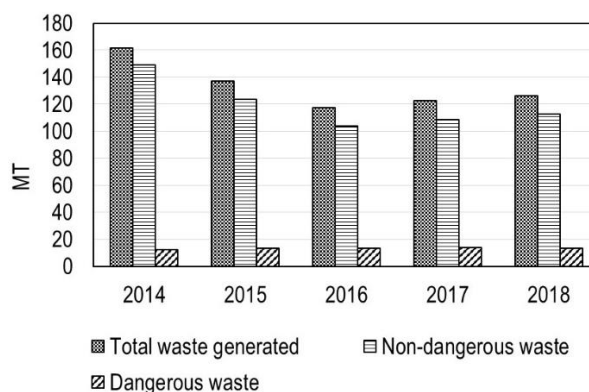


**Fig.1. Total volume of generated waste in Bulgaria for the 2014-2018 period**

The results, represented on Figure 1 show that during the last three years of the examined period the total volume of generated waste has changed insignificantly from 3,03% to

4,27%. Nevertheless, when there is a possibility for waste treatment, it should be conducted so that the negative consequences of their dumping and accumulation are reduced. According to the waste types, the different courses of waste treatment are their utilization, hazard neutralization or export (fig. 2).

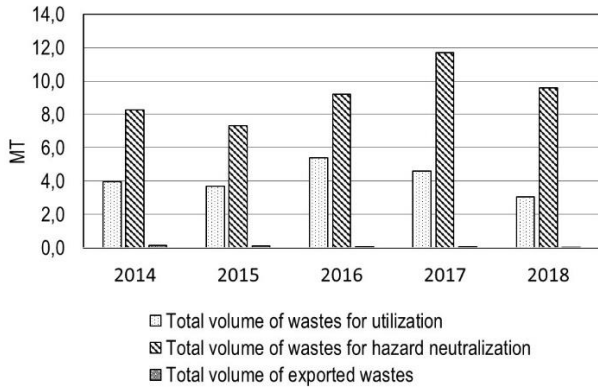


**Fig.2. Distribution of the waste volumes, designated for utilization, hazard neutralization and export for the 2014 – 2018 period**

After analyzing the data from Figure 2 it can be pointed out that the average annual waste volumes, designated for utilization are 4,14 million tons, which is approximately 3,12% from the total generated waste volumes (hazardous and non-hazardous) – 132,8 million tons.

A relatively higher part goes to the waste volumes, designated for hazard neutralization: 6,9%. Statistic data shows that only an insignificant part of the waste volumes in Bulgaria are exported: 0,07%.

The volumes of waste which are generated by the mining and processing industry, as well as the possibilities for their complex management are considered to be perspective. Figure 3 represents a diagram of the relative parts for the generated waste volumes according to their originating economic activity.

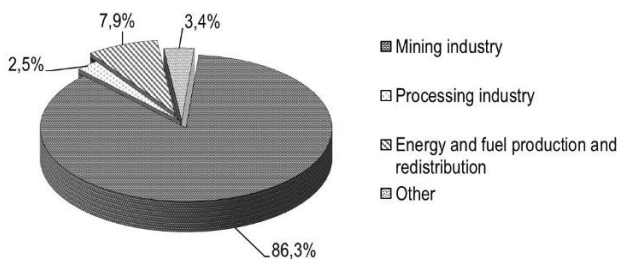


**Fig.3. Distribution for the generated waste volumes according to their originating economic activities for the 2014 – 2018 period**

The highest relative part goes to the mining industry – 86,3%, followed by the production and distribution of energy and fuel – 7,9%. The third place goes to the processing industry – 2,5%.

After extracting and processing mineral resources, their respective wastes are to be dumped in specialized facilities, which are classified as waste dumps (overburden embankments) and tailings. (Grigorova et al., 2014). They differ from each other significantly due their mineral and granular consistency. Overburden waste dumps are intended for mining

waste (overburden) accumulation and the waste size varies with an average size of few centimeters. The ore content in these kinds of dumps is very low, which leads to the increased interest for the waste utilization as a construction material. Dumps of this type are built in open spaces and have a different special shape: pyramid-like shape, a truncated- cone-like shape, etc.

Waste material from ore and mineral resources processing with a medium particle size from several microns to several millimeters. Depending on the processing technology, they could include some quantities of ore content, which is bigger than the cut-off grade. The tailing may be “wet” or “dry”. While this type of waste is dry, it can be stored similar to waste dumps in depots. For the wet tailing waste, in order to reduce the necessary storage areas, tailing dams have to be made with safety ditches, which prevent their spread to the surface. A suitable place for their construction can be river valleys or gulches. In time the water level inside the tailings declines due to water filtration through the bed.

The distribution of waste depots around our country’s territory is highly uneven. Usually they are situated right next to mining companies. Depending on the structure of the waste, they correspond with the extracted mineral resources during the mining and processing operations. Near the quarrying sites, which are extracting limestone sand, several outdoor depots are situated, which accumulate the overburden, clay rocks and part of the substandard mining reserves. In general, these waste dumps do not contain hazardous materials and the acting European laws does not enforce high technologic requirements towards them (National strategy for development of the mining industry, 2015).

The total number of dumps (hydraulic and granular) is 227. This means, then in each administrative region of Bulgaria, there are 10 waste dumps on average. During the reclamation of the areas in the sector of “Non-metallic mineral resources”, there is a tendency of a gradual increase of these areas. During 2018 about 132,6 ha are reclaimed, while during 2019 – 176,5 ha. This is an indicator that the mining business from this sector is oriented towards the preservation of the environment and local ecosystems.

To this moment, 518 concessions for mineral resources are provided in Bulgaria, some which have been provided from 1997. While taking into consideration the term until each one lasts, in the next few years it is expected that mining will conclude in quarries such as: “Hristovo” deposit for filnstone concretions, Vetovo municipality (2024), „Iskar“ deposit for quartz-feldspar sands, Dolna Mitropoliya municipality (2024), „Krivina“ deposit for sands and gravel (2026), „Ahmatovo“ deposit for sands, Sadovo municipality (2021), „Shishmantzi“ deposit for limestones, Rakovski municipality, „Belashtitsa“ deposit for marble, Rodopi municipality (2021), “Devnya” deposit, “Lyulyaka” sector и “Snezhno pole yugoiztok” sector for quartz sands (2025), „Yurt-dere“ deposit, Dimitrovgrad municipality (2020), „Probuda“ marl deposit, Targovishte municipality (according to the data from the Register of the active concessions for mineral resources mining and quarrying, updated to 16th July 2020). Each of the pointed quarrying sites has a potential for hard rock waste dumping and the site for building an environmentally friendly integrated waste facility.

## Complex solutions for dumping solid wastes inside the stoped-out areas in open-pit mines

One of the promising possibilities for complex utilization of the natural resources, the waste treatment, the rational land usage and the disturbed areas reclamation is for that the stoped-out areas in open-pit mines should be used for their filling with solid industrial and household waste. Usually this is done when in the mining regions the soil layer is absent and the reclamation of the natural landscape is virtually impossible. This way some of the quarries are situated in the neighboring territories of towns or very close to industrial companies, which is an additional argument for transforming the stoped-out areas for waste depots. In addition, the problem with dumping and storing solid household wastes (SHO), especially for densely populated areas is difficult to be resolved. On the whole, transforming the stoped-out areas has a further practical usage and the initial landscape restoration is possible. For this purpose, it is required that during the mine site (or quarry site) design phase the volumes of the processed and utilized household wastes are taken into account, as well as the different stages of waste dumping for every waste type and their respective parameters with a consideration of the environmental protection. The waste

dump body, as a base part of the integrated waste facility must ensure the hazard neutralization of the waste, while at the same time it does not threaten the health conditions of the working staff, as well as the neighboring populated areas. In addition, it must not induce a risk for polluting the air, the underground water sources, the soil, the flora and the fauna. A monitoring for noise and dust pollution has to be considered as well as the control of bad smells from the waste facility.

The placement of the solid wastes inside the depot have to be organized in such a manner, that ensured the stability of the waste material on the slopes in order to prevent landslides. The waste dump body is tested for its general stability in order to ensure its stability during the different stages of its utilization: construction until reaching 1/3 of its design height, 2/3 and the maximum design height. In order to determine the deformations (subsidence, failure, etc.) it is necessary that certain computational checks are made for forecasting the stability of the facility.

The construction of an integrated waste facility in the stoped-out areas of the mining (or quarrying) site starts with the following preparation (<https://sites.google.com>, fig.4):

- Slope adjustment for the open-pit mine (a frequent practice for open-pit mines and quarries land reclamation).

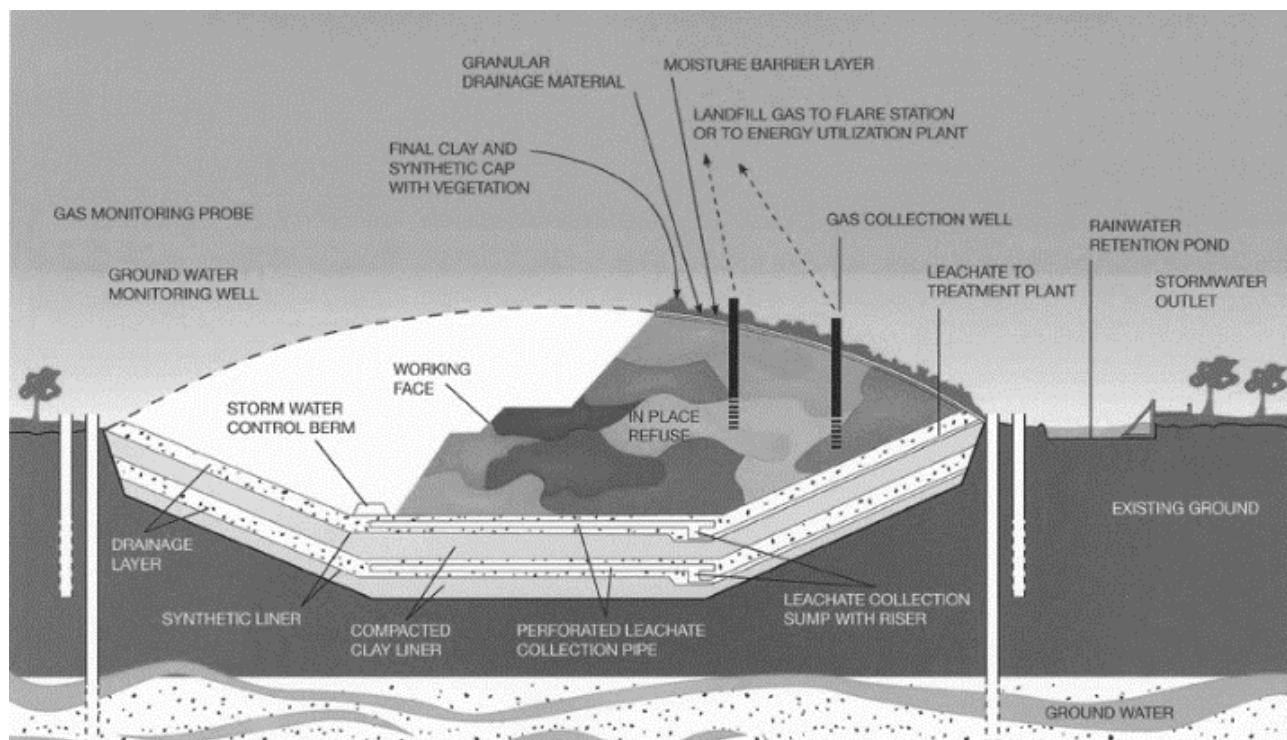


Fig.4. Technology for building an integrated waste facility in the stoped-out areas of an open-pit mine

- Consolidation of the dump's fundament by constructing a lower isolating screen for sealing the bed and the slopes. This is necessary for the case when the dump base does not suit the requirements for ensuring the sufficient resistance for preventing the risk of polluting the soil and waters. In this case the filtration index (coefficient) -  $K_f$  (determined by experimental from water assaying from a drill well) – does not suit the normative geological barrier requirements  $K_f < 1 \times 10^{-6}$  m/s (Regulation №6). The lower isolation screen of the depot, in combination with the geologic basis must satisfy the

requirements for permeability and thickness and the requirements for protecting the underground waters from the negative impact of the waste dump body and its satisfactory stability. It is designed as a system for sealing the bed and the slopes of the depot, which includes a mineral sealing layer, mineral obturation, an isolation geomembrane and a protecting layer of a drainage (fig.4).

- The placement of an isolation geomembrane takes place for absorbing the deformations and the subsidence of the mineral in the sealing layer and the geological base. Its purpose

is that combined with the sealing layer, they ensure a protection for the soil and underground waters from leaks of the formed infiltrate inside the body of the waste dump. The geomembrane's main feature is that is chemically resistant to the infiltrating chemicals inside the body of the waste dump.

- In order to mechanically protect the foil, it is covered with a layer of geotextile;

- Placement of a drainage system in the lower isolating screen for collecting and leading the infiltrate from the dump body. It includes an area drainage with a thickness of at least 0,50 m from washed rubble with a granular composition which ensures  $K_f \geq 1.10^{-3}$  m/s; a drainage pipe for collecting and leading the infiltrate to a collecting shaft; a collecting and revision shaft; a submerged pump; a pipeline, leading the infiltrate outside the body of the waste depot. The drainage pipes (farically perforated) are placed on the bed of each cell over the isolation layer. They lead the infiltrate to the collecting shaft. The free end of the drainage pipes is lead to the outer boundary of the ditch for revision and possible flushing.

- The network of drainage systems across the bed of the depot is covered with an area drainage – a two-layered filter of river gravel (5-40 mm with a thickness of 0,30 m) and coarse-grained sand (0,20 m thick over a layer of gravel) only around the pipes. The drainage system is designed to accumulated the maximal daily infiltration flow-off.

- Collecting the atmospheric waters on the upper boundary of the pit's surface is done by placing drain ditches.

- The infiltrating waters (IF) formed inside the body of the depot as drained to a drainage network inside a concrete shaft. The collected water from the shaft are lead to a pumping station with a retention volume for the IF.

- If it required, a passive or an active degasification system is built for the waste gas, which should lead to the burning of the collected gas (turning  $CH_4$  into the less harmful  $CO_2$ )

- Building on a surface isolating screen on the parts of the depot, which are full;

- The closing processes of the solid waste dump take place when it reaches its design height. The last layer of waste is covered with a layer of soil which is 1-2 m thick. The covering layer has to intact and firm across the whole area. In order to avoid erosion, the whole dump is reclaimed and grass is planted. For the kinds of waste dump which emit  $CH_4$  a gas drainage layer is considered, which has the purpose of collecting the emitted gases.

A long-term monitoring is required for this type of integrated waste facility, which takes place during its construction and utilization, as well as its final reclamation. The monitoring project includes the following activities:

- 1) Control of the dumping activities – input control and technological control, isolation of the drianage system and the stability of whole dump facility. The dump's operator keeps track of a "Report book", which contains the information of the input control;

- 2) A system for independent monitoring – it includes the monitoring the research during the period of the waste dump exploitation, as well after its close down:

- meteorological date – information about the quantity of rainfall water, the air's teperature, the wind direction and force, as well as the evaporation and air humidity. This information is required for tracking the processes in the waste body and is gathered by the closes hydrometeorological service in the region.

- surface waters – they drain throught the ditches and follow the direction of the natural surface drainage.

- the condition of the waste depot body – for tracking the deformations of the body, certain observation points have to be chosen on the reclaimed grasses area of the waste dump.

## Conclusion

The modern level of technologica ladvancement cannot ensure that each industry is waste-free. Therefore, in the near-future research for the reduction in the waste generation for different types of technology as well as their safe keeping in suitable conditions. The presented complex decisions for the waste dumping of hard material in the stoped-out mining areas in open-pit mines are only a part of the perspective tendencies for reducing the environmental impact from the generation of hard waste.

## References

- Grigorova, I., M. Ranchev, I. Nishkov. 2014. Lasting tendencies for dumping final technological wastes from mineral resources processing. *Minno delo i geologiya (Mining and Geology) magazine*, 2014/9-10, 37-41 (in Bulgarian).
- Regulation №6 from 27.08.2013 for the conditions and requirements of depots and other facilities and installations construction and utilization for the use and hazard neutralization of wastes, amended and supplemented, Vol. 13 from 7th February 2017. (In Bulgarian)
- National strategy for development of the mining industry, 2015 (In Bulgarian).
- <https://nsi.bg> (last opened on 29th July 2020)
- <https://sites.google.com/a/comell.edu/municipal-solid-waste/environmental-impacts> (last opened on 29th July 2020).

## DRILLING AND BLASTING TO FORM THE WALL OF THE NON-OPERATIONAL BENCHES OF ELLATZITE MINE

**Radoslav Asenov, Pavel Nedkov, Penko Karamihov**

Mining Complex, "Ellatzite-Med" AD, 2180 Etropole; r.asenov@ellatzite-med.com; p.nedkov@ellatzite-med.com; p.karamihov@ellatzite-med.com

**ABSTRACT.** Ellatzite Open Pit Mine is remarkable for its variable lithology, specific geotechnical areas and a wide variety of rock strengths in the processed rock body. This variety is a challenge when it comes to designing, drilling and blasting for they need to cover a large scope of criteria. Having in mind the scale of processing (space and depth), it is necessary to sustain a long lasting wall stability. After multiple consultations and knowledge exchange, Mine Management made a decision to use 24-meter-long pre-split holes which changed the design for drilling and blasting of fields at a final project contour of the operational benches and helped securing the wall stability.

**Keywords:** lithology, design for drilling and blasting

### ПРОБИВНО-ВЗРИВНИ РАБОТИ ЗА ОФОРМЯНЕ НА ОТКОСА НА НЕРАБОТНИТЕ СЪТПАЛА В РУДНИК „ЕЛАЦИТЕ“

**Радослав Асенов, Павел Недков, Пенко Карамихов**

Рудодобивен комплекс, „Елаците-Мед“ АД, 2180 Етрополе

**РЕЗЮМЕ.** Рудник „Елаците“ се отличава с многообразна литология, специфични геотехнически зони и широк диапазон от стойности на якост на разработвания масив. Това разнообразие е предизвикателство при проектирането на пробивно-взривни работи, които да покриват множество критерии. Предвид мащабите на разработване (по площ и дълбочина) е необходимо осигуряването на дълготрайна устойчивост на откосите. След проведени консултации и обмяна на опит, ръководството на рудника взема решение за изпълняването на 24-метрови контурни сондажи, които променят проектирането на паспортите за ПВР при взривни полета до проектен краен контур по работните хоризонти и спомагат за осигуряването на стабилитета на откосите.

**Ключови думи:** литология, паспорт за ПВР

## Introduction

When excavating ore deposits, it is of primary importance to secure the walls of the benches for the whole lifetime of the mine. The output data for determining the wall stability are complexity of information about the nature and technical mining conditions and factors, characterizing the objects in question. There are many methods to calculate the stability profile of the walls, but none of them gives precise results. This is due to their imperfection and the probabilistic nature of the output data. The majority of those methods are based on the assumption for the existence of a certain slip motion surface in the wall slope where the rock movement can occur.

In Ellatzite Open-pit Mine, the wall profile is with terrace-like form, consisting of non-operational benches, whose parameters, based on the physio-mechanical properties of the rock diversities, are as follows: project height of the benches at final contour  $H=15$  m or  $H=30$  m; safety berms width  $B=12-20$  m and slope angle  $\alpha=65^{\circ}-75^{\circ}$  (in weak rock zones  $\alpha=55^{\circ}$ ).

There are two stages of processing to achieve non-operational benches with project height of  $H=30$  m (1<sup>st</sup> and 2<sup>nd</sup>), with sub benches whose height is  $H=15$  m. Providing long term wall stability in Ellatzite Mine ensures safe processing and potentially long term exploitation.

## Rock mass geology in Ellatzite Open-pit Mine

When designing the drilling and blasting activities there is a need to consider the geological and geotechnical information for the processed rock diversities which will give the main directions when choosing:

- o Boreholes diameters and boreholes patterns
- o Blasting technology
- o Explosives
- o Necessary quantities of explosives in a series for detonation
- o Delay grades (surface, when applying NONEL technology and delays for the electronic detonators when applying ELECTRONIC technology) for detonation of the different explosive charges.

For this purpose, all production benches of the mine, be it ore or waste, are mapped by the Geotechnical Department of Ellatzite Mine and described in terms of: lithology of the rock body, physio-mechanical properties of the rocks, tectonic faults, block structure and cracks of the rock bodies, mainly consisting of: granodiorites, porphyrites, shists and phillites. The compression strength values are different with the different rock types. Most of them have values of  $s=120-150$  MPa. A blastability matrix has been created, based on the information of

all mapped benches in the mine (table 1). This matrix divides the rock bodies into nine different classes, depending on their block structure and compression strength, that determine the borehole patterns, technology of detonation (NONEL or Electronic) and the quantities of explosives when creating the drilling and blasting design.

The main statement is structured into different sections, possibly divided by a separate title each. Each statement needs: research thesis and hypothesis, applied methods, main achieved results and discussion. The conclusion should not match the resume word by word.

Table 1. Rock bodies classification in Ellatzite Open-pit Mine according to the blastability matrix

BLOCK STRUCTURE			Mpa	COMPRESSION STRENGTH
0m - 0,3m	0,3m - 1m	1m <		
PHILITES (40 Mpa)	PHILITES (40 Mpa)	PHILITES (40 Mpa)	0 - 60	
SHISTS IN WET CONDITIONS (87 Mpa)	SHISTS IN WET CONDITIONS (87 Mpa)	SHISTS IN WET CONDITIONS (87 Mpa)	60 - 120	
SHISTS IN DRY CONDITIONS (123 Mpa) PORPHYRITES (126 Mpa) GRANODIORYTES IN DRY CONDITIONS (147 Mpa) GRANODIORYTES IN WET CONDITIONS(133 Mpa)	SHISTS IN DRY CONDITIONS (123 Mpa) PORPHYRITES (126 Mpa) GRANODIORYTES IN DRY CONDITIONS (147 Mpa) GRANODIORYTES IN WET CONDITIONS(133 Mpa)	SHISTS IN DRY CONDITIONS (123 Mpa) PORPHYRITES (126 Mpa) GRANODIORYTES IN DRY CONDITIONS (147 Mpa) GRANODIORYTES IN WET CONDITIONS(133 Mpa)	120 <	

On Figure 1, you can see the lithology of one of the workout benches with tectonic faults and the orientation of their space distribution. There is a structural geological diagram (left part of the figure), which represents the crack distribution in the rock mass and their frequency. For each of the workout benches there could be several diagrams of that kind but there are not randomly situated in the bench plans. They are placed in the areas with supposed deformation processes and the space distribution direction in case of activation. The engineers engaged in drilling and blasting design take this information into account when preparing the drilling and blasting design.

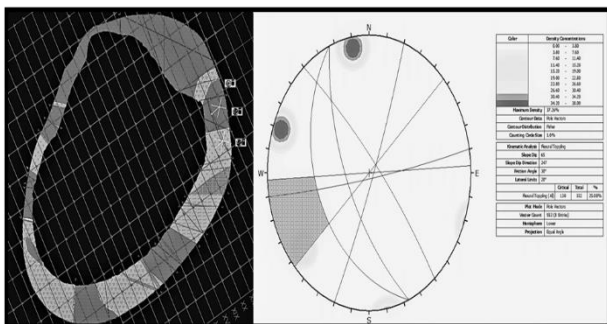


Fig. 1. Plan view of a mapped production bench -1090 – in Ellatzite Mine and structural geological bench diagram

### Drilling and blasting activities to form the wall of the non-operational H=30 m benches

The idea of a good drilling and blasting design, providing quality of board formation with minimal damage is to undertake certain measures to: reduce wall damage (defining the

quantities of explosive in the boreholes and the optimal timing for initiation of the charges); protecting the integrity of the upper crest of the safety berms (no boreholes are situated in the project upper crest of the safety berms) which increases the capacity of the safety berms to “take up” the falling rocks and to provide the necessary protection for the machines and the staff, working underneath.

On Figure 2, you can see a comparison between wall formation of the non-operational benches with pre-split holes in both stages of workout (a) and using pre-split holes only in the first stage (b). With option (a) from Fig. 2, you can see the formation of the berm between the two sub benches along the non-operational bench, whose width varies between B=1.5 – 2.5 m. The pre-split holes in this wall formation model have a designed depth of L=16 m, designed angle  $\alpha=75^\circ$  and spacing  $a= 1.5 – 2.5$  m.

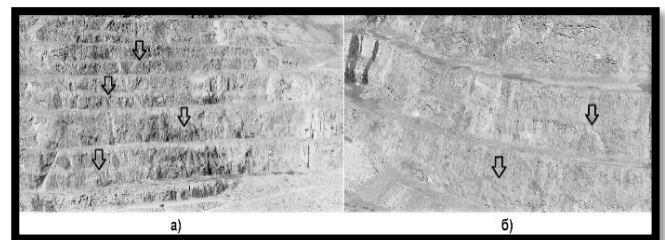


Fig. 2. a) results after using pre-split holes in 1<sup>st</sup> and 2<sup>nd</sup> stages of working with sub benches; b) results after using pre-split holes only in 1<sup>st</sup> stage of working with sub benches.

With option (b) from Fig. 2, to form the wall of the non-operational bench with height of H=30 m, the pre-split holes are done once. This wall formation model has been applied in the recent few years, showing considerably better results in the formation of the wall geometry of the non-operational benches. The berm, characteristic for option (a) from Fig. 2 is no longer available. The wall is a bit more inclined giving opportunities for a more even distribution of the possible deformation processes in the rock mass. Having in mind the diversity of the lithology in Ellatzite Mine and the rock classification according to the blastability matrix (table 1), there are different borehole patterns in the drilling and blasting designs, with different quantities of explosives and different blasting technologies (NONEL or Electronic). In the present report there will be presented drilling and blasting activities for wall formation of non-operational benches with height of H=30 m and wall angle of  $\alpha=65^\circ$ , in a rock body of granodiorite. The diameters used for drilling are d=165 mm (push-button bits) and d=250 mm (triple-roller bits). Hole networks: for pre-split  $a=1,8$  m; for production 5,5 x 6,5 m. For the purposes of the drilling and blasting, checkered patterns are used.

### Use of explosives

Ellatzite Mine have their own Explosives factory that produces the necessary quantities of explosives for its production purposes. The explosive used for the pre-split holes loading is cartridge emulsion Ellatzit 710. The sleeve of the cartridge explosive is a three layered, antistatic cross-shaped foil with a diameter of d=40 mm and L=10 m. The weight of the explosive Ellatzit 710 for a cartridge with the given size is Q=16

kg. Two cartridges of Ellatzit 710 are put alongside each pre-split hole, taking up 20 m of its length (83%). Only Electronic technology is used to detonate the explosives in the presplit holes, produced by Austin Powder. The explosive is sensitive to detonators and there is no need for boosters. The time interval for detonation of the charges in the pre-split holes is in milliseconds, in accordance with the physio-mechanical and geotechnical properties of the rock body where the pre-split holes are. In this case of a rock body, consisting of granodiorites, 160 kg of Ellatzit 710 is used in a series, where the interval between the different series is  $t=15$  ms. The time intervals for both pre-split and production holes are analyzed in terms of the caused seismic through investigations made by Explosivprogres – GTM Ltd.

Table 2. Explosives used in the 1<sup>st</sup> and 2<sup>nd</sup> stage of working a non-operational bench H=30 m in Ellatzite Mine

Explosive	Type of explosive	Bulk density, kg/m <sup>3</sup>	Critical diameter, mm, not more than	stable diameter, mm not more than	Optimal middle detonator	Velocity of detonation, m/s
Ellatzit 710	cartridged emulsion	1100-1220	до 51*	над 51**	not less than KD №8	not less than 5000
ANFO E	naphtrinitrate roughly disperse	750-820	60	100	400 g cartridge TNT	not less than 3000
Ellatzit 3400	emulsion	1150-1280	80	120	400 g cartridge TNT	not less than 4300

\* - with hot emulsion density =  $1.08 \pm 0.03$  g/cm<sup>3</sup>; with cooled emulsion density =  $1.12 \pm 0.03$  g/cm<sup>3</sup>

\*\* - with hot emulsion density =  $1.14 \pm 0.03$  g/cm<sup>3</sup>; with cooled emulsion density =  $1.18 \pm 0.03$  g/cm<sup>3</sup>

The technological capacity of the Explosives Plant in Ellatzite Mining Complex allow the production of cartridges of Ellatzit 710 with different diameters, length and weight. There are several sizes according to diameter: 28 mm; 32 mm; 36 mm; 50 mm; 65 mm и 90 mm.

### Drilling throughout the stages of wall formation of a non-operational bench in Ellatzite Mine with H=30 m height, using sub benches of H=15 m

One of the conditions for wall control and damage decrease is to use pre-split holes in order to disperse the energy and sending part of it vertically up when blasting final board designs. The pre-split holes are drilled with diesel-hydraulic drilling machines with  $d=145$  mm or  $d=165$  mm push-button bits. According to the compression strength of the rock types, where the pre-split holes will take place and the diameter of the drilling instrument, the distances between them are described in Tables 3 and 4.

Table 3. Spacing between pre-split holes in different rock types, made with  $d=165$  mm drill bit.

Drill bit Rock body	Compression strength, MPa	Spacing, m
Philites	40	2,5
Shists	87	2
Porphyrites	126	1,8
Granodiorites	147	1,8

Table 4. Spacing between pre-split holes in different rock types, made with  $d=142$  mm drill bit.

Rock body	Compression strength, MPa	Spacing, m
Philites	40	1,8
Shists	87	1,6
Porphyrites	126	1,5
Granodiorites	147	1,5

After drilling and blasting of the pre-split holes, the rest of the holes needed for the final wall formation are done. For these purpose diesel-hydraulic drilling machines are used with diameter  $d=142-250$  mm. The applied hole patterns are checked. The location of the holes is set by the surveyors after importing the coordinates of each hole in GNSS- receiver. The majority of diesel-hydraulic drillers in Ellatzite Mining Complex that use  $d=250$  mm drill bits have integrated system for positioning over the design coordinates of the holes, with accuracy of positioning up to 10 cm. Fig. 3 and Fig. 4 show the applied types of boreholes and the spacing between them.

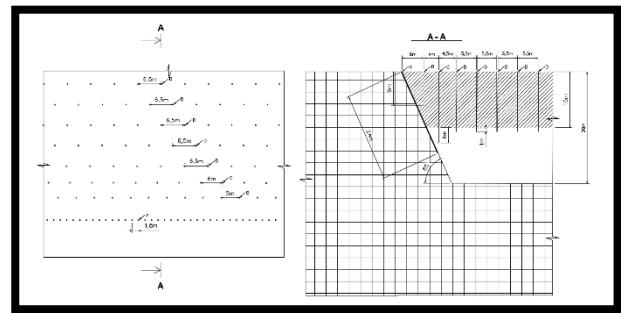


Fig. 3. Wall formation drilling, performed in the 1<sup>st</sup> stage of working the non-operational bench with H=30 m height in Ellatzite Mine

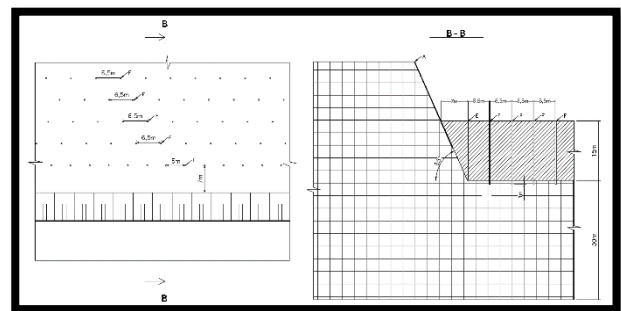


Fig. 4. Wall formation drilling, performed in the 2<sup>nd</sup> stage of working the non-operational bench with H=30 m height in Ellatzite Mine

When the resistance line (W) is too high the production holes (categories D and F) are done with design angle different than 90° (from 75° to 85°).

Table 5. Realized boreholes, used for wall formation of non-operational bench with H=30 m height in Ellatzite Mine

Blasthole category	Stage of working	Blasthole type	Diameter, mm	Project angle, ...°	Depth, m	Cartridge, pcs.	Quantity of explosive per hole (dry or wet), kg			Charge construction	Stemming, m
							E-710	E-3400	ANFO		
A	1st	presplit	165	65	24	-	32	-	-	continuous	-
B	1st	buffer	165	90	9	1	-	120	-	continuous	-
C	1st	buffer	165	90	19	2	-	400	-	continuous	5
D	1st	production	250	90	16	2	-	770	440	continuous	5
E	2nd	buffer	165	90	15	2	-	220	-	continuous	-
F	2nd	production	250	90	16	2	-	770	440	continuous	5

In the 2<sup>nd</sup> work stage (fig. 4), the buffer holes, category E, are placed over the toe of the safety berms with no subdrilling. The stemming material for both work stages is a fraction with rock pieces size up to 20 mm. The material for the stemming is mine mass from Ellatzite pit, crashed by a mobile crusher situated on the territory of the pit itself.

### Control seismic research for the impact of blasting on the walls of Ellatzite Mine

In Ellatzite Open-pit Mine there is a large variety of the geological, hydrogeological and other conditions that reflect the behavior of the rock masses forming the pit walls. When making seismic researches, they use seismic waves generated by the blastworks in the mine.

The control seismic researches are made by Explosiveprogres-GTM Ltd. They use equipment from „Instantel“(Canada) and „Nomis“ (USA). They provide with the opportunity of the immediate result speed of movement (vibration, fluctuation) V. The explosive seismic impact on the pit

walls is a result of dynamic pressure and release from the seismic waves through the rocks, caused by the production blasting. In these cases the dynamic pressure and release of the rock body goes according to the same physical law, in the scope of the elastic behavior of the rocks which doesn't lead to residual deformations. For rates above this tension, the pressure and release of the rock body happens according to different physical laws, leading to formation and accumulation of residual deformations. This accumulation is typical for multiple blasting and can lead to loss of stability and rock downfall.

The deformational properties of the rocks are of crucial significance when choosing the allowed speed of movement (vibration, fluctuation) V. The speed of movement (vibration, fluctuation) V, depending on the rock break characteristics, shows that when V is up to 20 cm, there are no observed breaks (damages) in hard rocks.

### Conclusion

This drilling and blasting model has one key element that plays an important role in DB designing and it is the pre-split holes with L=24 m depth. They have more advantages compared to the no longer applied L=16 m,  $\alpha=75^\circ$  ones (used for double benches). This type of boreholes helps avoiding drilling underneath the walls according to designed toe in the 2<sup>nd</sup> stage of the working with sub benches. There are also economic advantages since this helps reducing the amount of drilling. Last, but not least, their main purpose to form the walls of the non-operational benches is fulfilled and the results are technically and economically efficient.

## COMPARATIVE ANALYSIS OF STATE SUPPORT PROGRAMMES FOR CLUSTERS: EXPERIENCE OF THE REPUBLIC OF KAZAKHSTAN AND THE RUSSIAN FEDERATION

**Bozhko L.L., Turgel I.D., Sapanova R.K.**

*Rudny Industrial Institute, Rudny, bozhkoll70@gmail.com*

**ABSTRACT.** In the modern world, subject to active globalisation processes, the need to identify competitive advantages of territories is growing. One of the sources of such advantages is regional economy's clustering. At the same time, the question of effectiveness of state support measures aimed at industrial clusters development remains open. Based on the foregoing, study's relevance is determined by the need to develop a system of criteria for state support measures, allowing regional and cross-national comparisons. The research objective includes a comparative analysis of the legal regulation of cluster policy in the Republic of Kazakhstan and the Russian Federation; and development and testing of criteria for state support measures classification. The following methods of systemic and comparative analysis, formalised methods of regulatory acts analysis were used in the research. The novelty of the author's approach is the universality of the selected criteria, the possibility of their usage for state support measures analysis in various countries. The research information base was made up of programme documents, as well as strategies for socio-economic development of the regions of Kazakhstan and Russia, available at the official websites of regional administrations. During the research, an analysis of regulatory legal acts was carried out that form the basis of cluster policy in the Republic of Kazakhstan and the Russian Federation; the evolution of programme documents aimed at clusters development was studied; criteria for state support measures classification were established; and classification of state programmes according to the specified criteria was carried out. The practical significance of the research lies in the development of approaches that allow a comparative analysis of state regulation mechanisms for accelerated clustering of regions. The results obtained during the research can be used to determine priority areas for cluster policy development in the region.

**Keywords:** clusters, cluster policy, state programmes classification, Kazakhstan, Russia

### КОМПАРАТИВНЫЙ АНАЛИЗ ПРОГРАММ ГОСУДАРСТВЕННОЙ ПОДДЕРЖКИ КЛАСТЕРОВ: ОПЫТ РЕСПУБЛИКИ КАЗАХСТАН И РОССИЙСКОЙ ФЕДЕРАЦИИ

**Божко Л.Л., Сапанова Р.К.**

*Рудненский индустриальный институт, 111500 Рудный*

**РЕЗЮМЕ.** В современном мире, подверженном активным процессам глобализации, возрастает необходимость выявления конкурентных преимуществ территорий. Одним из источников таких преимуществ является кластеризация региональной экономики. При этом остается открытым вопрос эффективности мер государственной поддержки, направленных на развитие промышленных кластеров. Исходя из вышесказанного, актуальность исследования обуславливается необходимостью разработки системы мер государственной поддержки, позволяющей осуществлять региональные и кросс-национальные сравнения. Цель исследования включает проведение компаративного анализа нормативно-правового регулирования кластерной политики в Республике Казахстан и Российской Федерации, выработку и апробацию критериев для классификации мер государственной поддержки. В исследовании использованы методы системного и сравнительного анализа, формализованные методы анализа нормативно-правовых актов. Новизна авторского подхода состоит в универсальности отобранных критериев, возможности их использования для анализа мер государственной поддержки в различных странах. Информационную базу исследования составили программные документы, а также стратегии социально-экономического развития регионов Казахстана и России, представленные на официальных сайтах региональных администраций. В ходе исследования был проведен анализ нормативно-правовых актов, составляющих основу кластерной политики в Республике Казахстан и Российской Федерации; изучена эволюция программных документов, направленных на развитие кластеров; установлены критерии для классификации мер государственной поддержки, проведена классификация государственных программ по заданным критериям. Практическая значимость исследования заключается в разработке подходов, позволяющих провести компаративный анализ механизмов государственного регулирования ускоренной кластеризации регионов. Полученные в ходе исследования результаты могут быть использованы для определения приоритетных направлений развития кластерной политики в регионе.

**Ключевые слова:** кластеры, кластерная политика, классификация государственных программ, Казахстан, Россия

### Introduction

Clusters are drivers of modern economy development. Regardless of the specialisation of the clusters, their activities also affect the general indicators of socio-economic development of the territory. The presence of clusters contributes to an increase in such important parameters of economic development of territories such as employment, level of wages, the number of enterprises, their stability and development. At present, it is becoming especially important to study the place and significance of cluster policy in the socio-economic development of regions. Each of them is unique in its own way, combining presence of a variety of resources, technologies, potential capabilities. That is why it becomes so

important to develop an approach to classification of the clusters studied according to certain criteria. This allows us to identify general trends in the clustering of regional economy and to focus on development priorities.

The purpose of the study includes conducting a comparative analysis of legal regulation of cluster policy in the Republic of Kazakhstan and the Russian Federation, developing and testing criteria for classifying government support measures.

Achievement of the research goal is ensured by consistently solving the following tasks:

- to analyse regulatory legal acts that form the basis of cluster policy in the Republic of Kazakhstan and the Russian Federation;

- to propose criteria for classification of state support measures;
- to classify state programmes according to the criteria specified.

### Theoretical basis

The existing body of literature on the development of cluster initiatives and cluster policy can be divided into two groups. The first group of works is devoted to the issues of determining the essence of clusters and cluster policy, assessing its impact on the development of regional economy. Variants of definitions were proposed by L.S. Markov, V.B. Kurmashev, A. Yu. Nizkovsky, who came to the conclusion that "cluster policy is used as a generalised name for various methods of supporting and creating network associations of enterprises" [1]. Systematisation of the approaches of Russian and foreign scientists to the definition of the concept of "cluster" was carried out by M.S. Kokareva, who concludes that a cluster in general is a spatial form of organisation of productive forces, factors of production and social (economic and social) relations, which is characterised by the following characteristics: geographic location; specialisation of manufacturing firms; diversity and plurality of participants, their interdependence and complementarity; competition and cooperation "[2]. Furre H. emphasises the importance of impact of clusters on the economy and, in this regard, the need for a full study of such a concept as cluster policy and its components. The author himself defines a cluster as "a geographically close group of interconnected companies and associated institutions in a particular area, linked by common features and complementarities." The author refers to the cluster policy all policies that fall into one of three categories: those aimed at creating, mobilising or strengthening a specific cluster; using clusters to improve efficiency; aimed at creating an optimal environment for development and creating clusters [3].

Reflections on cluster policy and its role in economic development are contained in the works of Brakman, S., van Marrewijk, R.; Corrado, L., Martin, R., Weeks, M. Brakman, S., van Marrewijk, R. identify in their study a number of reasons why cluster policy is not always effective. Among them are the lack of a precise definition of the concept of "cluster"; difficulties in limiting a cluster in space; Porter's model is only partial [4]. Corrado, L., Martin, R., Weeks, M. in their study used a methodology that allows endogenous selection of regional clusters using a multidimensional stationarity criterion, where the number and composition of clusters are determined by applying pairwise criteria of regional differences in production volumes per capita in time [5].

Especially interesting is the study by E. Kozonogova [6], in which the author conducts economic and mathematical assessment of the impact of cluster policy on the quality of solving the tasks set by the Government: improving quality of life on the territory where the cluster is located; contribution to attracting investments to the territory; development of small and medium-sized businesses; development of international scientific and technical cooperation. As a result, it was proved that the fact of existence of a cluster in the territory is reflected in the amount of wages in it; with an increase in the number of clusters, the level of investment in fixed assets also increases. Ketels, C. in his study proves that development of clusters is closely related to changes in indicators' development of the

region. The article presents the opinions of foreign authors on the most significant criteria affecting cluster policy. Among them are the location of a cluster, its specialisation, size, etc. [7]. The aim of the study, conducted by DiMariaE., CostalongaG., was to find common theoretical foundations of the cluster concept in economics and concepts of internationalisation of business activity. The author notes that the internationalisation of clusters opens up wide opportunities for reorganisation of innovation processes in the regions, which are based on new forms of division of labour and cooperation among cluster members from different countries of the world. Using the example of Italian industrial regions, it is proved that clusters open their borders through expansion of production and distribution chains, both nationally and internationally. There are two main scenarios for development of internationalisation of clusters: production and commercial [8]. E. Kutsenko and D. Meissner [9] developing ideas about approaches to analysing the impact of clustering on the development of territories emphasize that the cluster approach makes innovation policy more systemic, coordinating measures aimed at supporting various participants in comprehensive efforts linking the most promising localised industries " ... The second group of studies is devoted to selection of criteria for classification of clusters. The importance of using the analysis of regulatory legal acts to study cluster policy was emphasised by L. Bozhko [10]. The work of M.N. Nikonova [11] should also be noted. The study is an analytical review of a modern package of documents, definitions, main institutional factors and concepts that determine cluster policy in the Russian Federation. In his research E.S. Kutsenko analyses characteristic features of a successful cluster (quality of urban environment; critical mass of specialised companies; domination of private initiative; internal competition and openness; presence of specialised independent governing bodies and active working groups; formalisation of rights, responsibilities and decision-making mechanisms; implementation of joint innovative projects and the formation of a belt of innovative start-ups around large companies or universities), correspondence of pilot innovative clusters in Russia to these characteristics, makes quantitative comparisons between Russian and foreign clusters [12].

Assessment of the impact of national cluster policy, age of a cluster, benchmarks for clusters development in neighbouring regions and aggregate level of regional innovation potential on the number and quality of cluster initiatives in Russia was carried out by E.V. Kutsenko, E. Islankina, V. Abakshin [16]. Certain issues of cluster policy were considered in the works of Delgado M., Porter M., Stern S. [17], K. Beshimbaev [18], O.V. Kostenko [19], Karlsson Ch. [20], E.E. Kolchinskaya, L.E. Limonova, E.S. Stepanova [21], O.A. Vasilyeva [22], E. Islankina [23], A.K. Akhmetovna, D.M. Serikovna, B.T. Sovetovich [24], EngelJ.S., I. del-Palacio [25]. Experience of Russia and Kazakhstan in the field of regional cluster policy was considered by I.D. Turgel, L.L. Bozhko, E.V. Prachevoy [26].

Thus, having considered several approaches to the task at hand, it can be noted that there is fairly large experience in the study of cluster policy at the national and regional levels, and variants of cluster classification have been developed. At the same time, the issues of analysing state programmes aimed at supporting clusters remain insufficiently studied.

## Methods and data

This study is based on analysis of key documents in the field of cluster policy in the Russian Federation and the Republic of Kazakhstan. The object of the research are state programmes aimed at the development of clusters. The choice of Russia and Kazakhstan for comparison is justified by a high degree of economic interconnections, similarity of trends in the social, economic and political development of these countries.

The work is based on a set of methods used to determine the main aspects of cluster policy. In addition to the analysis of regulatory legal acts, the study investigated information portals of the Russian Federation and the Republic of Kazakhstan, dedicated to the implementation of cluster policy. Particular attention was paid to information posted on the official portal of the project of "Map of Russian clusters". The collected statistics became the basis for further analysis.

The research includes three consecutive stages. At the first stage, the main normative legal acts in the sphere of cluster policy of the Russian Federation and the Republic of Kazakhstan were analysed. First of all, it was determined in which documents the main provisions of cluster policy were fixed. Conclusions are drawn about the general and distinctive features, developmental features. At the second stage, criteria for classification of the state support measures are proposed. These criteria were selected according to the principle of universality, as well as the possibility of combining clusters into groups or categories for the purpose of analysis. At the third stage, classification of state programmes was carried out according to the criteria specified.

## Results

### Legal regulation of cluster policy in Russia and Kazakhstan

Analysis of main regulatory legal acts in the field of cluster policy showed that the key directions of cluster development in Russia are determined by such regulatory legal acts as the Strategy for Innovative Development of the Russian Federation until 2020 and the Strategy for Spatial Socio-Economic Development of the Russian Federation until 2025. One of the 6 key tasks of the Strategy for Innovative Development of the Russian Federation until 2020 is associated precisely with the development of clusters: intensification of activities to implement innovation policy carried out by the authorities of the constituent entities of the Russian Federation and municipalities, formation of territories for innovative development, development of innovation clusters.

The need for cluster development is also emphasised in the Strategy for Spatial Socio-Economic Development of Russia. According to the Strategy, "innovative and social directions of the long-term socio-economic development of the Russian Federation are manifested in the following: formation of territorial production clusters (at least 6 - 8), focused on high-tech industries in priority sectors of the economy, with concentration of such clusters in urbanised regions; formation of territorial-production clusters in underdeveloped areas, focused on deep processing of raw materials and energy production using modern technologies."

The need for cluster policy is mentioned in many regulatory legal acts of the Republic of Kazakhstan. Importance of the work in this direction was emphasised in the Address of the

President of the Republic of Kazakhstan - the leader of the nation N.A. Nazarbayev to the people of Kazakhstan. In the Strategy "Kazakhstan-2050", the President sets a priority on the work on "road maps" for formation of promising national clusters.

*Implementation of cluster policy was carried out within the framework of the State Programme for Industrial and Innovative Development (SPIID) of the Republic of Kazakhstan for 2015-2019 and the project between the Government of the Republic of Kazakhstan and the World Bank "Increasing the competitiveness of small and medium-sized enterprises in Kazakhstan". Within the framework of the project, 6 pilot territorial clusters were identified, for which a cluster analysis was carried out in order to implement a cluster initiative, as well as accompanying measures of state support and necessary basis for the further implementation of cluster policy in the Republic of Kazakhstan were developed.*

The normative legal act that fixes the main provisions of cluster policy on the territory of the Republic is the Concept of formation of promising national clusters of the Republic of Kazakhstan until 2020. According to the Concept, cluster policy is focused on two areas: National clusters in traditional sectors of economy and clusters in the sectors of "economy of the future".

After analysing the documents in the field of cluster policy in Russia and Kazakhstan, we can conclude that it plays a significant role in building a strategy for development of territories. Support measures for cluster initiatives are very similar. First of all, in the regulatory legal acts of the Russian Federation, an emphasis is placed on the allocation of subsidies and co-financing of regional programmes, financing of research and development of cluster members, i.e. financial assistance, however, considerable attention is paid to the recognition of the need to establish relationships between participants in cluster policy.

### Classification of government programmes that promote cluster development

The following issues were identified as the main criteria for classification of state programmes contributing to intellectual and innovative clusters development:

- assistance in increasing the level of readiness of a cluster for transition to Industry 4.0 solutions through technological development, expansion of production and increase in exports;
- promoting innovative and technological development of a cluster through introduction of elements of Industry 4.0, which have technological, market and managerial readiness;
- creating basic conditions for smart cluster formation and ensuring digital synergy;
- assistance in re-employment of the labour resources released in connection with the intellectual and innovative clusters development (development of automation and digitalisation) (Table 1).

In the Republic of Kazakhstan, much attention is paid to the introduction of elements of 4.0 Industry. Accordingly, the criteria selected contain a set of measures related to technological development, expansion of production, increasing exports, development of automation and digitalisation, as well as introduction of elements of Industry 4.0, which have technological, market and managerial readiness. Among these criteria, the initiatives aimed at creating smart clusters and ensuring digital synergy are identified. But in this case, it should be noted that mechanisms

for financing the introduction of a concept of smart clusters have not been formed in the country yet. There is a deep gap

between the priorities declared at the national level and real actions.

Table 1. Classification of state programmes contributing to intellectual and innovative clusters development

Classification feature	Main purpose of support	State programme
Facilitating an increase in the level of readiness of a cluster for transition to Industry 4.0 solutions through technological development, expansion of production and increase in exports	sales growth	1. State programme for industrial and innovative development of the Republic of Kazakhstan for 2020 - 2025 2. Concept of industrial and innovative development of the Republic of Kazakhstan for 2020 - 2025 3. State programme for development of agro-industrial complex of the Republic of Kazakhstan for 2017-2021 4. Export strategy 5. Local content policy state programme "Otandykty Goldau", aimed at creating a strong base of local producers and their integration into the supply chain of large enterprises.
	investments growth	1. State programme for industrial and innovative development of the Republic of Kazakhstan for 2020 - 2025 2. Concept of industrial and innovative development of the Republic of Kazakhstan for 2020 - 2025 3. State programme for development of agro-industrial complex of the Republic of Kazakhstan for 2017-2021 4. Export strategy
	acceleration of technological modernisation	1. State programme for industrial and innovative development of the Republic of Kazakhstan for 2020 - 2025 2. Concept of industrial and innovative development of the Republic of Kazakhstan for 2020 - 2025 3. State programme for development of agro-industrial complex of the Republic of Kazakhstan for 2017-2021
Promoting innovative and technological development of a cluster through introduction of elements of Industry 4.0 that have technological, market and managerial readiness	development of digital competencies	Package of measures 2025
Creation of basic conditions for formation of a smart cluster and ensuring digital synergy	digital creation	1. State programme "Digital Kazakhstan" 2. Improving the position of the Republic of Kazakhstan in the rating of network infrastructure development of the WEF
Promoting re-employment of released labour resources in connection with intellectual and innovative clusters development	levelling of negative effects	1. Employment and Entrepreneurship Programme 2017 - 2021 2. Business Roadmap 2025

The following criteria were identified as the main ones for classification of government programmes that contribute to the development of industrial clusters in the Republic of Kazakhstan:

- promoting development of industrial cooperation and cooperation of cluster members;

- creation of basic conditions for ensuring import substitution;

- promoting innovative and technological development of a cluster (table 2).

Table 2. Classification of government programmes contributing to industrial clusters development

Classification feature	Main purpose of support	State programme
Promoting the development of industrial cooperation and cooperation of cluster members	development of cooperation	1. State programme for industrial and innovative development of the Republic of Kazakhstan for 2020 - 2025 2. Concept of industrial and innovative development of the Republic of Kazakhstan for 2020 - 2025 3. State programme for development of agro-industrial complex of the Republic of Kazakhstan for 2017-2021 4. Economy of simple things (2018-2020)
Creation of basic conditions for ensuring import substitution	growth of localisation	1. Local content policy state programme "Otandykty Goldau", aimed at creating a strong base of local producers and their integration into the supply chain of large enterprises
Promoting innovative and technological development of a cluster	investments growth	1. State programme for industrial and innovative development of the Republic of Kazakhstan for 2020 - 2025 2. Concept of industrial and innovative development of the Republic of Kazakhstan for 2020 - 2025 3. State programme for development of agro-industrial complex of the Republic of Kazakhstan for 2017-2021 4. Export strategy 5. Economy of simple things (2018-2020)

The following criteria were identified as the main ones for classifying government programmes that contribute to pilot innovative territorial clusters development in the Republic of Kazakhstan:

- promoting development of innovation infrastructure;

- creating business climate;  
- creation of an infrastructure for collective use of a cluster (laboratories, centres of competence, service centres, showrooms, etc.) (Table 3).

Table 3. Classification of state programmes contributing to pilot innovative territorial clusters development

Classification feature	Main purpose of support	State programme
Promoting innovative infrastructure development	creation of an innovation ecosystem	1. State programme "Innovative Kazakhstan"
Creating business climate	shaping business environment	1. Local content policy state programme "Otandykty Goldau" aimed at creating a strong base of local producers and their integration into the supply chain of large enterprises 2. "Enbek" Programme (2017-2021) 3. Tourism Industry Development Programme (2019-2025)
Creation of infrastructure for collective use of a cluster (laboratories, competence centres, service centres, show rooms, etc.)	development of scientific infrastructure	1. State programme for industrial and innovative development of the Republic of Kazakhstan for 2020 - 2025 2. Concept of industrial and innovative development of the Republic of Kazakhstan for 2020 - 2025 3. State programme for development of agro-industrial complex of the Republic of Kazakhstan for 2017-2021 4. Export strategy

In general, we can distinguish 3 classification features that allow identifying a set of measures aimed at supporting all types of clusters in the Republic of Kazakhstan:

- measures of state support;  
- targets of state support;  
- sectoral focus of state support (table 4).

Table 4. Classification of a set of measures aimed at supporting all types of clusters in the Republic of Kazakhstan

Classification feature	Types of clusters		
	Intellectual and innovative clusters	Pilot innovative territorial clusters	Industrial clusters
State support measures	Comprehensive support cluster development (export, attraction of investments, commercialisation of technology, training of managers cluster, etc.)	Possibility of introducing fiscal incentives, as well as revising the rules on failed innovations. Establishing international cooperation and building partnerships with international organisations in the field of industrial and innovative development and technology transfer. Measures to stimulate creation of venture capital funds will be taken that will focus on solving industry-based venture funds in the manufacturing industry. Tools to attract players of the start-up ecosystem to solving technological problems and problems of manufacturing enterprises will be developed. Measures to stimulate the market for technology brokerage services, creation of cluster competence centres, service centres for equipment maintenance, as well as centres for the exchange of experience and information, including the development of local competencies suppliers will be developed.	Information and analytical support and state support aimed at the development of cooperation and cooperation of participants. Human resource development (trainings, education, professional development). Cluster expansion (attracting foreign investors, conducting an information and advertising campaign). Innovative and technological development, including stimulating creation of specialised regional engineering organisations. Creation of infrastructure, including on the basis of public-private partnership. Stimulation of improving manufactured products quality (testing facilities, laboratories).
State support targets	On increase in the volume of non-resource exports, attraction of investments, implementation of 4.0 Industry	Development of innovation infrastructure and innovation cycle	Strengthening industrial cooperation, import substitution course
Sectoral focus of state support	Information and communication technologies, advanced technologies (clean and green technologies, smart industry, smart environment, e-commerce and media) Production of new materials, advanced technologies (energy saving, 3D printing, biotechnology) and design.	Development of universities and business incubators	Manufacturing industry

Thus, government measures to support clusters in the Republic of Kazakhstan are linked to the country's overall development strategy. The complex of key state programmes defined by the Plan of the Nation - 100 Concrete Steps is aimed at accelerating the technological modernisation of the country's economy. Key policy documents include as follows:

- SPIID-3 (2020-2025) - continuation of SPIID-2 (2015-2019), focusing on manufacturing industry;
- Economy of simple things (2018-2020) - focusing on the agro-industrial complex and manufacturing industry;

- Agro-industrial complex development programme (2017-2021) - a set of measures for agro-industrial complex development;

- DKB-2025 (2020-2024) - continuation of the DKB-2020, development of entrepreneurship in villages and priority sectors;

- The Enbek programme (2017-2021) - stimulation of mass entrepreneurship.

In addition, most cities in the Republic of Kazakhstan and the Russian Federation seek to consolidate cluster policy priorities in strategic urban development plans (Table 5).

Table 5. Priorities of cluster policy in accordance with the strategy of socio-economic development of cities in Russia and Kazakhstan

City	Cluster policy priorities
Kazan	- formation of "smart" economy clusters; - implementation of technical re-equipment of the production base of the clusters being formed; - promoting creation of creative campus clusters, co-working spaces for innovative and creative entrepreneurship, attracting international partners; - promoting effective interaction between business, science and government within clusters.
Yekaterinburg	"IT-cluster" as a project within the framework of the strategic programme of "Digital Yekaterinburg".
Novosibirsk	- development of scientific and industrial clusters as one of the opportunities to develop the city of Novosibirsk; - information cluster development as one of the ways to implement of digital economy.
Rostov-on-Don	- activation and expansion of cluster policy in key areas of industry; - launching cluster projects in the fields of mechanical engineering, food industry and digital media communications; - participation in the development of existing and creation of new cluster interactions for development of information and communication infrastructure.
Voronezh	- creating conditions for activation of city's universities in the creation of technology parks, clusters, and other forms of integration interaction; - activation of cluster policy in the industry; - formation of scientific and educational, and scientific and industrial clusters in high-tech sectors of the economy.
Samara	- launching the process of regular elaboration of product, technological and managerial prospects for development of industrial sectors and clusters as one of the goals of innovative and technological production; - development of tourism and aerospace clusters.
Krasnoyarsk	- ensuring development of the tourist and recreational cluster; - creation of conditions for high-tech competitive clusters development; - creating conditions for formation and development of a medical cluster.
Perm	ensuring coordination of plans and development programmes for the city of Perm and large enterprises, including formation of clusters to assist the city's enterprises in obtaining resources for modernisation and development as one of the key tasks of functional-target direction of "Economic Development".
Krasnodar	Economic development objectives: Development of a cluster of "creative industries", a financial cluster, a transport and logistics cluster, an industrial and construction cluster, an agro-scientific cluster, a tourism cluster, an educational and scientific cluster, an "Olympic" cluster
Volgograd	- formation of transport and logistics cluster as one of the development goals of the city's transport and logistics complex; - creation of favourable environment for activities of the subjects of tourism industry, formation and development of a full-fledged tourist cluster on the territory of Volgograd.
Nur-Sultan	- development of the educational cluster as a means of providing highly qualified personnel staff and a way to attract investment; - development of a cluster of financial services as a means of improving their quality, stimulating development of financial technologies, transfer of knowledge and technologies.
Almaty	- development of tourism cluster to world level; - creation of scientific, educational and industrial clusters together with coordination training centres for training, retraining, advanced training and certification of personnel at organisations of technical and vocational education.
Shymkent	- development of greenhouse clusters in the peripheral territory as a way to form an agro-zone with intensive technologies; - implementation of "Food Clusters" Concept with characteristics of the agricultural park.

It should be noted that not all urban strategies mention cluster policy. For example, the cities of Ufa, Omsk, Chelyabinsk and Nizhny Novgorod have not specified it in the strategy of socio-economic development.

## Conclusion

The interest in the issues of cluster policy and its impact on socio-economic development of the territory led to the creation of many methods for studying clusters, depending on their distinctive features. The research is based on the analysis of clusters located on the same territory. In our study, we

identified a specific algorithm by which one can analyse governmental programmes aimed at developing clusters.

The regulatory legal acts that form the basis of cluster policy in the Russian Federation and the Republic of Kazakhstan were investigated during the study. We managed to determine the vectors of further development of cluster policy in Russia and Kazakhstan, its priorities and measures of state support. The analysis showed that the cluster policy is an integral and promising part of the further development of territories. In both Russia and Kazakhstan, innovation clusters are a priority.

Criteria for classification of state programmes aimed at the development of intellectual and innovative, industrial and pilot innovative territorial clusters were established.

It has been determined that the strategy of socio-economic development is the main document in the sphere of cluster policy on the territory of cities.

The study has confirmed that cluster policy plays a crucial role in the socio-economic development of the countries studied. Competent selection of criteria for clusters' classification will allow obtaining qualitatively new results and making a conclusion about the further development of the researched object.

## References

1. Markov L. S., Kurmashev V. B., Nizkovskiy A. Yu. (2017). Federal and regional cluster policy of the Russian Federation. *World of Economics and Management*, 17 (4), doi 10.25205/2542-0429-2017-17-4-107-121 (In Russ.)
2. Kokareva M.S. (2008). Theoretical aspects of clusters formation: essence and classification. *Economy of Region*, S4, 136-148. (In Russ.)
3. Furre H. (2008). Cluster Policy in Europe-A Brief Summary of Cluster Policies in 31 European Countries, Oxford Research AS, Norway.
4. Brakman, S., van Marrewijk, C. (2013). Reflections on cluster policies. *Cambridge Journal of Regions, Economy and Society*. 6 (2), 217-231.
5. Corrado, L., Martin, R., Weeks, M. (2005). Identifying and Interpreting Regional Convergence Clusters across Europe. *The Economic Journal*, 115 (502), 133-160.
6. Kozonogova E.A., Dubrovskaya J., Goncharova N., Elokhova I. (2018, November). Does state cluster policy really promote regional development? The case of Russia. IOP Conference Series: Materials Science and Engineering. Paper presented at the 2nd International Scientific Conference on Digital Transformation on Manufacturing, Infrastructure and Service. Saint-Petersburg: IOP Publishing.
7. Ketels C. (2013). Recent research on competitiveness and clusters: what are the implications for regional policy? *Cambridge Journal of Regions, Economy and Society*, 6 (2), 269-284.
8. Di Maria E., Costalonga G. (2004). Internationalization and innovation in CADSES SMEs and clusters: the INDE results. Internationalisation processes and virtual cluster promotion in the CADSES area (INDE project final document), 3, 48-70.
9. Kutsenko E. S., Meissner D. (2013). Key Features of the First Phase of the National Cluster Programme in Russia. Series: science, technology and innovation. Working papers by NRU Higher School of Economics. Series WP BRP Science, Technology and Innovation.
10. Naizabekov A., Bozhko L. (2018, May). Future development of cluster initiatives in the Republic of Kazakhstan. Paper presented at the International Scientific Conference Environmental and Climate Technologies, CONECT 2018, Riga (654-659).
11. Nikonova M. N. (2016). Cluster policy in the Russian Federation: basic documents, regulations, institutional factors and concepts. *Political Science Issues*, 4(24), 229-239. (In Russ.)
12. Kutsenko E. S. (2015). Pilot Innovative Territorial Clusters in Russia: A Sustainable Development Model. *Foresight and STI Governance*, 9, 32-55. (In Russ.)
13. Rodionova I., Krejdenko T., Cezary Madry (2018). Cluster policy in the Russian Federation: a case study of industrial clusters. *Quaestiones Geographicae*, 37 (2), 61-75.
14. Mitrofanova I.V., Sheikin D.A., Ivanov N.P., Trilitskaya O.Y. (2019). Quality management of cluster institutional development: new trends and the best practices in regions of the world and Russia. *International Journal for Quality Research*, 13(2), doi: 24874/IJQR13.02-01
15. Zemtsov S.P., Pavlov P.N., Sorokina A.V. (2016). Specifics of Cluster Policy in Russia. *Quarterly Journal of Economics and Economic Policy*, 11(3), 499-536.
16. Kutsenko E.V., Islankina E., Abashkin V. (2017). The evolution of cluster initiatives in Russia: the impacts of policy, life-time, proximity and innovative environment. *Foresight*, 19 (2), 87-120.
17. Delgado M., Porter M., Stern S. (2014). Clusters, convergence, and economic performance. *Research Policy*. 43(10), 1785-1799.
18. Kuandyk Beshimbaev (2004, November). Industrial and territorial clustering as a vehicle for industrial restructuring. Paper presented at the Regional forum Public-private Co-operation in Industrial Restructuring. Kazakhstan: Organisation for Security and Co-operation in Europe. (In Russ.)
19. Kostenko O.V. (2016). The main directions and priorities of the cluster policy of Russia. *Problems of modern science and education*. (In Russ.)
20. Karlsson Ch. (2008). Handbook of Research on cluster theory. Cornwall: Edward Elgar Publishing, 316.
21. Kolchinskaya E. E., Limonov L. E., Stepanova E. S. (2018). The role of clusters and cluster policy in the development of Russian regions: statement of the problem and a possible approach to assessment. *Proceedings of the Russian Geographical Society*, 150 (3), 1-11. (In Russ.)
22. Vasileva O. A. Cluster policy in Kazakhstan: preconditions and peculiarities of cluster agrarian. *State Advisor*, 2(10), 16-20. (In Russ.)
23. Islankina E. (2015). Internationalization of Regional Clusters: Theoretical and Empirical Issues. *Science, Technology and Innovation*.
24. Akhmetovna A. K., Serikovna D. M., Sovetovich B. T. (2018). Assessment and identification of the possibility for creating it clusters in Kazakhstan regions. *Economy of Region*, 14(2), 463-473.
25. Engel J.S., I. del-Palacio. (2009). Global networks of clusters of innovation: Accelerating the innovation process. *Business Horizons*, 52 (5), 493-503.
26. Turgel I.D., Bozhko L.L., Pracheva E.V. (2019). Special economic zones as a tool for regional and cluster policies (experience of Russia and Kazkhstan). *Scientific works of the Freedom economic society of Russia*, 215 (1), 385-400. (In Russ.)
27. Кластерный подход: почему одни регионы успешнее других (2019). Получено из: <https://cluster.hse.ru/news/341473882.html> (по состоянию на 27 февраля 2020 года).
28. И. Тургель, Л. Божко, А. Ойхер. Кластерная политика индустриального региона / Экономика и управление: Научно-практический журнал, № 1 (151), 2020, с.32-36, DOI: 10.34773/EU.2020.1.8
29. Turgel, I.D., Bozhko, L.L., & Pandzhiyeva, V.T. (2020). Cluster policies of large cities in Russia and Kazakhstan. *R-economy*, 6 (1), 28-39. doi: 0.15826/recon.2020.6.1.003.

## INTERPHASE FORMATIONS IN COPPER EXTRACTION SYSTEMS

**T.A. Chepushtanova<sup>1</sup>, M. Yessirkegenov<sup>2</sup>, K.K. Mamyrbayeva<sup>3</sup>, A. Nikoloski<sup>4</sup>, V.A. Luganov<sup>5</sup>**

<sup>1,2,3,5</sup> Satbayev University, Kazakhstan, Almaty, 050013, str. Satpayev 22; T.chepushtanova@satbayev.university, tanya2305@list.ru

<sup>4</sup>Murdoch University South St, Murdoch WA 6150, a.nikoloski@murdoch.edu.au

**ABSTRACT.** The technology of Solvent extraction-electrowinning is widely used for the production of copper from poor oxidized ores. The main problem in solvent extraction is the formation of interfacial formations (crud) on the liquid/liquid interface. Many factors influence the formation of crud and their study of which is currently an actual problem. For research, we took the primary ore from the Oxide Ore Process plant in Kazakhstan with a copper content of 0.37%. As a result of ore leaching with sulfuric acid (30 g/l), we obtained a productive leach solution (PLS) of the composition, g/L: Cu 3.5-4.93; SiO<sub>2</sub> 0.6; Fe<sup>2+</sup> 3.0-3.1; S<sub>общ</sub> 54,3-62,1; Mn 0.5-0.55. To determine the phase separation time and the effect of the organic phase composition on the formation of crud, laboratory extraction tests were carried out with extractants ACORGA M5640 (with modifier) and LIX984N (without modifier) in diluent ShellSol D70. PLS contained Cu - 3.5 g/L and 370 mg/L of; pH - 1.2. It was established that the formation of crud in both extractants is the same. However, the phase separation time in experiments using the LIX984N extractant was 10 seconds shorter than in experiments using the ACORGA M5640 extractant and amounted to 110 and 120 sec, respectively.

**Keywords:** Solvent extraction, copper, liquid/liquid interface, crude, PLS, extractant

### МЕЖФАЗНЫЕ ОБРАЗОВАНИЯ В ЭКСТРАКЦИОННЫХ СИСТЕМАХ МЕДИ

**T.A. Чепуштанова<sup>1</sup>, М. Есиркегенов<sup>2</sup>, К.К. Мамырбаева<sup>3</sup>, А. Николоски<sup>4</sup>, В.А. Луганов<sup>5</sup>**

<sup>1,2,3,5</sup> Satbayev University, Казахстан, Алматы, 050013, ул. Сампаева 22; T.chepushtanova@satbayev.university, tanya2305@list.ru

<sup>4</sup> Университет Мёрдока, Южная ул. Мёрдок WA 6150, a.nikoloski@murdoch.edu.au

**РЕЗЮМЕ.** Для производства меди из труднообогатимых бедных окисленных руд широко применяют технологию «жидкостная экстракция, электролиз». Основной проблемой при экстракции меди является формирование на поверхности раздела жидкость/жидкость межфазных образований (крада), которая приводит к снижению производительности всего предприятия. На образование крада влияют многие факторы и изучение которых является в настоящее время актуальной проблемой. Для исследований нами была взята исходная руда с производственного комплекса Актогай с содержанием меди 0,37%. В результате выщелачивания руды серной кислотой концентрацией 30 г/л нами был получен продуктивный раствор состава, г/дм<sup>3</sup>: Cu 3,5-4,93; SiO<sub>2</sub> 0,6; Fe<sup>2+</sup> 3,0-3,1; S<sub>общ</sub> 54,3-62,1; Mn 0,5-0,55 и др. С целью определения времени расслоения фаз и влияния состава органической фазы на образования крада лабораторные тесты по экстракции были проведены с экстрагентами ACORGA M5640 (с модификатором) и LIX984N (без модификатора). Опыты проводились в условиях: концентрация экстрагента 16 %, разбавитель - ShellSol D70; соотношение водной и органической фаз - 1:1; продолжительность экстракции 180 сек, температура - 20°С. Состав РЛС: Cu - 3,5 г/л и 370 мг/л растворенных взвесей; pH - 1,2. Установлено, что образование межфазовой взвеси (крада) в обоих экстрагентах одинаково. Однако, время расслоения фаз в опытах с применением экстрагента LIX984N было на 10 секунд короче, чем в опытах с применением экстрагента ACORGA M5640 и составили 110 и 120 сек соответственно.

**Keywords:** Solvent extraction, copper, liquid/liquid interface, crude, PLS, extractant

### Introduction

Due to the depletion of reserves of copper-bearing ores in modern Kazakhstan, poor oxidized and mixed ores are increasingly involved in copper production. The copper content in the ore of the deposits that are currently being developed in Kazakhstan is on average 0.36-0.45% versus the average 0.95% worldwide. To extract copper from such poor raw materials, it is necessary to use new efficient technologies and processing facilities. These methods, in particular, include the technology Solvent Extraction - Electrowinning (SX-EW) with the use of modern extractants with high technological properties.

The advantage of extraction lies primarily in the organization of a continuous high-performance process, and, consequently, in reducing capital and operating costs and improving working conditions. It should also be noted that the extraction in most cases is carried out at normal pressure and

temperature. The extraction technology is characterized by high selectivity in relation to the recovered metal, which allows the process to be carried out with a short duration of the technological cycle, relatively low costs and expenses of chemical reagents. In accordance with this, it becomes possible to process poor raw materials, the extraction of metals from which was previously considered economically unprofitable. The extraction technology for producing copper is more complicated than the cementation of copper with iron scrap, but as a result of its application, cathode copper is immediately obtained, iron does not accumulate in the circulating solutions, and, in addition, sulfuric acid is regenerated. The latter allows saving up to one and a half kilograms of acid on each kilogram of copper. In this regard, experimental studies on the extraction method using new highly effective, readily available and relatively inexpensive extractants are relevant.

Since 2007, 4 projects have been implemented in Kazakhstan on the technology of solvent extraction and electrowinning. However, at the moment, two projects are suspended due to the problem of processing productive leach solutions (PLS) of complex composition.

The main problem during extraction is the formation of interfacial formations (crud) of a certain thickness at the liquid-liquid interface, which leads to a decrease in the productivity of extraction processes and the quality of the obtained cathode copper, and the consumption of expensive reagents.

Crud is the material formed at the interface, when the emulsion formed due to mixing with the organic phase is mixed with the solid phase or dissolved elements in the PLS production solution.

The emulsion is a stable third phase at the interface between the organic and aqueous phases in settling separators. It prevents normal phase separation and contributes to additional losses of the organic phase: "This data are published by David J. Readett (1997)".

The formation of crude is influenced by many factors, the study of which is an urgent problem. Therefore, the proposal of schemes for the extraction stage, measures to prevent the formation of crude at each of them is impossible without preliminary individual testing and solving problems.

The aim of our research was to study the formation of interfacial formations (crud) at the interface between the aqueous and organic phases during the extraction of copper with extractants ACORGA M5640 (with a modifier) and LIX984N (without a modifier).

## Experiment

### Materials

We took oxidized ore and a productive solution (PLS) from a cathode copper plant in Kazakhstan as the initial ore.

Physicochemical methods of analysis have established the material composition of the original ore (Table 1).

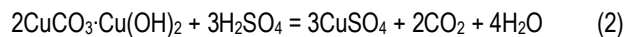
Table 1. Results of the analysis of oxidized ore

Component	Content, %
Cu – average	0.36-0.41
SiO <sub>2</sub>	51-67
Al <sub>2</sub> O <sub>3</sub>	13-22
FeO	0.3-5.5
Fe <sub>2</sub> O <sub>3</sub>	0.55-4.9
MnO	0.03-0.18
CaO	2-6
MgO	0.5-4
Chlorides	0-0.08

As the results of the analysis show, the copper content in the ore is low and averages 0.39 %, the ore is dominated by silicon. The main copper minerals in the ore are malachite, azurite, tenorite and chrysocolla.

Leaching of this type of raw material is efficiently carried out with mineral acids, and the most cost-effective is non-oxidative sulfuric acid leaching.

The process of leaching malachite, azurite, tenorite and chrysocolla with sulfuric acid can be described by the following reactions:



Under conditions of excess sulfuric acid in the leaching solution, the dissolution of chrysocolla can proceed with the formation of colloidal silicic acid, the increased content of which in solutions complicates the processing of these solutions by extraction.



At the process plants of Kazakhstan, leaching of the original ore is carried out by the heap method with a solution of sulfuric acid with a concentration of 20-35 g/l to obtain productive solutions. The main factor causing the formation of crud is the properties of the original PLS and the mode of operation of solvent extraction. For the study, samples of PLS and solid crud were taken from the cathode copper plant, the compositions are given in Tables 2 and 2.1.

Table 2. Chemical analysis of PLS and crud

№	Component	SiO <sub>2</sub>	Fe <sup>2+</sup>	S <sub>tot</sub>	Ca	Mg	Na
1	PLS, g/l	0,6	3,1	54,3	0,09	7,81	2,5
2	PLS, g/l	0,6	3,0	62,1	0,09	7,3	2,2
3	Crud, %	41,44	0,65	3,21	0,11	0,51	0,14
4	Crud, %	41,62	0,69	3,4	0,19	0,56	0,16

Table 2.1. Chemical analysis of PLS and crud

№	Component	K	Al	Fe	Mn	Cu
1	PLS, g/l	0,034	14,5	8,24	0,55	4,93
2	PLS, g/l	0,033	13,2	7,8	0,5	4,78
3	Crud, %	<0,05	1,15	0,55	0,03 5	0,3
4	Crud, %	<0,05	1,27	0,61	0,03 8	0,33

As the chemical analysis of PLS shows, a solution was obtained during leaching that is quite suitable for the extraction of copper by (4.78-4.93 g / l) solvent extraction.

According to studies, the main factors causing the occurrence of interphase formations are the composition of the initial solution (PLS), the organic phase, suspended solids in the PLS and the operating mode of the solvent extraction stage.

The chemical composition of the productive solution obtained by leaching the original ore shows that, in addition to dissolving copper as the base metal, undesirable impurity metals such as silicon, aluminum, magnesium, iron and manganese are present in the solution.

It is known that the dissolved silicon oxide, entering the liquid extraction cycle, forms crud due to the polymerization reaction, and dissolved aluminum and magnesium, interacting with sulfuric acid, increase the viscosity of the solution "This result is published by P. Cole and T. Bednarski \* (2016)".

The presence of manganese impurities in the productive solution negatively affects both the extraction rates and the copper electrolysis process. This is due to the fact that manganese ions are prone to oxidation and the formed MnO<sub>4</sub>-

and other high-valence manganese ions increase the electrolyte oxidation potential, and upon contact with the organic phase lead to its oxidation, thereby forming interfacial suspensions.

$Fe^{3+}$ ,  $Mg^{2+}$ , fine air bubbles and suspended particles in the leach solution contribute to the formation of crud.

The authors noted that at  $pH > 2.5$   $Fe^{3+}$  enters into hydrolysis and polymerization reactions with the formation of complex ions  $FeOH^{2+}$ ,  $Fe_2(OH)_2^{4+}$ . Reference needed is needed

The volume of crud formation also increases with an increase in the pH of the solution and decreases with an increase in the phase ratio: This data are published by R.F.Dalton, C.Maes (1983).

*Reagents:* organic phase containing ACORGA M5640 extractant (16 %) and ShellSol D70 diluent (400 ml); organic phase containing LIX984N extractant (16 %) and ShellSol D70 diluent (400 ml); PLS solution, Table 3.

Table 3. *Properties of extractants*

Extractants for copper	LIX984N	ACORGA M5640
Chemical components	Aldoxime + Ketoxim	Aldoxime + modifier
Selectivity (Cu/Fe)	Medium	High
PpH	Medium acidity	Acidic
Cu	Average content	High content
Manufacturer	BASF	SOLVAY

As a productive solution, a solution from a copper cathode plant was used, with a copper content of 3.5 g/l and PPH -1.2 and 370 mg/l of dissolved suspensions. The test was carried out at room temperature.

### Crud formation studying

To study the effect of the organic phase on the formation of interfacial formations (crud) at the boundary between the aqueous and organic phases, we used the extractants ACORGA M5640 (with a modifier) and LIX984N (without a modifier). Some experts on solvent extraction of copper, argue that modified extractants lead to the formation of interfacial suspension (crud) in the process of liquid extraction, which aroused interest in this work.

Extractant ACORGA M5640, consists of an active molecule aldoxime mixed with an ether modifier, while extractant LIX984N, consists of active molecules aldoxime and ketoxime without the addition of a modifier.

As a diluent, a dearomatized hydrocarbon solvent ShellSol D70, consisting mainly of naphthenes and paraffins C 11 - C 14, and with a high boiling point ( $> 190$  °C) was used.

The experiments were carried out under the following conditions: the concentration of the extractant in the diluent was 16 %, the volume of the organic phase was 400 ml, the ratio of the organic and aqueous phases was 1: 1, the temperature was 20 °C, the stirring rate of the phases was 600 rpm, the duration of stirring was 180 sec.

## Results and discussion

The experimental results are shown in table 4. The copper content in PLS was 3.5 g/l, pH was 1.2.

Table 4. *Results of studying the effect of the organic phase on the formation of interphase formations (crud)*

No	Organic phase	Aqueous phase	Mixing time	Separation time, s	Visually observation
1	ShellSol D70 + 16% LIX984N	PLS (Cu – 3.5 g/L, pH - 1.2)	180 se	110-115	A gray film was observed at the boundary between the aqueous and organic phases
2	ShellSol D70 + 16% ACORGA M5640	PLS (Cu – 3.5 g/L, pH - 1.2)	180 s	120 s	A gray film was observed at the boundary between the aqueous and organic phases

On the basis of the experiments carried out, it can be concluded that the appearance of interfacial formations (crud) occurs in the two experiments in the same way, and the phase separation in the first experiment with the use of the extractant LIX984N is 10 seconds shorter.

The formation of interfacial suspensions is clearly seen in Figure 1.

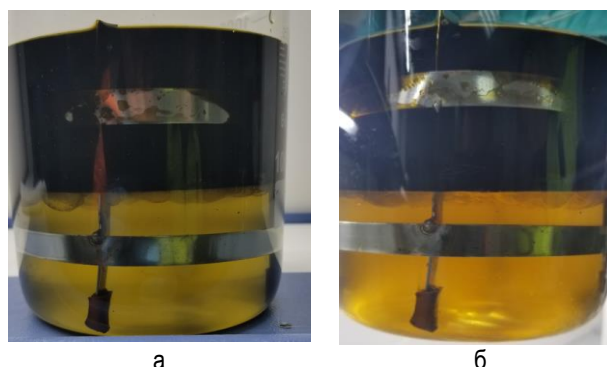


Fig. 1. *Formation of interfacial suspensions (crud) during copper extraction with extractants LIX984N (a) and ACORGA M5640 (b)*

During research, it was found that the formation of crud is promoted by:

- the presence of organic phase oxidation products.
- unfavorable composition of product solutions (increased content of solid slime particles, increased content of dissolved silicon in the solution, etc.);
- excessive intensity of mixing during extraction.

Thus, on the basis of our studies, we can conclude that the ratio of interfacial suspension (crud) in both extractants is the same, and the phase separation in the experiments using the LIX984N extractant (without the modifier) was 10 seconds shorter than in the experiments using extractant ACORGA M5640 (with modifier). The presence of the modifier in the organic phase did not affect the formation of interfacial suspension.

### Study of the effect of silicon on PLS solutions

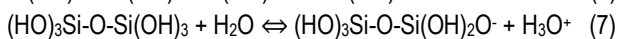
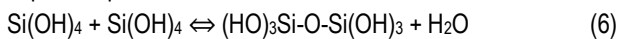
We have studied the effect of various impurities on the formation of interfacial suspension. Silicon in solution appears during leaching of silicon ores as a result of the interaction of silicon ores with sulfuric acid, especially at low pH values, or during the dissolution of copper silicon minerals such as chrysocolla. Dissolved silicon can affect the properties of the organic / water interface by interacting with the active components of the organic phase, resulting in the appearance of suspended solids.

Natural silicon dioxide, found in minerals, has a low aqueous solubility. However, when these minerals are dissolved in strong acids, large amounts of silicic acid are released. This can then polymerize in solution to form colloidal silicon dioxide. This colloidal silicon dioxide can be stable in solution at high levels and over time.

The colloidal silicon can pass through the leaching process without affecting any performance in weak solution irrigation and copper recovery in extraction. However, this can cause several problems when mixing with organic matter, settling, and the dynamics of solutions in extraction. When mixed with an organic solution, they can form a waste mass and significantly interfere with the flow of the aqueous phase of the solvent extraction.

In the water continuity mode of the SX mixer and in the presence of dissolved silicon, long periods of disruption of phase interaction often occur, which leads to a significant increase in the entrainment of organic and aqueous phases (up to 200 mg / L and above).

The stability of dissolved silicon depends on chemical and physical factors. Certain cations such as aluminum, manganese and molybdenum are very effective in stabilizing colloidal silicon and pH is very important, with stability maximizing around pH 2. Silicic acid undergoes a complex series of interrelated condensations (equation 6) and ionizations (equation 7) depending on temperature, pH and impurities present:



In the solvent extraction process, silicon can have the most dramatic effect. With the transition of the mixer operation to water continuity, the phase separation time increases several times, respectively, the dispersed belt in the settler shifts to the organic and aqueous phase gutters. These changes upset the stability of the compacted crud and then this crud is poured through the chute into the next stages. This phenomenon is considered undesirable, since when crud goes to the next stage, the mode of operation of the mixer of the next stage switches to water continuity, which can effect dramatically to organic loses or process cost.

Study of the physical properties of the crud. Increasing the viscosity of the solution. When designing SX-EW plants, it is important not only to control the content of iron, chlorides, silicon and so on, but also the presence of aluminum and magnesium in the productive solution, which can increase the PLS viscosity, leading to a deterioration in the physical parameters of the solution, as well as to a decrease in copper recovery. due to low extraction efficiency. The efficiency of the extraction process depends on many factors, some of them are listed below: temperature, separation time, stirring speed / mixer rotation speed, quality of the organic phase, impurities in

PLS solutions, PLS solution viscosity, phase ratio, extractant formula etc.

Table 5. Datas on the values of the viscosity of solutions with the corresponding extraction efficiency

Dilution with water, %	Solution viscosity, Poise	Extraction efficiency, %
0	7,8	91,6
25	4,2	94,1
50	2,8	95,6
75	1,7	98,3

It was found that with an increase in the viscosity of the solution, the time of phase separation increases, which in turn leads to significant carryover of the organic phase together with the aqueous phase, and most of it is irretrievably lost in the process of heap leaching.: The data are published by Alexis Soto L. and Hector Yáñez F. (2017).

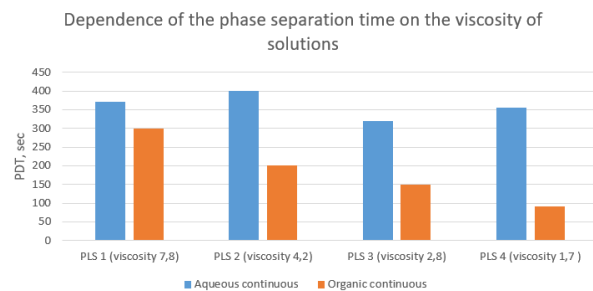


Fig. 2. Dependence of the phase separation time on the viscosity of the solutions

Thus, the conducted technological studies show that control of the viscosity of the aqueous phase can provide a low cost of the extraction processing in the SX-EW process.

To clarify the composition, we carried out X-ray diffraction studies of samples of interfacial suspensions (crud) formed during extraction. The survey was carried out on a D8 Advance (Bruker) apparatus, Cu K $\alpha$  radiation, voltage across the tube 40 kV, current 40 mA. The processing of the obtained data of diffraction patterns and the calculation of interplanar distances were carried out using the EVA software.

Phase analysis (diffractometer DRON-3) shows that the waste mass is partially in an amorphous state, the compositions of interfacial suspensions (crud) in both extractants differ in composition by decimal fractions. The main components of crud are aluminum and magnesium hydrogen sulfates. The silica content in the crud formed when using the ACORGA M5640 extractant is 0.9% higher compared to the LIX984N extractant.

In order to study the microstructure of the samples, the waste mass samples were examined using a JEOL ISM - 25S 3 scanning electron microscope. The Figure 3 shows images in backscattered electrons at a magnification of x100.

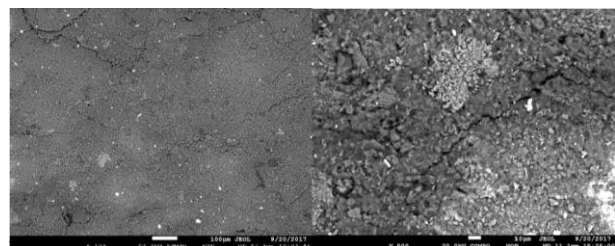


Fig.3. Microscopic structure of crud mass

A high silicon content and amorphous structure are recorded. This silicon content causes swelling, difficulty in separation. It is possible that the silicon itself in the samples is amorphous, which affects the viscosity of the structure.

Electron microscopic studies in backscattered electrons have established that the tetrahedral coordination of silicon with respect to oxygen is due to the value of the ratio of the ionic radii of silicon and oxygen, equal to 0.29. As is known, the quadruple coordination of the cation is most stable in the range of  $k = 0.225-0.414$ . The Si-O distance is 0,162 nm, and the distance is 0-0-0.265 nm. The angle inside the O-Si-O tetrahedron is approximately 109-110°. The Si-O bond is predominantly covalent, and in the transition from crystalline substances to glassy, the degree of covalence can increase from 50 to 80 %. Which explains the alignment of the oxygen scaffolds during crate formation.

### Tests of waste mass removal using coagulants

In this experiment, a Polysil coagulant was used to precipitate dissolved silicon in PLS production solutions. Polysil coagulants are intended for use in the mining industry for treating fine particles in aqueous suspension. Polyester coagulants are one of the few that are effective against colloidal silicon dioxide formed during acid leaching of ores or slags containing silicates.

Coagulants of the POLYSIL® RM1250 and POLYSIL® RM2050 brands were used to carry out the dissolved silicon precipitation tests.

An experimental extraction unit was launched for testing. Extraction with the addition of POLYSIL® RM1250 was started on one line and extraction on the other without the addition of coagulant. Dosing of POLYSIL® RM1250 was carried out at a continuous dosage of 250 g/m<sup>3</sup>. This dosage has been calculated and determined from laboratory tests.

Crud in the test circuit formed after 5 hours of operation and the circuit was stopped due to the resulting waste mass. The crud began to break through to overflows and disrupt the extraction process. Table 6 shows the operating mode of the experimental extraction plant. As can be seen from the data, both lines were tested in organic continuity.

Table 6. Operating conditions of the extraction plant

Parameters	Control line	Test line
PLS flow (l/min)	6	6
Organic phase flow (l/min)	8,5	8,5

The extraction plant was rebooted and operated with POLYSIL® RM2050 at 300 g / m<sup>3</sup>, in this chain, too, after 6-7 hours of operation, levels of waste mass were created to such an extent that they led to overflows of the organic phase and disrupted the extraction process.

The fast waste mass formation rate in the test circuits was since the coagulated silicon solids were not efficiently separated from the PLS before it was fed to the SX. The settling time of the solutions after adding coagulants was chosen 4-5 hours. The current conditions for the addition of coagulants did not allow the sedimentation of coagulated particles, so an alternative sedimentation method was investigated in the laboratory to speed up this process and propose an alternative strategy for the addition of coagulants.

The extraction unit was cleaned and replaced with fresh organic phase for a second test with a POLYSIL® RM2050

coalescer. The control line, as in the previous test, remained without adding any new organic substances (coagulants). POLYSIL® RM2050 was added to PLS at a dosage of about 330 g / m<sup>3</sup>. The coagulant treated PLS solution was left overnight to calm the coagulated particles.

After starting the pilot plant, a crud was again formed in the E1 test line after 4-5 hours of continuous operation, the raffinate solution with the addition of coagulants (lean solution after the extraction plant) was contaminated than the control line indicating that there was poor sedimentation of coagulated solids silicon.

An alternative technique for the precipitation of coagulated silicon dioxide was developed - the addition of a surfactant (bentonite) in combination with a flocculant. Surfactants help as reaction points for coagulation and as a medium to promote flocculation as the silicon coagulates, chlorinates on its own. Samples of the PLS solution from coagulant testing were sent for the analysis of silicon and other elements.

The laboratory program consisted of the following items: 1 L PLS; adding a coagulant (330 g / m<sup>3</sup>); addition of bentonite at a dosage of 10 kg/m<sup>3</sup>; addition of flocculant at 200 g/t; settling for 2 hours before taking a sample for analysis.

The addition of POLYSIL® RM1250 and POLYSIL® RM2050 shows that both coagulants decrease silicon levels with increasing dosage, Table 7. POLYSIL® RM1250 reduced silicon from 0.72 g/dm<sup>3</sup> to 0.37 g/t at a dosage of 200 g/m<sup>3</sup>. Dependence of the concentration of dissolved silicon dioxide on the amount of addition of coagulants introduce in Figure 3.

Table 7. Chemical analysis of PLS saturated solutions with the addition of coagulants POLYSIL® RM1250 and POLYSIL® RM2050

Coagulant	Cu	Al	Mg	Na	Ca	Si
PLS solution without coagulant	4,63	18,17	8,91	3,77	0,93	0,72
POLYSIL® RM1250, 50 g/m <sup>3</sup>	4,41	17,16	8,56	3,59	0,97	0,62
POLYSIL® RM1250, 100 g/m <sup>3</sup>	4,47	17,33	8,79	3,68	0,97	0,44
POLYSIL® RM1250, 200 g/m <sup>3</sup>	3,58	17,60	8,89	3,58	0,98	0,37
POLYSIL® RM1250, 500 g/m <sup>3</sup>	4,10	16,21	8,24	3,35	0,94	0,26
POLYSIL® RM2050, 50 g/m <sup>3</sup>	4,43	17,39	8,64	3,67	1,18	0,81
POLYSIL® RM2050, 100 g/m <sup>3</sup>	4,36	17,14	8,76	3,63	1,02	0,73
POLYSIL® RM2050, 200 g/m <sup>3</sup>	4,28	16,58	8,55	3,61	0,99	0,46
POLYSIL® RM2050, 500 g/m <sup>3</sup>	4,11	16,09	8,19	3,42	0,96	0,3

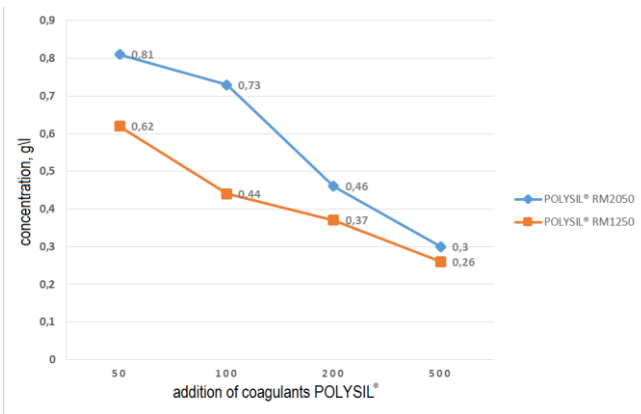


Fig. 4. Dependence of the concentration of dissolved silicon dioxide on the amount of addition of coagulants

The poor raffinate solution was also tested with the addition of POLYSIL® coagulants. The dosage of coagulants was 200 and 500 g/m<sup>3</sup>. Adding POLYSIL® coagulant to the lean raffinate solution will require a solid-solution separation step to remove coagulated particles before the raffinate is fed back to the heap leach. Coagulated particles not removed by the solid / solution separation step are likely to lead to plugging in the heap leach irrigation system.

Samples of the saturated PLS and the lean raffinate solution were taken for chemical analysis. Table 8 shows analyzes that show that during sampling, no significant change in silicon levels was observed during solvent extraction.

Table 8. Chemical analysis of solutions

Samples	Content of elements, g/l					
	Cu	Al	Mg	Na	Ca	Si
PLS	4,63	18,17	8,91	3,77	0,93	0,72
Raffinate solution from E2	2,58	17,8	8,96	3,76	0,9	0,71
Raffinate solution from E3	1,85	17,99	9,03	3,85	0,94	0,74
Raffinate solution from E1	3,4	17,86	8,86	3,73	0,9	0,73

In conclusion, we can say that both POLYSIL® coagulants tested in an experimental setup showed an effect on the solvent extraction process with the formation of a rapidly dissolving fraction in E1 and an unstable processing operation.

It was found that the formation of waste mass was caused by poor deposition of coagulated silicon. It was found that an increase in suspended solids in the PLS before the test line results in the formation of a cloudy raffinate.

To quickly remove finely dispersed coagulated silicon dioxide, a solid liquid separation stage is required; an additional filter is required to purify the solution prior to extraction.

When 1 g per 500 ml of flocculant is added, flocs are precipitated, but during extraction the crud in flocs floats to the surface and makes it difficult to separate the organic and aqueous phases.

Studies have shown that an increase in pH to 2 leads to a decrease of crud by up to 15 %, while colloidal silicon becomes more passive.

The following technological recommendations have been developed: monitoring the phase separation zone, controlling the phase disengagement time in extraction and stripping, continuously treatment of crud from the separation zone in the settlers of SX, study and tests for crud reduction with chemical reagents.

## Conclusion

The work solved the problems of the Cathode Copper Plant, determined the optimal technological parameters for the formation of waste mass (crud), proposed solutions to reduce the formation of waste mass (crud), proposed universal methods and conditions for processing similar copper raw materials for all countries of copper producers.

Economic calculations have established that when removing the waste mass from extraction, it is possible to increase the flow of the saturated solution to the design parameters and additionally produce cathode copper ~ 500 tons per year.

## References

- G.A. Kordovsky, 2002. «Copper recovery using leach/solvent extraction/electrowinning technology: Forty years of innovation, 2.2 million tonnes of copper annually.» – The Journal of The South African Institute of Mining and Metallurgy 450 p. (in English)
- David J. Readett and Greame M. Miller, 1997. «The impact of Silicon on Solvent Extraction: Girilambone Copper Company, Case Study» (in English)
- R.F.Dalton, C.Maes, and K.Severs, 1983. “Aspects of Crud formation in Solvent Extraction Systems” – Annual meeting of the Arizona Conference of AIME, Tucson. (in English)
- P. Cole\*, T. Bednarski\*, L. Thomas\*, D. Muteba\*, G. Banza\*, and M. Soderstrom. 2016. Understanding aqueous-in-organic entrainment in copper solvent extraction – In: Journal of the Southern African Institute of Mining and Metallurgy, 527 p.
- Alexis Soto L. and Hector Yáñez F. (2017) “HOW PLS VISCOSITY CAN AFFECT SOLVENT EXTRACTION OPERATION?” – Chile, Santiago (in English).

## TECHNOLOGY OF SULFIDIZING-PYRRHOTIZING ROASTING OF LEAD FLOTATION TAILINGS

**T.A. Chepushtanova<sup>1</sup>, I.Y. Motovilov<sup>1</sup>, Y.S. Merkiyayev<sup>1</sup>, M.S. Sarsenova<sup>1</sup>, G. Sumedh<sup>2</sup>**

<sup>1</sup> Satbayev University, Kazakhstan, Almaty, 050013, str. Satpayev 22; T.chepushtanova@satbayev.university, tanya2305@list.ru

<sup>2</sup> American Air Liquide, USA, 200 GBC Dr, Newark, DE, 19702; sumedh2014@gmail.com

**ABSTRACT.** Processing of refractory, pyrite-containing raw materials is most expediently carried out by a combination of pyrometallurgical and hydrometallurgical processes. During pyrometallurgical processing, pyrite undergoes changes leading to a change in the chemical and physical properties of the processed products. The results of the technology for the integrated processing of oxidized polymetallic ores and intermediate products by sulfidizing roasting with pyrite concentrate, followed by magnetic and flotation dressing, are presented. Based on thermodynamic calculations, it follows that the interaction of sulfate with pyrite proceeds at temperatures of 540 °C and higher with the formation of pyrrhotite (Fe<sub>7</sub>S<sub>8</sub>); Fe<sub>7</sub>S<sub>8</sub> interacts with sulfate at a temperature of 460 °C with the formation of lower iron sulfides; sulfidization of lead and zinc oxides and carbonates with pyrite with the formation of the corresponding sulfides is carried out at temperatures above 300 °C. The research results are aimed at solving the problem of additional extraction of lead and zinc. In this work introduced the conditions for Zn extraction up to 95 % and Pb to 80 % to sulfide concentrate.

**Keywords:** pyrite concentrate, sulfidizing roasting, thermodynamic calculations, sulfidization, lead flotation tailings

## ТЕХНОЛОГИЯ СУЛЬФИДИРУЮЩЕГО-ПИРРОТИНИЗИРУЮЩЕГО ОБЖИГА ХВОСТОВ СВИНЦОВОЙ ФЛОТАЦИИ

**Т.А. Чепуштанова<sup>1</sup>, И.Ю. Мотовилов<sup>1</sup>, Е.С. Меркибаев<sup>1</sup>, М.С. Сарсенова<sup>1</sup>, Г. Сумедх<sup>2</sup>**

<sup>1</sup> Satbayev University, Казахстан, Алматы, 050013, ул. Сампаева 22; T.chepushtanova@satbayev.university, tanya2305@list.ru

<sup>2</sup> American Air Liquide, США, 200 GBC Dr, Ньюарк, DE, 19702; sumedh2014@gmail.com

**РЕЗЮМЕ.** Переработку труднообогатимого, пиритсодержащего сырья наиболее целесообразно осуществлять комбинацией пирометаллургических и гидрометаллургических процессов. При пирометаллургической обработке пирит претерпевает изменения, приводящие к изменению химических и физических свойств продуктов обработки. Представлены результаты технологии комплексной переработки окисленных полиметаллических руд и промпродуктов сульфидирующим обжигом с пиритным концентратом, с последующим магнитным и флотационным обогащением огарка. На основании термодинамических расчетов следует, что взаимодействие сульфата с пиритом протекает при температурах 540 °C и выше с образованием пирротина Fe<sub>7</sub>S<sub>8</sub>; Fe<sub>7</sub>S<sub>8</sub> взаимодействует с сульфатом при температуре 460 °C с образованием низших сульфидов железа; сульфидирование оксидов и карбонатов свинца и цинка пиритом с образованием соответствующих сульфидов вероятно при температурах выше 300 °C. Результаты исследований направлены на решение проблемы дополнительного извлечения свинца и цинка. Разработаны условия извлечения в сульфидный концентрат Zn до 95 %, Pb до 80 %.

**Ключевые слова:** пиритные концентраты, сульфидирующий обжиг, термодинамические расчеты, сульфидирование, хвосты свинцовой флотации

## Introduction

Lead and zinc are important materials supporting modern society and nowadays, both of which are mainly extracted from sulfides by pyrometallurgy method, published by Balarini (2008). With the exploitation of resources in the world, the primary resources are soon going to be insufficient to meet the demand, and the Pb–Zn oxide ore usually containing 1 % – 5 % Pb and 1 % – 20 % Zn, may be the second source to offer the above metals. However, it seems to be difficult for valuable metal recovery from the refractory ore characterized by complex composition and high content of slime, published by Peng (2003).

The main use of lead is rechargeable batteries (automobile) of all types and sizes, with the exception of mobile devices. Car production in China over the past 5 years has increased from 18 million to 28 million units per year. Only China created a 13 % increase in world car production with a total increase of 19 %. And it was he who ensured the stability of lead prices (Liu, 2018). Lead is the only stock exchange metals with a share of recycling exceeding 50 % of the market.

The lead deficit in the world market in May 2017 amounted to 37.2 thousand tons and continues to persist.

Lead prices in 2019 rose to \$ 1.949.5 per tonne (London Metal Exchange, LME). Kazakhstan increased lead exports by 74 %. The main importers of raw materials are Vietnam and Spain. Extraction of lead in lead concentrate for 2 months of the current year amounted to 15 thousand tons - 8.7 % more than a year earlier. The production of lead concentrates increased by 18.7 % - up to 57.1 thousand tons. Lead use for domestic needs of the Republic of Kazakhstan immediately increased by 20 % year-on-year, to 24.2 thousand tons in 2018. Zinc is the fourth most used metal in the world. World zinc consumption amounts to about 13.0 million tons per year. The average annual growth rate of the zinc market is about 3.5 %. Between 2013 and 2018, zinc consumption in China more than doubled to 5.6 million tons, and the average annual growth rate was about 10 %, (Liu, 2018).

About 50% of the world's zinc is used as electroplated coatings to protect steel and other metals from corrosion, 17% is spent on the production of zinc alloys and 17% on the production of brass and bronze.

Currently, world zinc consumption is 11 million tons, and also grows annually regardless of the state of the world economy, and often outstrips the growth of gross national product. Despite the decrease in export volumes of zinc ores and concentrates in physical terms, in monetary terms, supplies to foreign markets brought Kazakhstan immediately \$ 239.5 million, which is 29.9 % more than in 2018. Due to rising zinc prices (\$ 2,351 per tonne), zinc export revenues in Kazakhstan increased 1.5 times. Zinc per capita consumption is growing at 1.8% per year, with zinc consumption growing in developed countries faster (International Zinc Association).

The best indicators for the processing of oxidized and mixed ores are achieved by using the preliminary activation of the feedstock by oxidizing or sulfating roasting followed by processing of the activated product, however, these methods have not been applied in industry (Ejtemaei, 2011).

New processing? Directions are formed, characterized by a selective change in the natural technological properties of minerals before enrichment. This is carried out by dosed physical and physico-chemical effects that change the composition, structure of the crystal lattice and surface properties of minerals. One of these areas is sulfidizing, which can be carried out both by hydrometallurgical and pyrometallurgical methods. Autoclave sulfidization due to the periodicity of the process and the low productivity of equipment for large-capacity production is ineffective. Sulfidization by sulfate-reducing bacteria allows the flotation activity of oxidized lead minerals to be restored due to the formation of sulfide and sulfur films on the surface of minerals (Hosseini, 2011). However, there are no recommendations on the use of such a method in industry, as a critical analysis of technologies has shown.

Sulfidization of polymetallic raw materials with elemental sulfur can be carried out both in melts and in the solid phase (Keqing, 2005). The Australian Bureau of Mines has developed a sulfidization process with elemental sulfur and sulfur dioxide gas with the addition of pyrite to the batch. The resulting cinder is subjected to flotation (Qiu, 2007).

In the process of beneficiation of mixed polymetallic ores, a significant amount of middlings and tailings are formed, the flotation processing of which is ineffective. At the same time, in the froth flotation products, in addition to oxidized compounds of zinc and lead, a significant amount of pyrite is concentrated, (Chepushtanova, 2012; 2015). We studied the possibility of thermal treatment of flotation middlings with zinc sulfidization due to pyrite contained in the middlings, the composition and magnetic properties of pyrrhotite formed as a result of roasting.

The paper presents the results of technological studies of the process of thermal treatment of flotation middlings with zinc sulfidization due to pyrite contained in the middlings, the composition and magnetic properties of pyrrhotite formed as a result of roasting, with the study of the effect of temperature, duration and composition of the gas phase on the process.

The aim of the research was to determine the possibility and conditions of magnetic enrichment of sulfidized cinders.

## Materials and methods

The following materials were used as starting materials: intermediate product of flotation concentration of lead-zinc ore, consisting of a foam product of lead cleaning (40 %) and

tailings of lead flotation (60 %), containing Pb - 1.86, Zn - 4.33, Fe - 34.88, S - 36.60, CaO - 3.50, SiO<sub>2</sub> - 14.27, Al<sub>2</sub>O<sub>3</sub> - 1.52, MgO - 1.30 %, (the pyrite content in the original samples was 71.48 %); pyrrhotite containing 96,5 % iron sulfide Fe<sub>0,855</sub>S.

Mineralogical characteristics of pyrite in the initial samples of the intermediate product:

1) free grains – 90 %; grain size from 5.0·10<sup>-6</sup> to 4.0·10<sup>-5</sup> m, prevailing 2.0·10<sup>-5</sup> m;

2) intergrowths with sphalerite – 6 %; the size of pyrite precipitates is from 5.0·10<sup>-6</sup> to 2.0·10<sup>-5</sup> m, of which the opening is 5%;

3) intergrowths with quartz – 2 %; the size of pyrite precipitates is from 2.0·10<sup>-6</sup> to 4.0·10<sup>-5</sup> m, mostly open;

4) intergrowths with galena - about 1%, the size of precipitates is from 5.0·10<sup>-6</sup> to 2.0·10<sup>-5</sup> m, mostly closed.

## Experiments of heat treatment of middlings in vacuum

The main factors affecting on the rate and completeness of thermal decomposition of pyrite are the conditions of heat transfer, i.e. temperature, and duration of heat treatment.

The grain size from 1.0·10<sup>-5</sup> to 6.0 10<sup>-4</sup> m does not affect the process speed. In studies in a fixed bed, the rate of the process is influenced by the layer thickness, therefore, in the experiments described below, the size of the sample and the method of its placement in the furnace were selected experimentally in order to minimize the effect of this factor (when carrying out decomposition in industrial continuous units, for example, in fluidized bed furnaces, the influence of this factor will not affect), (Sadowski, 2004).

The experiments were carried out with weights of 10·10<sup>-3</sup> kg in a fixed bed, the setup diagram is shown in Fig.1. The residual pressure during the experiments was 1-15 Pa. The time of the experiment was counted after reaching the specified temperature, which was maintained with an accuracy of ± 1 °C.

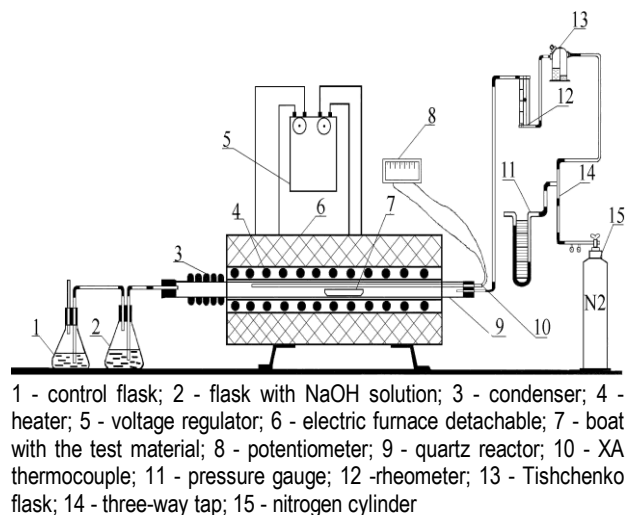


Fig. 1. The scheme of the sulfidizing pyrrhotizing roast setting

## Experiments of heat treatment of middlings in the air

The decomposition was carried out in a fixed bed in quartz test tubes in an atmosphere of gases formed during the decomposition of the middling product, which makes it possible to accurately control the oxygen consumption.

The weight of the sample was taken depending on the volume of the test tube, taking into account the reaction of oxygen from the air in the closed volume of the reaction space.

The amount of labile sulfur in the initial sample exceeded its amount theoretically capable of reacting with oxygen present in the reaction space at the beginning of the experiment.

**Microscopic studies**

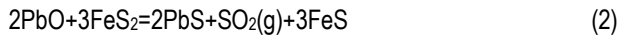
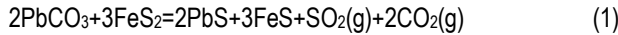
Microscopic studies (fig.3) were performed on a JEOL ISM - 25S 3 scanning electron microscope. Sample size was + 70 - 100 microns, magnification x1500.

**Thermodynamic research**

The calculations were performed using by thermodynamic calculation program of the Outokumpu Ou Company; using of phase equilibrium diagrams. On the basis of thermodynamic analysis, it was established that: the homogeneity region of the synthesized pyrrhotite is a continuous series of iron-sulfur compounds; in the Fe-S-O system, the formation of pyrrhotites of composition from FeS to Fe<sub>0,877</sub>S or Fe<sub>7</sub>S<sub>8</sub> is possible.

**Sulfidization of lead oxides and carbonates**

The reactions of sulfidization of PbCO<sub>3</sub> with pyrite (FeS<sub>2</sub>) were studied:



Standard changes in free energy (ΔG) for the above reactions in the range from 100 to 1000 ° C were calculated per 2 mol of PbCO<sub>3</sub> and PbO using HSC Chemistry 5. The results show that sulfidization of PbCO<sub>3</sub> and PbO with FeS<sub>2</sub> is thermodynamically possible in the studied temperature range, Fig.2. Regarding the transformation of the iron phases, equations 1 and 2 show relatively large negative values of ΔG, with the values becoming more negative with increasing temperature, and therefore the conversion of FeS<sub>2</sub> to FeSO<sub>4</sub> and Fe<sub>2</sub>O<sub>3</sub> / Fe<sub>3</sub>O<sub>4</sub> is predominant.

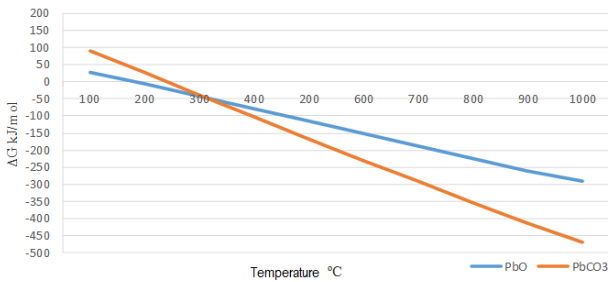


**Fig. 2. Standard changes in free energy of possible reactions depending on temperature in the range of 100-1000°C**

**Sulfidization of zinc oxides and carbonates**

The probability of the formation of various compounds of zinc and iron as a result of interaction and the influence of the process conditions on the composition of the products was studied. The analysis was carried out for oxidizing, reducing and neutral environments of zinc oxide sulfidization with pyrite.

The paper presents calculations of the thermodynamic characteristics of the process of sulfidization of ZnCO<sub>3</sub> to obtain zinc in the form of Zn, ZnO, ZnSO<sub>4</sub>, ZnS; iron - in the form of troilite FeS (the formation of pyrrhotites was not taken into account), FeO, Fe<sub>3</sub>O<sub>4</sub>, Fe<sub>2</sub>O<sub>3</sub> FeSO<sub>4</sub>.

During heat treatment, ZnCO<sub>3</sub> dissociates with the formation of ZnO and CO<sub>2</sub> at temperatures of 573 K and higher (ZnCO<sub>3</sub> = ZnO + CO<sub>2</sub> ΔG<sub>0</sub>, kJ / mol S<sub>2</sub> at a temperature, K 973: -93.4), therefore, in the calculations, oxide ZnO was used as the initial compound.

Since, at high temperatures, thermal decomposition of pyrite occurs with the formation of pyrrhotite and elemental sulfur, we calculated the thermodynamic characteristics of sulfidization of zinc oxides with elemental sulfur.

**Sulfidization in an inert atmosphere**

In an inert atmosphere, sulfidizing of zinc oxide in the temperature range 573-973 K is thermodynamically possible in the entire temperature range under study.

Depending on the ZnO / FeS<sub>2</sub> ratio under the initial conditions, the reaction can form various iron compounds - with a decrease in the ZnO / FeS<sub>2</sub> ratio, the reaction products can be not only FeS, but also oxides (from FeO to Fe<sub>3</sub>O<sub>4</sub> and Fe<sub>2</sub>O<sub>3</sub>, and sulfate. At temperatures above 793 K ferrous sulfate is sulfided by pyrite to form FeS.

**Sulfidization in an oxidizing environment**

The participation of oxygen in the sulfiding process increases the thermodynamic probability of zinc oxide sulfiding with the formation of iron oxides and sulfates. However, an increase in the amount of oxygen in the reaction shifts the equilibrium of the reaction towards the formation of zinc sulfate (Table 1).

At the same time, it is practically impossible to obtain zinc sulfide as a result of the interaction.

**Table 1. Thermodynamics of the interaction of ZnO and FeS<sub>2</sub> at the O<sub>2</sub> presence**

N	Reaction	ΔG <sup>0</sup> , kJ/моль S <sub>2</sub> , 973, K
1	ZnO+FeS <sub>2</sub> +O <sub>2</sub> =ZnS+FeO+SO <sub>2</sub>	-245.5
2	ZnO+FeS <sub>2</sub> +3O <sub>2</sub> =ZnSO <sub>4</sub> +FeO+SO <sub>2</sub>	-760.3
3	ZnO+2FeS <sub>2</sub> +6O <sub>2</sub> =ZnSO <sub>4</sub> +Fe <sub>2</sub> O <sub>3</sub> +3SO <sub>2</sub>	-801.1
4	ZnS+3Fe <sub>2</sub> O <sub>3</sub> +1.5O <sub>2</sub> =ZnSO <sub>4</sub> +2Fe <sub>3</sub> O <sub>4</sub>	-332.9
5	ZnS+2O <sub>2</sub> =ZnSO <sub>4</sub>	-904.0
6	ZnO+2FeS <sub>2</sub> +6O <sub>2</sub> =ZnSO <sub>4</sub> +Fe <sub>2</sub> O <sub>3</sub> +3SO <sub>2</sub>	-1602.2
7	ZnO+3FeS <sub>2</sub> +8.5O <sub>2</sub> =ZnSO <sub>4</sub> +Fe <sub>3</sub> O <sub>4</sub> +5SO <sub>2</sub>	-2313.6
8	2ZnO+4S+O <sub>2</sub> =2ZnS+2SO <sub>2</sub>	-111.6

Thus, sulfidization of lead and zinc oxides and carbonates by pyrite with the formation of the corresponding sulfides is thermodynamically probable at temperatures above 300 °C. In this case, pyrite decomposes to FeS, Fe<sub>7</sub>S<sub>8</sub> or Fe<sub>0,877</sub>S.. Those, during sulfidization of oxidized compounds of lead and zinc, pyrrhotite may form within its homogeneity region.

On the basis of thermodynamic analysis, the technological parameters of sulfidizing-pyrrhotizing roasting with the production of non-stoichiometric pyrrhotites were selected and they are???

**Results and discussion**

**Heat treatment of middlings in vacuum**

The experimental results are presented in table 2.

Table 2. Dependence of the decomposition completeness of pyrite in vacuum on the temperature, at time?

Temperature, °C	Weight of the cinder, kg · 10 <sup>-3</sup>	Content in the cinder, weight, %		Fe/S in the cinder	% extraction of labile sulfur to gas
		Fe	S		
650	8.0	34.3	28.7	1.25	60
700	7.0	34.8	29.0	1.30	67
750	7.7	35.3	28.9	1.40	77
800	7.5	36.9	27.4	1.47	83
850	7.8	37.2	27.9	1.46	83
900	7.5	38.1	24.1	1.53	87
950	7.5	37.5	27.1	1.50	84

After the end of the experiment, the sample was cooled under vacuum. The weight of the sample after decomposition and the content of iron and sulfur in the processed product were monitored.

In a vacuum with the duration of the decomposition process of 30 minutes, it is possible to drive away up to 84-87 % of the labile sulfur of pyrite. An increase in the decomposition temperature above 800 °C does not increase the extraction of sulfur into the gas, in addition, at temperatures above 850 °C, the initial product is enlarged. This means that increasing the process temperature above 900 °C is impractical, since it does not lead to an increase in sulfur recovery.

The increasing of duration more than 15 minutes, as can be seen from the data (table 3), does not significantly affect the degree of sulfur recovery in the gas. This suggests that at constant temperature and gas phase composition are obtained pyrrhotite approximately the same composition, and hence properties of pyrrhotite should be close.

Mineralogical studies of samples of industrial products obtained by decomposition in vacuum gave the following results: during the decomposition process at a temperature of 750 °C, pyrite is 75-80 % replaced by pyrrhotite, which forms semi-oval sinuous-oblong and worm-like secretions??? ranging from 5.0·10<sup>-6</sup> to 1.0·10<sup>-5</sup> m, grouped into aggregative clusters (several dozen pieces) ranging from 4.0·10<sup>-5</sup> to 8.0·10<sup>-5</sup> – 1.0·10<sup>-4</sup> m across. The resulting pyrrhotites have a composition of Fe<sub>0.892</sub>S - Fe<sub>0.869</sub>S.

Table 3. Dependence of the completeness of pyrite decomposition in a vacuum on the duration of the experiment, at temperature?

Duration, min	Weight of the cinder, kg · 10 <sup>-3</sup>	Content in the cinder, weight, %		Fe/S in cinder	% extraction of labile sulfur to gas
		Fe	S		
15	7.9	35.1	28.1	1.36	72.0
30	7.9	34.8	29.0	1.30	67.0
60	7.9	35.6	28.4	1.40	76.0
90	8.0	35.6	28.2	1.37	73.0
120	7.9	35.4	28.0	1.37	74.5

Sphalerite undergoes minor changes: the same sharp-angled fragments of its grains as in the original (not subjected to heat treatment) product; their size and distribution pattern does not change in the cinder – in aggregate and other

complex aggregates, sphalerite occupies the same position. The contours of the boundaries between sphalerite grains and semi-oval pyrrhotite secretions that replaced pyrite are still complex, sinuous and have the character of close contact.

The behavior of sphalerite is characterized as follows:

- 1) free grains - 49 %; of them the size from 5.0·10<sup>-6</sup> to 2.0·10<sup>-5</sup> m - 37 %, from 2.0·10<sup>-5</sup> to 4.0·10<sup>-5</sup> m -12 %;
- 2) accretions with pyrrhotite – 19 %; the size of sphalerite secretions from 5.0·10<sup>-6</sup> to 2.0·10<sup>-5</sup> m. single grains up to 4.0·10<sup>-5</sup> m of them open - 12 %. closed - 7 %;
- 3) splices with pyrrhotite and galenite – 13 %; the size of the splices from 4.0·10<sup>-5</sup> 8.0·10<sup>-5</sup> before 8.0·10<sup>-5</sup> · 1.2·10<sup>-4</sup> m. sphalerite size up to 3.0·10<sup>-5</sup> m mostly closed;
- 4) accretions with quartz-12 %; size of sphalerite discharge from 7.0·10<sup>-6</sup> to 3.0·10<sup>-5</sup> m. open - 8 %. closed - 4 %;
- 5) accretions with pyrrhotite and quartz – 7 %. the size of sphalerite discharge from 5.0·10<sup>-5</sup> to 2.0·10<sup>-5</sup> m. mostly closed.

The color of sphalerite grains becomes slightly lighter than in the original industrial product, they appear thin, but quite bright reflexes, and at large magnifications (x 950 and x 1425) in the immersion oil, even without structural etching, the internal structure of individual large grains of sphalerite secretions is clearly visible: it is visible that they are composed of the thinnest (2.0·10<sup>-6</sup> – 5.0·10<sup>-6</sup> m) xenomorphic grains with prizing boundaries between them, which create internal reflexes. Obviously, part of the iron entering the sphalerite lattice leaves the crystal lattice during firing???. Zinc sulfide has a β-modification.

Thus, it is established that the sulfidizing roasting of oxidized ore allows to obtain zinc sulfides similar in their properties to those obtained from pure compounds, while pyrrhotites of the composition Fe<sub>0.892</sub>S - Fe<sub>0.869</sub>S with pronounced magnetic properties are formed. Sulfidizing roasting is advisable to be carried out at a temperature of 650-700 °C, for a duration of 30 minutes.

When the temperature of heat treatment of industrial products increases to 950 °C, the nature of changes in the mineralogical composition is similar. Pyrite is completely replaced by pyrrhotite, which is present almost exclusively in the form of separated semi-oval and dump secretions and inclusions sized from 5.0·10<sup>-6</sup> – 8.0·10<sup>-6</sup> up to 4.0·10<sup>-5</sup> m. Hematite was not detected.

As can be seen from the mineralogical analysis, pyrite is almost completely replaced by pyrrhotite, such results indicate the possibility of applying enrichment methods to the heat-treated product. An increase in the temperature of heat treatment above 900 °C leads to some enlargement of the material, to its partial agglomeration, which indicates that it is not advisable to increase the temperature of the process to this level.

#### Heat treatment of industrial middlings in the air

The results of the experiments showed that during of the 30 minutes at a temperature of 700-750 °C, the decomposition of pyrite, which is part of industrial products, occurs by 89-98 % (table 4). There is no sintering of the products. Pyrrhotites of the composition Fe<sub>0.892</sub>S - Fe<sub>0.869</sub>S are formed, the magnetic susceptibility of which is equal to 1330 - 1020 ·10<sup>-6</sup> SI / g.

Table 4. The dependence of the completeness of the decomposition of pyrite from the temperature

Temperature, °C	The content in the cinder, %		Fe/S in the cinder	% extraction of labile sulfur to gas
	Fe	S		
700	41.67	24.40	1.70	89.0
750	42.50	22.75	1.8	98.0
800	41.57	24.43	1.70	88.0
900	41.52	24.52	1.69	87.0

Mineralogical analysis shows that the replacement of pyrite with pyrrhotite occurred by 95-98 %, and all free grains were completely replaced. The presence of a small amount of hematite, which replaces pyrrhotite, was detected.

The results of electron microscopic analysis confirm the results of the mineralogical analysis of the roasted middling, Fig.3.

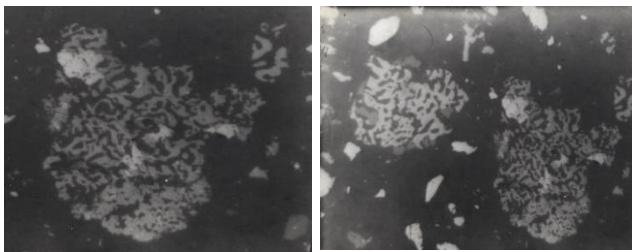


Fig. 3. Large skeletal-frame allocation of pyrrhotite

As a result of thermal decomposition, there is no noticeable decryption of pyrite particles, but it transforms into pyrrhotite of the skeletal-frame form, which can be seen from Figure 3.

**Enlarged tests on magnetic separation of sulfidizing roasting products of lead flotation middlings**

Literature data and our research indicate that pyrrhotites obtained during thermal dissociation have magnetic properties and can therefore be separated into a separate product by magnetic separation. According to research results, 95-98 % of pyrite is converted to pyrrhotite during heat treatment of industrial flotation products.

For the parameters determination of dry and wet magnetic enrichment were performed the research with a mechanical mixture of pyrrhotite (30 %) and lead flotation tailings (70 %) and products of sulfidizing roasting of industrial products of enrichment.

The researches were carried out for separating of the mechanical mixture of pyrrhotite and lead flotation tailings for the establishing of the operating parameters of the magnetic separator.

Pyrrhotite contained 96,5 % iron sulfide  $Fe_{0,855}S$  and had a magnetic susceptibility of  $1000 \cdot 10^{-6}$  SI/g. Particle size in pyrrhotite was 15 % - 44 microns, and in tailings 30 % - 44 microns. The initial pyrrhotite product contained 56 % iron, and the lead flotation tailings contained 20,75 %, in the form of non-magnetic pyrite and 2,93% zinc. The content of the mixture: zinc-2,15 %, iron-30,34 %.

The field strength at the electromagnetic separator varied from 40-80 kA/m (500-1000 Oersted), and the current strength – from 0.25 to 2.0 A (table 5).

Table 5. Results of experiments on magnetic separation of an artificial mixture of pyrrhotite and lead flotation tailings

Name of produce	Current, A	Exit, %	$Fe_{1-x}S$ , %	Extraction $Fe_{1-x}S$ , %
Magnetic fraction	0,25	35.15	77.7	91.15
Non-magnetic fraction		64.85	4.10	8.85
<b>TOTAL</b>		100.0	-	100.0
Magnetic fraction	1,0	32.15	81.20	87.29
Non-magnetic fraction		67.85	5.60	12.71
<b>TOTAL</b>		100.0	-	100.0
Magnetic fraction	2	33.40	81.70	91.11
Non-magnetic fraction		66.60	4.0	8.89
<b>TOTAL</b>		100.0	-	100.0

From the data shown in table 5, it can be seen that the separation of pyrrhotite and tailings practically does not depend on the current strength and magnetic field strength on the separator and is carried out with a high degree. Extraction of pyrrhotite in the magnetic product is 91.15 %.

Further, enlarged tests were carried out for wet magnetic separation of the stub obtained from the sample product. The initial sample contained, %: lead cleaning (40 %) and tails of lead flotation (60 %), Pb – 1.86, Zn – 4,33, Fe – 34.88, S – 36.60, CaO – 3.50,  $SiO_2$  – 14.27,  $Al_2O_3$  – 1.52, MgO – 1.30 %. The pyrite content in the initial samples is 71-72 %.

The original sample was subjected to heat treatment at a temperature of 700 °C for 30 minutes without air access to the reaction zone. The sample was cooled together with the furnace, the resulting cinder was sent to magnetic separation. The content of pyrrhotite in the cinder is 42,0 %. Magnetic field strength 40-80 kA/m (500 -1000 Oe) (table 6).

Table 6. Results of experiments on wet magnetic separation of cinder

Name of produce	Current, A	Exit %	Content $Fe_{1-x}S$ , %	Extraction, $Fe_{1-x}S$ %
Magnetic fraction	0.25	30.50	85.50	62.40
	0.5	27.50	98.10	64.20
	1.0	35.30	79.60	66.90
	2.0	30.0	97.0	69.20

The results show that when the magnetic field strength increases from 40-80 kA/m (500 to 1000 e), the extraction of pyrrhotite in the magnetic fraction increases from 62.4 to 69.20 %.

Thus, magnetic separation of a mixture of ferromagnetic pyrrhotite and intermediate products of flotation enrichment, polymetallic ores allows 91 % of the compacted pyrrhotite to be separated into the magnetic product.

As a result of roasting industrial products in a non-oxidizing atmosphere and subsequent magnetic separation of the cinder, more than 69.20 % of iron in the form of pyrrhotite can

be extracted into the magnetic fraction, the content of pyrrhotite in the magnetic fraction is at the level of 85-97 %. At a magnetic field strength of 40-80 kA/m (500-1000 Oe), it is possible to extract up to 69.20 % of pyrrhotite into the magnetic fraction.

## Conclusion

Enlarged tests of the magnetic separation of sulfidizing roasting products in an environment with a limited amount of oxygen in lead flotation middlings confirm the possibility of separating up to 69 % of iron in the form of pyrrhotite into the magnetic product, with a pyrrhotite content in the magnetic product of up to 97-98 %. The technical and economic efficiency from the introduction of the technology of processing roasting-magnetic beneficiation with sulfidizing roasting on the example of processing tailings with subsequent magnetic separation is achieved through additional extraction of zinc from the lead flotation by-product.

## References

- Balarini J. C., Polli L., Miranda T., Castro R., Salum A. Importance of roasted sulphide concentrates characterization in the hydrometallurgical extraction of zinc [J]. *Minerals Engineering*, 2008, 21(1): 100-110.
- Liu, Wei, Zhu, Lin, Han, Junwei, Jiao, Fen, Qin, Wenqing. Sulfidation mechanism of ZnO roasted with pyrite. *SCIENTIFIC REPORTS*. Web of science. Vol. 8. Article number: 9516 (2018).
- Peng Rong-qiu, Ren Hong-jiu, Zhang Xun-peng. *Metallurgy of lead and zinc* [M]. Beijing: Science Press, 2003. (in Chinese).
- Ejtemaei M., Irannajad M., Gharabaghi M. Influence of important factors on flotation of zinc oxide mineral using cationic, anionic and mixed (cationic/anionic) collectors [J]. *Minerals Engineering*, 2011, 24(13): 1402-1408.
- Hosseini S., Forssberg E. Studies on selective flotation of smithsonite from silicate minerals using mercaptans and one stage desliming [J]. *Mineral Processing and Extractive Metallurgy*, 2011, 120(2): 79-84.
- Keqing F.A., Miller J. D., Jiang Tao, Li Guang-hui. Sulphidization flotation for recovery of lead and zinc from oxide-sulfide ores [J]. *Transactions of Nonferrous Metal Society of China*, 2005, 15(5): 56-79.
- Qiu X., Li S., Deng H., He X. Study of heating surface surface sulfurized flotation dynamics of smithsonite [J]. *Nonferrous Metals Mineral Processing*, 2007, 1: 6-10.
- Sadowski Z., Polowczyk I. Agglomerate flotation of fine oxide particles [J]. *International Journal of Mineral Processing*, 2004, 74(1): 85-90.
- Chepushtanova T.A., Luganov V.A., Mamyrbayeva K., Mishra B. Mechanism of Nonoxidizing and Oxidative Pyrrhotites Leaching. *Minerals & Metallurgical Processing Journal*. August 2012, Thomson Reuter, ISI Web of Knowledge. Vol. 29 № 3. – P. 159-164.
- Chepushtanova T.A., Luganov V.A., Ermolayev V.N., Mishra B., Gyseinova G.D. Investigation of the magnetic and flotation properties of synthesized hexagonal pyrrhotites. *Mineral processing and extractive metallurgy review: an international journal*. 2015, Thomson Reuter. Vol. 36 № 4. – P. 237-241. ИФ – 0,690.

## WASTE MANAGEMENT IN KOSTINBROD AREA

**Krasimir Debelyashki, Marina Nicolova**

University of Mining and Geology "St. Ivan Rilski", 1700 Sofia; k.debelyashki@gmail.com

**ABSTRACT.** The goals of this doctrine encompass the municipalities of the Regional waste management administration Kostinbrod, including the municipalities: Kostinbrod, Bozhurishte, Svoge, Slivnitsa, Godech and Dragoman and intend to decompose the running condition of waste management. The main struggle and matters that appear for municipalities in the implementation of the regulations at the local level are related to the realization of the set goals in the Waste Management law (legislation). It is obligatory to decrease the deposited quantities by 50% of the total general weight of waste materials including: paper, paperboard, metal, plastic and glass from the housekeeping

**Keywords:** waste, management, environment.

### УПРАВЛЕНИЕ НА ОТПАДЪЦИТЕ В РЕГИОН КОСТИНБРОД

**Красимир Дебеляшки, Марина Николова**

Минно-геоложки университет „Св. Иван Рилски“, 1700 София

**РЕЗЮМЕ.** Целите на настоящото проучване обхващат общините от Регионалното сдружение за управление на отпадъци Костинброд, включващо общините: Костинброд, Божурище, Своге, Сливница, Годеч и Драгоман и целят да се анализира съществуващото състояние по управление на отпадъците. Основните трудности и проблеми, които възникват пред общините при прилагането на нормативната уредба на местно ниво са свързани с изпълнението на поставените цели в Закона за управлението на отпадъците. Необходимо е да се намалят депонираните количества с 50% от общото тегло на отпадъчните материали, включващи хартия и картон, метал, пластмаса и стъкло от домакинствата.

**Ключови думи:** отпадък, управление, околна среда.

### Introduction

The article discusses the prerequisites for creating a system for separate collection of green and/or biodegradable waste and construction of installations for their processing, as well as an installation for pre-treatment of mixed municipal waste in the **Kostinbrod Regional Waste Management Association**.

To this end, the waste management practices in the area are presented and an alternative related to the reduction of the quantities intended for disposal, which meets the requirements of the legislation and is cost-effective.

As an outcome of taking measures to establish the system and with the development of technologies for repair, an increasing part of the landfilled waste will be able to be re-incorporated into the production of new products by using them as an alternative raw material and power source and increasingly -small part will be deposited.

The mechanism and equipment will also make an important input reducing the unsafe properties of waste, reducing the risk to human health and restricting the noxious effects on the environment engendered by the straight disposal of waste during the life cycle of the landfill.



**Fig.1. Administrative map of Sofia Region**  
Source: National Statistical Institute

## Priorities, objectives and conformities in waste management in Bulgaria

The Waste Management Law (WML) introduces the requirements of the Waste Framework Directive 2008/98/EU into the Bulgarian legislation and regulates the measures and control for the protection of environment and human health by preventing or reducing the harmful effects of waste generation and management, as well as by reducing the overall impact of resource use and by increasing the efficiency of that use. According to Article 52 of the WML: Municipalities must develop and implement waste management programs for the territory of the respective municipality for a period that should coincide with the period of validity of the National Waste Management Plan and the National Waste Management Program as its essential part, and to develop them in accordance with the structure, objectives and provisions of the NWMP (Waste Management Law 2012). In addition, the WML requires that municipal waste management programs shall include the necessary measures to meet the obligations of municipalities resulting from this law.

According to the national targets, the share of disposed biodegradable waste should be reduced to 35% and the quantity of recycled waste should be increased to 50% by 2020. The National Waste Management Plan (NWMP) provides for achieving a regional target for separate collection and recovery of municipal bio-waste – not less than 50 percent of the quantity of municipal bio-waste generated in the region in 2014 (National Waste Management Plan 2014).

To prevent the generation of municipal waste (MA) in Bulgaria, regulatory and economic instruments are used – deductions for waste disposal; producer responsibility schemes for specific waste streams/product charges/royalties to organizations for the recovery of widespread waste (WsW); municipal waste fee; fee for limiting the use of polymer bags with certain parameters.

The Operational Program "Environment 2014 – 2020" provides to contribute to the implementation of the country's commitments in the "Waste" Sector and the achievement of the objectives arising from European and national legislation. The criminal proceedings initiated against the country for non-compliance with Directive 1999/31/EC on the waste disposal has also been taken into consideration.

The Waste Sector is financed through Priority Axis 2 of the Operational Program "Environment", financed by the European Regional Development Fund. The objective of the priority axis is to achieve consistency with the waste management hierarchy (Directive 2008/98/EC) and with the objectives of national legislation. According to the hierarchy, priority is given in the sector to measures aimed at reducing the quantity of deposited municipal waste by reuse, recycling and recovery.

### Current situation/Practices in waste management in the Municipalities in the Kostinbrod Regional Waste Management Association

The study shows that currently the municipalities in the Kostinbrod Regional Waste Management Association: Kostinbrod, Bozhurishte, Godech, Slivnitsa, Dragoman and Svoge deposit their municipal waste at a regional landfill, complying with the regulatory requirements, with a valid

Complex Permit but there is no installation for pre-treatment of municipal waste and/or composting installation, as required by the national legislation in the field of waste management.

The waste generated by the Kostinbrod Regional Waste Management Association is mainly non-hazardous waste. Mixed non-hazardous household waste, production waste from companies engaged in production activities, green waste from households, maintenance of green areas, parks, gardens, and construction waste from repair and construction works are generated. The existing practice in the municipalities of Kostinbrod Regional Waste Management Association, as well as in all municipalities in the Republic of Bulgaria is waste disposal when deposited at landfills.

According to data provided in recent years by the National Statistical Institute (NSI, www.nsi.bg), the trend is to reduce the total quantity of disposed waste in the country.

The reports kept over the years in the municipalities of this area show that waste is significantly increasing due to the developing economy and production activities, and the variety of products that are a serious generator of waste after consumption is increasing at the market.

The main index in defining municipal waste is the accumulation rate (Table 1), showing the quantity of waste generated by one person for a certain period of time, usually a year. The accumulation rate can be expressed in weight (kg/year/per capita) or in volume units (m<sup>3</sup>/year/ per capita).

Table 1. Accumulation rate by groups of settlements

Inhabitants	Over 150 000	50 – 150 000	25 – 50 000	3 – 25 000	Under 3 000
kg/year/per capita	410,3	349,6	334,9	295,5	241,7

The average accumulation rate for the municipalities of the Kostinbrod Regional Waste Management Association for the last 5 years is 592.08 kg/year/per capita, which is higher than the average for the country (375 kg/year/per capita).

The morphology of the generated waste from the municipalities in the area shows that the most serious share is reported in green and food waste (Table 2) as only the Bozhurishte Municipality is an exception where the percentage of generated inert waste is the highest.

The municipalities of the Kostinbrod Regional Waste Management Association have implemented effective systems for organized waste collection in their settlements by placing containers. The vessels are replaced and supplemented, if necessary. The special machinery for their service is provided by the respective municipalities. The number of placed waste containers is calculated according to the "Guide for determining the number and type of necessary containers and machinery for waste collection and transportation", developed by the Ministry of Environment and Water (MEW).

The municipalities have organized the separate collection of larger waste streams on their territory. They have organized independently and/or in cooperation with organizations using various waste collection systems. They also manage to implement the new legal requirements for their activities.

There is still a lack of infrastructure in their territories for the treatment of plant and biodegradable waste.

Table 2. Morphological composition of waste in the municipalities of Kostinbrod Regional Waste Management Association for 2016

Fraction	Unit	Kostinbrod Municipality	Svoege Municipality	Slivnitsa Municipality	Godech Municipality	Bozhurishte Municipality	Dragoman Municipality
<b>Municipal waste, Total</b>							
Paper and cardboard	%	17.49	14.71	7.69	10.01	6.91	5.71
Plastics	%	12.83	12.18	6.68	9.89	7.31	2.13
Glass	%	3.28	5.17	3.92	6.82	8.24	2.45
Metal	%	3.81	1.85	7.11	2.65	3.57	0.52
Wood	%	4.48	6.97	2.62	2.65	1.71	5.51
Rubber	%	1.24	1.69	0.09	0.28	0.32	0.35
Textiles and leather	%	3.82	3.92	2.28	3.3	4.25	1.66
Hazardous municipal waste	%	2.14	0.75	0.24	1.28	0.09	0.35
Inert waste	%	11.27	9.55	8.97	20.15	33.74	7.95
Food waste	%	17.19	19.89	6.02	10.42	13.26	5.45
Green waste	%	22.45	23.32	54.38	32.55	10.69	67.93

On the territories of the municipalities there is no installation for pre-treatment of waste/separation.

Currently the sludge from the Wastewater Treatment Plant (WWTP) is in small quantities and the construction of infrastructure for their treatment would be inexpedient. It is advisable to look for an option for another recovery that is economically feasible.

### Possibilities for reducing the quantity of deposited waste

According to Article 38, paragraph 1 of Ordinance No. 6 dated 27.08.2013 on the conditions and requirements for construction and operation of landfills and other facilities and installations for recovery and disposal of waste at landfills, pre-treated waste is accepted (Ordinance No. 6/2013). In accordance with the definition of "*polluter pays*", the costs of pre-treatment are borne by the persons in whose activities they are incurred.

The pre-treatment of mixed municipal waste generated by households is the responsibility of the Municipal Administration, as the population pays a "Municipal Waste Fee" for them. The responsibility for the treatment of other waste generated outside the organized system of waste collection and disposal lies with the perpetrators and their owners.

According to § 1 of the above-mentioned Ordinance No. 6, "Pre-treatment" means all physical, thermal, chemical or biological processes, including sorting, that change the characteristics of waste in order to reduce its volume or hazardous properties in order to facilitate further treatment or to increase the waste utilization.

The pre-treatment aims at separating recoverable components from the total waste stream before their final disposal or preparation for recovery. Through separation, the volume of waste for disposal is significantly reduced, which extends the service life of landfills.

The analysis of the need for the construction of additional infrastructure for pre-treatment of mixed municipal waste proves the need for the construction of such, as:

1. The objectives under Article 31, paragraph 1, item 1 of the WML shall not be achieved at regional level. The systems for separate collection, reuse, recycling and recovery of municipal waste shall ensure at least the fulfilment of the following objectives:

- by January 1, 2020 at the latest, preparation for re-use and recycling of waste materials, including paper and cardboard, metal, plastics and glass from households and similar waste from other sources of not less than 50 percent of the total weight of this waste
  - by December 31, 2020 at the latest, limiting the quantity of deposited biodegradable municipal waste to 35 percent of the total quantity of the same waste generated in the Republic of Bulgaria in 1995.
2. The targets for limiting deposited waste quantities by 2020 must be met.
3. There is no infrastructure developed for pre-treatment of the mixed collected municipal waste at municipality level and at area level, which has a capacity guaranteeing the fulfilment of the set objectives.

### Conclusions

In accordance with the set national and European objectives for reducing the quantities of deposited waste and based on the presented data on their management in the municipalities of Kostinbrod Area, the following conclusions are imposed:

- It is necessary to implement a system for separate collection of green and biodegradable waste on the territory of the Municipalities and construction of composting plants for biodegradable and/or green waste;
- The pre-separation of the mixed collected municipal waste will separate the recoverable components from the total

flow and at the same time will reduce the quantities intended for depositing. In this regard, the construction of a pre-treatment plant will also extend the service life of the existing regional landfill;

- It is necessary to take action on the treatment of construction waste in the region. The establishment of a temporary storage site will greatly facilitate their further management.

The construction of a pre-treatment installation for mixed municipal waste and composting installations, as well as waste management measures will contribute to reducing the environmental impacts caused by the generated waste, improving resource efficiency, increasing the responsibilities of polluters, and stimulating investment in the field of waste management.

## **References**

Directive 1999/31/EC (in Bulgarian)

Directive 2008/98/EC (in Bulgarian)

Guide for determining the number and type of necessary containers and machinery for waste collection and transportation, Sofia, 2011 (in Bulgarian)

National Statistical Institute ([www.nsi.bg](http://www.nsi.bg)) (in Bulgarian)

National Waste Management Plan 2014 – 2020 (in Bulgarian)

Ordinance No. 6 dated 27.08.2013 on the conditions and requirements for construction and operation of landfills and other facilities and installations for recovery and disposal of waste at landfills, pre-treated waste is accepted, MEW, amended and supplemented No. 13 of 07.02.2017 (in Bulgarian)

Waste Management Law, Promulgated in State Gazette, issue 53 of July 13, 2012, amended and supplemented in State Gazette, issue 81 of October 15, 2019 (in Bulgarian)

## ZnO-BASED NANOMATERIALS FOR ORGANIC POLLUTANTS REMOVAL FROM WASTEWATER

**Gospodinka Gicheva, Neli Mintcheva, Lyubomir Djerahov**

University of Mining and Geology "St. Ivan Rilski", Department of Chemistry, 1700 Sofia;  
e\_gospodinka@yahoo.com; nnmintcheva@mgu.bg; lubomirdjerahov@abv.bg

**ABSTRACT.** This paper presents a comprehensive literature overview on synthesis, morphology and properties of ZnO nanoparticles, metal-doped ZnO nanomaterials and ZnO-supported zeolite nanocomposites and their application for organic pollutants removal from wastewater. ZnO is among semiconductor photocatalysts widely explored and used for treatment of harmful contaminants in wastewater, due to its low toxicity, reasonable price, facile synthesis and tunable morphologies. However, some drawbacks arise from its wide band gap and fast recombination rate of photogenerated electron/hole pairs, which might be overcome by synthesis of ZnO doped with metals. Such materials demonstrate enhanced photocatalytic activity in comparison with pure ZnO. The relatively poor adsorption capability of ZnO and difficulties in recovering and recycling of nanoparticles provoke the development of nanocomposites of semiconductor nanoparticles supported on zeolites and other substrates. Thus, the adsorption ability and selectivity of nanomaterials ZnO-zeolite for dyes and toxic metals elimination are also discussed.

**Keywords:** ZnO, ZnO-based nanocomposites, zeolites, photocatalytic activity, adsorption capability.

## НАНОМАТЕРИАЛИ НА ОСНОВАТА НА ZnO ЗА ОТСТРАНЯВАНЕ НА ОРГАНИЧНИ ЗАМЪРСИТЕЛИ ОТ ОТПАДЪЧНИ ВОДИ

**Господинка Гичева, Нели Минчева, Любомир Джерахов**

Минно-геоложки университет „Св. Иван Рилски“, Катедра Химия, 1700 София

**РЕЗЮМЕ.** В тази статия е представен литературен обзор върху синтеза, морфологията и свойствата на наночастици от ZnO, ZnO дотиран с метали и нанокompозити ZnO-зеолити, и тяхното приложение за отстраняване на органични замърсители от отпадъчни води. ZnO е полупроводник и фотокатализатор, който е широко изследван и използван за третиране на опасни вещества в отпадъчни води, поради неговата ниска токсичност и цена, лесен синтез и промяна на морфологията на материала. Обаче, от неговата широка забранена зона и бързата рекомбинация на фотогенерираната двойка електрон/дупка възникват определени недостатъци при използването му, които могат да се преодолеят чрез синтез на ZnO, дотиран с различни метали. Такива материали показват по-висока фотокаталитична активност в сравнение с чистия ZnO. Относително слабата адсорбционна способност на ZnO и трудностите при отделянето и рециклирането на наночастиците пораждат интерес към разработването на нанокompозити от полупроводникови наночастици, нанесени върху зеолити и други подложки. Ето защо, адсорбцията и селективното задържане на багрила и токсични метали от нанокompозити ZnO-зеолит са също дискутирани в статията.

**Ключови думи:** ZnO, нанокompозити, зеолити, фотокаталитична активност, адсорбционна способност.

## Introduction

The implementation of nano-sized materials in the past years has gained a tremendous popularity in many aspects of modern technology – electronics (Liu et al., 2015), medicine and life sciences (Mirzaei et al., 2017), environmental protection (Hoffmann et al., 1995) and sustainability (Oskoei et al., 2016). The list of different materials (metals, metal oxides, sulfides, carbides, etc.) in nanoscale that has been applied as photovoltaics (Aissat et al, 2015), dyes for bioimaging and target drug delivery as well as photocatalysts, is really long and constantly increasing. The used nanomaterials vary in composition depending on the intended application – polymer, metal, oxides and halides. Special interest has been paid to semiconductor metal oxides nanoparticles and their use in the environmental protection and water treatment (Zhang et al, 2012; Lee et al., 2016). The ever increasing demand for fresh drinking water is an issue worldwide. The most affected areas are countries with limited supply of natural water resources like

Africa and Arabian Peninsula. The applications of cost effective methods at large scale for water treatment are most desired and widely investigated. In this aspect, as a promising candidate appears the method of photocatalysis, which is based on photo-induced generation of electron-hole pair in the semiconductor nanoparticles and formation of strong oxidizing species that are able to oxidize and decompose organic pollutants in the wastewater. The potential of photocatalysts depends on the type of semiconductor, particle's size, surface area and morphology of material, pH of the media as well as the characteristics (wavelength, intensity) of the light source used for irradiation.

In order to be applied in practice the photocatalytic material should be efficient, cost effective and environmentally friendly. One of the preferred choice for photocatalyst is ZnO. It is cheap and non-hazardous material which is very efficient in degradation of organic contaminants under UV radiation (Moezzi et al., 2012; Kolodziejczak-Radzimska et al., 2014).

Here we present a review on different methods for synthesis of ZnO nanoparticles, metal-doped ZnO nanomaterials and ZnO-supported zeolite nanocomposites, their morphology, properties and applications for organic pollutants removal from wastewater.

## ZnO nanoparticles

ZnO is n-type II–VI semiconductor material with band gap of 3.37 eV and high exciton binding energy (60meV). Nanosized ZnO materials has gained popularity in the recent years due to their versatile use in different areas like biomedicine (Steffy et al., 2018; Zhu et al., 2020), environmental protection (Daneshvar et al., 2007), cosmetics, optics and electronic.

ZnO nanoparticles (ZnO NPs) are very promising candidates for large scale application purposes because they are inexpensive to manufacture, non-hazardous and easily synthesized. One of their advantages is that they have been categorized by the U.S. Food and Drug Administration (FDA) as GRAS (generally recognized as safe) metal oxide nanoparticles (21CFR182.8991).

ZnO NPs raise particular interest as a photocatalyst and antibacterial agent since nanoparticles have suitable band gap width for UV light excitation and a large surface area due to the small size of the nanoparticles, which strongly depend on the synthesis method (Ahmed et al., 2017; Kumar et al., 2019). It is reported that ZnO NPs have been applied for disposal of Gram-positive (*Bacillus megaterium*, *Bacillus pumilus* and *Bacillus cereus*) and Gram-negative (*Escherichia coli*) bacteria resistant to all other type of eradication techniques (Nagajyothi et al., 2014).

Major impact on the efficiency of ZnO NPs as a photocatalyst has their size, shape and surface morphology, which makes the method for their synthesis very important. The ability to tune and control NPs properties by controlling their size and shapes is of great importance when method for preparation is developed. (Basnet et al., 2020).

A different shapes of ZnO NPs have different morphologies like nanoflake, nanoflower, nanobelt, nanorod and nanowire (Ong et al., 2018). The methods for their preparation can be summarized in two major divisions – chemical and biological. The chemical methods usually involve a controlled precipitation of zinc salt while biological methods are based on the use of plant extracts (from different parts such as leaves, roots, rhizomes, bark, fruits, flowers) and microbes (Basnet et al., 2018).

The so-called wet chemical methods include hydrothermal, sol-gel, precipitation, microemulsion, solvothermal, electrochemical deposition process, which are among most popular approaches. The precipitation methods developed for preparation of ZnO NPs in solution use zinc salts like  $Zn(NO_3)_2$ ,  $ZnCl_2$ ,  $Zn(CH_3COO)_2$ ,  $Zn(C_2O_4)$  and precipitation agents like  $NH_4OH$ ,  $NaOH$  and  $KOH$  for formation of  $ZnO/Zn(OH)_2$ , followed by further annealing at high temperature in order to improve the crystallinity of the ZnO NPs. At such conditions a wurtzite hexagonal structure is often formed. A capping agent can be added to improve the control over the size and shape of the obtained ZnO NPs.

The precipitation method is very attractive because it is cost effective, uses non-toxic solvent (as water), allows good control over the obtained NPs during the precipitation. The

addition of surfactants with various structures, for example sodium dodecyl sulphate (SDS) (Juabrum et al., 2019) and cetyl trimethyl ammonium bromide (CTAB) (Sun et al., 2003), amino acids (Wu et al., 2008), polymers (polyethylene glycol (PEG) and polyvinyl pyrrolidone (PVP) (Tachikawa et al., 2011; Vidyasagar et al., 2016) and polysaccharides (starch) (Vidhya et al., 2015), would not only restrict the NP size but also would prevent aggregation of the obtained NPs and would stabilize them in the dispersion (Vijayakumar et al., 2020). That's why the synthesis of NPs is often carried out in the presence of surfactants in the reaction media.

ZnO nanoparticles have a lot of applications that were listed above but two of them attract our interest – their photocatalytic and antibacterial activity. ZnO is very effective photocatalyst used in treatment of water and degradation of model organic compounds (dyes) like methylene blue, reactive black, congo red as well as some pharmaceutical and agricultural pollutants like furosemide, glyphosate-based herbicide, tartrazine, diclofenac and others.

Páez et al. (2019) have reported removal of a glyphosate-based herbicide from water using ZnO nanoparticles. They have applied a method of controlled precipitation where acidified water solution of zinc acetate  $Zn(CH_3COO)_2$  as Zn precursor and ammonium hydroxide ( $NH_4OH$ ) as precipitant were mixed at room temperature and constant stirring. This method resulted in ZnO NPs with uniform particle size (<100 nm), spheroidal morphology and formed soft agglomerates with well-defined wurtzite structure. The material was successfully tested for removal of the herbicide glyphosate (Monsanto herbicide Roundup 747 SG) without UV irradiation. The decrease in herbicide concentration was monitored by using UV–Vis absorption spectroscopy. Removal from 70% to 90% was calculated depending on the ratio glyphosate to ZnO NPs in herbicide solution, indicating the nanomaterial as very effective sorbent. The equation for removal of glyphosate by ZnO NPs followed kinetics of a pseudo second order reaction (chemisorption process).

## ZnO-doped nanoparticles

A drawback of ZnO as a photocatalyst is its wide band gap (3.2 eV) which requires UV light for generation of electron-hole pair and activation of photocatalytic process, as well as the fast recombination rate of photogenerated electron/hole pairs, which hinder the catalytic efficiency. The lowering of its band gap would allow a sunlight photo-induction and would provide very cheap and convenient way to use ZnO in sun-driven devices and settings.

The band gap of semiconductors can be altered by introduction of a new energy states. The incorporation of metal ions in ZnO structure causes the formation of additional energy level, either within or beyond the band gap of ZnO, which decreases the recombination of electron/hole pairs since the metal ions act as an electron trap, thus reducing the band gap energy. This results in more effective separation of electron/hole pairs and enhancement of photocatalytic activity under visible light (Nouri et al., 2014; Sitthichai et al., 2017).

There are different types of dopant that has been used for ZnO NPs, like alkali metals, alkaline earth metals, transition metals and post-transition metals (Adam et al., 2020; Chandekar et al., 2020). The effect of each type of dopant is different, but they generally improve the optical and electronic

properties of the ZnO NPs. The most studied dopants are Mg, Fe, Co, Ni, La and some others. Precipitation method is very suitable for preparation of doped ZnO nanostructures since it allows to use conditions and synthesis schemes applied and already known for pure ZnO NPs.

Metal oxides are also used as dopants, for example  $V_2O_5$ -ZnO nanostructures. Authors have reported a facile sol-gel method for successful preparation of ZnO and  $V_2O_5$ -ZnO nanostructures that had flake-type structure of  $V_2O_5$ -ZnO obtained from ZnO nanorods (Shukla et al., 2018). It was found decrease in the band gap from 3.28 eV for ZnO to 2.64 eV for  $V_2O_5$ -ZnO detected by UV-Visible spectroscopy. The authors applied the  $V_2O_5$ -ZnO nanomaterial for methylene blue (MB) dye photodegradation which showed improved photocatalytic efficiency of the composite under visible light irradiation.

Other interesting and promising results were reported for the preparation of Ag/ZnO photocatalysts by the deposition of Ag on the surface of the ZnO by a simple immersion reduction method (Wang et al., 2021). The Ag load in the material was controlled by the concentration of Ag ions, immersion time and the amount of the reducing agent. A decrease in the band gap of the Ag/ZnO compare to the ZnO was observed due to the surface plasma resonance effect caused by Ag modification. The Ag/ZnO NPs were tested in the decolorization of Rhodamine B where they showed improved photocatalytic efficiency under UV irradiation.

## ZnO-zeolite nanocomposites

For development of methods for water treatment and environmental protection non-expensive, non-toxic, abundant and easy-recyclable materials are needed.

ZnO is excellent material for utilization in photocatalytic process but the inconvenience in practice is caused by the fact that it forms very fine suspension which makes it hard to retrieve from the treated water media. Some techniques like thin films or membrane impregnation have been use in order to secure the easier handling of the photocatalyst.

Other approach is preparation of composite materials where ZnO is combined with a suitable substrate. In this aspect a very good candidate is the natural zeolite. It is abundant in the nature and non-expensive. The zeolite itself has been used for water treatment for heavy metal ions removal and it is expected that it would demonstrate a synergetic effect with ZnO NPs.

In the literature, there are a few general approaches for preparation of such composites – by impregnation, by precipitation and by ion-exchange.

Karimi-Shamsabadi et al. (2017) report the preparation of photo-catalyst NiO-ZnO doped onto nano zeolite X (NZX) and its use in the photocatalytic degradation of Eriochrome Black T (EBT) and Methyl Orange (MO) under UV-light irradiation. The method used for preparation of nano-zeolite crystals was hydrothermal crystallization. The composite was prepared by Ni(II) and Zn(II) ions exchange on zeolite in an aqueous solution and following by calcination at 450 °C. Thus, the formed catalyst NiO-ZnO-NZX showed significantly enhanced photo-degradation activity when tested towards EBT and MO. This activity was attributed to the synergistic effect of mixed p-type NiO and n-type ZnO oxides. It was reported that about 80% of photodegradation of EBT and MO dyes was achieved in 90 min under UV light irradiation, confirmed by

spectrophotometry and chemical oxygen demand (COD). The factors that affected the degree and rate of degradation efficiency were pH of solutions,  $Ni^{2+}$  and  $Zn^{2+}$  loading onto NZX, dosage of photocatalyst, and initial EBT and MO concentrations. Mohammadi et al. (2020) report a composite based on novel ZnO-magnetic/ZSM-5 material with high adsorption capacity and magnetic separation capability which was tested on the adsorption of disperse blue 56 dyes. It was found that the optimal conditions for dye removal process were as follows adsorbent dosage 0.015 g, pH 3, stirring time 15 min and initial dye concentration  $10^{-5}$  M for maximum removal percentage (>91.0 %). The benefit of the composite ZnO-magnetic/ZSM-5 was its magnetization saturation value equal to 3.2 emu/g. This is a good indication that magnetically separation technologies can be used in its utilization, marking it as an efficient recoverable adsorbent. The authors reported that ZnO-magnetic/ZSM-5 in their experiments can be used up to 3 times without noticeable diminishing of adsorbent activity (yield of removal) and no obvious decrease of magnetic intensity. Kinetic and isotherm models of disperse blue 56 can indicate pseudo first-order model and the Freundlich isotherm based on high  $R^2$  (0.980) and  $R^2$  (0.989), respectively. The maximum adsorption capacity of disperse blue 56 obtained based on the Langmuir model was 6.23 mg.g<sup>-1</sup>. Other authors have engaged Faujasite X zeolite in their studies as a support for ZnO nanoparticles, incorporating them into its 3D channels and supercages. This type of zeolite was chosen because its structure naturally limits the growth of ZnO NPs and ensure control over their size. The method for preparation was via impregnation of the zeolite in aqueous solution of  $Zn(NO_3)_2$  with different concentrations and subsequently calcination under  $O_2$  flow. BET analysis showed a difference in  $N_2$  adsorption-desorption which is an indication that ZnO is inside the zeolite structure. A blue-shift of the emission band in PL spectrum was detected which was attributed to the quantum size effect of ZnO NPs inside the Faujasite X matrix.

Cheng et al. (2012) also have chosen the method for impregnation and in situ formation of composite material. They have selected a simple route for incorporation of ZnO in mesoporous ZSM-5 zeolite. A commercial H-ZSM-5 (Si/Al = 50) initially treated with NaOH solution has been used in the experiment. This was meant to evoke a partial desilication which would lead to a large number of intracrystal mesopores. After this pre-treatment the ZnO nanoparticles were successfully incorporated in the mesopores using wet impregnation method. By different modern methods for characterizations (XRD, UV-visible absorption spectra, TEM and  $N_2$  adsorption) authors were able to establish the location of ZnO nanoparticles. It was found that only mesopores can be loaded (about 15%) with ZnO NPs with average size of 20 nm, while micropores remained unchanged and cannot be loaded.

By using similar technique Lim and Ryu (2009) have reported the preparation of ZnO/TMA-A zeolite nanostructured composite. Applying anion exchange method then a hydrothermal method a nanoparticles ZnO were obtained into TMA-A zeolite. Its structure and morphology was confirmed by XRD, SEM and HR-TEM, respectively. Since it was of essence to obtain ZnO NPs with controlled size and properties, a study on the optimal heat-treatment condition for oxidation of zinc was conducted. It indicated that temperature range from 500 to 550 °C was appropriate for crystal ZnO/TMA-A zeolites formation. The ZnO NPs with size 5–10nm were well

distributed among 100–150nm nanoparticles of TMA-A zeolite. The microstructure and crystalline analyses revealed that ZnO NPs were evenly incorporated into TMA-A zeolite nanostructure. The XRD analyses have shown the sodalite cage size of 12.389 Å for ZnO/TMA-A zeolite sample treated at 500 °C.

Li M. et al. (2013) have reported the preparation and enhanced antimicrobial properties of nano-ZnO-supported zeolite filled polypropylene random copolymer (PPR) composites. Nano-ZnO-supported zeolite particles were prepared by chemical precipitation of ZnO on zeolite suspended in zinc chloride solution and following addition of 1mol/L NaOH under constant stirring. After separation and washing of the product it was dried in vacuum oven for 1 h, in muffle furnace at 200°C for 4h and 500°C for 2 h, respectively. After detailed analyses (fluorescence and UV-Vis spectra, inductive coupled plasma and scanning electron microscopy) it was demonstrated that ZnO with flower-like morphology was formed on the surface of zeolite particles. The composite PPR filled with nano-ZnO-supported zeolite was prepared by mixing them at 170 °C and stirring with 50 rpm for 7min. These inorganic-organic composites were tested for antimicrobial activity. It was demonstrated that nano-ZnO-supported zeolite filled PPR composites show higher antimicrobial activity to the *S. aureus* and *E. coli* than the PPR composite filled with corresponding amount of only nano-ZnO. A great advantage for the application of this nano-ZnO-supported zeolite composite is that the nanostructured content does not significantly influence the mechanical properties of PPR composites. This is a good indication that PPR composites with high antimicrobial activity and mechanical stability can be obtained by using nano-ZnO-supported zeolite as functional filler for PPR.

Alcantara-Cobos et al. (2020) reported the preparation and subsequent testing of ZnO nanoparticles (nanZnO) and a zeolite-ZnO nanoparticles composite (Ze-nanZnO) for the removal of Tartrazine. The method they used was chemical precipitation for both nanoparticles and nanocomposite which is facile, cheap and easily to scale-up. The procedure they employed consists of contacting clinoptilolite type zeolite with a zinc acetate solution, then adding drop wise NaOH solution (1 mL/min) and stirring the mixture for 2 h and reflux. The ZnO nanoparticles-zeolite composite (Ze-nanZnO) was washed with deionized water and ethanol, dried at 80 °C and calcined at 300 °C. The same procedure was used for ZnO nanoparticles (nanZnO) preparation. These materials were tested for the removal of tartrazine from aqueous solutions by an adsorption combined with photocatalysis process. The experiments have shown that the adsorption of Tartrazine onto nanZnO follows a fast decrease of the concentration while the adsorption onto the composite Ze-nanZnO was slower. The following process of degradation of tartrazine applying both materials under ultraviolet light irradiation seems to be a highly efficient process for both of them, 87 and 81% degradation were observed for nanZnO and Ze-nanZnO respectively. Strictly speaking the first material shows better efficiency than the second, but first material is difficult to remove from the aqueous solution after the process. The results from the mineralization process were obtained by measuring the total organic carbon (TOC) at different contact and irradiation times. The estimated degradation of the tartrazine was between 85 and 90%, noting that higher degradation was observed using

Ze-nanZnO as catalyst compared to nanZnO. It was estimated that nanZnO affects "Lactuca sativa" species, but judging by the results the material produces "low toxicity" to this species.

Du G. et al. (2017) demonstrated the preparation of efficient photocatalyst by immobilization of zeolitic imidazolate framework-8 (ZIF-8) derived ZnO on Zeolite A. This type of organometallic compounds known as metal-organic frameworks (MOFs) are hybrid structures consisting of inorganic connectors and organic linker molecules (Jiang Z. et al., 2013). In the case of zeolitic imidazolate framework-8 (ZIF-8), inorganic connectors are Zn(II) ions and organic linker molecules are 2-methylimidazole ligands. By applying the sonochemical synthesis the authors used pre-prepared zeolitic imidazolate framework-8 (ZIF-8) as precursors and zeolite A as support to successfully obtain ZIF-8@Zeolite A (ZIF-8@Z). The following calcination at different temperatures lead to formation of ZnO@Z photocatalysts at different temperatures by removing the organic functional groups of ZIF-8. The prepared photocatalyst, ZnO@Z was studied for application in the degradation of rhodamine B (RhB) aqueous solution under UV light irradiation and ZnO@Z showed higher photocatalytic activity than simply ZnO derived from ZIF-8. This observation can be attributed to the synergistic effect between ZnO and Zeolite because since zeolites are sorbents and can adsorb RhB dye. This prolongs the contact time with catalysts and increase its efficiency. The most active nanocomposite ZnO@Z was obtained by calcination at 550 °C for 5 h and demonstrated the highest photocatalytic efficiency (99.4 %).

Heidaria Z. et al. (2020) reported the synthesis of novel ZnO nanorods over ion exchanged clinoptilolite (ZnO/ICLT) by sonoprecipitation. This material was investigated and found efficient as a catalyst for the photocatalytic degradation of the drug furosemide (FRS). The composite's enhanced photocatalytic activity was attributed to its higher surface area (due to decreasing the particle size) in comparison to ZnO NPs prepared by conventional precipitation method. By the means of various analyses (TEM, EDX, BET, UV-visible spectroscopy techniques, XRD, etc.) was shown that the average particle size of ZnO in ZnO/ICLT prepared by sonoprecipitation was 20.5 nm, while without sonication the size increases up to 34.8 nm. Additionally, the sonication during the precipitation process prevents the agglomeration of nanoparticles. The effects of different parameters such as amount of ZnO on the zeolite, catalyst dosage, initial FRS concentration, pH of reaction media on the photocatalytic degradation were studied. It was found that the maximum degradation rate of FRS was achieved by using 15 wt% ZnO on ICLT, catalyst loading of 0.75 mg.L<sup>-1</sup> at pH 7. It was shown that ICLT has a synergetic effect on ZnO photocatalytic ability as calculated from Langmuir-Hinshelwood equation for photocatalytic degradation over 15%ZnO/ICLT, which has twice higher value than the one for ZnO photocatalysis. The good photocatalytic activity of 15%ZnO/ICLT makes it an excellent candidate for nanophotocatalyst in wastewater treatment applications.

Nezamzadeh-Ejehieh A. et al. (2014) reported also the use of natural zeolite clinoptilolite as a support for ZnO and its photocatalytic degradation of 4-nitrophenol. Nano-sized powder clinoptilolite was prepared via planetary ball mill mechanical method. The ZnO NPs were synthesized by ion exchange of nano-clinoptilolite in a 0.1 M zinc nitrate aqueous solution for 24 h followed by calcination at 450 °C for 12 h, thus forming the nanocomposite material ZnO/natural clinoptilolite

(ZnO/NCP). The photocatalytic tests of ZnO/NCP in the degradation of 4-nitrophenol under UV light irradiation prove the efficiency of the catalyst. The results from the experiments showed that the photodegradation rate of 4-nitrophenol was affected by a few parameters such as the initial 4-nitrophenol concentration, the pH of solution and the amount of catalyst. The process of photocatalysis was accelerated by addition to the system of an electron acceptor, namely hydrogen peroxide and potassium bromate, the latter was the more effective one. The comparison of photodegradation efficiency of the composite ZnO/NCP and pure phases of ZnO or zeolite, showed the enhanced activity of the composite and the advantage of a combination between zeolite and ZnO.

## Conclusions

ZnO is a very promising material with enormous potential in terms of large scale processes for water treatment and practical usage. Its high efficiency in photocatalytic degradation of dyes, pharmaceutical products and herbicide combined with its low cost and simple synthesis marks it as an excellent candidate for integration in advanced and environmentally friendly technologies and settings for water treatment and remediation. Keeping in mind that ZnO has also good antibacterial properties which is advantageous combination when speaking of clean water. One of its disadvantages is that ZnO requires UV light irradiation (its band gap is 3.2-3.3 eV) to operate as effective photocatalysts, which can be easily overcome by doping ZnO with metals. Such incorporation of metal ions into the ZnO lattice leads to formation of additional energy levels that narrow the band gap and makes possible the activation of photocatalyst by sun light. This is a major leap since it will significantly lower the cost for processes when doped ZnO is applied. However, technically speaking the small size of ZnO and ZnO-doped NPs causes difficulties in catalyst removal from the treated water, so it is more convenient if ZnO NPs are attached on suitable support. Good candidate is a zeolite (synthetic and natural) because it is non-toxic material with good sorption properties and high surface area due to its micro porosity. It has been shown that ZnO supported zeolite nanocomposites have a high photocatalytic efficiency in degradation of different organic compounds demonstrating synergetic effect between ZnO and zeolite.

**Acknowledgements.** The authors thank the National Science Fund of Bulgaria, project number DN-17/20 for the financial support.

## References

- Adam, R.E., Alnoor, H., Pozina, G., Liu, X., Willander, M., Nur, O. 2020. Synthesis of Mg-doped ZnO NPs via a chemical low-temperature method and investigation of the efficient photocatalytic activity for the degradation of dyes under solar light. – *Solid State Sciences*, 99, 106053.
- Ahmed, S., Chaudhry, A.S.A., Ikram, S. 2017. A review on biogenic synthesis of ZnO nanoparticles using plant extracts and microbes: A prospect towards green chemistry. – *Journal of Photochemistry and Photobiology B: Biology*, 166, 272-284.
- Aissat, A., Ghomrani, M.A., Belil, W., Benkouider, A., Vilcot, J.P. 2015. The doping effect on the properties of zinc oxide (ZnO) thin layers for photovoltaic applications. – *International Journal of Hydrogen Energy*, 40 (39), 13685–13689.
- Alcantara-Cobos, A., Gutierrez-Segura, E., Solache-Ríos, M., Amaya-Chavez, A., Solís-Casados, D.A. 2020. Tartrazine removal by ZnO nanoparticles and a zeolite-ZnO nanoparticles composite and the phytotoxicity of ZnO nanoparticles. – *Microporous and Mesoporous Materials*, 302, 110212.
- Basnet, P., Chatterjee, S. 2020. Structure-directing property and growth mechanism induced by capping agents in nanostructured ZnO during hydrothermal synthesis—A systematic review. – *Nano-Structures and Nano-Objects*, 22, 100426.
- Basnet, P., Inakhunbi Chanu, T., Samanta, D., Chatterjee, S. 2018. A review on bio-synthesized zinc oxide nanoparticles using plant extracts as reductants and stabilizing agents. – *Journal of Photochemistry and Photobiology*, 183, 201-221.
- Chandekar, k.v., Shkir, M., Khan, A., Al-Shehri, B.M., Hamdy, M.S., AlFaify, S., El-Toni, M.A., Aldabahi, A., Ansari, A.A., Ghaithan H. 2020. A facile one-pot flash combustion synthesis of La@ZnO nanoparticles and their characterizations for optoelectronic and photocatalysis applications. – *Journal of Photochemistry and Photobiology A: Chemistry*, 395, 112465.
- Cheng, X., Meng, Q., Chen, J., Long, Y. 2012. A facile route to synthesize mesoporous ZSM-5 zeolite incorporating high ZnO loading in mesopores. – *Microporous and Mesoporous Materials*, 153, 198–203.
- Daneshvar, N., Rasoulifard, M.H., Khataee. A.R. 2007. Removal of C.I. Acid Orange 7 from aqueous solution by UV irradiation in the presence of ZnO nanopowder. – *Journal of Hazardous Materials*, 143(1–2), 95–101.
- Du, G., Feng, P., Cheng, X., Li, J., Luo, X. 2017. Immobilizing of ZIF-8 Derived ZnO with Controllable Morphologies on Zeolite A for Efficient Photocatalysis. – *Journal of Solid State Chemistry*, 255, 215-218.
- Heidaria, Z., Alizadeha, R., Ebadia, A., Oturan, N., Oturan, M.A. 2020. Efficient photocatalytic degradation of furosemide by a novel sonoprecipitated ZnO over ion exchanged clinoptilolite nanorods. – *Separation and Purification Technology*, 242, 116800, 1-13.
- Hoffmann, M.R., Martin, S.T., Choi, W., Bahnemann, D.W. 1995. Environmental applications of semiconductor photocatalysis. – *Chemical Reviews*, 95 (1), 69–96.
- Jiang, Z., Li, Z.P., Qin, Z.H., Sun, H.Y., Jiao, X.L., Chen, D.R. 2013. LDH nanocages synthesized with MOF templates and their high performance as supercapacitors. – *Nanoscale*, 5(23), 11770-11775.
- Juabrum, S., Chankhanittha, T., Nanan, S. 2019. Hydrothermally grown SDS-capped ZnO photocatalyst for degradation of RR141 azo dye. – *Materials Letters*, 245, 1-5.
- Karimi-Shamsabadi, M., Behpour, M., Babaheidari, A. K., Saberi, Z. 2017. Efficiently enhancing photocatalytic activity of NiO-ZnO doped onto nanozeoliteX by synergistic effects of p-n heterojunction, supporting and zeolite nanoparticles in photo-degradation of Eriochrome Black T

- and Methyl Orange. – *Journal of Photochemistry and Photobiology A: Chemistry*, 346, 133–143.
- Kolodziejczak-Radzimska, A., Jesionowski, T. 2014. Zinc oxide-from synthesis to application: a review – *Materials*, 7, 2833–2881.
- Kumar, M.R.A., Ravikumar, C.R., Nagaswarupa, H.P., Purshotam, B., Gonfa, B.A., Murthy, H.C.A., FSabir, F.K., Tadesse S. 2019. Evaluation of bi-functional applications of ZnO nanoparticles prepared by green and chemical methods. – *Journal of Environmental Chemical Engineering*, 7(6), 103468.
- Lee, K.M., Lai, C.W., Ngai, K.S., Juan, J.C. 2016. Recent developments of zinc oxide based photocatalyst in water treatment technology: a review. – *Water Research*, 88, 428–448.
- Li, M., Li, G., Jiang, J., Tao, Y., Mai, K. 2013. Preparation, antimicrobial, crystallization and mechanical properties of nano-ZnO-supported zeolite filled polypropylene random copolymer composites. – *Composites Science and Technology*, 81, 30–36.
- Lim, C. S., Ryu, J.H. 2009. Synthesis and characterization of TMA-A zeolite nanocrystals incorporating ZnO nanoclusters. – *Journal of Crystal Growth*, 311, 486–489.
- Liu, M., Li, K., Kong, F., Zhao, J., Yue, Q., Yu, X. 2015. Improvement of the light extraction efficiency of light-emitting diodes based on ZnO nanotubes. – *Photonics and Nanostructures - Fundamentals and Applications*, 16, 9–15.
- Mirzaei, H., Darroudi, M. 2017. Zinc oxide nanoparticles: biological synthesis and biomedical applications. – *Ceramics International*, 43, 907-914.
- Moezzi, A., McDonagh, A.M., Cortie, M.B. 2012. Zinc oxide particles: synthesis, properties and applications. – *Chemical Engineering Journal*, 185–186, 1-22.
- Mohammadi, R., Feyzi, M., Joshaghani, M. 2020. Synthesis of ZnO-magnetic/ZSM-5 and its application for removal of disperse Blue 56 from contaminated water. – *Chemical Engineering and Processing - Process Intensification*, 153, 107969.
- Nagajyothi, P.C., Sreekanth, T.V.M., Tettey, C.O., Jun, Y.I., Mook, S.H. 2014. Characterization, antibacterial, antioxidant, and cytotoxic activities of ZnO nanoparticles using *Coptidis Rhizoma*. – *Bioorganic and Medicinal Chemistry Letters*, 24, 4298–4303.
- Nezamzadeh-Ejhieh, A., Khorsandi, S. 2014. Photocatalytic degradation of 4-nitrophenol with ZnO supported nanoclinoptilolite zeolite. – *Journal of Industrial and Engineering Chemistry*, 20(3), 937-946.
- Nouri, H., Habibi-Yangjeh, A. 2014. Microwave-assisted method for preparation of Zn<sub>1-x</sub>Mg<sub>x</sub>O nanostructures and their activities for photodegradation of methylene blue. – *Advanced Powder Technology*, 25, 1016-1025.
- Ong, C.B., Ng, L.Y., Mohammad, A.W. 2018. A review of ZnO nanoparticles as solar photocatalysts: Synthesis, mechanisms and applications – *Renewable and Sustainable Energy Reviews*, 81(1), 536-551.
- Oskoei, V., Dehghani, M.H., Nazmara, S., Heibati, B., Asif, M., Tyagi, I., Agarwal, S., Gupta, V.K. 2016. Removal of humic acid from aqueous solution using UV/ZnO nanoparticle photocatalysis and adsorption. – *Journal of Molecular Liquids*, 213, 374–380.
- Páez, R., Ochoa-Muñoz, Y., Rodríguez-Páez, J.E. 2019. Efficient removal of a glyphosate-based herbicide from water using ZnO nanoparticles (ZnO-NPs) – *Biocatalysis and Agricultural Biotechnology*, 22, 101434.
- Shukla, P., Shukla, J.K. 2018. Facile sol-gel synthesis and enhanced photocatalytic activity of the V<sub>2</sub>O<sub>5</sub>-ZnO nanoflakes – *Journal of Science: Advanced Materials and Devices*, 3(4), 452-455.
- Sitthichai, S., Phuruangrat, A., Thongtem, T., Thongtem, S. 2017. Influence of Mg dopant on photocatalytic properties of Mg-doped ZnO nanoparticles prepared by sol-gel method – *Journal of the Ceramic Society of Japan*, 125, 122-124.
- Steffy, K., Shanthi, G., Markyb, A.S., Selvakumar, S. 2018. Enhanced antibacterial effects of green synthesized ZnO NPs using *Aristolochia indica* against Multi-drug resistant bacterial pathogens from Diabetic Foot Ulcer – *Journal of Infection and Public Health*, 11 (4), 463-471.
- Sun, X., Chen, X., Deng, Z., Li, Y. 2003. A CTAB-assisted hydrothermal orientation growth of ZnO nanorods – *Materials Chemistry and Physics*, 78, 99-104.
- Tachikawa, S., Noguchi, A., Tsuge T., Hara, M., Odawara, O., Wada, H. 2011. Optical properties of ZnO nanoparticles capped with polymers – *Materials (Basel)*, 4, 1132-1143.
- Vidhya, K., Saravanan, M., Bhoopathi, G., Devarajan, V.P., Subanya, S. 2015. Structural and optical characterization of pure and starch-capped ZnO quantum dots and their photocatalytic activity – *Applied Nanoscience*, 5, 235-243.
- Vidyasagar, C.C., Arthoba Naik, Y. 2016. Surfactant (PEG 400) effects on crystallinity of ZnO nanoparticles – *Arabian Journal of Chemistry*, 9, 507-510.
- Vijayakumar, S., Saravanakumar, K., Malaikozhundan, B., Divya, M., Vaseeharan, B., Durán-Lara, S.F., Wang M.H. 2020. Biopolymer K-carrageenan wrapped ZnO nanoparticles as drug delivery vehicles for anti MRSA therapy – *International Journal of Biological Macromolecules*, 144, 9-18.
- Wang, Z., Ye, X., Chen, L., Huang, P., Wang, Q., Ma, L., Hua, N., Liu, X., Xiao, X., Chen, S. 2021. Silver nanoparticles decorated grassy ZnO coating for photocatalytic activity enhancement – *Materials Science in Semiconductor Processing*, 121, 105354.
- Wu, Q., Chen, X., Zhang, P., Han, Y., Chen, X., Yan, Y., Li, S. 2008. Amino acid-assisted synthesis of ZnO hierarchical architectures and their novel photocatalytic activities – *Crystal Growth and Design*, 8, 3010-3018.
- Zhang, L., Mohamed, H.H., Dillert, R., Bahnemann, D. 2012. Kinetics and mechanisms of charge transfer processes in photocatalytic systems: a review – *Journal of Photochemistry and Photobiology C*, 13, 263–276.
- Zhu, S., Xu, L., Yang, S., Zhou, X., Chen, X., Dong, B., Bai, X., Lu, G., Song, H. 2020. Cobalt-doped ZnO nanoparticles derived from zeolite imidazole frameworks: Synthesis, characterization, and application for the detection of an exhaled diabetes biomarker – *Journal of Colloid and Interface Science*, 569, 358-365.

## STUDY OF THE PHYSICO-MECHANICAL PROPERTIES OF THE ROCK MASSIF IN THE SHUMACHEVSKI DOL DEPOSIT, THE ANDROW SECTION

**Mitko Hristov**

University of Mining and Geology "St. Ivan Rilski", Sofia, Bulgaria; avile900819@gmail.com

**ABSTRACT.** In underground mining of vein deposits of minerals, it is necessary to know the physico-mechanical properties of the rock massif around the ore bodies. The lack of adequate knowledge of the state of the rock mass leads to deficiency in the bearing capacity or to over-reliability that result in the choice of support or lining structures, in the selection of design sections of the mine working grid, or in activities related to the management of such mining processes as host rock caving, back filling of stoped-out spaces, etc. The current work demonstrates a sequence of field and laboratory methods whose aim is to characterise the rock mass in terms of properties and condition.

**Keywords:** physico-mechanical properties, laboratory and field research, rock massif

### ИЗСЛЕДВАНЕ НА ФИЗИКО МЕХАНИЧНИ СВОЙСТВА НА СКАЛНИЯ МАСИВ В НАХОДИЩЕ „ШУМАЧЕВСКИ ДОЛ”, УЧАСТЪК „АНДРОУ“ РУДНИК ЕРМА РЕКА

**Митко Христов**

Минно-геоложки университет „Св. Иван Рилски“, 1700 София

**РЕЗЮМЕ.** При подземно разработване на жилни находища на полезни изкопаеми е необходимо да се познават физико-механичните свойства на скалния масив около рудните тела. Липсата на адекватни познания за състоянието на скалния масив води до дефицит на носеща способност или прекален запас на сигурност обуславящ се в избор на крепежни конструкции, избор на проектни сечения на мрежата минни изработки или мероприятия свързани с управлението на минните процеси като обрушаване на вместващите скали, запълване на иззетите пространства и др. Настоящата публикация цели да демонстрира една последователност от полеви и лабораторни методи с цел характеризация на скалния масив по свойства и състояние.

**Ключови думи:** механични свойства, лабораторни и полеви изследвания

### Introduction

The *Androw* section of the *Shumachevski Dol* deposit is represented by vein hydrothermal lead and zinc mineralisation. The major mining operations are carried out along the following ore bodies: apophysis III/towards ore body 7I, ore body 7, ore body "Androw North", and ore body 5. The ore bodies are represented by quartz-carbonate sulphide veins with well-defined contacts. The specific conditions in the *Androw* section are the relatively great depth, the high temperature, the high moisture content, the approximation of the stopes to the piezometric level of hydrothermal pressure water with a temperature between two marble layers and manifestations of primary rock pressure as a result of the redistribution of the stresses in the massif during mining workings.

To determine the physico-mechanical properties of the host rocks in ore body 7 and ore body 5, a series of experimental works were performed near the ore bodies (apophysis and vein) along horizons 450 and 550 respectively.

Suitable locations were selected from these two main horizons for the deposit that best represent the geometrical position of the under host rocks, the hanging host rocks, and the enclosed ore body. For the purposes of characterising the massif, a pre-selection of platforms was made and platforms were determined and marked with the appropriate designations. The platforms were localised in sublevel workings, orts and cut-off entries.

Each of the platforms was specified in such a manner as to cover the three major lithological varieties (host rocks and ore body) as close as possible. Some of the platforms whereby cylindrical samples have been taken are presented in Figure 1.

Rock sampling was carried out by a *Hilti* mobile drill with a penetrating capacity of 50 cm in depth and a diameter (d) of 50 to 150 mm. The above activities were carried out on ten work platforms in order to cover most of the host rocks and ore bodies in the respective above-mentioned horizons (450 and 550). As a photographic application, Figure 2 shows the mobile drilling machine while operating and taking core samples.

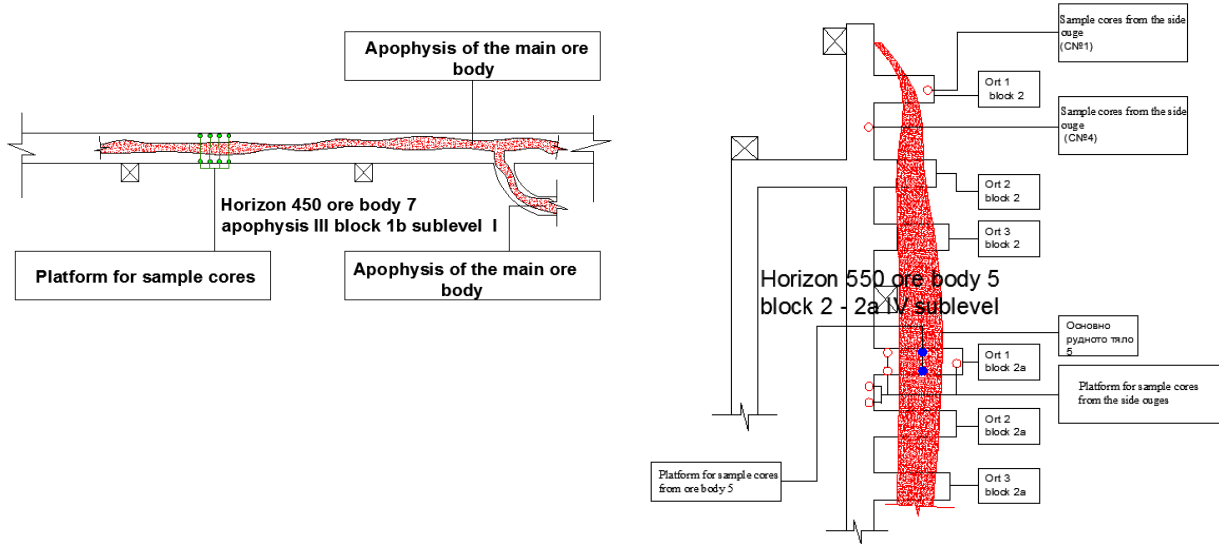


Fig. 1. Location of the working platforms along: a) level 450, ore body 7, apophysis III, stope 1b, sublevel 1; b) level 550, ore body 5, stope 2, sublevel 4

The core samples taken after drilling have a total length of 4.2 m and a diameter of  $d=50$  mm, i.e. NX. The specimens have different lengths depending on the disturbance of the individual selected ore bodies as well as of the host massif. The angle of inclination and the orientation of the main cracks

in the extracted rock specimens were also determined immediately after the sample was taken out of the borehole. All these studies and measurements are presented as a photographic application in Figure 2.



Fig. 2. Drilling core samples out of the host massif

In order to characterise the rock massif, the following necessary laboratory and field studies (ISRM, 1981; Dachev and Ivanov, 2016) concerning the density, strength and deformation parameters of the rocks are planned to be performed:

- Testing in laboratory conditions of the mechanical properties of specimens with a correct geometric shape in terms of strength and deformation;
- Preparation of cuts for determining the distribution of the main rock types in the production sections;
- Determining the orientation and location of structural disturbances (cracks, faults, etc.)

### Laboratory research for determining the physico-mechanical properties of the host massif

As a result of the field experiments carried out, core samples (Fig. 3) were selected from the three lithological varieties of the rock massif. The core samples were tested in the accredited laboratory of *Eurotest-Control EAD* where their face surfaces were pre-formed. The individual sequences of rock specimens were grouped. Out of the test pieces with correct geometrical shape, 30 standard rock specimens were prepared in compliance with the recommendations of ISRM (ISRM, 1981; Dachev et al. 2018). Those were distributed in three sequences corresponding to the properties of the massif in one production section, i.e. hanging rock massif, ore body, under rock mass around the ore body.



Fig. 3. Grouping of a sets of rock specimens taken from the individual ore bodies in laboratory conditions

➤ **Strength tests**

The first series of laboratory samples has revealed that the samples taken from stope 1b, sublevel 1 are composed of varieties of hydrothermal alterations of two-mica gneisses with embedded quartz-sulphide mineralisation. The obtained results of the strength tests that were performed (ISRM, 1981) for the individual varieties of gneisses are given in Table 1 and Table 2.

The second series of laboratory samples has revealed that the samples taken from stope 2, sublevel 4 are composed of varieties of hydrothermal alterations of two-mica gneisses with embedded quartz-sulphide mineralisation.

Table 1. Laboratory data on the physico-mechanical properties of the host rocks and of ore body 7, apophysis III at block 1b of horizon/ 450

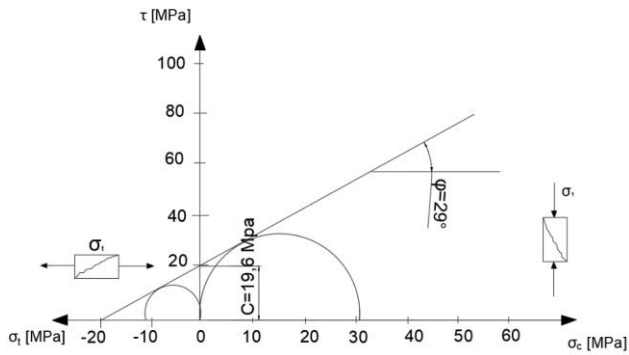
Location	Hanging ouge	Under ouge	Ore body
Parameters			
Volume density min/max, [MN/m <sup>3</sup> ]	0.0275 ±0.0002	0.0273±0.0002	0.0342/0.0469
Uniaxial pressure strength, σucs [MPa] min/max	46.2/51.6	63.9/70.3	45.5/60.2
Tensile strength, σt [MPa] min/max	12.5/17.2	18.1/20.4	15.3/19.5
Cohesion C [MPa]	15.4	10.4	11.2
Angle of internal friction, [°]	32	30	28.9
Elasticity modulus, E [MPa] min/max	23480/34515	40363	14817/17660
Poisson's ratio ν [-]	0.10	0.09	0.08

Table 2. Laboratory data on the physico-mechanical properties of the host rocks and of ore body 5 in block 2 of horizon 550

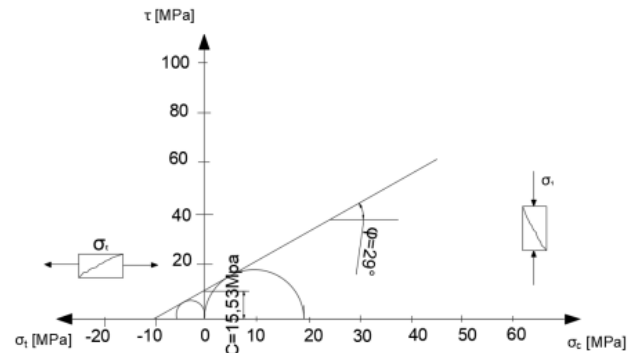
Location	Hanging ouge	Under ouge	Ore body
Parameters			
Volume density min/max, [MN/m <sup>3</sup> ]	0.0255 ±0.0002	0.0257/0.0268	0.0291/0.0312
Uniaxial pressure strength, σucs [MPa] min/max	19.5/21.7	24.7/36.9	20.7/38.9
Tensile strength, σt [MPa] min/max	4.5/7.2	9.8/13.1	6.1/8.5
Cohesion C [MPa]	5.63	18.3	14.7
Angle of internal friction, [°]	34	34	33
Elasticity modulus E [MPa]	6820	12138	10450
Poisson's ratio ν [-]	0.24	0.14	0.12

The test results presented in Tables 1 and 2 show that the rocks of the ore body are with the highest density, they have the lowest porosity. The strength parameters of the rocks from the hanging ouge are the lowest. The laboratory study has shown that during the test, the strength properties of the three characteristic groups of rock varieties have a range of variation from 20 to 30%. At the stage of each strength study, a strength

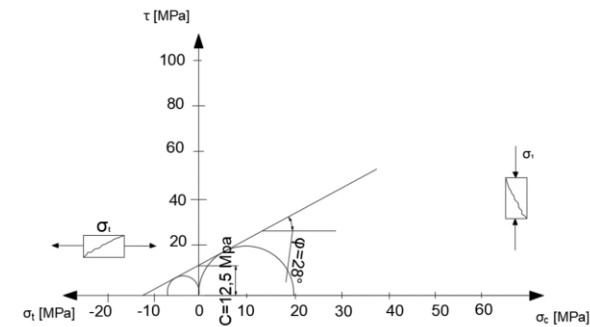
layout for the particular type of rock variety needs to be designed. One of the most famous strength layouts is that of Mohr-Coulomb (Hoek, 2001; Brady and Brown, 2004). Using the Mohr-Coulomb criterion, the relationship between normal and tangential stress is given. Strength layouts were outlined in the studies performed. Part of the strength layouts based on laboratory test data is shown in Figure 4.



a) amphibole-biotite gneisses – lying host massif



b) hydrothermally altered amphibole-biotite gneisses – hanging host massif



c) hydrothermally altered two-mica amphibole-biotite gneisses - ore body

Fig. 4. a, b, c - strength layouts of the rocks from the gneiss variants in the production section of horizon 550

### Study of the structural disturbance of the rock mass

The structural disturbance of the massif provides the amount of information necessary to determine the state of the rock massif (Brady and Brown, 2004). The study of this information is a continuous process which begins with the stage of mineral survey and exploration and goes through all mining phases, thus resulting in a large amount of factual material amassed (Brady and Brown, 2004). The study of the structural disturbance of the massif in the *Androw* section is prompted by the need to determine the mechanical condition of the host massif around the ore bodies. The purpose is to provide stability in compliance with the applied development system in the individual ore bodies. The DIPS ver. 7.0 (Rocscience, 2018) software package was used to analyse the results related to the structural disturbance of the massif. Figure 5 shows the overall structural disturbance of the massif on horizon 450. Based on the results obtained, two groups of crack systems have been identified. The first crack system (which is the main one) is in the direction of 130°-310° and is embedded in the southeast-northwesterly direction; the second crack system is in the direction of 10°-190° and is embedded from the northeast to the southwest. Based on the measured cracks in terms of orientation and dip, the systems of cracks are determined (see Figure 5). One characteristic feature of the cracks on horizon 550 is that they are grouped into two or up to three main groups of systems: the first system is 125-305°, the second is 5-185°, and the third, which is pronging, is 160-340°.

The orientation of the crack in depth was determined after the extraction of the pieces of the oriented drill core.

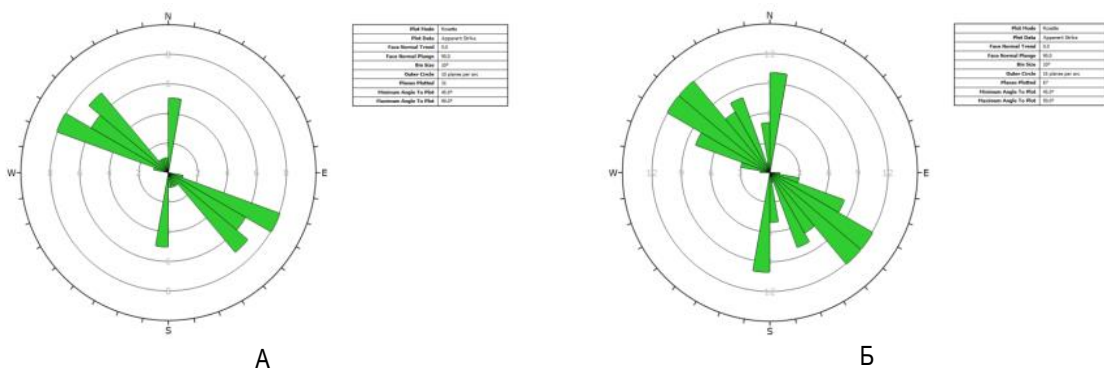


Fig. 5. Results from the study of overall structural disruption/disturbance of the cracks - the three systems of cracks are displayed in the "rose-type diagram of cracks: A) on horizon 450; B) on horizon 550

### Rock quality designation

Standard research on the rock quality designation (RQD) has not been carried out so far (Dachev and Ivanov, 2016). Determining the quality of the rock, i.e. RQD, is not performed by the classical method, but by one of the alternative methods (Brady and Brown, 2004), instead. The assessment of the rock quality is made in Fig. 6. The results of the structural disturbance of the massif are used and the parameters of average number of cracks per meter are determined (Brady and Brown, 2004).

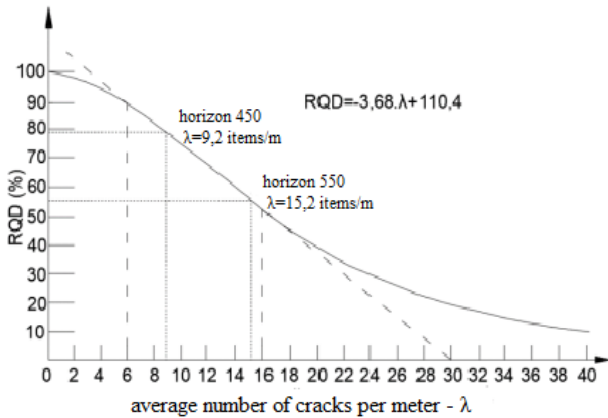


Fig. 6. Results of the quality of the massif RQD obtained through the method of Brady and Brown

#### For horizon 450

According to the results shown in Fig. 7, the RQD concerning the quality of the massif from the structural disruption/disturbance is 77% and ranges from 75% to 90%.

The results are shown by means of the bar chart in Fig. 7A); thus, it is possible to determine the average for the RQD, which is:

$$RQD_{cp.} = 77\% \rightarrow (75 \div 90) \Rightarrow R_{RQD} = 17$$

#### For level/horizon 550

As for the second region on level/horizon 550 studied, the results are also shown in Fig. 7. The RQD concerning the quality of the massif from the structural disruption/disturbance is 54.5% and ranges between 50% and 75%.

The results are shown by means of the bar chart in Fig. 7B); thus, it is possible to determine the average for the RQD, which is:

$$RQD_{cp.} = 54,5\% \rightarrow (50 \div 70) \Rightarrow R_{RQD} = 13$$

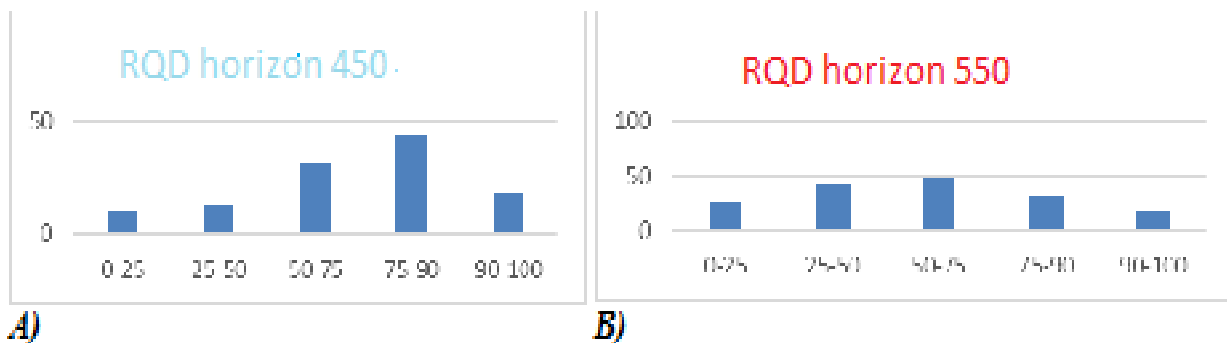


Fig. 7. Bar charts for the distribution of the RQD values for a geomechanical region on: A) horizon 450; B) horizon 450

The results for the RQD have been processed with the help of Table 3 offered by Deere.

Table 3. Quality of the massif RQD, after Deere

RQD %	class/grade	Quality of the massif	
0-25	A	Very poor	
25-50	B	Poor	
50-75	C	Fair	The massif on horizon 550
75-90	D	Good	The massif on horizon 450
90-100	E	Excellent	

### Results of the research work

The obtained results concerning the mechanical condition of the massif are new for the Androw section. Based on them, several significant conclusions can be drawn:

- Complex laboratory tests have been carried out on samples of the rock varieties that make up the host massif. The strength and deformation characteristics of the various

lithological varieties of rock that form the host massif in the experimental production section have been determined. Mohr-Coulomb strength layouts have been outlined for each lithological type of rock in the regions studied. New geomechanical software has been used to study the deformation behaviour and to determine the elastic constants.

- The structural disturbance (RQD) of the respective horizons has been studied and a geomechanical classification

of the massif has been offered. As a result of laboratory, field, and structural studies, a multidimensional database has been made for the purposes of the integrated characterisation of the massif.

## Conclusion

Due to the extensive geomechanical research carried out, a database has been provided. Classification assessments have been made. Several significant conclusions can be drawn from the research applied. Those could serve as recommendations for the future development of the *Androw* section:

- Keeping a database of the physico-mechanical properties of the lithological varieties of host rocks around the ore bodies is imperative at the stage of the penetration in depth and the subsequent development and mining.
- The database should comprise information on the strength and deformation properties of the massif, data on the density properties, and mandatory data on the structural disturbance. This would lead to an adequate interpretation of the condition of the massif at each stage of the production or the construction of mining workings.

## References

- Hoek E.T. Rock Engineering AA Balkema. Rotterdam, 2001.
- ISRM Suggested Methods. Rock Characterisation Testing and Monitoring. Pergamon, Press, 1981.
- B. H. G. Brady, E. T. Brown- Rock mechanics and underground mining, third edition-Canada 2004.
- Dachev G., Ivanov, V., Kompleksnata I dostovernata harakterizatsia na masiva – osnoven etap na geomehanichnoto osigurivane na poszemnia dobiv na polesni iskopaemi, VII Mejdunarodna konferenzia po geomehanika 27-01.07.2016, “Sv. Konstantin i Elena”, Varna, Bulgaria, 205-211. (in Bulgarian)
- Dachev G., Ivanov, V., Geomehanichna obosnovka na optimalen variant za izzemvane na zamasite v uchastak “Marzyan” ot rudnik “Erma reka”, V Nauchno-tehnicheska konferenzia s mejdunarodno uchastie, Devin, 04-07.10.2016, 141-148. (in Bulgarian)
- Dachev G., Kutsarov K., Georgiev D. The safe and effective acquisition of geo-resources as the main objective of geomechanics. XI<sup>th</sup> Expert counseling with international in the area of underground and surface exploitation and geological exploration of mineral resources Podelks Poveks 2018, Struga, R. of Macedonia 09-11 November 2018, page 143-149.
- Rocscience, Dips, v7.0. Toronto, Canada 2018.

## APPLICATION OF NON-DETONATING CHARGES FOR CAUTIOUS BLASTING OF CONCRETES

**Neno Ivanov<sup>1</sup>, Petar Shishkov<sup>2</sup>**

<sup>1</sup> University of Mining and Geology "St. Ivan Rilski", 1700 Sofia; nenoiv.ivanov@gmail.com

<sup>2</sup> University of Mining and Geology "St. Ivan Rilski", 1700 Sofia; sfxman86@yahoo.com

**ABSTRACT.** Usually, when carrying out special blasting works for demolition of concrete elements and structures in construction, the so-called "Small Charges Method" is applied. Traditionally, explosives with higher brisance and a shorter period of increasing the rate of explosive conversion are preferred. This ensures the completeness of the detonation and the optimal size of the "sphere of destruction" around each charge. In some specific situations, the shattering effect of explosives provides more damages to the surroundings, than benefits from blasting treatment of the concrete element. It often happens, that there are existing protected objects next to the demolished element or structure, even in the immediate vicinity. There are cases when, despite expensive measures to protect against the harmful effects of the explosion, some damages from the effects of detonation are unavoidable. In such situations, two approaches are applied in practice: non-explosive destruction or use of "low-energy" charges. The report discusses a real task for explosive crushing of hardened concrete in the body of a self-propelled concrete mixer, without deforming or damaging the technical means. Non-detonating metal-containing pyrotechnic mixtures have been used for explosive charges with reduced energy.

**Keywords:** non-detonating blasting cartridges, propellants, cautious blasting, blasting demolition

### ПРИЛОЖЕНИЕ НА НЕДЕТОНИРАЩИ ЗАРЯДИ ЗА ПРЕЦИЗНО РАЗДРОБЯВАНЕ НА БЕТОНИ

**Нено Иванов<sup>1</sup>, Петър Шишков<sup>2</sup>**

<sup>1,2</sup> Минно-геоложки университет „Св. Иван Рилски“, 1700 София

**РЕЗЮМЕ.** Обикновено, при провеждане на специални взривни работи за разрушаване на бетонни елементи и конструкции в строителството се прилага така наречения "Метод на малките заряди". Традиционно се предпочитат експлозиви с повишена бризантност и по-кратък период на нарастване на скоростта на взривно превръщане. Така се гарантира пълнотата на детонация и оптимален размер на "сферата на разрушение" около всеки заряд. В някои специфични ситуации, бризантното действие на взривните вещества нанася повече вреди по оръжаващата среда, отколкото са ползите от взривното третиране на бетонния елемент. Често се случва до подлежащия на разрушаване елемент или конструкция да има охраняем(и) обект(и), дори в непосредствена близост. Има случаи, когато въпреки скъпите мероприятия по защита от вредните въздействия на взрива, пораженията от ефектите на детонацията се оказват неизбежни. При такива ситуации, в практиката се прилагат два подхода: безвзривно разрушаване или използване на "нискоенергийни" заряди. В доклада е разгледана реална задача за взривно раздробяване на втвърден бетон в корпуса на самоходен бетонов миксер, без техническото средство да се деформира или поврежда. За заряди с понижена енергия са използвани недетониращи метало-съдържащи пиротехнически смеси.

**Ключови думи:** недетониращи взривни патрони, металелни взривни вещества, предпазливо взривяване, взривно разрушаване

### Introduction

Modern industrial and civil construction is associated with an increasing need of demolishing of parts of buildings and entire facilities for reconstruction or complete clearing of terrains. Explosion is the fastest and most cost-effective way, but it is often accompanied by inconveniences, caused by the harmful effects of detonation. Carrying out blasting operations in urban areas, close to sensitive industries and critical infrastructure requires a specific approach for protection against seismicity, vibrations, shock wave and fly-rocks. The blasting technique is placed in an unfavorable competitive race with various non-explosive methods of destruction. Complicated working conditions are a prerequisite for developing a new generation of explosives and technological approaches for their application. They can be based on non-detonating energetic compositions. The processes for crushing of consolidated cement mixtures and ordinary concrete are identical to those in the fragmentation of rocks. In them, intense cracking can be caused even only under the influence

of rapidly expanding gaseous products. The destruction of reinforced concrete and composite materials is complicated by the presence of reinforcement of different nature, spatial location and degree of crosslinking. The rupture of the reinforcing elements requires a brizant action of the explosion, which is inevitably associated with the detonation. The main purpose of this study is to research the possibilities of using pyrotechnic compositions for the destruction of concrete elements and structures in construction, without the risk of side effects caused by detonation of charges. Experiments for blasting of hardened concrete with non-detonating charges are the next step in the study of the potential of low-speed energetic compositions for delicate blasting not only in the extraction of dimension stones, but also for special blasting works.

Knowledge of the theoretical basis of explosive action in a solid medium, about the differences between the action of high-explosives and low-explosives, as well as the processes of crack formation in metamorphic rocks, plays a leading role in scientific and experimental activities.

### About explosives and their impact on hard medium

The explosives are high-energetic chemical compounds or mixtures of chemical compounds that, when properly initiated, instantly turn into gaseous products with high temperature and pressure. This process is called "explosion". During that rapid decomposition, one kilogram of explosive turns into hot gases in just a part of milisecond, creating a pressure of about 10,000 MPa (1,450,000 psi) inside the blast hole. The explosion temperatures of the various explosives are between 1,500 °C to 4,500 °C. Detonation velocities for civil and military explosives varies in the range from 2,500 to 8,000 m/s.

The rate of explosive's chemical reaction (combustion, deflagration or detonation) is one of the parameters determining their classification. This parameter has a direct influence on the brizancy of the explosive, respectively for the fracture formation in the treated rock. The type of explosive decomposition is decisive for the choice of explosives and the appropriate explosive technology in special blasting works. The detonation velocity is the speed at which the shock wave travels through the length of the charge. The higher this speed, the greater is the strength of the explosive's shredding effect. High-speed explosives are suitable for blasting hard rocks and strong reinforced concrete. The blasting agents with a lower detonation rate are used to break up soft rocks and weak concrete. The propellants emits their gaseous products for a longer time and therefore exert a better throwing action.

The detonation pressure is the pressure in the reaction zone when the explosive decomposes at supersonic speed. It causes the primary shock wave of compression. That compression wave propagates in the environment and is an important indicator of the ability of the explosive to perform good fragmentation.

Deflagration is a subsonic reaction of chemical decomposition of explosives. It is typical for all types of gunpowder and other propellants, which work by means of the pressure, generated by the compressed gaseous products of the explosion. Practically, they haven't a brizant action.

### Experimental part

The occasion for the experiment was a road accident with a concrete truck, overturning when driving off-road. The accident ended with uncontrolled hardening of the concrete solution in the mixer body (Fig. 1).



Fig. 1. Concrete truck

### The task

Explosive fragmentation and crushing of hardened concrete solution inside the mixer's body of a concrete truck (Fig. 2 and 3) without allowing deformations of the metal housing.



Fig. 2. Concrete mixer exterior

Available concrete in the mixer - 6 m<sup>3</sup>. Brand of the concrete mixture - "B-20", with receipt according to BDS EN 206 - 1.

Standard containing for 1 m<sup>3</sup>:

- Variegated river gravel or crushed stone - 1250 kg. ~ 1300 kg.
- Washed sand - 650 kg. ~ 700 kg;
- Portland cement brand M 250 - 465 kg .;
- Water - 180 l. ~ 200 l.

Approximate weight of 1 m<sup>3</sup> of the described concrete solution = 2550 kg. Weight of 6 m<sup>3</sup> concrete "B-20" = 15 300 kg.



Fig. 3. Concrete mixer interior

### Site conditions

The steel body of the mixer (barrel) is made of wear-resistant steel sheets brand DILLIDUR 400/500 with a thickness of 12 mm. The individual sheets of the housing are welded with an automatic welding machine with internal and external welding seam. Inside the mixer are welded screw ribs made of wear-resistant steel sheets 4 mm., designed for mixing the concrete solution and for its unloading. There is an inspection hole with a diameter of 500 mm., which is covered with a removable cover, in the front compartment of the barrel (Fig. 4). Outlet diameter 900 mm.

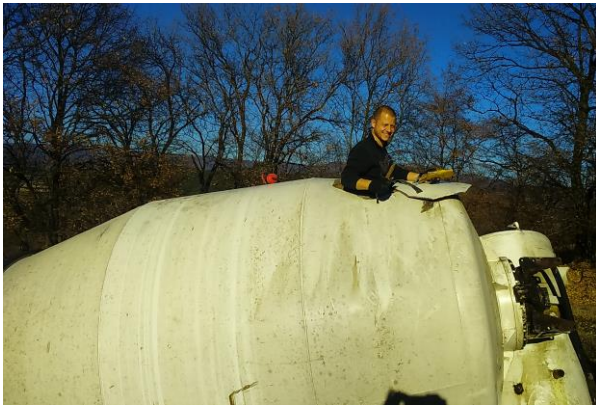


Fig. 4. Concrete mixer revision hole

The available hardened concrete mixture was distributed along the entire length of the barrel, filling 37.2% of its total geometric volume. The remaining free volume of 62.8% was inconvenient, but sufficient to carry out the processes of preparation of special blasting works (Fig. 5). Due to the narrow space in the mixer housing for the preparatory processes for drilling and blasting works and the difficult access to the site, it is not possible to use perforators with compressed air. Another reason to avoid the pneumatic drilling technique is that a large amount of dust is released when working with a pneumatic perforator. Under these conditions (small free volume, lack of open space, poor ventilation, even with personal protective equipment) it was not appropriate to work with pneumatic tools. For this purpose, an electric drill BOSSH GBH 5-40 DCE was selected, with the necessary accessories to it (crushing awls and drill bits for boring of blast holes). The electric drill was powered by a portable gasoline single-phase generator model IMER EXPLORER 4010 - 3000W.

#### Coefficient of strength of the concrete mixture

The uniaxial compressive strength class of concrete is indicated by the letter "B" and numbers after it, showing the minimum strength in MPa. These indicators mean strength with a guaranty of 95%.

For example, for the most used concrete B-20, this means that when testing a reference cube of this brand of concrete, its strength is good at 95% of the results with a pressure of 20 MPa. The compressive strength of the concrete is determined on reference (test bodies) cubes with size 150 x 150 mm, which harden at the prescribed technological time.

According to the European standard to which the Bulgarian BDS EN 206 - 1 is synchronized, the strength classes are marked with "C" and two groups of numbers after it. For the most used concrete C - 20/25 this means that its minimum strength determined on test specimens (cylinders with a diameter of 150 mm and a height of 300 mm) is with a pressure of 20 MPa, and the minimum strength determined on cubes) with a size of 150 x 150 mm. is 25 MPa.

In the present case, the concrete mix had not reached its standard strength, but was still brittle and with high moisture content. The strength coefficient according to M.M. Protodyakonov was accepted:  $f = 10 - 12$ .

#### Selection of technological method of blasting and construction of the charges

Given the specific conditions of the site and the irregular shape of the concrete body, which is located in the lower part of the steel barrel of the mixer, the blasting for swelling the concrete was carried out in stages in several sectors in order to preserve the structural integrity of the mixer. In the design of blasting, the concrete body was considered as similar to a dug foundation of non-reinforced concrete. In order to achieve a more gentle blasting effect with successive opening of free surfaces, a model of bench blasting by the method of small charges was provided.

#### Selection of the explosive

Having into account the delicate technical conditions of the site, an opportunity was sought for a choice between explosives that do not detonate. In selecting the appropriate formulations, as a starting point were used the results of the laboratory tests of explosive mixtures published in „*Innovative formulations for a new generation of low-speed explosive compositions, designed for blasting in tender conditions and for extraction of rock-cladding materials*” – Journal of Mining and Geological Sciences, p.94 – 99, vol.62, Nr.2, 2019.



Fig. 5. Blasting field

In this particular case, a pyrolant explosive was chosen - a pyrotechnic mixture with a working form of chemical reaction "combustion". The so-called "Sound-light gas-generating pyrotechnic composition" provides a relatively large volume of gaseous products per kilogram of explosive and a sufficiently short period of rate increase to deflagration. During the ongoing chemical process, the contained metal powder fuel raises the temperature, which contributes to the greater expansion of the gaseous products (Table 1). Charge construction – continuous type.

Table 1. Non-detonating explosive mixtures

Characteristics	Black powder	Flash powder for SFX	Noise-light gas generating mixture
1. Ingredients, %:			
- KNO <sub>3</sub>	75	-	-
- KClO <sub>4</sub>	-	-	50
- Ba(NO <sub>3</sub> ) <sub>2</sub>	-	50	20
- charcoal	15	-	-
- S	10	-	10
- Al/Mg powder	-	50	20
2. Estimated characteristics:			
- oxygen balance, %	- 20,3	- 23,4	- 8,5
- heat of blast, MJ/kg	3	4,5	4
- volume of gases, l/kg	280	260	340
3. Experimental characteristics:			
- moisture & volatile <sup>3</sup> , %	-	-	-
- bulk density, kg/m <sup>3</sup>	0,4 ÷ 0,5	0,5 ÷ 0,7	0,6 ÷ 0,8
- efficiency, cm <sup>3</sup>	30	28	35
- brizance <sup>1</sup> , mm	-	-	-
- critical diameter in bulk density <sup>1</sup> , mm	-	-	-
- stable diameter in bulk density <sup>1</sup> , mm	-	-	-
- velocity of chemical decomposition, m/s	300÷600	600÷900	400÷700
- optimal loading density <sup>2</sup> , kg/m <sup>3</sup>	Does not compact	Does not compact	Does not compact

**Notes:**

1. Brizance, critical diameter and stable diameter are not determined because the charges are not initiated by a detonator and do not detonate in the site conditions.
2. The charges are not sealed in the blast holes in order not to create preconditions for their explosive combustion to pass into detonation.
3. Moisture and volatile components reduce the burning rate and performance of the described pyrotechnic compositions.

**Type of the blast pattern**

The decision for application of non-detonating charges deprives from the convenience of relying on the brizance action of the blasting. Respectively, the typical "spheres of explosive destruction" around the charges become practically unattainable. The expansion of the heated gaseous products causes only a few single radial cracks from the point of explosion, without areas of grinding and active fragmentation. In order to achieve sufficient cracking of the concrete body, it was necessary most of the cracks from the individual charges to be crossed. For this reason, the relative distance between the individual blast-holes should have been the same. A staggered layout of the blasting pattern was chosen.

**Determination of the face burden (average)**

Due to the fact, that the construction of the barrel was complicated by internal screw ribs, the blasting was carried out in seven separate stages in order to prevent deformation of these elements. Therefore, in the first round, a preliminary manual breaking was made, in order to form an additional free face. In the sections of concrete, that were located immediately behind the auger fins, the charges worked in unfavorable conditions - with only one open surface (in the vertical direction). The construction of these charges was with a reduced concentration of explosive to prevent damage on the fin-ribbing. With the first cut holes in the mentioned stages, the effect of low explosive performance of "cracking charge" was sought. The burden of the next charges (second, third and fourth rows of blast-holes) appears in a horizontal direction to the newly discovered surface from the first cut-holes. According to the Method of the small blasting charges, when destroying a buried foundation, described on page 218 by N. Paunov and B. Barbulov "V pomoshit na vzrivnika", burden was accepted in the range  $W_b = 0.30 \div 0.85$  m. Due to the fact, that in the present case non-detonating pyrotechnic charges were used, the burden of the first cut-hole was determined to be 0.30 m.

**Initiation technique**

Electric igniters for professional pyrotechnic purposes with a resistance of 2.5  $\Omega$  and a guarantee amperage of 1 A connected in a series circuit, were preferred as the most suitable means for inflammation. The number of electric igniters was determined depending on the blasting rounds parameters. The main goal was to avoid overloading the structure of the concrete-mixer caused by instantaneous expansion of the solid material during blasting. Separated step blasting was chosen due to the impossibility of the electric igniters to work in series of delay.

**Loading method**

Manual loading with individual approach to the blast holes were preferred.



Fig. 6. Loading of the charge in the blast-hole

The drill-holes for phased loading were pre-checked for their design depth. Residual material from the drilling works was cleaned. The electric igniters were calibrated using an ohmmeter, with a difference in resistance values not exceeding 10%. During the preparation of the charges, the pyrotechnic composition was weighed with an electronic scale to correspond to the quantity set in the project. The electric igniter

and the weighed pyrolant were wrapped and fastened in a thin polyethylene foil tube. The prepared charge was placed to the bottom of the blasthole with the help of a tamping-rod (Fig. 6). No excessive pressure was applied to the charge, so that it would not be deformed or dead-pressed. A sand stemming was applied. At each blasting round, the ends of the wires of the respective number of igniters were connected in a series to the firing cable.

## Results and discussion

Excellent swelling fragmentation of treated concrete was performed after blasting with pyrolant charges (Fig. 7 and 8). No damages on the construction of the mixer were registered.



Fig. 7. Swelled concrete inside the mixer interior after blasting

The absence of seismic action is explained by the fact, that the blasting was carried out above the ground and no high explosives were used to cause supersonic shock waves and compressive stresses.

Due to the fact, that the blasting demolition was performed in a closed space, as well as due to the used pyrotechnic composition with a low deflagration rate (up to 400 m/s.), distributed in small charges (up to 50 g.), no air-blast with overpressure was formed.

The enclosed space and the well-calculated charges were a prerequisite for the lack of fly-rocks.



Fig. 8. Grain sizes of the fragmented concrete

The total used explosive weight was less than 5 kg. No dangerous amount of toxic gases and harmful chemical compounds were released.

## Conclusions

It was made investigations for application of fast combusting pyrotechnic composition for obtaining of non-detonating explosive charges, suitable for blasting activities at tender and complicated conditions. Results from blast-splitting of consolidated concrete in the volume of the mixer was satisfactory. There was no fumes emission, air-blast or fly-rocks after explosion of pyrolant composition. The velocity of propagation of the reaction of chemical destruction of used high-energetic composition was between 400 and 700 m/sec. depending on the diameter of the charges, moisture and density. Usually, noise-light gas-generating mixture shows higher velocities of deflagration and in bigger diameters of the charges is inclined to pass from combustion to detonation. The authors doesn't noticed any tendency for transition from deflagration to detonation in case of ignition of 50 g. charges with soft burning electric fuse-head in drill-holes with diameter 38 mm.

Such energetic compositions could replace both the widely used industrial explosives and blasting gunpowder in cases of cautious blasting in tender conditions. One of the disadvantages is their increased sensitivity to external influences, which could be prevented by usage of suitable charge casings. Another drawback is relatively high cost, which can be compensated by the reliefs in the mode of acquisition, transportation, storage and use, resulting from the lower hazard class of the products.

**Aknowledgements.** Cordial thanks to the management and employees of "OGNENA HRIZANTEMA" Ltd. – Panagiyurishte for provided territories, workers, equipment and data during field experiments!

## References

- Boychev Y., Asenov S., 2018. "Pirotehicheski sastavi za neletalni svetlinnozvukovi sredstva", ISBN:978-619-7246-20-9, ISSN:2367-7481, 614-620, National Academic Publishing House (in Bulgarian).
- Paunov N., Barbulov B., 1989. "V pomosht na vzrivnika", Izdatelstvo "Tehnika", 292 p. (in Bulgarian)
- Mitkov V. 2014. Novyye vodoustoychivyye vzryvchatyye veshchestva na osnove energeticheskikh materialov utiliziruyemykh boyepripasov.- *Mining informational and analytical bulletin*, Moskva, № 11, 312-316, ISSN: 0236-1493. (in Russian)
- Mitkov, V. 2010. Bezopasnost pri proizvodstvo i upotreba na eksplozivi. Sv. Ivan Rilski, Sofia - 343 p. ISBN 978-954-353-131-8 (in Bulgarian).
- Mitkov V., 2010. Assessment and risk management of malicious acts aimed at potentially hazardous Hydrotechnical constructions. *Conference proceedings from the International conference of Blasting techniques*, Stara Lesna, Slovak Republic, pp. 212-220, ISBN 978-80-970265-2-3.
- Mitkov V., 2010. Metodika za kompyutarno proektirane na parametrite na PVR pri karieren dobiv.- *Annual of the University of Mining and Geology "St. Ivan Rilski"*, 53, Part 2: Dobiv i prerabotka na polezni surovini, pp. 88-94, ISSN 1312-1820. (in Bulgarian).

- Mitkov, V. 2011. Razrabotvane i izsledvane na novi zariadi ot utilizirani boepripasi, *Geology and mineral resources* Nr. 4, p. 30-33, ISSN 1310-2265 (in Bulgarian).
- Stoilova S., Mitkov V., Belin V., 2014. Analiz na vuzdeistvieto na vazdushnata udarna valna za usloviyata na kariera "Tselovizhda" , *Annual of the University of Mining and Geology "St. Ivan Rilski"* – Sofia, v. 57, Part II: Dobiv i prerabotka na polezni surovini, pp.108-110, ISSN 1312-1820, (in Bulgarian with English abstract).
- Stoycheva N., Shishkov P., 2019. Innovative formulations for a new generation of low-speed explosive compositions, designed for blasting in tender conditions and for extraction of rock-cladding materials – *Journal of Mining and Geological Sciences*, p.94 – 99, vol.62, Nr.2.
- Shishkov P., Stoycheva N., 2018. Savremenni vzrivni tehniki za dobiv na skalno-oblicovachni materiali - *Mining and geology magazine*, 10-11, p.42-49, ISSN 0861-5713 (in Bulgarian with English abstract).

## TOOTH WEAR ON A TWO-SHAFT SHREDDER

**Malina Ivanova**

University of Mining and Geology "St. Ivan Rilski", 1700 Sofia, malina\_vatz@abv.bg

**ABSTRACT.** The article is devoted to the wear of shredding chamber teeth of a two-shaft shredder for crushing of technological and building waste materials. The factors influencing the wear process are regarded. The studies of the mechanical load and behavior of the teeth have been conducted through solving the equations describing the mechanical processes in working conditions under the finite element method. For this purpose, there has been generated a three-dimensional geometrical model of the teeth, which has been discretized (digitized) to a planned network of finite elements in the programming environment of ANSYS MECHANICAL APDL programming environment

**Keywords:** teeth of a two-shaft shredder, technological waste materials, wear process, three-dimensional geometrical model

### ИЗНОСВАНЕ НА ЗЪБИТЕ НА ДВУВАЛОВ ШРЕДЕР

**Малина Иванова**

Минно-геоложки университет „Св.Иван Рилски“, 1700 София

**РЕЗЮМЕ.** Статията е посветена на износването на зъбите на двувалов шредер като основна машина при раздробяване на техногенни и строителни отпадъци. Разгледани са факторите, влияещи на процеса износване. Изследванията на механичното натоварване и поведение на зъбите са проведени чрез решаване на уравненията, описващи механичните процеси при работни условия по метод на крайните елементи. За целта е генериран триизмерен геометричен модел на зъбите, който е дискретизиран на планирана мрежа от крайни елементи в програмната среда на ANSYS MECHANICAL APDL.

**Ключови думи:** зъби на двувалов шредер, техногенни отпадъци, износване, триизмерен геометричен модел

### Introduction

Plastic is one of the most important engineering materials used for various applications. Biodegradable plastic is produced but its share in global production is very small. Most polymeric materials are not biodegradable. They are used in the form of foil, bottles, packaging, pipes, etc. such as packaging and preserving foods and drinks (Tegegne et al., 2019). The lifetime of polymers has a disadvantage, too- the waste, including industrial waste, generated after their use and the fact that it must be disposed of. Storage in landfills, utilization or burning plastic causes an irreparable damage to the environment. Therefore polymer producers and the companies producing and generating plastic waste aim at recycling. This is a number of measures, as follows:

- collecting and sorting waste;
- reprocessing into secondary raw materials;
- production of end products.

The plastic waste used can be converted into raw materials by using a suitable mechanic technology such as crushing or extrusion. As an integral part of the reprocessing processes, the waste material is ground to sizes suitable for further transportation, measuring, dosing and using in the production chain. In some cases grinding is required in order to reduce the bulk density of the material during reprocessing, polystyrol foam for example; in some cases, on the other hand, to increase the bulk density and reduce transportation costs. In other cases, for example in treating a polymer film, waste needs to be ground (and also agglomerated) so that the resulting material can be easily and smoothly fed into the extruder for further treatment. Crushing is performed for further

plastification but also as a necessary step of warehouse logistics and even the waste burning process since waste requires uniformity of the fraction composition for uniform feeding and dosing during treatment.

Typical grinding technologies include crushing, compaction, agglomeration and atomization (micronization-sputtering). The type of equipment is determined based on the material to be crushed. A combination of various types of equipment is very often used in the grinding process. For example, when processing big, dense and thick-walled waste material, they are first crushed in shredders, as shown in fig. 1, after that in cracker machines and then in micronizers if dust-like fractioning is required.



**Fig.1. Different types shredders**  
(a) Single-shaft shredder, working by scraping; (b) Single-shaft shredder, working by cutting; (c) Two-shaft and (d) Four-shaft shredders (Vatskicheva, Grigorova, 2017)

The grinding process is often used when a composite or a multilayer material needs to be separated into components, such as different coatings, laminated materials. Crushing in combination with air allows multicomponent plastic waste such as hoses reinforced with textile fibers, partition foil, mats with one layer of foam, etc. to be sorted and separated. The basic thing is that the grinding process of the composite material leads to breaking the physical connection among most heterogenic particles. After that the resulting scrapped composite material can be divided into air flows based on different density and geometry of the materials included in it. In such a division light particles go up and heavy particles fall down as a result of gravitation. Such methods are used for separating scrub rubber from hard thermoplastic materials and aluminium from thermoplastic materials (Nasr, Yehia, 2019).

The second step is melting and finally transformation into new products. The shredder blade plays the main part in the plastic shredder machine. There are many types and forms of shredder blades (VijayAnanth at al., 2018), fixed to rotating shafts and shown in figure 2.



Fig.2. Types of shredder blades (Nasr, Yehia, 2019)

Machines with a high rotating speed are used for light and thin plastic, and for hard waste and for such with big dimensions – machines with low rotating speed. Here the uniformity of grinding, the absence of dust and too big pieces depends on a number of parameters of polymer materials:

- physical and mechanic properties - resistance, impact resistance, friction factor, softening temperature;
- structure- they are continuous, fibrous, cellular, composite;
- shape and sizes.

Plastic materials can be divided into three groups:

Group 1: film /foil/- polypropylene, acrylic, polyethylene and PVC films are highly elastic. They need to be cut in order to be ground.

Group 2: small and thin-walled- they include PET containers, small fuel boxes and lubricants and coatings, plastic pipes. The shredders need to be equipped with more powerful blades or teeth for them.

Group 3: such with big dimensions and thick walls- they are crushed by hitting, compression /pressure/ or abrasion.

Waste is initially crushed by shredders and a granulating machine is used for secondary grinding. The two stages are divided with a view to production optimization. The two-level crushing allows you to reduce power costs and to increase the speed of treatment. Machines that combine a shredder and a granulating machine are manufactured. For example the international group of companies TRIA has developed a series of combined machines for treatment of large units and thick-walled products. However, they are not suitable for small waste- PET containers, materials in the form of foil, etc.

Tegegne et al. (2019) have developed an electrically driven two-shaft machine for crushing waste plastic. The angle at the top of the blades, the space between the blades, etc. are considered. The blades have been manufactured from tool steel ASIS L-2.

Ekman (2018) has designed and manufactured a shredder machine for plastic waste material recycling. He has used an engine with capacity of 2,2 KW and 2820 r.p.m. of the exit shaft of the engine and a reduction gear with a gear reduction ratio  $i=40$  to reach a rotation speed of 7 r.p.m. which is required for crushing plastic bottles.

### Object of study

The object of study of this paper is the mechanic wear of the teeth of a two-shaft shredder for crushing plastic.

The shredder blades are manufactured from steel DIN1.1830. It is used for the production of blades operating in conditions that do not cause heating of the cutting edge. This steel is used mainly to manufacture blades operating under moderate load, for crushing materials that do not require high strength of the tool (soft metals, wood, plastic, polyethylene).

In this study the blades have three cutting edges used in a machine for shredding PE plastic. Polyethylene is composite thermoplastic plastic. There are many types of polyethylene but the most popular are: low-density polyethylene (LDPE) and high-density polyethylene (HDPE). In both cases the density is lower than  $1 \text{ g/cm}^3$  which means that they float on the surface of water. The items produced from them are shown in fig. 3.



Fig.3. Items from polyethylene /PE/

The geometry and shape of the blade are generated with the help of Solid Works 16. The blades have a hexagonal hole for fixing the shaft. The dimensions are illustrated in figure 4.

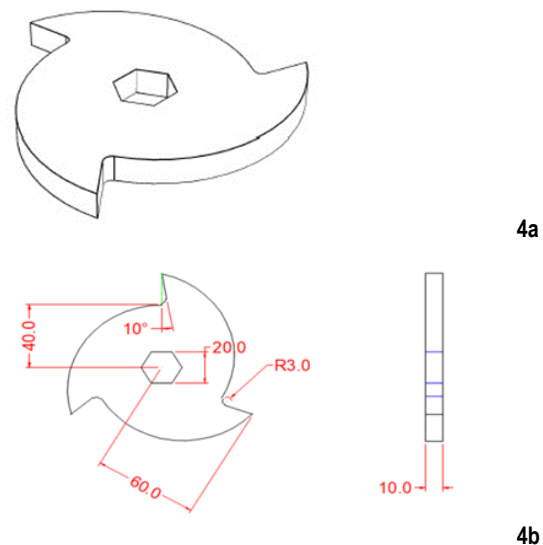


Fig.4. Detailed geometry of the shredder blade (The dimensions are in mm)  
4a) Isometric; 4b) Plane view (Nasr, Yehia, 2019)

The procedure for determining the distributed applied cutting (shredding) force at the edge of the blade is illustrated in the flow chart given in figure 5.

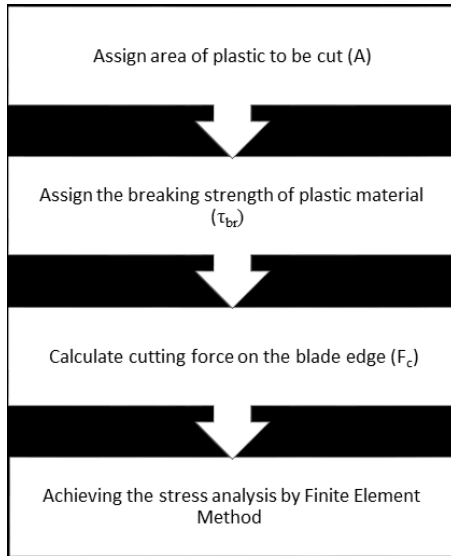


Fig.5. Flow chart for calculating the shredding force (Nasr, Yehia, 2019)

The mechanical properties of polyethylene (PE) are presented in table 1 (Shackelford, Alexander, 2001).

Table 1. Main properties of PE

No	Parameter	Method	Unit of measurement	Value
Mechanic properties				
1	Density	DIN 53479	g/cm3	0.96
2	Tensile strength	DIN 53455	MPa	27
3	Elastic modulus	DIN 53457	MPa	850
4	Friction factor			0.29
5	Poisson's ratio (u)			0.37- 0.44
6	Hardness	DIN 53482	RC	94 - 101
7	Yield strength	DIN 53484	MPa	24
8	Surface energy	DIN 53476	mN/m	31

Table 1 presents the values of the mechanical properties of the material in the linear area. As a polymer, polyethylene as a whole has non-linear mechanical behaviour. For this specific case it has been considered as a linear material for modelling purposes. In table 1 for most of the values only one number from a range of values has been selected according to the loading and brand of polyethylene.

Breaking strength can be calculated as the ultimate strength multiplied by a factor of safety 1.5. It is set based on the tensile strength but for most materials the shearing strength is lower. The calculation in this way is in the direction of safety.

The admissible strength of PE plastic material is:

$$\tau_{br,plastic} = 27 \times 1,5 = 40,5 \text{ MPa}$$

The cross-sectional area of the material to be cut is:

$$(1) \quad S = B \times t, \text{ where:}$$

B is the width of cutting blade edge,

t is the thickness of the plastic material.

The cutting force required for cutting the plastic bottles is:

$$(2) \quad F_c = \tau_{br,plastic} \times S$$

### Case study concept

The studies of the mechanic load and wear of the teeth of a two-shaft shredder have been made by solving the equations that describe the mechanic processes under working conditions by finite elements method. For this purpose a three-dimensional geometrical model of the blades has been generated which has been discretized on a planned finite elements network in the program environment of ANSYS MECHANICAL APDL.

The boundary conditions reflecting the mechanical load and wear of the teeth include the following parameters.

#### Blade geometry

The blade is assigned with (refer to fig. 4):

$$B = 0,01 \text{ m}; R_o = 0,06 \text{ m}; R_{omeop} = 0,01 \text{ m}$$

The thickness of plastic bottles is assumed to be

$$t = 1 \times 10^{-3} \text{ m.}$$

The cutting area of plastic is

$$S = B \times t = 0,01 \times 1 \times 10^{-3} = 1 \times 10^{-5} \text{ m}^2.$$

#### Material for manufacturing the blades

The blades are made of low carbon steel (as per DIN 1.1830, as per ГОСТ У8Г) with tensile strength = 1860 MPa /at 20°C/ and 710 MPa /at 100°C/; elastic modulus E = 209 GPa, and Poisson's ratio of 0,29.

#### Cutting force

The cutting force is:

$$F_c = \tau_{br,plastic} \times S = 40,5 \times 10^6 \times 1 \times 10^{-5} = 405 \text{ N.}$$

### Results obtained

The stress analysis of the teeth of a two-shaft shredder for crushing plastic has been performed with the help of the finite elements method (Braess, 2007), using ANSYS MECHANICAL APDL software, there being only static stress and strains, without any vibrations.

Figure 6 presents the 3-D model of the teeth of a two-shaft shredder.



Fig.6. 3-D model of a two-shaft shredder tooth

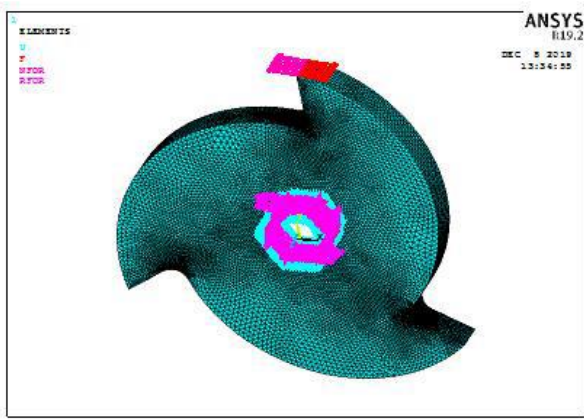


Fig.7. Shredder blade with applied loads and boundary conditions

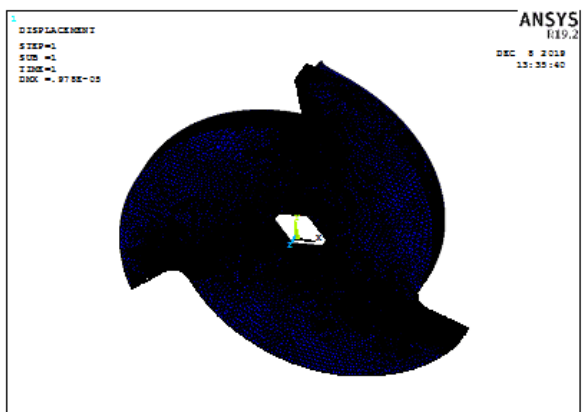


Fig.8. Summary of deformations / Shredder blade deformed shape

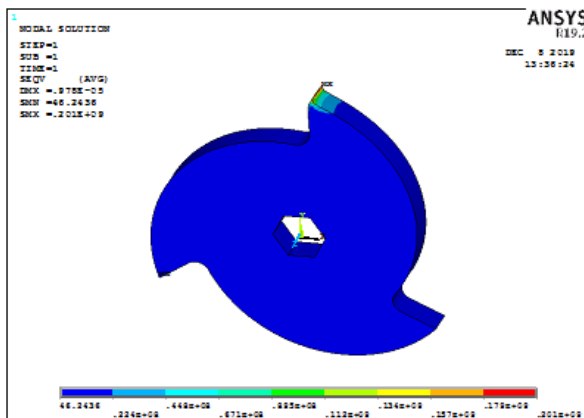


Fig.9. Von Mises Stress

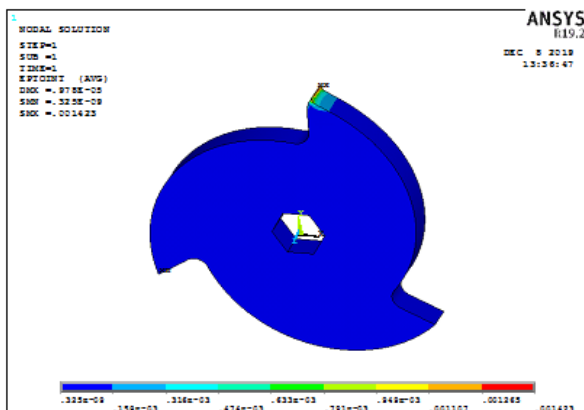


Fig.10. Summary of strains / Total mechanical strain

The results obtained from ANSYS (as illustrated in figures 8, 9 and 10) show that the applied stress is lower than the Von Mises Stress for the blades material.

The maximum total mechanical strain is  $1,4 \times 10^{-3}$ , and the maximum deformation is  $0,97 \times 10^{-5}$  m.

## Conclusions

The results obtained from the case studies give grounds to make the following conclusions with respect to the wear of the teeth of a two-shaft shredder:

- The shredder for crushing waste plastic is widely used in the plastic waste management industry.
- In this study a crushing blade has been developed using Solid Works.
- A strain analysis has been conducted using ANSYS MECHANICAL APDL.
- The places of wear of the blades have been indicated according to the results obtained for the applied strains and deformation.
- The material for manufacturing the blades has been analyzed.
- The results obtained by the finite elements method indicate that the stress to be applied to the blades in the process of crushing of the PE plastic material is far below the stress of destruction of the material of the blades.
- The analysis of vibrations and dynamic stress applied when the shredder blades work are guidelines for future investigation.

**Acknowledgment:** The author expresses her gratitude to the University of Chemical Technology and Metallurgy, the city of Sofia, for the opportunity to use hardware systems and licensed software to perform the calculation procedures.

## References

- Tegegne, A., A. Tsegaye, E. Ambaye, R. Mebrhatu "Development of Dual Shaft Multi Blade Waste Plastic Shredder for Recycling Purpose", International Journal of Research and Scientific Innovation (IJRSI) | Volume VI, Issue I, 2019.
- VijayAnanth, S., T.N. Suresh Kumar, C. Dhanasekaran, A. Aravinth Kumar A. "Design and Fabrication of Plastic Shredder Machine for Clean Environment", International Journal of Management, Technology and Engineering, Volume 8, Issue XII, 2018.
- Vatskicheva, M., I. Grigorova. Study of two-shaft shredder for crushing of concrete, rubber, plastic and wood, Journal of International Scientific Publications: Materials, Methods & Technologies, Vol. 11, Accepted, 2017.
- Nasr, M. F., K. A. Yehia. Stress Analysis of a Shredder Blade for Cutting Waste Plastics, Journal of International Society for Science and Engineering Vol. 1, No. 1, 09-12, ISSN: 2636-4425, 2019.
- Ekman, R. "Development of a Plastic Shredder", master thesis, Sweden, Lund University, 2018.
- Shackelford, F. J., W. Alexander. "Materials Science and Engineering Handbook", CRC Press LLC, 2001.
- Braess, D. Finite Elemente – Theorie, schnelle Löser und Anwendungen in der Elastizitätstheorie. 4. Auflage. Springer, ISBN 978-3-540-72449-0, 2007.

## IDENTIFYING THE DIG LINES FOR ORE EXTRACTION IN THE CASE OF OPEN-PIT MINING

*Dimitar Kaykov<sup>1</sup>, Daniel Georgiev<sup>2</sup>*

<sup>1</sup>University of Mining and Geology "St. Ivan Rilski", 1700 Sofia; dimitar.kaykov@gmail.com

<sup>2</sup>University of Mining and Geology "St. Ivan Rilski", 1700 Sofia; daniel.georgiev.hip@gmail.com

**ABSTRACT.** Based on the implementation of the contemporary Blast Movement Monitoring markers (BMMs) for tracking the movement of ore boundaries in the volume of a blasted rock pile, the post-blast ore boundaries can be determined with a satisfying accuracy. The calculated and visualized post-blast ore boundaries can be used for determining and calculating the boundaries of the improved dig lines for each flitch in the post-blast bench. The purpose of the improved dig lines is to acquire a maximal volume of ore, while preserving the initial ore grades as much as possible by tolerating the excavation of some waste volumes. Following the new dig lines, the amount of ore dilution is minimal, while maintaining a low level of ore loss at the same time.

**Keywords:** BMMs, dig lines, losses, dilution

## ОПРЕДЕЛЯНЕ НА ГРАНИЦИТЕ НА ДОБИВНИЯ БЛОК В УСЛОВИЯТА НА ОТКРИТ ДОБИВ НА РУДНИ ПОЛЕЗНИ ИЗКОПАЕМИ

*Димитър Кайков, Даниел Георгиев*

*Минно-геоложки университет „Св. Иван Рилски“, 1700 София*

**РЕЗЮМЕ.** Въз основа на използването на съвременната BMM технология (Маркери за мониторинг на отместването на взривното поле) за проследяването на отместването на рудните зони в рамките на взриввания блок, сравнително точно могат да бъдат определени крайните им граници в обема на скалния развал след извършено взривяване. Използването на отместените граници на орудяванията може да послужи за определянето на границите на добивните блокове за всяко подстъпало в рамките на работното стъпало, като се цели в границите им максимално да бъде запазено средното съдържание за всяка рудна зона. По този начин може се минимизира обедняването на рудата и да се проследят загубите на полезен компонент при добива на руда.

**Ключови думи:** BMM датчици, добивен блок, загуби, обедняване

## Introduction

Modern-day ore mining practices have started including more and more sophisticated methods for improving the ore grade control due to the ever-changing economical situation as well as the accelerated scientific and technical progress. Using samples from pre-blast and post-blast mining surfaces prove to be a rational and a reliable source of information for the ore zones and their grade estimates. However, this type of technology has the drawback that the information of ore zone grades may take too long to be acquired from the chemical laboratory, which leads to complex organization of the mining process. In-situ ray logging of ores also proves to be a quick way of getting a both for pre-blast and post-blast grade information from the mining surfaces. However, its drawback is that the margin of error is not always satisfactory. Therefore, these two practices should be combined whenever the mining companies has the chance in order to make more precise estimates (Konstantinov, 1997). Another alternative is using a different type of technology for ore grade estimation in post-blast ore strings. One such successful method around the world is the use of the so called Blast Movement Monitors (BMMs) from Blast Movement Technologies. The targeted types of ores which use this type of technology include gold, copper, lithium, iron ore,

nickel, platinum, silver, uranium and zinc. So far this technology has reached 133 mining companies in 41 countries around the world (blastmovement.com).

## Purpose of Blast movement monitors (BMMs)

In open-pit mining the ore and waste flows are a part of two key processes: 1) the formation of stockpiles with different ore grades which are later used for blending and achieving the targeted ore grade, required for the processing plant; 2) the formation of waste dumps for poor ore grades below the cut-off grade and for overburden. However certain ore and waste mislocations may occur due to the unknown places of the post-blast ore and waste zones. Figure 1 represents the three main types of ore and waste mislocations.

Blast movement monitors (BMMs) prove to be helpful for gathering information on how the ore strings have moved after production blasting and for pinpointing their approximate location in the blasted rock pile (Fig. 2). So far many case studies around the world from Blast Movement Technologies have shown that using the post-blast ore strings for dig lines the avoided ore misclassification and dilution ensure a better economic result reaching up to several thousands of USD per blast.

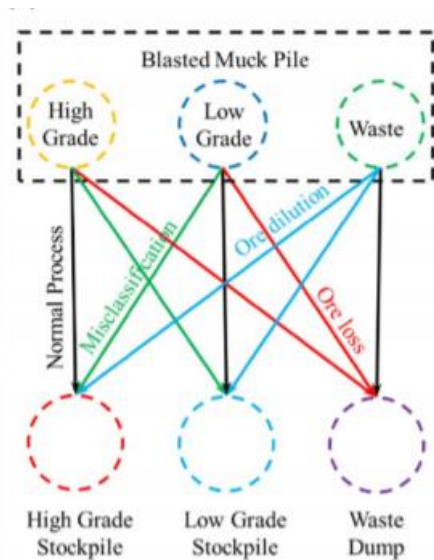


Fig. 1. The impact of blast-induced rock movement (Yu et al., 2019)

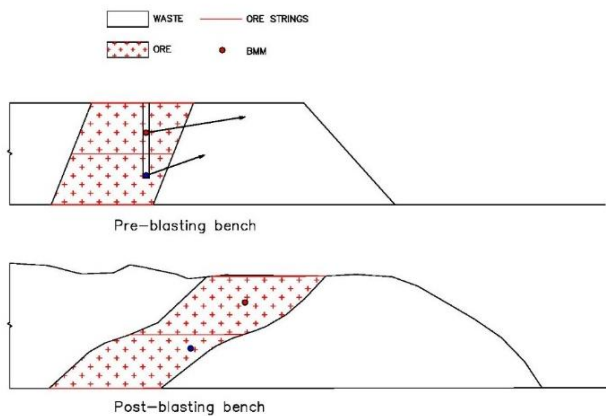


Fig. 2. The effect from using BMMs (ocblasting.com), (seequent.com)

### Defining feasible dig lines using post-blast bmm ore strings

Most mining practices rely on using the same string boundaries as their dig lines. However, certain unwanted situations are likely to occur, which are not accounted for. These dig lines could lead to diluting the mined ore with overburden as well as realizing partial ore losses (Fig. 3).

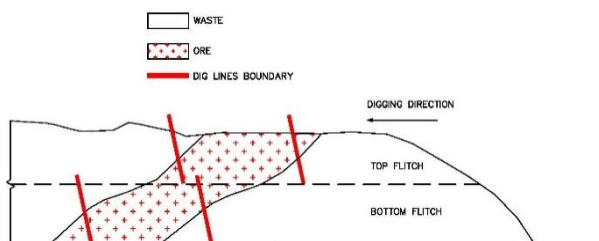


Fig. 3. Commonly used dig lines for each ore string (ocblasting.com), (seequent.com)

A different approach can be taken into consideration in order to properly define the dig lines for the post-blast ore strings. The

strings regarding the same ore zone in the top flitch and the bottom flitch overlap each other in the view plane which lead to the formation of two main zones: 1) Inner Ore Zone (IOZ = TFS ∩ BFS) and 2) Outer Ore Zone (OOZ = TFZ ∪ BFZ) (Fig. 4).

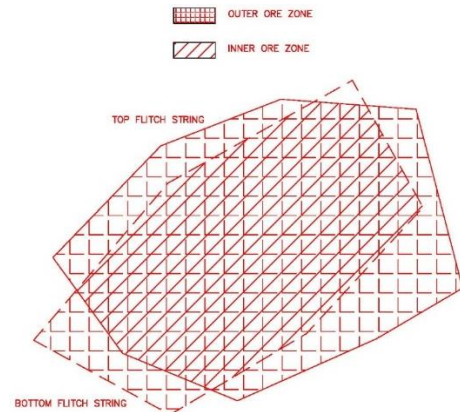


Fig. 4. Inner ore zone and Outer ore zone

One can notice that there are different zones inside the dig lines, where the ore remains with the same grade, while in other zones, the ore grade is diluted by the waste volumes. This required the Outer Ore Zone to be divided to certain elementary volumes (Fig. 5).

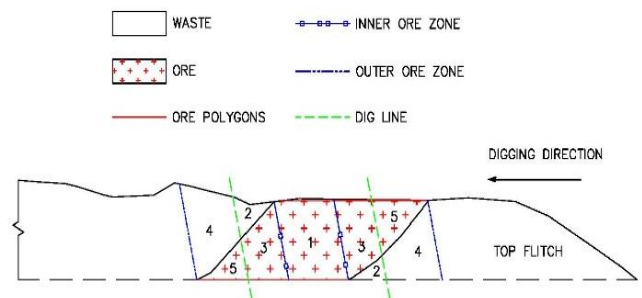


Fig. 5. Elementary volumes inside the Outer Ore zone

- 1 –  $V_{i.o.z.}$  – volume of ore in the Inner Ore Zone,  $m^3$  (if the Top Flitch String and the Bottom Flitch strings do not overlap,  $TFS \cap BFS = \emptyset$ , then  $V_{i.o.z.} = 0 m^3$ );
- 2 –  $V^{o.b.}_{dil}$  – volume of overburden from the diluted area outside the Inner Ore Zone,  $m^3$ ;
- 3 –  $V^{ore}_{dil}$  – volume of ore from the diluted area outside the Inner Ore Zone,  $m^3$ ;
- 4 –  $V^{o.b.}_{loss}$  – volume of overburden above or below the ore losses outside the dig lines,  $m^3$ ;
- 5 –  $V^{ore}_{loss}$  – volume of ore losses outside the dig lines,  $m^3$ ;

The figure shows that this method is applied for the top flitch. Nevertheless, the same logic could be applied while excavating the bottom flitch or mining the whole bench with its full height. In addition, the same logic can be applied for every string in the blasted rock pile.

The volume of the Outer Ore Zone inside the blasted rock pile can be represented with the equation:

$$V_{o.o.z.} = V_{i.o.z.} + V^{ore}_{dil} + V^{o.b.}_{dil} + V^{ore}_{mis.} + V^{o.b.}_{loss} + V^{ore}_{loss}$$

where  $V_{o.o.z.}$  – volume of each Outer Ore Zone,  $m^3$ ;

$V_{mis.}^{ore}$  – volume of misclassified ore from neighboring ore strings inside the digging block boundary ( $V_{mis.}^{ore} = 0 \text{ m}^3$  if there are no neighboring strings),  $\text{m}^3$ ;

In general, the volume of the blasted area includes the volumes of ore from each string as well as the waste volumes in between the strings. After the blasting process is concluded the different elementary volumes preserve a weight balance. The volume of the post-blasted rock pile can be calculated the following way:

$$V_{b.r.p.} = V_{b.r.p.}^{o.b.} + \sum_{i=1}^n V_{o.o.z.i}$$

where  $V_{b.r.p.}$  – volume of blasted rock pile,  $\text{m}^3$ ;

$V_{b.r.p.}^{o.b.}$  – volume of overburden in the blasted rock pile (outside every Outer Ore Zones),  $\text{m}^3$ ;

$V_{o.o.z.i}$  – volume of ore and overburden for Outer Ore Zone  $i$ ,  $\text{m}^3$ ;

$i$  – sequential number for the Outer Ore Zones;

$n$  – total number of Outer Ore Zones in the blasted rock pile;

**The shape of the dig line boundaries depends on the ore strings geometry as well as the blast movement distance and direction. Another important factor is the excavator's digging direction.** Nevertheless, the dig lines are used to identify whether the ore inside the dig lines are to be mined in a selective or bulk manner. There are three main goals which should be met in order to determine the optimal dig lines for each Outer Ore Zone:

- 1) a **maximum profit** should be achieved from the dig lines;
- 2) the **ore content for each dig block** should be either have a maximum value or it should not be lower than the initial category, in which the contents of ore strings belong to;
- 3) the **ore losses** should not be lower than an initially determined percentage;

In order to determine the dig line boundaries for each digging block a feasibility check has to be made in order to

identify where it is feasible to excavate the diluted ore blocks and to determine whether the dilution is too high that it is more profitable to dilute and lose some of the post-blast ore via bulk mining. When applying selective mining the goal is to ensure a digging process where the blasted ore is excavated in its supposed contact zones with the overburden. Therefore, this ensures that the different elementary volumes of ore and overburden are transported to their correct place (stockpile for ores and waste dump for overburden).

The expected revenue for each blasted rock pile is determined by the two formulas for bulk and selective mining:

$$\text{Revenue}_{bulk i} = (V_{i.o.z. i} + V_{dil. i}^{ore} + V_{mis. i}^{ore}) \cdot \gamma_{ore} \cdot P_m \cdot \frac{\epsilon}{100 \cdot \beta}$$

$$\text{Revenue}_{selective i} = (V_{i.o.z. i} + V_{dil. i}^{ore} + V_{mis. i}^{ore} + V_{loss i}^{ore}) \cdot \gamma_{ore} \cdot P_m \cdot \frac{\epsilon}{100 \cdot \beta}$$

where  $\text{Revenue}_{bulk i}$  – revenue from bulk mining technology for the Outer ore zone, USD (BGN);

$\text{Revenue}_{selective i}$  – revenue with from selective mining technology for the Outer ore zone, USD (BGN);

$\gamma_{ore}$  – density of the ore,  $\text{t/m}^3$ ;

$P_m$  – metal price per ton, USD/t (BGN/t);

$\epsilon$  – percentage of concentrate extraction from the ore in the processing plant, %;

$\beta$  – content of the metal product in the final processed concentrate, %

The costs for excavating each blasted rock pile includes the blasting costs, the excavation costs, transportation costs, ore processing costs and overburden waste dump building. Depending on the excavation technology (bulk or selective), the costs are determined by the formulas:

$\text{Costs}_{bulk} =$

$$\begin{aligned} & \left[ \sum_{i=1}^n \gamma_{ore} \cdot V_{i.o.z.i} + \gamma_{ore} \cdot V_{dil. i}^{ore} + \gamma_{o.b.} \cdot V_{dil. i}^{o.b.} + \gamma_{ore} \cdot V_{mis. i}^{ore} \right] \cdot [L^{ore} \cdot C_{tr}^{ore} + C_{pr}] + \\ & + \left[ \gamma_{o.b.} \cdot V_{o.o.z.}^{o.b.} + \sum_{i=1}^n \gamma_{ore} \cdot V_{loss i}^{ore} + \gamma_{o.b.} \cdot V_{loss i}^{o.b.} \right] \cdot L^{o.b.} \cdot C_{tr}^{o.b.} + \\ & + \left[ V_{o.o.z.}^{o.b.} + \sum_{i=1}^n V_{loss i}^{ore} + V_{loss i}^{o.b.} \right] \cdot C_{w.d.} + \\ & + V_{b.r.p.} \cdot [C_{blast} + C_{exc}] \end{aligned}$$

$\text{Costs}_{selective} =$

$$\begin{aligned} & \left[ \sum_{i=1}^n V_{i.o.z.i} + V_{dil. i}^{ore} + V_{loss i}^{ore} + V_{mis. i}^{ore} \right] \cdot \left[ \gamma_{ore} \cdot K_{tr}^{\frac{s}{b}} \cdot L^{ore} \cdot C_{tr}^{ore} + \gamma_{ore} \cdot C_{pr} \right] + \\ & + \left[ V_{o.o.z.}^{o.b.} + \sum_{i=1}^n V_{dil. i}^{o.b.} + V_{loss i}^{o.b.} \right] \cdot \left[ \gamma_{o.b.} \cdot K_{tr}^{\frac{s}{b}} \cdot L^{o.b.} \cdot C_{tr}^{o.b.} + C_{w.d.} \right] + \\ & + V_{b.r.p.} \cdot [C_{blast} + K_{exc}^{\frac{s}{b}} \cdot C_{exc}] \end{aligned}$$

where  $\gamma_{o.b.}$  – overburden density, t/m<sup>3</sup>;  
 $C_{blast}$  – blasting costs, USD/m<sup>3</sup> (BGN/m<sup>3</sup>);  
 $C_{exc}$  – excavation costs, USD/m<sup>3</sup> (BGN/m<sup>3</sup>);  
 $L^{ore}$  – distance for ore transportation, km;  
 $C_{tr}^{ore}$  – relative costs for ore transportation, USD/t.km (BGN/t.km);  
 $C_{pr}$  – relative ore processing costs, USD/t (BGN/t);  
 $L^{o.b.}$  – distance for overburden transportation, km;  
 $C_{tr}^{o.b.}$  – relative costs for overburden transportation, USD/t.km (BGN/t.km);  
 $C_{w.d.}$  – relative costs for waste dump building, USD/m<sup>3</sup> (BGN/m<sup>3</sup>);  
 $K_{exc}^s$  – multiplier indicating how many times selective mining costs for excavation exceed the ones for bulk mining (due to preliminary operations of the excavator for moving overburden or ore volume aside);  
 $K_{tr}^s$  – multiplier indicating how many times selective mining costs for transportation exceed the ones for bulk mining (due to idle time for trucks while waiting for the excavator).

The potential profit which every blasting generates can be calculated by subtracting the revenues and the costs respectively for bulk mining and selective mining.

$$Profit_{bulk_i} = Revenue_{bulk_i} - Costs_{bulk_i}$$

$$Profit_{selective_i} = Revenue_{selective_i} - Costs_{selective_i}$$

However, in order to determine whether it is feasible to excavate each mining block via a selective mining or bulk mining, the parameter  $\Delta_i$  had to be defined to determine the difference between the profits from bulk mining to selective mining.

$$\Delta_i = Profit_{bulk_i} - Profit_{selective_i}$$

When  $\Delta_i < 0$  selective mining is the more profitable alternative for the whole Outer Ore Zone. In this case each elementary volume is transported to its respective stockpile (for ore) or waste dump (for overburden). However, this may prove to be a very time-consuming and difficult task for the excavator's operator and his spotter and therefore it could be applied only in special occasions such as: 1) when the ore grade is high, 2) the grade estimation and the ore body geometry model is reliable, 3) the rock types for the ore and the overburden differ from each other visually, 4) the time-bound constraints are defined as a wide interval, etc.

When  $\Delta_i > 0$  bulk mining is the more feasible type of mining technology for string  $i$  and the Outer Ore Zone is not fully mined. However, this could lead to unwanted ore losses and grade misclassification between neighboring ore strings. Hence, certain constraints have to be adopted in order to ensure the ore losses ( $OL_{max}$ ) and dilution percentage ( $D_{max}$ ) do not exceed a certain percent (Koprev, 2018):

$$1) \frac{V_{i.o.z.i}^{ore} + V_{dil.i}^{ore} + V_{mis.i}^{ore} + V_{loss.i}^{ore}}{V_{i.o.z.i}^{ore} + V_{dil.i}^{ore} + V_{mis.i}^{ore} + V_{loss.i}^{ore}} \leq OL_{max_i}$$

$$2) \frac{\gamma_{ore} \cdot (V_{d.b.i}^{in} + V_{dil.i}^{ore} + V_{mis.i}^{ore})}{\gamma_{ore} \cdot (V_{d.b.i}^{in} + V_{dil.i}^{ore} + V_{mis.i}^{ore}) + \gamma_{o.b.} \cdot V_{dil.i}^{o.b.}} \leq D_{max_i}$$

or

$$2) \frac{q_i \cdot \gamma_{ore} \cdot (V_{i.o.z.i} + V_{dil.i}^{ore} + V_{mis.i}^{ore})}{\gamma_{ore} \cdot (V_{i.o.z.i} + V_{dil.i}^{ore} + V_{mis.i}^{ore}) + \gamma_{o.b.} \cdot V_{dil.i}^{o.b.}} \rightarrow max$$

When  $\Delta_i = 0$  both types of mining technology are equally feasible which leads to the need of preliminary adoption of further criteria, such as time-bound requirements for the selective mining technology as well as the levels of ore losses, misclassification and ore dilution.

### Improving bulk and selective mining dig lines

Although these two alternatives seem to be simple and intuitive, they prove to be two totally opposite alternatives, which treat the content of every Outer Ore Zone either by achieving full selective mining (as much as possible) or full bulk mining. However, there is a third alternative which utilizes partial selectivity of the excavation process for each ore block. This could be achieved by dividing the outer dig lines in several inscribed boundaries which form halo-like zones of diluted ore around the Inner Ore Zone, which belong to one of the ore grade categories (Low Grade, Medium Grade, High Grade or Very High Grade) or fall into the zone below the cut-off grade (Fig. 6).

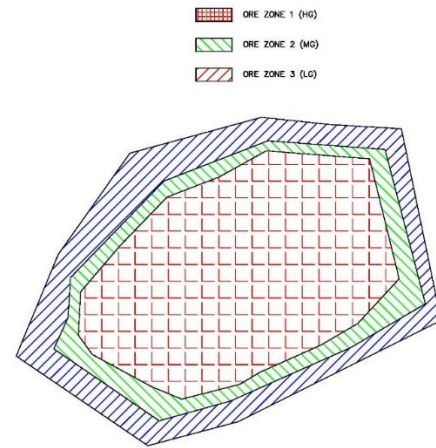


Fig. 6. Inscribed dig lines for the different ore zones deriving from the Inner and Outer Ore Zone boundaries

Following the excavation of the different ore zones from every Outer Ore Zone ensures that several volumes form with different grades of ore and they are separately transported and accumulated in their respective stockpile. Theoretically, this lowers the possibility of blending the ore while mining it and then mixing it once more with the ore grade from the stockpile, which could lead to misclassification in the respective stockpile. There are infinite number of solutions to this problem, so in order to reach satisfactory results, a heuristic approach is used for the solution. In order to achieve bigger volumes of higher grade ore, the innermost dig line assumes the lowest possible grade from the category of the inner boundary  $B_{in}$ . For example, if  $q = MG$  (medium grade), then the ore grade for the first ore zone is  $q^{MG_{min}}$ . Generally, this could be written with the equation:  $q^j = q^{c_{min}}$ . This equation ensures that the content from the excavated ore inside the dig lines is not in a lower category than the initial ore content of the ore string.

Where  $q^j$  – ore grade for diluted ore zone  $j$ , % (or g/t);  
 $j$  – consecutive number of the diluted ore zone ( $j \geq 1$ );  
 $q^{c_{min}}$  – ore grade for ore category  $c$ , % (or g/t);  
 $c$  – consecutive number of the ore grade category ( $c=1$  is LG;  $c=2$  is MG;  $c=3$  is HG;  $c=4$  VHG).

The following optimization function must be valid:

$$V_{d.b. ij}^{in} + V_{dil. ij}^{ore} + V_{mis. ij}^{ore} + V_{dil. ij}^{o.b.} \rightarrow \max$$

while

$$\frac{q_i \cdot \gamma_{ore} \cdot (V_{i.o.z. ij} + V_{mis. ij}^{ore} + V_{dil. ij}^{ore})}{\gamma_{ore} \cdot (V_{i.o.z. ij} + V_{dil. ij}^{ore} + V_{mis. ij}^{ore}) + \gamma_{o.b.} \cdot V_{dil. ij}^{o.b.}} = q_{min}^c$$

The solution of the optimization problem is reached at the limit of the set and therefore the location of the dig lines are determined by solving the latter equation.

Let us define the volume of ore zone  $j$  as  $V_{o.z. ij}$ , where

$$V_{o.z. ij} = V_{i.o.z. ij} + V_{mis. ij}^{ore} + V_{dil. ij}^{ore} + V_{dil. ij}^{o.b.}$$

$$q_{min}^{c'} = \frac{q_i \cdot \gamma_{ore} \cdot (V_{i.o.z. ij} + V_{mis. ij}^{ore} + V_{dil. ij}^{ore} - \partial^{ore}_{ij})}{\gamma_{ore} \cdot (V_{i.o.z. ij} + V_{dil. ij}^{ore} + V_{mis. ij}^{ore}) + \gamma_{o.b.} \cdot (V_{dil. ij}^{o.b.} - \partial^{ore}_{ij} - \partial^{o.b.}_{ij})}$$

where  $\partial^{ore}_{ij} + \partial^{o.b.}_{ij} = V_{o.z. ij} - V'_{o.z. ij}$

$\partial^{ore}_{ij}$  - volume of subtracted ore for reaching the integer requirement, m<sup>3</sup>;

$\partial^{o.b.}_{ij}$  - volume of subtracted overburden for reaching the integer requirement, m<sup>3</sup>.

In order to find out the geometric position of the dig lines - either of the approaches could be assumed - 1) representing the blasted volume of ore and waste as an approximation with smaller blocks; 2) geometric interpretation of the post blast ore zones with elementary figures (prisms, pyramids and tetrahedrons). In both cases the zones outside the Inner Ore Zone and inside the Outer Ore Zone are projected as an area in the view plane. When applying the dig lines there is a dependency between this area and the volume whose projection is the same area.

After solving the following equation, the dig lines for block  $z$  are considered to be adjusted.

This calculation is repeated until one of the two cases is reached:

1) Either there is no volume left from the outer dig line boundary and the last ore zone has a higher grade than its respective grade category,

2) or the current diluted ore zone has an ore grade which below the cut-off grade.

If case 1 is reached, then the algorithm stops and new dig lines can no longer be generated and the existing ones no longer have to be adjusted.

If case 2 is reached, then the last amount of volume has to be added the volumes of either of the previous one, two, three or four zones until the sum reaches a grade equal to the value of LG ore content. After the previous volumes and borders are corrected, no new dig lines are generated, as well as the existing ones no longer have to be adjusted.

This process has to be repeated independently for every ore top and bottom string inside the blasted rock pile. Once the algorithm is repeated for every string and optimal dig lines have been generated, the optimal solution for the blasted rock pile

In order to ensure that the number of trucks, required for transporting this volume the following requirement has to be fulfilled:

$$n_{min} \cdot E \cdot K_{s.f.} \leq V_{o.z. ij} \leq n_{max} \cdot E \cdot K_{s.f.} \cdot N_s$$

where  $E$  - capacity of the excavator shovel, m<sup>3</sup>;

$N_s$  - number of trucks, required for transporting the ore volume;

$K_{s.f.}$  - swelling factor (dependent on the rock type);

$n_{min}$  - minimum number of shovels, required for reaching the truck's capacity, m<sup>3</sup>, ( $n_{min} = 4$ );

$n_{max}$  - maximum number of shovels, required for reaching the truck's capacity, m<sup>3</sup>, ( $n_{max} = 6$ ) (Djbov, Koprev, 2017)

In addition, integer programming problem has to be solved in order to achieve an integer value for  $\frac{V_{o.z. ij}}{K_{s.f.}}$ . After the adjusted

ore zone volume solution  $V'_{o.z. ij}$  is determined, the dig lines have to be adjusted by finding out the value for the adjusted ore grade  $q_{min}^{c'}$  from the equation:

has been reached, as the optimization problem is separable. The sequential operations for solving the dig lines problem are shown as a flowchart on Figures 7a and 7b.

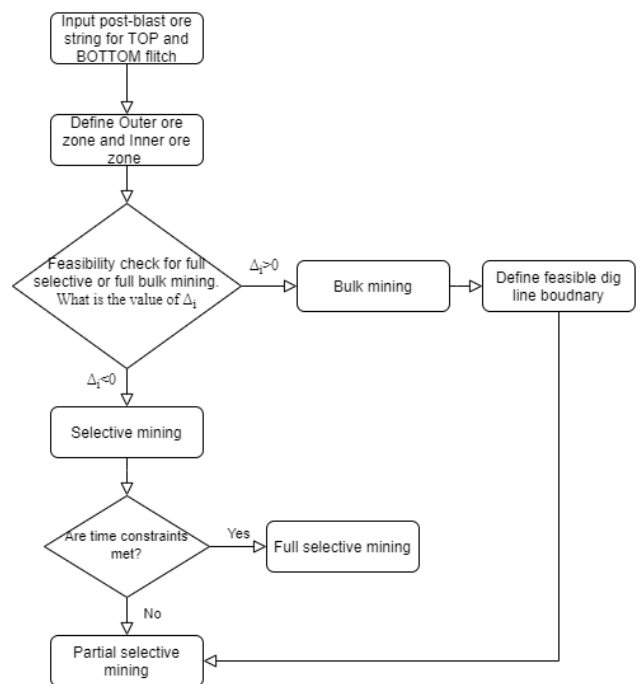


Fig. 7a. Flowchart of feasibility check for dig lines

This approach for solving the problem of differentiating the different dig lines for the different ore dilution/misclassification zone is also known as a "greedy algorithm" as it follows the problem-solving process of making locally optimal choices at each stage. Although this algorithm is not generally preferred, it serves a satisfactory job for the current problem, due to its ability to give the higher grade zones bigger volumes of ore, and the remaining volumes are considered either of low grade ore or below the cut-off. Therefore, the requirement for extracting the

largest possible amount of volumes with higher ore grades is fulfilled.

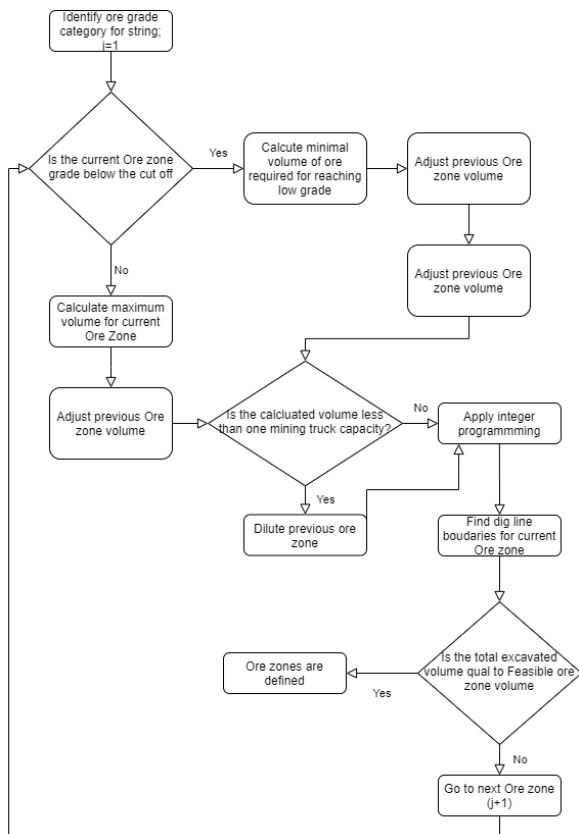


Fig. 7b. Flowchart of principles for defining lines for the partial selective ore mining

## Conclusion

This paper serves as a theoretical examination of the feasible dig lines identification and has to be further examined by taking samples for chemical analysis and grade estimation from the supposed halo-like grade zones. A serious drawback of the proposed way for defining rational dig lines is that they are heavily dependent on the ore strings, defined by the geologists, the ore grade estimation for each string, as well as the string shape, the movement accounted by the BMM results and the digging direction. However, this way of ore excavation is expected to prove itself as more feasible than the currently used dig lines which follow the exact shape of the post-blast ore strings or flags markers distinguishing different ore grade zones.

## References

- Djbov, I., I. Koprev. 2017. Handbook for processes in open-pit mining, Sofia. (in Bulgarian)
- Konstantinov, G. 1997. Quality management for open-pit mining production, Sofia. (in Bulgarian)
- Koprev, I. 2018. Mathematic modelling in open-pit mining, Sofia. (in Bulgarian)
- Yu, Z., X. Shi, J. Zhou, et al. 2019. Feasibility of the indirect determination of blast-induced rock movement based on three new hybrid intelligent models. Engineering with Computers.
- <https://blastmovement.com/the-bmt-solution/case-studies/> (last opened on 29<sup>th</sup> July 2020)
- <https://www.ocblasting.com/orepro3d-software> (last opened on 29<sup>th</sup> July 2020)
- <https://www.seequent.com/to-flitch-or-not-to-flitch-using-post-blast-3d-optimization-to-make-the-decision/> (last opened on 29<sup>th</sup> July 2020).

## BIOTECHNOLOGIES APPLICATION AT ARSENIC-BEARING MATERIALS PROCESSING

V.A. Luganov<sup>1</sup>, T.A. Chepushtanova<sup>1</sup>, G.D. Guseynova<sup>1</sup>, B. Mishra<sup>2</sup>

<sup>1</sup> Satbayev University, Kazakhstan, Almaty, 050013, str. Satpayev 22; T.chepushtanova@satbayev.university, tanya2305@list.ru  
<sup>2</sup> Worcester polytechnic institute. USA, 100 Institute Road, Worcester, MA 01609; bmishra@wpi.edu

**ABSTRACT.** The arsenic problem is a global problem. Results obtained in this research allow us to formulate directions for development of environmentally friendly technologies for processing arsenic-bearing ore and technogenic materials. Behavior of autotrophic thionic bacteria was studied (*Thiobacillus thiooxidans*, *Thiobacillus thiooxidans*, *Thiobacillus ferrooxidans*), as well as arsenite-oxidizing and arsenate-reducing bacteria. Their influence on soil, different calcium arsenate cakes and cinders were studied. Model tests in laboratory conditions for determination of possibilities for development of microbiological processes with formation of versatile arsenic forms at the presence of arsenate cakes, sulfide sublimates and soils at various temperatures were conducted. It was established that the development of arsenate-reducing bacteria is associated with the presence of higher arsenic oxides in sulfide sublimates, which play the role of electron acceptors in inactive chains of bacteria and reduce  $As_2O_5$  until trivalent form. Experiments were carried out with pure cultures of bacteria potentially capable of transforming arsenic in arsenic-containing products. In variants using arsenate-reducing bacteria, arsenic content decreased from 11.6-17.0 mg / l to 3.0-11.6 mg / l, which indicates that calcium arsenate-cake does not affect the viability of arsenate-reducing bacteria, which can precipitate soluble arsenic into insoluble arsenic compounds.

**Keywords:** micro-bioleaching, arsenic cake, cinders, sulfide sublimates, thionic bacteria, solubility

### ПРИМЕНЕНИЕ БИОТЕХНОЛОГИЙ ПРИ ПЕРЕРАБОТКЕ МЫШЬЯКСОДЕРЖАЩИХ МАТЕРИАЛОВ

V.A. Луганов<sup>1</sup>, Т.А. Чепуштанова<sup>1</sup>, Г.Д. Гусейнова<sup>1</sup>, В. Мешра<sup>2</sup>

<sup>1</sup> Satbayev University, Казахстан, Алматы, 050013, Ул. Самнаева 22; T.chepushtanova@satbayev.university, tanya2305@list.ru  
<sup>2</sup> Worcester polytechnic institute. США, 100 Institute Road, Вочестер, МА 01609; bmishra@wpi.edu

**ABSTRACT.** Проблема мышьяка является общемировой проблемой. Полученные результаты позволяют сформировать направления развития экологически безопасных технологий переработки мышьяксодержащих рудных и техногенных материалов. В работе изучалось поведение автотрофных тионовых (*Thiobacillus thiooxidans*, *Thiobacillus thiooxidans*, *Thiobacillus ferrooxidans*), а также мышьякоксиляющих и мышьяквосстанавливающих бактерий. Проведены модельные испытания для определения возможности развития микробиологических процессов с образованием подвижных форм мышьяка в лабораторных условиях в присутствии арсенатных кеков, сульфидных возгонов и почв при различных температурах. Установлено, что развитие арсенатвосстанавливающих бактерий связано с наличием в сульфидных возгонах высших оксидов мышьяка, которые играют роль акцептора электронов в натальной цепи бактерий и восстанавливают  $As_2O_5$  до 3-х валентной формы. Выполнены эксперименты с чистыми культурами бактерий, потенциально способными к трансформации мышьяка в мышьяксодержащих продуктах. В вариантах с использованием арсенатвосстанавливающих бактерий содержание мышьяка снижалось от 11.6-17.0 мг/л до 3.0-11.6 мг/л, что свидетельствует о том, что арсенат-кальциевый кек не влияет на жизнеспособность арсенатвосстанавливающих бактерий, которые способны осаждать растворимый мышьяк в нерастворимые соединения мышьяка. Установлено, что результаты микробиологических исследований должны учитываться при выборе способа и условий захоронения техногенных мышьяковых продуктов.

**Ключевые слова:** микробиологическое выщелачивание, арсенатный кек, огарки, сульфидные возгоны, тионовые бактерии, растворимость

### Introduction

The current practice of arsenic-containing wastes (cakes) recycling in special facilities does not prevent the possibility of soil, air, etc. getting into them, which can cause or inhibit the transformation of some compounds into others.

Long-term storage of arsenate cakes in landfills can lead to their transformation under the influence of external conditions and microorganisms capable of oxidizing and / or reducing arsenic. This will cause a change in the solubility of arsenic compounds and will affect the possibility of arsenic transfer to the environment.

A similar transformation of arsenic can also occur in sulfide sublimates obtained during sulfidizing roasting of arsenic raw materials. For example, arsenic sulfide  $As_2S_3$  (orpiment) is very slightly soluble in water, while  $As_2S_5$  is practically insoluble in water, (Xian-Chun, 2018). At the same time, during long-term storage in air under the influence of moisture and microorganisms, even such poorly soluble arsenic compounds as arsenic sulfides can transform into soluble forms, Nguyen

(2015). The effectiveness of the use of biotechnology is also described in the works about arsenic tolerance and bioleaching from realgar based on response surface methodology, published by Lei Yan (2017) and about column bioleaching of arsenic and heavy metals from gold mine tailings by *Aspergillus fumigates*, published by Bahi Jalili (2012).

The purpose of this work was to conduct model tests to determine the possibility of the development of microbiological processes with the formation of versatile forms of arsenic in laboratory conditions in the presence of arsenate cakes, sulfide sublimates, and soils at different temperatures, as well as to conduct laboratory model experiments with pure cultures of bacteria, potentially capable of transferring hardly soluble arsenic compounds into a versatile form.

The studying of autotrophic thionic bacteria, as well as arsenic-oxidizing and arsenic-reducing bacteria, which changing the valence of arsenic can form arsenic compounds with different solubility are objects of interest.

## Methods and materials

For the studies, we used soil that did not contain arsenic, washed out and not washed from oxides, sublimates of sulfidizing roasting of arsenic concentrate and arsenate-calcium cakes, as well as initial technological cakes. Mineralogical composition of unwashed fumes (%):  $As_2S_3$  - 45,  $As_4S_4$  - 32,  $As_2S_5$  - 10,  $As_2O_3$  - 13, their chemical composition (%): As - 62.4, S - 32.5, O - 5.1. The washed sublimates contained traces of oxides.

The number of microorganisms was determined by plating samples on elective media. The experiment was carried out in duplicate. Experimental vessels were filled with 100 g of soil, 1 g of sublimate or cake, 500 ml of distilled water with pH 7.0-7.2. Half of the test vessels were incubated at room temperature (+ 18-20 °C), and the other half at +4 °C.

The work studied the behavior of autotrophic thionic bacteria (*Thiobacillus thrioparis*, *Thiobacillus thiooxidans*, *Thiobacillus ferrooxidans*), as well as arsenic-oxidizing and arsenic-reducing bacteria.

Thionic bacteria differ in their ability to grow at different pH of the environment. In the presence of sulfur-containing compounds, thionic bacteria gain advantage, for which environmental conditions (pH, temperature, and humidity) will be optimal. A decreasing of pH as a result of the activity of one group of bacteria can suppress the activity of this group of bacteria, and this niche will be occupied by another group for which the formed conditions will be optimal.

The influence of the composition of the medium on the behavior of arsenite-oxidizing and arsenate-reducing bacteria in systems with sublimates was studied using media of various compositions (Table 1).

Table 1. Composition of media in vessels

№	Environment	Additive amount, g/l
1	Soil without additives	-
2	Soil + Calcium Lactate	3.5 g/l
3	Soil + Sodium Acetate	3 g/l
4	Soil + yeast extract	1 g/l
5	Soil + glucose	5 r/n
6	Soil + sulfur	1 g per 100 g soil
7	Soil+ $Ca(OH)_2$	1 g/l

In all experiments, the content:  $(NH_4)_2SO_4$  - 1g/L,  $KH_2PO_4$  - 1g/l. In all solutions, the pH was 7.5. In experiments with the addition of  $Ca(OH)_2$ , the initial pH value was 9-10.

## Results and discussion

### Influence of microorganisms on the arsenic behavior at materials storage in soil

**Arsenate calcium cake.** The experiment was carried out in duplicate for 7 months. In each of the four experimental vessels, 100 g of soil was introduced, then 10 g of arsenate-calcium cake. Each vessel was added to 500 ml of sterile water with a pH of 7.0-7.2. Half of the test vessels were incubated at room temperature (+ 18-20 °C), and the other at +4 °C. The room temperature was recorded and the experimental vessels were mixed daily.

Thionic bacteria were not detected throughout the experiment, while the number of arsenite-oxidizing bacteria increased during the first 4 months, and by the end of the experiment (after 7 months), a decrease in their number was observed (Fig.1). The development of arsenite-oxidizing bacteria confirms the presence of a certain amount of arsenite in the arsenate-calcium cake. In the ionic form, the ongoing reaction is described by the equation:  $As^{3+} - 2e^- = As^{5+}$ .

As can be seen from fig. 1, during the first four months, the amount of arsenic that passed into the solution increased.

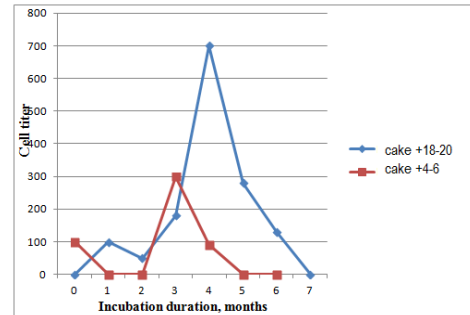


Fig. 1. Content of arsenite-oxidizing bacteria in vessels with arsenate-calcium cake (cells/ml) - at + 18-20 °C, - at + 4-6 °C

The solubility of  $3Ca_3(AsO_4)_2 \cdot 2Ca(OH)_2$  is higher than that of  $3Ca(AsO_2)_2$ , which led to an increase in the content of soluble arsenic in the solution. Determination of the number of arsenate-reducing bacteria is shown in Fig. 2. The arsenic content in the model solution at a temperature of +4 °C slowly increased throughout the experiment.

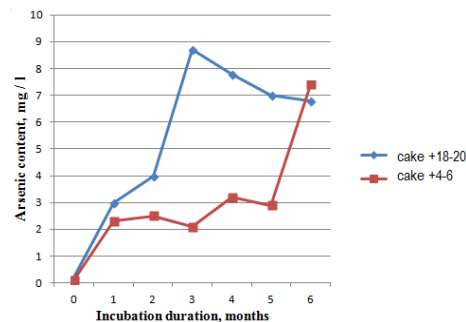


Fig. 2. The content of soluble arsenic in model solutions with arsenate calcium cake (- at + 18-20 °C, - at + 4-6 °C)

Arsenate-reducing bacteria are anaerobic bacteria capable of using arsenate as the final electron acceptor and reducing it to trivalent arsenite. In the presence of sulfate ions in the medium, which can also be reduced by bacteria to sulfide ion, the formation of practically insoluble arsenic sulfide  $As_2S_3$  is possible, Fig.3.

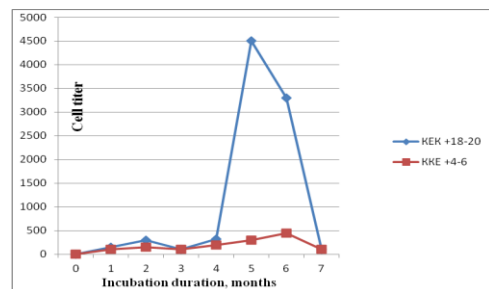


Fig. 3. The content of arsenate-reducing bacteria in the vessels with arsenate calcium cake (- at + 18-20 °C, - at + 4-6 °C)

The reaction can proceed in accordance with the equations:

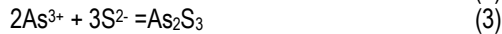


Table 2. pH of media and the content of microorganisms in samples after a month of incubation

Arsenite oxidizing bacteria		Arsenate-reducing bacteria	
pH	cells / ml	pH	cells / ml
Soil without additives (Sample 1)			
7.45/6.95*	50/9.0*	6.95/6.95*	0/0*
Soil + calcium lactate (Sample 2)			
7.42/7.48*	140/25.5*	7.08/7.0*	1.1/0*
Soil + sodium acetate (Sample 3)			
7.53/7.65*	140/0*	7.2/6.9*	0/0*
Soil + yeast extract (Sample 4)			
7.57/7.56*	0.5/0*	7.24/7.0*	0/0*
Soil + glucose (Sample 5)			
7.53/7.46*	5.0/1.2*	7.7/6.8*	0/0*
Soil + sulfur (Sample 6)			
7.5/7.66*	0/0*	7.2/7.0*	0/0*
Soil + Ca (OH) 2 (Sample 7)			
7.0/6.25*	0.4/2*	7.2/7.15*	0/0*

\* Numerator - at room temperature. Denominator - at 4 °C.

Thus, in the presence of arsenate-calcium cake, arsenite-oxidizing bacteria first begin to develop, which oxidize trivalent arsenic to a soluble pentavalent form, and then anaerobic arsenate-reducing bacteria develop, which reduce arsenate and convert it into insoluble arsenic sulfide. Due to this, the observed decrease in the arsenic content in the test vessels occurs by the end of the experiment at a temperature of + 18-20 °C. At the same time, during the incubation of the vessels at + 4 °C, the amount of arsenate-reducing bacteria is very low. Therefore, the formation of arsenic sulfide does not occur, and by the end of the experiment the content of soluble arsenic increases to 6.3 mg/l.

The results obtained allow us to say that in experiments simulating the storage of arsenate-calcium cake in soil under high humidity conditions, autotrophic thionic bacteria are unable to affect the mobility of arsenic. At the same time, the active growth of arsenite-oxidizing bacteria and the subsequent development of arsenate-reducing bacteria indicate that these bacteria affect the mobility of arsenic. The subsequent development of arsenate-reducing bacteria is associated with the presence of arsenates in the cakes, which play the role of an electron acceptor in the respiratory chain of bacteria and reduce arsenate to the trivalent form with the formation of arsenic sulfides. A decrease in the concentration of soluble arsenic by the end of the experiment suggests that the formation of a sparingly soluble arsenic compound is possible under the influence of arsenate-reducing bacteria.

### Sulfide sublimates

The results of studies of the behavior of bacteria in the presence of washed sulphide sublimates showed that thionic bacteria were not detected during the experiment, i.e. sulfide forms of arsenic are inert with respect to the studied microorganisms. Next, we checked the survival of arsenite-oxidizing and arsenate-reducing bacteria under conditions of prolonged contact with washed sulfide arsenic sublimates in various environments (Table 2). As follows from the results obtained, arsenate-reducing bacteria are not detected in samples as early as 1 month after the start of the experiment, i.e. they do not participate in the processes.

In the second series of experiments, the behavior of arsenite fumes in the presence of arsenite-oxidizing bacteria was studied. As a result of the experiments performed, it was found that various additives in the form of calcium lactate, sodium acetate, yeast extract, glucose do not have a noticeable effect on the transition of arsenic into solution.

The transition to the solution of arsenic is mainly associated with the oxides contained in the sulfide fume. Oxidation from As<sup>3+</sup> oxides to As<sup>5+</sup> promotes the transfer of arsenic into solution. As is known, As<sub>2</sub>O<sub>5</sub> has a higher solubility than As<sub>2</sub>O<sub>3</sub> - the solubility of As<sub>2</sub>O<sub>3</sub> at 25 °C in 100 g of water is 2.1 g and As<sub>2</sub>O<sub>5</sub> is 65.8 g.

The transition of arsenic into solution is more noticeably influenced by the presence of elemental sulfur. The results of studies on the behavior of arsenite-oxidizing and arsenate-reducing bacteria under conditions of long-term contact (within 7 months) with washed and unwashed sulfide arsenous sublimates in the presence of soils are presented in Fig.4-6.

As can be seen, at 20 °C the number of arsenite-oxidizing bacteria remained almost unchanged during the first three months (Fig 4).

After four months, the number of arsenite-oxidizing bacteria reached a maximum and gradually decreased to zero by the end of the experiment.

The development of arsenite-oxidizing bacteria is apparently associated with their participation in the oxidation of arsenic oxide (As<sub>2</sub>O<sub>3</sub>) in accordance with the equation  $\text{As}_3 + -2\text{e} = \text{As}_5^+$ . This is also indicated by a sharp increase in the content of arsenic in the solution in the first three months of the experiment (Fig 5).

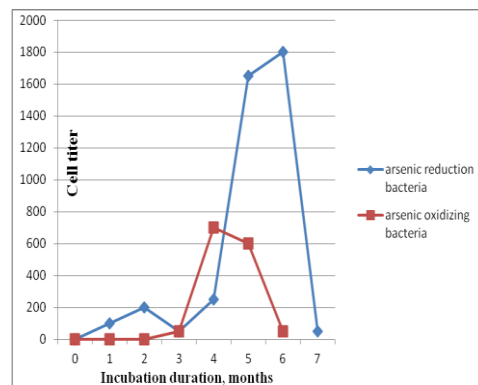


Fig. 4. Change in the number of bacteria depending on the duration

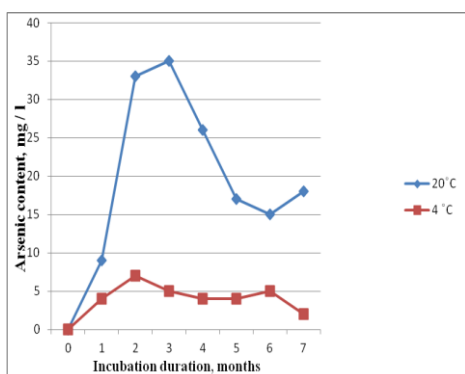


Fig. 5. Change in the content of arsenic in the solution depending on the duration (sample of unwashed fumes)

At room temperature, arsenate-reducing bacteria develop intensively starting from the fourth month (Fig. 4) and reach their maximum numbers by the sixth month of the experiment. By the end of the experiment, the number of arsenate-reducing bacteria gradually decreased.

In model vessels with the introduction of sulfide fumes, the content of arsenic passing into the solution increased during the first three months: starting from the fourth month, a tendency to decrease in its amount was observed (Fig.5).

Thus, in the presence of unwashed sulfide sublimate, arsenite-oxidizing bacteria first begin to develop, which oxidize trivalent arsenic oxide to a soluble 5-valent form, and then anaerobic arsenate-reducing bacteria develop, which restore pentavalent arsenic compounds and convert it into sparingly soluble arsenic forms 3-valent. Due to this, the observed decrease in the arsenic content in the test vessels by the end of the experiment occurs. The decrease in the concentration of bacteria by the end of the seventh month is due to the fact that the nutrient medium introduced into the samples at the beginning of the process was exhausted. No additional soil was introduced into the system.

In order to exclude the effect of arsenic oxide forms, a study was carried out of the possibility of the development of microbiological processes under similar conditions in the presence of sulfide fumes washed from arsenic oxides. The change in the content of arsenic in solutions depending on the duration (Fig.6) indicates that in the absence of oxide forms of arsenic, the solubility of fumes decreases sharply and the content of arsenic does not exceed 0.15 mg/l. And this amount of arsenic went into solution due to the dissolution of arsenic oxides present in the sublimates). The development of microbiological processes is not observed, i.e. the sulfide forms of arsenic are inert with respect to the microorganisms under study.

The results obtained allow us to say that in experiments simulating the storage of sulfide fumes in soil at high humidity, autotrophic thionic bacteria are unable to affect the mobility of arsenic. At the same time, the active growth of arsenite-oxidizing bacteria and the subsequent development of arsenate-reducing bacteria indicate that these bacteria affect the mobility of arsenic.

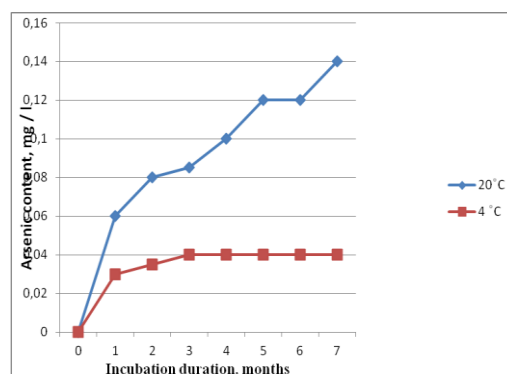


Fig. 6. Change in the content of arsenic in the solution depending on the duration (sample of the washed sublimate)

The fact that arsenite-oxidizing bacteria develop first indicates the possibility of the 3-valent oxide forms of arsenic present in arsenic products to be oxidized by bacteria to the highest forms. It can be assumed that the partial dissolution of sulphide sublimate is associated with the properties of the soil used, because humic and fulvic acids present in the soil can affect the solubility of metal ions. This is also confirmed by the fact that the maximum increase in the arsenic content in the solution is noted after two months of experiments, when the active growth of arsenite-oxidizing bacteria has not yet begun. The subsequent development of arsenate-reducing bacteria is associated with the presence of higher arsenic oxides in sulfide sublimates, which play the role of an electron acceptor in the underwear chain of bacteria and reduce  $As_2O_5$  to the 3-valent form. The results show that the studied microorganisms under the studied conditions practically do not affect the sulfide forms of arsenic, participating in the transformation of only oxide compounds contained in sulfide sublimates.

To obtain stable sulfide fumes, it is advisable to carry out additional sulfidization before disposal.

### The effect of pure cultures of bacteria on the transformation of arsenic in arsenic-containing products

#### Arsenate calcium cake

This study included experiments with arsenate-calcium cake and fume after sulfidizing roasting of the concentrate to determine the possibility of the effect of pure cultures of bacteria on the solubility of arsenic from these products. For this purpose, the vessels containing the media optimal for the development of the corresponding group of bacteria were inoculated with pure cultures of bacteria. Every 1.5 months, an analysis was carried out for the content of thionic bacteria, arsenate-reducing and arsenite-oxidizing bacteria in these vessels, changes in pH and the content of total arsenic in the solution. The studies were carried out with non-sterile arsenic-containing products. 1 g of arsenate-calcium cake or sublimate after sulfidizing roasting of the concentrate was added to the vessels with the appropriate medium. 400 ml of the appropriate medium and pure cultures of bacteria were added to each vessel. The experiment was carried out in 2 replicates.

Analysis of the results obtained indicates that bacteria *T.thiooxidans* were not detected after 1.5 months and until the end of the experiment. The abundance of *T.ferrooxidans* decreases to 10 cells / ml after 4.5 months, and by the sixth month they are also not detected. *T.thioparus* bacteria with an initial content of 109 cells / ml were not detected after 1.5 months and until the end of the experiment. The content of  $As_3$  + oxidizing bacteria gradually decreases, but even after six months it is 103-4 cells / ml. The number of  $As_5$  + reducing bacteria at their initial content of 106 cells / ml decreases and by the end of the experiment is 102-3 cells / ml.

After 1.5 months of the experiment, practically in all variants, including the control variants without the introduction of bacteria, an increase in the pH of the medium is observed, which, apparently, is associated with the transition of hydroxyl groups present in the arsenate-calcium cake into the solution. Therefore, every 1.5 months after sampling, the pH of the media in all variants was brought to the level corresponding to each medium.

The data on the content of soluble arsenic showed that in the variant with *T.thiooxidans*, an increase in its amount from 20 mg/L at the beginning of the experiment to 150 mg/L after 4.5 months and a slight decrease by the sixth month is observed.

The arsenic content in the variant using *T.ferrooxidans* is approximately the same both in the control and in the experiment. The increase in the arsenic content during the experiment is apparently associated with the low pH of the medium (2-2.5), in which the culture was grown, which contributed to the dissolution of a part of the arsenate-calcium cake.

In experiments with  $As_3^+$  oxidizing bacteria, the concentration of arsenic in the solution slightly increases during the experiment, and this is noted both in the variants without bacteria, and with bacteria.

When *T.thioparus* is grown, the content of soluble arsenic increases from 0.2 mg / l at the beginning of the experiment to 10-90 mg/l after 6 months. A similar trend was observed in the variants without bacteria, although in this case the arsenic content was lower. When growing  $As_5$  + reducing bacteria, a decrease in the content of soluble arsenic was noted throughout the experiment in the variant with bacteria and an increase in its content in the control.

Thus, the results showed that the thionic bacteria *Thiobacillus thiooxidans*, *Thiobacillus thioparus*, and *Thiobacillus ferrooxidans*, despite the creation of optimal conditions for their growth, are unable to grow in the presence of calcium arsenate cake. Therefore, these bacteria cannot influence the mobility of arsenic in arsenate calcium cake. At the same time, the growth of arsenite-oxidizing and arsenate-reducing bacteria under such conditions indicates that they can influence the transformation of arsenic in arsenate-calcium cake.

With the aim of a more detailed study of the effect of arsenite-oxidizing and arsenate-reducing bacteria on the mobility of arsenic in arsenate-calcium cake, additional studies were performed with these microorganisms.

The objective of this stage of research was to study the effect of arsenite-oxidizing and arsenate-reducing bacteria on the mobility of arsenic in arsenate-calcium cake under optimal conditions for the growth of the studied bacteria.

The results of the work showed that after three months of the experiment, the number of arsenite-oxidizing bacteria decreased slightly from 108-9 cells / ml in the initial sample to 106-7 cells / ml. The number of arsenate-reducing bacteria did not change and amounted to 103-4 cells / ml.

The content of arsenic in vessels with arsenite-oxidizing bacteria increased from 6.4-7.4 in variants with bacteria to 20-26.6 mg / L, while in the control variants this value increased from 8.0-9.4 to 38-44.4 mg / L after three months.

In variants with the use of arsenate-reducing bacteria, the arsenic content decreased from 11.6-17.0 mg / L to 3.0-11.6 mg / L after three months of the experiment, which indicates that arsenate-calcium cake does not affect the viability of arsenate-reducing bacteria, which are able to precipitate soluble arsenic into insoluble arsenic compounds.

The results of the X-ray phase analysis - Table 4.

The analysis of the obtained results showed that arsenite-oxidizing bacteria practically do not change the cake composition in comparison with the original untreated cake.

In all variants, both in the control without bacteria and in the variants with bacteria, the disappearance of arsenic acid  $H_3AsO_4 \cdot 3H_2O$  is noted, which, apparently, is associated with its dissolution.

It was found that when arsenic acid goes into solution, then pentavalent arsenic is reduced by bacteria with the subsequent formation of arsenic-calcium complexes. In variants with the use of arsenic-reducing bacteria, all sodium sulfur-containing salts ( $Na_2S_5O_{16}$ ,  $Na_2SO_4$ ) and  $\beta-NaCaAsO_4$  disappear, although they are present in the original untreated cake and in controls without bacteria. It is known that arsenate-reducing bacteria are able to use sulfur from these compounds in the process of metabolism with its subsequent reduction.

Thus, arsenate-reducing bacteria influence the composition of the arsenate-calcium cake. They are able to reduce all water-soluble arsenic salts contained in the cake, with the formation of insoluble arsenic complexes with calcium, and can reduce sulfates and polysulfates, using them as the final electron acceptor.

#### Sulfide sublimates

Studies have shown that throughout the experiment, the number of the studied groups of bacteria changed in different ways. Thus, bacteria with *T.thiooxidans* were not detected after 1.5 months of the experiment.

Analysis of the data on changes in pH showed that during incubation of vessels with *T.thiooxidans*, no change in the pH of the medium was observed in comparison with the control variants without bacteria, which also confirms the absence of viable cells in the medium. There were also no visual differences between the experimental and control variants. It should be noted that after 1.5 months the content of soluble arsenic increased in the variant with the *T.thiooxidans* culture to 400-600 mg/L in the test vessels and 800 mg/L in the control vessels without bacteria, and then gradually decreased.

In experiments with *T.thioparus*, the arsenic content increased from 9-20 mg/L at the beginning of the experiment to 1000 mg/L after 1.5 months in the variant with bacteria and 1200 mg/L in the control. Perhaps this is due to the solubility of sublimate polysulfides under slightly alkaline conditions.

The number of *T.ferrooxidans* bacteria began to decrease from 103 cells/ml in the initial sample to 0-102 cells/ml by the

third month of the experiment, and after 4.5 months of the experiment, bacteria were not detected.

Table 4 - Results of X-ray phase analysis of microbiological samples of arsenate-calcium cake \*

Culture under study	Nutritional supplement	Compound	Approximate content, %
Arsenite oxidizing bacteria	Glucose	$\text{Ca}_5(\text{AsO}_4)_3\text{OH} \cdot \text{H}_2\text{O}$	30
		$\text{Ca}_5(\text{AsO}_4)_3\text{OH}$	10
		$\text{CaSO}_4$	20
Control without bacteria	Glucose	$\text{Ca}_5(\text{AsO}_4)_3\text{OH} \cdot \text{H}_2\text{O}$	30
		$\text{Ca}_5(\text{AsO}_4)_3\text{OH}$	30
		$\text{CaSO}_4$	10
Arsenate-reducing bacteria	Calcium lactate	$\text{Ca}_5(\text{AsO}_4)_3\text{OH} \cdot \text{H}_2\text{O}$	25
		$\text{Ca}_5(\text{AsO}_4)_3\text{OH}$	25
		$\text{CaSO}_4$	10
Control without bacteria	Calcium lactate	$\text{Ca}_5(\text{AsO}_4)_3\text{OH} \cdot \text{H}_2\text{O}$	30
		$\text{Ca}_5(\text{AsO}_4)_3\text{OH}$	20
		$\text{CaSO}_4$	10

\* Calcium arsenate cake (original, untreated) contains, %:  $\text{Ca}_5(\text{AsO}_4)_3\text{OH} \cdot \text{H}_2\text{O}$  – 10;  $\text{Ca}_5(\text{AsO}_4)_3\text{OH}$  – 10;  $\text{CaSO}_4$  – 5;  $\text{CaCO}_3$  – 40;  $\text{Ca}(\text{OH})_2$  – 20;  $\beta\text{-Na-CaAsO}_4$  – 5;  $\text{H}_3\text{AsO}_4 \cdot 3\text{H}_2\text{O}$  – 5;  $\text{Na}_2\text{S}_5\text{O}_{16}$  – 5.

It should be noted that in the variants with the culture of *T.ferrooxidans*, after 4.5 months, upon visual examination, the sublimate, which was a light suspension on the surface of the medium, dissolved, and only precipitates of iron hydroxides formed in the oxidation of iron by the culture of *T.ferrooxidans* were visible in the vessels. In the control variants without bacteria, the sublimation practically did not change and was on the surface of the medium. Apparently, *T.ferrooxidans*, under favorable conditions, is able to use sulfur from the sublimate polysulfides, thereby dissolving the sublimate. This is confirmed by the results of chemical analysis, according to which, after 1.5 months of the experiment, the arsenic content in the variant with *T.ferrooxidans* bacteria was 600-800 mg/l, while in the control variants this figure was 200 mg/l.

Arsenite-oxidizing bacteria grew well in the presence of sublimate and their number increased from 103-4 cells/ml in the initial sample to 107-8 cells/ml throughout the experiment. The content of soluble arsenic in the experimental variant after 1.5 months was 200 mg/l, while in the control it was 900-1000 mg/l. It is difficult to explain why the experimental variant after 1.5 months found 5 times less arsenic than the control one. As a result, it was established that arsenite-oxidizing bacteria practically do not affect the solubility of fumes.

Of greatest interest are the results obtained in experiments with arsenate-reducing bacteria. The content of arsenate-reducing bacteria was approximately at the same level throughout the experiment and amounted to 103-6 cells / ml. If the content of soluble arsenic forms at the beginning of the experiment in the variant with bacteria was 40-50 mg/l, and

after 1.5 months it increased to 200 mg/l, then in the control variant this value increased from 10 to 300 mg/l. Three months later, in the variant with bacteria, the content of soluble arsenic decreased to 20 mg/l, while in the control variant this value increased to 400-500 mg/l. The formation of a finely dispersed yellow-orange sediment, presumably arsenic sulfide, was visually observed, which settled to the bottom and walls of the experimental vessels. In the experimental vessels, an increase in the pH of the medium was noted, which also indicated a good development of bacteria and their reduction of arsenate to arsenite.

## Conclusion

The study of the influence of microorganisms on the transformation and solubility of arsenic in arsenate-calcium cake and sublimate of sulphiding roasting shows that thionic bacteria have no significant effect on the stability of these products during long-term storage. Arsenite-oxidizing and arsenate-reducing bacteria affect the stability of arsenic compounds in the studied materials: in sulfide sublimate, oxygen-containing arsenic compounds undergo the main transformation, in arsenate cakes, successive oxidation processes occur - reduction of the corresponding arsenite-arsenate forms of arsenic. To regulate the activity of these bacteria in order to reduce the solubility of arsenic, certain nutrient additives are required in the soil. The stabilization of sulfide fumes is also facilitated by a decrease in the content of arsenic oxide forms in their composition, which are most susceptible to microbiological dissolution.

The results of microbiological studies can be useful in choosing the method and conditions for the disposal of technogenic arsenic products.

## References

- Xian-Chun Zeng, Ye Yang, Wanxia Shi, Zhaofeng Peng, Xiaoming Chen, Xianbin Zhu, Yanxin Wang, 2018, Microbially Mediated Methylation of Arsenic in the Arsenic-Rich Soils and Sediments of Jiangnan Plain. *Front. Microbiol.*
- Nguyen, Van Lee, Jong-Un, 2015, A comparison of microbial leaching and chemical leaching of arsenic and heavy metals from mine tailings. *Biotechnology & Bioprocess Engineering.*, Vol. 20 Issue 1, 91-99.
- Lei Yan, Huixin Hu, Shuang Zhang, 2017, Arsenic tolerance and bioleaching from realgar based on response surface methodology by *Acidithiobacillus ferrooxidans* isolated from Wudalianchi volcanic lake, northeast China. *Electronic Journal of Biotechnology*. Volume 25, 50-57.
- Bahi Jalili Seh-Bardan, Radziah Othman, Samsuri Ab Wahid, 2012, Column Bioleaching of Arsenic and Heavy Metals from Gold Mine Tailings by *Aspergillus fumigatus*. *CLEAN. Soil. Air. Water*. Volume 40, Issue 6, 565-666.

## GEOTECHNICAL ASSESSMENT OF THE BENCHES IN THE ELATZITE OPEN PIT MINE AFTER BLASTING

**Stefan Nachev, Georgi Georgiev, Ivan Vasilev, Marieta Takeva**

Mining Complex, "Ellatzite-Med" AD, 2180 Etropole; s.p.nachev@ellatzite-med.com; g.georgiev@ellatzite-med.com; i.vasilev@ellatzite-med.com; m.takeva@ellatzite-med.com

**ABSTRACT.** The geotechnical assessment of the mine slopes is part of the monitoring of controlled blasting performed at the „Elatzite“ Open-pit Mine in the design of the final geometry of the mine board. The structural integrity and geometry of the benches formed by the blasting as well as their long-term stability are analysed. An essential part of this assessment are the specific recommendations for blasting designs that take into account the influence of geological and technological factors on the design of the benches for each area of the mine pit. The publication deals with 12 types of deviations from the design geometry of the slopes and three types of violations of their structural integrity.

**Keywords:** geotechnical assessment, open pit mine

### ГЕОТЕХНИЧЕСКА ОЦЕНКА НА ОТКОСИТЕ НА РУДНИЧНИТЕ СЪПАЛА В РУДНИК „ЕЛАЦИТЕ“ СЛЕД ПРОВЕЖДАНЕ НА ВЗРИВНИ ДЕЙНОСТИ

**Стефан Начев, Георги Георгиев, Иван Василев, Мариета Такева**

Рудодобивен комплекс, „Елаците-Мед“ АД, 2180 Етрополе

**РЕЗЮМЕ.** Геотехническата оценка на рудничните откоси е част от мониторинга на контролираните взривните дейности, извършвани в рудник „Елаците“, при оформянето на крайната геометрия на рудничния борд. При извършването ѝ се анализира структурната цялост и геометрията на рудничните стъпала, получени в следствие на взривните дейности, както и дългосрочната им устойчивост. Съществена част от тази оценка е изготвянето на специфични препоръки към проектите за взривни работи, отчитащи влиянието на геоложките и технологичните фактори, върху дизайна на рудничните стъпала за всяка една зона от рудничния котлован. В публикацията са разгледани 12 типа отклонения от проектната геометрия на откосите и три типа нарушения на структурната им цялост.

**Ключови думи:** геотехническа оценка, открит рудник

### Introduction

Ellatzite Open-pit Mine belongs to the company Ellatzite-MED AD (part of the GEOTECHMIN Group), that specializes in producing copper-gold and molybdenum concentrates. It is situated in the ridge parts of the Northern flank of stara Planina near the town of Etropole. It is situated about 60 kilometers east from Sofia, in the northern foot of Etropolska Baba Peak (1 787 m). The topography of the region of the deposit is typically mountain like, from elevation 840 m to elevation 1510 m. It is connected to the town of Etropole via 14-kilometer long asphalt road, providing access all year long, as well as to the towns of Zlatitza and Pirdop via Zlatitza Passage (fig. 1).

The region of the pit consists of three main rock types:

- Paleozoic metamorphic complex (phyllite, sphilitriped and spotted schists, hornfels);
- Paleozoic granodiorites and concomitant strings of dike rocks;
- Upper cretaceous granodiorite, diorite and quartz monodiorite porphyllite rocks, intervening the two upper complexes.



**Fig. 1. Location of Ellatzite Open-pit Mine**

The geometry and stability of the pit walls depends on the geological factors, the factors connected with the design of pit benches and the blasting activities in the present publication we will mainly consider the geotechnical estimation of the controlled blast works and their impact on the geometry and stability of the pit benches.

The influence of the different factors is specific for each area of the pit and this is why it is necessary to be taken into account when preparing blast designs. One of the possible approaches to reduce this influence is the use of specific techniques of controlled blasting, such as: different timing, different hole diameters and spacing, variety in the quantity of explosives, stemming length etc. With the help of the controlled blasting one can achieve the steepest possible angles of the single or double benches and safe digging and clearing of the mine mass is guaranteed. It allows to keep the strength and structural integrity of the pit walls, minimizes the technogenic cracks in the rock body, situated right next to the blasted mine mass and achieves the project geometry of the pit bench.

Too much damage on the wall can be described as the impact of blast activities gone beyond the planned blast area or crack distribution in the rock body outside the deflecting line. In the scope of the blast field there is an expectancy of about 80% reduction of the rock strength (Peterson, 2001). This strength reduction can be distributed outside the area of the blastfield over some weak structures (contacts, faults and cracks) (Krolikowski, 2015). In addition to the vibrations, the movement caused by gas swelling of the rock body and pressure changes have equal probability to affect the shearing strength along the cracks. Reducing the shearing strength benefits the movement along them which leads to possibilities of creating slide surfaces and wedge rockslides. The reduction of the rock strength is caused by the blast mechanics thorough the outcoming vibrations and by the gas expansion. Overdamaging the rock integrity can often lead to violation of the wall stability of pit benches and mine mass downfall (Hoek, 2007).

**Methods**

When making geotechnical assessment of the pit bench walls after controlled blasting activities in Ellatzite Pit, the geotechnical experts document and analyze the state of integrity of the walls, situated in right next to the blasted mine mass, and the achievement of the project geometry of the pit bench. The characteristics of the deformations after blasting is based on the information achieved by the special mapping and analysis according to the methods of Cebrian (2017), Marshall-Mohr (2005), Rock-mass ratings system (RMR –

2. Level – Moderate deformations	The weak stowing material of the cracks has been broken. Very rare occasions of block movement and the cracks are slightly open	Slope angle from 65° to 75°. The slope is smooth, some of the pre-split holes can be seen. There is slight break and a little technogenic cracking of the wall by blasting	Excavation and loading material slightly behind the project gowl line going through the center of the pre-split holes. Bucket teeth of the excavator grind noisily over the rock
3. Level – High deformations	Some of the blocks are moved and the cracks are wide/open	Slope angle from 60° to 65°. The slope is relatively smooth. Minimal break, moderate technogenic and visible radial cracking by the blasts	Excavation and loading material up to 1.5 m behind the project gowl line going through the center of the pre-split holes.
4. Level – Very high deformations	Thick net of open cracks and some blocks are lose and moved	Slope angle from 55° to 60°. Uneven slope with smal breaking and highly cracked wall in depth	Excavation and loading material до 3 m behind the project gowl line going through the center of the pre-split holes.
5. Level – Extreme deformations	The blocks are moved and highly lose and reoriented. Large open cracks with visible damage from blasting	Slope angle < 55°. Very uneven slope highly broken and open technogenic cracks in the wall	Excavation and loading material more than 3 m behind the project gowl line going through the center of the pre-split holes.

Bieniawski (1989) and ISRM (1981), modified 6/98), Mining Rock-mass ratings system (MRMR – Laubscher (1990)) и Q-slope (Bar & Barton, 2018). It is also a very important part of the process of creating a stable and economically efficient profile of the mine.

The scope of geotechnical assessment includes the following tasks:

- check up right after blasting, as well as mapping, photographing and describing the deformations (parallel cracks) behind the deflecting line;
- five-stage quality assessment of the deformations along the slope of the benches (Cebrian, 2017, changed) as a result of blasting according to three criteria for excavating the blasted ore (table 1);
- mapping, photographing and description of the deformations along the benches after excavation of the ore mass;
- geodesic survey of the achieved upper and toe crests of the benches after digging the blasted ore and comparison with their designed locations in search of inaccuracies;
- update of the bench plans for the strength and structure of the rock body in the areas where the next blasting activities are about to take place;

Table 1.

Level of deformations	Cracks and blocks	Slope angle and rock body status	Excavation and loading and wall geometry
1. Level – Slight deformations	The cracks are closed and the stowage is still intact	Slope angle >75°. The pre-split holes are clearly seen on the wall. There is no damage and there is minimal technogenic cracking by the blasts.	Traces of bucket teeth of the excavator in softer rocks. Excavation and loading material to the prject gowl line going through the center of the pre-split holes

- preparation of recommendations for better efficiency of the blasting activities in problematic zones and areas.

In the high hypsometrical levels of Ellatzite mining is done by working of a single bench with 15 m height. In depth (going into harder rocks) those benches become double. Due to the big variety of rock types with wide diversity of physio-mechanical properties, there are specific designs for every different area or elevation. They are structured in different sections, each with a title of their own if possible. Each statement should contain: thesis and hypothesis of the research, applied methods, main results achieved and discussion. The conclusion should not match completely the resume.

In Figure 2 there is an exemplary situation of blasthole pattern. You can see a combination of pre-split row, stab row, or as often called - short buffer row, buffer row as well as three production rows.

The production rows, depending on the physio-mechanical properties of the rocks, can be vertical, with diameters 142, 165 or 250 mm and 16 m length, and the rest of the holes are with diameter 142 or 165 mm, with variable length and inclination. Depending on the length of the resistance line in the bottom of the wall, however, the production holes can be drilled with inclination. Stab holes are 9 m long and the buffer ones – 19 m. They are left without stemming (air deck), with the upper few meters remaining empty. The combination of different types of pre-split, stab and buffer holes is a main element for controlling the blastwork and is essential for maintaining the structural integrity of the ore bench and reducing the deformations and damages of its final board.

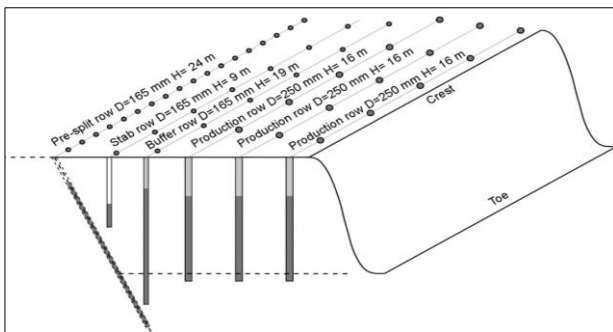


Fig. 2. Example of a blast pattern in Ellatzite Mine

## Results

The summarized results from the geotechnical assessment of the bench walls after performing controlled blasting activities are illustrated with 12 examples for different wall geometries. The difference of the geometry before designed and real bench wall after excavating the blasted material is due to the combination between the strength characteristics and the structures (faults, cracks) of the rock body. The angle between these structures and the wall, as well as the design blasting parameters, are shown in Figure 3 and in Table 2.

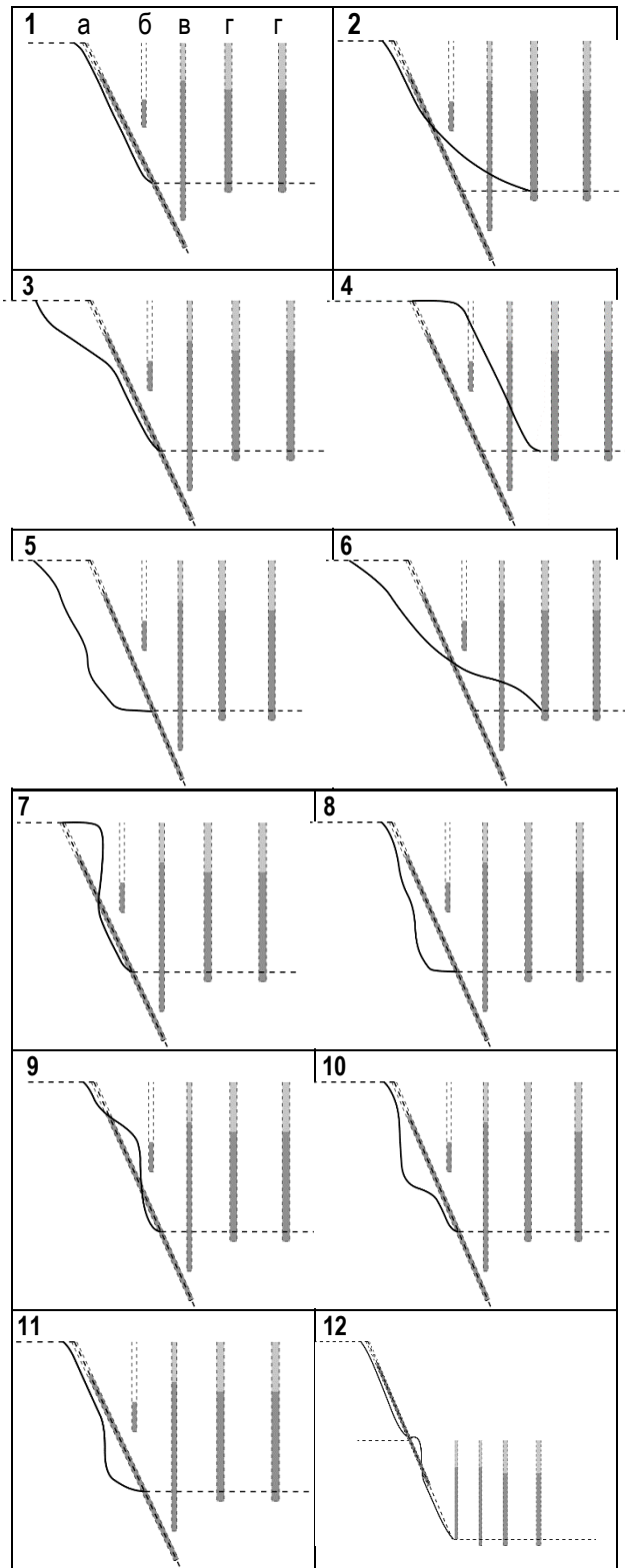


Fig. 3. Grafical representation of the 12 examples for the achieved pit wall compared to designed (Cebrian, 2017 c with changes) Legend: designed wall geometry of the bench; — achieved wall geometry after excavation; a – pre-split hole; б – stab hole; в – buffer hole; г – production holes. Dark grey color shows the explosive material, light grey – stemming.

Description of the twelve examples for achieved geometry of the pit wall profile compared to the design, after finishing with excavation and loading:

- Example 1. The board matches the design – this can happen when there is some damage from blasting level 1 or 2, which means slight to moderate. There is no need for minimal modification of the next project for controlled blasting in the examined area. This is the prevailing type of geometry of the actually achieved walls and it is observed with all rock types;
- Example 2. The toe of the real slope is in front of the project one – this happens in very rare occasions and mainly with vertical change of the lithology in the bench or when there are horizontal or slightly inclined tectonic breaks that screen the blasting energy. The harder rock at the toe of the slope has remained unbroken. There is a need to increase the blasting energy. In this example, the space between the buffer row and the production holes is correct. The necessary changes for the next projects might be some of the following:
  - o increase of the charge in the buffer road;
  - o decrease of spacing between buffer row holes;
  - o moving the buffer row closer to the pre-split holes.

Table 2.

Rock types/Example	1	2	3	4	5	6	7	8	9	10	11	12
Phyllite	X		X		X							
Shists	X		X		X		X		X	X		
Homfels	X	X	X		X	X						X
Quarz monodiorit porphyrites	X	X	X		X	X			X	X		
Granodiorites	X			X		X	X	X			X	X

- Example 3. The crest of the actual slope is behind the project one – this happens when there is some damage from blasting level 3 to 5, which means high to extreme. This is observed at slopes with cracks with slight inclination going inside the wall, as well as in layered types of rock (phyllite and shists). It is necessary to decrease the energy in the upper part of the area of project slope. Usually this geometry happens because of some unfavorable geological structures and/or excessive energy in the stabilizing buffer row, as well as too much subdrilling from the upper bench. The slope toe is in the right position that is why the location of the buffer row should not change. In this case the downfall could be avoided through:

- o increasing the stemming interval (decreasing the length and quantity of explosive respectively) of the stab and buffer rows;
- o decreasing the load of explosives only in the stab row;
- o increasing the distance between the stab row and the pre-split holes;

- o increasing the spacing in the stab and buffer rows, as well as increasing the burden between those two rows;
- o double decked charge (divided) in the stab and buffer rows with two independent levels and blasting of the upper charge 80 - 100 ms before the lower one, i.e. formation of two separate, independent blasts in the upper and lower level.

- Example 4. The actual slope is in front of the design one – this happens when the rock body strength is not reduced enough due to the high rock strength or the insufficient blast energy. It is necessary that the energy from the blast in the design slope area is increased. The design might be corrected through narrowing the distance between stab and buffer row and the pre-split holes equal to the difference between the project and the actual wall crest, and reducing the time delays between the rows.

- Example 5. The real slope is far behind the designed one – this happens when there is some damage from blasting level 3 to 5, which means high to extreme. This can be observed in benches with highly damaged tectonic areas, mainly in phyllite and shists. It is necessary to reduce the energy from the blasting to be reduced. This can be achieved (contrary to the example above) through increasing the distance between the stab and buffer rows and the pre-split equal to the difference between the actual and designed wall crest, as well as through increasing the time delays between the rows.

- Example 6. The real slope in its upper part is behind the designed one, and in its lower part is in front – this happens when there is some damage from blasting level 3 to 5, which means strong to extreme. These are pretty rare in our mine. Almost every time they are due to gravitation processes of the type slide along slope cracks and faults. It is necessary for the accumulated energy to be reduced in the upper part and increased in the lower part. The design of the following blast works must be modified for fragmentation improvement in the lower part of the bench while at the same time reducing eventual damages in the upper part. In this case it is necessary to use the following steps for improvement of blasting activities:

- o reduce of spacing in the buffer row;
- o increase the charge in the buffer row;
- o increase the distance of the stab row and reduce the distance of the buffer row to the pre-split holes;
- o double deck the stab row and the buffer row in two independent levels and blasting the upper deck slightly before the lower, for example 25 ms.

- Example 7. The actual slope in its upper part is before the designed – this can happen when the upper part of the slope the rock strength is not reduced enough due to the better rock strength of the upper part of the rock body, change of the lithology in depth. It is necessary that the released energy in the upper part to be increased. This can be achieved through the following:

- o increasing the charge of the stab row;
- o increasing the charge in both stab and buffer rows;
- o reducing the distance between the stab row and pre-split holes;
- o reducing the spacing between stab row holes.

- Example 8. The actual slope is with a bigger angle and its lower part is behind the designed one – this can happen with really hard rocks or when there are tectonic faults with sinking angle larger than 65° towards the air slope. It is necessary that the energy released with the blasting of the lower parts of the

designed slope to be reduced as well as some changes in the buffer row through:

- o reducing the charge in it;
- o increasing the spacing;
- o increasing the distance between it and the pre-split holes.

- Example 9. The actual slope's middle part is in front of the designed one – this can happen when there is a lens or dike from a harder rock. It is necessary that the released energy from blasting the middle part of designed slope to be increased. In the mine such cases, although very rare, can happen at the borders between shists and quartzmonodiorite porphyrite. This can be corrected by increasing the charge or narrowing the spacing of the stab row;

- Example 10. The actual slope in its middle part is behind the designed slope – this is due to the presence of tectonic faults or when there is a lens or dike body from a weaker rock. It is necessary that the energy released during blasting in the middle parts of the slope to be reduced. This can be corrected by reducing the charge or increasing the spacing in the stab row;

- Example 11. When achieving the designed location of the toe and the designed slope angle of the bench, the actual slope, in its lower part, is behind the designed one – this can happen when there is a more cracked and broken area in the lower part of the slope. This happens when there is some damage from blasting level 3 and 4, which means high to very high. This usually happens with granodiorites. It is necessary that the energy released during blasting in the lower parts of the area of the designed slope to be reduced. With this type of damage on the wall the charge in the buffer row should be reduced or the spacing in it to be increased;

- Example 12. The real slope of the lower bench in its upper part is in front of the actual slope of the upper slope leaving a small berm between them – this happens with double benching, mostly because of the drilling specifics for the pre-split row. It is necessary that the energy released when blasting in the upper part of the designed slope of the lower bench to be reduced. This can be corrected through increasing the charge or narrowing the spacing of the stab row in the lower bench.

## Conclusion

The way the blasting is performed, especially the last bench blasting that forms its final configuration, respectively – its final slope angle, can be crucial for the final stability of the pit wall. The correct application of the controlled blasting technique allows to lower to the minimum the explosive seismic impact on the slopes and the precise contouring of the benches' crests and toes. This is how optimization of the slope angles and maximum width of the final berm are achieved. For example, by increasing the slope angle in hard rocks from 65° to 70° ÷ 75° allows berm widths to be increased by 1 m to 3 m or to increase the angles between the ramps and the general board angles that, respectively, reduces the waste coefficient.

The timely provision of detailed and precise information about the geotechnical properties of the rock body has a huge impact on the optimization and improvement of the drilling and blasting activities in the mine.

The results of the recommendations described in the 12 examples need to be carefully investigated. The follow up blasting designs need to be changed singularly and in random

combinations between changing the burden to the pre-split holes, the spacing in different rows and the burden between the rows, the quantity of explosive and the timing in the holes, the amount of stemming and the number of holes left without stemming. This should be done until achieving the optimal designed slopes of the mine benches in the examined area.

Using a pre-split row with preliminary blasting, as well as the positioning and charging of the inside and outside buffer rows reduces the explosive seismic impact on the wall behind, by restricting the influence of the typical geology. Using stab row of holes (to improve material movement in the upper part of the slope) is especially needed in cases of blasting harder rocks. When there are deviations from the designed walls, in the toe and lower part of the ore bench, some improvement can be achieved by changes in the holes of the buffer row.

The faults are having a destructive impact on the surrounding rock body and the rocks in the hanging wing of the fault are considerably more damaged. This is the main reason for extremely damaged surfaces in the upper part of the wall.

It is noteworthy that you can participate with a more intense contact change, near magmatic rocks, a larger gravitational case with the nature of wedge-shaped landslides and sliding surfaces is formed. This is due to the loss of flow properties of these metamorph rocks and formation of cracks in them. There is a narrow protruding berm formed in the middle of the slope at some of the double 30m benches.

Something that is characteristic for the quartzmonodiorite porphyrite and the hornfels is the development of some gravity processes in it that look like wedge slides in cases when the top of the pyramid, formed by the prismatic cracking, points at the airy part of the bench slope. Such slides with different scale often occur in these rocks. Sometimes they cover the wall surface from crest to toe.

In the granodiorite slopes there can be seen almost everywhere the traces of the presplit holes which shows that the design and the actual wall surface match. In some areas these rocks, however, form slopes that are steeper than the designed ones. This is due to some subvertical cracks with direction that is parallel or sub-parallel to the slope. In these rocks, the main gravitation processes have the characteristics of flat slide

## References

- Bar, N., N. R. Barton. 2016. *Empirical slope design for hard and soft rocks using Q-slope*. In Proc. 50th US Rock Mechanics/ Geomechanics Symposium, Houston 26–29 June 2016. ARMA, 8p.
- Bar, N., N. R. Barton. 2018. *Rock Slope Design using Q-slope and Geophysical Survey Data*. Periodica Polytechnica Civil Engineering. doi:10.3311/PPci.12287.
- Barton, N.R., N. Bar. 2015. *Introducing the Q-slope method and its intended use within civil and mining engineering projects*. In Schubert W (ed.), Future Development of Rock Mechanics; Proc. ISRM reg. symp. Eurock 2015 & 64th Geomechanics Colloquium, Salzburg 7–10 October 2015. OGG, 157-162.
- Cebrian, B. 2017. *Short course of Wall Control Optimization*. Blast Dynamics Inc., 251 p.
- Cebrian, B., M. Rocha, B. Morales, J. L. Castañón, J. Floyd. 2018. *Full Wall Control*. The Journal of Explosives Engineering, July/August 2018, 6-14.

- Dick, R. A., L. R. Fletcher, D.V. D'Andrea. 1982. *Explosives and Blasting Procedures Manual*. Bureau of Mines, Washington, D.C.
- Hoek, E., C. Carranza-Torres, B. Corkum. 2002. *Hoek-Brown Failure Criterion - 2002 Edition*. Proc. NARMS-TAC Conference, Toronto, 1, 267-273.
- Hoek, E. 2007. *Blasting Damage in Rock*. Practical Rock Engineering book.
- Hoek, E., E.T. Brown. 2018. *The Hoek–Brown failure criterion and GSI – 2018 edition*. Journal of Rock Mechanics and Geotechnical Engineering, Volume 11, Issue 3, June 2019, 445-463.
- Krolikowski, Ch. 2015. *Summary of Surface Blasting and Damages with Analysis of Two Mitigation Techniques – Presplit and Smooth Blasting*. Department of Civil and Environmental Engineering University of Michigan.
- Langefors, U., B. Kihlström, 1978. *The Modern Technique of Rock Blasting*. 3rd Ed., Wiley and Sons Inc., NY.
- Marshall, N., N. Mohr. 2005. *Ellatzite open pit – slope design project*. SRK project number U2645, SRK Consulting, 292 p.
- Peterson, J. A. 2001. *Blast Damage Mechanisms at Ekati(TM) Mine (Order No. MQ69811)*. Available from ProQuest Dissertations & Theses A&I; ProQuest Dissertations & Theses Full Text; ProQuest Dissertations & Theses Global. (304744467).
- Rajmeny, P. et al. 2012. *Improving pit wall stability by minimizing blast damage vis a vis rock characterization at RAM*. 10th International Seminar on Rock fragmentation by blasting, At New Delhi, India.

## ELECTRICITY GENERATION BY DIFFERENT MICROBIAL STRAINS

**Marina Nicolova, Irena Spasova, Plamen Georgiev, Stoyan Groudev**

University of Mining and Geology "St. Ivan Rilski", 1700 Sofia; mnikolova@mgu.bg

**ABSTRACT.** Microbial strains of iron reducing bacteria from the genera *Geobacter* and *Shewanella* were used in experiments for electricity generation by means of a microbial fuel cell. The cell was a plexiglass cylindrical column 45 cm high and with 10 cm internal diameter. The cell consisted of two sections separated by a permeable barrier of glass wool of 5 cm thickness. The feed stream, i.e. the solution subjected to treatment by the microorganisms, was supplied to the bottom anodic section of the column and the effluents passed through the cathodic section and exited at the top. Air was injected to the cathodic section. Several microbial strains from the two genera mentioned above were tested in these experiments. Some of the microbial strains, even those from the same taxonomic species, differed considerably in their ability for electricity generation.

**Keywords:** electricity generation, microorganisms, iron reducing bacteria

### ГЕНЕРИРАНЕ НА ЕЛЕКТРИЧЕСТВО ЧРЕЗ РАЗЛИЧНИ МИКРОБНИ ЩАМОВЕ

**Марина Николова, Ирена Спасова, Пламен Георгиев, Стоян Грудев**

Минно геоложки университет „Св. Иван Рилски“, София 1700; mnicolova@mgu.bg

**РЕЗЮМЕ.** Микробни щамове на желязо редуциращи бактерии от родовете *Geobacter* и *Shewanella* са използвани за производство на електричество с помощта на микробна горивна клетка. Клетката представляваше плексигласова цилиндрична колона с височина 45 см и вътрешен диаметър 10 см. Клетката се състоеше от две секции, разделени от пропусклива преграда от стъклена вата с дебелина 5 см. Захранващият поток, т.е. разтворът, подложен на обработка от микроорганизмите, се подаваше в долния аноден участък на колоната и изтичащите вещества преминават пред катодната секция и излизат в горната част. Въздух се инжектираше в катодната секция. В експериментите бяха тествани няколко микробни щамове, като дори тези от един и същ таксономичен вид, значително се различаваха по способността си за производство на енергия.

**Ключови думи:** генериране на електричество, микроорганизми, желязо редуциращи бактерии

### Introduction

The natural contacts of rainfalls with heaps, dumps and even with the relatively stable deposits of the relevant ores are connected with the presence, growth and activity of different microorganisms. Some of these microorganisms, mainly the chemolithotrophic bacteria and archaea, are the prevalent inhabitants of these biotopes. At present, such microorganisms are largely used for leaching of useful components from different mineral substrates such as low-grade ores and mineral wastes but also concentrates and rich ores. These technologies are connected with efficient measures for conservation of the nature and its inhabitants. A special attention is paid to the development of efficient technologies for the electricity generation by means of microorganisms.

The ability of some microorganisms to generate electricity in constructed fuel cells is based on the microbial transfer of electrons from different organic substrates to the surface of electrodes located in the anoxic sections of the relevant fuel cells. Some of these microorganisms (mainly bacteria and archaea) are able to form biofilms on the anodic surface and to transfer the electrons directly, through microscopic pipes located in the pili of the microbial surface. The most active microorganisms using this mechanism are some bacteria possessing the so called anaerobic iron respiration. These bacteria are typical heterotrophs able to remove electrons from some organic compounds and to transfer them via microbial respiratory chains to ferric ions acting as final electron acceptors. The most studied from these bacteria are some

species related to the genera *Geobacter* and *Shewanella*. They are able to form stable biofilms on the anodic electrodes in the constructed microbial fuel cells. In these cells, the electrons are removed from the anode by means of wires (usually from copper) and are transferred to contact with a resistance located outside the anodic section. As a result of such treatment, a portion of the chemical energy of electrons is converted to electricity and the electrons reach the aerobic cathodic section of the fuel cell in which they react with the protons to form water molecules (Rabaey and Verstraete, 2005; Lovely, 2008).

Apart from the iron-reducing bacteria mentioned above, anaerobic microorganisms using sulphates as electronic acceptors and the typical fermenting bacteria are also used in investigations of this type.

This article is related to investigations on the ability of typical iron reducing bacteria to generate electricity by means of a constructed fuel cell.

### Materials and Methods

The microorganisms used in this investigation were isolated from a natural wetland located in a territory in the proximity of Sofia. The experiments for electricity generation presented in this study were performed in the laboratories of the University of Mining and Geology in Sofia.

The constructed wetland was a plastic basin 1.50 m long, 1.2 m wide and 0.6 m deep. The bottom of the wetland was covered by a 0.2 m thick layer, consisting of a mixture of soil

rich in biodegradable organic compounds, plant compost, manure, crushed limestone and sand. A permeable barrier consisting of the mixture mentioned above and with the following dimensions - 0.6 m height, 1.2 m width and 0.5 – 0.2 m length (at the bottom and the top, respectively), was constructed in the wetland perpendicularly to the direction of water flow.

The wetland was characterised by abundant vegetation and diverse microflora. *Typha angustifolia*, *Phragmites australis* and *Scirpus lacustris* were the dominant species in the wetland but representatives of the genera *Juncus*, *Eleocharis*, *Potamogeton* and several algae (mainly from the genera *Scenedesmus* and *Eudoria*) were also present.

Microbial strains of iron reducing bacteria from the genera *Geobacter* and *Shewanella* were used in experiments for electricity generation by means of microbial fuel cell. The cell was a plexyglass cylindrical column 45 cm high and with internal diameter of 10 cm. The cell consisted of two sections separated by means of a permeable barrier of glass wool of 5 cm thickness. The feed stream, i.e. the solution subjected to treatment by microorganisms, was supplied to the bottom anodic section of the column and the effluents passed through the cathodic section located in the top part of the column and exited outside. Air was injected to the cathodic section. Several microbial strains from the two genera mentioned above were tested in these experiments. Some of these strains, even such from the same taxonomic species, differed considerably in their ability for electricity generation.

The elemental analysis of the waters was performed by means of atomic absorption spectrometry and inductively coupled plasma spectrometry.

The isolation, identification and enumeration of the microorganisms was carried out by the classical physiological and biochemical tests (Karavaiko et al., 1988) and by the molecular PCR methods (Sanz and Köchling, 2007; Escobar et al., 2008; Dopson and Johnson, 2012). The measurement of the produced power was carried out by digital multimeter.

## Results and Discussion

The treatment of the polluted waters by means of the constructed wetland was connected with an efficient cleaning of these waters (Table 1). The content of the toxic elements (mainly heavy metals and arsenic) was decreased below the permissible levels (Ordinance № 12, 2002). At the same time the content of dissolved organic was considerably increased even above the relevant permissible level. The pH was also increased but within the relevant levels. These changes were related to the deep changes of the microorganisms present in these waters (Table 2). The numbers of acidophilic chemolithotrophs (mainly *Acidithiobacillus ferrooxidans* and *Acidithiobacillus thiooxidans*) was negligible and in some samples these acidophiles were not even present.

Table 1. Data about the polluted waters before and after the treatment by means of constructed wetland

Parameters	Before treatment	After treatment	Permissible levels
pH	1.90 – 2.84	6.20 – 7.38	6 – 9
Solids, mg/l	48 – 176	28 – 60	100
Diss. O <sub>2</sub> , mg/l	1.4 – 2.1	0.2 – 0.5	20
Diss. org. C, mg/l	2.3 – 8.2	45 – 82	40

Sulphates, mg/l	415 – 1085	215 – 392	400
Fe, mg/l	314 – 1085	1.4 – 6.8	5
Cu, mg/l	4.1 – 23	0.21 – 0.42	0.5
Mn, mg/l	14 – 41	0.2 – 0.8	0.8
Zn, mg/l	11 – 51	0.28 – 0.59	10
Cd, mg/l	0.2 – 0.8	< 0.01	0.02
As, mg/l	0.8 – 6.4	< 0.1	0.2

Table 2. Microflora of the polluted waters before and after their treatment by means of the constructed wetland

Microorganisms	Before treatment	After treatment
	Cells/ml	
Fe <sup>2+</sup> - oxidising chemolithotrophs	10 <sup>5</sup> – 10 <sup>8</sup>	0 – 10 <sup>2</sup>
S <sup>0</sup> - oxidising chemolithotrophs	10 <sup>5</sup> – 10 <sup>7</sup>	0 – 10 <sup>3</sup>
Aerobic heterotrophic bacteria	10 <sup>1</sup> – 10 <sup>3</sup>	10 <sup>2</sup> – 10 <sup>4</sup>
Cellulose-degrading aerobes	0 – 10 <sup>2</sup>	10 <sup>1</sup> – 10 <sup>4</sup>
Anaerobic heterotrophic bacteria	0 – 10 <sup>3</sup>	10 <sup>2</sup> – 10 <sup>3</sup>
Cellulose-degrading anaerobes	0 – 10 <sup>1</sup>	10 <sup>4</sup> – 10 <sup>6</sup>
Sulphate-reducing bacteria	0 – 10 <sup>2</sup>	10 <sup>6</sup> – 10 <sup>8</sup>
Fe <sup>3+</sup> - reducing bacteria	0 – 10 <sup>2</sup>	10 <sup>3</sup> – 10 <sup>6</sup>

At the same time the numbers of some microorganisms were considerably increased. The sulphate-reducing bacteria and the ferric iron reducing bacteria were the dominant microorganisms in the waters subjected to treatment by means of the constructed wetland. These microorganisms were very efficient for electricity generation in the microbial fuel cells (Table 3).

Table 3. Maximum Fe<sup>3+</sup> - reducing rates by means of different mesophilic iron-reducing bacteria

Iron-reducing bacteria	Number of the strains tested	Maximum Fe <sup>3+</sup> - reducing rate, mg/l.24 h
Shewanella genus		
<i>S. odeinensis</i>	4	123 – 335
<i>S. loihica</i>	10	140 – 321
<i>S. putrefaciens</i>	5	87 – 235
<i>S. alga</i>	12	77 – 182
Geobacter genus		
<i>G. ferrireducens</i>	10	125 – 203
<i>G. metallireducens</i>	6	140 – 212
<i>G. sulfurreducens</i>	6	62 – 140
<i>G. hydrogenofilus</i>	4	41 – 104

It must be noted that the highest production of electricity by such cells was achieved by means of mixed populations of sulphate-reducing and ferric iron reducing bacteria (Table 4).

Table 4. Electricity generation by means of different anaerobic microorganisms present in the anodic section of the microbial fuel cell

Microbial populations	Cells/ml	COD, mg O <sub>2</sub> /l.h	Power, mW/m <sup>2</sup>
Sulphate-reducing bacteria	>5.10 <sup>8</sup>	680 – 2350	2150 – 3750
Ferric iron-reducing bacteria	>3.10 <sup>8</sup>	750 – 1940	1540 – 2860

Mixed sulphate-reducing bacteria and iron-reducing bacteria	$>3 \cdot 10^8$	820 – 2640	1580 – 4060
Mixed populations of anaerobic bacteria	$>5 \cdot 10^8$	440 – 1720	1420 – 3140

## Conclusion

The investigations on the electricity generation by the constructed microbial fuel cell revealed that this process was possible by using different anoxic microorganisms (sulphate-reducing, ferric iron-reducing and mixed populations of these anaerobic bacteria). It must be noted that some strains of these bacteria differ considerably from other strains of the same species. These conclusions reveal that the selection of the more active strains from the different microbial taxonomic species is an efficient way to make this approach very efficient for the future industrial application.

**Acknowledgements.** The authors would like to express their gratitude to the Scientific Research & International Partnership Unit of the University of Mining and Geology "St. Ivan Rilski", Sofia (under the frame of GPF-229/2020 project) for the financial support for publishing of this article.

## References

- Dopson, M. and Johnson, D., 2012. Biodiversity, metabolism and applications of acidophilic sulphur-metabolizing microorganisms, *Environ. Microbiol.*, 14, 2620 – 2631.
- Escobar, B., Bustos K., Morales, G. and Salazar, O., 2008. Rapid and specific detection of *Acidithiobacillus ferrooxidans* and *Leptospirillum ferrooxidans* by PCR, *Hydrometallurgy*, 92, 102 – 106.
- Karavaiko, G.I., Rossi, G., Agate, A.D., Groudev, S.N. and Avakyan, Z.A. (eds.), Biogeotechnology of Metals, *Manual GKNT Centre for International Projects*, Moscow, 1988.
- Lovely, D.R., 2008. The microbe electric conversation of organic matter to electricity, *Current Opinion in Biotechnology*, 19, 1 – 8.
- Ordinance № 12, 2002. Quality requirements for surface waters intended for drinking and domestic water supply, *State Gazette* 63, 2002, Corr. SG 15, 2012.
- Rabaey K. and Verstraete W., 2005. Microbial fuel cells: novel biotechnology for energy generation, *Trends in Biotechnology*, 23, 291 – 299.
- Sanz, J.L. and Köchling, T., 2007. Molecular biology techniques used in wastewater treatment: An overview. *Process Biochemistry* 42, 119–133.

## DESIGN OPTIMIZATION OF DRILLING AND BLASTING OPERATIONS: A CASE STUDY ON COPPER ORE MINING IN ASAREL

Vladimir Penev<sup>1</sup>, Zdravka Mollova<sup>2</sup>

<sup>1</sup>University of Mining and Geology "St. Ivan Rilski", 1700 Sofia; vladimir.penev@mgu.bg

<sup>2</sup>University of Mining and Geology "St. Ivan Rilski", 1700 Sofia; mollova.zdravka@gmail.com

**ABSTRACT.** Drilling and blasting are significant technological operations in open-pit mines. They directly affect the cost of extraction and processing of the rock mass and indirectly through the impact of the fragments' size of the blast material on the efficiency of the subsequent processes of loading, hauling and crushing. The purpose of this paper is to explore a methodological approach for optimization of blasting parameters based on the reduction of the specific consumption of explosives. This is achieved by examining the influence of a geometric parameter - the burden between the drill rows on the explosive effect. In addition, the correlation between the relative consumption of explosives for extraction and fragmentation per ton of mine mass and geometric parameters of blasting. Data from in-situ experiments is used for assessment according to criteria for stability of the rock massif and seismic actions caused by blasting operations.

**Keywords:** optimization; drilling and blasting operations; open-pit mines

### ОПТИМИЗАЦИЯ НА ПРОБИВНО – ВЗРИВНИТЕ РАБОТИ ПРИ ДОБИВА НА МЕДНА РУДА В РУДНИК АСАРЕЛ

Владимир Пенеv<sup>1</sup>, Здравка Моллова<sup>2</sup>

<sup>1</sup>Минно-геоложки университет „Св. Иван Рилски“, 1700 София

<sup>2</sup>Минно-геоложки университет „Св. Иван Рилски“, 1700 София

**РЕЗЮМЕ.** Пробивно – взривните работи са ключов технологичен процес в добива на руда. Те повлияват директно върху себестойността на добитата и преработена скална маса и косвено - чрез въздействието на зърнометричния състав на раздробения материал върху ефективността на последващите процеси - товарене, транспорт и трошене. Авторите са насочили изследването си към методологичен подход за оптимизиране параметрите на взривяване, който се основава на намаляване на специфичния разход на взривно вещество посредством изследване влиянието на геометричен параметър – разстоянието между сондажните редове, върху взривния ефект и изследване на относителния разход на взривно вещество за добив и раздробяване на тон минна маса в зависимост от геометричните параметри на взривяване. Използвани са данни от полеви опити, които са проведени за оценка по критерии за устойчивост на скалния масив и взривно – сеизмичното въздействие.

**Ключови думи:** оптимизация; пробивно-взривни работи; добив по открит способ

### Introduction

Drilling and blasting operations have a significant role in mining since the rock mass contains useful minerals that must be first broken, then crushed, and finally ground in mills. Drilling and blasting operations influence directly the cost of extraction and processing of the rock mass and have an indirect influence on the following technological processes.

This determines the core objectives of technological blasting, namely:

- complete removal of the rock mass within the design contour of the blasting field with a desired grain size distribution of the blasted material;

- to preserve the environment from the harmful effects that arise from the explosion to a level, considered practically safe.

The relation "mining conditions - primary explosive effect – side effects of the explosion" are complex, and some of the factors remain unknown or uncertain with a sufficient degree of reliability. This predetermines the need for constant monitoring and research in order to ensure safety, easy implementation and economic profitability of the processes.

This research is aimed at improving the parameters of technological explosions to:

- optimize the parameters of the blasting works to achieve maximum fragmentation effect, compliant to state-of-the-art mining practices worldwide.

- achieve the desired granulometric composition (particle size distribution) of the blast-cause fragmented mining mass.

- define the relationship between blast parameters and the level of seismic action of the blast.

According to the established state-of-the-art blasting practice, detailed research is carried out to determine the prime factor influencing the explosive effects - the structure of the rock mass.

The blastability zones are clearly drawn by both research and the investigated experimental blasting. For each blast field, the design of the drilling and blasting parameters is performed on the basis of:

- an expert assessment of the location of the field and

- an assessment of the structure of the exposed surface of the working field. That is the distance between the visible damages in the vertical and horizontal directions.

For each blastability zone, the integral indicator characterizing the blasting effect is determined, represented by the "optimal relative consumption of explosive (sc. specific charge)" for blasting per unit volume of rock mass and fragmentation of the rock mass with the desired grain size distribution (granulometry).

## Research methodology

Rock fragmentation resulting from blasting operations has an influence on secondary fragmentation, loading, hauling, and crushing. The concept on optimum fragmentation is an interesting topic in mining engineering. There is no proper definition on optimum fragmentation, but it is considered such if it fulfils all of the following conditions:

- Minimum cost from drilling to grinding in the fragmentation chain: drilling-blasting-crushing-grinding.
- Maximum ore recovery.
- High productivity.
- Minimum impact on safety and environment.

The chosen methodology for optimization is "reduction of the specific consumption (sc. charge concentration) of explosive per linear meter of blasted mine mass" through examination of the influence of a geometric parameter, the burden between the drill rows, on the blasting effect. In addition, the correlation between the relative consumption (sc. specific charge) of explosive for extraction and fragmentation per ton of mine mass ( $q$ , kg/t) and geometric parameters of detonation – average (burden) for 1st row boreholes, spacing between boreholes in the row, burden between drill rows, is considered to evaluate the different optimization results.

This was achieved by designing and performing a test blasting in a predefined zone, in accordance to the following parameters:

- acreage of the blasting field in accordance to the development of the mining works on the defined section.
- diameter of the boreholes.
- energetic parameters of the explosive charge in the drill hole - number of the charges, length of the main and upper charge; length of the intermediate stemming; length of the upper stemming; schedule of commutation of the charges in time and space.

The drilling and blasting processes on the test field are in accordance to the established practice of the copper mine. The actual parameters of the blasting are determined when loading the boreholes.

Expert assessment is executed after test blasting by visual examination of the blasted pile. The grain size distribution of the fragmented rock mass (percentage of oversized rock fragments and average piece size) is investigated.

The excavation of the material is monitored closely. After the loading, the ejection distribution of the rock mass is documented at the level of the floor and inside the borders of the blasting field.

The quantitative indicators of the test blasting - extraction of mining mass per linear meter of drilling and relative consumption of explosive are determined.

## In-situ test

Copper ore mine Asarel-Medet is a world leader in the open-pit development of copper deposits with a content of less than 0.5%.

Asarel copper porphyry deposit is located in the Razslatitsa area, Sredna Gora, 8 km northwest of the town of Panagyurishte, Pazardzhik region.

The geological structure of the Asarel deposit consists of Proterozoic metamorphites, Paleozoic granites, Turonian sediments, upper cretaceous andesites, tuffs, tuff breccias, diorite, quartz-diorite, granodiorite porphyrites and monzodiorite porphyrites.

The local tectono-structural position of the Asarel deposit is quite complex. The Asarel graben - syncline, locked between the Mial and Petrich faults and the area of the deposit are strongly torn by three systems of faults with different age relationships - northwestern, northeastern and meridional. The mutual intersection of the disturbances from these systems has formed a block-fault character of the deposit.

The blasting works in the Assarel mine are performed in complex geological conditions. The combination of multiple fault zones, inhomogeneous rocks, rock massifs with varying degrees of cracking and alternation of dry with waterlogged boreholes (even within a single blast field), springing and flowing water through boreholes complicate daily blasting and require an unique approach for almost every blast.

## Mining and technical conditions:

- semi-trench excavation in the presence of a free surface parallel to the length of the borehole.
- bench height from  $H = 11$  m to  $H = 15$  m.
- angle of inclination of the bench  $\alpha = 75^\circ$ .
- design diameter of the blasting boreholes -  $d = 251$  mm.
- design relative consumption of explosive -  $q = 0.190$  kg / t (determined for difficult for blasting zone).

The relationship "relative explosive consumption - explosive effect" is explored by adjusting the distance between boreholes in accordance to the adopted approach.

The test is limited in the area of the blast field with a bench height  $H \geq 11.5$  m to take into account the requirements for normal operation of the drilling charges (ratio between geometrical parameters and diameter of the drilling).

Expert analysis found that the rock mass in the slope of the bench is intensely cracked to a large block structure.

An established practice when performing blasting operations in the Asarel open-pit mine is to make control measurements of the charge length in case of doubt for leakage or washout of explosives through cracks in the massif. In case of a detected problem, the borehole is recharged with additional explosives. In this way, the blasting squad secures achievement of the planned results in terms of ejection and comminution of the rock mass. This practice increases the relative cost of blasting and the risk of harmful effects. In this regard, it is recommended, that when performing blasting works in the fault zones of the Asarel open-pit mine (in the presence of running water) explosive loading should be applied in the boreholes through a strong polymer liner. The liner will protect the explosive from leaching and will prevent it from being displaced into the borehole by the sand carried by the running water. This will contribute to the improvement of the economic indicators of the blasting technological process, due to the elimination of the need for recharging.

## Blast effect

The evaluation of the explosive effect is made by the following steps:

1. overview of the blasting pile – visual assessment: normal compared to previous blasting works in this area; oversized rock pieces and average grain size.
2. operation of the excavator - assessment of granulometry and level of the floor when the field is completely excavated.
3. quantitative indicators - design volume - 90624 t; total amount of explosives - 15950 kg (mass of charge explosive); relative consumption of explosive - 0.176 kg/t; mining yield per linear meter of drilling - 183.08 t/m.

**Comparison and evaluation of results**

The test blasting is performed according to a new blasting pattern with a change of the following parameters:

- Spacing between boreholes in the row.
- Burden between drill rows. In a rectangular grid 9,50 x 9,00 m (relative distance = 1.055) and boreholes with lengths from 5 m to 10 m (Figure 1).

The newly designed blasting field is with an area equal to the regular but it reaches design savings as follows:

- Field drilling: 34 m.
- Quantity of explosives per field: 834.5 kg.
- Relative consumption difference: - 0.006 kg/t.

**Analysis and conclusions**

The results of the test blasting pattern prove the suitability of the methodology. The same granulometry of the fragmented rock mass was achieved with the reduced relative consumption of explosives. This new approach can lower the cost of blasting operations, reduce the side effects on the environment due to the lower quantity of explosives used and increase the productivity by reducing the boreholes. Therefore, the used methodology, based on "reduction of the specific consumption of explosive per linear meter of blasted mine mass" fulfils the criteria for optimization.

Table 1. Comparison between the results of regular blasting and test blasting

	Number of boreholes	Σ length of boreholes	Σ length of the explosive charge	Quantity of explosives for the blast field	Relative consumption of explosives
	-	[m]	[m]	[kg]	[kg/t]
[1]	[2]	[3]	[4]	[5]	[6]
Regular grid (9mx9m)	43	400.0	163.6	9818.2	0.121
Test grid (9.5mx9m)	41	366.0	149.7	8983.6	0.115
Difference	-2	-34.0	-13.9	-834.5	-0.006

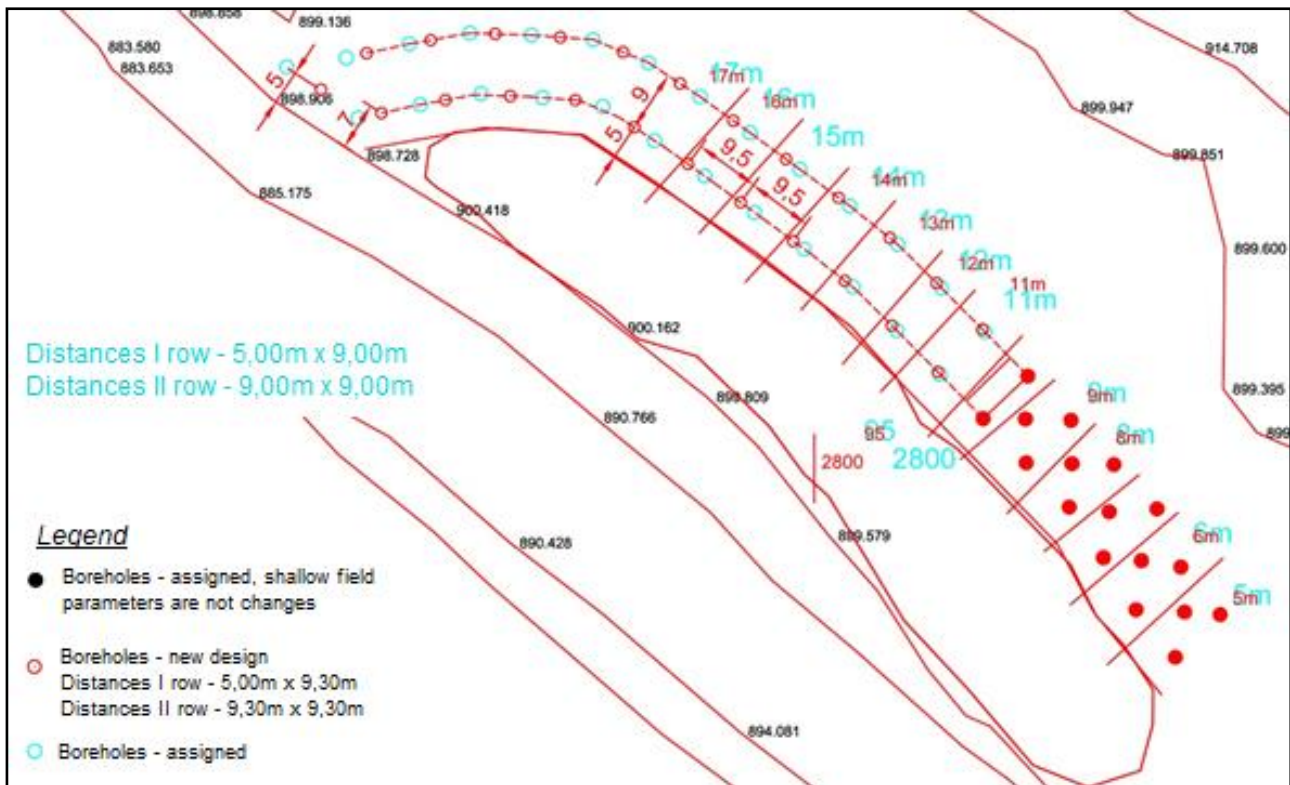
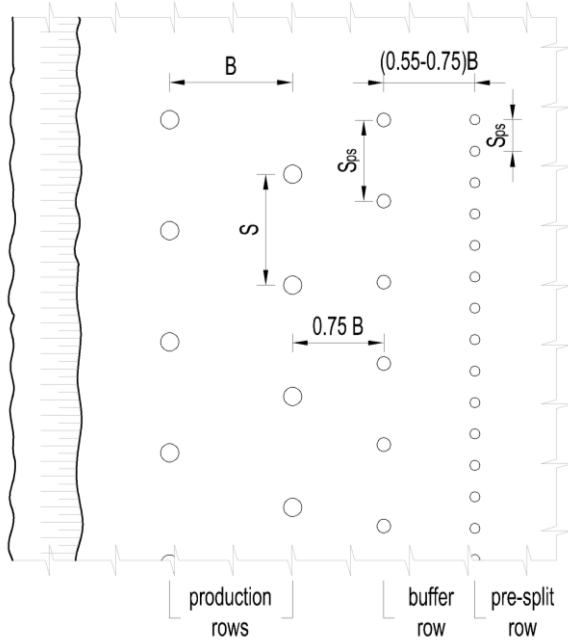


Fig. 1. Plan of the blasting field for the in-situ test – Asarel mine

**Design recommendations**

Contour blasting by the method of pre-splitting of the rock massif is recommended in order to preserve the integrity of the massif. Blasting technology includes blasting the pre-split row and blasting the production rows to eject the rock mass in front of the pre-split crack (Figure 2)

The boreholes for the pre-split row are drilled with a diameter  $d_c \leq 110$  mm above the design angle of the slope of the non-working bench.



**Fig.2. Recommended drilling pattern (pre-shielding of the rock massif)**

The recommended diameter of the boreholes from so-called buffer row is  $d_c = 165$  mm. The blasting parameters: B and S of buffer row of boreholes are with values of 75% of the determined for the given diameter of the production boreholes. The amount of charge is 55-75% of the defined boreholes for the production. The blasting parameters of the pre-split row are presented in Table 2.

**Table 2. Comparison between the results of regular blasting and test blasting**

Diameter of Drilling	Diameter of Charge (cartridge)	Spacing	Parameters of the blasting contour						
			Bottom charge		Multi-deck chained charge			Stemming	
			weight	length	weight	length	quantity	main	intermediate
[mm]	[mm]	[m]	[kg]	[m]	[kg]	[m]	pcs	[m]	[m]
$\leq 110$	$\leq 0.5d_c$	1.00	2.50	0.50	0.50	0.30	14.00	1.50	0.70

According to the established blasting practice, the parameters are determined as follows:

- the charges from the pre-splitting row are detonated first, following the production boreholes of no less than 100ms.
- the boreholes for pre-splitting row are drilled with the same angle and plane of the non-working bench.
- blasting sequence – instantaneous.

- the initiation of the charges is carried out by means of detonating cord - /two parallel pieces/.
- Intermediate stemming - air.

The decoupled chained multi-deck blasting charge is constructed of water resistant explosive cartages /pack/ „Elatzit 710“ with diameter  $\varnothing 50$  mm and length 400 mm.

The charge should be centered along the axis of the borehole. The configuration of the explosive charge inside the blast-hole is given on figure 3.

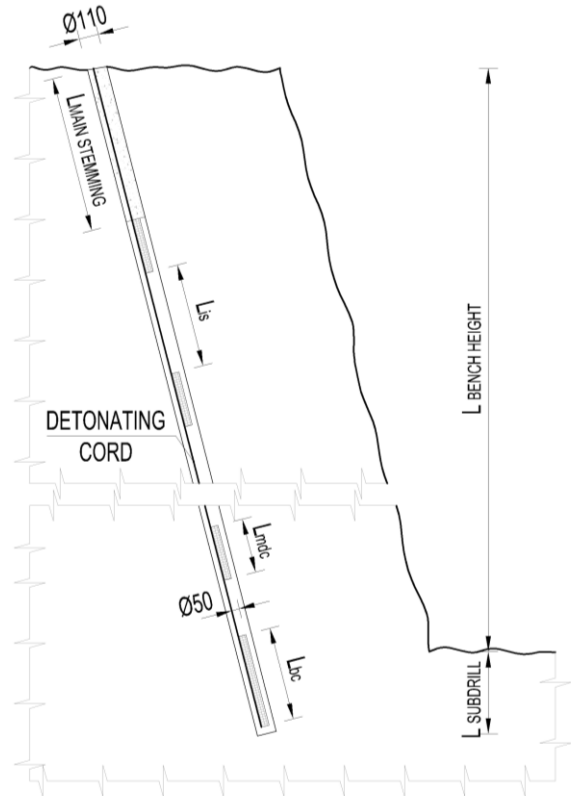


**Fig.3. Configuration of the decoupled chained multi-deck blasting charges for pre-splitting**

**Recommendations**

Based on the study, the following recommendations are proposed:

4. In a blasting field the distance between a drilled borehole and the next (i.e. geometrical parameters) shall be adjusted depending on the established properties of the rock massif obtained from the previous borehole.

5. Special attention must be given to boreholes in severely cracked structures and/or in the presence of water. Such cases would require an individual approach with appropriate technology and measures, e.g. applying a polyethylene liner.

6. In some cases, accommodating an alternative approach, such as the "Hydrox" system can be beneficial. Applying this methodology can assist to:

- reduce the impact of plastic deformations in the rock massif and thus,
- improve the overall and local stability of individual steps and benches.
- reduce the harmful impact on the environment.
- decrease explosive consumption and so the total cost of the process.

## References

- Mitkov, V. 2010. Bezopasnost pri proizvodstvo i upotreba na eksplozivi. Sv. Ivan Rilski, Sofia - 343 p. ISBN 978-954-353-131-8 (in Bulgarian)
- Mitkov, V et al. 2015. Task report: Process Audit of Drilling and Blasting Operations in Copper Ore Mine Asarel. Sv. Ivan Rilski, Sofia (in Bulgarian)
- Mitkov, V. 2007. Za bezopasnostta na eksplozivite za grazhdanski tseli.- *Annual of the University of Mining and Geology "St. Ivan Rilski"*, 50, Part 2, 109-114 ISSN 1312-1820. (in Bulgarian).
- Mitkov V. 2010. Improvement of the technology for performing blasting works in Studena Quarry.- *Proceedings of the Thirty-Sixth Annual Conference on Explosives and Blasting Technique*, ISEE-Orlando, FL USA, Vol. 1 p. 247-256, ISSN 0732-619X (in English).
- Mitkov, V. 2010. Metodika za kompyutarno proektirane na parametrite na PVR pri karieren dobiv.- *Annual of the University of Mining and Geology "St. Ivan Rilski"*, 53, Part 2, 88-94. ISSN 1312-1820. (in Bulgarian).
- Mitkov, V. 2011. Tehniko- ikonomicheska otsenka na efektivnostta pri izpolzване na vzrivnite veshtestva.- *Annual of the University of Mining and Geology "St. Ivan Rilski"*, 54, Part 2, 79-82. ISSN 1312-1820. (in Bulgarian)
- Mitkov, V., Kamburova, G. 2007. Izsledvane, sazdavane i vnedryavane na grubodispersni amoniti sas sensibilizator vtorichen bezdimen barut.- *Annual of the University of Mining and Geology "St. Ivan Rilski"*, 50, Part 2, 115-120. ISSN 1312-1820. (in Bulgarian).
- Shiskov, P. 2019. *Spravochnik na vzrivnika*. Izdatelska kashta Sv. Ivan Rilski, Sofia - 244 p. ISBN 978-954-353-378-9 (in Bulgarian)
- Shishkov P., Stoycheva N., 2018. Savremenni vzrivni tehniki za dobiv na skalno-oblicovachni materiali - *Mining and geology magazine*, 10-11, 42-49, ISSN 0861-5713 (in Bulgarian with English abstract)
- Shishkov P., Stoycheva N., 2019. Application of long term stored single and double based propellants in advanced blasting methods for dimension stone extraction – *NTREM 2019 - New trends in research of energetic materials*, Pardubice, 09 – 11.04.2019, CZ, Proceedings Part 1, pp.619-629, ISBN 978-80-7560-210-7(in English).

## POLLUTION OF GROUNDWATER AND SURFACE WATER FROM THE MINING INDUSTRY

**Sotir Plochev, Stefan Zeinelov**

*University of Mining and Geology "St. Ivan Rilski", 1700 Sofia; plo4ev@mail.bg*

**ABSTRACT.** The pollution of groundwater and surface waters from the mining industry is a very serious ecological problem worldwide. The article overview various examples from world practice, related to the research, monitoring and the applied measures to reduce this pollution. The causes and conditions, under which these environmental problems occur, are thoroughly analysed. Potential and real sources of pollution - landfills, and abandoned mines, specific mineralization in the sites, pollution from accumulated sediments and sludge, etc. are studied. The possibilities for assessment and predicting of this type of pollutions with the help of mathematical models are presented, and some typical examples of pollution areas around uranium mines in Bulgaria and Germany are overviewed. Pollution with heavy metals around mine in Morocco is another presented example.

**Keywords:** groundwater contamination, acid mine drainage, heavy metals, mass transport model and water quality.

### ЗАМЪРСЯВАНЕ НА ПОДЗЕМНИТЕ И ПОВЪРХНОСТНИ ВОДИ ОТ МИННО-ДОБИВНАТА ДЕЙНОСТ

**Сотир Плочев, Стефан Зейнелов**

*Минно-геоложки университет „Св. Иван Рилски“, 1700 София*

**РЕЗЮМЕ.** Замяряването на подземни и повърхностни води от минно-добивна дейност е много сериозен екологичен проблем в световен мащаб. В статията са разгледани различни примери от световната практика, свързани с изследването, мониторинга и прилагането на мерки за ограничаване на това замърсяване. Направен е обзорен анализ на причините и условията, при които възникват тези екологични проблеми. Разгледани са потенциалните и реални източници на замърсяване – отпадъкохранилища и изоставени минни, специфична минерализация в обектите, замърсявания от натрупани наноси и утайки и др. Представени са възможностите за оценка и прогнозиране на този тип замърсявания посредством математически модели и специализирани компютърни програми. Направен е преглед на някои типични примери на замърсяване на повърхностни и подземни води при добива на метални руди и естествен уран в Германия и България. Разгледан е и друг случай на замърсяване с тежки метали в района на мина в Мароко.

**Ключови думи:** замърсяване на подземните води, кисели руднично води, тежки метали, миграционен модел и качество на водите.

### Introduction

The protection of the environment, the biosphere and the natural resources is connected with the sustainable progress. The surface and the interior of the Earth, the atmosphere and the water are basic natural resources, providing conditions for emerging, development and existence of organisms and humans. The presence of pollutants, in concentration over the regulated limits, could cause negative consequences for the whole food chain, the ecosystems and other natural resources. The environmental pollution directly affects the society, and is harmful for the people's health. It also has negative impact on tourism, fishing and agriculture. In addition to monitoring, analyzing and control of the surface water and groundwater condition is required.

Contamination of surface water and groundwater in result of ore mining operations is quite complex ecological problem worldwide. The analysis of a huge number of scientific publications shows, that the biggest impact over the nature and the peoples is from the toxic and radioactive type of pollutants (Casagrande et al., 2019; Arranz-González et al., 2016; Wang et al., 2019; Aleksander-Kwaterczak et al., 2016; Olías et al., 2019; Luo et al., 2020; Andonov et al., 2019; Stoyanov, 2019; and Stoyanov et al., 2018). The list of toxic pollutant is long -

some of the most common are the metals Cd, Ni, Hg, Pb, As, Cr, Cu, Zn, Fe, Mn. The radioactive contaminants include radionuclides and products from fission of the uranium (isotopes of elements). The main sources of toxic pollution are related with mining activities and the processing of metal ore, tailing ponds, etc. Sources of radioactive contamination are the uranium mines, the processing of the uranium ore and the storage facilities. The negative impact continues after the the period of exploitation. The pollution could come from underground and open pit mines, extraction with reinjection, geotechnological and product enrichment facilities, temporary storage of hazardous materials, etc. In fact, the extraction of uranium ore is also connected with intensive pollution with various heavy metals, but also can cause long lasting contamination with a lot of others inorganic and organic contaminants as sulfates, chlorides, ammonium ions, oil products, cyanide, etc.

The text below includes some typical examples, with the results of the conducted research of the processes leading to pollution due to the mining of metal ores and uranium ore in Germany, Morocco and Bulgaria (Bain et al., 2001; Moye et al., 2017; Kolev and Hristov, 2019; Stoyanov et al., 2019).

## Materials and methods

1. During the second half of the last century, significant quantities of uranium ore were mined in Bulgaria. In 1988 the extracted ore is 662 t (1,5% of the world total yield). The uranium reserves on the territory of Bulgaria in 2014 are about 35,374 tons.

One of the uranium ore sites is a mine called Druzhba, near Eleshnitsa village, in the southwest part of Bulgaria, operated in the period 1955 - 1992. After cessation of mining activities, the drainage pumps (with approximate pumping rate of 300 m<sup>3</sup>/h) were shut down in December 1995, and since then the discharged water flows directly into Zlataritsa river with initial rate of about 10 l/s. During the excavation work, three different confined aquifers (upper, medium and lower) were registered in the region of the deposit - respectively at approximate altitudes of 805, 730 and 630 m, recharged exclusively from infiltration of atmospheric precipitation. The filtration parameters of the massif are adopted by archive data as follows: cumulative thickness of the aquifers 146 m; hydraulic conductivity  $k = 0,5$  m/d, water yield coefficient  $\mu = 0,005$ . The galleries volume is respectively 980000 m<sup>3</sup> between 520 and 620 m height, equivalent radius 56 m; 1150000 m<sup>3</sup> between 620 and 712 m height, equivalent radius 56 m; 325000 m<sup>3</sup> between 712 and 738 m height, equivalent radius 63 m.



Fig.1. Photo of the area of Druzhba mine (Google Earth, 2020)

The tailing pond collecting the wastewaters from the mining activities is located 2,6 km southeast of Eleshnitsa village, and is used since 1969 (Fig.1). The height of the dam is 74 m, and the total area of the tailing pond is 250000 m<sup>2</sup>. The pond contains about 9000000 t of wastes, 730 t of them uranium, with total radioactivity =  $1,5 \cdot 10^{15}$  Bq. Rehabilitation of the pond was conducted from 2003 to 2005 (project PHARE). Since then a water treatment plant downstream from the tailings pond collects all the drainage water and treats it for possible uranium pollution (Kolev and Hristov, 2018).

2. Another area in Bulgaria impacted by pollution with metals is the Madjarovo ore field. The mining operations began in 1958 and finished in 1997. The ore field includes the mines Arda, Harman kaya, Momina skala and Brousevtsi (Fig.2). The parts of the rock massif that are affected by mining activities are characterized by very high water permeability and play the role of complex drainage systems. Data from the system monitoring, as well as hydro-chemical studies carried out in 2015, revealed increased contents of Fe, Mn, Zn, Pb, Cd, As, Ni, and other heavy metals in the mine and in the surface waters in the region. The main pollution is caused by zinc, lead, cadmium and nickel. The harmful effects of the pollutants are health disorders, such as damage to body cells, kidney damage, cancer, skin inflammation, negative impact on plants and animals.



Fig.2. Map of the area of the Madjarovo ore field (Stoyanov et al., 2019).

Applying the Modflow and MT3D-MS computer programs (McDonald and Harbaugh, 2000), (Zheng and Wang, 1998), several 3D numerical models are composed. The studied area is divided in five hydrogeological units:

I - parts of the rock complex affected by the mining activities – galleries, shafts, shattered zones, pillars (hydraulic conductivity  $k = 3$  m/d; volumetric mass = 1850 kg/m<sup>3</sup>; longitudinal dispersion 3 m; coefficient of molecular diffusion  $D_M = 5 \cdot 10^{-4}$ );

II - tectonic zones (hydraulic conductivity  $k = 4,5$  m/d; volumetric mass = 1850 kg/m<sup>3</sup>; longitudinal dispersion 4,5 m; coefficient of molecular diffusion  $D_M = 5 \cdot 10^{-4}$ );

III - regionally fractured and secondary altered parts of the rock complex down to elevation 110 m (hydraulic conductivity  $k = 0,35$  m/d; volumetric mass = 2150 kg/m<sup>3</sup>; longitudinal dispersion 10 m; coefficient of molecular diffusion  $D_M = 7 \cdot 10^{-4}$ );

IV - weakly affected by secondary changes parts of the rock complex (hydraulic conductivity  $k = 0,02$  m/d; volumetric mass = 2150 kg/m<sup>3</sup>; longitudinal dispersion 10 m; coefficient of molecular diffusion  $D_M = 7 \cdot 10^{-4}$ );

V - river terrace - cobblestones, gravels, and sands (hydraulic conductivity  $k = 100$  m/d; volumetric mass = 2100

kg/m<sup>3</sup>; longitudinal dispersion 5,5 m; coefficient of molecular diffusion  $D_M = 3.10^{-4}$ ).

The 3D mass transport model simulates the movement of the main pollutants, and follows the prepared filtration model of the studied area. Convection, reversible elimination, dispersion, diffusion and mixing are taken into account. The transverse dispersion is 1/10 of the value of the longitudinal dispersion. The vertical dispersion is 1/100 of the longitudinal dispersion. The simulated period is from 1995 to 2030 (Stoyanov N. et al., 2019).

3. The uranium mine Koenigstein is located in the Saxony Region of eastern Germany near the River Elbe, about 20 km south of the City of Dresden. The ore is not very rich - about 0,03 % (mass), mainly as UO<sub>2</sub>. The study area consists of a series of sandstone aquifers separated by clay. The ore body is located in a lower sandstone layer, designated as the fourth aquifer. This aquifer has about 10 m average thickness. The overlying aquifer is used as a potable water supply. From 1950 through to the end of 1990, uranium ore was extracted at this mine by means of an underground in situ leaching process, which involved passing a sulfuric acid leaching solution through isolated blocks of the ore body. Since closure of the mine in 1990, the level of the underground waters has been maintained at low level.

The groundwater flow system for complex multi-aquifer system has been modeled by WASY software and FEFLOW software. The two profiles (sections), showing the uranium transportation, are presented on Fig. 3. The longer is 5 km and the short is 1 km long. The flowing direction of the underground waters is N - NE. A simplified model of a one-dimensional profile parallel to the direction of groundwater is used. The choice for 1D model is appropriate because the ratio between length and thickness of the fourth aquifer (1000 - 5000 m in length, 10 m thick).

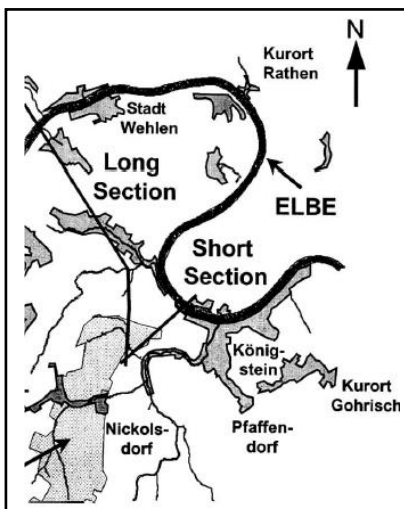


Fig.3. Two sections (Long Section и Short Section), oriented accordingly to the underground flow direction (Bain J. et al., 2001)

The filtration parameters of the lowest aquifer are: hydraulic conductivity 0,86 m/d; porosity 0,19; volumetric mass = 2100 kg/m<sup>3</sup>; coefficient of molecular diffusion  $D_M = 9.10^{-5}$  m<sup>2</sup>/d).

In 1993, an experiment was carried out in which the pumping of groundwater was stopped and the mine was flooded. Water samples from the site were taken after 190

days from the beginning of the flooding. The predicted period for the long section is 50 years, and 100 years for the shorter section. The studied data is for the following contaminants: Fe, U, Pb, Ni, Cd, Cr и Zn and sulfates (Bain J. et al., 2001).

4. Ketara mine is located nearby Ketara village, 35 km northwest from Marrakech city, in Morocco (Fig.4). The mine extracted sulfide minerals from pyrrhotite ore, and currently the mining operations are ceased. The area around the mine is polluted with Mn, Fe, Zn, As, etc., which affect the quality of groundwater.

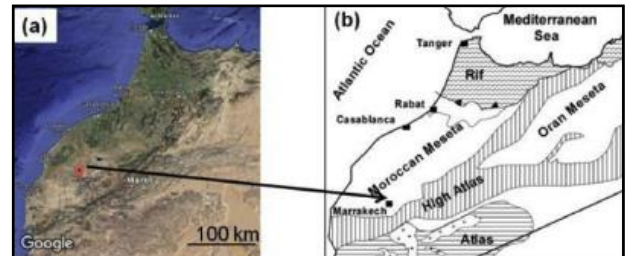


Fig.4. Location of Ketara mine, Morocco (a - photo; b - map)

Two aquifers have been established on the territory of the site - one in the Sarhlef shale, and one in the granite rocks called Bamega. The study is focused on the aquifer in the shale with hydraulic conductivity 78 m/d and storage coefficient 5.10<sup>-2</sup>.

After collecting the necessary data, models for the underground water levels and electrical conductivity were created using the computer program Golden software. The concentrations of contaminants from the water samples are presented in Table 1 (Moye et al., 2017).

Table1. Concentration of contaminants

Pollutant	Concentration min-max (ppb)	Average concentration (ppb)	Standart deviation
As	0,25 - 22,12	3,35	6,52
Fe	43,5 - 668	168,71	189,35
Mn	5,36 - 1184,5	88,8	302,28
Zn	5,92 - 29,54	-	-

## Results and discussion

1. The concentration of the pollutant in water samples taken from gallery №9 (point 34 of the monitoring) in the period from 2012 to 2016 is shown in Fig.5. Gallery №9 is the lowest exit of the mine at level 738 m and is discharging the flow (10 l/s) in Zlataritsa river.



Fig.5. Concentration of the uranium (mg/l) in the waters from gallery №9 (Kolev and Hristov, 2018)

At this flow rate, the amount of uranium poured into the Zlataritsa river for the period 2012 - 2018 is about 5 tons, with average concentration of 2,8 mg/l. Over time, concentrations decrease, due to flooding of the mine, leading to limited contact with oxygen and reduced mobility of the pollutant.

2. The model of pollution in the Madzharovo ore field is based on a filtration model, which determines the spatial distribution of pressures, gradients and velocities. The problematic pollutants are Zn, Pb, Cd, and Ni. The range of the pollution is determined with 3D mass transport model. The largest contamination by area is caused by the element nickel (Fig.6), but the zinc has the strongest exceeding of the permissible norms (Fig.7).

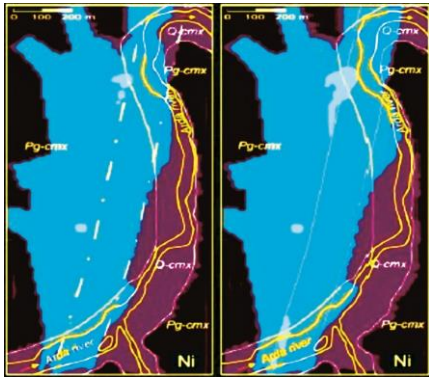


Fig.6. Nickel pollution for period of 15 and 30 years (Stoyanov et al., 2019). Concentration (mg/l):



The results show a significant impact on the area between the town of Madzharovo and the large meander of river Arda. The wastewater flow is significant (about 40 l/s), and the pollution covers an area of the river terrace with a length of over 1 km (Stoyanov et al., 2019).

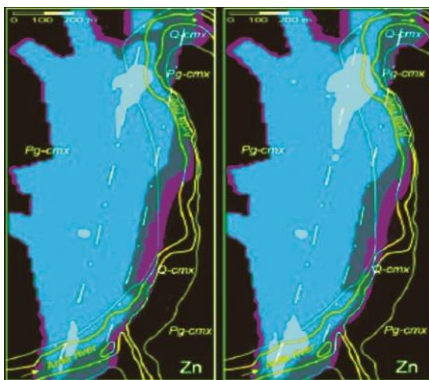


Fig.7. Zinc pollution for period of 15 and 30 years (Stoyanov et al., 2019). Concentration (mg/l):



3. Koenigstein mine in Germany - the prediction data for the two profiles are in Fig.8 and Fig.9. For the "Short Section" are presented data which take into account the reactions between the pollutant and the aquifer, and data calculated without the influence of the reactions with the underground aquifers (conservative model).

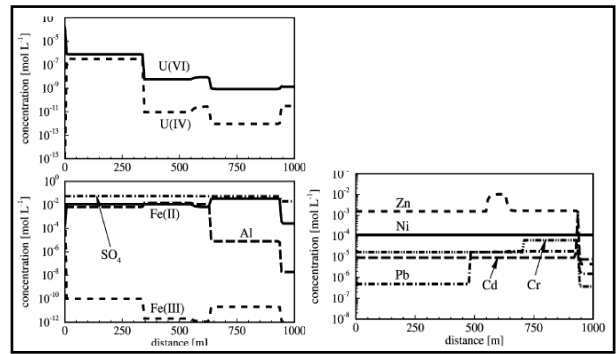


Fig.8. "Long Section" profile concentrations for 50 year period (Bain et al., 2001)

The predicted concentrations for the short profile (Fig.9) are for point located at 1000 m from the pollution source (Bain et al., 2001).

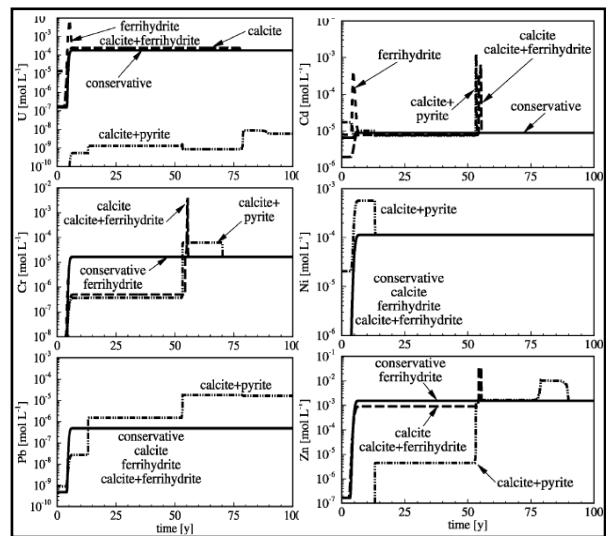


Fig.9. "Short Section" profile concentrations for point at 1000 m distance of the contaminant source. Prediction period - 100 year (Bain et al., 2001)

4. The analysis of data from the Ketara mine site was used to determine the concentrations of pollutants that may affect the quality of groundwater.

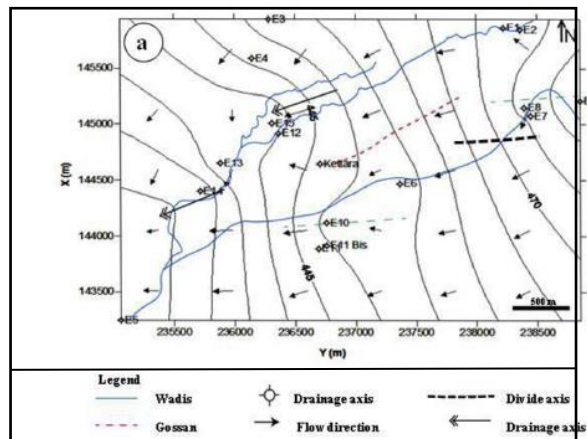


Fig.10. Piezometric levels in the area of the mine (Moye et al., 2017)

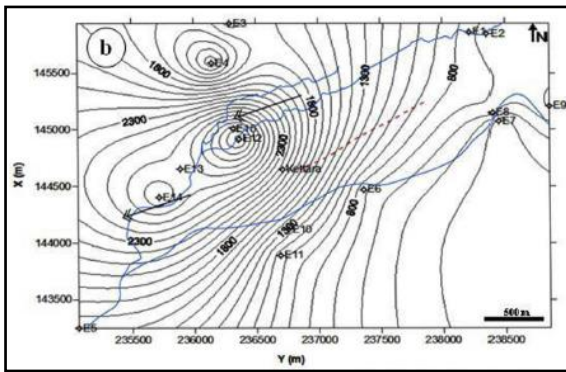


Fig.11. Electrical conductivity in the area of the mine (Moye et al., 2017)

The results of the model for the filtration field and the calculated electrical conductivity are presented in Fig.10 and Fig.11. The concentrations of the pollutants are in Fig.12 and Fig.13.

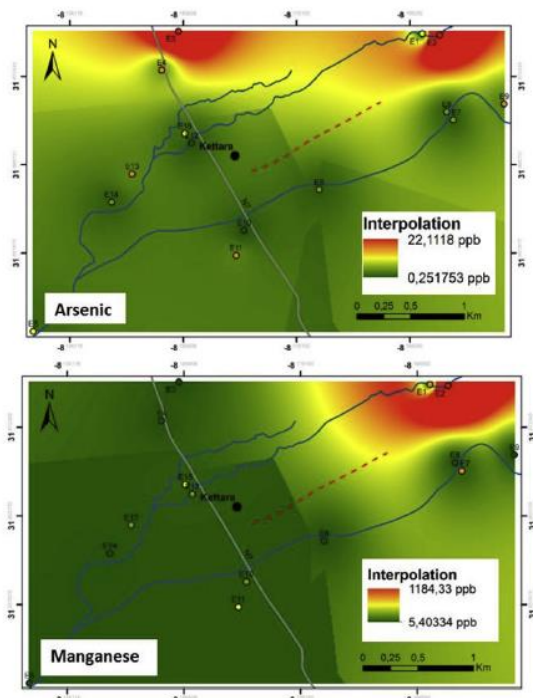


Fig.12. Pollutant concentration in the area around Ketara mine (Moye et al., 2017)

The major problem in the area around the mine is caused by arsenic. The high levels of pollution are most likely due to the presence of a regional fault, the high values of evaporation in the area and possibly to reaction with organic substance or iron oxide (Moye et al., 2017).

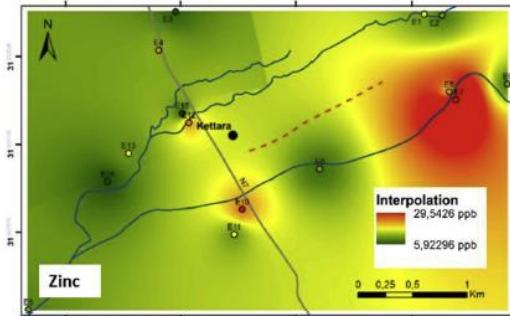
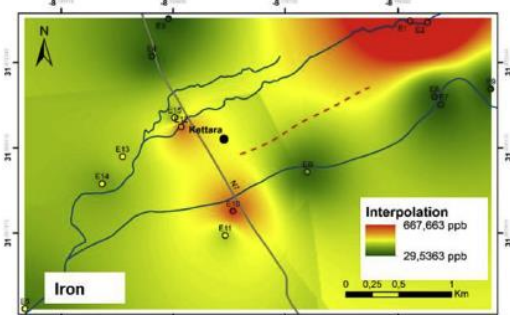


Fig.13. Pollutant concentration in the area around Ketara mine (Moye et al., 2017)

### Conclusion

The presented examples above clearly show that mining activities are very often the cause of long-term, large-scale and very intense pollution with toxic, radioactive and other pollutants of groundwater and surface water. Solving the problem requires a very detailed scientific hydro-geoecological study of each specific site. The study should involve a set of field, laboratory, and study models. The main purpose of this study is long-term forecast and quantitative assessment of the negative processes related to the pollution with metals, and the identification of appropriate recovery measures. Undoubtedly, such a study must precede any investments in mining and mineral processing activities.

**Acknowledgments:** This work has been carried out in the framework of the National Science Program "Environmental Protection and Reduction of Risks of Adverse Events and Natural Disasters", approved by the Resolution of the Council of Ministers № 577/17.08.2018 and supported by the Ministry of Education and Science (MES) of Bulgaria (Agreement № DO-230/06-12-2018).

### References

Aleksander-Kwarczak, U., D. Ciszewski. 2016. Pollutant dispersal in groundwater and sediments of gaining and losing river reaches affected by metal mining. – *Environmental Earth Sci.*, 75, 9, 15 p. doi:10.1007/s12665-015-4859-8.

Antonov, D., N. Stoyanov, A. Benderev. 2019. Using Pedotransfer Function (PTF) analysis in the assessment of the parameters of potential radionuclide transport through the vadose zone of PRAW "Novi Han" – an initial stage of a model case study. – *Geologica Balcanica*, 48, 2, 3-12.

- Arranz-González, J. C., V. Rodríguez-Gómez, E. del Campo, L. Vadillo-Fernández, F. Fernández-Naranjo, J. Reyes-Andrés, R. Rodríguez-Pacheco. 2016. A methodology for ranking potential pollution caused by abandoned mining wastes: application to sulfide mine tailings in Mazarrón (Southeast Spain). – *Environmental Earth Sci.*, 75, 656. doi:10.1007/s12665-016-5495-7.
- Bain, J. G., K. Mayer, D. Blowes, E. Frind, J. Molson, R. Kahnt, U. Jenk. 2001. Modelling the closure-related geochemical evolution of groundwater at a former uranium mine. – *Journal of Contaminant Hydrology*, 52, 1-4, 109-135. doi:10.1016/s0169-7722(01)00155-3.
- Casagrande, M. F. S., C. Moreira, D. Targa. 2019. Study of generation and underground flow of acid mine drainage in waste rock pile in an uranium mine using electrical resistivity tomography. – *Pure and Applied Geophysics*, 177, 2, 703–721. doi:10.1007/s00024-019-02351-9.
- Kolev, S., V. Hristov. 2018. Groundwater rebound in "Druzha" uranium mine (SW Bulgaria) after cessation of mining activities. – *Proceedings of 18th international multidisciplinary scientific geoconference SGEM 2018*, Vol. 18, Issue 12, 317-324.
- Luo, C., J. Routh, M. Dario, S. Sarkar, L. Wei, D. Luo, Y. Liu. 2020. Distribution and mobilization of heavy metals at an acid mine drainage affected region in South China, a post-remediation study. – *Science of the Total Environment*, 724, Art. 138122, 18 p., doi:10.1016/j.scitotenv.2020.138122/s0169-7722(01)00155-3.
- Moyé, J., T. Picard-Lesteven, L. Zouhri, K. El Amari, M. Hibti, A. Benkaddour. 2017. Groundwater assessment and environmental impact in the abandoned mine of Kettara (Morocco). – *Environmental Pollution*, 231, 899–907. doi:10.1016/j.envpol.2017.07.044.
- Oliás, M., C. Cánovas, M. Basallote, F. Macías, R. Pérez-López, R. González, J. Nieto. 2019. Causes and impacts of a mine water spill from an acidic pit lake (Iberian Pyrite Belt). – *Environmental Pollution*, 250, 127-136. doi:10.1016/j.envpol.2019.04.011.
- Stoyanov, N., S. Kolev, V. Petrov. 2018. Prognosis of contaminants mass transport in groundwater after cessation of uranium mining in Momino deposit (South Bulgaria). – *Proceedings of 18th international multidisciplinary scientific geoconference SGEM 2018*, Vol. 18, Issue 12, 593-600.
- Stoyanov, N., S. Bratkova, S. Dimovski. 2019. Mathematical models of contamination with heavy metals from the abandoned mines in the Madjarovo ore field, Eastern Rhodopes. – *Journal of Mining and Geological Sciences*, 2, Number 1, 95-100.
- Stoyanov, N. 2019. *Matematischesko modelirane v hidrogeologiyata. Chisleni 3D modeli po metoda na krainite razliki*. Vanio Nedkov, Sofia, 246 p. (in Bulgarian)
- Wang, Y., R. Dong, Y. Zhou, X. Luo. 2019. Characteristics of groundwater discharge to river and related heavy metal transportation in a mountain mining area of Dabaoshan, Southern China. – *Science of the Total Environment*, 679, 346–358. doi:10.1016/j.scitotenv.2019.04.273.

## TYPES PASSPORTS FOR ROOFBOLTING FOR CROSSES ON BROAD ROADS WITH HYDRAULIC TILTING FRICTION ANCHORS IN THE CONDITION OF THE MINE „KOSHAVA“, „GYPSUM“, JSC

**Georgi Stoyanchev<sup>1</sup>, Krastyu Dermendzhiev<sup>2</sup>, Georgi Dachev<sup>3</sup>**

<sup>1</sup> University of Mining and Geology “St. Ivan Rilski”, 1700 Sofia; g.stoyanchev@mail.bg

<sup>2</sup> University of Mining and Geology “St. Ivan Rilski”, 1700 Sofia; krderm@mgu.bg

<sup>3</sup> University of Mining and Geology “St. Ivan Rilski”, 1700 Sofia; georgidachev87@gmail.com

**ABSTRACT.** As a result of studies and expert evaluations carried out of different types anchors been preferred the hydraulically expending anchor is selected as the preferred in mine conditions for Koshava. Based on this anchor have been proposed, analyzed and investigated different schemes of passports for roofbolting the crosses of the main mine workings. As finally results was suggested four types passports linked to the specific geomechanical mining conditions.

**Keywords:** rock bolting, geomechanical condition, gypsum

### ТИПОВИ ПАСПОРТИ ЗА ЗАКРЕПВАНЕ НА КРЪСТОВЕ НА КАПИТАЛНИ ИЗРАБОТКИ С ХИДРАВЛИЧНО РАЗПЪВАЩ СЕ ФРИКЦИОНЕН АНКЕР ЗА УСЛОВИЯТА НА МИНА „КОШАВА“, „ГИПС“ АД

**Георги Стоянчев<sup>1</sup>, Кръстю Дерменджиев<sup>2</sup>, Георги Дачев<sup>3</sup>**

<sup>1,2,3</sup> Минно-геоложки университет „Св. Иван Рилски“, 1700 София

**РЕЗЮМЕ.** В резултат от извършени изследвания и експертни оценки на различни типове анкери в условията на мина „Кошава“, като предпочитан за основен крепежен елемент е избран хидравлично разпъващ се фрикционен анкер. На базата на този анкер са предложени, изследвани и анализирани различни схеми на паспорти за крепене на кръстовете на главните минни изработки. Като краен резултат са предложени четири типа паспорта на крепене обвързани с конкретното геомеханично състояние на масива около кръстовете.

**Ключови думи:** анкери, геомеханични условия, гипс

### Passports for fastening the crosses of the capital constructions in the conditions of the Koshava mine

For the conditions of the mine, two standard passports have been developed and applied for fastening the crosses of the capital mines (Stoyanchev and Dermendzhiev, 2019).

The applied calculation scheme for determining the expected rock pressure is based on the hypothesis in which a peeling plate with a thickness of about 1.1 m is formed in the ceiling of the workpiece over time. This plate is sewn to the rest of the sturdy top with „Koshava“ anchors. The volume and weight of this detached part also form the expected rock pressure. According to the calculated rock scale, the scheme of placement of the anchors in the ceiling and the fastening passport is formed.

The anchors used in the type passports consist of a plastic anchor and an anchor steel rod 1.2 m long and 16 mm in diameter. They are accompanied by a rectangular plate with dimensions 100x100x10 mm. The anchors have a density of 0.69 pcs / m<sup>2</sup>. The available scheme is square with a distance between the anchors of 1.2 m. The distance between the anchors is determined on the basis of the expected bearing capacity of the anchor from 25 to 30 KN.

The application of this type passport is for relatively strong and stable tops without expected peeling and destruction of the top. For strong tops but with expected partial delamination of the top, another standard scheme of fastening passport is applied.

This scheme has the same elements and parameters of the anchor network as in the first scheme, but also includes the undertaken network-garden type. The application of this passport is for relatively strong tops but with expected partial delamination of the top.

Both passports ensure a stable condition of the crosses of the capital works in the mine. Their application is based on a detailed assessment of the mining-geological and mining-technical conditions and the behavior of the massif in the cross.

### New anchor fasteners

In the period October 2018, February 2019 in the conditions of the Koshava mine a wide study of the behavior and bearing capacity of different types of friction anchors was conducted (Stoyanchev and Dermendzhiev, 2019). Based on the results of these studies (Stoyanchev and Dermendzhiev, 2019; Design of a standard passport..., 2019; Dermendzhiev and Stoyanchev, 2019), it was decided for the conditions of the mine to develop new standard passports for fastening the

crosses of the capital works. The best-performing hydraulically extensible friction anchor "HR" should be used as the basis of standard passports.

For the development of different variants of passports for fastening with a hydraulically extensible friction anchor, specialized model studies were made on the interaction of the array with the anchor fastening systems and the expected condition of the crosses. The research systems were performed on the basis of average for the mine mining-geological and mining-technical conditions and physical-mechanical properties of the gypsum layer, as an accommodating array of capital mining.

The gypsum layer includes different types of gypsum. Its thickness is in the range, 25.0 to 29.0 m. Classification tests of the gypsum layer according to the international standard have not been performed. The data obtained in 1989 presented in Table 1 can be considered as the most reliable. The strength of uniaxial pressure  $\sigma_{ucs}$  varies from 14 to 17 MPa. The tensile strength  $\sigma_t$  from 1.3 to 1.5 MPa.

The depth of development is Haver. = 300 m, at average volume weight of the weaker rocks  $\gamma_{aver.} = 22,5 \text{ kN} / \text{m}^3$ . The average strength of the gypsum layer at uniaxial pressure is 15 MPa. The coefficient of structural weakening is  $K_{str.} \approx 0,5$ , and the angle of internal friction,  $\varphi \approx 45^\circ$ .

The deformation parameters of the gypsum massif are characterized by:

- Dynamic modulus of elasticity,  $E_d \approx 15 - 35 \text{ GPa}$ ;
- Poisson's ratio,  $\mu \approx 0,3 - 0,35$ ;
- Modulus of elasticity  $E \approx 13,5 \text{ GPa}$ .

The average volume weight of the gypsum layer varies in the range  $\gamma_{aver.} \approx 22 - 23 \text{ kN} / \text{m}^3$ , average  $\gamma_{aver.} \approx 22,1 \text{ kN} / \text{m}^3$ .

The main top is about 14.5 m and is made of clays, marls of clay limestones with a volume weight of about  $22 \text{ kN} / \text{m}^3$ . The upper part is made of light gray clay with a thickness of about 5 m. immediately below it is a gypsum with clay solder with a thickness of 2.5 m.

Table 1. Strength characteristics of the gypsum layer

No in order	Type of gypsum	Uniaxial compressive strength $\sigma_{ucs}$ , MPa	Uniaxial tensile strength $\sigma_t$ , MPa	Ratio $\sigma_{ucs} / \sigma_t$
1	Shell gypsum	14,32	1,30	11,03
2	Layer gypsum	16,75	1,36	12,22
3	Medium to wholesale layer gypsum	14,77	1,39	10,66
4	Medium layer gypsum	14,81	1,45	10,18
5	Marl in the bottom	2,88	0,92	2,26

➤ The fastening system is based on friction hydraulically extending anchors "HR" with the following characteristics:

1. Load-bearing capacity - 50 KN;

2. Length of the anchor - 1.5 m;

➤ Anchor tube thickness  $\delta = 3.2 \text{ mm}$ , diameter  $\phi = 42 \text{ mm}$ ; anchor The fastening system is based on friction hydraulically extending anchors "HR" with the following characteristics:

3. Load-bearing capacity - 50 KN;
4. Length of the anchor - 1.5 m;
5. Anchor tube thickness  $\delta = 3.2 \text{ mm}$ , diameter  $\phi = 42 \text{ mm}$ ; anchor hole 45 mm;
6. The cross-sectional area of the anchor pipe is  $235 \text{ mm}^2$ ;
7. Modulus of elasticity of steel  $80\,000 \text{ MPa}$ ;
8. Bound Strength -  $40 \text{ kN} / \text{m}$  or (45). Limit tensile strength;
9. Out of plane Spacing - 1.5 m (distance between anchors);
10. Bound Shear Stiffnes -  $38 - 40 \text{ kN} / \text{mm}$  (cut-off force).

Preliminary studies have found that it is very difficult to form a calculation scheme to determine the load-bearing capacity and parameters of a combined fastening with anchors. The tested anchors of the "Koshava" type have a bearing capacity of 2.5 t - 3.0 t (axial force) but do not work in a system that ensures the overall stability and safety of the upper waist in case of possible stratification of the upper.

In the first variant of anchor fastening systems with "HR" anchors, the anchors are mounted with a bearing plate independently without connecting them with grips.

The anchors are at a distance of 1.0 m from the wall, and the distance between them is 1.5 m. The total number of anchors in the proposed scheme is 31 anchors, of which 24 outside the intersection and 9 inside the intersection. In fig. 1 shows the scheme of disposal of the "HR" anchors on the ceiling of the capital construction.

➤ The second considered fastening system consists of a combined fastening - hydraulically extending anchors "HR" and connecting grips. The grips are metal rails supported by the anchors at both ends by means of planks. The software of the Canadian company Rocscience was used for the research for geomechanical analysis of the proposed variants of fastening passports. The studied parameters through the analysis are mainly acting pressure (vertical) stress -  $\sigma_1$  in the waist ceiling and coefficient of stability (factor of safety)  $K_{stab.}$  on the massif around the waist.

Phase<sup>2</sup> software ver. 9.0 makes it possible to study various fastening structures, as well as to study the condition of mine workings in unattached massifs. The main stages in the formation of the crossroads and the change in the state of the massif ( $\sigma_{ij}$ ,  $K_{stab.}$ ) In the formation of the crossroads are studied.

The analysis of the visual results from the research of the crosses of the capital works shows the following:

In the ceiling of the crosses of the unmounted work, pressure stresses with a value of 1.0 to 1.5 MPa occur. In the corners, the values are larger, but cover larger areas of the array. When fastened, the values of the normal voltage decrease below the above values, and the safety factor of the array increases from 1.0 to 1.5 and more. In general, in the case of loose and anchored construction, the values of the normal stress are less than the compressive strength of the gypsum mass, it is stable and the coefficient of resistance is from 1.0 to 1.3. This shows that the top of the crosses is stable

at the time of construction, as well as after fastening with anchors.

When carrying out the workings - development of the waist in area and length, changes occur both in the size and the area of influence of the main normal voltage and in terms of the coefficient of resistance. The main stress increases from 1.0 to 2.6 MPa in height from 1.5 to 1.6 m in the top. The coefficient of resistance is different in different fastening systems. In the case of anchor fasteners of the first type, without grips, only with plates, the influence of the fasteners on the normal stress and stability is represented by  $K_{stab}$ . is insignificant. In the presence of grips and connection of anchors in the fastening system, the influence of the fasteners on the stresses and their distribution by area and height is positive, and the stability of the fastening-array system is significantly better,  $K_{stab}$ . 2-2.5.

Based on these main results and conclusions, we propose to apply in the crosses of the Koshava mine a fastening system of a hydraulically extending anchor "HR" in combination with grips (metal rail), plates and, if necessary, to use a net.

The realization of the bearing functions of the anchor fastening in the conditions of the mine is expected to take place in time, during the development of the deformation process, delamination and less frequent destruction of the top.

With these expectations, we recommend that the hydraulically extending anchors be 1.5 and 2.0 m long, depending on their position in a cross area.

### **Model schemes for passports for securing capital works in the conditions of Koshava mine**

Based on the analyzed models for geomechanical condition of the crosses of the capital works, it was found that the applied type of anchor "Koshava", as well as other types of anchors in a network with a distance between the anchors more than 0.5 m does not achieve the desired support effect do not work as a fastening system. Therefore, in the future system based on anchors, it is necessary to connect them by means of techniques and form on this basis a fastening system. Based on this scheme, 7 different models of anchor fastening systems are considered, which are used to ensure the stability and safety of the crosses in the mine.

Six of the schemes use "HR" type anchors with a length of 1.5 m, located in a square mesh of 1.5x1.5 m. The differences in the schemes are in the presence of anchoring elements and the type of these elements (approaches, self-tensioning plates, different types of nets), (Design of a standard passport..., 2019).

In the seventh scheme, the distance between the anchors is 1.2 m, as in the passports of the mine. The anchor elements are taken in rows as in schemes 5 and 6 (Design of a standard passport..., 2019). In addition to grips, a garden net used by the anchor plates is also used.

This scheme is designed for complex geomechanical conditions with expected peeling of the top and collapse over time.

During the discussion of the options, the conditions under which the expected stability and security of the fixed space should be applied were assessed. The possibility of applying anchors of different lengths is not excluded. The schemes can be combined with anchors with a length of 1.5, 2.0 and more meters.

### **Discussion of model schemes and proposals for type passports**

The developed model schemes differ from the ones applied in the mine by the type of the applied anchor. The hydraulically extending anchor has a higher bearing capacity /60-70kN/ and has certain technological advantages (Design of a standard passport..., 2019; Dermendzhiev and Stoyanchev, 2019). The use of this type of anchor makes it possible to reduce the number and density of anchors at the same expected rock pressure. Therefore, it was decided to dilute the anchor net to 1.5x1.5 m. This dilution maintains larger areas over which the anchor does not have a large impact. Therefore, the anchor nets must have approaches, through which an anchor fastening system is formed, which will provide the necessary bearing capacity and safety in case of different behavior of the array from the top.

When discussing the expected behavior of the array in the crosses of the capital works, four types of geomechanical conditions were formulated, such as:

Slight / №1 /, Sturdy resistant massifs in the top without expected stratification of the layered layers and subsequent destruction;

Medium / №2 /, Medium strong, but steadily layered massifs with expected exfoliation on planes of stratification in time;

Heavy / №3 /, Medium resistant to unstable layered massifs with expected exfoliation on planes of stratification and self-collapse in time;

Very heavy / №4 /, Unstable layered massifs with expected destruction and exfoliation on planes of stratification and self-collapse in time. Expected increase in the height of the peeling arch.

Based on the standard conditions formulated above, it was decided to design four standard passports for fastening the crosses. The passports should be based on the hydraulically extending "HR" anchor (Stoyanchev and Dermendzhiev, 2019; Dermendzhiev and Stoyanchev, 2019). Depending on the assessment and conditions, the anchors should be 1.5 and 2.0 m long. For geomechanical conditions №4, the length of the anchors is assumed to be 2.0 m.

The proposed solutions for standard passports for fastening crosses in the capital mining works of the Koshava mine for the different type of mining geological and mining technical conditions are presented in more detail in Design of a standard passport..., 2019, Annexes №1-№3.

The analysis of the expected behavior of the array from the production ceiling and the technological capabilities of the passport using busbar grips connecting the anchors shows the following: the installation of the anchors connected to the rails is labor intensive due to the standard sizes of the rails and the distances between the anchors; when interconnecting the anchors with rails, it is necessary to perform disassembly and assembly works. This will slow down the fastening operations and will require a longer stay of the fasteners in an unsecured space; presence of many fasteners that need to be connected; need for precise aiming and drilling of the anchor holes.

The above-mentioned shortcomings of the fasteners in the recommended passports presented in (Design of a standard passport..., 2019) led to the decision to replace the connecting plates with a special type of steel mesh with increased load-bearing capacity.

Under the first type of geomechanical conditions, the parameters of the anchor network are preserved using a "reinforced hexagonal mesh" as a connecting element. Under the second type of conditions, a lighter type of electric welded mesh is used as the connecting anchor unit. In the third type of "heavy" conditions, the connecting anchor unit is a heavier type of electric welded network. Under very severe conditions, the length of the anchors is 2.0 m and the distance between them is 1.2 m. The connection between the anchors is with an electrowelded mesh.

The general scheme of the type passports and the characteristic fastening parameters are given in Fig.1. The parameters of the type passports and the geomechanical conditions for their application are given in Table №2.

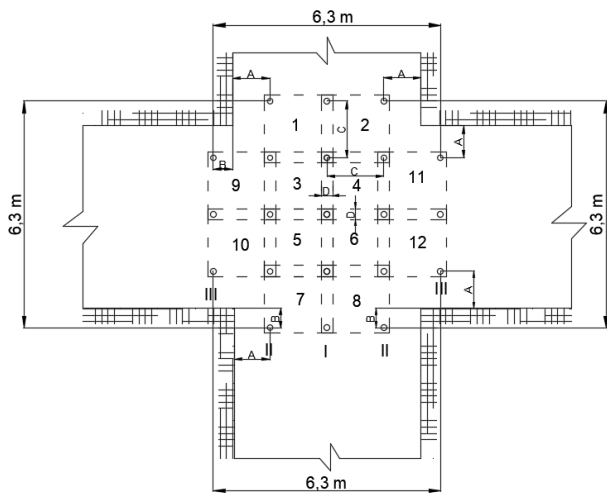


Fig. 1. General scheme of the type passports and the characteristic fastening parameters

Table 2. Parameters of the type passports and the geomechanical conditions for their application

Typical conditions and parameters of the passport	Types of passports			
	№1	№2	№3	№4
Geomechanical type conditions	Slight /№1/	Medium /№2/	Heavy /№3 /	Very heavy /№4/
Anchor type	HR	HR	HR	HR
Anchor length, m	1,5/2,0	1,5/2,0	1,5/2,0	2,0
Parameters available on the anchors, m :A	1,0	1,0	1,0	1,0
B	0,5	0,5	0,5	0,2
C	1,5	1,5	1,5	1,2
Overlap D	0,15	0,15	0,10	0,10
Plank, dimensions m x m	0,15 x 0,15	0,15 x 0,15	0,15 x 0,15	0,15 x 0,15

Mesh, type	Hexagonal	Electrowelded		
		1,7 x 1,7	1,7 x 1,7	1,5 x 1,5
Canvas dimensions mech m x m	1,7 x 6,5	1,7 x 1,7	1,7 x 1,7	1,5 x 1,5
Mesh dimensions: Diameter of bodies, mm	3,0	4,0	5,0	5,0
Dimensions of the holes, m x m	0,1 x 0,1	0,15 x 0,15	0,1 x 0,1	0,1 x 0,1

### Conclusions

When sizing the anchor fasteners according to the so-called "set load" scheme and its placement in a network with a distance between the anchors of 0.8-1.0 m, the anchors do not work as a system and do not have a stabilizing effect on the fixed array. In these cases, regardless of the load-bearing capacity of the anchors used, they must be connected in a network by the use of various connecting units, such as grips, plates and nets. In this way, the fastener is formed as a system that provides the necessary load-bearing capacity and security of the fixed space.

The proposed standard passports for fastening the crosses of the capital constructions of the Koshava mine, developed on the basis of the hydraulically extending friction anchor / HR / and the additional connecting elements, create a real opportunity to ensure high stability and safety of the crosses in different mining and technical conditions.

The standard fastening passports are to be applied and adapted in the conditions of the mine.

### References

Nikolaev N, V. Parushev, Anchors and anchor fasteners for underground facilities "Technique", Sofia, 1985, 24 p.

Stoyanchev G., Kr. Dermendzhiev, Study of the behavior and bearing capacity of different types of anchors in the conditions of mine "Koshava", "Gypsum" AD. Research project report, 2019 Koshava Mine Archive.

Design of a standard passport for fastening the crosses of the capital works with hydraulically extending fasteners in the conditions of the mine "Koshava", "Gypsum", AD., Report under contract I-285, Director G. Stoyanchev, Archive of MSU, December 2019.

Dermendzhiev Kr., G. Stoyanchev, Investigation of the parameters and capabilities of a pipe anchor with hydraulic tensioning. Fourth nat. scientific and technical conf. Technologies and practices in underground mining and mining, Devin, September 23-26, 2019: Sat. report pp. 121-126.

## COMBINED METHODS FOR EXTRACTION OF LARGE DIMENSION STONE BLOCKS FOR DECORATIVE PURPOSES

**Nadezhda K. Stoycheva**

University of Mining and Geology "St. Ivan Rilski", 1700 Sofia; nandy\_f@abv.bg

**ABSTRACT.** The report discusses combined methods for extraction of large rock blocks. For primary separation of the lamellae from the main rock body and its splitting into smaller blocks, suitable for transportation and subsequent processing to finished products, different types of stone cutting machines and precise drilling and blasting activities are used. The main problem when working with high-speed or industrial explosives for extracting large blocks of expensive stone is the aggressive impact of the shock wave on the solid medium. The overpressure of the shock wave front during detonation shatters the rock around the blast hole and can cause cracks in unwanted directions. Under complicated conditions, it is necessary to interrupt the rock environment in advance to shield the propagation of pressure waves caused by the detonation of larger explosive charges. Techniques that combine the simultaneous use of explosive and mechanical methods to separate rock blocks from the massif are discussed. Emphasis is placed on various methods for protecting the surfaces of the rock block and the main massif from unwanted cracking during blasting activities.

**Keywords:** extraction of rock cladding materials; splitting of dimension stone blocks; precise blasting; low explosives; stone cutting machines

### КОМБИНИРАНИ МЕТОДИ ЗА ДОБИВ НА ЕДРОГАБАРИТНИ ОРАЗМЕРЕНИ КАМЕННИ БЛОКОВЕ ЗА ДЕКОРАТИВНИ ЦЕЛИ

**Надежда К. Стойчева**

Минно-геоложки университет „Св. Иван Рилски“, 1700 София

**РЕЗЮМЕ.** В доклада са разгледани комбинирани методи за добив на едрогабаритни скални блокове. За първично отделяне на ламелите от основното скално тяло и разцепването му на по-малки блокове, подходящи за транспортиране и последваща обработка до готови продукти се използват различни видове каменорезни машини и прецизни пробивно-взривни работи. Основен проблем при работа с високоскоростни експлозиви за извличане на големи блокове от качествен материал е агресивното въздействие на ударната вълна върху твърдата среда. Свърхналягането на фронта на ударната вълна при детонацията раздробява скалата около взривната дупка и може да причини пукнатини и в нежелани посоки. При усложнени условия е необходимо предварително прекъсване на скалната среда за екраниране на разпространението на вълни на натиск, причинени от детонацията на по-големи заряди. Обсъдени са техники, които комбинират едновременното използване на експлозивни и механични методи за отделяне на скални блокове от масива. Акцентира се върху различни методи за защита на повърхностите на скалния блок и на основния масив от нежелано напукване при взривно въздействие.

**Ключови думи:** добив на скално-облицовъчни материали; отцепване на оразмерени блокове; прецизно взривяване; ниско-скоростни експлозиви; каменорезни машини

### Introduction

The modern techniques and technological schemes in the extraction of ornamental stone aim at high-performance and efficient extraction with minimal losses of valuable raw material. Therefore, it is crucial to select the most rational way to discover the deposits, as well as to apply the appropriate technology for the specific conditions with relevant mechanization. The use of modern technologies and their rapid development, which has been observed over the last 50 years, is a clear sign of the need for this type of minerals. The technologies and methods considered in the present study are focused on separating the rock blocks by cutting from the massif.

#### Technologies for quarry extraction of dimension stone

The quarry stage of production has the following phases: preparation of the bench, separation of the primary lamella (whose size varies from ten to one hundred cubic meters) and finally dismantling of the rock lamella on the pit floor to be cut

into smaller blocks with commercial sizes. The technologies for extraction of natural stones are:

**Technology with drilling mechanization and wedge separation of the blocks from the massif.** In this method, the separation of the blocks from the massif is done by drilling and wedge works, which overcome the cohesion forces of the rock particles and disrupt their integrity. The main operations in this technology are two - drilling holes at a certain distance (vertical, horizontal or inclined) and splitting with different types of wedges. Nowadays, hydraulic wedges are used - both manual and automated. The holes are drilled along the contours of the block. The depth, diameter and distance between them depend exclusively on the physical and mechanical properties of the rocks. The desired splitting occurs in the area between the perforations - the distance of least resistance on the rock.

**Technology with chain saw cutting machines.** Chainsaws are driven by electric engine. The essence of this technology is to make vertical and horizontal cuts with a cutting chain, which

is equipped with teeth made of hard steel or diamond. In a technological plan with chain saw stone-cutting machines, high productivity and large block sizes are achieved, if the mining and geological conditions allow it.

**Diamond wire cutting technology.** In general, this method is cutting the rocks by movement and applying the principle of abrasive wear on the rocks. The cutting element of the machine is the so-called "Diamond" wire. It is formed in a closed loop around the section which has to be cut. The cooling of the wire and the cleaning of the cut are guaranteed by a constant water supply. To ensure a closed loop, it is necessary to drill two intersecting holes in the massif. The wire passes through them so as to obtain a closed circle. During the cutting itself, the machine, which most often travels on a rail track, moves away from the massif. In this way the wire is stretched and cuts optimally. Diamond wire stone cutting machines can operate in a wide range of angles to the face. They can change the directions of the "diamond" wire in terms of the type of cut and the specific situation.

**Technology with drilling mechanization and chemical agents.** This technology is based on the property of certain chemical compounds when wet to "absorb" water by binding it to their own molecules in the so-called "chelate coordination complexes". Upon apparent drying of the material, the water molecules appear to be part of the crystal lattice of the compound. This leads to a drastic increase in the coefficient of volumetric expansion. Thus, these substances, when placed in the drilled holes and in contact with water, are able to harden and expand after a period of time. In this way, they create stresses in the rocks up to 40-45 MPa. The essence of the technology is the same as in the drilling-wedge and drilling-blasting method. With the drilling mechanization (perforators, drilling rig boomers, jumbo drillers or borers) vertical and horizontal holes with a diameter of 30-50 mm are perforated along the contours of the block. The distance between the holes depends on the specific conditions, the type of rocks extracted and the expansion capacity of the chemical compound.

**Technology with flame-jet cutting.** Thermal "cutting" of rocks is an effective non-contact method. The so-called thermo-cutters (thermal burners, flame-jets, air-jet burners, etc.). They are used for the destruction of hard rocks, such as granite, granodiorite, sandstones and others with quartz content. Flame-jets are mainly used for making incisions in the rock massif, but can also be used for drilling in the massif and secondary fragmentation of rocks.

**Technology with water jet cutting.** In general, this technology is the destruction of rocks by means of a high-pressure water jet (about 350 MPa). The cutting of the rocks itself is not done by friction, impact or chemical reaction, but by breaking and separating the constituent compounds of the material. The bonds between the minerals in the rock medium are literally falling apart due to the thrust of the high water pressure. The system of the water jet cutting machine consists of two main components - a pressure generator and a nozzle.

**Technology with drilling equipment and energy of the explosion.** This method of extraction comes into use when the application of stone cutting machines from a practical, economic and environmental point of view are irrelevant. It is workable for extraction of ornamental stones with compressive

strength greater than 100 MPa, strongly cracked rocks, with the content of hard and highly abrasive inclusions in the rock mass, as well as in the presence of horizontal cracks in rocks such as granite, gabbro, limestone and others. In the presence of layers over 1.5 m thickness, when mechanical splitting methods are not effective, as well as in the development of inclined layers up to 40°, this technology is applicable also.

The sequence of the technology is as follows: blastholes (horizontal and/or vertical) are drilled in the chosen direction for splitting the rocks. Drilling mechanization is the same as in the drilling-wedge method. The diameter of the blast-holes is between 20 and 50 mm. In some cases drillings with larger sizes are applied. Then, a multi-deck charges of high-explosive or a certain number of detonating cord threads, could be loaded in the drilled holes.

**Combined technologies for extraction of rock cladding materials.** They are a blend of some of the methods already mentioned. The parameters and the construction of the quarry with applied combined technology depend on the specific mining and geological conditions of the deposit and the technical characteristics of the used mechanization. The complex technology is flexible and allows to use the advantages of the separate technologies, which when properly matched with appropriate equipment can afford very good results for obtaining higher quality blocks and higher yield. One of the most popular/common combined methods is those between mechanical pre-cutting and controlled blasting with various explosive.

### Advantages and drawbacks when using high explosives or non-detonating charges

Knowing the assets and shortcomings of using various explosives is crucial for managing blasting energy and preventing the harmful effects of the detonations.

The main advantage of high explosives is the low price. They easily cause the formation of a crack in the rock thanks to the energy of the pressure shock wave. This is achieved by drilling a series of blast holes in a given plane, which are charged and detonated simultaneously. The resulting shock waves are superimposed along the line between the boreholes, increasing the compressive forces generated in this plane. The compressive forces cause tensile forces in the rock perpendicular to the direction of action. In this way, splitting takes place along the line between the holes as a result of exceeding the tensile strength of the rock. With a small amount of industrial explosive, the necessary clefts for separation of the dimension stone could be achieved. Their disadvantage is the difficult control of the explosive energy, released by the detonation. In many cases, this energy causes the formation of parasitic cracks, which degrade the performance of the material and lead to a decrease in yield.

Modern non-detonating explosives combine the throwing properties of the blasting gunpowder with preferences such as: water resistance, improved energy, reduced emissions of harmful gases and solid particles. An important advantage of deflagrating charges is their non-aggressive impact on rock splitting. It is obtained due to the slower chemical reaction. The expansion of the hot gaseous products creates compressive forces on the walls of the blast holes that overcome the tensile strength of the rock. The result is a smooth slit in the specified direction, without unnecessary cracking of the material.

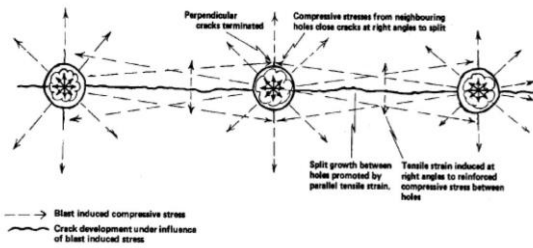


Fig.1. Crack-formation process

Another asset of ready-made non-detonating explosive cartridges is their low hazard class in accordance with international agreements and the national laws of most countries. A lighter conditions for acquisition, transportation, storage and use contributes to cost reduction. Their application is accompanied by the absence of air blast, insignificant fly-rocks and lack of seismic vibrations. For these reasons, quarries for decorative rock materials in developed countries are gradually putting into operation the new generation of propellant based blasting devices. These charges are a successful solution against damages, caused by conventional explosives during the extraction. At the same time, they are the better substitute for blasting gunpowder.

A drawback when working with non-detonating charges is the relatively higher cost of the products, compared to traditional explosives. Another negative is the relatively higher consumption of explosives to form one square meter of sloping surface. As a disadvantage, it can also be noted the need for a reliable plug, which ensures the retention of exhaust gases to achieve optimal blasting effect.

### Methods for limiting the harmful effects of the propagation of the pressure wave in the rock medium

In the extraction of dimension stones, drilling and blasting activities are applied for removal of soil layers and rocks of poor quality (overburden), as well as for primary separation of the lamella from the massif and its splitting into smaller blocks, suitable for transportation and post-processing to finished products. In these operations, a risk of creating compressive stresses and irreversible deformations in the valuable raw material is existing. This requires additional measures to protect the windrow surfaces and the rock body in depth.



Fig.2. Bench blasting for removal of waste rock in dimension stone quarry

The most effective method for limiting the propagation of a pressure wave in the massif is to break the rock medium by creating a shielding surface for wave reflection. The ways for intersection of the rock are: mechanical cutting with diamond-wire cutters, cutting with chain-saw cutters, cutting with a series of overlapping perforations and by presplit blasting.



Fig.3. Decoupled multi-deck chained charge loading

Presplit blasting with industrial explosives in the separation of rock blocks has been used less and less in recent years. The blasting action caused by the detonation and the high energy of the shock wave are prerequisites for the formation of unwanted cracks in the extracted lamella and the residual massif. The danger of damaging high-quality material forces quarry owners to look for alternative approaches with reduced risk. Presplit blasting finds greater application in removing the overburden.



Fig.4. Pre-split blasting preparation

The methodology is based on the creation of a shielding surface to separate low-quality material from the deposit, which is intended for extraction. It is performed before the main blasting to break up the overburden. This surface is usually performed in the vertical direction.



Fig.5. Split-blasting for removal of waste rock close to high quality material



**Fig.6. Pre-splitting crack and displacement of the low quality limestone after split-blasting**



**Fig.7. Effect of smooth blasting on the limestone wall after excavation**

Under suitable conditions for access of drilling equipment in the face, a presplit row can also be perforated in the horizontal direction. The horizontal shielding surface is performed over an existing vein or over the visual boundary between the overburden layer and the high quality material layer, parallel to the occurrence direction.



**Fig.8. Horizontal drill holes for pre-split blasting**

Depending on the diameter of the drilling chisel and the calculated specific explosive consumption, it is desirable to drill the horizontal holes at a distance of 1.0 - 1.5 m above the extraction layer. Presplit blasting is carried out with garland charges of high explosives.



**Fig.9. Horizontal split crack in limestone**

The section with a curve contoured by shielding surfaces is considered as prepared for fragmentation with blasting drill-holes. The charges in production blast-holes on the periphery of the blast field should be with 40-60% less mass than the others. It is recommended that the horizontal shielding row to be perforated 1.5 - 2 m below the level of the bottoms of the production drill-holes. All this is done to ensure that when the overburden is fragmented by detonation, the cracking will not reach the high quality stone. In cases where no clear boundary is observed and there is no natural crack that separates the quality material from the unnecessary material in the massif, it is recommended that it should be cut mechanically. This interruption of the rock environment is a reinsurance against the transmission of compressive stresses from the presplit blasting to the deposit, intended for subsequent extraction.

### Combined methods for removing the overburden during extraction of dimension stones

In some deposits of dimension stones, the ledges with high quality raw material are not compact, but are surrounded by rocks with poor exploitation characteristics. The quarry is developed in areas around the relevant ledges, and the unnecessary rock mass is excavated and removed. Each section is developed with faces and trenches on extraction benches to provide open surfaces and easy access. Proximity to the valuable raw material requires more attention and precision in removing the useless rock. The last remaining volumes of the overburden are approached literally as a quality material - taken out in large blocks. Subsequently, they are crushed on the pit floor and transported. In such situations it is necessary to use a combination of mechanical and explosive methods for separation and fragmentation of the blocks with waste rock.

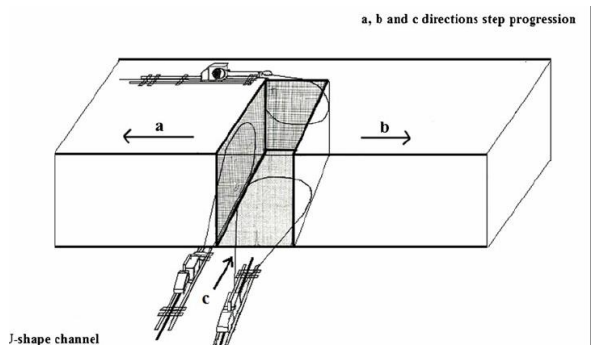


**Fig.10. Diamond saw cutting for separation of the stone-volume to be crushed**

The maximum volume of the block is determined according to the parameters of the bench and the capabilities of the available mechanization. Depending on the access, the contours are cut with chain-saw cutters and diamond-wire cutters. If any of the pre-cuts cannot be made, it should be replaced with pre-splitting blast holes in a row. If a wider protective crack is required, pre-split blast holes could be perforated parallel to the finished cuts along the inner contour of the block. The distance from the pre-splitting row to the pre-cut should not be less than 0.50 m. The blast field has to be perforated with vertical boreholes, and the parameters of the blasting pattern should be calculated for a "charge of low swelling", depending on the diameter of the chisel of the drill. This reduced explosive effect is achieved by decreasing the relative consumption of the explosive.



**Fig.11. Pre-cutted along the perimeter block of overburden, repaired for loading with explosives.**

The distance from the peripheral production blastholes to the mechanical pre-precision should not be less than the distance between two production blastholes. It is preferable to form oversized boulders, rather than transmitting a shock wave when shrinking the narrow pre-cut.



**Fig.12. Effect of mechanical pre-cutting**

For a more even distribution of the explosive energy along the perforation, a multi-deck design of the charges in the blastholes is recommended. To better control the propagation of the blast-induced seismic vibrations in the massif, the individual charges should be initiated with a millisecond delay. When using an inert intermediate stemming, the bottom charge

in each of the blastholes explodes 25 ms before the upper charge. Depending on the shape of the undermining cut, the smallest possible number of blastholes has to be initiated simultaneously in a series. To achieve really low levels of vibration, it is allowed the blastholes to be sequentially initiated one after another. When the charges work individually, the fragmentation of the muckpile also decreases. There are practically no strict requirements for the granulometry of the overburden. The size of the boulders is determined by the cargo space and the technical parameters of the available transport equipment.



**Fig.13. Muckpile of waste rock after blasting of the pre-cutted block**

Due to the weak blasting effect, the crushed rock remains as a compact pile within the bench. During the excavation, a perfect separation along the perimeter of the preliminary cuts was observed. There are no visible traces of damage and deformation on the smooth vertical walls of the residual massif.

## Conclusions

In developed countries, ornamental stone quarries are using high explosives only to remove overburden. For the fine work of displacement the primary lamella and the splitting operations for its cutting into commercial-sized blocks, they rely mainly on combined methods and partly on low-speed explosive charges. Thus, the losses from the cracked outer layer of the rock materials with first-class decorative characteristics are drastically reduced.

The desired splitting with high-speed explosives is achieved through the optimal balance of the distance between the holes and the power of the explosive. The tensile strength of the rock is exceeded only where there is an accumulation of shock waves, ie. along the line between the holes.

The application of combined methods, which include pre-contouring with mechanical cuts of the volume of waste rock intended for explosive crushing and removal, is a successful way to protect the deposit from cracking during blasting.

## References

- Belin V., Mitkov V., 2015. Vliyanie kachestva vzrivotnih materialov promishlenogo naznacheniya na effektivnosti drobleniya gomoy masi vzrivom, Informatsionno-analiticheskiy biyuletin ANO "Natsionalnaya organizatsiya

- inzhenerov-vzrivnikov v podderzhku profesionalnogo razvitiya”, № 2, pp. 37-39, ISSN 2411-491X. (in Russian)
- Boychev Y., Asenov S., 2018, “Pirotehicheski sastavi za neletalni svetlinnozvukovi sredstva”, ISBN:978-619-7246-20-9, ISSN:2367-7481, 614-620, National Academic Publishing House. (in Bulgarian)
- Boychev Y., 2018, “Pirotehicheski neletalni sredstva za zashtita”, National conference with international attendance “Defence Industry – Leader of the Innovations in Bulgaria”, 20.09.2018, Sofia, Bulgaria. (in Bulgarian)
- Mitkov V., 2007. *Proizvodstvo na eksplozivi za grazhdanski tseli*, ISBN 978-954-353-049-6. (in Bulgarian)
- Mitkov V., 2010. *Bezopasnost pri proizvodstvoto i upotrebatata na eksplozivi*, ISBN 978-954-353-131-8. (in Bulgarian)
- Shishkov P., Stoycheva N., 2018. “Savremenni vzrivni tehniki za dobiv na skalno-oblicovachni material” - *Mining and geology magazine*, 10-11, p.42-49, ISSN 0861-5713. (in Bulgarian with English abstract)
- Shishkov, P. 2019. *Spravochnik na vzrivnika*. Izdatelska kashta Sv. Ivan Rilski, Sofia - 244 p. ISBN 978-954-353-378-9. (in Bulgarian)
- Stoilova S., Mitkov V., Belin V., 2014. Analiz na vuzdeistviето na vazdushnata udarna valna za usloviyata na kariera “Tselovizhda” , *Annual of the University of Mining and Geology “St. Ivan Rilski”* – Sofia, v. 57, Part II: Dobiv prerabotka na polezni surovini, pp.108-110, ISSN 1312-1820, (in Bulgarian with English abstract).
- Stoyanov D., 1994. *Rakovodstvo za uprazhneniya po probivno-vzrivni raboti v otkriti rudnici, karieri i stroitelstvoto*, MGU, Sofia. (in Bulgarian)
- Stoycheva N., Shishkov P., 2019. „Innovative formulations for a new generation of low-speed explosive compositions, designed for blasting in tender conditions and for extraction of rock-cladding materials” – *Journal of Mining and Geological Sciences*, p.94 – 99, vol.62, Nr.2 (in English).

## ULTRASOUND-PROPELLED BIOMIMETIC NANOROBOT FOR TARGETING AND ISOLATION OF PATHOGENIC BACTERIA FROM DIVERSE ENVIRONMENTAL MEDIA

Svetlin Toshev<sup>1</sup>, Alexandre Loukanov<sup>1,2</sup>

<sup>1</sup> Laboratory of Engineering NanoBiotechnology, Department of Eng. Geoecology, University of Mining and Geology "St. Ivan Rilski" – Sofia, Bulgaria, svetlio\_13@abv.bg

<sup>2</sup> Division of Strategic Research and Development, Graduate School of Science and Engineering, Shimo – Ohkubo 255, Sakura – Ku, Saitama 338-8570, Japan, loukanov@mail.saitama-u.ac.jp

**ABSTRACT.** The artificial nanomachines have been demonstrated with their useful applications in the fields of bioanalytical diagnostics and environmental remediation. We designed ultrasound-propelled nanorobot, which was functionalized with cell membrane for targeting and isolation of pathogenic bacteria (e.g. *Escherichia coli*) from complex and diverse environmental media. Since the artificially prepared device was covered with cell membrane, i.e. membrane receptors were immobilized on its surface the resulted nanoscale invention was known as biomimetic nanorobot. It displayed rapid detection ability and prolonged acoustic propulsion in aqueous solution. The proposed design opens the possibilities for creation of a broad-spectrum detoxification and remediation robotic platforms.

**Keywords:** Biomimetic nanorobot, ultrasound-propelling, pathogenic bacteria isolation

### БИОМИМЕТИЧЕН НАНОРОБОТ ЗАДВИЖВАН ЧРЕЗ УЛТРАЗВУК ЗА НАСОЧВАНЕ И ИЗОЛИРАНЕ НА ПАТОГЕННИ БАКТЕРИИ ОТ РАЗНООБРАЗНИ ПРИРОДНИ СРЕДИ

Светлин Тошев<sup>1</sup>, Александър Луканов<sup>1,2</sup>

<sup>1</sup> Лаборатория Инж. Нанобиотехнология, Катедра „Инженерна геоекология“, Минно-геоложки Университет „Св.Иван Рилски“ – София, България, svetlio\_13@abv.bg

<sup>2</sup> Отдел за стратегически изследвания и развитие, Факултет по наука и инженерство, Университет Сайтама, Шимо-Окубо 255, Сакура-ку, Сайтама 338-8570, Япония, loukanov@mail.saitama-u.ac.jp

**РЕЗЮМЕ.** Изкуствените наномашини са демонстрирани с техните полезни свойства в области, като биоаналитична диагностика и екологично възстановяване. Ние проектирахме наноробот, задвижван от ултразвук, който беше функционализиран с клетъчна мембрана за насочване и изолиране на патогенни бактерии (например *Escherichia coli*) от комплексни и разнообразни природни среди. Тъй като изкуствено конструираното устройство беше покрито с клетъчна стена, т.е. мембранните рецептори бяха имобилизирани на повърхността му, полученото изобретение беше известна, като биомиметичен наноробот. Той показа способност за бърза детекция и продължително акустично задвижване във воден разтвор. Предложеният дизайн отваря възможности за създаване на широкоспектрни роботизирани платформи за детоксикация и ремедиация.

**Ключови думи:** Биомиметичен наноробот, ултразвуково задвижване, изолиране на патогенни бактерии

### Introduction

The development of artificial nanomachines and nanorobotics with wide range of applications has raised substantially during the last decade (Loukanov et al., 2019). Nowadays the micro- and nanorobots are already commonly used in numerous and diverse biotechnological processes (Bogue, 2010). However, a critical issues is still their way of powering and locomotion in terms of bio-application. Most of them can be actuated through various chemical methods for propulsion, which require energy from proceeding of chemical reactions in the solution (Yang et al., 2019). So in all these cases the environment must contain fuel (e.g. hydrogen peroxide, acid, etc.), which often is harmful for the living organisms (Soto & Chrostowski, 2018). Due to this reason, the efforts were focused on the research, where the triggering and control of nanorobots might occur in fuel free environment. The most references in this novel scientific field have reported about the externally powered nanodevices with magnetic force

(microswimmers) or ultrasound, e.g. highly-porous nanomotors (Xu et al., 2017). The ultrasound has been found as especially promising way to drive nanomachines in biological fluids or media, because of its deep penetration and less harmful effect to the tissues. The ultrasound-propelled nanodevices can be built from gold nanowires and then propelled by the induced ultrasound mechanical waves (Garcia-Gradilla et al., 2014). The gold nanostructures have also received considerable interest due to their attractive plasmonic, catalytic and thermal properties (Lee et al., 2018). If biomaterial as proteins, receptors or plasma membrane is immobilized on their surface, they can be considered as robust biomimetic nanorobots with multipurpose programmed applications (de Ávila et al., 2018).

The purpose of current report was to design ultrasound-propelled biomimetic nanorobot for removal of pathogenic bacteria from broth environment. Our nanorobot was fabricated from acoustic gold nanowires. Their surface was coated with monoclonal antibodies, which inherently mimic the surface

properties of the cells that have been used as a source. In such a way, our resulted biomimetic nanorobots possess the advantages of both functional biomolecules of cellular membrane, as well as the dynamic movement induced by the ultrasound propulsion. The presented integration resulted also in broader and more robust application in respect to the complicated and complex tasks performance. This statement was proved by our programmed hybrid fuel-free nanorobot, which was able to simultaneously target and removal the pathogenic *E. coli* through ultrasound and adhesion, thankful to its functionalized layer of monoclonal antibodies. *Escherichia coli* O157:H7 was chosen in the conducted experiments as a model and target pathogenic bacterium, because it is known and well-characterized microorganism (Lim et al., 2010). The advantage of coupling between the biological function of antibodies and the ultrasound fuel-free navigation in our design enables a dynamic and multifunctional platform that might represent a unique tool for movement and manipulation of biological objects at cellular level. In addition, all processes in the sample occurred for relatively short time, which was measured within minutes. And last but not least, the designed nanorobot might be considered as a robust technique for potential use in different biological fields, including immune modulation, drug delivery, cellular imaging and detoxification.

## Materials and methods

### Reagents and materials

Commercial gold plating solution (Technic Inc., Anaheim, USA) was used for fabrication of the nanorobot. (3-Mercaptopropionic acid used for coating of the gold nanowires was purchased from Sigma-Aldrich. Methylene chloride, ethanol and isopropanol were purchased from WAKO. The PC membrane template was purchased from Whatman Nuclepore (catalog № 110407). It contained 400 nm in diameter nanopores. The nanorobot was functionalized with monoclonal antibody (anti-*E. coli* O157:H7) purchased from Meridian Life Science, Inc (Saco, ME). The acoustic cell consisted of a piezoelectric transducer (Ferroperm), which generated ultrasound waves. 4',6-diamidino-2-phenylindole (DAPI) was used as a fluorescent stain for quantitative measurement of the cells by photoluminescence spectrophotometer (Jasco analytical photoluminescence UV-VIS, model No FP-6300). Aqueous solution of 2 % uranyl acetate  $UO_2(CH_3COO)_2$  was used as a reagent for the negative staining of the samples observed in the transmission electron microscope.

### Nanorobot fabrication

The gold nanowires were prepared by a common electrodeposition method. For that purpose, thin film of elemental gold was sputtered on porous PC membrane template. After that the membrane was assembled in a plating cell (Teflon) with Al foil. The gold was plated and the resulted sputtered layer was removed by mechanical polishing. Thus gold wire nanorobot was created with concave shape and average size distribution between 2 – 7  $\mu\text{m}$ . PC membrane residues were dissolved in methylene chloride and the nanorobots were separated from the mixed solution through centrifugation and washing with isopropanol and ethanol. The resulted precipitation was stored in ultrapure water at 4°C. The functionalization of the nanorobot with monoclonal antibody (anti-*E. coli* O157:H7) was done in phosphate-buffered saline

(PBS) solution. The gold nanowires were first coated with 0.20 mM 3-mercaptopropionic acid (MPA) for overnight and then reacted with monoclonal antibody in a buffered solution through conjugation reaction. The fabricated biomimetic nanorobot were mixed with bacterial suspension (taken at the mid log phase) and were activated by ultrasound (frequency of 2.60 MHz and 2.0 V amplitude).

### Bacterial culture

*Escherichia coli* O157:H7 was used for the performance of ultrasound-propelled biomimetic nanorobot. The bacterial colonies were stored  $-70^\circ\text{C}$  and cultivated on trypticase soy agar plates (BD Bioscience, MD). A single colony was inoculated in tryptic soy broth medium (BD Bioscience, MD) and grown for 24 hours at  $37^\circ\text{C}$ . At the mid log phase 100 L of the microbiological suspension was transferred to a fresh broth media and incubated for 6 hours at  $37^\circ\text{C}$  before labeling experiment.

### Transmission electron microscopy observation and analysis of the attached *E. coli*

The attached bacteria were removed from the suspension by centrifugation. They were washed with PBS solution to avoid the formation of artifacts and dropped on a micro-grid coated with amorphous carbon film. The buffer drop was removed with filter paper and the sample was frozen rapidly in a cryogenic storage (Loukanov et al., 2018).

## Results and discussion

The biomimetic nanorobot was fabricated by using of electrochemical deposition protocol for template-assisted gold nanowires (Garcia-Gradilla et al., 2013). Its surface was modified with MPA before coating with monoclonal antibodies. It was characterized by transmission electron microscope. As shown on the micrograph (Fig. 1) the nanorobot diameter is about 400-500 nm and length up to 6000-7000 nm. Its shape is asymmetric, which is a condition for the ultrasound propulsion. The presented geometrical asymmetry enables to the gold nanowires to convert the acoustic steady streaming into axial motion with independent trajectory, as shown on Fig. 1A. Another key factor which affect the acoustic energy conversion into propulsion is the material density and its dimension. The elemental gold is relatively dense material, and therefore, the designed size is enough large to achieve autonomous propulsion in agreement with the low Reynolds number (Jarell & McBride, 2008). Thus, the acoustically propelled biomimetic nanorobot demonstrated a synergistic effect of enhancing both mass transport and directional collisions with the target bacteria. The thin coating of nanorobot with monoclonal antibody (as shown on the scheme Fig. 1B) was observed by TEM observation (Fig. 1C). The protein contained layer coated on the gold surface was visible due to the negative staining of the sample with uranyl acetate. The presence of protein contents was also proved qualitatively by ninhydrin test, which reacts with the amino groups of amino acid residues. The protein coating might remain conjugated on the nanorobot for relatively long period of time (at least 5-6 months) if stored in refrigerator at  $4^\circ\text{C}$ .

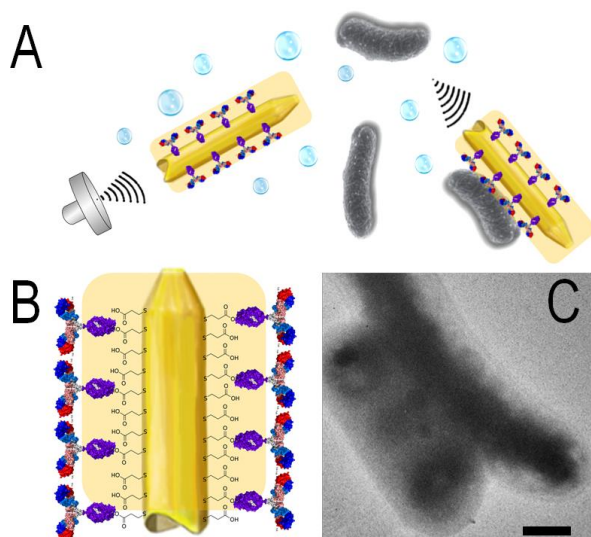


**Fig. 1.** Illustration of the way of operation of the ultrasound-propelled biomimetic nanorobot (A). Schematic of the nanorobot modified with MPA and coated with monoclonal antibody layer (B). TEM images of pathogenic *E. coli* O157:H7 attached on the nanorobot surface

As demonstrated, the presented mobile nanorobot enables both enhanced binding to pathogen in broth sample and its effective neutralization. The presence of monoclonal antibody enables selective targeting, effective adhering or binding of the pathogen to the nanorobot and its following isolation from the microbial environment. The whole process occurred in a short contact time (i.e. within 5-10 min incubation) and 2.60 MHz ultrasound (2.0 V). If the nanorobot is applied without coating with antibodies as control experiment, there was absence of the process of bacterial adhesion in the suspension. This was demonstrated by fluorescent staining (by DAPI) of the bacterial cells and measuring of the overall normalized photoluminescence intensity of the isolated cells in suspension by spectrophotometer. As shown on Fig. 2 the absence of bacteria on the bare nanorobot (in control experiment) was displayed as a negligible fluorescent intensity. In the case of antibody coated nanorobot the photoluminescence intensity was remarkable high, which is indication for successful occurred processes of biorecognition and binding.

All results demonstrated the unique characteristic of the designed ultrasound-propelled biomimetic nanorobot to achieve selective and rapid isolation of the pathogens microorganisms. However, the coating with monoclonal antibodies opens also other diverse biological function applications, which could be demonstrated with binding of existing toxins in the bacterial environment. The ability our nanorobots for absorbing and neutralization of toxins is still under investigation. The reason is that the monoclonal antibody is not able to bind the toxins molecules and accomplish their removing in the manner as the bacterial cells. Nevertheless, the possibilities for future accelerated detoxification of various produced toxins in real environment could be another important application of the designed ultrasound propelled nanorobotics.

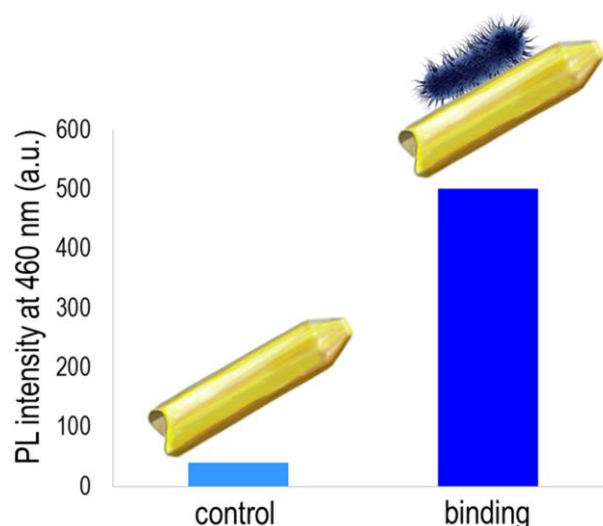


**Fig. 2.** Normalized photoluminescence intensity at 460 nm of DAPI-stained *E. coli* O157:H7 retained on a bare nanorobot (left side as control) and antibody-coated biomimetic nanorobot (right side, binding experiment)

## Conclusion

Since the acoustic propulsion is used as a model of fuel-free propulsion, the reported nanorobot can be used for other diverse applications.

## References

- Bogue, R. 2010. "Microrobots and nanorobots: a review of recent developments", *Industrial Robot*, 37 No. 4, pp. 341-346.
- de Ávila et al. 2018. Hybrid biomembrane-functionalized nanorobots for concurrent removal of pathogenic bacteria and toxins. *Sci. Robot.* 3, eaat0485.
- Garcia-Gradilla et al. 2014. Ultrasound-Propelled Nanoporous Gold Wire for Efficient Drug Loading and Release, *small* 2014, 10, No. 20, 4154-4159.
- Garcia-Gradilla, V., J. Orozco, S. Sattayasamitsathit, F. Soto, F. Kuralay, A. Pourazary, A. Katzenberg, W. Gao, Y. Shen, J. Wang. 2013. Functionalized ultrasound-propelled magnetically guided nanomotors: Toward practical biomedical applications. *ACS Nano* 7, 9232-9240.
- Jarrell, K. F., McBride, M. J. 2008. The surprisingly diverse ways that prokaryotes move, *Nature Reviews Microbiology* v6, 466-476.
- Lee et al. 2018. Spontaneous formation of gold nanostructures in aqueous microdroplets, *Nature Communications* volume 9, Article number: 1562.
- Lim et al. 2010. A Brief Overview of *Escherichia coli* O157:H7 and Its Plasmid O157, *J Microbiol Biotechnol.*; 20(1): 5-14.
- Loukanov, A., H. Gagov, S. 2020. Nakabayashi. *Artificial Nanomachines and Nanorobotics. The Road from Nanomedicine to Precision Medicine.*
- Loukanov et al. 2018. Visualization of the native shape of bodipy-labeled DNA in *Escherichia coli* by correlative microscopy, *Microsc Res Tech.*; 81: 267-274.
- Soto, F., R. Chrostowski. 2018. *Frontiers of Medical Micro/Nanorobotics: in vivo Applications and Commercialization Perspectives Toward Clinical Uses*, *Front. Bioeng. Biotechnol.*, 14 November.
- Xu et al., 2017. Ultrasound propulsion of micro-/nanomotors, *Applied Materials Today* 9, 493-503.
- Yang et al. 2019. Development of micro- and nanorobotics: A review, *Sci China Tech Sci*, Vol.62 No.1.

## TRANSIENT, THREE-DIMENSIONAL, HYDROGEOLOGICAL NUMERICAL MODEL OF ELLATZITE OPEN PIT MINE

**Nikola Toshkov, Ivan Vasilev, Lyubomir Svilenov**

Mining Complex, "Ellatzite-Med" AD, 2180 Etropole; [n.toshkov@ellatzite-med.com](mailto:n.toshkov@ellatzite-med.com); [i.vasilev@ellatzite-med.com](mailto:i.vasilev@ellatzite-med.com); [l.svilenov@ellatzite-med.com](mailto:l.svilenov@ellatzite-med.com)

**ABSTRACT.** The nature of the groundwater behaviour in active open pit mines is transient due to the constant mining and installation of active dewatering/depressurisation systems. Prediction of the groundwater flow in such a conditions is mainly important in two aspects - assessment of the pit inflow in order to design dewatering/depressurisation systems for normal operation and investigation of the slope stability in order to design the optimum geometry. In Ellatzite Open Pit Mine a three-dimensional, hydrogeological numerical model is developed that has the ability to do transient calculation not only with reference to the dewatering systems but also to the change in the pit geometry, hydraulic parameters, recharge zones and climate changes.

**Keywords:** numerical modelling, mine dewatering

### ТРИМЕРЕН, ХИДРОГЕОЛОЖКИ ЧИСЛЕН МОДЕЛ НА РУДНИК ЕЛАЦИТЕ В РЕЖИМ НА НЕСТАБИЛИЗИРАНА ФИЛТРАЦИЯ

**Никола Тошков, Иван Василев, Любомир Свиленов**

Рудодобивен комплекс, „Елаците-Мед“ АД, 2180 Етрополе

**РЕЗЮМЕ.** Поведението на подземните води в активни открити рудници е променливо или в състояние на постоянна нестабилизирана филтрация, поради минните дейности и инсталирането на различни отводнителни системи. Прогнозирането му в такива условия е важно в два аспекта – оценка на водопритока към рудника за проектиране на отводнителни системи с цел нормална експлоатация и изследване на устойчивостта за проектиране на оптимална геометрия. В рудник „Елаците“ е разработен тримерен хидрогеоложки числен модел, с възможност да извършва изчисления в режим на нестабилизирана филтрация по отношение не само на отводнителните системи, но и по промяната в рудничната геометрия, хидрогеоложките параметри, зоните на подхранване, и климатичните условия.

**Ключови думи:** числено моделиране, минно отводняване

## Introduction

Groundwater dewatering and control under operation of large open pits is a complex and challenging process that requires design and construction of drainage tunnels, pumping wells, sub horizontal boreholes, ditches, sumps, pumping stations and pipelines. The main purposes of these systems are to sustain the normal operation work of people and machines, increase stability and design optimal pit geometry (Read and Beale 2014). In order to achieve that we need to determine the climatic, hydrological, geological, hydrogeological and mine exploitation settings.

If we assume that climate conditions and geological settings are known during the lifetime of a pit, the rest have transient character because of the active mining activities. They constantly change the surrounding topography and create new watersheds in different scale. Due to the large mass being excavated, the rock near the pit slope is under relaxation. This causes the processes of swelling and joint opening, which are changing the hydraulic properties of the rock mass (Liu 2013; Ugorets 2015). Moreover, the installation of new drainage systems alters the groundwater flow and its boundary conditions.

The Ellatzite open pit mine is located about 1.5 km north of the main ridge of the Balkan mountain in the region of Etropole and consists of a single large excavation. At present, the highest bench is at 1510 m.a.s.l. while the lowest at 865 m.a.s.l. The shape of the pit in plan is elliptical with the longest and shortest axes being 2100 and 1500 m, respectively (Figure 1). The mining activities are carried out with the help of a third drainage tunnel under the pit bottom and slope toes. The tunnel has four adits and it is connected to the bottom of the pit through vertical boreholes. While the tunnel transmits the surface water and part of the groundwater flow, several horizontal drainage boreholes depressurise the slope.

Those dynamic and complex specifics of large open pit mines impose the use of a numerical three dimensional hydrogeological model that is able to do transient calculations. Such a model was accomplished in 2019 together with the specialists from the mine and consultancy company Itasca with the software MineDW that is specially adapted for mines (Liu 2013; Ugorets 2015). The geological and structural models of the pit, the drainage tunnels and dewatering boreholes, all the historical surfaces of the pit are implemented in the model. Discharge data from surface and groundwater flows, in-situ filtration tests and data from monitoring systems are also used.

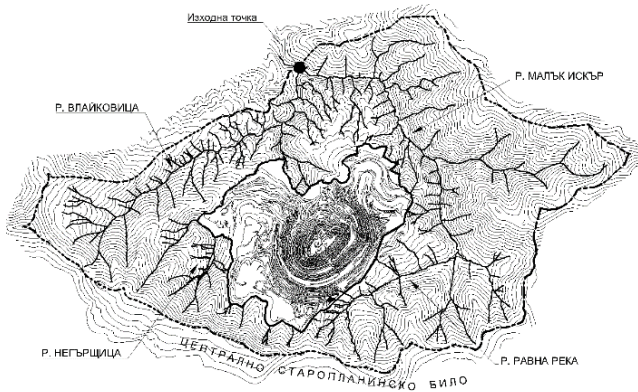


Fig. 1. Ellatzite open pit mine and its surrounding areas. Mining activities' extent, hydrogeological model boundaries and river streams are shown with thicker lines. The point of the model drainage is indicated in the northern part

### Hydrogeological conditions and conceptual model

The surface and base runoff in the hydrogeological model is drained by the Maluk Iskar River and its main tributaries, the rivers Ravna and Negarshitzta. The former surrounds the pit area from southeast while the latter is partially covered by the west waste dumps of the mine. The Vlaicovitza River is the main tributary of the Negarshitzta River and the Dascalski Polqni ridge is their watershed divide (Fig. 1). The river is located in the most western part of the model area. The south boundary of the model is the main ridge of the Balkan mountain. A section of Maluk Iskar after the Negarshitzta River flows in it as a drainage point of the model. The watershed area of this section is 31 km<sup>2</sup> and it is used as an external boundary of the model.

The terrain around the area of mining activities is natural and it is characterised by steep slopes and various forestation type. The lowest elevation in the model is 760 m.a.s.l. at the drainage point, while the highest is 1822 m.a.s.l. and it is located at Korduna peak. In the area with mining activities the terrain is considerably changed. The waste dumps are constructed with horizontal levels that are filed up to the projected extent, whereby slopes with heights of 10m to 50m, rarely 100 m are formed. The surface water which could enter the piles is caught and diverted with surface and underground drainage systems and it is later released in natural streams. The polluted water that discharge from them is also caught, but this time it is diverted to the purification plant at elevation 840 m.a.s.l. and the floatation plant (Hristov et al. 2014, 2016).

The region of the mine is characterised by mountainous climatic conditions of the continental climatic zone (Belda et al. 2014; Hristov et al. 2014), which means that the temperature fluctuations are considerable in the range of 25-30° C. In January, the average monthly temperature is below 0° C, while during the summer the temperature is above 20° C. For the last ten years, the average annual precipitation, measured by a meteorological station located at elevation 1103 m.a.s.l. in the centre of the hydrogeological model, is 1110.5 l/m<sup>2</sup>. For the groundwater budget (1) the precipitation (P) is the only recharge for the model, since there are no other water bodies to recharge the system (Hristov et al. 2016). After estimating the evaporation (E) and the surface run off (Qs) the quantity of the rain that

enters the groundwater system (Qu) is calculated. The values are used for recharge of the hydrogeological model and it is different for the pit and waste dump areas.

$$Q_u = P - Q_s - E \quad (1)$$

The evaporation (E) is calculated using the analytical formula of Turk (2), which is widely used for various conditions and takes into account the values of the temperature (t). The applied formula estimates that the annual average evaporation is from 35% to 48% depending on the year (Hristov et al., 2016).

$$E = \frac{P}{\sqrt{0.9 + \frac{P^2}{L^2}}} \quad (2)$$

where:

$$L = 300 + 25t + 0.05t^3 \quad (3)$$

Estimating the surface run off and groundwater discharge is a challenging task, if there is not enough detailed data of the daily river stage at the discharge point. However, it is empirically assessed that the groundwater recharge (Qu) as a part of the precipitation is about 23% to 42% depending on the year (Hristov et al., 2016). The percentage is higher for the area of the waste dump and it can reach up to full infiltration of the precipitation (100%).

Six lithological units comprise the hydrogeological model – granodiorites, hornfelses, monzodiorite porphyries, schists, phyllites and sandstones. In most of them the groundwater movement is due to the fracture system. Major faults have considerable influence over the formation of the groundwater flow, acting as an aquiclude or transmitting the water depending on the flow direction. This effect in the model is achieved by grouping the elements of the mesh in fault zones (like the faults on Fig. 4a) and applying their hydraulic conductivity parameters. In such a manner the model can reproduce the observed (by monitoring systems) vertical pore pressure gradient.

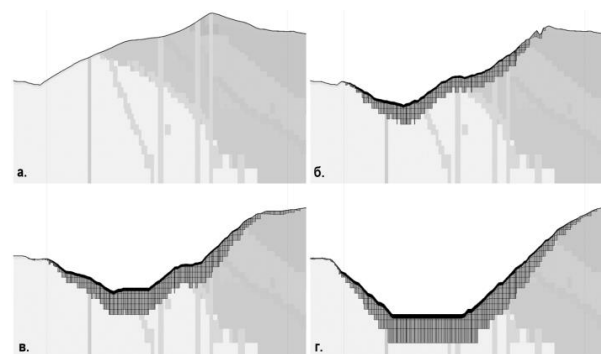


Fig. 2. ZOR extent in the section oriented north-south across the middle of the mine – before the start of the mine (a), at the beginning of year 2005 (b), 2015 (c) and 2031 (g). The two ZOR are with black and grey (covered with the mesh) with 1/10 and 1/3 from the excavation thickness. Different geological units are also illustrated with dim colours (without calculation mesh)

The conductivity change of the rock mass close to the pit surface caused by active mining is modelled with zones called Zones of Relaxation (ZOR). There are two in the model divided by a vertical extent and are dependent on the pit excavation (fig.

2). They are simulated as elements with increased hydraulic conductivity. The first zone has ten times higher hydraulic conductivity compared to the unchanged rock mass and encompasses elements with depth of 1/10 the thickness of excavation mass above. The second zone reaches a depth of up to 1/3 of the excavation thickness and has three times higher hydraulic conductivity. The extent of the ZOR and their hydraulic conductivities are based on Itasca experience (Xiang and Sterrett 2019).

The constitutive law that calculates the groundwater flow budget in each element is the Darcy's law for transient flow in three dimensions (4).

$$S_s \frac{\partial h}{\partial t} = k \left( \frac{\partial^2 h}{\partial x^2} + \frac{\partial^2 h}{\partial y^2} + \frac{\partial^2 h}{\partial z^2} \right) + w \quad (4)$$

where:

- $S_s$  – specific storage, [m<sup>-1</sup>];
- $k$  – hydraulic conductivity, [m/s];
- $h$  – head, [m];
- $x, y, z$  – directions in the model;
- $w$  – recharge from precipitation, [m/s];
- $t$  – time, [s].

All external boundary conditions of the model, rivers, pit excavation, drainage galleries and horizontal drain boreholes are represented with their particular boundary condition. The flow rate is calculated in the nodes of the elements of the external boundary conditions by analytical solution for a semi-infinite aquifer. This allows to reduce the size of the model and decrease the influence of the external boundary condition on the calculation ("MineDW, User's Manual" 2018). On a pre-defined river stream route the nodes of the elements are made as drainage nodes and the groundwater that recharge them is taken out. If the head of the groundwater system (H) becomes higher than the surface topography elevation (H<sub>s</sub>) of the river nodes the model discharges groundwater that does not infiltrate back. The nodes of the pit excavation are also drain nodes, whose elevation varies with time (the elevation is reduced for excavations). The drainage galleries are drainage nodes that are activated at the time of completion. The flow rate of the rivers, the pit excavation and the galleries nodes are calculated by formulas (5) and (6) and the pit can be assessed by lithological units.

$$Q_{seepage} = CL * (H_s - H), \quad (5)$$

when  $H > H_s$ ,

otherwise  $Q_{seepage} = 0$

$$CL = \frac{K * D_2 * D_3}{D_1} \quad (6)$$

where:

- $Q_{seepage}$  – drainage nodes flow rate, [m<sup>3</sup>/d];
- $H$  u  $H_s$  – nodes calculated head and elevation, [m];
- $CL$  – leakage factor, [m<sup>2</sup>/d];
- $K$  – hydraulic conductivity, [m/d];
- $D_1, D_2$  u  $D_3$  – dimension of an element, [m].

The excavation is simulated by changing the elevation of the pit nodes between the known pit geometries over time (Fig. 3).

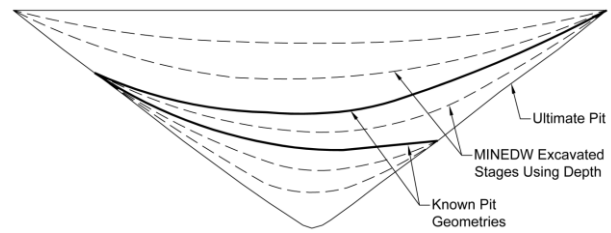


Fig. 3. Reduction of the node elevations in the pit vicinity, by interpolation between the know geometries ("MineDW, User's Manual" 2018)

### Input data

The initial heads that are required at the beginning of the transient simulation are obtained by steady state calculation (with time  $\partial t = 0$  (4)). After finding the pre-mining groundwater condition for the year 1978, the model starts to reduce the pit nodes elevations and to add drainage nodes for the galleries on a monthly base. The model recharge is also changed for the same time period. Moreover, the annual recharge over the waste dump area is 41% from the precipitation, while in the rest of the model it is 34%. The end of the simulation is the year 2031.

The hydraulic conductivity for all six lithological units is listed in Table 1. Higher hydraulic conductivity values are used for phyllites, schists and granodiorite units at the surface of the model to simulate the effect of rock mass weathering. The hydraulic conductivity of all faults is the same - 1.0 e<sup>-5</sup> m/d. All units hydraulic conductivity is isotropic ( $k_x = k_y = k_z$ ).

Overall twelve underground mining structures are implemented in the model. Eight of them are exploration galleries constructed between elevation 1160 and 1285, between 1960 and 1968 before the start of the mining activities. Three out of the four other structures are made on elevations 1030, 950, 840 m.a.s.l to dewater the pit. The last is at elevation 1050 and it has an ecological purpose. Apart from the underground structures, eighteen sub-horizontal boreholes also acting as drainage nodes are implemented in the model.

Table 1. Filtration parameters of the lithological units

Lithological Unit	Hydraulic conductivity, m/d ( $k_x = k_y = k_z$ )	Specific storage, m <sup>-1</sup>
Granodiorites (weathered)	2.0e-1	5.0e-6
Granodiorites	2.0e-3	5.0e-6
Porphyries	3.0e-3	5.0e-6
Hornfels	2.0e-3	5.0e-6
Schists (weathered)	2.0e-1	5.0e-6
Schists	1.0e-2	5.0e-6
Phyllites (weathered)	1.0e-3	5.0e-6
Phyllites	1.0e-5	5.0e-6
Sandstones	3.0e-2	5.0e-6

To calibrate the transient simulation data, thirty-five vibrating wire sensors (recording pore-water pressure) and twenty eight piezometers (recording water level) are used. Records of the

flow rates of galleries, river streams and sub-horizontal boreholes are also used. Mapped locations and measured flow rates of seepages in the pit are compared with those calculated from the model.

### Hydrogeological model and calibration

The simulated steady state head and the boreholes measured from the exploration are shown on Fig. 4. In both cases, northeast from the main fault zone (Ellatzí 1) a convex water level is formed, while southwest from it the shape is concave. The flow rate at the model drainage point (Fig. 1) is 270 l/s, while the measured flow rate of the base flow in the same point in years 2014 and 2015 is in the range of 200 to 400 l/s. Right before the inflow of the Ravna River in Maluk Iskar the measured flow rates of the base flow are around 34 l/s, while the simulated are 32 l/s.

The simulated by the transient simulation and the measured groundwater pressures are in accordance. The comparison between the measured and the simulated water levels for some monitoring boreholes is illustrated on Fig. 5. The calculated flow rates for the drainage gallery at elevation 840 are from 38 l/s to 77.5 l/s, while the measured ones for the same period are 38 l/s to 128 l/s. The measured flow rate for the drainage gallery at elevation 950 is from 22 to 95 l/s, while the simulated one is from 66 to 128 l/s. For five sub-horizontal boreholes located on two benches in the pit the calculated flow rates are in the range of the same magnitude as the measured.

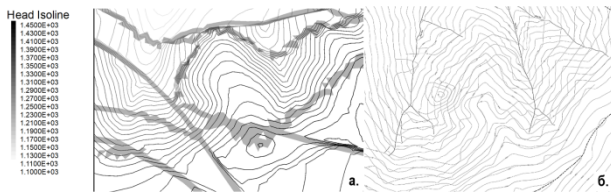


Fig. 4. Simulated (a) and measured (b) water levels before the mining activities being used for calibration and initial head of the transient simulation. In grey in (a) the major fault zones with elements of the calculation mesh are represented. Isolines of the groundwater head on the same plot are visualised between 20 m, from 1100 m to 1450 m. The measured head in (b) is visualised between 25 m, from 1175 m to 1425 m

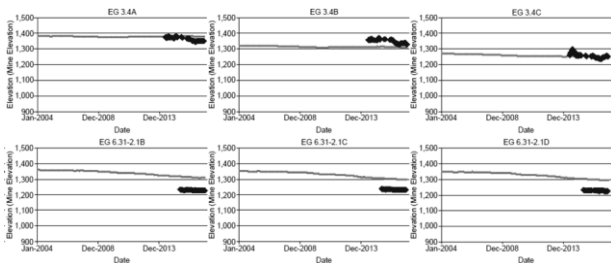


Fig. 5. Simulated (continuous lines) and measured (black symbols) by vibrating wire sensor pore pressure (illustrated as head)

The model recharge is 0.28% higher than the water quantity of the model discharge from the drain point. This shows that the model drainage point is discharging the whole model and negligible water quantity is recharged to the model from the

external boundaries. The simulated groundwater budget for December 2017 is as follows: flow rate of the model drainage point 270 l/s (99.76%); groundwater recharge to the rivers 178 l/s (66%); flow rate to the drainage galleries 34 l/s (13%); inflow to the pit 23 l/s (23%); discharge from groundwater storage 33 l/s (12%) (Xiang and Sterrett 2019). The measured seepages flow rate during the dry season in 48% of the pit benches in 2015 is 10 l/s, while during the wet season in 57% of the benches the flow rate is 72 l/s (Hristov et al. 2016)

Fig. 6 clearly shows how the drainage tunnel at elevation 840 and the fault zones change the groundwater dynamics. Along with the reduced pore pressures in the lower part of the pit and under the bottom of the mine above the drainage gallery 840, in the upper sectors of the pit slope, behind the tectonic zones (playing the role of aquicludes), conditions for groundwater accumulation are formed that cause additional pore-pressures. This is prominent for the southern mine sector (Fig. 6, profile line A-A'), which in its upper parts consists mainly of weak geological units (phyllites and schists) with low filtration properties. This fact has an additional negative impact on the stability of the slope. In this regard, a conceptual drainage system has been developed.

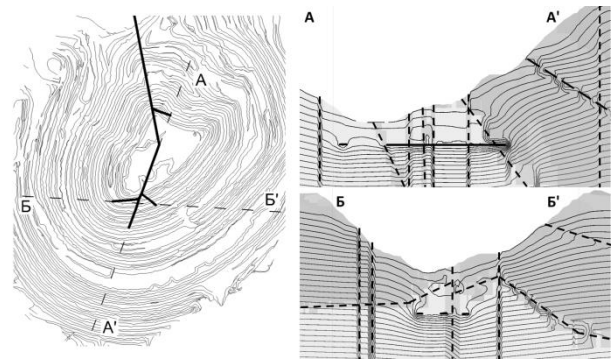


Fig. 6. Longitudinal (A-A') and transverse (B-B') section along the drainage gallery at elevation 840, with pore-pressure distribution in depth for year 2015. The isolines are between 250 kPa, starting from 0 kPa, the gallery location is illustrated with a continuous black line, while the major fault zones are marked with dashed line

### Conceptual drainage system

The developed conceptual drainage system (Fig. 7) consists entirely of sub-horizontal boreholes, simulated on pit benches with elevation from 1200 to 1400 m, and the time of their activation in the model (from 2020 to 2022) is consistent with the project development of mining activities. For the purposes of the initial simulation, the boreholes were modelled with a length of 220 to 250 m and an average horizontal distance of 40 m between them on each bench. After stabilisation of the groundwater levels in the area, the calculated total flow rate of the system gradually decreases to about 12 l/s after year 2022.

Similar simulations are to be performed with modelling of future underground drainage galleries, as well as a combined drainage system, including galleries, sub-horizontal and/or inclined drilling, sumps and ditches.

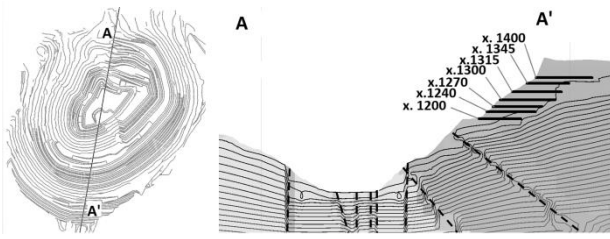


Fig. 7. Conceptual drainage system in phyllites and schists with horizontal drainage boreholes from elevation 1200 to 1400 m. The left plot shows a plan of the Ellatzite mine at the end of 2022 with the position of the section shown in the right diagram. The section shows the horizontal drainage boreholes and the isolines of the pore pressure distribution in depth, with difference of 250 kPa, starting from 0 kPa

## Conclusions

The following more important conclusions can be summarised from the performed transient three-dimensional hydrogeological numerical simulation:

- The used software product MineDW is able to take into account the change of the hydrogeological conditions in the dynamically changing environment, such as the open pit mines;
- The constructed three-dimensional model is able to reliably simulate both the spatial and quantitative distribution of groundwater, and can be successfully used for the design of various drainage systems, depending on the operational needs of the mine;
- It is necessary to continuously upgrade and calibrate the model through the newly gathered meteorological, hydrological, structural-geological and hydrogeological information, for the acquisition of which it is necessary to

expand the monitoring system of the mine by building new observation points;

- To more accurately dimension and design the future drainage systems of the mine, it is necessary to perform pilot in-situ experimental-filtration investigation, through which to validate the design parameters of the sub-horizontal boreholes.

## References

- Belda, M, E Holtanová, T Halenka, and J Kalvová. 2014. *Climate Classification Revisited: From Köppen to Trewartha*. *Climate Research* 59 (1): 1–13.
- Liu, H. 2013. *Using MINEDW to Simulate Pore Pressure as Input for FLAC3D and 3DEC*. 9.
- MineDW, User's Manual*. 2018. Itasca International Inc.
- Read, John, and Geoff Beale. 2014. *Guidelines for Evaluating Water in Pit Slope Stability*. Boca Raton, Florida: CRC Press.
- Ugorets, VI. 2015. *Benefits of MINEDW Code for Mine Dewatering Projects in Complex Hydrogeological Settings*, 10.
- Xiang, Jianwei, and Robert Sterrett. 2019. *Three-Dimensional Groundwater Flow Model and Conceptual Dewatering Programme at Ellatzite Med Mine, Bulgaria*. 4003. Denver, Colorado, USA.
- Hristov, V., Benderev, A., Kolev, S., et al. 2016. *Hydrogeological site investigations carried out in Ellatzite open pit mine and surrounding areas during years 2014 and 2015*, Sofia, GI BAS "Strashimir Dimitrov"
- Hristov, V., Benderev, A., Shanov, S., et.al. 2014. *Hydrogeological site investigations carried out in Ellatzite open pit mine and surrounding areas during years 2013* Sofia, GI BAS "Strashimir Dimitrov".

## A STUDY OF HORIZONTAL DISTRIBUTION PATTERN OF PARTICULATE POLLUTANTS NEAR A HIGHWAY

**Maya Vatzkitcheva<sup>1</sup>, Kalinka Velichkova<sup>2</sup>, Nikolay Kolev<sup>3</sup>, Plamen Savov<sup>4</sup>**

<sup>1</sup> University of Mining and Geology "St. Ivan Rilski", 1700 Sofia; mayavack@gmail.com

<sup>2</sup> University of Mining and Geology "St. Ivan Rilski", 1700 Sofia; k.velichkova@mgu.bg

<sup>3</sup> University of Mining and Geology "St. Ivan Rilski", 1700 Sofia; nic\_k@abv.bg

<sup>4</sup> University of Mining and Geology "St. Ivan Rilski", 1700 Sofia; psavov@mgu.bg

**ABSTRACT.** Understanding vehicle-generated emissions, their dispersion near roads and their potential impact on the near-roadway populations is an area of growing environmental interest. This article presents the horizontal dispersion of coarse and fine particulate matter pollutants in places located near a busy highway (such as the Trakia highway) at the exit of the city of Sofia, over flat terrain, where the predominant dispersion mechanisms are atmospheric turbulence and the turbulence created by traffic. Four sites (at distances of 25, 50, 100 and 200 m from the highway) were selected to study the concentration profiles of pollutants. Under conditions of low wind speed, particles from the highway are established even in areas located far away upwind from the highway. Experimental results show that two dimensional modelling of particle flows produced by highway traffic is needed, and it is important to take into account the turbulence caused by traffic in order to accurately predict the dispersion of particulate pollutants near roads.

**Keywords:** vehicle-generated particulate matter emissions, particulate matter dispersion, concentration profiles, pollution near highway, dispersion mechanism

### ИЗУЧАВАНЕ НА МОДЕЛ НА ХОРИЗОНТАЛНО РАЗПРЕДЕЛЕНИЕ НА ПРАХОВИТЕ ЗАМЪРСИТЕЛИ БЛИЗО ДО МАГИСТРАЛА

**Майа Вацкичева, Калинка Величкова, Николай Колев, Пламен Савов**

*Минно-геоложки университет „Св. Иван Рилски“, 1700 София*

**РЕЗЮМЕ.** Стремежът към по-добро разбиране на процесите на дисперсия на генерираните от превозни средства емисии, в близост до пътищата и потенциалното им въздействие върху населението, живеещо близо до тях, е област с нарастващ екологичен интерес. Настоящата статия представя хоризонталната дисперсия на едри и фини прахови замърсители на места, разположени в близост до натоварена магистрала (като магистрала Тракия) на изхода на град София, над равен терен, където преобладаващите механизми на дисперсия са атмосферната турбулентност и тази, създадена от трафика. Четири площадки (на разстояния 25, 50, 100 и 200 м от магистралата) бяха избрани за измерване на концентрацията на замърсителите. Когато скоростта на вятъра е ниска, частици от магистралата се установяват дори и на места, разположени сравнително далеч откъм подветрената страна на магистралата. Експерименталните резултати показват, че е необходимо при двумерно моделиране на потоците от прахови частици, генерирани от трафика по магистралите, да се вземе предвид турбулентността, причинена от трафика, за да се предвиди по-точно дисперсията на праховите частици в близост до пътищата.

**Ключови думи:** прахови частици от автомобилни емисии, дисперсия на прахови частици, концентрационен профил, замърсяване до пътища, дисперсионни механизми

### Introduction

Road transport is globally recognized as a significant and constantly increasing source of air pollution.

The increased traffic has resulted in more pollutant emissions and the deterioration of environmental quality and human health in cities.

Vehicles in major cities are estimated to account for 70% of the respective total pollution loads there.

Particulate matter (PM) pollution in these cities near major roads was often found to be more severe than that in urban areas.

Motor vehicle emissions, however, usually constitute a significant source of coarse and fine particles, such as PM10 and PM2.5. (Batterman et al., 2010; Dallmann et al., 2012 and Gerardin et al., 2016)

It is necessary to quantify the emission levels of the gaseous pollutants and particles with different size fraction (PM10, PM2.5) near heavy traffic road and also to determine their behavior after emission as they are transported away from the road.

Thus the present study is designed to measure the horizontal concentrations of particulate pollutants PM10, PM2.5 and CO<sub>2</sub> levels aside the highway with the effect of meteorological parameters on them.

This study will help the authority boards in most cities to know about the status of pollutants concentration adjacent to highways (Halonen et al., 2016; He et al., 2012).

Particulate matter is the name used for a complex mixture of liquid droplets and solid particles suspended in the atmosphere such as dust, soot, black smoke and volcanic ash.

Particulate matter varies greatly in composition, and for this reason it is usually classified by size. The most common way

to refer to particles is by classifying them into ultra-fine, fine and coarse particles, or by attaching the number in the subscript of the abbreviation, PM, that refers to the upper limit of the particle size taken into account. For example, PM10 encompasses all particles up to the size of 10 micrometers ( $\mu\text{m}$ ).

Coarse particulate matter includes particles sized 2.5–10  $\mu\text{m}$  in aerodynamic diameter or, as they are commonly referred to, PM2.5 – PM10. Fine particles are those with aerodynamic diameter smaller than 2.5  $\mu\text{m}$  (PM2.5) and ultra-fine – less than 100 nm.

Depending on their origin, different sources result in different types of particulate matter with regards to their chemical composition. It should also be noted that while transported in the atmosphere, their chemical and physical characteristics may change as they encounter and react with other particles.

Generally speaking, especially in urban environments, coarse particles are most often of natural origin, while fine particles seem predominantly to have anthropogenic origin.

Primary PM emissions from road traffic come from vehicle exhaust, brake linings, tire wear, as well as road wear and resuspension of road dust. Resuspension, which is the renewed suspension of particles after their deposition, is affected by factors such as the road surface and traffic intensity, and weather conditions like humidity, wind speed and precipitation (Huertas et al., 2017; Ignacio et al., 2017; Savov et al., 2016; Wua Ye et al., 2002).

In the present study, the relationship between concentration of air pollutants and distance from a busy highway was observed. Relation was found between distance and concentrations of PM10 and PM2.5.

The horizontal gradients at the highway suggested that pollutants concentrations were affected significantly by re-suspended road dust and tailpipe exhaust from motor vehicles.

The present study is aimed at assessing the parameters that affect PM number and mass concentration and horizontal dispersion in places located near a busy highway (such as the "Trakia" highway) at the exit of the city of Sofia, Bulgaria.

## Experiment

### Instruments

The number and mass concentrations were measured by a portable laser particle counters BQ20 (TROTEC, Germany) laser particle counter (LPC) capable of measuring in two-channel: channel 1 (0 - 2.5  $\mu\text{m}$ ) and channel 2 (2.5 - 10  $\mu\text{m}$ ) denoted further in the paper as PM2.5 and PM10, respectively. The concentrations were measured instantly with time step 10 minutes. The sampling rate was 0.9 l/min. The accuracy of the devices is in the range of 15-20%.

The meteorological data were obtained from the multi-functional weather station with five sensors (temperature, precipitation, relative humidity, air pressure, wind direction and speed).

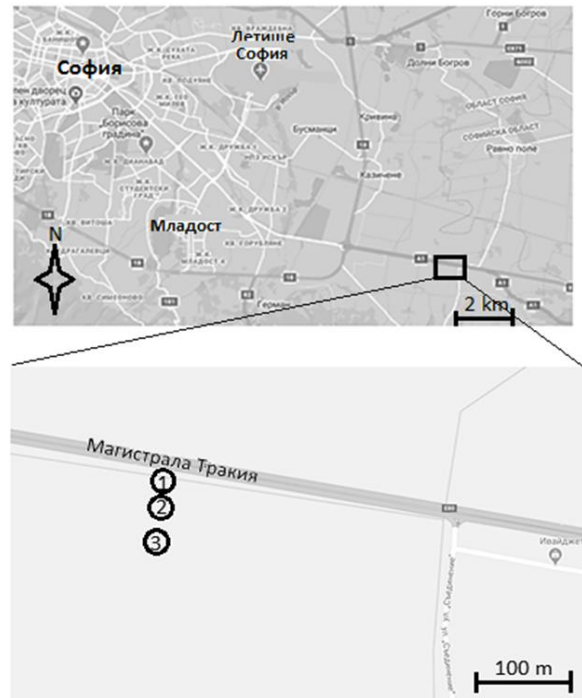


Fig. 1. Measurement sites 1, 2 and 3 near by Trakia highway

### Site description

The site selected for the present study was conducted in the vicinity of "Trakia" highway about 4 km from Sofia (Fig. 1). The location selected is ideal both for the absence of residential areas and of local traffic. The highway has four lines and is approximately 20 m wide. Orientation is W–E direction. Measurements were made at three sampling sites, at distances of 25, 50, and 100 m to the highway, hereafter referred to as site 1, site 2, and site 3, respectively.

The traffic on the main road was estimated by counting the numbers of cars, light trucks, and heavy trucks passing by in random 15 min periods during the measurements. The average traffic densities per hour during the measurements were: cars 2452, and heavy trucks 630, total vehicles 3082.

### Methodology

For the purposes of the present study, the dependence of the mass concentration of PM on the class of atmospheric stability was determined by

$$C(x,0,0) = \frac{Q}{\pi\sigma_z u} e^{-\frac{H^2}{2\sigma_z^2}} \quad (1)$$

The power of the source (traffic)  $Q = 7 \mu\text{g}/\text{m}\cdot\text{s}$  is determined by the measured number of vehicles and the ratio of cars to heavy trucks. For the base values we accepted 5  $\mu\text{g}/\text{m}\cdot\text{s}$  for cars and 20  $\mu\text{g}/\text{m}\cdot\text{s}$  for trucks.  $H = 0.5 \text{ m}$ , which is the predominant height of the sources of pollutants above the ground (the exhaust system of vehicles);  $u$  - the wind component perpendicular to the roadway, and  $\sigma_z$  - coefficient depending on the stability class of the atmosphere and the distance  $x$  from the linear source. The values of  $\sigma_z$  are determined as follows (Colls, 2002):

class A  $\sigma_z = 0.20x$   
 class C  $\sigma_z = 0.08x(1 + 0.0002x)^{-0.5}$  (2)  
 class D  $\sigma_z = 0.06x(1 + 0.0015x)^{-0.5}$

**Results and discussions**

The results of the measurement of solar radiation show that its values vary between 720 and 880 W m<sup>2</sup> (Fig. 2). Based on these data, as well as the magnitude of the wind speed (Fig. 3), we determined the atmospheric stability as corresponding to class A.

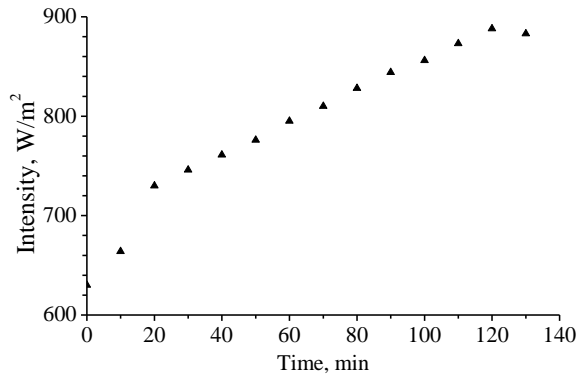


**Fig. 2. Solar radiation**

Wind speed and direction play an important role in pollution distribution and should be considered as key factors in most measurements (Fig. 3).

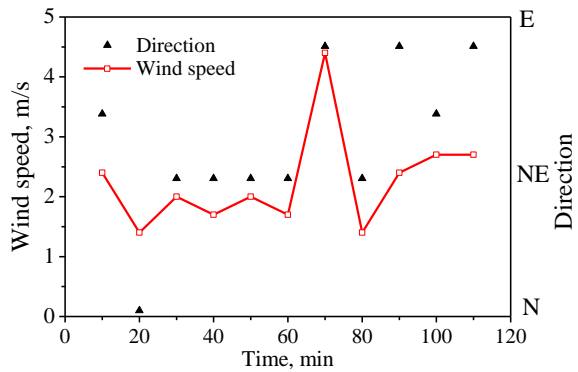


**Fig. 3. Wind speed and direction**

The numerical concentration of PM10 is low, between 1 and 2 m<sup>-3</sup>, and decreases to 1 m<sup>-3</sup> with increasing distance to 100 m (Fig. 4). Concentration fluctuations over time are more related to wind orientation - when the wind orientation is perpendicular to the road, the PM10 concentration values are higher. This is more pronounced in PM10 and very weak in PM2.5. After the first 30 minutes, the wind becomes mostly northeast (NE), and at the end of the measurement - east, parallel to the road. At a distance of 100 m from the highway, the wind orientation has no effect on the PM10 concentration. When the wind blows directly from the source towards the receptor, the concentration gradient is more pronounced and extends further away than when the wind blows parallel to the road, or away from it. According to some research, the concentration of fine and ultra-fine particles drops by half at a

distance of 100-150 m from the source when measurements are taken downwind. The reduction to half the concentration happens 50-100 m from the road when the wind is blowing parallel to the line source (Batterman et al., 2010; Dallmann et al., 2012 and Gerardin et al., 2016).

Different behavior in particle distribution is observed in the present study.

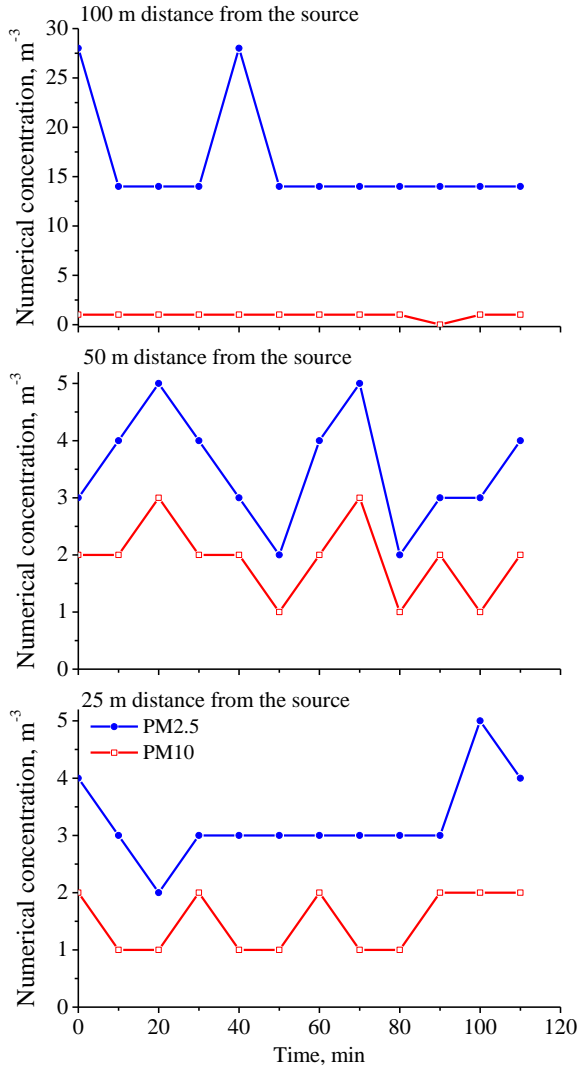


**Fig. 4. Numerical concentration of PM 2.5 and PM 10 at different distances from the source**

Fig. 6 presents the evolution of the mass concentration of aerosols as a function of distance and time. Although after about 60 minutes the wind direction changes from northeast to east, no significant change in concentrations is observed. The average values of the concentration as a function of the distance are given in fig. 8, as bars. It can be seen that even 100 m from the source the mass concentration is still high. This could be due to wind erosion of the soil from the open field and/or from the bioaerosol, which is inevitably emitted by the plantings (sunflower). This background effect is added to the residual aerosol from the highway and maintains high levels of pollution.

The CO<sub>2</sub> concentration is close to the background value, being slightly above it (410 ppm) near the road and decreasing to 380 ppm (Fig. 6). When the wind turns from the northeast

and east (30th and 70th minute) the concentration at both distances decreases. This result shows that the main source of CO<sub>2</sub> above the background are vehicles.

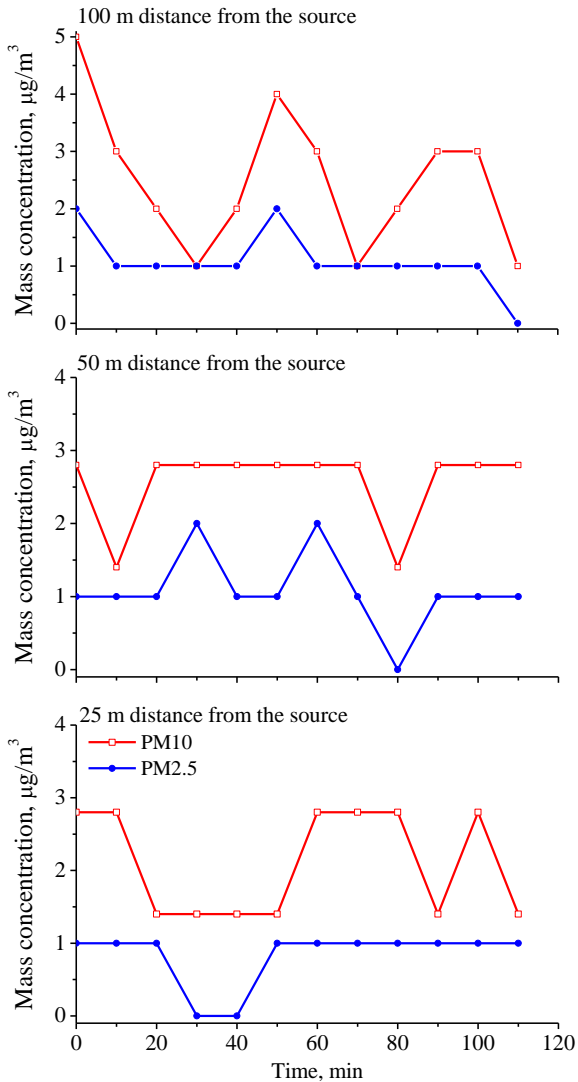


Fig. 5. Mass concentration of PM 2.5 and PM 10 at different distances from the source

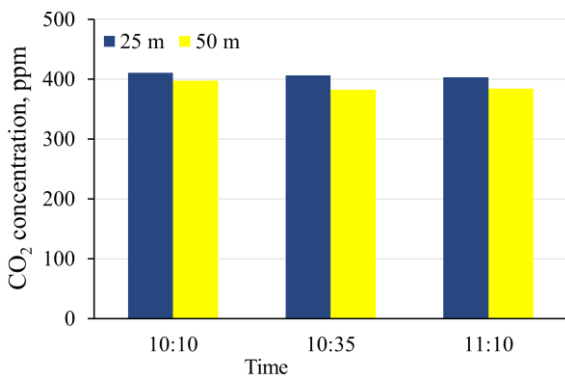


Fig. 6. CO<sub>2</sub> concentration at different distances from the source

In Fig. 7 the dependence of the mass concentration on the wind speed for stability class A, as observed during our measurements, is presented.

The same figure shows the measured concentration for PM<sub>10</sub> at 25, 50 and 100 m of the highway. The values are averaged over a time interval in which the wind has a relatively constant speed and direction - between the 30th and 60th minute (Fig. 3). It was taken into account that the wind blows at an angle of 45° to the road during this period. In this sense a comparison should be made with the graph for  $u = 1$  m/s.

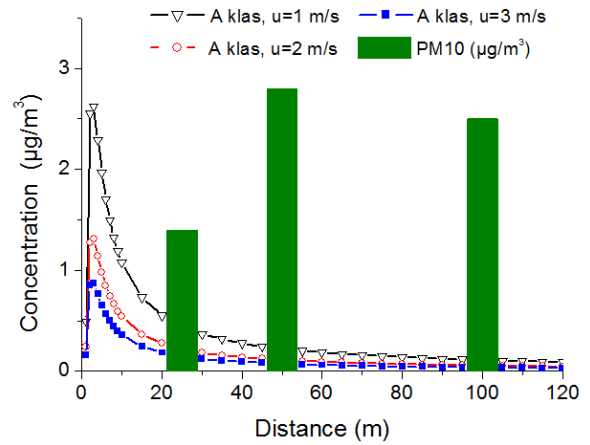


Fig. 7. Wind dependence of mass concentration for stability class A and comparison with the measured values of PM<sub>10</sub>

The experimental profiles of particle concentration close to the highway are significantly different from model calculated. This behaviour could be due to a combination of three processes. First, the effect of bushes and trees barrier in near-roadway neighborhoods reduce air flow, leading to increased pollutant concentrations behind the trees. Second, the plume is likely to ascend near the highway because of the thermal buoyancy associated with the temperature gradient between traffic exhaust and ambient air.. Three, the vortices by traffic-produced turbulence and ground surface friction can help to facilitate the mixing of particles in the air mass in the lower heights. The first process explains the lower particle concentration in site 1. The second process explain the peak plume displacement away from highway in comparison withcalculated one. The third process explains the relatively higher concentrations in experimental plume in comparison with calculated.

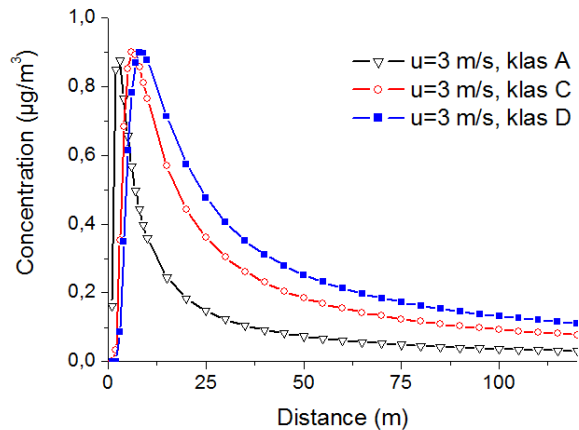


Fig. 8. Mass concentration dependence on atmospheric stability class A, C and D

In Fig. 8. the dependence of the mass concentration on the atmospheric stability class at wind speed 3 m/s, perpendicular to the highway, is presented. The calculations were made according to (1) and (2) under the mentioned conditions for  $Q$  and  $H$ .

There was no significant difference in the maximum concentration for the three classes.

In the comparison of Fig. 8 and Fig. 9 it is seen that the combination of weak wind and strong instability or strong wind and neutral stratification of the atmosphere contribute to the strongest dispersion of pollutions away from the source. In a situation with light wind (about 1 m/s) and strong instability, the pollution levels around the source are the highest.

## Conclusion

The purpose of this study is the characterization of the "Trakia" highway in terms of evolution of particle mass and number concentration at different distances from the highway. Mass concentrations of large particles measured were significantly lower than the average values for the urban environment.

The discrepancy between experimental and calculated mass and number concentration is establish. This is do for three main reasons:

- the effect of bushes and trees barrier in near-roadway neighborhoods;
- thermal buoyancy associated with the temperature gradient between traffic exhaust and ambient air;
- the vortices by traffic-produced turbulence and ground surface friction.

All this factors cause displacement and stretch in particle dispersion profile from highway in comparison with Gauss's profile.

An additional result we got is that the main source of  $CO_2$  above the background are vehicles.

The experimental results suggest the need for three-dimensional modelling of particle plumes from highways and the importance of considering enumerate phenomenon for accurate prediction of particle dispersion near roadways.

**Acknowledgements.** This work is supported by contract № GPF-231 /2020 University of Mining and Geology is "St. Ivan Rilski".

This work has been carried out in the framework of the National Science Program "Environmental Protection and Reduction of Risks of Adverse Events and Natural Disasters", approved by the Resolution of the Council of Ministers № 577/17.08.2018 and supported by the Ministry of Education and Science (MES) of Bulgaria (Agreement № Д01-322/18.12.2019).

## References

- Batterman S., Zhang K., Kononowech R., 2010, Prediction and analysis of near-road concentrations using a reduced-form emission/ dispersion model, *Environmental Health*, 9-29, <http://www.ehjournal.net/content/9/1/29>
- Colls, J. 2002, *Air pollution*. Taylor & Francis Group
- Dallmann, T.R.; DeMartini, S.J.; Kirchstetter, T.W.; Herndon, S.C.; Onasch, T.B.; Wood, E.C.; Harley, R.A., 2012, On-road measurement of gas and particle phase pollutant emission factors for individual heavy-duty diesel trucks. *Environ. Sci. Technol.* 46, 8511–8518.
- Gerardin, F., & Midoux, N. 2016. Attenuation of road dust emissions caused by industrial vehicle traffic., 25 *Atmospheric Environment*, 127, 46–54.
- Halnen, J.I.; Blangiardo, M.; Toledano, M.B.; Fehst, D.; Gulliver, J.; Anderson, H.R.; Beevers, S.D.; Dajnak, D.; Kelly, F.J.; Tonne, 2016, C. Long-term exposure to traffic pollution and hospital admissions in London., *Environ. Pollut.* 208, 48–57.
- He, M., and Dhaniyala, S. 2012. Vertical and horizontal concentration distributions of ultrafine particles near a highway. *Atmospheric Environment*, 46, 225–236.
- Huertas, M. E., Huertas, J. I., a Valencia, A. 2017. Vehicular road influence areas. *Atmospheric Environment*, 151, 108–116.
- Ignacio J., Cardozo H., Fernando D., Sánchez P., 2017, Air pollution near arterial roads: An experimental and modeling study, *Atmos. Chem. Phys. Discuss.*, <https://doi.org/10.5194/acp-2017-753>
- Savov, P., Kolev, N., Evgenieva, Ts., Vatzkitcheva M. 2016. Correlations Between Particle Number Concentrations, Boundary Layer Height, Meteorological Parameters and Urban Environments. *Comptes Rendus de l'Academie Bulgare des Sciences*, 69, 19-24.
- Wua Ye, Haoa J., Fua L., Wangb Z., Tangb U., 2002, Vertical and horizontal profiles of airborne particulate matter near major roads in Macao, China, *Atmospheric Environment* 36 4907–4918.

## STRESS AND STRAIN STATE AROUND ELLIPTIC OPENING IN TRANSVERSALLY ISOTROPIC ROCK MASS – 2

**Rayna Vucheva, Violeta Trifonova – Genova**

*<sup>1</sup>University of Mining and Geology “St. Ivan Rilski”, 1700 Sofia; r.wutschewa@abv.bg, violeta.trifonova@yahoo.com*

**ABSTRACT:** This article discusses the question of analytical determining the stresses and strains around opening. Its cross section is an ellipse. The rock mass has inclined plane of isotropy. This class of plane tasks is solved by complex function method. The behavior surrounding the opening is described by differential equation of function for stresses. This function is represented by two functions of complex variables. They took part in expressions of stresses and strains in the point of examined medium.

The expressions of complex functions in condition for plane strain are given on contour of the opening. The analytical expressions of stresses and strains are presented in points on contour of opening. These expressions are written in natural and orthogonal coordinates systems.

**Keywords:** elliptical opening, transversally isotropic rock mass, analytical solution, complex function method

### НАПРЕГНАТО И ДЕФОРМИРАНО СЪСТОЯНИЕ ОКОЛО ЕЛИПТИЧНА ИЗРАБОТКА В ТРАНСВЕРЗАЛНО ИЗОТРОПЕН МАСИВ - 2

**Райна Вучева, Виолета Трифонова – Генова**

*Минно-геоложки университет „Св. Иван Рилски“, 1700 София*

**РЕЗЮМЕ:** Тази статия се разглежда въпросът за аналитично определяне на напреженията и деформациите около изработка. Нейното напречно сечение е елипса. Масивът притежава наклонена равнина на изотропия. Този вид равнинни задачи се решават с метода на комплексна функция. Околността около отвора се описва с диференциално уравнение на функция за напрежението. Тя е представена посредством две функции на комплексни променливи. Те участват в изразите за напреженията и деформациите в точка от разглежданата област.

По контура на отвора са дадени изразите за комплексните функции в условие на равнинна деформация. Представени са аналитичните изрази за напреженията и деформациите в точки от контура на отвора. Тези изрази са записани в естествена и декартова координатни системи.

**Ключови думи:** елиптична изработка, трансверзално изотропен масив, аналитично решение, метод на комплексна функция

### Introduction

The behavior of the rocks is influenced by the mechanical properties when underground construction works are performed and materials are extracted. These properties describes by mechanical models. They idealize the rock mass. In each of the models only basic essential properties are reflected. Depending on the properties of the rock mass and the nature of the processes, different theories are applied. The theory of elasticity is used here. She applies the following models of rock mass (Bulichev, 1984): elastic, viscoelastic, elastoplastic nonhomogeneous, viscoplastic and elastoplastic model and etc.

The rock mass has natural empty space and fissure. It is considered as a system of macro blocks. The relations of the contact between them are destroyed. Then the rock mass is modulated as stochastic medium. For her two group models are typical (Vulkov, 2016): linear and nonlinear. The first group includes: parabolic (Trifonova, 2008; 2010), hyperbolic, elliptic and generalizing model. The second group encloses: nonlinear model of Litwiniszyn, nonlinear parabolic model (Vulkov, 1987-88), nonlinear hyperbolic and nonlinear generalizing model.

The refinement of these models and methods for determination of stresses and displacements around opening is the goal of researchers. The opening may be close to the earth's surface or at a considerable depth.

In this article elastic model of theory of elasticity is used. The stresses and the strains are related by linear dependence for transversally isotropic rock mass. The mechanical properties of medium are the same in the plane of isotropy and are different in direction, perpendicular to her.

### Methods

#### Formulation of the problem

Horizontal opening in the shape of an ellipse is drawn at a great depth  $H$  (fig.1). The rock mass has inclined plane of isotropy. This plane forms an angle  $\varphi$  with the horizontal axis.

The width of the opening is  $2a$  and the height is:  $2b$ . The rock mass has volumetric weight:  $\gamma$ .

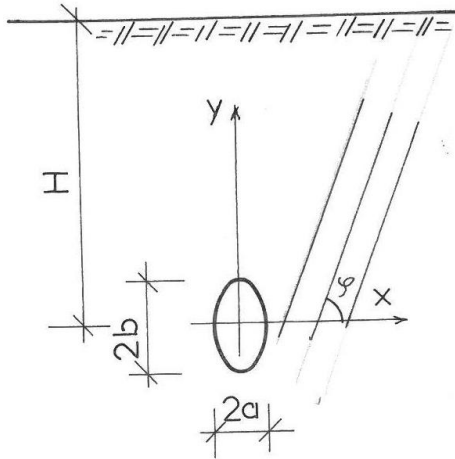


Fig.1. Horizontal elliptical opening in rock mass with inclined plane of isotropy

**Stresses in natural coordinate system**

The stresses are the sum of stresses in indestructible rock mass and the supplemental stresses that take into account the influence of the opening:

$$\sigma_n = \sigma_n^o + \sigma_n'; \quad \sigma_t = \sigma_t^o + \sigma_t'; \quad \tau_{nt} = \tau_{nt}^o + \tau_{nt}'. \quad (1)$$

The stresses in indestructible rock mass are given in (Trifonova-Genova, 2019). The supplemental stresses have the form:

$$\begin{aligned} \sigma_n' &= \frac{2}{c_o} \operatorname{Re} [\Phi_1'(z_1)c_1^2 + \Phi_2'(z_2)c_2^2]; \\ \sigma_t' &= \frac{2}{c_o} \operatorname{Re} [\Phi_1'(z_1)c_3^2 + \Phi_2'(z_2)c_4^2]; \\ \tau_{nt}' &= \frac{2}{c_o} \operatorname{Re} [\Phi_1'(z_1)c_1c_3 + \Phi_2'(z_2)c_2c_4]. \end{aligned} \quad (2)$$

where

$$\begin{aligned} c_o &= a \sin^2 t + b \cos^2 t; \quad c_1 = s_1 a \sin t + b \cos t; \\ c_2 &= s_2 a \sin t + b \cos t; \quad c_3 = a \sin t - s_1 b \cos t; \\ c_4 &= a \sin t - s_2 b \cos t. \end{aligned}$$

In these expressions  $s_1$  and  $s_2$  are roots of the characteristic equation given in (Ivanova et al., 2018):

$$s_j = \alpha_j + i\beta_j. \quad (3)$$

Here  $i$  is imaginary unit and  $j=1,2$ .

The parameter  $t$  in the trigonometric dependencies in (2) is related to the polar angle  $\theta$  by means of the relation (Trifonova-Genova, 2019) (fig. 2):

$$\operatorname{tg} t = \frac{a}{b} \operatorname{tg} \theta. \quad (4)$$

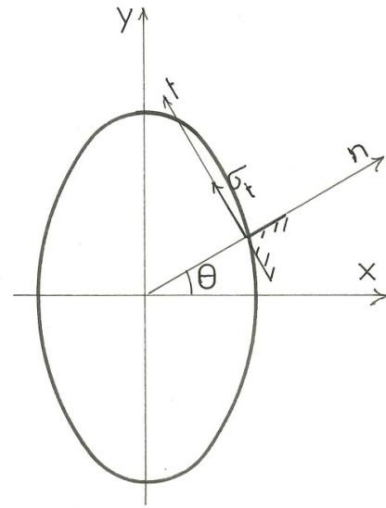


Fig.2. Contour stresses in natural coordinate system

The area occupied by the rock mass around the elliptical opening is transformed into the outer region of a unit circle. The functions of the complex variables from (1) along the contour of this circle have the form:

$$\Phi_1(z_1) = \frac{A_1}{e^{it}}; \quad \Phi_2(z_2) = \frac{B_1}{e^{it}}. \quad (5)$$

According to the method, described in (Minchev, 1960), the coefficients in (5) are:

$$A_1 = A_{11} + iA_{12}; \quad B_1 = B_{11} + iB_{12}, \quad (6)$$

where

$$\begin{aligned} A_{11} &= A_{01}a(\lambda_x - \lambda_y s_2); \quad A_{12} = A_{01}b(\lambda_x - \lambda_y s_2); \\ B_{11} &= A_{01}a(\lambda_y s_1 - \lambda_x); \quad B_{12} = A_{01}b(\lambda_y s_1 - \lambda_x); \\ A_{01} &= 0,5Q(s_2 - s_1)^{-1}; \quad Q = \gamma H. \end{aligned}$$

The expressions for the coefficients  $\lambda_x, \lambda_y, \lambda_z$  are given in (Trifonova-Genova, 2019).

Expressions (6) are replaced by (5). The first derived of functions (5) are replaced by (1). The contour stresses are:

$$\begin{aligned} \sigma_t &= \sigma_t^o + \frac{2}{c_o} \operatorname{Re} \left[ \frac{A_1 i}{e^{it}} c_3^2 + \frac{B_1 i}{e^{it}} c_4^2 \right]; \\ \sigma_n &= 0; \quad \tau_{nt} = 0, \end{aligned} \quad (7)$$

where

$$c_5 = a \sin t + s_1 b \cos t; \quad c_6 = a \sin t + s_2 b \cos t.$$

**Stresses in orthogonal coordinate system**

Formulas are used to transform stresses from natural to orthogonal coordinates given in (Trifonova-Genova, 2019). The stresses in orthogonal coordinate system on the contour of the opening are (fig.3):

$$\sigma_x = \frac{\Delta_1}{\Delta} \sigma_t; \sigma_y = \frac{\Delta_2}{\Delta} \sigma_t; \tau_{xy} = \frac{\Delta_3}{\Delta} \sigma_t, \quad (8)$$

where

$$\begin{aligned} \Delta &= \frac{1}{c^3} [\Delta_4 c_7 + \sin^2(2t) a^2 b^2 \Delta_5]; \\ \Delta_1 &= \frac{a^2}{c^3} [0,5 b^2 \sin^2(2t) - \Delta_4 \sin^2 t]; \\ \Delta_2 &= \frac{b^2}{c^3} [0,5 a^2 \sin^2(2t) + \Delta_4 \cos^2 t]; \\ \Delta_3 &= -\frac{ab}{c^3} \sin(2t) \Delta_5; \Delta_4 = b^2 \cos^2 t - a^2 \sin^2 t; \\ \Delta_5 &= b^2 \cos^2 t + a^2 \sin^2 t; \\ c_7 &= b^4 \cos^4 t - a^4 \sin^4 t; c = b^2 \cos^2 t + a^2 \sin^2 t. \end{aligned}$$

In expressions for stresses in the top expressions participate the tangential normal stresses of (7).

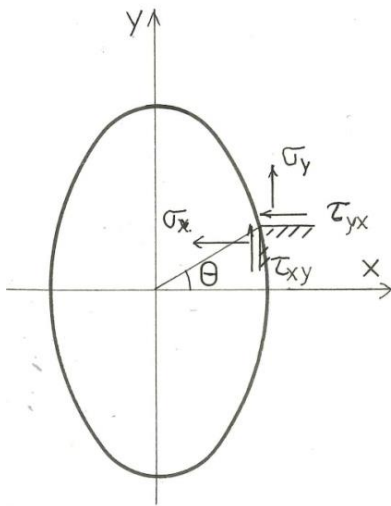


Fig.3. Contour stresses in orthogonal coordinate system

**Strains**

The strains on contour of the opening in natural coordinate system are:

$$\varepsilon_n = b_{13} \sigma_t; \varepsilon_t = b_{33} \sigma_t; \gamma_{nt} = b_{35} \sigma_t. \quad (9)$$

The stresses on contour of the opening in orthogonal coordinate system are:

$$\begin{aligned} \varepsilon_x &= \frac{\sigma_t}{\Delta} (b_{11} \Delta_1 + b_{13} \Delta_2 + b_{15} \Delta_3); \\ \varepsilon_y &= \frac{\sigma_t}{\Delta} (b_{13} \Delta_1 + b_{33} \Delta_2 + b_{35} \Delta_3); \\ \gamma_{xy} &= \frac{\sigma_t}{\Delta} (b_{15} \Delta_1 + b_{35} \Delta_2 + b_{55} \Delta_3). \end{aligned} \quad (10)$$

The expressions of the strains of (9) and (10) involve the tangential normal stress. The coefficients with small letters in these expressions are given in (Ivanova et al., 2018), and those with capital letters are presented in (8).

**Conclusion**

The analytical expressions for stresses and strains, given in this paper, are applied to elliptical opening. It is drawn in a transversally isotropic rock mass. These expressions will write to detail. That will permit the numerical determination of stresses and strains.

These results should correspond to the strains observed in the rock mass. Theoretical studies (formulations) can be compared with other methods used to track strains. Modern photogrammetric methods are suitable for such purposes. In abroad and in Bulgaria there are developments related to the creation of numerical models in underground mines, using digital photogrammetry (Gospodinova, 2019; Gospodinova et al., 2018). These methods are not vector but tensor descriptions of geometric changes that give a better idea of the rock movements and the potential danger to the integrity of the rock. It may be interesting in the future to conduct a study related to the application of digital photogrammetry to track the strains, after then compare the results with the analytically determined stresses and strains along the contour of the opening.

**References**

Bulichev, N. S. 1982. *Mechanika podzemni soorujenii*, M., "Nedra", 282p. (in Russian)

Gospodinova, V. 2019. Research on creating a digital photogrammetric model by using different number of control and check points. - *Journal of Mining and Geological Science*, Volume 62, Number 2, 29-33. (in Bulgarian with English abstract)

Gospodinova, V., P. Georgiev, P. Ivanov. 2018. Generating of photogrammetric model in underground mines, - *Sixth National Scientific Technical Conference with International Participation "Technologies and Practices in Underground Mining and Mining Construction*, Devin, Bulgaria, 155-161. (in Bulgarian with English abstract)

Ivanova, M., V. Trifonova-Genova. 2018. Protecting the people, drawing on elliptic opening in transverse isotropic rock. - *Processing in Annual University Scientific Conference, National Warming University "V. Levski"*, 25-26 October, 656-660. (in Bulgarian with English abstract)

Minchev, I. T. 1960. *Mehanika na anizotropnoto tyalo v minnoto delo*, S., "Tehnika", 126p. (in Bulgarian)

- Trifonova, M., 2008. A method for determination of physical and mechanical characteristics of Kandaurov's earth stochastic medium. - *Annual of University of Mining and Geology "St. Iv. Rilski", S., Volume 51, Part II*, 141-144. (in Bulgarian with English abstract)
- Trifonova, M., 2010. Impact of mining layer depth on physical and mechanical characteristics of Kandaurov's earth stochastic medium. - *Annual of University of Mining and Geology "St. Iv. Rilski", S., Volume 53, Part II*, 58-60. (in Bulgarian with English abstract)
- Trifonova-Genova V. 2019. Stress and strain state in transversally isotropic rock – 1. - *Processing in Annual University Scientific Conference, National Warming University "V. Levski", 27-28 June*, 403-411. (in Bulgarian with English abstract)
- Vulkov M., 2006. *Stochastichni modeli v kinematica na muldata*, S., Izdatelska Kachta "St. Iv. Rilski", 135p. (in Bulgarian)
- Vulkov M., 1987-88. For general equation of nonlinear stochastic geomechanic, S., *Annual of Higher Mining and Geological Institute, Volume 34, Part II*, 357-363. (in Bulgarian with English abstract).

## ON THE DETERMINATION OF THE FUNCTION FOR STRESS IN TRANSVERSALLY ISOTROPIC ROCK MASS WITH ELLIPTIC OPENING

**Rayna Vucheva, Malina Ivanova**

University of Mining and Geology "St. Ivan Rilski", 1700 Sofia; r.wutschewa@abv.bg, malina\_vatz@abv.bg

**ABSTRACT:** The opening with form of ellipse is drawn in transversally isotropic rock mass. He owns the plane of isotropy, which is inclined. Stresses in the point of the medium surrounding the opening are determined with complex function method. The conduit of rock mass in condition of plane strain is described with partial differential equation. The main integral of this equation is function for stress. She depends by roots of characteristic equation. This equation is of fourth degree. To determine the roots of equation are applied iterative method.

The characteristic equation and his complex roots are obtained for real rock mass. The roots take part in expressions of function for stress and for stresses in point on opening.

**Keywords:** elliptical opening, transversally isotropic rock mass, analytical solution, complex function method

### ВЪРХУ ОПРЕДЕЛЯНЕ НА ФУНКЦИЯТА ЗА НАПРЕЖЕНИЕТО В ТРАНСВЕРЗАЛНО ИЗОТРОПЕН МАСИВ С ЕЛИПТИЧЕН ОТВОР

**Райна Вучева, Малина Иванова**

Минно-геоложки университет „Св. Иван Рилски“, 1700 София

**РЕЗЮМЕ:** Изработка с форма на елипса е проколана в трансверзално изотропен масив. Той притежава равнина на изотропия, която е наклонена. Напреженията в точка около отвора се определят с метода на комплексна функция. Поведението на масива в условие на равнинна деформация се описва с частно диференциално уравнение. Общият интеграл на това уравнение е функция за напрежението. Тя зависи от корените на характеристичното уравнение. Последното е от четвърта степен. За определяне на корените на уравнението се прилага итеративен метод.

За реален масив са определени характеристичното уравнение и комплексните му корени. Последните участват в изрази за функция за напрежението и за напреженията в точки от отвора.

**Ключови думи:** елиптична изработка, трансверзално изотропен масив, аналитично решение, метод на комплексна функция.

### Introduction

The distribution of stresses in rock mass around the opening is problem, solved by analytical, numerical, geological and surveying methods. Between analytical methods, the most applying is complex variable method. The rock mass is modulated by isotropic medium. The relation between the stresses and strains are linear.

In this research the transversally isotropic rock mass is examined. For her it will be applied the algorithm for determining the function for stresses.

### Methods

#### Formulation of the problem

The elliptic opening is drawn in rock mass with the plane of isotropy. She is inclined by angle  $\varphi$  to horizontal axis (fig.1). The stresses, the strains and the displacements are expressed by the function for stresses:  $F(x, y)$ . She depends of the coordinates  $x$  and  $y$  of the point of the medium around the opening. This function fulfills the partial differential equation:

$$D_1 D_2 D_3 D_4 (F) = 0 \quad (1)$$

and the boundary conditions of the contour of the opening .

The symbol in (1)  $D_k$  ( $k=1, 2, 3, 4$ ) notes with the operator

$$D_k = \frac{\partial}{\partial y} - s_k \frac{\partial}{\partial x}, \quad (2)$$

Here  $s_k$  are the roots of characteristic equation:

$$b_{11}s^4 - 2b_{15}s^3 + b_{17}s^2 - 2b_{35}s + b_{33} = 0, \quad (3)$$

where

$$b_{17} = (2b_{13} + b_{55}).$$

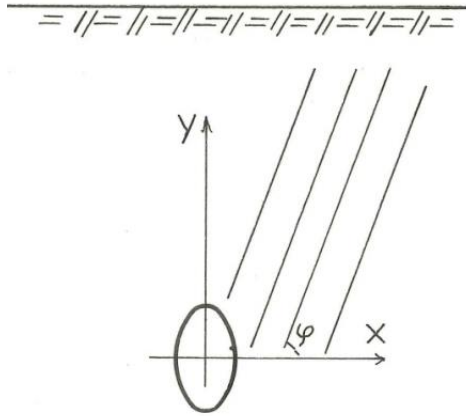


Fig.1. Horizontal elliptic opening in rock mass with inclined plane of isotropy

The coefficients in this equation can be seen in (Ivanova et al., 2018; Trifonova-Genova, 2019). The equation (3) can be written as:

$$s^4 + A_3s^3 + A_2s^2 + A_1s + A_0 = 0, \tag{4}$$

where

$$A_3 = \frac{2b_{13}}{b_{11}}, \quad A_2 = \frac{2b_{13} + b_{55}}{b_{11}}, \quad A_1 = \frac{-2b_{35}}{b_{11}},$$

$$A_0 = \frac{b_{33}}{b_{11}}.$$

By the algorithm given in (Ivanova et al., 2018), equation (4) is replaced with multiplication of two polynomials of the second degree:

$$(s^2 + e_{11}s + e_{10})(s^2 + e_{21}s + e_{20}) = 0, \tag{5}$$

where

$$e_{11} = B_1 + C_1, \quad e_{10} = B_0 + C_0, \quad e_{21} = B_1 - C_1,$$

$$e_{20} = B_0 - C_0.$$

The expressions above are given in recommended source. The roots of (5) are:

$$s_j = \alpha_j + i\beta_j, \tag{6}$$

where  $i$  is an imaginary unit and  $j=1,2$ .

**Numerical example**

The rock mass has the plane of isotropy, inclined by angle  $\varphi = 70^\circ$  (fig. 1). For this plane Young's modulus is  $E_1 = 14,5 \cdot 10^3 \text{ N/m}^2$  and Poisson's ration is

$\mu_1 = 0,105$ . In the direction perpendicular to this plane the parameters are:  $E_2 = 41,5 \cdot 10^3 \text{ N/m}^2$ ,  $\mu_2 = 0,3$ . In the same direction the shear modulus is  $G_2 = 8,24 \cdot 10^3 \text{ N/m}^2$ . When calculating the coefficients of polynomials (5), an accuracy equal to:  $\varepsilon_o = 1\%$  is assumed.

The elements of matrix A are calculated using formulas presented in (Trifonova-Genova, 2019):

$$[A] = 10^{-5} \begin{bmatrix} a_{11} & a_{12} \\ a_{21} & a_{22} \end{bmatrix},$$

where

$$a_{11} = \begin{bmatrix} 3,8193 & -1,9117 & -2,6838 \\ -1,9117 & 6,8966 & -0,8814 \\ -2,6838 & -0,8814 & 7,2566 \end{bmatrix};$$

$$a_{12} = \begin{bmatrix} 0 & 1,9117 & 0 \\ 0 & 0,8645 & 0 \\ 0 & 0,6748 & 0 \end{bmatrix};$$

$$a_{21} = \begin{bmatrix} 0 & 0 & 0 \\ 1,2094 & 0,8645 & 1,6748 \\ 0 & 0 & 0 \end{bmatrix};$$

$$a_{22} = \begin{bmatrix} 14,9207 & 0 & 0,8811 \\ 0 & 10,0405 & 0 \\ 0,8811 & 0 & 12,8206 \end{bmatrix}.$$

The coefficients of equation (3) are obtained by formulas given in above literary source:

$$b_{11} = 3,2894 \cdot 10^{-5}; \quad b_{12} = -4,3688 \cdot 10^{-5};$$

$$b_{22} = 7,144 \cdot 10^{-5}; \quad b_{26} = 1,5644 \cdot 10^{-5};$$

$$b_{66} = 9,9321 \cdot 10^{-5}.$$

The coefficients in equation (4) are presented in the following table:

Table 1. Coefficients in characteristic equation

$A_0$	$A_1$	$A_3$	$A_3$
2,1718	-0,9512	0,3631	-0,8810

By the first two step of algorithm, described in (Trifonova-Genova, 2018) are obtained:  $D_I = -0,08455$ ,  $D_{II} = 1,47371$ .

The third step includes the subroutine for calculating:  $B_0$ . She compounded of two parts. Since the coefficient  $D_I$  is smaller than the coefficient:  $D_{II}$ , the required coefficient  $B_0$

is determined by the second part. Its value is final after the second iteration.

The modulus of  $C_0$  and  $C_1$  and their multiplication are obtained according to fourth step of algorithm. The multiplication is negative. For that the coefficient  $C_0$  has plus sign and  $C_1$  - minus sign.

The coefficients in two polynomials of equation (5) are calculated following fifth step. The results of last three steps are given in following table:

Table 2. Coefficients in equation (5)

$B_0$	$B_1$	$C_0$	$C_1$
1,4774	-0,4405	-0,1043	1,6690
$e_{10}$	$e_{11}$	$e_{20}$	$e_{21}$
1,3731	1,2285	1,5817	-2,1095

The determination of the roots of characteristic equation (5) is the last step of algorithm. These roots are:

$$s_1 = -0,6143 + i0,9979, s_2 = 1,0548 + i0,73, \\ s_3 = -0,6143 - i0,9979, s_4 = 1,0548 - i0,73.$$

## Conclusion

The obtained roots participated in the function for stresses  $F(x, y)$  of (1). This function is compounded by two functions of complex variables (Trifonova-Genova, 2018). By them the stresses on contour of elliptic opening are obtained. When the stress values are small, the stability of the opening is guaranteed.

## References

- Ivanova, M., Trifonova-Genova, V. 2018. Protecting the people, drawing on elliptic opening in transversal isotropic rock. - *Processing in Annual University Scientific Conference, National Warming University "V. Levski"*, 25-26 October, 656-660. (in Bulgarian with English abstract).
- Trifonova-Genova, V. 2018. Functions of stresses around of elliptic opening, drawn in transversal isotropic rock. - *Resumes of XVIII - Anniversary International Scientific Conference "Construction and Architecture" VSU'2018*, 18-20 October, section 2, 65. (in Bulgarian with English abstract).
- Trifonova-Genova, V. 2019. Stress and strain state in transversally isotropic rock – 1. - *Processing in Annual University Scientific Conference, National Warming University "V. Levski"*, 27-28 June, 403-411. (in Bulgarian with English abstract).

## ADOPTED APPROACHES AND PRACTICES DURING THE STRUCTURAL-GEOLOGICAL INVESTIGATION OF THE ROCK MASS IN ELLATSITE OPEN PIT MINE, FOR THE PURPOSE OF NUMERICAL MODELLING AND MINE DESIGN

**Zhelyazko Yalamov, Nataliya Hadzhieva**

Mining Complex, "Ellatzite-Med" AD, 2180 Etropole; zh.yalamov@ellatzite-med.com; n.hadzhieva@ellatzite-med.com

**ABSTRACT.** The rapid development of software products and the improved computational power of the computer technologies over the last two decades allowed spatial georeferencing of the geological information and the ability of more complex three-dimensional geological and structural modelling of the rock mass. The article contains the applied approaches during the geological mapping, the data processing and interpretation for the deposit's geological model construction and update. Briefly discussed is the applicability of the results to the activities, related to the mining process.

**Keywords:** geological mapping, geological wireframing

### ВЪЗПРИЕТИ ПОДХОДИ И ПРАКТИКИ В ХОДА НА СТРУКТУРНО-ГЕОЛОЖКОТО ИЗУЧАВАНЕ НА СКАЛНИЯ МАСИВ В РУДНИК „ЕЛАЦИТЕ“ ЗА ЦЕЛИТЕ НА ЧИСЛЕНОТО МОДЕЛИРАНЕ И МИННО ПРОЕКТИРАНЕ

**Желязко Ялъмов, Наталия Хаджиева**

Рудодобивен комплекс, „Елаците-Мед“ АД, 2180 Етрополе

**РЕЗЮМЕ.** Бурното развитие на софтуерните продукти и повишената изчислителна мощност на компютърните технологии през последните две десетилетия позволи пространствено привързване на геоложката информация и възможността за по-детайлно триизмерно моделиране на геоложките тела и разломните нарушения в скалния масив. Статията съдържа възприетите подходи при теренното събиране на данни за прекъснатостите в масива, необходимата обработка и интерпретация на тази информация при изграждането и актуализацията на структурния модел на находището. Засегната накратко е приложимостта на резултатите при дейностите, свързани с миннодобивния процес.

**Ключови думи:** геоложко картиране, геоложко моделиране

## Introduction

The management of Ellatzite-Med AD commenced a campaign in 2013, aiming to develop a geomechanical and hydrogeological numerical models of the rock mass of Ellatzite mine. Another project for updating the existing model of the deposit, which had been built in the *Datamine* software suite, began in 2015. The update was performed by the newly implemented *HxGN MinePlan 3D* software for mine planning and design. Firstly, the available geological information was analyzed and a spatial tectonic faults model (structural model) together with a spatial lithological model have been developed as a base for these two projects.

The modelling of tectonic faults and geological boundaries within the deposit and its vicinity, and the discussion on them herein do not aim to solve any problems keen to the regional geology. A guiding line was as precisely as possible to define the tectonic faults surfaces, by accounting the available field and drill-hole data, while minimally judge over their location – predominantly in the model's peripheral regions. This article mainly aims to describe the preliminary activities and adopted approaches for processing and analyzing the existing geological data, which has been used for developing of the geomechanical, hydrogeological and block models of the deposit.

## Geology

The Ellatzite deposit is the northernmost one of the Upper Cretaceous copper-porphyry systems, part of the Panagyurishte Ore Region. The deposits in this region are arranged in an en-echelon array. They are located in the western parts of Central Sredna Gora and Central Balkan Mountains. Some regional summary tectonic works on the Upper Cretaceous magmatic arc development in the Sredna Gora region, interpret the deposits as a result of an oblique subduction at the front side of Rhodope Massif. Deep seated strike slip faults are considered as a main cause for structural placement of the deposits (Von Quadt et al., 2001).

Rock varieties present at Ellatzite deposit could be divided in two main groups: *Paleozoic metamorphic and intrusive igneous rocks* and *Upper Cretaceous intrusive to subvolcanic and sedimentary rocks*. The first group consists of low-grade metamorphic varieties from the Vezhen pluton collar – phyllites, contact-altered schists and hornfelses, and the granodiorites of Vezhen pluton. The second group consists of quartz-monzodiorite porphyries, granodiorite porphyries and Turonian sandstones. The latter are outcropped at the southernmost parts of the deposit, close to the mountain ridge.

## Input data types, their processing and outcomes

### Detailed sketches of rock slope outcrops, M 1:500

An approach for detailed data collection from the newly outcropped slopes has been adopted at Ellatzite mine. This is achieved by detailed sketches of the slopes in M 1:500 (Figure 1)

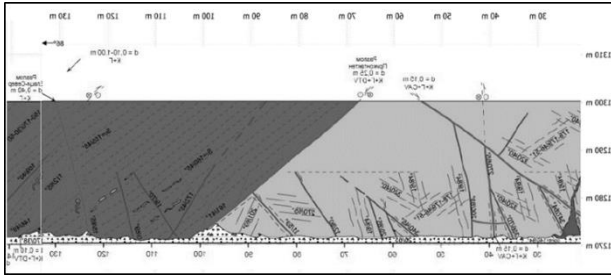


Fig.1. Part of a large sketch of a rock slope outcrop, M 1:500

The field structural and geological data collection has been established during the last 17 years. Firstly, paint marks are placed at every 5 m along a slope being mapped and marks' coordinates are recorded. Then all geological and structural features are spatially related to the paint marks. This detailed geological and structural mapping has been completed year by year by a team of geologists from NIS at Sofia University "St. Kliment Ohridski", under the supervision of prof. Zhivko Ivanov (2003-2015) and assoc. prof. Neven Georgiev (2015-2020). The field study results are presented in a sequence of applied science reports. The authors of this article participated in the field works from 2007 to 2012.

Field works especially accented on:

- the lithology and spatial interrelation between different geological bodies (incl. the degree of alteration underwent by rocks – hydrothermal, weathering, etc.);
- the texture of different segments along the rock slope – features of tectonic faults and shear zones, jointing, etc.;
- detailed study of brittle structures – separation of all joint sets in a particular segment of the slope, their spatial orientation and elements (length, frequency, joint profile morphology, joint surface alteration, fill, and degree of openness);

The brittle structures description (Ivanov et al. 2008) defines three different types, depending on their scale and role for rock mass rupturing: faults (F), master joints (GF) and joints (P).

Faults (F) are large discontinuities, accompanied by tectonic brecciation, cataclasis, fault gouge, while their thickness exceeds 2-3 cm. The boundaries between lithologic bodies are frequently delineated by such faults.

Master joints (GF) are large discontinuity planes, along which there is no visible displacement. Their traces could be often followed in 1-2 benches. Sometimes they are kinematically connected (splay structures) to the main faults. In other cases, they are parts of a well-defined joint set, having similar features and orientation. Master joints are accompanied by thin frictional zones of grinding, up to 1-2 cm in thickness.

Joints (P) are the smallest discontinuities. They tend to form separate sets with similar orientation and morphology. Several (from 2 to 4-5) joint sets are reported in different mapped slopes,

independently of their host rocks and having different spatial and morphological parameters.

Metamorphic rocks, affected by regional green-schist metamorphism, are mapped in rock slopes. They show three foliation generations –  $S_{0-1}$ ,  $S_2$  and  $S_3$ . Georgiev et al (2017) interpret them as a results of at least three different deformational events.

All field measurements through the yearly campaigns are accompanied by their coordinates. They are summarized in a tabulated spreadsheets. The spatial orientation of faults, master joints and foliation surfaces are coupled to the coordinates along the metric scale of the outcrops, at the slope heel. Joint sets are centered to the middle point coordinates of each studied rock slope segment. Each mapped discontinuity is accompanied by attributive columns for: coordinates (X, Y, Z), dip, dip direction, host rocks, type of the structure (F, GF, P, S), kinematics, thickness (openness), trace length along the slope, fill, litho-tectonic domain, open pit sector, metric location along the bench, and year of measurement.

The so catalogued structures allow their comparatively fast integration into different software applications and implementation of statistical, stereographic, and kinematic analyses. Spatial analysis is also possible by applying different sub-data sets and criteria. The most used software application for such spatial analysis at Ellatzite-Med AD is *Move*. It allows criteria searches – after different attributive data, location, or relative position to some other geometric objects. Examples for such objects are: a 3D surface of the open pit (real or designed), a directional line or a cross-sectional plane for stability analyses. The current volume of data consists of: 3320 fault measurements (Figure. 2a), 6060 master joints (Figure 2b), 7040 joint sets measurements (Figure 2c), and 5360 foliation surfaces (Figure 2d). It is important to note, that the number of fault measurements does not represent 3320 different fault structures. There are tens of measurements for each structure, which are collected at different bench levels, and different sequential push-ups (3 to 4 in number) of the mine.

The possibility to render different structural types with their spatial orientation is useful and has its own advantages. On the other hand, the simultaneous viewing of thousands of spatial measurements often is misleading and not very informative. This prompted the authors to develop a methodology for coupling of raster images of field sketches. The information contained therein helps to figure out the interrelationship between different discontinuities and their subordination (Figures 3 and 4).

For this purpose, again in the *Move* application, the metric paint marks along the mapped slope, with their coordinates, are imported in a 3D mode (Figure 3) and a continuous polyline is constructed. In the ideal case, it coincides with the slope heel line. The polyline is used for a cross section generation, which follows the polyline. The metric scale is projected over the generated cross section. In a 2D mode of operation, the raster image of the complete sketch or a part of it is imported and properly scaled.



Fig.2a.

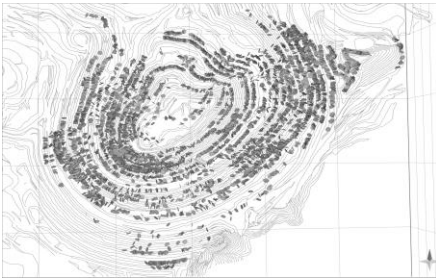


Fig.2b.

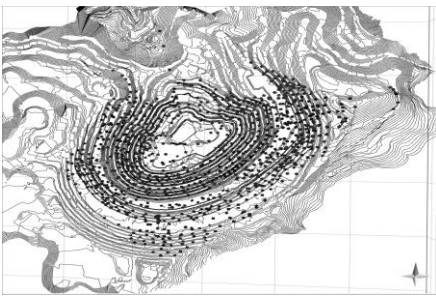


Fig.2c.

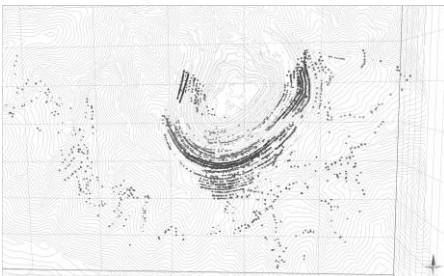


Fig.2d.

**Fig.2. Location and distribution of structural measurements of faults (2a), master joints (2b), joint sets (2c) and foliation surfaces (2d)**

#### Drill-hole data

The undertaken lithologic and structural modelling demanded an upgrade and supplementing with the existing drill-hole data. It has been summarized and complemented by data for all underground exploration and drainage galleries. The latter were modelled as a sub-horizontal drill lines. Different terms used through the years of study, by different teams, have been standardized and unified – different descriptive terms for rock varieties, especially for metamorphic ones. As a result, the outcropped within the open pit rocks have been divided into six main varieties: hornfelses, schists, phyllites, granodiorites, quartz-monzodiorites, and granodiorite porphyries. These

varieties possess clear differences in their physical and mechanical properties, structural anisotropy, and location along the deposit stratification.

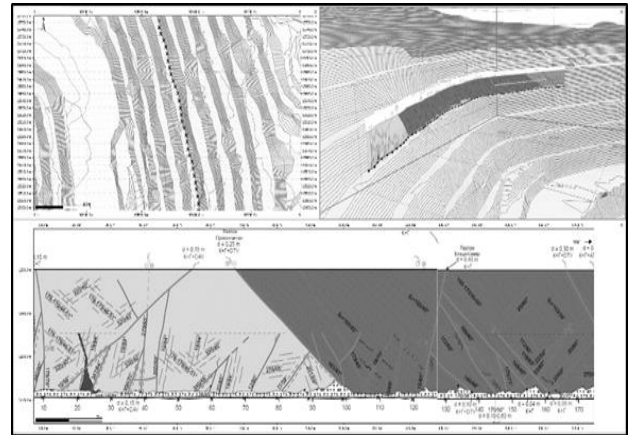


**Fig.3. Spatial coupling of a large sketch. Top left – metric scale points along the bench in a plan view. Bottom – scaled raster image of the sketch, placed along the constructed cross section. Top right – 3D view of the sketch, viewed to SE.**



**Fig.4. General view of the spatially coupled scaled sketches of rock slopes, from the eastern sector of the open pit, viewed to NE.**

The lack of data or the scarcity of oriented drill cores did not help much to define the spatial orientation of penetrated by drilling faults. Therefore the intersections were imported in the models only as points in space, accompanied by attributive data for the apparent fault zone thickness along the drill-hole, fill features and the angle between the drill-hole axis and the fault planes. The adopted approach is also appropriate if we take into account the difficulties to collect oriented drill cores out of the tectonically altered and disintegrated sections of the drill cores. Our experience from recent drilling campaigns show some 80-90% oriented core out of the whole drilled length, while the presence of faults discontinuities in the drill-hole prevents the successful core orientation or only allows low reliability in it.

#### Geophysical prospecting

Applied geophysical exploration has been performed in the higher peripheral levels of the southern and eastern sectors of the open pit, from 2013 to 2015, which aimed to fill up some lack of knowledge there. This included electric resistivity and

polarization profiling, together with vertical electric sounding (Yaneva et al., 2015). The results were accomplished and interpreted by a team from Geology of Earthquakes Department, Geological Institute, Bulgarian Academy of Sciences, under the supervision by assoc. prof. Marlena Yaneva, PhD and prof. Stefan Shanov, PhD.

The interpreted geophysical profiles (Figure 5a) were placed in their corresponding location by using the same methodology, described above. The results of this exploration were also analyzed and interpreted by the team in 24 horizontal plan views, vertically separated by 15 m, from levels 1510 to 1165 m. The raster images were georeferenced and digitized. The interpreted fault and geological boundary trace lines on each of the plan views were used for constructing of triangulated surfaces (Figure 5b).

The results were used for modelling of boundary surfaces, part of the lithological model, as well as of fault surfaces in the structural model, at the particular sector of the open pit.

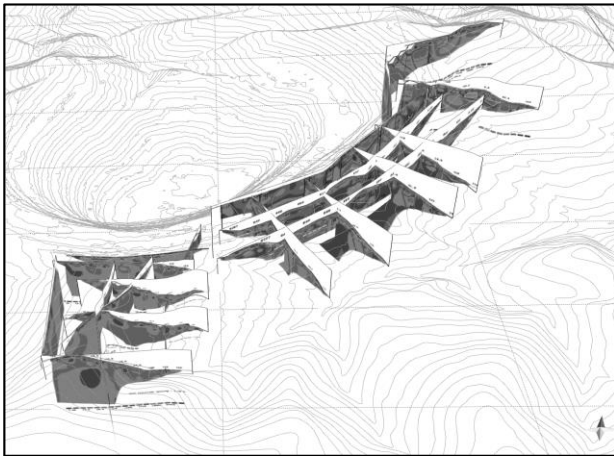


Fig.5a.

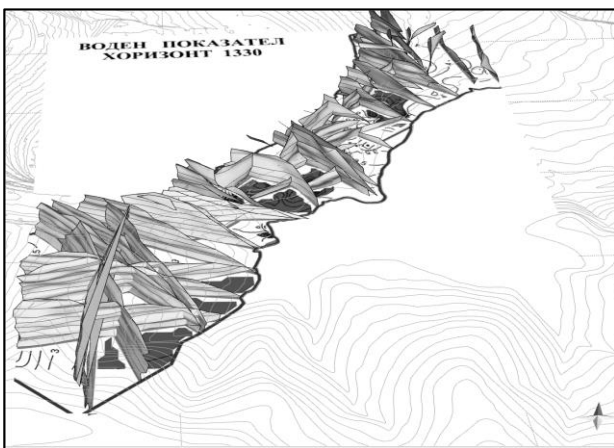


Fig.5b.

Fig.5. Location of processed geophysical profiles (5a) and the corresponding plan views, with their constructed 3D surfaces, viewed to the North.

#### Archived maps, cross-sections and plan views of the detailed exploration of the deposit

Raster images of the available maps, not in vectorized format, were georeferenced and digitized. Later, vectorized

objects, bearing geological information, were spatially placed by their projecting over preliminary prepared 3D surfaces, representing the open pit geometry (Figure 6a). The existing digital, 2D maps were spatially oriented.

The scanned geological cross sections and plan views of the detailed exploration of the deposit (Hadzhiiski, 1968), were placed along vertical and horizontal cross sections, generated in Move (Figure 6b), with their corresponding orientation and level.

These geological data were used as auxiliary to the drill-hole information, mainly for modelling the rock mass, which had been mined out, up to the natural landscape.

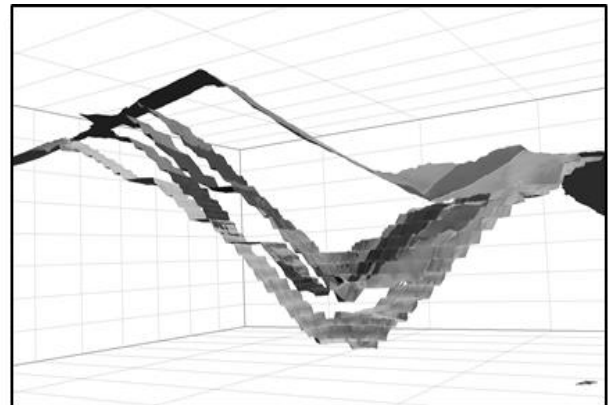


Fig.6a.

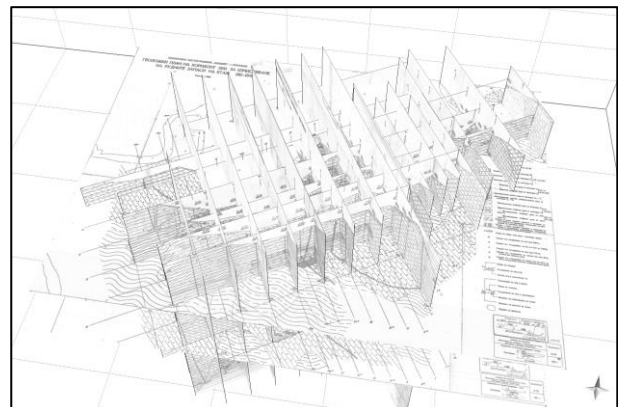


Fig.6b.

Fig.6. A part of the digitized and spatially oriented archived map data (6a) and a set of vertical and horizontal cross sections from the detailed exploration of the deposit (6b)

#### Lithological and structural modeling

The summarized geological information was interpreted along 58 2D profiles, SE-NW oriented. They were separated at 50 m in the central parts of the deposit and at 100 and 200 m in the periphery. The geological boundaries and first order faults were interpreted in a solid, 4930 x 4770 x 1400 m in size, for the necessities of the geomechanical and hydrogeological models of the deposit. The rock mass has been divided into four main tectonic blocks (Figure 7a), which are separated by two first

order fault structures – Elatsi-1 and Elatsi-2. These structures show larger vertical and horizontal displacements. The two faults, according to their kinematics, are classified as dextral strike-slip faults, bearing a superimposed normal faulting displacement (Georgiev et al., 2017).

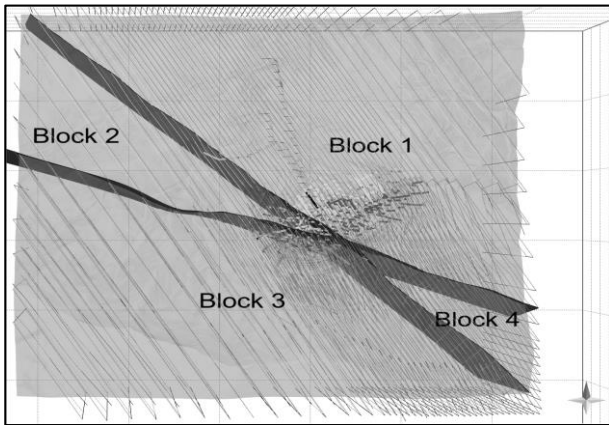


Fig.7a.

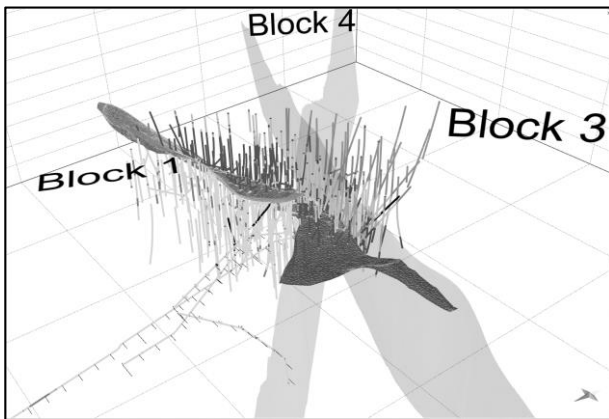
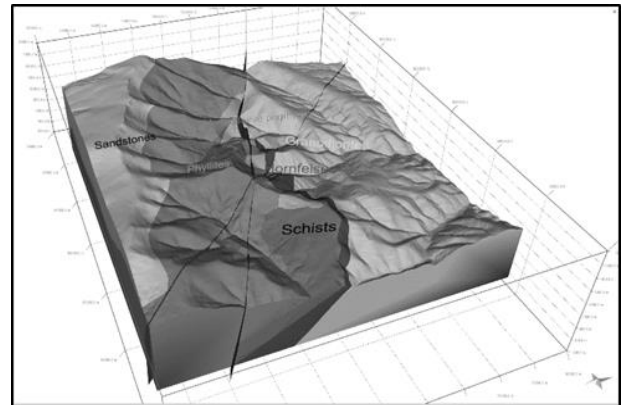


Fig.7b.

**Fig.7. Location of the interpreted profile lines in a plan view, with four tectonic blocks denoted (7a). Three-dimensional view of the boundary surfaces modelled between granodiorites and hornfelses, tectonic blocks 1 and 2, viewed to SE (7b).**

The geological boundaries are mostly tectonically reactivated magmatic contact surfaces. They are drawn as polylines, for each tectonic block. The resulting polylines are used for constructing triangulated boundary surfaces, separating different rock varieties, at each tectonic block (Figure 7b). The so constructed surfaces are edited in 3D working space, by several iterations of geometric files, between *Move* and *HxGN MinePlan3D* applications. The editing consists of simplification or addition of more nodes on surfaces, as well their coupling to lithologic boundaries, detected by drilling or surface mapping. The surfaces are extended along their strike and dip toward the open pit peripheral areas, so that the surfaces to pass through the whole solid, in which they are in. That is to allow easy work with Boolean operators. All surfaces have been checked for possible gaps, overlaps or intersecting facets.

As a result from the whole modelling, the six main rock varieties (Figure 8) are divided into 23 litho-tectonic domains. This detailed classification gives the opportunity for more thorough statistical (geostatistical) analysis, for different types of studies and structural measurements, which fall in different domains. It also provides flexibility when different properties and parameters are set for the geomechanical, hydrogeological and block modelling. This is also helpful for finding of optimal conceptual boundaries of the deposit, as they are constructed within the *HxGN Mine Plan Economic Planner* module, for long-term mine planning.



**Fig.8. Three-dimensional view of the spatial lithologic model of the deposit. Left to right: sandstones, phyllites, schists, quartz-monzodiorite porphyries, hornfelses, and granodiorites, viewed to NW.**

Part of the fault surfaces were modelled during interpretation of geological data along 2D cross sections. The remaining ones were constructed in a 3D working mode at *Move* and *HxGN MinePlan3D* applications. All drill-hole and mapped data were used for construction of triangulated surfaces. Spatially referenced large- and middle-scale archived geological maps, together with corresponding cross sections in M 1:5000, 1:10000 и 1:25000, were very useful for the peripheral areas around the open pit. The interpretation of interrelations between different fault surfaces is based on scaled field sketches of rock slopes, archived mapping campaigns, and the field experience of the authors, working within the open pit.

The current structural model of the deposit consists of 70 3D fault surfaces (Figure 9). They are ranked according to their size: first-order (21), second-order (34), and third-order (15). The first-order faults cross-cut the whole open pit or are present in one of the sectors, but also play a role of a lithologic boundary. Second-order faults pass through the entire single wall of the open pit, in a particular sector. Third-order faults are present across several benches (inter-ramp scale). Excluding two of the first-order faults, all others are modelled as singular surfaces. Ellatzi-1 and Ellatzi-2 faults are modelled as having certain thickness, varying between 4-5 and 10-12 m. These two main structures are modelled by a couple of subparallel fault wall surfaces, representing their brittle boundaries. The geometric files for the lithologic and structural models are annually updated with the newly collected drilling and mapped data.

## Conclusions

The summarized geological information considered in this article is a good foundation for all activities, necessary for the geomechanical, hydrogeological and block modelling of the deposit. Results obtained from the accumulated data base, together with the 3D geological model, are used on a daily base for planning and design of drilling and blasting works. They are used as input data for: geotechnical plan views, which reflect the rock mass zoning according to its blastability; preparation of text and graphic files, containing geological bedrock information and constructing 2D cross sections for stability analyses; preparation of entire or local model designs for stability purposes.

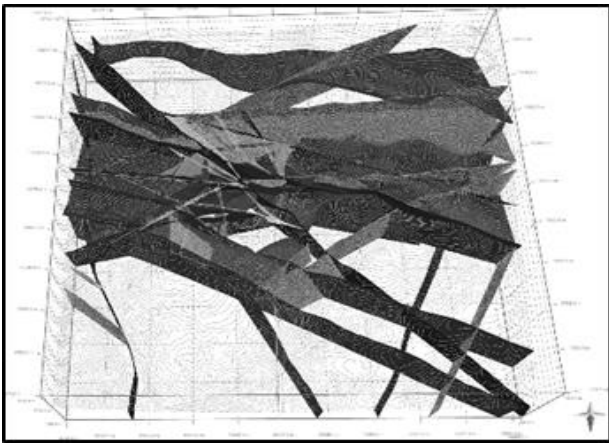


**Fig.9. Three-dimensional view of the modelled surfaces, part of the structural model of the deposit, viewed to the South.**

These results are also used for preparation of the geological base, which is integrated into the radar system software, used for real time slope stability monitoring. Another application goes for design of exploration and drainage drilling. The detailed classification of the rock domains allows the assessment of

different rock slope geometries, within those domains. The models described in this article are used for strategic mine planning and design, while searching for economically feasible deposit boundaries. The importance of the described here modelling requires a critical thinking over the spatial models, a permanent pursue for their upgrade with good quality data and improving their reliability.

## References

- Ivanov, Z., Z. Yalamov, M. Ivanov, I. Mitzev, P. Vasileva, N. Hadzhieva, G. Milanova. 2008. *Geological and structural mapping of newly outcropped and accessible levels, in M 1:500 – stage 2007*. Geotechmin OOD's archive (in Bulgarian).
- Georgiev, N., K. Naydenov, I. Krumov, Z. Nanov, A. Gadzhev, Tz. Gorinova, P. Petkova, A. Keskinova, V. Vasileva. 2017. *Supplementary notes to a geological map and cross sections of the Ellatzite open pit and its surrounding areas (b)*. Ellatzite-Med AD's archive (in Bulgarian).
- Hadzhiiski, G., K. Angelkov, Tz. Tzvetkov. 1968. *I-744 Report for the results of the geological exploration of Ellatzite Cu deposit*. Ellatzite-Med AD's archive (in Bulgarian)
- Yaneva, M., S. Shanov, K. Kostov, V. Nikolov, G. Nikolov, Y. Donkova. 2015. *Report for the results of the applied geophysical exploration of the Ellatzite open pit and its surrounding areas, during 2014-2015*. Ellatzite-Med AD's archive (in Bulgarian).
- Von Quadt, A., Z. Ivanov, I. Peycheva. 2001. *The Central Srednogorie (Bulgaria) part of the Cu (Au-Mo) Belt of Europe: A review of the geochronological data and the geodynamical models in the light of the new structural and isotopic studies. - Mineral Deposits at the beginning of the 21st Century* (Eds. A. Piestruzynski et al.), Proceedings of the Joint 6th Biannual SGA-SEG Meeting, 2001, A.A. Balkema Publisher, Netherlands, p.p. 555-558.

**SECTION**

**MECHANISATION, ELECTRIFICATION AND  
AUTOMATION OF MINES**

## ANALYSIS OF THE HYDROGEN CONCENTRATION ON NETWORKS FOR GAS SUPPLY

**Martin Boyadjiev**

University of Mining and Geology "St. Ivan Rilski", 1700 Sofia; martinb@mgu.bg

**ABSTRACT.** Restrictions on the planet's carbon footprint are becoming a motivating measure to limit the use of fossil fuels in the European Union. One of the measures to decarbonize the economy is to reduce the use of hydrocarbon fuels (oil, gas, coal). Increasing the potential for hydrogen use in energy is a key point in the conversion of fuels into energy. How the concentration of hydrogen is reflected in the gas supply is an analysis that the energy sector must consider to determine the safe operation and quality of operation of the appliances. Increasing the concentration of hydrogen in gas mixtures by up to 5% does not change the key parameters that determine the interchangeability of used gases in the gas industry. At hydrogen concentrations above 10% in the gas mixtures, the gas-dynamic properties of the gas also change, which also affects the design parameters of the gas supply systems.

**Keywords:** natural gas, hydrogen, gas supply, gas appliances

### АНАЛИЗ НА ВЪЗМОЖОСТИ ЗА ИЗПОЛЗВАНЕТО НА ВОДОРОД В ГАЗОСНАБДИТЕЛНИТЕ СИСТЕМИ

**Мартин Бояджиев**

Минно-геоложки университет „Св. Иван Рилски“, 1700 София

**РЕЗЮМЕ.** Намалението на въглеродният отпечатък върху планетата, става мотивираща мярка за ограничаване на използването на фосилните горива в Европейския съюз. Една от мерките за декарбонизация на икономиката е намаляване на използването на въглеводородни горива (нефт, газ, въглища). Увеличението на възможностите за използване на водород в енергетиката е ключов момент при конверсията на горива в икономиката. Как се отразява концентрацията на водорода при газоснабдяването е анализ, който енергийния сектор трябва да вземе предвид за определяне на безопасната експлоатация и качеството на работа на газовите уреди. Увеличаване на концентрацията на водород в газовите смеси до 5% не променят ключовите параметри определящи взаимозаменяемостта на използваните газове в газовата промишленост. При концентрации на водорода над 10% в газовите смеси се променят и газодинамичните качества на газа, което се отразява и на проектните параметри на газоснабдителните системи. Предмет на този доклад е възможността за използване и пренасяне на водорода в газоснабдителните системи.

**Ключови думи:** природен газ, водород, газоснабдяване, газови уреди

### Introduction

Protecting the environment and preserving the ecological climate of the planet is society's duty to the next generation and an investment in the future.

Joint multi-layered efforts are needed to achieve a sensitive effect and real benefits for clean air, climate and public health. The extractive and processing industries, together with transport, are the sectors of the economy that will undergo the most profound changes in the realization of the goals set for society to reduce the carbon footprint of the planet.

The main changes are expected to be in the direction of changing the fuel base in the energy and transport sectors. The task is to limit fossil fuels at the expense of an increasing share of hydrogen (green and blue), obtained by electrolysis or reforming, respectively from water or fuels that contain it. The European Community expects that by 2040 the reduction of greenhouse gases will be 5 Gt compared to the current situation.

In the process of replacing fossil non-renewable fuels with hydrogen produced by the two main technologies, at least three problems have been identified. One is related to the production of sufficiently significant quantities of this gas, and

the others are related to the transmission, distribution and use by consumers. The last two issues and related issues are addressed in this report.

### Possibilities for hydrogen use in gas supply systems

European politicians are increasingly recognizing the important role that hydrogen will play in existing gas networks in order to achieve decarbonization targets with minimal disruption to consumers. Existing gas infrastructure is a vital advantage for energy supply and security of supply, capable of long-term and reliable energy storage. Mixing hydrogen with natural gas in existing gas supply systems is a possible advantage over companies in the gas sector. Some idea of the market can be obtained by studying the theory of imbalance, as a balanced center of gravity presented by (Radev, 2011). Technologically in the supply chain from the production of hydrogen to its combustion at consumers three technical-technological tasks are distinguished, corresponding to the chain of production and supply to customers (Fig. 1).

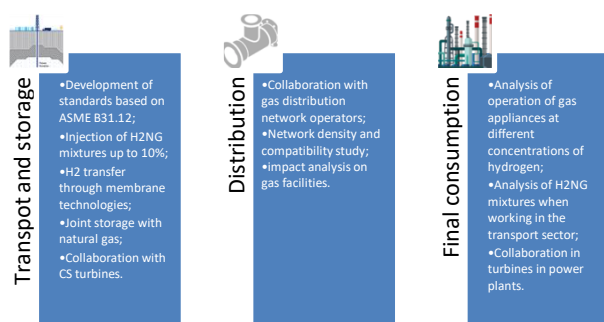


Fig. 1. Technical problems in hydrogen supply

The first problem is related to transport, where the subproblems are divided into the linear (pipeline) part, gas storages and compressor stations. In the transmission network the research is in the direction of: development of standards based on ASME B 31.12, which should prepare specifications of the admissible equipment, technical means for injection of high pressure hydrogen in the transport systems, research and study of membrane technologies for steel protection pipelines of high hydrogen concentration during transmission. A promising direction in storage is the possibility of capturing carbon dioxide from thermal power plants and in combination with hydrogen to obtain methane, which is traditionally stored and used in gas transmission systems. In the case of compressor stations, research is of interest to establish the effect of increased hydrogen concentration during the operation of gas turbine units.

In the distribution of gas, the analysis of the intensity of the diffusion processes of hydrogen in the pipes is in principle important for establishing the criteria for limiting the amounts of hydrogen used in urban networks. A separate type of research is devoted to its impact on gas facilities.

In the use of hydrogen gas mixtures (H2NG) by consumers, the efforts of the scientific community are aimed at establishing the impact of the mixture on the combustion process in order to maintain the design power of gas appliances and the quality of the combustion process. The possibility of using hydrogen in transport also belongs to this segment of research. The models adopted there are based on internal combustion engines using hydrogen as fuel or on the basis of hydrogen cells to generate electricity for electric vehicles and heavier vehicles. The well-known technology for obtaining hydrogen-oxygen mixtures in our country at the beginning of the new millennium, known as "brown gas" on behalf of its developer, is a third form, but is not based on scientific and theoretical popularity and is currently not widespread and applicable.

### Hydrogen injection into gas supply systems

Hydrogen is a gas that differs greatly in its physicochemical characteristics from natural gas and other biogases that are compatible in the gas network. Its pure use, in concentrations above 90%, can impair the mechanical properties of steel pipelines, gas storage facilities and customer installations. It can definitely be argued that pure hydrogen is not compatible with existing networks. However, hydrogen may be transferred to the gas networks if it is in quantities at the network entry point mixed with natural gas which do not adversely affect the

interoperability of the gas supply network. This follows from the interpretation of Articles of Directive (EU) 2018/2001 of the European Parliament of the Council of 11 December 2018 on the promotion of the use of energy from renewable sources. These possibilities are to be described in detail in standards and working documents of the network operators, so that other gases can be supplied to the network as "additional gas" to natural gas ("main gas") in existing gas supply networks. In addition, the supplementary gas must be injected in a manner that meets the requirements for the public natural gas supplier at the point of entry. This means that hydrogen can be supplied as far as permitted and as far as possible to ensure the safety and interoperability of the input network in question, of each transmission network along the chain, and of the storage facilities connected to the affected sections along it.

On the other hand, the network operator is not required to increase the hydrogen resistance of the existing network. In this case, the rules on minimum availability and minimum injection capacity do not apply. Nor are measures requiring the network operator to take action to increase the capacity of its network. This means that while there may be sufficient gas capacity in the system, the gas injected into the system may not necessarily be compatible with that system.

### Network connection

In Directive 2014/94/EU, hydrogen is classified as an alternative fuel and Art. 6 allows its transmission on available infrastructure. This assessment does not contradict the inclusion of hydrogen in the definition under Art. 171, para. 5 of the Energy Act. This can be seen by comparing the legal situation applicable to the supply of raw biogas (called raw biogas), which may also be incompatible when injected into gas systems. The rules for the supply of biogas also apply to the injection of raw biogas, as the definition of biogas covers for raw materials any possible form of biogas, ie. gas obtained from biomass, gas from waste water treatment plants, landfill gas and mine gas, regardless of the degree of treatment in each case, its specific composition or its compatibility with the system. On the other hand, if, contrary to the current legal situation, the connection requirements of network operators are required to ensure that the injected biogas meets the requirements of the system and is compatible, then in the case of injected hydrogen, crude biogas or other non-compliant gases, which fall within these definitions are incompatible with the network. In these cases, the network operator would be required to either improve its network or, if technically impossible or economically unprofitable, to build and operate the necessary biogas or methanization plants itself. However, this is not the purpose and intention of Art. 6 of Directive 2014/94 / EU. As the comparison specifically with raw biogas shows, it is not the purpose or intention to include renewable hydrogen and renewable synthetic methane. An interpretation in this direction would be in breach of the principles laid down in the provisions for the connection of gas sources to transmission systems, according to which the supplier should ensure that the gas injected into the system is compliant and compatible with it.

### **System compatibility assessment**

Upon receipt of a request for connection, the network operator, as part of the analysis of the current situation and possible changes in the operator's system already foreseeable at the time of the request, must first determine the maximum volume of hydrogen that its network can will take over. According to accepted principles in the EU, the costs of this assessment are always borne by the connecting party, provided that the assessment does not relate to capacity building measures within the meaning of the provisions of the Energy Act. As part of the assessment of connectivity, the network operator must in particular calculate the maximum permissible hydrogen content in its network and the permissible supply volume or capacity. To do this, the network operator must determine the factors of its network and other networks in the chain that could limit the amount of hydrogen that can be injected. In this context, a distinction must be made between restrictions that arise in relation to total gas supply and restrictions that relate only to the requirements of specific customer groups (eg the use of natural gas as a production material in the chemical industry). In practice, the provisions only protect the requirements related to the total gas supply. The requirements for the total gas supply and hence the interoperability of the gas supply network also cover the requirements for the system and storage activities, and the general and normal use of gas in the production of heat and electricity. This relates in particular to the quality of gas and hydrogen concentration required for gas turbines, cogeneration engines and gas storage installations, as well as the non-capture of hydrogen concentrations by gas chromatographs (GC).

Exceptions in this context are HGs used in the calibrated measurement of fuel value for the purposes of correct gas charging. According to European standards, the network operator is required to exchange the HTG if this is necessary to meet the gas charging requirements under the Connection and Trade Rules for Natural Gas and if the associated costs do not make the whole connection economically unjustified. The costs incurred in this connection shall always be borne by the network operator in whose network they are incurred, even if such costs arise as a result of a transformation in an upstream network area. This means that if new GCs have to be deployed in a network at customer entry points as a result of hydrogen injection, this is the responsibility of the downstream operator. On the other hand, this operator may pass on these costs where this would be economically justified and subject to cost-effectiveness considerations in the company's annual investment programs.

It is not normatively determined whether it is necessary to set further requirements for the quality of gas for charging stations with compressed natural gas (CNG) before the provisions on the interoperability of the gas supply network. It is unclear given the relatively small volumes of natural gas currently consumed as automotive fuel compared to the volumes used to generate heat and even electricity. The current situation, not future or expected developments, is crucial in this regard. On the other hand, the protection in the form of interoperability of the gas supply network is supported by the fact that in the presence of about 100 charging stations a large number of end customers are directly affected, and in the presence of more than 69,000 cars powered by natural gas in Bulgaria, and about one million such cars in Europe as a

whole, even more end customers are indirectly affected. A final assessment of the hydrogen injection situation remains to be considered in more detail, taking into account that the requirements for existing CNG charging stations should in any case be taken into account when setting the maximum permissible hydrogen content. As pure hydrogen is not compatible with the system and can only be supplied after it has been sufficiently mixed with natural gas, a current customer who is not protected by the interoperability requirements of the gas supply network must be able to at least rely on receiving of gas compatible with the system, which meets the thresholds provided in the working documents of the Bulgarian legislation.

After identifying the hydrogen-sensitive applications in the system, the network operator must - taking into account the binding data from the hydrogen supplier and in the connection request for the planned injection purposes - determine the required data from its network and whether and to what extent degree hydrogen may come into contact with sensitive applications or interconnection points in downstream or upstream networks (in the case of reverse feed). If this is the case, it may be necessary for the network operator to assess, where applicable with the affected customer, whether the application or the affected customer (eg storage or power plant operator) may exceptionally be able to accept higher hydrogen content or a larger volume of hydrogen (for example, very short-term excesses); on the other hand, the customer concerned is not required to accept a higher hydrogen content for a short period if damage cannot be completely ruled out, even if such content is only increased for a very short period of time. If this is not the case, the network operator must calculate the amount of hydrogen that can be injected at the requested connection point. If hydrogen is to enter downstream or upstream networks, the network operator must determine how much hydrogen can enter the network up or down the chain through the relevant interconnection point and must report this finding to the relevant network operator. It must then make a separate assessment to determine whether, in anticipating that it is possible to supply higher levels of hydrogen at certain times, the network operator must allow the supplier to do so. If this requires the installation of a chromatograph with a hydrogen reading column, the costs should be borne by the network operator.

The network operator needs to assess whether the replacement of hydrogen-sensitive equipment with hydrogen-compatible equipment or the modification of existing facilities to withstand higher hydrogen concentrations will be able to increase the hydrogen mixture without to disrupt or jeopardize the fulfillment of its obligation to operate a secure, reliable and efficient system.

On one hand, the network operator is not required to modify or install new equipment or accept the costs involved, but on the other hand it must provide the provider with all the information that will enable it to decide whether it would be more efficiently from a business point of view to transform customer installations in order to optimize the injection of hydrogen at the expense of the supplier, and not to carry out the required increase of the hydrogen mixture or not to use additional installation for methanization.

This may be relevant if several hydrogen suppliers would benefit from such measures and if retrofitting costs are shared between them.

### Changes in parameters after connection evaluation

Hydrogen injection may also be subject to change after the assessment of connectivity as a result of a change in gas flow at the network entry point. This may be due to changed import / export flows or commissioning / decommissioning, changed mode of operation of gas storage installations, changed reception structure (such as loss or attraction of customers), conversion of L-type gas into type H gas, market conversion from L gas to H gas and decentralized supply or reverse supply of gases (such as biomethane), or the injection of hydrogen at a later stage (if the permissible injection is to be distributed between several installations).

Imposing restrictions on hydrogen injection may result in additional hydrogen injection being linked at a later stage. On the other hand, limiting hydrogen injection on the basis of injection at a later stage would run counter to the principle of priority of earlier coupling or request for coupling. By deviating from the priority principle, it would be possible to achieve a higher (overall) level of hydrogen injection, as feed points that would be technically and commercially acceptable would not be neglected simply due to the existence of earlier submission projects. On the other hand, the operator of an installation that is connected earlier would make its investment decision based on arguments that will be undermined if the priority principle is disregarded. In this respect, the legitimate expectations of an earlier connecting party must be protected and take precedence over technically optimized maximum injection into a network or part of a network. Finally, this should also apply to connection requests, the network of this operator has applications that are sensitive to hydrogen, and must calculate how much hydrogen can be fed to the relevant point. The conclusion of the evaluation should be communicated to the network operator. The network operator (on supply) must then use this information to assess how much hydrogen can be injected at the required connection point. As part of this assessment, the network operator (where applicable in cooperation with the downstream or downstream network operators concerned) should also take into account foreseeable changes that may occur during the year. If it can be done at an earlier stage, in cases where the connection assessment has not yet been completed

In addition, the network operator must take into account any subsequent changes in the framework conditions under which hydrogen is injected. In particular, the network operator is not entitled - if a change in gas flow is expected at a later stage as a result of the supply or re-supply of a system-compatible gas (such as biogas that has been improved to natural gas quality) - to refuse such changes to facilitate unchanged hydrogen injection. Any such refusal may be based only on technical impossibility, economic unreasonableness or lack of compatibility with the system. On the other hand, such grounds for refusal do not apply in the circumstances described.

If circumstances arise that the network operator must take into account, the network operator should assess whether this would also have an effect on hydrogen injection. The evaluation should be undertaken in the same way as the evaluation of a request for connection. The assessment may lead to an increase or decrease in the amount of hydrogen injected. If the network operator concludes that the hydrogen injection needs to be reduced in order to maintain the

interoperability of the gas supply network, the network operator must check whether alternative measures (change in transmission settings, change of installation) would provide a way to reduce to avoid. On the other hand, the costs of such measures that may be required are borne by the hydrogen supplier. If these measures would be extremely costly for the hydrogen supplier, the network operator has the right, as a last resort, to reduce the amount of hydrogen injected or to stop the injection altogether if necessary. Therefore, the network operator has the right to retain the right of limited injection if the technical framework conditions change or, as a result of such changes, it becomes necessary to reduce the amount of hydrogen injected on the grounds of safety and interoperability of the gas network.

As the potential for change in gas flows as a result of changing supply and consumption patterns increases, it is becoming increasingly important for the hydrogen supplier to choose a location that fully guarantees the planned injection or gas flow that can be reliably planned on an ongoing basis. year and the network operator to notify the connecting party as soon as it becomes aware of even the slightest possibility of a negative change in gas flows and then to support the connecting party, as far as its knowledge and ability allow, to minimize the risk of damage that comes from stopping or reducing the injection. The allocation of risks in this way will make it possible to create energy-related business incentives for the relocation of hydrogen injection installations to such grid locations that provide high and reliable levels of long-term hydrogen compatibility. At network topological positions where there is a high probability of injection limitation, the risk distribution is such that it creates incentives in favor of methanization.

### Influence on the operation of gas appliances

To ensure safety and determine the operation of a system with increasing hydrogen concentration, an effort is needed to develop regulatory studies and constraints.

The University of Mining and Geology, together with the gas sector, has launched a number of studies relate to this. These projects aim to develop and publish a detailed study of the impact of mixtures of natural gas and hydrogen on end-use applications, in particular in the household and commercial sectors.

Our task is to study the possibility of widespread use of H<sub>2</sub>CH<sub>4</sub> (hydrogen in natural gas) mixtures and their impact on household and commercial gas appliances.

According to the European standard EN 16726: 2015 "it is not possible to determine a hydrogen limit value valid for all parts of the European gas infrastructure, therefore a case-by-case analysis is recommended". Eligibility limits vary for the United Kingdom from 0.1% to 6 and 10% in France and Germany respectively. The current levels of hydrogen in mixtures of hydrogen with natural gas do not indicate the need for additional safety requirements. For increased hydrogen concentrations, the prospect is to increase the requirements for monitoring, sensors and safety rules in installations. There are additional restrictions related to national provisions or areas of application. For example, the calorific value of the gas changes after the injection. In Germany, there is a formal agreement for the monitoring and invoicing of H<sub>2</sub>NG mixtures, where the

calorific value can be determined with gas quality measuring instruments (gas chromatographs are currently used).

The EU Gas Appliances Directive 90/396/EEC and derivative Gas Appliances Regulations (EU) 2016/426, which cover all Member States, already sets out (in a common format) the requirement to prove the safety of any gas appliance that will be sold in the EU.

The regulations for gas appliances apply equally to all gaseous fuels that will be used in a gas appliance - hydrogen, biogas, natural gas, propane and / or butane. The conducted research showed that at the moment the operation of gas appliances with the used mixtures of hydrogen and natural gas up to 10% by volume of hydrogen is possible without adaptation of the devices.

Table 1. Influence of hydrogen concentration

% H <sub>2</sub>	d, kg/m <sup>3</sup>	Hlcv kWh	Hgcv kWh	Wlcv MJ/m <sup>3</sup>	Wgcv MJ/m <sup>3</sup>
0	0,67	9,156	10,165	43,73	48,546
5	0,641	8,69	9,65	42,547	47,235
10	0,608	8,22	9,13	41,333	45,89
15	0,575	7,75	8,61	40,08	44,5
20	0,542	7,29	8,09	38,793	41,59
25	0,51	6,82	7,57	37,46	41,59
50	0,345	4,48	4,979	29,93	33,23

The table presents the results of a study of the concentration of hydrogen in a methane mixture. The step is 5 percent, and the variations studied are from 0 to 50 percent hydrogen content in a methane mixture. Indicators such as: density, d (kg / m<sup>3</sup>), upper and lower limit of combustion heat, H (kWh) and lower and upper value of the Wobbe number, W (MJ / m<sup>3</sup>) were evaluated. The calculations are based on the methodology and requirements of the BDS ISO 6976 standard, and software used for these purposes by the Natural Gas Association.

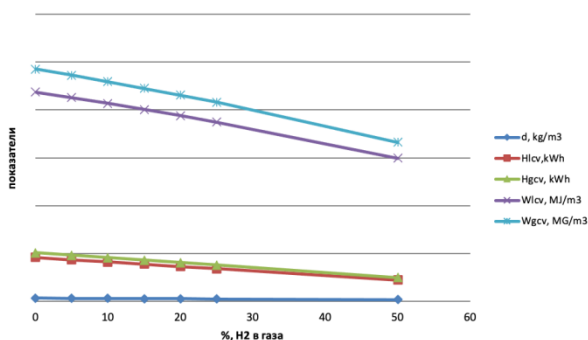


Fig. 2. Change in gas mixture parameters due to increase in hydrogen concentration

Due to the lower density of hydrogen and volumetric heat of combustion with increasing its concentration, the values of the studied parameters of the gas mixture also decrease.

## Conclusion

The requirement for the use of 32% renewable energy, defined in the Renewable Energy Directive and the requirement for an annual increase in the share of renewable energy sources in heating and cooling compared to what was

achieved in 2020. by 1.3%, puts the issue of hydrogen use in an important position for their implementation. There are many technical, legislative and other barriers that need to be overcome for this implementation.

An example of this we can, as usual, take from Germany. What has been achieved there shows that some of the pan-European barriers can be overcome quicker at a national level, before waiting for the EU Directives.

Gaps and inconsistencies at the regulatory level relate to:

- The lack of a uniform definition of renewable gases of non-biological origin - the only existing definition applies only to fuels in the transport sector. To overcome this barrier, Germany includes hydrogen produced by electrolysis of water with renewable energy in the definition of biogas (Energy Industry Act).
- The existence of a single Guarantee of Origin system for renewable gases of non-biological origin would encourage end-users to buy renewable hydrogen. In this regard, Regulation № RD-16-1117 of 14 October 2011 is a good basis that can be applied in such future situations.
- Adoption of standards for permissible concentration of hydrogen in the gas mixture. Based on the current study and future projects in this direction, definitions of gas quality can be developed at national level to be allowed, including norms for the concentration of hydrogen in gas mixtures.

**Acknowledgements.** The author expresses his sincere gratitude to the gas companies of the Natural Gas Association, which have accepted the topic of decarbonization and environmental protection as their mission and in this sense have given full support and empathy to the research and analysis.

We gratefully accept the suggestions for follow-up activities and results, believing that real results in scientific activity can be obtained only if they are related to applied projects that will benefit society as a whole.

## References

- Radev, J., Theory of Imbalance: Perspectives for the Gas Sector in Europe, IC "St. Iv. Rilski", 2011.
- Radev, J., Model of natural gas demand from households in Europe, Journal of Economic Alternatives, 2011, №1, p.58-81.
- Radev, J., Empirical analysis of natural gas demand from Households in Europe, Journal of Economic Research, pp.154-183, 2012.
- Georgiev L., Application of a hybrid mathematical model for expert technical and economic assessment of gas deposits with limited reserves. Technical conference „Automatization in mining industry and metalurgy”, Sofia. ISSN 1314-4537, 2016.
- Georgiev L., Mathematical models for forecasting the development of gas deposits in the initial stage. Technical conference, стр.197-200, ISBN -10:954-91547-4-2, 2006;
- EWRC, Rules for management and technical rules of the gas transmission networks, 2014
- ORDINANCE No. RD-16-1117 of 14.10.2011 on the terms and conditions for issuing, transferring, revoking and recognizing guarantees for the origin of energy from renewable sources.

## ORE LOAD INFLUENCE ON BALL MILLS SPECIFIC ELECTRICITY CONSUMPTION

**Stoyan Chetyov<sup>1</sup>, Kiril Dzhustrov<sup>2</sup>**

<sup>1</sup>University of Mining and Geology "St. Ivan Rilski", 1700 Sofia; chetyov@gmail.com

<sup>2</sup>University of Mining and Geology "St. Ivan Rilski", 1700 Sofia; justrov@mgu.bg

**ABSTRACT.** The mill productivity and therefore the specific electricity consumption depends on the right choice of the ore load. Both the increased and the reduced ore load leads to decrease of mill productivity, which causes an increase in the specific electricity consumption. With an optimal mill load, operating in a closed cycle, an increase in the circulating load can be allowed while increasing the mill productivity, reducing the specific electricity consumption and improving the technological indicators. Data were processed from the operation of ball mills and experimental studies were performed to determine the specific electricity consumption at different loads, to analyze the influence of the ore quantity on the specific electricity consumption.

**Keywords:** mill productivity, specific electricity consumption

### ВЛИЯНИЕ НА НАТОВАРВАНЕТО ПО РУДА ВЪРХУ СПЕЦИФИЧНИЯ РАЗХОД НА ЕЛЕКТРОЕНЕРГИЯ НА ТОПКОВИ МЕЛНИЦИ

**Стоян Четъев<sup>1</sup>, Кирил Джустров<sup>2</sup>**

<sup>1</sup>Минно-геоложки университет „Св. Иван Рилски“, 1700 София

<sup>2</sup>Минно-геоложки университет „Св. Иван Рилски“, 1700 София

**РЕЗЮМЕ.** От правилния избор на натоварването по руда зависи производителността на мелницата и следователно специфичния разход на електроенергия. Както завишеното, така и заниженото натоварване с руда, води до намаляване на производителността на мелницата, което предизвиква повишаване на специфичния разход на електроенергия. При оптимален натоварване на мелницата, работеща в затворен цикъл, може да се допусне повишение на циркулационния товар при едновременно увеличение на производителността на мелницата, снижавайки специфичния разход на електроенергия и подобрявайки технологичните показатели. За анализ на влиянието на количеството руда върху специфичния разход на електроенергия са обработени данни от работата на топкови мелници и са направени експериментални изследвания за определяне на специфичният разход на електроенергия при различни натоварвания.

**Ключови думи:** производителност на мелница, специфичен разход на електроенергия

### Introduction

Two Process plants have been studied in which the grinding of copper ore takes place in ball mills driven by synchronous motors 2.5 MW and voltage 6 kV. The mills are identical in both enterprises, differing only in the physical and mechanical properties of the ore.

The technological operation of grinding is the most energy-intensive. It consumes 60-70% of the electricity consumed by the process plant. Therefore, it is necessary to establish such a mode of operation that the specific consumption of electricity is minimal at maximum productivity of the mill in the specified class of the finished product.

As it is known, the specific consumption of electricity for grinding in ball mills is closely related to the technological process and depends on a number of factors: the weight of the ball load, the size of the mill, rotation speed, pulp density, size of the source material, lining type, physical and mechanical properties of the ore, productivity of the mills, etc.

Experimental studies have shown that the main power in the ball mill is spent on lifting the ball load - about 80%.

Increasing the productivity of the mill leads to a slight increase in the extracted power. The striving to increase the productivity of the mills is obvious, which will reduce the specific consumption of electricity.

### Experimental research

All experimental studies were performed with modern digital network analyzers FLUKE 437-II, FLUKE 435-II and FLUKE-43B.

The influence of the ore load at constant ball load on the energy characteristics has been studied.

Figure 1 shows the results of the experimental study of increasing the ore load by 5 t / h at an interval of 30 minutes on a mill unit M4. Until the beginning of the experiment at 14:00 h, the M4 mill operated only with a load of about 157 t/h. From 14:00 to 14:30 the mill worked with a reduced load - 150 t/h. In the next 30 minute intervals the load was increased to 165 t/h and 170 t/h.

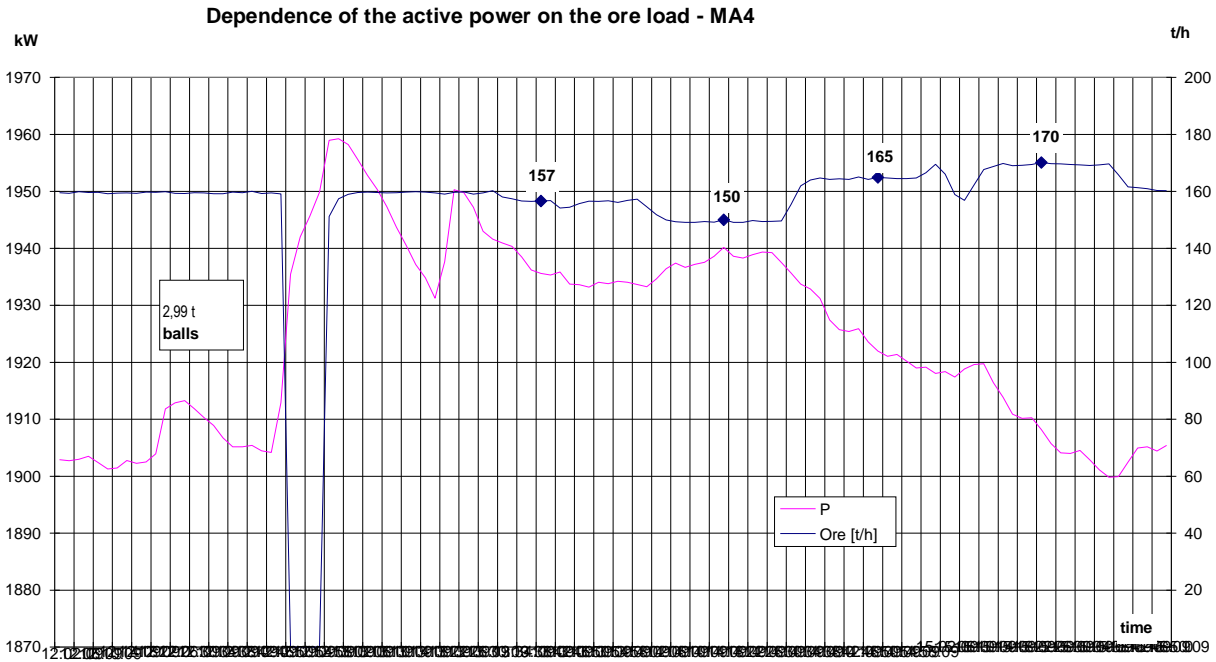


Fig.1. Dependence of the active power on the load on the ore - M4

The power drawn from the motor was recorded by the FLUKE 437-II instrument, and the results for the ore load were reported at one-minute intervals from the SCADA system. After about an hour and 35 minutes, the percentage of the class - 80

microns fell from 56.97% to 54.02 and the ore load was reduced to 160 t / h. In fig. 2 shows the change of the starting product from the mill during the experiment.

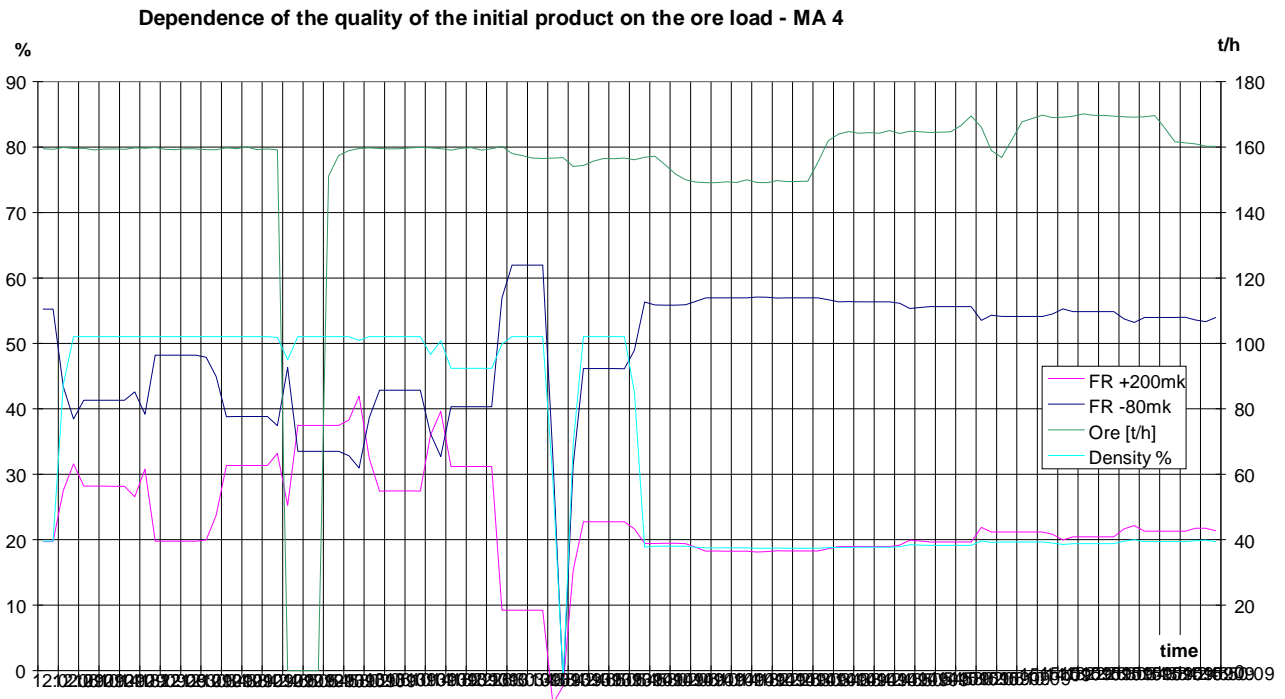


Fig.2. Dependence of the quality of the initial product on the ore load - M4

The results of the experiment give reason to draw an important conclusion:

The load on the ore, at a relatively constant ball load leads to a reduction of the active power drawn from the electric motor. At a load of 150 t / h ore, a registered power of 1940 kW

was registered. From the moment of increasing the load on the ore, the power drawn from the motor gradually decreases and after 1 hour and 30 minutes reaches its minimum value of 1900 kW.

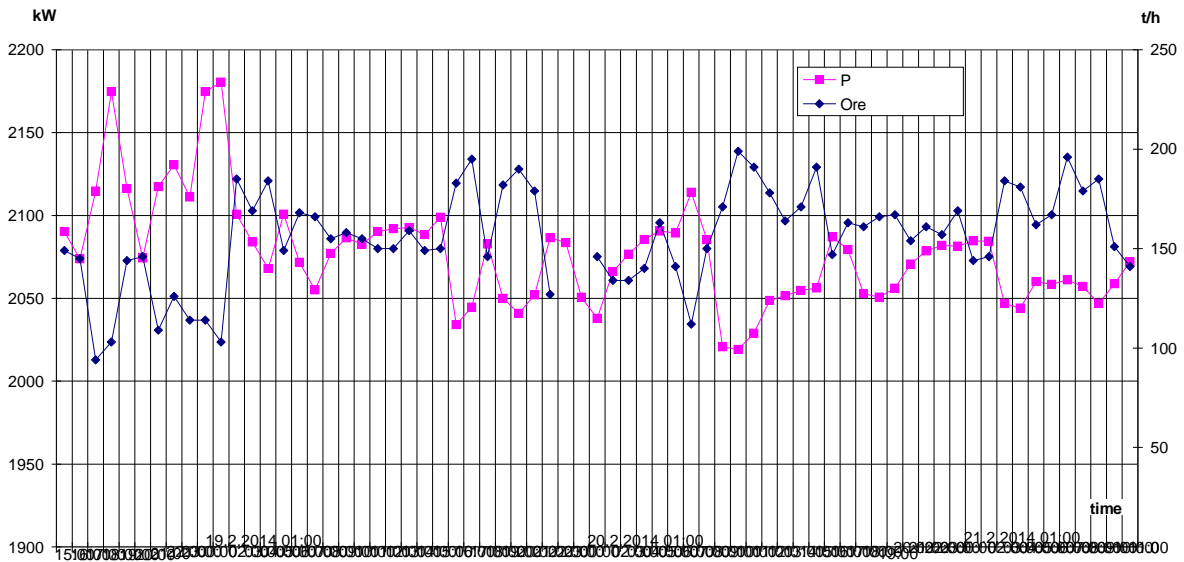


Fig.3. Dependence between the drawn active power and the load on the ore - M3

Figure 3 compares the hourly load of the ore mill and the average hourly power, at constant ball load of the mill unit M3 in the same enterprise. Here the fact recorded by other measurements is also confirmed that as the load on the mill increases, the power drawn from the motor decreases. This shows that for the entire measurement period the operating

mode of the mill was after the extremum of the function  $P = F(G_{cm})$ , i.e. the ball load was optimal or above the optimal.

Figure 4 shows the results of the experimental study in the other process plant, with an increase in the load on the ore by 38 t / h. Until 11.00 h mill №3 worked only on the plum with a load of about 200 t / h.

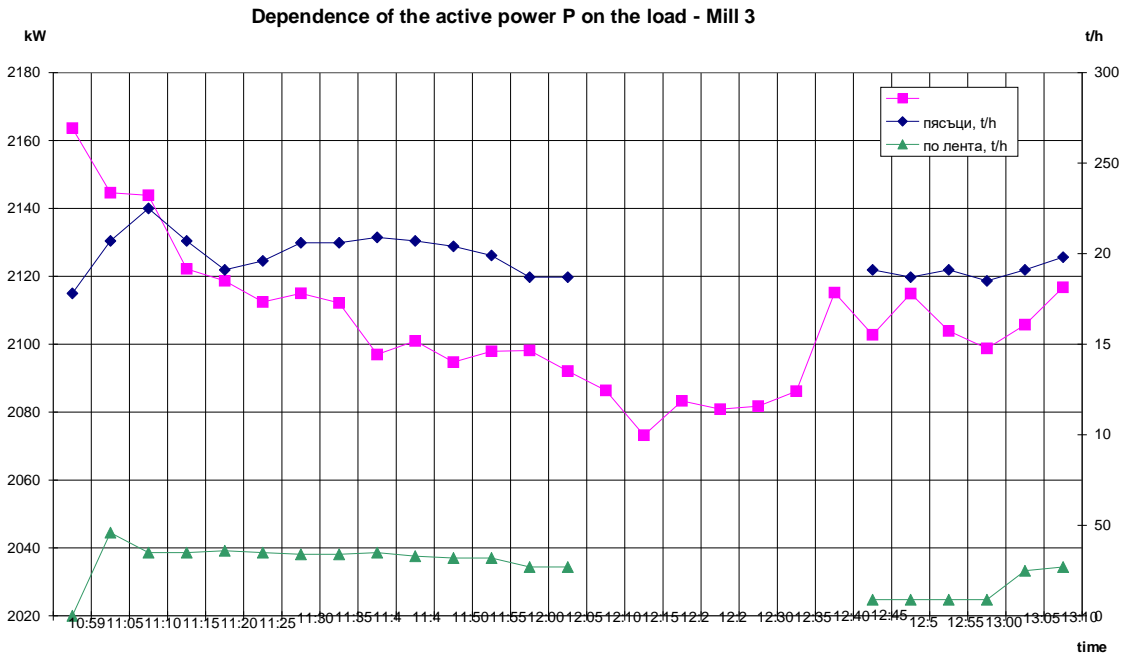


Fig.4. Dependence of the active power on the ore load - M3

Data from the SCADA system were missing for some of the five-minute intervals, but this does not prevent important conclusions from being drawn:

- The load on the ore, with a relatively constant load on the sands, leads to a reduction in the active power drawn from the electric motor. Before the ore mill was loaded, a power of 2160 kW was registered. From the moment of ore supply (38 t / h),

the power drawn from the electric motor gradually decreases and after 1 hour and 15 minutes reaches its minimum value of 2080 kW.

About one hour and 35 minutes later, the percentage of the class - 100 microns fell below 70% and the ore load was reduced to 10 t / h, at which the starting product from the mill returned to normal values. The power drawn from the electric motor increased on average by about 30 kW.

The explanation of this fact can be sought by analogy with the dependence of the magnitude of the ball load and the power drawn. This dependence is known to be nonlinear. As the ball load increases, the power drawn from the motor increases to its maximum value (extremum) and then gradually decreases. This is explained by the fact that with increasing ball load, after the extremum, the center of gravity of the grinding medium moves closer to the axis of rotation of the machine (Dzhustrov 2019).

As it is known, in the case of a waterfall mode of operation of the ball mill, the useful power  $P_o$  includes the power for raising the grinding medium and for transmitting the necessary and kinetic energy.

$$P_o = Mw, W;$$

where:  $M$  is the moment created by the grinding medium removed by the rotation of the drum,  $Nm$ ;

$w$  - actual angular velocity,  $rad / s$ .

$$M = Gcm.l,$$

where:  $Gcm$ - weight of the digestion medium,  $N$ ;

$l$  - distance between the center of gravity of the grinding medium and the axis of rotation of the drum,  $m$ .

From the conducted experiment it was established that the introduced additional load on ore  $38 t / h$  (particle size distribution  $+5 \div -10 mm$ ) leads to displacement of the center of gravity of the grinding medium, respectively reduction of the moment  $M$  and reduction of the extracted power. From the graphically presented data from the experiment in fig. 4 it can be tentatively determined that the loading of 1 ton of ore on the ball mill leads to a reduction of about 2 kW of the active power drawn from the electric motor at the existing ball load. This statement is valid only if before the introduced load on the ore the mode of operation of the mill on ball load and load on the drum was after the extremum of the dependence  $P = F(Gcm)$ .

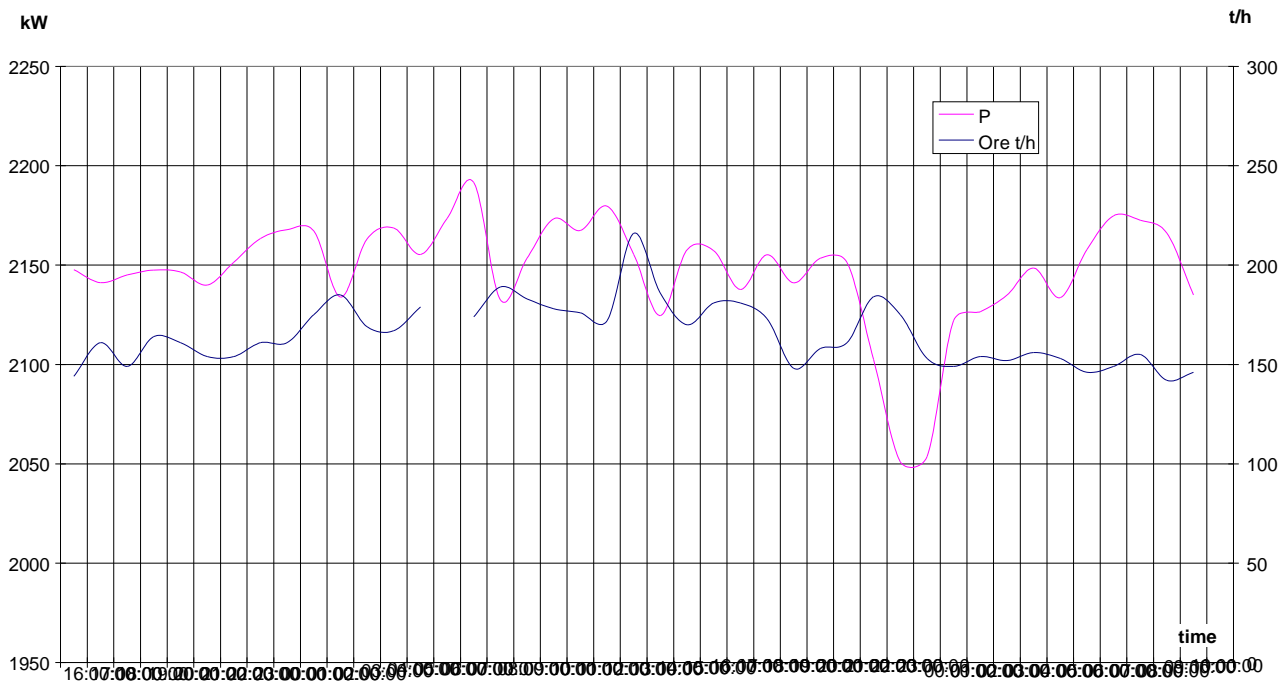


Fig.5. Dependence of the active power on the load on the ore - mill 3

Figure 5 shows a record of the average hourly active power of a mill № 3, compared with the hourly load of the mill on sands and ore. For a period of 44 hours, the dependence described above is confirmed.

With each increase in the load of the mill, the active power drawn from the electric motor decreases and vice versa - with decreasing load, the power increases. When removing the dependences shown in fig. 5, the mill worked with a normal technological process and the starting product was with normal indicators.

## Conclusions

The results of the conducted experimental researches give grounds for the following conclusions:

- the active power drawn from the electric motor of the ball mill is not an unambiguous indicator of the load of the mill;
- the determination of the active power losses in the stator

winding for generating reactive power from the synchronous electric motor must not be done by the change of the drawn active power;

- the specific consumption of electricity decreases not only from the increased productivity of the mill, but also from the reduced active power drawn from the electric motor;
- it is necessary in each specific production conditions by changing the load of the mill to seek the optimal load of the mill to minimize energy costs in compliance with the imposed limit on the grain size distribution of the starting product.

## References

- Dzhustrov K. 2019. Influence of the ball load on the specific power consumption of ball mills. – *Journal of Mining and Geological Sciences*, 62, Part 3, 77–81.

# ELECTRICAL LOSSES IN THE ELECTRICITY DISTRIBUTION NETWORKS WHEN CONNECTING NEW GENERATOR POWER

Kiril Dzhustrov<sup>1</sup>, Nikolay Haralambiev<sup>2</sup>

<sup>1</sup>University of Mining and Geology “St. Ivan Rilski”, 1700 Sofia; justrov@mgu.bg

<sup>2</sup>University of Mining and Geology “St. Ivan Rilski”, 1700 Sofia; nikolay.haralambiev@cez.bg

**ABSTRACT.** The report considers the possibility of connecting new generating powers in a cascade of HPP. The flow distribution of powers at different powers of the power plants is determined, as well the voltages at the connection points in the power supply scheme of the power lines. The losses of power and electricity under different operating conditions are determined analytically.

**Keywords:** electrical losses

## ЗАГУБИ В ЕЛЕКТРОРАЗПРЕДЕЛИТЕЛНИТЕ МРЕЖИ ПРИ ПРИСЪЕДИНЯВАНЕ НА НОВИ ГЕНЕРАТОРНИ МОЩНОСТИ

Кирил Джустров<sup>1</sup>, Николай Хараламбиев<sup>2</sup>,

<sup>1</sup>Минно-геоложки университет „Св. Иван Рилски“, 1700 София

<sup>2</sup>Минно-геоложки университет „Св. Иван Рилски“, 1700 София

**РЕЗЮМЕ.** В доклада се разглежда възможността за присъединяване на нови генераторни мощности в каскада от ВЕЦ. Определено е потокоразпределението на мощностите при различни мощности на централите, а така също и напреженията в точките на присъединяване в електроснабдителната схема на електропроводите. Аналитично са определени загубите на мощност и електроенергия при различни условия на експлоатация.

**Ключови думи:** електрически загуби

An analysis was made of the possibility for connection of “Opletnya” MHPP with a capacity of 2,6 MW to the existing 20 kV power lines “Milanovo” and “Izdrintets”. “Lakatnik” MHPP and “Svrazhen” MHPP, each of them with a capacity of 3,2 MW, are connected to the same power lines. The single-line diagram is shown in fig. 1. The flow distribution of powers at different generated powers of the power plants is determined, as well the voltages at the connection points in the power supply scheme of the power lines.

As output data additionally are given:

- voltage of the busbars at substation Bov – 20,5 kV;

- minimum power factor of the connected consumers -  $\cos\varphi = 0,90$ ;

- power factor of the connected power plants -  $\cos\varphi = 0,95 \div 1,00$ .

In the article are discussed four options of connecting.

### First option: the two power lines are in parallel at both ends

In this variant, a case is considered, in which the two power lines are considered as single, but with a cross sectional area of the conductors in the main feed, equivalent to ACSR 190 mm<sup>2</sup> (2 x ACSR 95).

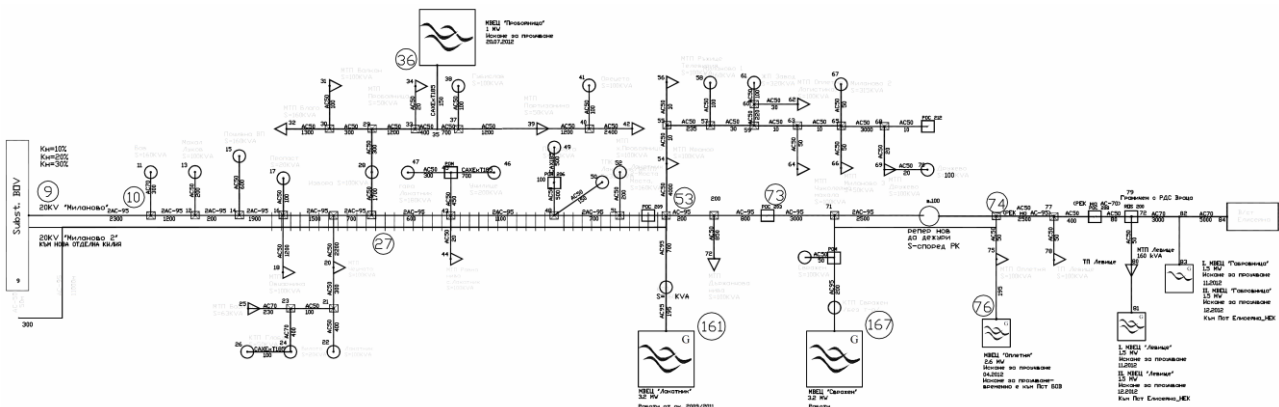


Fig. 1. Single-line diagram.

The calculation model also envisages the operation of a new MHPP "Proboynitsa" with a power of 1 MW. In the scheme considered this way, three values of the generated power and two values of the electric energy consumed by the consumers are set. The results of the calculations at some specific points are shown in tables 1 to 4.

From table 1 obviously the generated power at any moment exceeds the consumed by the consumers connected to the power network and the flow of power along the main power line will be in the direction of substation Bov. From the point of view of the allowable current load, the conductors will not be overloaded.

Table 1 - power lines are in parallel at both ends 100% generator power,  $K_n = 10\%$ ,  $\cos\varphi = 0,95$

Losses	$\Delta P$ , kW	$\Delta Q$ , kVAr			
	467	519			
Point	Generator power kW	Difference kW	Main feed power kW	Curr ent, A	U, kV
9					20,50
10	10000	9534	466	269	20,87
27	9000	8622	379	243	21,76
36	1000	1000		28	21,75
53	9000	8810	191	248	22,13
161	3200	3200		90	22,11
167	3200	3200		90	22,74
74	2600	2590	10	73	23,03
76	2600	2600		73	23,05

Power losses in the entire power network (including to consumers) will be  $\Delta P = 467$  kW and  $\Delta Q = 519$  kVAr. The voltage at the connection points (including in the connections of the consumers) will be significant, as the maximum exceedance will be 2,55 kV (at busbar voltage in the substation  $U = 20,5$  kV). This will be 15,25% higher, compared to the nominal voltage. Obviously even if the additional terminals of the transformers are used ( $\pm 5\%$ ), the end users will receive a significantly higher voltage than the allowable one.

Table 2 - power lines are in parallel at both ends 50% generator power,  $K_n=10\%$ ,  $\cos\varphi=0,95$

Losses	$\Delta P$ , kW	$\Delta Q$ , kVAr			
	110	121			
Point	Generator power kW	Difference kW	Main feed power kW	Curr ent, A	U, kV
9					20,50
10	5000	4534	466	128	20,68
27	4500	4122	379	116	21,10
36	500	500		14	21,10
53	4500	4310	191	121	21,28
161	1600	1600		45	21,27
167	1600	1600		45	21,59
74	1300	1290	10	36	21,73
76	1300	1300		37	21,74

In this mode, the maximum voltage increase will be 1,24 kV. This is 8,7% higher, compared to the nominal voltage. The highest voltage will be in MTP "Derzhanchova Niva" with a value of 21,60 kV, or 8,00% higher than nominal. For the other transformers the voltage will be in the range from 20,68 kV to 21,25 kV. This voltage will be relatively acceptable, if the transformers are switched to voltage 21 / 0,4 kV. Power losses in the entire power network (including to consumers) will be  $\Delta P = 110$  kW and  $\Delta Q = 121$  kVAr.

Table 3 - power lines are in parallel at both ends 30% generator power,  $K_n=10\%$ ,  $\cos\varphi=0,95$

Losses	$\Delta P$ , kW	$\Delta Q$ , kVAr			
	29	33			
Point	Generator power kW	Difference kW	Main feed power kW	Curr ent, A	U, kV
9					20,50
10	3000	2534	466	71	20,60
27	2700	2322	379	65	20,84
36	300	300		8	20,84
53	2700	2510	191	71	20,94
161	960	960		27	20,94
167	960	960		27	21,03
74	780	770	10	22	21,10
76	780	780		22	21,10

In this mode the maximum voltage increase will be 0,60 kV. This will be 5,5% higher, compared to the nominal voltage. In MTP "Derzhanchova Niva", will be the highest voltage with a value of 21,04 kV, or 5,02% higher than nominal. For the other transformers, the voltage will be in the range of 20,60 kV to 20,91 kV. This voltage will be within the variable range of the transformers. Power losses in the entire power network (including to consumers) will be  $\Delta P = 29$  kW and  $\Delta Q = 33$  kVAr.

Table 4 - the power lines are in parallel at both ends 30% generator power,  $K_n=30\%$ ,  $\cos\varphi=0,95$

Losses	$\Delta P$ , kW	$\Delta Q$ , kVAr			
	17	18			
Point	Generator power kW	Difference kW	Main feed power kW	Curr ent, A	U, kV
9					20,50
10	3000	1603	1397	45	20,56
27	2700	1565	1136	44	20,72
36	300	300		8	20,72
53	2700	2129	572	60	20,81
161	960	960		27	20,80
167	960	960		27	20,89
74	780	750	30	21	20,96
76	780	780		22	20,96

Voltages, similar to the previous one mode are obtained. That shows, increasing the power, consumed by consumers will reduce the voltage at their connection points, but their relative value is small. As a general conclusion, it can be noted, that the reduction of the generated and the increase of

the consumed electricity, will increase quality of the power supply. Power losses in the entire power network (including to consumers) will be  $\Delta P = 17$  kW and  $\Delta Q = 18$  kVAr.

**Option 2 - Lakatnik to Izdrinets, Svrazhen and Opletnya to Milanovo**

In the considered scheme are set three values of the generated power and two values of the electricity consumed by the consumers. The results of the calculations at some specific points are shown in Tables 5 to 8.

Table 5 - Lakatnik to Izdrinets, Svrazhen and Opletnya to Milanovo 100% generator power,  $K_n = 10\%$ ,  $\cos\varphi = 0,95$

Losses	$\Delta P$ , kW	$\Delta Q$ , kVAr			
	442	498			
Point	Generator power kW	Difference kW	Main feed power kW	Curr ent, A	U, kV
9					20,50
10	6800	6334	466	150	20,92
27	6800	6422	379	153	21,92
53	5800	5610	191	158	22,40
161	3200	3200		90	21,72
167	3200	3200		90	23,01
74	2600	2590	10	73	23,35
76	2600	2600		73	23,38

In this mode, the maximum voltage increase will be 2,88 kV. This is 16,9% higher, compared to the nominal voltage. Obviously, this excess of the voltage will be unacceptable for consumers. The power losses in the entire power network (including to the consumers) will be  $\Delta P = 442$  kW and  $\Delta Q = 498$  kVAr.

Table 6 - Lakatnik to Izdrinets, Svrazhen and Opletnya to Milanovo 50% generator power,  $K_n = 10\%$ ,  $\cos\varphi = 0,95$

Losses	$\Delta P$ , kW	$\Delta Q$ , kVAr			
	102	115			
Point	Generator power kW	Difference kW	Main feed power kW	Curr ent, A	U, kV
9					20,50
10	6800	6334	466	150	20,92
27	6800	6422	379	153	21,92
53	5800	5610	191	158	22,40
161	3200	3200		90	21,72
167	3200	3200		90	23,01
74	2600	2590	10	73	23,35
76	2600	2600		73	23,38

In this mode the maximum voltage increase will be 1.37 kV. This is 9,35% higher, compared to the nominal voltage. The highest voltage will be in the MTP "Derzhanchova Niva" with a value of 21,69 kV, or 8,45% higher than nominal. For the other transformers the voltage will be in the range of 20,69 kV to 21,35 kV. This voltage will be within the variable range of the transformers. Power losses in the entire network (including to consumers) will be  $\Delta P = 102$  kW and  $\Delta Q = 115$  kVAr.

Table 7 - Lakatnik to Izdrinets, Svrazhen and Opletnya to Milanovo 30% generator power,  $K_n = 10\%$ ,  $\cos\varphi = 0,95$

Losses	$\Delta P$ , kW	$\Delta Q$ , kVAr			
	39	43			
Point	Generator power kW	Difference kW	Main feed power kW	Curr ent, A	U, kV
9					20,50
10	2040	1574	466	44	20,62
27	2040	1662	379	47	20,93
53	1740	1550	191	44	21,05
161	960	960		27	20,87
167	960	960		27	21,24
74	780	770	10	22	21,34
76	780	780		22	21,34

In this mode, the maximum voltage increase will be 0,84 kV. This is 6,7% higher, compared to the nominal voltage. The highest voltage will be in MTP "Derzhanchova Niva" with a value of 21,24 kV, or 6,2% higher than nominal. For the other transformers the voltage will be in the range of 20.62 kV to 21.02 kV. This voltage will be within the variable range of the transformers. Power losses in the entire power network (including to consumers) will be  $\Delta P = 39$  kW and  $\Delta Q = 43$  kVAr.

Table 8 - Lakatnik to Izdrinets, Svrazhen and Opletnya to Milanovo 30% generator power,  $K_n = 30\%$ ,  $\cos\varphi = 0,95$

Losses	$\Delta P$ , kW	$\Delta Q$ , kVAr			
	25	27			
Point	Generator power kW	Difference kW	Main feed power kW	Curr ent, A	U, kV
9					20,50
10	2040	643	1397	18	20,55
27	2040	905	1136	25	20,70
53	1740	1169	572	33	20,78
161	960	960		27	20,86
167	960	960		27	20,96
74	780	750	30	21	21,06
76	780	780		22	21,07

In this mode, the maximum voltage increase will be 0,57 kV. This is 5,35% higher, compared to the nominal voltage. The highest voltage will be in MTP "Derzhanchova Niva" with a value of 20,97 kV, or 4,85% higher than nominal. For the other transformers the voltage will be in the range of 20,55 kV to 20,69 kV. This voltage will be within the variable range of the transformers. Power losses in the entire power network (including to consumers) will be  $\Delta P = 25$  kW and  $\Delta Q = 27$  kVAr.

**Option 3 - Separation of generators on one power line and consumers on the other**

This is the optimal mode for electricity consumers. For them, the received power will be from substation Bov, in which voltages at the connection points will depend on the voltage drop in the feed line and the busbar voltage in the substation. In particular, even if a new cell is not equipped

and the two power lines are separated, practically the increase (decrease) of voltage at the point of connection of the two power lines will be negligible.

Table 9 - Separation of generators on one power line and consumers on the other 100% generator power,  $K_n = 30\%$ ,  $\cos\varphi = 0,95$

Losses	$\Delta P$ , kW	$\Delta Q$ , kVAr				
	800	886				
Point	Generat or power kW	Curre nt, A	dU %	$\Delta P$ kW	$\Delta Q$ kVAr	U kV
9	9000	253				20,50
27	9000	253	2,39	496	552	22,89
53	9000	253	0,77	159	177	23,65
53_1	3200	84	0,08	5	5	23,73
161	3200	90	0,02	2	2	23,75
200	5800	161	0,04	5	6	23,69
72		4	0,00	0	0	23,69
73	5800	162	0,16	21	23	23,85
71	5800	162	0,59	78	86	24,43
71_1	3200	86	0,01	1	1	24,44
167	3200	90	0,02	2	2	24,46
74	2600	72	0,11	6	7	24,54
75	2600	70	0,01	0	0	24,55
76	2600	73	0,03	2	1	24,57

The table shows, that at full power of the generators, the voltage will significantly exceed the nominal. In addition to the transformer for own needs to the respective power plants (items 53\_1, 71\_1, 75), MTP "Derzhanchova Niva" will also be at a higher voltage with a value of 23,69 kV. These voltages are unacceptable for the transformers and the consumers connected to them. In addition, the over-voltage protection of 20 kV feeders from the power plants ( $U_{set} = 22$  kV) will be activated.

The power losses in power line will be  $\Delta P = 800$  kW and  $\Delta Q = 886$  kVAr.

Table 10 - Separation of generators on one power line and consumers on the other 30% generator power,  $K_n = 30\%$ ,  $\cos\varphi = 0,95$

Losses	$\Delta P$ , kW	$\Delta Q$ , kVAr				
	117	130				
Point	Generat or power kW	Curre nt, A	dU %	$\Delta P$ kW	$\Delta Q$ kVAr	U kV
9	4500	98				20,50
27	4500	98	0,92	74	82	21,42
53	1600	98	0,29	24	26	21,72
53_1	1600	30	0,03	1	1	21,74
161	2900	36	0,01	0	0	21,75
200		59	0,01	1	1	21,73
72	2900	4	0,00	0	0	21,73
73	2900	60	0,06	3	3	21,79
71	1600	60	0,22	11	12	22,00
71_1	1600	32	0,00	0	0	22,01
167	1300	36	0,01	0	0	22,02
74	1300	25	0,04	1	1	22,04
75	1300	22	0,00	0	0	22,04
76	2600	26	0,01	0	0	22,05

And in this case, the voltage increase will be higher than allowable. The power losses in power line will be  $\Delta P = 117$  kW and  $\Delta Q = 130$  kVAr.

### Conclusion

The best option for power supply, is when the two power lines are in parallel and generator power is 30% (table 3 and table 4), even with the future connection of MHPP "Proboynitsa" with a power of 1 MW. In this option, the voltages at the individual points of the power network, as well as the electricity losses, will be the lowest.

"Option 2 - Lakatnik MHPP to Izdrinets, Svrazhen MHPP and Opletnya MHPP to Milanovo" is also a good option if the generators operate with 30% generator power at each of the power plants (Table 7 and Table 8). The voltages at the detached points of the power network will be within the permissible limits, and the losses of power and electricity will be in the same order, as in parallel operation of the power lines.

## PLATFORM FOR EXPERIMENTAL STUDY OF A SWITCHED RELUCTANCE MOTOR

**Yassen Gorbounov<sup>1</sup>, Romeo Alexandrov<sup>2</sup>**

<sup>1</sup>University of Mining and Geology "St. Ivan Rilski", 1700 Sofia; y.gorbounov@mgu.bg

<sup>2</sup> University of Mining and Geology "St. Ivan Rilski", 1700 Sofia; romeo.alexandrov@mgu.bg

**ABSTRACT.** Switched reluctance motors (SRM) are among the first rotating electric machines, but they are little known in Bulgaria and are rarely mentioned, mainly in the courses on electric machines and special electric motors. However, they have great potential because they are environmentally friendly, highly efficient and can work in harsh environments. Although they have a simple construction, there are difficulties in their control due to the highly nonlinear nature of the magnetic circuit resulting from their salient pole structure. In this article, a laboratory model for studying low-power SR motors is presented. The key problems related to their principle of operation and control are discussed and a method for identifying the non-linear inductance is introduced which allows for implementing sensorless control algorithms. A small modification of the motor winding is made, which makes the simulation of phase winding faults possible.

**Keywords:** Switched Reluctance Motors, Electrical Drives, Nonlinear Magnetic Circuit

### ПЛАТФОРМА ЗА ЕКСПЕРИМЕНТАЛНО ИЗСЛЕДВАНЕ НА ПРЕВКЛЮЧВАЕМ РЕАКТИВЕН ДВИГАТЕЛ

**Ясен Горбунов, Ромео Александров**

Минно-геоложки университет „Св. Иван Рилски“, 1700 София

**РЕЗЮМЕ.** Превключваемите реактивни двигатели (ПРД) са сред първите въртящи се електрически машини, но са слабо познати в България като за тях се споменава рядко, предимно в курсовете по електрически машини и специални електрозадвижвания. Те крият обаче, голям потенциал, тъй като са екологични, с висок коефициент на полезно действие и могат да работят в тежки условия. Макар че имат просто устройство, съществуват трудности при тяхното управление, свързани със силно нелинейния характер на магнитната верига, произтичащ от явнополюсната им конструкция. В настоящата статия е представен лабораторен макет за изследване на ПРД с малка мощност. Дискутирани са основните проблеми, свързани с техния принцип на работа и управление и е представен метод за идентификация на нелинейната индуктивност, с чиято помощ може да бъде реализирано безсензорно управление. Извършена е малка модификация на фазната намотката, която позволява да бъдат симулирани аварийни режими на работа.

**Ключови думи:** Превключваеми реактивни двигатели, Електрозадвижване, Нелинейна магнитна верига

### Introduction

The Switched Reluctance Motors (SRM) are synchronous machines that have salient poles and simple construction with a rotor made of laminated steel (Krishnan 2001). They are easy to be manufactured and are ecological due to the reduced amount of copper in the windings and the absence of impregnating resins. They feature high power and also a very high level of safety and reliability due to the complete lack of arcing which is a result of their brushless operation and their inherent ability to work with one, and in some cases with even more disconnected phases. Although the broad majority of SRM applications range in the field of household appliances as well as in automotive and industrial machinery, the advantages just mentioned above make the electrical drives built with SR motors extremely suitable for use in mining. There are specific requirements for the electrical drives used in the mining sector such as smooth adjustable speed control, high torque, operation in harsh and explosive environments, high degree of protection and high reliability.

In the mining industry there are known few cases of application of SRM mainly for locomotives and drives of belt conveyors (Gorbounov 2019; Ptakh 2015) but in Bulgaria their usage is still very limited and is virtually absent. The main

reason for their relatively small distribution are the increased requirements for the power and control electronics, especially in terms of computing speed. To be able to realize continuous movement of the rotor it is necessary to continuously monitor its position and just before reaching the so called aligned position it is necessary to switch off the phase of the motor. The precise control of the advance angle of phase switching is crucial for the efficient motor control and is heavily dependent on the quite non-linear shape of the stator inductance which is a function of three variables namely the angle of rotation of the rotor, the current through the winding and the temperature. With the lack of control of the SRM, which takes into account the position of the rotor, the motor efficiency falls below 50%. In the same time with proper electronic control the real efficiency can reach 90% and above. This makes all developments related to increasing the power and control efficiency of SRM drives highly relevant and significant in view of the upgrading of mining machinery. The development of new algorithms and tools for energy management can lead to improved power efficiency, which is crucial for the whole mining industry.

The basic structure of a typical rotating 3-phase SR motor of type 12-8 is depicted in Fig. 1. This type of motor is used in

the current experimental platform. For clarity only a single phase is shown.

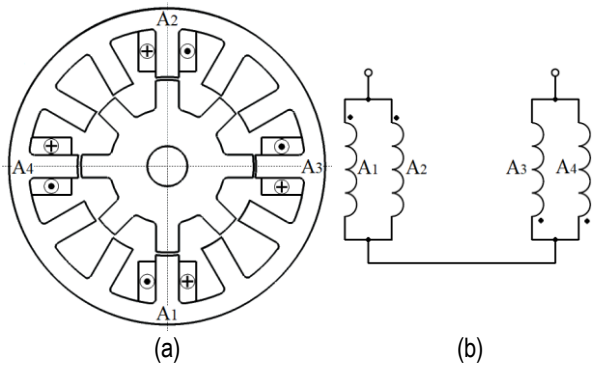


Fig. 1. Basic configuration of a typical SRM of type 12-8: salient pole structure (a), and windings arrangement (b)

The torque is produced due to the tendency of the rotor to transition to the so called aligned position, i.e. a position with minimum reluctance (minimal magnetic resistance, respectively a maximum inductance). The windings are wound on the opposite poles of the yoke and they are coupled in pairs to form the phase sections of the inductor. They are connected so that the total magnetic flux is increased.

The motor is said to be of type 12-8 because it has 12 stator poles  $Z_s$  and 8 rotor poles  $Z_r$ . The phase count  $m$  is equal to the number of stator teeth divided by the number of poles  $2p$  which for the SR motors with central axial symmetry is  $2.p = Z_s - Z_r$ . Knowing that  $Z_s = 2.p.m$ , the angular distance between the closest stator and rotor poles (from the unaligned to the aligned position) can be expressed either using poles number or using pole pairs and the number of phases, and it is given by the expression (1). For the SRM12-8 it is  $\epsilon = 15^\circ$ .

$$\epsilon = 2.p \left( \frac{1}{Z_r} - \frac{1}{Z_s} \right) = \frac{\pi}{p} \left( \frac{1}{m-1} - \frac{1}{m} \right) \quad (1)$$

The motor is being controlled by square wave pulses that energize each phase. The control voltage and current shape for single phase commutation is shown in Fig. 2.

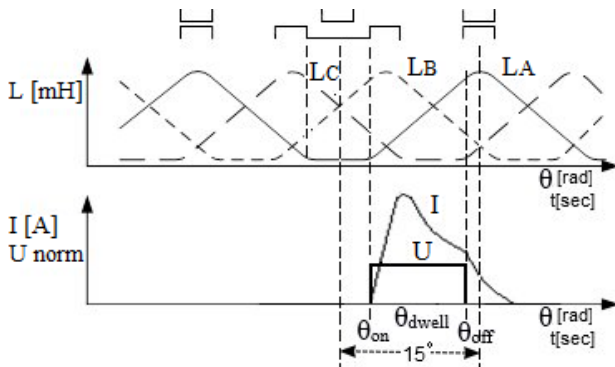


Fig. 2. Idealized inductance shape and control signal profile

As it has been already mentioned the inductance is a function of three variables of which the rotor position and the current flowing through the phase winding are the most important. This dependence is due to the saturation of the magnetic circuit and the air gap that changes during rotation

and is the cause of the highly nonlinear inductance shape. In order to implement efficient control and to minimize torque ripples the most important parameters are the switching angles. The start of the commutation angle is  $\theta_{on}$  which have to be slightly delayed from the ideal unaligned position (Kjaer 1997). Next it is the switch-off angle  $\theta_{off}$  which determines the instant of de-energizing the phase. In order to not produce a braking torque this angle must come with some advance before reaching maximum inductance. To achieve the goal of efficient control it is crucially important to obtain the correct rotor position information. This can be done either by using some position sensor such as an encoder or by identifying the inductance profile in real time thus implementing sensorless control algorithm.

The current paper aims to introduce an experimental platform built using a real SRM which can help for conducting research on the digital control algorithms and the identification of the stator inductance. Since the SRM is known for its high fault tolerance a modification of the phase winding is done which allows for introducing phase faults.

### Mathematical description

The mathematical modeling of the SRM drive can be derived by taking into account the voltage equations, the motion equation and the equation of the torque. The phase voltage can be written by observing the equivalent circuit in Fig. 3 and is given in (2).

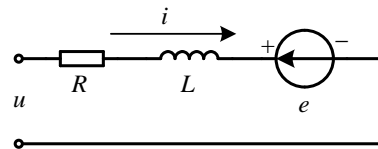


Fig. 3. Equivalent circuit of one phase

$$u = Ri + \frac{\partial \psi}{\partial i} \frac{di}{dt} + \frac{\partial \psi}{\partial \theta} \omega \quad (2)$$

In this expression  $u$  is the control voltage,  $R$  is the active phase resistance,  $i$  is the current through the winding,  $\theta$  represents the angular position,  $\psi$  denotes the flux linkage and  $\omega$  is the angular velocity (3).

$$\omega = \frac{d\theta}{dt} \quad (3)$$

Substituting (3) in (2) and taking into account that the derivative of the flux linkage with respect to the current is in fact the inductance (4) it can be obtained (5).

$$\frac{\partial \psi}{\partial i} = L(i, \theta) \quad (4)$$

$$u = Ri + L(i, \theta) \frac{di}{dt} + i \frac{\partial L(i, \theta)}{\partial \theta} \frac{d\theta}{dt} \quad (5)$$

The motion equation is given in (6) assuming the following conditions.

- the drive is presented for a single-mass system, without taking into account the elasticity of the elements of the mechanical system;
- the moment of inertia  $J$  of the system is constant and does not change during the movement;
- the equation refers to the motoring mode, the electromagnetic torque acts in the direction of motion, and the load counteracts.

$$J \frac{d\omega}{dt} = T_{em} - T_L \quad (6)$$

The torque equation is derived by the method for analysis of the magnetic energy and the co-energy of the SRM taking into account the effect of the saturation of the magnetic system. For the most of the motors, the saturation region of the magnetic circuit is reached. Usually the motors are not designed to work in the linear region of the dependence between the field strength  $H$  and the magnetization  $M$ , because the achievement of a certain torque will be at the expense of very large dimensions.

The magnetization curve profile as a function of the stator current is given in Fig. 4. In the figure  $U$  denotes the unaligned position and  $A$  is the aligned position of the rotor.

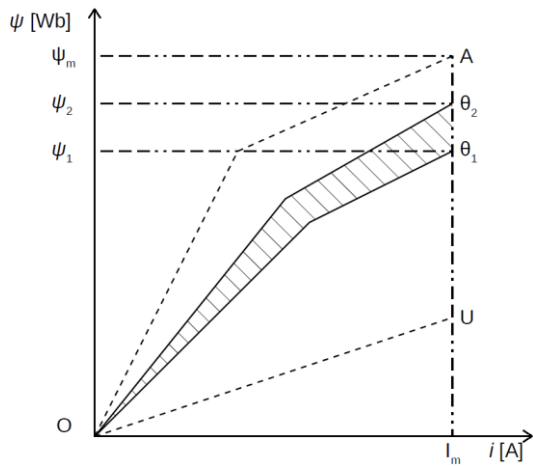


Fig. 4. A family of magnetization curves at particular rotor positions  $\theta$

The torque of the motor is determined by the magnetic field created by the motor windings. Under its pull, the rotor rotates from some angular position  $\theta_1$  to the next one  $\theta_2 = \theta_1 + \Delta\theta$  for a time of  $\Delta t$ . The analysis is made on the basis of the characteristics of the total magnetic flux  $\psi$  as a function of the current  $i$  for different values of the angle  $\theta$ , provided that during the movement, the current does not change its value. To simplify the analysis, heat losses are neglected. The energy of the electric source for time  $\Delta t$  is used to increase the magnetic energy and the energy of the system.

For the change in the electric field energy it can be written (7).

$$\Delta W_{el} = \Delta W_{mag} + \Delta W_{co} = I_m(\psi_2 - \psi_1) = I_m \cdot \Delta\psi \quad (7)$$

The change in the electric field energy  $\Delta W_{el}$  is in fact the area of the rectangle  $\theta_1\theta_2\psi_2\psi_1$ .

On the other hand, under the law of energy storage it turns out that the change in the electric field energy is equal to the change in the mechanical energy (8).

$$\Delta W_{el} = \Delta W_{mag} + \Delta W_{meh} \quad (8)$$

The change in the mechanical energy is the mechanical work done and it is given in (9).

$$\Delta W_{meh} = \Delta W_{co} = T_{em}(\theta_2 - \theta_1) = T_{em} \cdot \Delta\theta \quad (9)$$

The change in the co-energy  $\Delta W_{co}$  is (10). It corresponds to the shaded area in Fig. 4 which is the area of  $O\theta_1\theta_2$ .

$$\begin{aligned} \Delta W_{co} &= \int_0^{I_m} \psi(\theta_2, i) di - \int_0^{I_m} \psi(\theta_1, i) di = \\ &= \Delta \int_0^{I_m} \psi(\theta, i) di \end{aligned} \quad (10)$$

This way the motoring torque equates to (11).

$$T_{em} = \frac{\partial}{\partial \theta} \int_0^{I_m} \psi(\theta, i) di \quad (11)$$

## Measurement of the magnetization curves

The magnetization curves measurement is important for implementing optimal control strategies for maximum energy efficiency and minimum torque ripples as well as for validating the simulation tools performance. There exist many methods for obtaining flux linkage curves (Shehata 2018) either in a direct or indirect fashion. Some of them include measuring and recording the transient current profile (Gobbi 2006, Radimov 2005), static torque measuring at an arbitrary position (Zhang 2006), applying alternating current source with auxiliary search coil and next recording the induced voltage in the auxiliary coil together with the excited stator instantaneous current (Szabo 2013).

In this paper the magnetization curves measurement is made using the technique described in (Cossar 2001) which is a direct method. For this purpose the SR motor is coupled with a dividing head which is capable of holding the motor shaft at a desired angle as shown in Fig. 5. For each angular position from the unaligned to the aligned position a square pulse of the nominal motor voltage is being applied to a single stator phase using the pulse generator PG. Measurement samples of the voltage and current are being taken with the aid of an oscilloscope and are stored in memory. After all the curves are collected they are processed offline using a mathematical software package such as Matlab or SciLab.

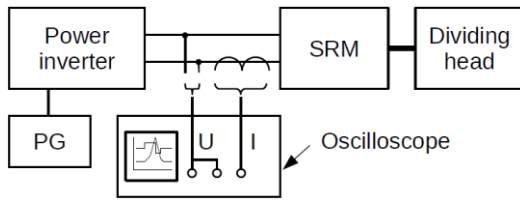


**Fig. 5. Magnetization curves measurement direct method test setup**

Using this setup the flux linkage calculation can be evaluated using equation (12).

$$\psi(t) = \int (u(t) - i(t) \cdot R) \cdot dt \quad (12)$$

The magnetization curves family is shown in Fig. 6.

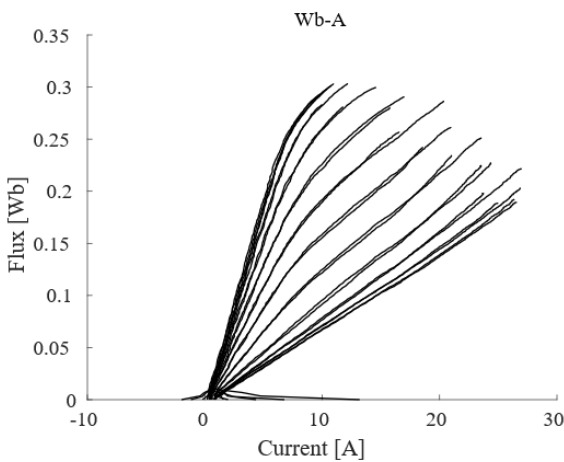


**Fig. 6. Switched reluctance motor magnetization curves**

The lowest curve in the figure corresponds to the unaligned position, i.e. the one where no saturation is observed because of the maximum air gap (minimum inductance). The top curve corresponds to the aligned position where the nonlinearity is obvious and is due to the maximum inductance value.

According to Faraday's Law it is known that the self-induced voltage across the inductor coil due to a current is proportional to the rate of change of the total magnetic flux. This means that if the above procedure is transformed to a continuous online measurement, the inductance as a function of the angular position and the current can be obtained by solving (13).

$$L = \frac{d\psi}{di} \quad (13)$$

Being able to calculate the flux linkage and the inductance means that the angular position information can be obtained from the magnetic characteristics of the motor itself which is of great benefit especially for SR motors where the magnetic circuit is highly nonlinear. This way it can be synthesized a sensorless control algorithm which eliminates the external mechanical sensors.

## The experimental platform

As stated in the previous chapter in order to measure the magnetization curves the motor shaft have to be fixed at desired angle. This is done by the aid of the dividing head shown in Fig. 7. The measurements are taken at a resolution of 1° although a significantly higher resolution is possible.

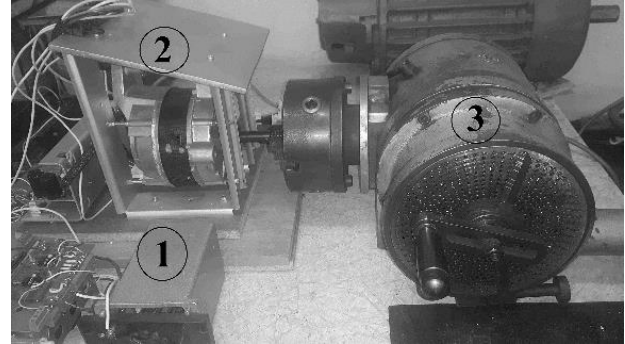


**Fig. 7. The SR motor shaft coupled with a dividing head**

In the figure (1) denotes the pulse generator, (2) is the switched reluctance motor and (3) is the dividing head.

After taking the measurements a loading machine is coupled in the place of the dividing head (not shown).

The salient pole construction of the motor can be visually observed by using the hole cut in the back side of the housing (Fig. 8).



**Fig. 8. An opening in the motor housing exposing the salient pole construction of the rotor**

Although useless at high speeds of rotation this modification is very useful for educational purposes when explaining the working principle of the motor and in observing the degree of alignment during rotor positioning by the dividing head.

## Fault injection capabilities

The SR motor is known as a robust and reliable machine in which faults can occur predominantly in its windings and bearing (Miller 1995; Nandi 1999; Szabo 2013). In the majority of the fault cases the motor remains operational, which is critical for some applications. Common winding faults include short circuit in an entire phase or between two different

phases, short circuit from a coil to ground, an interrupted phase and open circuit in one coil of a phase.

In order to simulate some of the possible faults a small modification in a section of the winding is made which is shown in Fig. 9.

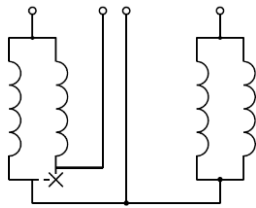


Fig. 9. Modification of a coil in a single phase winding

As it can be seen the coil is interrupted and its leads are exposed so they can be externally connected. A pole coil can be eliminated or connected in various configurations that allows to simulate different faults in the phase winding. Some of the possible connections are shown in the next figures.

In Fig. 10 (a) the broken coil is reconnected to its normal state by the aid of the bridge B while in Fig. 10 (b) the bridge is removed thus disconnecting the coil.

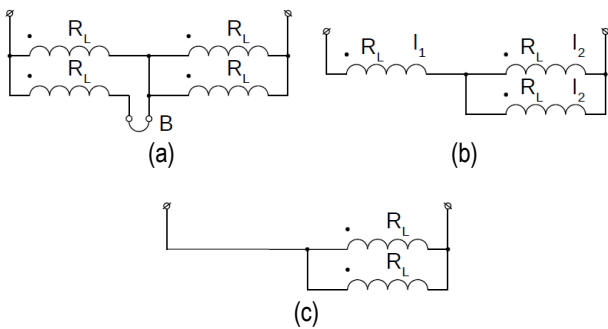


Fig. 10. Normal (healthy) connection (a), a disconnected coil (b) and a short in two opposite coils (c)

If all the coils are assumed to be equal and to have an active resistance  $R_L$ , the steady state current flowing through the phase winding according to Ohm's law is  $I=U/R_L$ . The nominal current through each section is half that value because the sections are connected in pairs in parallel. If the bridge is removed (Fig. 10 (b)) that would mean an interrupted coil. In this case the nominal phase current will equal  $I=2U/3R_L$ . This in turn will lead to increase in the current  $I_1$  with 1.33 times compared with the same current in healthy mode while the total current is slightly decreasing. It is also possible to short-circuit the left-hand coil (Fig. 10 (c)). In this case the current through the coils becomes equal to  $I_2=U/R_L$  which is an increase by a factor of two comparing with the previous case.

The measurement of the magnetization curves family is repeated under the condition in Fig. 10 (b) and the new plot is shown in Fig. 11. Comparing the results with Fig. 6 it can be seen that the current is decreased and it becomes harder to reach saturation.

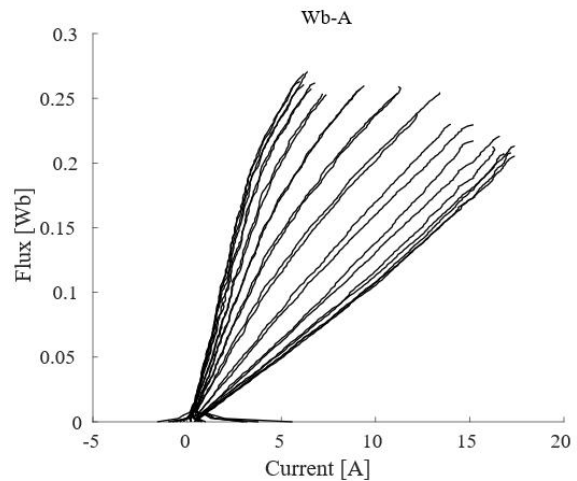


Fig. 11. Switched reluctance motor magnetization curves with an interrupter coil.

The proposed modification allows for few several faults to be injected and examined such as the ones shown in Fig. 12.

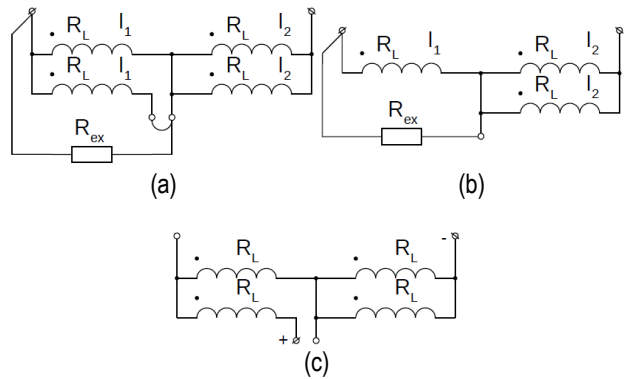


Fig. 12. Faulty situation with decreased coil resistance: case 1 (a) and case 2 (b), and simulation of a reversed coil (c)

A (variable) external resistance can be added either as shown in Fig. 12 (a) or in Fig. 12 (b) thus decreasing the equivalent active resistance of one or two opposite pole coils. This way a controllable value of the current can be achieved. The case shown in Fig. 12 (c) allows for increasing the equivalent active resistance or for applying external voltages of differing polarities and amplitudes to various sections of the circuit which provides additional flexibility to the proposed experimental platform.

## Conclusions

The proposed experimental platform provides a multifunctional setup which allows to find the electromagnetic quantities which are involved in the mathematical model of the SRM, both under normal operating conditions and in the case of a damaged phase winding. It has the following capabilities:

- the salient pole structure can be visually observed, which is very important when teaching the basics and the principle of operation of the SRM;
- the magnetization curves measurements can be taken at fixed angles with a resolution exceeding 1/12 of the degree;

- the influence of the vibrations that occur in this type of experiments is greatly reduced by the construction of the setup;
- the parameters of the control pulses can be adjusted such as the voltage amplitude, the repetition period and the pulse duration. This allows for experimenting with the commutation strategy by varying the switching angles thus examining the properties of the control algorithms;
- the proposed experimental platform offers a non-destructive method for the introduction of various types of faults related with the exploitation of the SRM.

The capabilities listed above provide prerequisites for creating an adequate mathematical model of the motor, which existence is critical for the efficiency of the control. The implemented method for measuring the magnetization curves is very important for the creation of a sensorless control system, which is associated with solving the opposite task – the inductance can be calculated online during the movement which allows for estimating the rotor position. This leads to a reduction in the cost and size of the SRM drive, while increasing its reliability and fault tolerance.

**Acknowledgements.** The support for this work is provided by the bilateral Chinese-Bulgarian scientific project of the National Science Fund of the Ministry of Education and Science with contract No KP-06-China/2 D-83/2018 between the China University of Mining and Technology and the University of Mining and Geology "St. Ivan Rilsky", Sofia.

## References

- Cossar C., Kelly L., 2001. Drive development and test, in Electronic Control of Switched Reluctance Machines by T. J. E. Miller, Oxford Newnes, pp. 201-226, ISBN 978-0-7506-5073-1
- Gobbi R., N. Sahoo, R. Rajandran, 2006. Rising and Falling Current Methods for Measurement of Flux-Linkage Characteristics of Switched Reluctance Motors: A Comparative Study, IEEE International Conference on Power and Energy (PECon), pp. 383 – 387, ISBN 1-4244-0273-5
- Gorbounov Y., H. Chen, 2019. Technological Aspects And Applications Of Large Power Switched Reluctance Motors In Mining, Journal Of Mining And Geological Sciences, Vol. 62, Number 3, pp. 86-92, ISSN 2682-9525
- Kjaer P., J. Gribble, 2001. Instantaneous torque control, 10.1016/B978-075065073-1/50008-0
- Krishnan R., 2001. Switched Reluctance Motor Drives: Modeling, Simulation, Analysis, Design, and Applications, CRC Press LLC, ISBN 0-8493-0838-0
- Miller T., 1995. Faults and unbalance forces in the switched reluctance machine, IEEE Transactions on Industry Applications, Vol. 31, pp. 319-328, ISSN 0093-9994
- Nandi S., H. Toliyat, 1999. Condition monitoring and fault diagnosis of electrical machines - A review, Proceedings of the IEEE International Conference on Electric Machines and Drives, pp. 197-204, ISBN 0-7803-5589-X
- Ptakh G., 2015. Switched Reluctance Drive Medium and High Power: Foreign and Domestic Experience (in Russian), Russian Internet Journal of Electrical Engineering, Vol. 2, No. 3, DOI 10.24892/RIJEE/20150305
- Radimov N., N. Ben-Hail, R. Rabinovici, 2005. Inductance measurements in switched reluctance machines, IEEE Trans. on Magnetics, Vol. 41, pp. 1296 – 1299, ISSN 0018-9464
- Shehata A., Y. Abdalla, A. Wakeel, R. Mostafa, 2018. Flux Linkage, and Inductance Measurement of a Fault Tolerant Switched Reluctance Motor Drive, 20th International Middle East Power Systems Conference (MEPCON), Cairo University, Egypt, ISBN 978-1-5386-6654-8
- Szabo L., R. Terec, M. Ruba, P. Rafajdus, 2013. Detecting and Tolerating Faults in Switched Reluctance Motors, Universal Journal of Electrical and Electronic Engineering Vol. 1, Number 2, pp. 16-25, DOI: 10.13189/ujeee.2013.010202
- Zhang J., A. Radun, 2006. A New Method to Measure the Switched Reluctance Motor's Flux, IEEE Transactions on Industry Applications, Vol. 42, pp. 1171 – 1176, ISSN 0093-9994

## ASPECTS OF ORIGIN MECHANISM FOR CONTINUOUS (IN SITU) HYDROCARBON ACCUMULATIONS

Jordan M. Jordanov

University of mining and geology "St. Ivan Rilski", 1700 Sofia, jordanjordanov45@gmail.com

**ABSTRACT.** The purpose of this work is to reveal the principal factors, controlling processes of origin mechanism of known nowadays certain continuous (in-situ) concentrations and those, known as "quasi-continuous. Through comparative analysis of the certain exploitation practice, and especially from Bakken Fm. (Williston Basin, USA), we discuss the role of kerogen concentration; migration processes; driving forces, including "constructive" type that initiate mobility and "unconstructive" or restrictive, acting against; rock hosted space, which consists of primary (matrix or mineral) and "organic" porosity and ratio of actual pore pressure vs. the normal hydrostatic pressure (pressure coefficient  $P_{pc}$ ) at the same depth.

As a result of the performed analyses, we conclude:

When the primary migration is 100 % restricted a certain continuous accumulation is formed;  $P_{pc} < 1.22$ .

In case of limited transfer of HC products, a quasi-continuous accumulation is expected;  $1.22 < P_{pc} < 1.9$ ;

When high level of expulsion efficiency is in force and petroleum products undergone notable buoyancy effect, than occur typical conventional accumulations;

If  $P_{pc} > 1.9$  more likely to occur natural hydro fracturing, changing the original tight rocks into the conventional fractured reservoirs.

**Keywords:** origin mechanism, continuous, quasi-continuous accumulations, shale gas

### АСПЕКТИ ОТ МЕХАНИЗМА НА ФОРМИРАНЕ НА НЕПРЕКЪСНАТИТЕ (IN-SITU) ПЕТРОЛНИ АКУМУЛАЦИИ

Йордан М. Йорданов

Минно-геоложки университет „Св. Иван Рилски“, 1700 София

**РЕЗЮМЕ.** Целта на работата е да се разкрие ролята на основните фактори, които контролират образуването на известните понастоящем същински непрекъснати петролни акумулации и разновидността, позната като „псевдо-непрекъснати“ акумулации. Посредством сравнителен анализ на данни от добивни полета и специално от практиката на формация Bakken (басейн Williston, САЩ), се обсъжда ролята на съдържанието на органично вещество в скалите; миграционните процеси; движещи сили, в това число „конструктивни“, които подпомагат движението на генерирани продукти и „рестриктивни“, които го ограничават; вместващия скален обем, който включва първична (матрична) и вторична – органична порестост; коефициента на свръхналягане ( $P_{pc}$ ), изразен като отношение на пластовото към хидростатичното налягане за дадена дълбочина.

В резултат на проведеня анализ са формулирани следните изводи:

При 100 % възпрепятствана първична миграция се формира същинска (In-situ) непрекъсната акумулация;  $P_{pc} < 1.22$ ;

Ако тя е частично реализирана, с ограничен миграционен път – са налице условия за „квази-непрекъсната акумулация“;  $1.22 < P_{pc} < 1.9$ ;

При мащабен трансфер на автономно сепарирана въглеродородна фаза се образува конвенционално насищане в геоклап от познатите конвенционални типове, може да бъде и с термо-баричен генезис, както това е доказано за газохидратните насищания;

Ако  $P_{pc} > 1.9$  е най-вероятно да настъпи естествен хидро-фракинг, съпроводен с трансформиране на първично плътните скални тела в конвенционални напукани резервоари.

**Ключови думи:** механизъм на формиране, непрекъснати, псевдо-непрекъснати акумулации, шистов газ

### Introduction

The registered remarkable results of shale gas and shale oil production worldwide have stimulated specialist to distinguish this kind of petroleum plays as a new specific ontogenetic branch. These natural hydrocarbon resources have been described later as "continuous petroleum accumulations", named also as "self-sourcing" plays (Schmoker, 1995; Qing Li et al., 2017; Jordanov, 2018, a, b and others). In order to achieve valuable growth in exploration efficiency, a lot of efforts have been made toward revealing their basic distinguished features. However, a range of important fundamental questions, regarding certain origin mechanism, have not been adequately answered. The purpose of this work is to reveal the principal factors, controlling processes of enrichment mechanism of known nowadays variety of continuous petroleum accumulations worldwide. The

analysis covers the certain continuous (in-situ) concentrations and those, known as "quasi-continuous", where the primary migration is partly realized and buoyancy forces have negligible effect. Because of fundamental differences in origin and enrichment pattern of methane-hydrates localizations, they have not been included into the scope of this work.

### Methodology

The methodological priority of the current analysis lies at the root of the petroleum-system fundamental principles. However, the main attention was placed only to those postulates, which can be used as a framework for model developing of continuous accumulations origin mechanism. As mentioned above, these types of natural petroleum products could be classified as: a) "curtain" (in-situ) and b) "quasi-

continuous" accumulations (Fig.1). From this point of view, the stress below is addressed on the role of:

- source rocks and organic matter (OM) contents;
- migration processes (physical constrains and acting forces);
- concentration (trapping) mechanism;
- origin and principal characteristics of the hosting rocks.

**Aspects of origin mechanism for continuous (in situ) petroleum accumulations**

**Source rocks and organic matter (OM) contents**

There is not considerable concept regarding critical content of rock OM as crucial control on the continuous accumulation origin. Therefore we chose to proceed from the assumption that such information could be extracted from the cases of worldwide organic rich basins, containing economically viable and producible continuous plays (Table 1). Through comparative analysis of the average lower limit values of OM of chosen examples, we assume that such approach could outline the framework of the problem. From this point of view, and from the certain exploitation practice, and especially from Bakken Fm. (Williston Basin, USA), we conclude that optimal weight % of kerogen concentration (or TOC) should hesitate near 6-8 %. Otherwise there are no suitable conditions for continuous plays origin. More precise arguments for this value (6-8 %) we shell give in the next sections below.

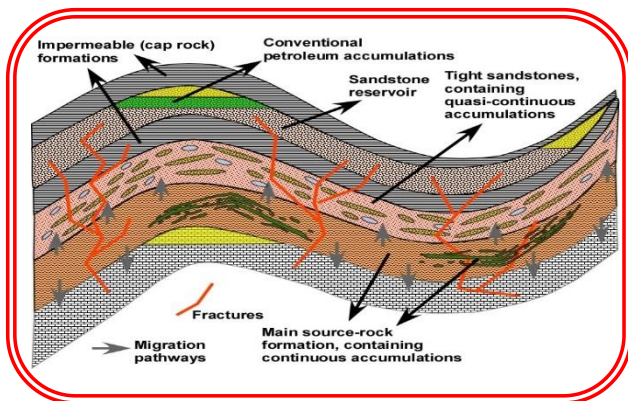


**Fig. 1. Schematic illustration of conventional and continuous petroleum accumulations**

Nevertheless of the precise analysis of the database from unconventional concentrations, we cannot identify any visible relationship between kerogen type and their enrichment mechanisms. The absence of mutual dependence of these parameters allows concluding that the influence of kerogen type on the enrichment pattern of continuous plays is negligible. As concerns the thickness of the charging source rocks intervals, there are some regularities which can develop

further stable trends through additional field data gathering. For widespread intracratonic basins like those of West Siberia, North Sea, as well as basins belonging to the large scale shelf areas (Maracaibo basin etc.), the thicknesses of the sourcing intervals are 30-120 m (averages near 30-40 m, Table 1). No such trends could be recognized for rift-controlled sedimentary basins, where exists high or rapid accumulation rates. In these cases it is supposed continuous plays to include thick rock suits (more than 1000 m), with typical multilayer architecture. The Mycopian Formation (late Oligocene-Miocene) from the ancient Peri-Tethyan basins is the quite proper examples. As results of the large scale field and exploration works performed in the Bulgarian Phanerozoic onshore territory, no widespread rock series have been identified, containing overcritical volume of kerogen (TOC), covering the requirement for continuous accumulations origin.

**Migration processes**

**Migration type and magnitude**

In order to develop more detailed model for unconventional localizations few principal attributes should be discussed, accounting for all aspects of acting (driving) forces. Such kind of analysis requires presenting the acceptable consistency regarding origin, expulsion and emplacement of petroleum. This phenomenon is known as "primary and secondary" migration. We consider that migration should be presented as tree-steps process, as pointed out below.

- Origin of autonomy hydrocarbon (HC) phases, as result of initial kerogen transformation and its separation into sorption and probable expulsion portions. The sorption processes can occur on the matrix as well as on the kerogen surface, whereas probable expulsion portions may fill existing matrix pores and pore space within the kerogen (organic porosity). This first episode we describe as very primarily expulsion step or "auftakt" migration. When this process ranges the space of the source rock body only, a certain (in-situ) accumulations are supposed to be formed.
- The migration of the generated HC products from the source rock into the adjacent host-strata we define as a certain primary migration. In this case, two scenarios are possible: if there is not visible mobility of the generated HC products, subsequently no buoyancy effect, than a "quasi-continuous" (or "source-contacting") accumulation is expected; otherwise a conventional play will occur (Fig.2).
- Secondary migration, which some researchers subdivide into "interior" and trans-reservoir transport of HC products. This kind of migration is typical for conventional plays.

**Table 1. Comparative data analysis of world leading continuous developments**

Basin (region)	Formation	Stratigraphy	Average TOC content (weight %)	Average thickness (m)
West Siberian	Bagenov	Tithonian-Berriasian	12	< 60
North Europe England-Paris basin	Posidonia	Early Jurassic, Toarcian)	10	30
Maracaibo	La Luna	Cenomanian-Santonian	4-5	< 100

Persian gulf (Saudi Arabia)	Hanifa	Oxfordian-Early Cimmerian	3-5	< 150
USA, North Dakota and Montana (Williston)	Bakken Shale	Devonian-Early Carboniferous	12-14	< 40
South Caspian region	Maikopian	Oligocene-Miocene	1.2-10 > 10 (Middle Maikopian formation)	70-250
North Sea	Kimmeridgian Clay	Late Jurassic	2-9 (средно 5)	15-30 for 'hot shales'

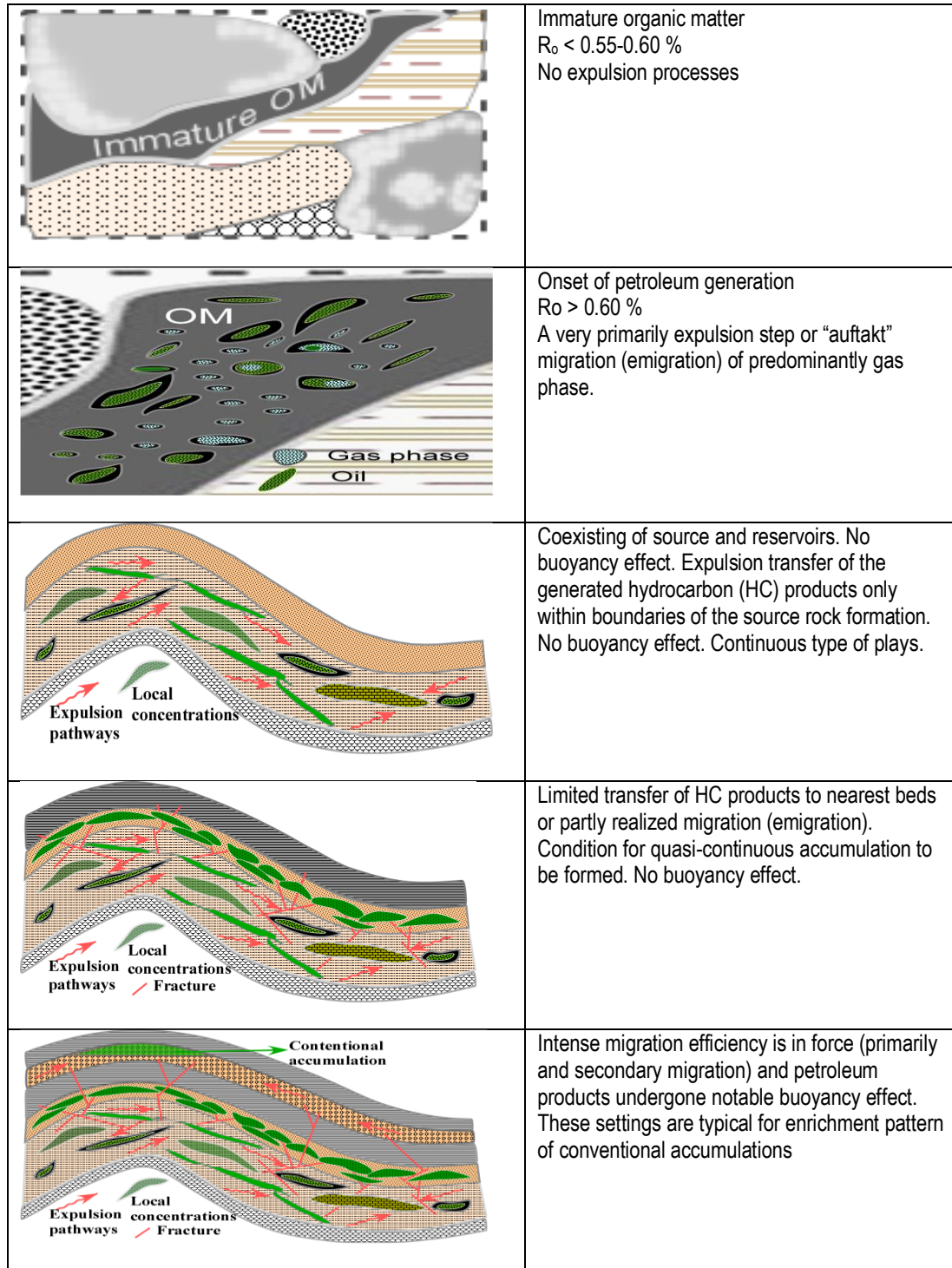
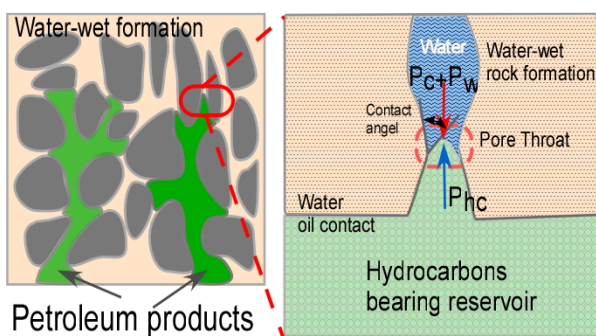


Fig. 2. Schematic illustration of the migration processes during petroleum accumulations origin

### Restrictive and constructive driving forces

There is a broad agreement regarding the crucial role of the rocks petrophysics on the processes of HC mobility. Therefore, the postulates of this concept were implemented in the current analysis of the main driving forces, acting during the continuous accumulations origin. The mobility of the generated HC occurs mostly in fine-grained, organic rich rock bodies, developed within subsiding sequences, undergoing increasing thermal load. The dominant feature of such type fine-grained layers is their limited filtration properties ( $< 0.1 \mu\text{D}$ ). These characteristics suggest presumably arising of two type driving forces: “constructive” that initiate mobility (chiefly formation overpressure and buoyancy effect) and “unconstructive” or restrictive, acting against (filtration barriers, capillary pressure, adhesion etc.). Consequently the magnitude of petroleum mobility entirely depends on the interaction between mentioned forces. It means that, if the restrictive forces are equal or greater than those presented as “constructive”, no common expulsion processes will take an effect. As a result a continuous play should occur (Fig. 3).



**Fig. 3. Schematic illustration of the “constructive” forces, mainly micro, mezzo and local formation overpressure pots ( $P_{hc}$ ), causing petroleum products mobility and restrictive forces (chiefly capillary and formation water pressure-  $P_c+P_w$ ), acting against**

Generally, the restrictive forces, it's believed to be depending mostly on the primarily diagenetic environment, i.g. on the initial properties of the fine-grained sedimentary fill. During the early subsidence episode these deposits underwent intensive changes of the rock matrix porosity and permeability (mainly through compaction and mineral transformation). This process continuous up to the depths of 800-1200 m and further subsidence will not lead to substantial changes. Consequently, the influence of burial at depth greater than 1000-1200 m, when the sediments enter into the oil window, has minor effect on the mobility of the generated HC products. Therefore we conclude that magnitude of restricted forces was almost stabilized at the end of this initial (very often rapid) compaction phenomenon (up to 800- 1200 depth). As a result, the migration ability of the generated HC products at the oil-window depths should have been govern chiefly by the size and shape of pore-throats, as well as capillary pressure values (Magara, 1982 and others). Additionally, to the end of the diagenetic rock transformation, the matrix surface it is expected to preserves its initial wettability; hence after the main compaction episode the capillary pressure depends only on the pore-throats radius, and remains relatively stable during the rest stages of the lithogenesis. Exceptional cases, when the fine-grained sequences are affected by the local or bulk

natural fracturing, should be addressed to the special petrophysical analysis.

A special attention to better understanding of the discussed above enrichment pattern should be addressed also to the behavior and treatment of the “constructive” forces (defluidization, buoyancy effect, diffusion, intra-formation pressure anomalies and others). The crucial importance belongs to the micro and local pressure anomalies, arising as a result of OM and some matrix minerals transformation. In the early stages of this process, i.g. when the source rocks enter into the oil window, local or point-size (embryonal) formation pressure anomalies arise. Coeval to subsidence, respectively to increasing thermal load, these anomalies expand, achieving magnitude of broader anomalies and finally to origin of overpressured strata. An outlook over this problem has been given in previous author's paper (Jordanov, 2013), where an attempt of calculations was made. These schematic calculations were focused on the fluid volume changes during the phase transformation of following couples: kerogen-oil; oil-gas; condensate-gas. Let us assume the following example: rock sample with  $2.45 \text{ g/cm}^3$  density contains 6 weight % kerogen,  $1.15 \text{ g/cm}^3$  density. Assume also that 50 % of kerogen will undergo conversion into oil of  $0.8 \text{ g/cm}^3$  density. Then this half part of kerogen will give only  $0.028 \text{ cm}^3 / \text{cm}^3$  additional (extra) volume, or near 3 %. Obviously this extra volume will generate insignificant pressure built-up anomaly. Quite different effect is expected when liquid phase (e.g. oil) is converted into gas. It is well known that 1 barrel of crude oil dives near  $85 \text{ m}^3$  gas phase and 15-18 % bituminous residue. Such types of transformations generate considerable by magnitude pressure anomaly. Compare presented above simplified calculations is clear that transformation “kerogen-to-oil”, even though higher degree of metamorphism, has no potential to generate overpressure that can act as a notable driving control. It is believed also that such kind of pressure anomaly should be absorbed by pore-rock system elasticity. Presented suggestion is supported by Tongwei Zhang et al. (2013) data from Bakken Fm. (USA). Cited authors have calculated generation of 13 mg/g rock oil and almost all oil volume was retained into the pore-rock system. Authors also consider that maximum expulsion efficiency do not exceed 41 %. An analogical pattern is in force probably for the prolific oil-prone Bagenov formation from West Siberia (Kalmikov & Balushkina, 2017 and others). The both petroleum producing regions contain minor volume of soluble gas phase. Presented above assumptions may arouse suspicion, but generally there is no notable inconsistency to the fluid-mechanical behavior of the source rocks contain I-II type kerogen.

As it was mentioned above, the formation pore pressure profile is quite different in case of abundant gas phase generation. The similar effect arise also when source rocks underwent intensive thermal load (temperature  $> 135\text{-}145 \text{ }^\circ\text{C}$ ), giving start for secondary conversion of generated oil into gas. This predominantly wet gas may exist as free volume, dissolved within the oil as well as adsorbed on the matrix and inert kerogen surfaces. Such model of multiphase rock saturation, it is believe to generate tremendous overpressure anomalies. In practice they act as a crucial “constructive” driving control. Obviously presented pattern can take place as local, zonal or regional anomaly, forming by this way overdressed formation of basin scale extent. The typical natural examples are the well-known basin-centered unconventional accumulations (Basin-centered gas systems

...2000; Fall, A. et al., 2012 and others). If the magnitude of formation overpressure, i.g. integral magnitude of “constructive” forces, exceeds the counteraction vector of “restricted” forces, conventional petroleum accumulations must be formed; otherwise unconventional pattern of petroleum concentrations should exist, being of certain “in-situ” continuous or quasi-continuous type. As results of the performed analyses, we conclude: *if filtration barriers restrict 100 % of primary migration, a certain continuous (in-situ) accumulation forms; if the primary migration is partly realized the quasi-continuous concentrations exist.* Under the conditions of scaled primary migration as well as good secondary migration within the reservoir rocks, a conventional accumulation is expected. We also consider that presented limitations for origin of a certain (in-situ) continuous accumulation should be addressed at extreme (endmost) environment, such as those shown in the Table 1.

### Trapping mechanism

The development of a reliable model of adequate trapping mechanism for discussed type of accumulations is still difficult because of their broad diversity, hence lack of reliable data base. It is widely accepted that the proper trapping mechanism is dominantly controlled by force equilibrium between hydrocarbon-generation pressure anomalies and capillary pressure barriers. The text below highlights some aspects of this problem for certain (in-situ) continuous and quasi-continuous accumulations.

### Aspects of trapping mechanism for certain (in-situ) continuous plays

It is believed that the oil/gas enrichment phenomenon for this type plays can be characterized by: a) broader, multi-points pseudo-migration process, instead of prevailing often single stream-like mechanism, typical for conventional accumulations; b) very short migration pathway; c) Darcy's law cannot be applied and buoyancy-driven forces may take an minor or negligible effect. Liu Guangdi et al. (2013) define this enrichment pattern as intra-formation “multi-point piston mechanism”.

In conjunction with presented above characteristics, there are important exceptions known as „sweet spots”. Practically they are localities, preserving higher porosity and permeability. Their petrophysics is closer to the reservoirs. As a rule they have diffusive contact in the environment and no detectable dependence on the formation water. We suggest for this special case invasive (repressive) charging, controlled by local or zonal pressure anomalies. Very often the „sweet spots” appear as lithological traps and are the main targets of the industrial interests. It is thought that presented scenario is inherent for the 40-50 m thick Bagenov Formation from West Siberia. This rock formation consists of fine-grained carbonate, shale and flint clastics, containing 8-12 % organic matter. Its lithological profile is quite heterogeneous with number of huge lens, equivalent to enigmatic „sweet spots”. They are the main producing objects. Additionally to the presented above model, Kalmikov & Balushkina (2017) consider that charging process of Bagenov's „sweet spots” occurs mainly by micro-fractures as well as by single, relatively bigger pores.

### II.3.2 Aspects of trapping mechanism for quasi-continuous plays

The main features controlling trapping mechanism of these type petroleum accumulations should be outlined from the specific characteristics of the hosted rocks. Practically, the matrix of such environment contains predominantly micro- and nano-sized pore space. Additional important feature of the quasi-continuous plays is also their direct and extensive contact to the main (chief) source rock body (Jordanov, 2018; Zhengjian Xu et al., 2017; Hua Yang et al., 2016; Jingzhou Zhao et al., 2012). This specific construction of “source rock-host strata” motivated some authors to introduce “source-contacting accumulations”. Following presented above basic principles, it seems correctly to assume analogous to “in-situ” plays trapping mechanism. It has to be governed by the same controls: generated overpressure due to OM conversion as follows: kerogen to gas; oil to gas; condensate to gas. Obviously, such model of charging will occur when the generated overpressure overcomes the filtration obstacles, developed on the boundary between source rocks and adjacent quasi-reservoirs (capillary pressure, adhesion forces and other minor of importance barriers). But, for this type of nano-pore system, accounting also for pore-throats abundance and its crucial role on the capillary pressure profile, it seems unacceptable to apply standard models of HC transition through pores and related its pore-canals. This is the reason to suggest that the main pattern of enrichment goes through micro-fractures and single pore-canals near or  $> 0.1 \mu\text{m}$  in size. Performed below simple calculations may argue for described idea. Let us take common Laplacian equation, assuming 40 mN/m surface tension on the “gas-formation water” boundary and effective pore radius of  $0.01 \mu\text{m}$  (10 nm) (Xiaojun Zhu et al., 2019; Cheng Zhang and Qingchun Yu, 2019 etc.). Then for the fully hydrophilic media, the capillary pressure ( $P_c$ ) value is 8 MPa. According to the published field data of number of authors (Zhengjian Xu et al., 2017 etc.), formation overpressure from the OM transformation may reach 5-10 MPa. Overpressure of such magnitude is enough to overcome capillary pressure counteraction. However, such breakthrough (displacement) pressure, that guarantees petroleum mobility, will be accompanied by opening of the principally closed fluid system. It unavoidable lead to pressure drop (pressure cooker principle). Such type of scenario may “push” the HC products to the places of accommodation (lithological traps), but the length of emigration will not exceed few to 10-20 m, charging practically number of local spots of the quasi-reservoirs beds. It is also important that such scenario of temporary “opening” of the pore-system, as a rule, suppose arising of multi-episode emplacement. Such pattern has been observed by many authors and as a typical case we give results of Zhengjian Xu et al (2017) for Ordos basin. The cited authors determine at least three episode of emplacement (Fig.12 of the paper).

Besides presented “invasive” enrichment pattern, it is necessary to account for possible diffusive mass transport. According to the Adolf Fick's law, given diffusion coefficient  $D = (1.5-2.5) \cdot 10^{-6} \text{ m}^2/\text{s}$ , seems logical to expect this effect. However, based on the performed large number of experimental works, J. Hunt (1995) concludes that mass transport by diffusion through tight porous media may take negligible effect. Cited author calculates that a volume of methane should pass by diffusion through 1740 m rock matrix for  $140 \cdot 10^6$  years (p.257).

Presented model of trapping (enrichment) mechanism for quasi-continuous plays principally requires strong dependence on the intensity of gas generation rate in order to give start of petroleum mobility. There are theoretical postulates giving a possible lower limit of generation rate. In the current analysis however an advantage is addressed to the certain field data, acquired from the real plays. Such a typical example is the working plays from Ordos basin (CN China), where at least 5 large tight gas/oil fields have been discovered. Through the last few decades, large number of detailed geochemical and petrophysical services have been done, focused on the Ordos's Carboniferous and Permian petroliferous strata, producing nowadays shale oil and shale gas from micro, nanopore hosted media (Jingzhou Zhao et al., 2012 et al.). Some researchers (Zhengjian Xu et al., 2017; Hua Yang et al., 2016; Jingzhou Zhao et al., 2012 et al.), have presented arguments allowing lower limit of gas generation rate to be defined. Data from more than 700 wells have been analyzed by the cited authors, which came to the conclusion that commercial saturation of quasi-continuous plays occur when intensity of gas generation exceeds  $10^8 \text{ m}^3/\text{km}^2$ . This lower limit value is close to the analogous regions from Russian Federation's continuous plays -  $20\text{-}30 \cdot 10^8 \text{ m}^3/\text{km}^2$ . Summarizing, it should be mentioned that essential element of the presented trapping pattern depends chiefly on the magnitude of generated formation overpressure, which should overcome all the filtration obstacles and fill invasively adjacent micro-, nano-pore system of the quasi-reservoirs. The absence of buoyancy effect as well as no visible trap boundaries is the dominant characteristics of this process, vice versa to the conventional analogues.

Independently of the presented above arguments supporting ideas for quasi-continuous plays enrichment, we consider that the development of the charging model, that will achieve reliable degree of adequacy to the real geological environment, requires lots of additional field and analytical efforts.

#### **Origin and characteristics of the hosted porous beds**

As it was mentioned above, the dominant feature of the continuous plays is their hosted space, which consists of *primary* (matrix or mineral) and "organic" porosity. The latter genetically arises as a result of OM (kerogen) conversion into HC products. Therefore it has to be classified as secondary. As a rule, the porosity volume is built up mainly by micro-nano pores. The initial matrix porosity (depositional pores) and its diagenetic rework totally is small (not exceeding 5-6 %), whereas the volume of organic pores may be equal or more than primarily. Due to the certain genetic differences of both type of hosted pore space, they are analyzed autonomy in the text below.

#### **Origin and characteristics of the matrix porosity in clastic deposits**

The hosted rocks most often are presented by tight clastic deposits (shale, siltstone, mudstone, chemogenic carbonates, silty sandstone, marl and others). In majority of the cases their matrix contains predominantly micro-nanoscale pore space. The total porosity of this kind of rock averages between 2-8 %, permeability do not exceeds 0.5 mD. The matrix voids include micro, nanopores, bounding its channels and deferent by geneses, size and extend micro-fractures. A detailed outlook on the variety of pore types that exist in the hosted beds of the

continuous plays is given by R. M. Slatt and N. R. O'Brien (2011). Based on the data from Barnett Shale in north Texas and the Woodford Shale in southeastern Oklahoma, cited authors specify: a) porous floccules, organopores, fecal pellets, fossil fragments, interpartical grain/pores and microchannel and microfractures (Fig. 16, p 227). In all these recognized pore spaces dominate microscale and nanoscale porosity. The pores cover an interval of 10-30 up to 300 nm in width.

Coeval with the dominating nanopore spaces there are small localities known as "sweet spots". These local reservoirs may arise due to depositional diversity as well as due to disequilibrium compaction in thick fine-grained sequences (Tingay et al., 2013; Jordanov, 2013). The latter phenomenon produces pressure anomalies, acting against compaction, respectively preserve porosity reduction and forming the enigmatic "sweet spots".

#### **Origin and characteristics of the matrix porosity in coal beds and coal-bearing strata**

The remarkable results of coal-bed-methane (CBM) production from number of USA and China developments, give strong contribution for better understanding of enrichment mechanism occurring in coal seams and coal-bearing strata (Tim A. Moore, 2012; Yu Liu, Yanming Zhu, 2016; Chenghua Ou et al., 2018 and others). The gas phase exists as free, adsorbed and dissolved form. The large number of investigation has shown that the volume of adsorbed gas has a greatest significance while the other both types have minor importance. Summarizing the observation of the enrichment patterns of the coal basins worldwide, including the great Zonguldag basin (Turkey), researchers define the statement that CBM fills chiefly nano-pores and micro-fractures. The latter is assumed to play important role as possible micro-migration pathways for gas phase movement into the direction of smaller formation pressure.

The common characteristics of the coal basins worldwide are their multilayer profile. It includes coal seams (beds, layers), coal-bearing strata, as well as non-coal intervals of different thicknesses. The latter consist more often of clastic deposits (sands, silts, conglomerates etc.), which should be addressed to the group of tight reservoirs. The typical examples of Bulgarian Paleozoic section are few Formations from the Greatest Dobroudja coal basin (Velkovo, Polianska Fm. and others (Hristov, Zd., et al., 1988)). Despite certain domination of the sandstones of their rock profile, they have not been assessed as promising targets for coal-bed-methane (CBM) resource.

Regarding CBM storage mechanism, Yu Liu & Yanming Zhu (2016) and others, argue the statement that in most of cases in coals dominate semi-closed micro pores (< 10 nm) and transitional (connecting) channels larger than 10-100 nm. The analogous pore size interval is typical also for clastic deposits which gives us motivation to conclude that the origin and characteristics of the coal pore space should follow the same principals as those of clastics.

#### **Origin and characteristics of the "organic" porosity volume**

This problem has been discussed in large number of papers (Jordanov, 2013; Maria-Fernanda Romero-Sarmiento et al., 2013; Vitaly Kuchinskiy, 2013; Zhuoheng Chen & Chunqing Jiang, 2016; Yuanjia Han et al., 2017 and others). The majority of authors consider origin of this type of porosity as results of rock OM (kerogen) transformation into HC

products due to thermal load from the Earth heat flow. During the burial the solid kerogen turns into liquid or gaseous phase (changes in kerogen density). This transformed part of the kerogen is considering as its labile content and usually account for 30-80 volume % of the initial volume. Being as labile HC phase, these products appear as moving substance, that occupy the "free" space, e.g. specific volume, named "organic" porosity. The published data, regarding the size interval of the new originated voids shows domination of nano-pores (20-50 nm). According to the Yuanjia Han et al. (2017) results, the pore shape depends on the kerogen maturation intensity. During the early stages of kerogen conversion isolated bubble-like pores start to occur. Further, coeval with increasing temperature, isolated bubble increase in volume and become more significant, taking a sponge-like appearance. Furthermore it is thought that organic voids occupied more and more space, forming by this way "micro-jails", possessing capacity for HC products retention.

The problem of dependence between organic porosity and kerogen content is of great importance for petroleum society. Comprehensive review on this matter dive Fernanda Romero-Sarmiento et al. (2013). The cited authors have modeled organic porosity evolution and tested the model on the world leading Barnett shale development. They assume that current average organic porosity of this shale is 4.3 % and it comes from the current TOC of 4.83 weight %. Summarizing, they have come to the conclusion that for every weight % of TOC may correspond 0.35-0.84 % porosity. Within this interval should be included also and the expected organic porosity of the most observed II type of kerogen. Formally we assume the value of 0,5 %/1 % TOC for this kind of kerogen. Even though, there are number of analytical technics for organic porosity calculation, we consider that there are lots of controls that cannot be assessed adequately (kerogen type, temperature profile, burial modeling and others). Therefore these efforts have not been widely accepted as a reliable decision.

In the context of the above presented understanding of the organic porosity origin, it should be of practical interest to develop an approach for TOC lower limit determination. Although it is possible to find out analytical (numerical) decisions, we prefer to give advantage to the data, extracted from the real field objects. On the base of the results obtained from the leading world etalons (Barnett shale, Bakken Form. from USA, Posidonia Form. from W. Europe, Bagenov Form. from W Siberia etc.), the measured organic porosity hesitates near 3-4 %. If formally assume 3 % as average value and implement Fernanda Romero-Sarmiento et al. (2013) findings, the critical TOC content (i.g. lower limit) for II type kerogen, should exceed 6 weight %.

**(6 % weight TOC X 0,5 = 3 % organic porosity)**

It should be mentioned that our perception for lower limit of 6 % TOC for source rocks should be accepted only for the current technical state-of-the-art and the future improvement will definitely introduce new modern decisions.

**Aspects of quantitative approach to determine overpressure control on the migration processes magnitude**

We assume that such a relation could be extracted from the following logical construction. As it was mentioned above, continuous accumulation is formed when filtration resistances

within the source rock could not be overcome by overpressure generated due to OM transformation. The main control on this process is attached to the capillary pressure ( $P_c$ ), which acting again formation fluids mobility. Basically it depends on the size (radius) of the biggest pore-throats. Consequently, the ratio of overpressure vs. capillary pressure appears as a chief parameter, controlling petroleum products mobility. The arising overpressure is an integral result of multiple impact of number of parameters that characterize principal stresses in the rock environments. They are: hydrostatic pressure ( $P_h$ ); formation (or pore) pressure ( $P_f$ ); overburden (or lithostatic) ( $P_l$ ) pressure. In order to justify  $P_f$  and  $P_h$  a pressure coefficient ( $P_{pc}$ ) was introduced. This coefficient is a ratio of actual pore pressure versus normal hydrostatic pressure at the same depth. There is general agreement that the regime is determined as overpressured if  $P_{pc} > 1.15-1.20$  (Tingay, M. et al., 2013 and others). It is well known that  $P_{pc}$  reaches 2.0-2.5 in number of basins worldwide. It corresponds to the super overdrressing regime, initiating natural hydro fracturing. From this point of view we suppose that it is possible to introduce lower and upper limit of  $P_{pc}$ , controlling petroleum products mobility.

Despite of all our efforts, we cannot find out reliable analytical or field data discussing the problem of  $P_{pc}$  lower limit. Therefore we speculate that common information of the pore-throat size of continuous plays could help in searching of a proper decision. As it was discussed above, this type of plays covers rock strata, containing nano-micro structure of the pore space. The size interval more often averages near 0.05-50 nm (0.005-0.05  $\mu\text{m}$ ). Consequently, implementing standard calculation procedure, capillary pressure is expected to be in the interval of 1.4-14.0 MPa. This suggestion is in agreement with Zhengjian Xu et al (2017) results, obtained for Triassic Chang 6 Member in the southwest Ordos Basin, China. Cited authors, performing modern techniques, have measured values for trapping pressure, which hesitate near 5-10 MPa excess pressure (Fig 5 and Table 5 of the work). Through recalculation of the author's data we obtain values for corresponding pressure coefficient 1.12-1.36 (average 1.22). Consequently, if the formation pressure of the source rocks forms  $P_{pc} > 1.22$ , generated petroleum products may leave the "birthplace". This suggestion is supported by the field data of the cited authors. They formulate the conclusion that calculated excess pressure overcomes filtration obstacles and gives start for filling the tight reservoirs of Member 6. Based on this, we conclude that the searching lower limit of the  $P_c$  may be drawn speculatively near 1.20-1.25.

As regards the upper limit, there is broad consensus that  $P_{pc}$  values  $> 1.8-1.9$  corresponds to the stress regime initiating process of natural fracturing that is, generating of filtration conduits, providing fluid mobility. Detailed information over this matter was provided by comprehensive investigation of Wanzhong Shi et al. (2013). They collect large scale field data from Qiongdongnan basin (China) and give evidences that  $P_c > 1.9$  leads to hydro fracturing.

The presented above logical construction, regarding lower and upper limit of  $P_{pc}$  may schematically be summarized as follows:

1. if  $P_{pc}$  within the formation source rocks  $< 1.22$ , then HC products mobility practically is negligible, which leads to the origin of a certain (in-situ) continuous accumulation;
2. if  $1.22 < P_{pc} < 1.9$  a quasi-continuous plays is likely to form;

3. if  $P_{pc} > 1.9$  more likely to occur natural hydro fracturing, changing the original tight rocks into the conventional fractured reservoirs.

Accounting for the broad diversity of principal stress profiles of rock sequences from basins worldwide, the presented above concept, regarding the role of  $P_{pc}$  values, should be accepted only as a preliminary attempt. However, we believe that the described rough ideas of a quantitative approach to determine overpressure control on the migration processes may help to better understanding of continuous play origin.

As final remarks to the presented above aspects of continuous accumulations origin, author is far away from the assumption that outlined postulates will address all the petroleum accumulations within the presented framework. The spectrum of petroleum localizations worldwide is too large, which unavoidably suggests vast existence of intermediate position and/or borderline field cases. It also means that the problem of continuous accumulation comprehensive description is still "open" and its decision appears as the main purpose of the future development of theoretical and practical petroleum geology.

## Conclusion

As a result of performed analysis, we propose a new model for continuous accumulation origin, in which the magnitude and style of primary migration have the leading role. These parameters, as an integral result of the cumulative influence of number of factors, may control the formation processes as follows:

- If the primary migration is 100 % restricted by filtration barriers a certain (in-situ) continuous accumulation is formed; in this case pressure coefficient ( $P_{pc}$ ) is more often  $< 1.22$ .
- In case of limited transfer of HC products to nearest beds or partly realized migration, there are condition for quasi-continuous accumulation to be formed; pressure coefficient is  $1.22 < P_{pc} < 1.9$ ;
- If  $P_{pc} > 1.9$  more likely to occur natural hydro fracturing, changing the original tight rocks into the conventional fractured reservoirs.
- When high level of expulsion efficiency is in force and petroleum products undergone notable buoyancy effect, than these settings are typical for enrichment pattern of conventional accumulations;
- The portion of the expelled products of continuous plays is quite smaller than the portion of the products not affected by the expulsion (e.g. in-situ products), which suggests broad genetic diversity of unconventional plays, compare to the conventional analogous.

**Acknowledgement.** We are grateful for ideas and constructive comments from prof. G. Georgiev and P. Nenkov, contributed to improvement of the earlier version of this manuscript.

## References

Basin-centered gas systems of the U.S. Project DE-AT26-98FT40031.2000. U.S. Department of Energy, National Energy Technology Laboratory Contractor: U.S. Geological Survey Central Region Energy Team DOE Project Chief:

- Bill Gwilliam USGS Project Chief: V.F. Nuccio Contract Period: April, 1998-November, 2000 Final Report.
- Cheng Zhang and Qingchun Yu. 2019. Breakthrough pressure and permeability in partially water-saturated shales using methane-carbon dioxide gas mixtures: An experimental study of Carboniferous shales from the eastern Qaidam Basin, China. AAPG Bulletin, v. 103, no. 2 (February 2019), pp. 273–301.
- Chenghua Ou, Chaochun Li, Dongming Zhi, Lie Xue, and Shuguang Yang. 2018. Coupling accumulation model with gas-bearing features to evaluate low-rank coalbed methane resource potential in the southern Junggar Basin, China. AAPG Bulletin, v. 102, no. 1 (January 2018), pp. 153–174.
- Fall, A., P. Eichhubl, St. Cumella, R. Bodnar, St. Laubach, St. Becker. 2012. Testing the basin-centered gas accumulation model using fluid inclusion observations: Southern Piceance Basin, Colorado. AAPG Bulletin, v. 96, no. 12 (December 2012), pp. 2297–2318.
- Hristov Z. et al. 1988. (in Bulgarian) Geology of the Dobrogea coal basin. Sofia, Technika, 170 pp.
- Hua Yang, Shixiang Li and Xianyang Liu. 2016. Characteristics and resource prospects of tight oil in Ordos Basin, China. Petroleum Research (2016) 1,27-38.
- Hunt, J. 1995. Petroleum geochemistry and geology. Second edition, New York, 743 pp.
- Jingzhou Zhao, Jinhua Fu, Xinshan Wei, Xinshe Liu, Xiaomei Wang, Qing Cao, Yanping Ma, and Yuanfang Fan. 2012. Quasi-continuous Lithologic Accumulation System: A New Model for Tight Gas Occurrence in the Ordos Basin, China. Search and Discovery Article #80210 (2012) Posted March 12, 2012.
- Jordanov, J. 2013. (in Bulgarian) Arising of abnormal pore pressure due to rock organic matter transformation. Assessment models. Annual of MGU, part III, Geology and geophysics, 56, 71-80.
- Jordanov, J. 2018 a. (in Bulgarian) Basic characteristics of the continuous (in-situ) petroleum accumulations. Journal of mining and geology, 4, 26-33.
- Jordanov, J. 2018 b. (in Bulgarian) Aspects of continuous (in-situ) petroleum accumulations origin mechanism. Journal of mining and geology, 9, 28-35.
- Kalmikov, G. A., N. S. Balushkina. 2017. (in Russian) A model of pore space saturation of Bagenov formation deposits, W. Siberia, for the purpose of resource potential assessment. GEOC, 2017, 247 c. ISBN 978-5-89118-763-4 <http://mmtk.ginras.ru/pdf>.
- Kuchinskiy, V. 2013. Organic Porosity Study: Porosity Development within Organic Matter of the Lower Silurian and Ordovician Source Rocks of the Poland Shale Gas Trend\* AAPG 2013 Annual Convention & Exhibition Pittsburgh, PA, USA May.
- Liu Guangdi, Sun Mingliang, Zhao Zhongying, Wang Xiaobo and Wu Shenghe. 2013. Characteristics and accumulation mechanism of tight sandstone gas reservoirs in the Upper Paleozoic, northern Ordos Basin, China. Pet.Sci.(2013)10:442-449.
- Magara, K. 1982. (in Russian) Compaction and fluid migration. Moscow, Nedra, 296 pp.
- Moore, T. A. 2012. Coalbed methane: A review. International Journal of Coal Geology 101:36–81, November 2012.
- Qing Li, Xuelian You, Zaixing Jiang, Xianzheng Zhao, and Ruifeng Zhang. 2017. A type of continuous petroleum

- accumulation system in the Shulu sag, Bohai Bay basin, eastern China. *AAPG Bulletin*, v. 101, no. 11 (November 2017), pp. 1791–1811.
- Romero-Sarmiento, M., M. Ducros, B. Carpentier, F. Lorant, M. Cacas, S. Pegaz-Fiornet, S. Wolf, S. Rohais, I. Moretti. 2013. Quantitative evaluation of TOC, organic porosity and gas retention distribution in a gas shale play using petroleum system modeling: Application to the Mississippian Barnett Shale. *Marine and Petroleum Geology* 45 (2013) 315-330.
- Schmoker, J. W. 1995. Method for Assessing Continuous-Type (Unconventional) Hydrocarbon Accumulations. In: Gautier, D. L., Dolton, G. L., Takahashi, K. I. and Varnes, K. L., Eds., National assessment of United States Oil and Gas Resources—Results, Methodology, and Supporting Data: U.S. Geological Survey Digital Data Series, 30, CD-ROM.
- Slatt, R. and N. O'Brien. 2011. Pore types in the Barnett and Woodford gas shales: Contribution to understanding gas storage and migration pathways in fine-grained rocks. *AAPG Bulletin*, v. 95, no. 12 (December 2011), pp. 2017–2030 2017.
- Tongwei Zhang, Xun Sun, and Stephen C. Ruppel. 2013. Hydrocarbon Geochemistry and Pore Characterization of Bakken Formation and Implication to Oil Migration and Oil Saturation. Search and Discovery Article #80321 (2013). Posted October 31, 2013. AAPG Annual Convention and Exhibition, Pittsburgh, Pennsylvania, May 19-22, 2013.
- Wanzhong Shi, Yuhong Xie, Zhenfeng Wang, Xusheng Li, Chuanxin Tong. 2013. Characteristics of overpressure distribution and its implication for hydrocarbon exploration in the Qiongdongnan Basin. *Journal of Asian Earth Sciences* 66 (2013) 150–165.
- Xiaojun Zhu, Jingong Cai, Qing Liu, Zheng Li, and Xuejun Zhang. 2019. Thresholds of petroleum content and pore diameter for petroleum mobility in shale. *AAPG Bulletin*, v. 103, no. 3 (March 2019), pp. 605–617.
- Yu Liu & Yanming Zhu. 2016. Comparison of pore characteristics in the coal and shale reservoirs of Taiyuan Formation, Qinshui Basin, China, *Int J Coal Sci Technol* (2016) 3(3):330–338.
- Yuanjia Han, B. Horsfield, R. Wirth, N. Mahlstedt, and S. Bernard. 2017. Oil retention and porosity evolution in organic-rich shales. *AAPG Bulletin*, v. 101, no. 6 (June 2017), pp. 807–827.
- Zhengjian Xu, Luofu Liu, Tieguan Wang, Kangjun Wu, Wenchao Dou, and Xingpei Song. 2017. Analysis of the charging process of the lacustrine tight oil reservoir in the Triassic Chang 6 Member in the southwest Ordos Basin, China. *Can. J. Earth Sci.* 54: 1228–1247 (2017) [dx.doi.org/10.1139/cjes-2016-0192](https://doi.org/10.1139/cjes-2016-0192).
- Zhuoheng Chen & Chunqing Jiang. 2016. A revised method for organic porosity estimation in shale reservoirs using Rock-Eval data: Example from Duvernay Formation in the Western Canada Sedimentary Basin. *AAPG Bulletin*, v. 100, no. 3 (March 2016), pp. 405–422.

## RELIABILITY FUNCTION IMPROVED FITTING USING GOODNESS-OF-FIT PROCEDURES

**Petko Nedyalkov**

UMG "St. Ivan Rilski" – Sofia, FMEM, dept. MM; petko.nedyalkov@mgu.bg

**ABSTRACT.** Presented research paper analyze assessments of reliability function using goodness-of-fit procedures. The analysis is deepen following the modern increased software and computational abilities which allows using better and accelerated mathematical procedures. Particularly goodness-of-fit /GOF/ procedures are compared with median rank estimation /MRE/ and maximum likelihood estimation /MLE/ in resolving fitted values for Weibull models in reliability function assessment. This study shows diagram CDF – ECDF comparison, as well as the criteria comparison using Kolmogorov-Smirnov, Anderson-Darling and Crammer-Von Mises distances. Data sets from jaw crusher lining plates repair periods are used. There are developed hazard and survival functions for reliability assessment based on fitted models.

**Keywords:** goodness-of-fit; liner plate wear; jaw crusher; Weibull model fit; Weibull reliability assessment

### ИЗВЕЖДАНЕ НА ФУНКЦИЯ НА НАДЕЖНОСТТА ЗА ОБЛИЦОВКИТЕ НА ЧЕЛЮСТНА ТРОШАЧКА

**Петко Недялков**

МГУ "Св. Иван Рилски" – София, МЕМФ, кат. MM, petko.nedyalkov@mgu.bg

**РЕЗЮМЕ.** Представената статия разглежда методите за интерполиране и оценка на показателите на функциите на надеждността. Ресурсните показатели на ремонтните въздействия поради естеството им са времево зависими дискретни данни, които при интерполиране към непрекъсната функция биха дали различни показатели в зависимост от използваните методи. Сравнени са класически методи: метод на ранга на медианата, максимум на функцията на възможността с метод максимизиращ метод на подобрението (goodness-of-fit). Оценката на показателите на функциите на надеждността е проведено с методите: Колмогоров-Смирнов, Андерсон-Дарлинг, Крамер-фон Мизес. Разработен е алгоритъм за приемане на показателите на функциите и оценъчните показатели на разпределенията и описващите ги модели. Представени са таблични и графични резултати за визуализация и оценка на моделите, оценките и сравнителните им показатели.

**Ключови думи:** goodness-of-fit; облицовъчни плочи, износване, челюстна трошачка, Вейбул модели, надеждностни модели

### Introduction

Operational properties of machines and their parts subjected to unsteady loading and abrasive wear tend to show variability despite the fact of strictly determined calculation design procedures. Following chain structure levels: part - sub-assembly - assembly- machine, the complete machine also tends to have inconsistency in its operational properties, repair periods and maintenance works. All this is enveloped in reliability model and has to be used in product lifecycle Minin (2017) management regarding the machine operation parameters aggravate in wear increasing Hristova (2016). Reliability model structure could be based on Weibull function, thoroughly described and proven in experimental scientific studies (Weibull (1951), Stephens (1974)) regarding such kind of problems.

The examined object Minin (2017) is a jaw crusher operating as gold ore sizing crusher in Bulgarian mine. Working process inconsistency depends mostly on the variance of ore fragment size and then on rock strength and abrasive properties, which vary with mineral-composite structure.

Although finding the proper reliability model, based on Weibull function could be a problem itself, the suitable function interpolation is equally important issue. The aim of this research is to resolve that issue with the significance and

the adequate values in Weibull function. The solution for estimated Weibull model values using median rank estimation /MRE/ and maximum likelihood estimation /MLE/ is expanded by goodness-of-fit tests (Delignete-Muller (2014), Murthy (2004), Krit (2014)), which assists the research engineer to choose between various valued models.

Some improvements in MRE algorithm with precise Bernard interpolation formula (eq. 6) can be found but that improvement averages in 0.1 % which is not valuable subject. Finding improved mathematical method is done successfully when goodness-of-fit functions are implemented as an algorithms in fitting software procedures (Delignete-Muller (2014), Krit (2014), Krit (2016)). That gives improved abilities in estimation of adequate and confident values in chosen reliability function. Presented research is focused in reliability function estimation improving and its application in real repair and maintenance of jaw crusher lining plates.

### Theory

Weibull probability distribution (density) function /pdf/ is defined as three parameter function but in reliability modeling the location parameter  $\gamma \in (-\infty, \infty)$  is often set to 0 ( $\gamma=0$ ), so the distribution is presented in following form:

$$f(\tau|\gamma=0) = \frac{\beta}{\eta} \cdot \left(\frac{\tau}{\eta}\right)^{(\beta-1)} \cdot \exp\left[-\left(\frac{\tau}{\eta}\right)^\beta\right] \quad (1)$$

and cumulative density function /CDF/ is:

$$F(t|\gamma=0) = \int_{-\infty}^t f(\tau) d\tau = 1 - \exp\left[-\left(\frac{\tau}{\eta}\right)^\beta\right] \quad (2)$$

Other important functional features are:

- survival function S(t) defined as admission life period to exceed some time interval P(T > t), as follows:

$$S(t) = 1 - P(T \leq t) = 1 - F(t) = \exp\left[-(t/\eta)^\beta\right] \quad (3)$$

- hazard function is defined by:

$$h(t) = \frac{f(t)}{S(t)} = \frac{f(t)}{1 - F(t)} = \frac{\beta}{\eta^\beta} \cdot t^{(\beta-1)} \quad (4)$$

- mean time to failure /MTTF/ or the expected time to failure as an mathematical expectation:

$$MTTF = E = \eta \cdot \Gamma\left(\frac{1}{\beta} + 1\right) \quad (5)$$

Computational application of MRE method with precise approximation Bernard algorithm formula for median rank is:

$$F_T(t_i) \cong Z_i \cong \frac{i - 0.3175}{N + 0.365} \quad (6)$$

, where:

N, number - total number of data;

i - data point ascending rank;

After double logarithm of upper formulas, with some idealizations it can be achieved:

$$\ln\{\ln[F_T(\ln t_i)]\} \cong y = \beta \cdot x - \beta \cdot \ln(\eta) = A_1 \cdot x + A_0 \quad (7)$$

, placed in linear interpolation, for example in spreadsheet, so the MRE non-iterative algorithm in calculation of Weibull function coefficients uses:

$$\begin{cases} \beta = A_1 \\ \beta \cdot \ln(\eta) = A_0 \end{cases} \Rightarrow \begin{cases} \beta = A_1 \\ \eta = \exp\left(-\frac{A_0}{A_1}\right) \end{cases} \quad (8)$$

The MLE method is accepted by Luciano [Luceno (2006)] as asymptotically optimal for large number of continuous distribution functions. Although Luceno (2006) and Krit (2014), Krit (2016) both based on their researches share the idea to use goodness-of-fit test as an algorithm in parameters estimation procedure. Initially the idea concerns any functions with large change in some intervals or points, which lead to large change in likelihood estimator and its impossibility of computing.

Goodness-of-fit estimation is based on algorithms that are previously developed as statistical methods proving the H0 hypothesis. Usually H0 hypothesis is about that two-samples of realizations are drawn from same distribution.

One-sample gof tests H0 hypothesis respects the realizations and theoretical function to have the same distribution. There are large amount of hypothesis testing functions but in previous researches (Luceno (2006), Delignete-Muller (2014), Krit (2016), Lazov (2014)) Kolmogorov-Smirnov and Anderson-Darling tests are recommended.

General form of Kolmogorov-Smirnov test is evaluated as:

$$KS_{nm} = \sup_t |F_n(t) - G_m(t)| \quad \text{or} \quad KS_n = \sup_t |F_n(t) - \hat{F}(t)| \quad (9)$$

, where:

KS<sub>nm</sub> - distance (statistic) value;

F<sub>n</sub>(t) - first CDF function with n - sample number;

G<sub>m</sub>(t) - second CDF function with m - sample number;

$\hat{F}(t)$  - estimated (theoretical) CDF. It was proven that the probability P of distance KS<sub>n</sub> to be smaller than chosen parameter lean to Kolmogorov distribution, as follows:

$$\lim_{n \rightarrow \infty} P(\sqrt{n} \cdot KS_n \leq x) = \frac{\sqrt{2} \cdot \pi}{x} \sum_{j=1}^{\infty} \exp\left(\frac{-(2 \cdot j - 1)^2 \cdot \pi^2}{8 \cdot x^2}\right) \quad (10)$$

, so the formal transformations have to be taken in attention:

$$P(KS_n > \delta_{n,1-\alpha}) = \alpha \Rightarrow P(KS_n < \delta_{n,\alpha}) = 1 - \alpha \quad (11)$$

, where:

$\alpha$  - significance level or -

CI = 1 -  $\alpha$  - confidence interval.

Statistic value (KS<sub>n</sub>) appraise the distance between CDF and ECDF (respectively theoretical function and observed) at the significance level. The p-value in that statistic (KS<sub>n</sub>) represents probability in finding the calculated distance value between CDF and ECDF. So the smallest distance (KS<sub>n</sub>) with high p-value means the smoothest and the most precise fit between observations and theoretical function.

It is known that Kolmogorov-Smirnov test Krit (2016), Delignete-Muller (2014), Luceno (2006) sensitivity to deviations from a cumulative distribution function /CDF/ is not variable independent which leads to more sensitivity of test around the median and less sensitivity at the extreme ends (tails) of the distribution, where cumulative distribution function get near 0 or 1. Anderson-Darling test remove these disadvantages with weighted statistic, but it is in integral form which is computational expensive. Real data application for Anderson-Darling is usually in the form of:

$$AD_n^2 = n \cdot \int_{-\infty}^{\infty} \frac{[F_n(x) - \hat{F}_0(x)]^2}{\hat{F}_0(x) \cdot [1 - \hat{F}_0(x)]} d\hat{F}_0(x) \quad (12)$$

, where: F<sub>n</sub>(x) - is empirical distribution function /ECDF/;

$\hat{F}_0(x)$  - theoretical (estimated) distribution function /CDF/;

The other test statistic placed upwards is Cramer - von Mises usually in the form of:

$$CM_n = n \cdot \int_{-\infty}^{\infty} [F_n(x) - \hat{F}_0(x)]^2 d\hat{F}(x) \quad (13)$$

, using same assignments as in the upper formulas, using same assignments as in the upper formulas.

Data and results

Here are used Kolmogorov-Smirnov and Anderson-Darling procedures in comparison to maximum likelihood estimation (mle) and median regression estimation (MRE). Checking procedure is done in one-sample Kolmogorov-Smirnov test and Crammer-Von Mises test conducted in different computational procedures.

There are used three data samples marked with D1 to D3 with different sample size and representing different maintenance periods for the considered parts. Data in D1 presents changing period for lining plate for movable jaw with 38 samples, D2 is for stationary jaw lining with 87 samples. Dataset D3 is chosen from data set D2 after 38-th row, so it has 50 samples. Dataset D3 is chosen from same samples in order to test computational procedures.

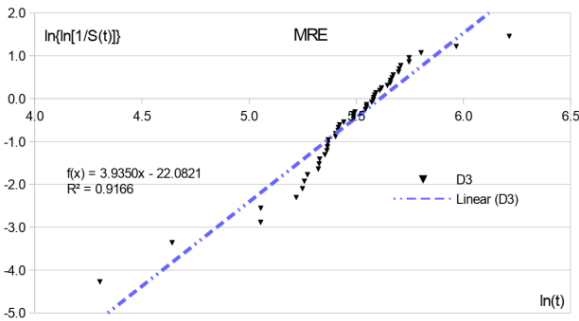


Fig.1. MRE regression for D1 with linear interpolation of MRE

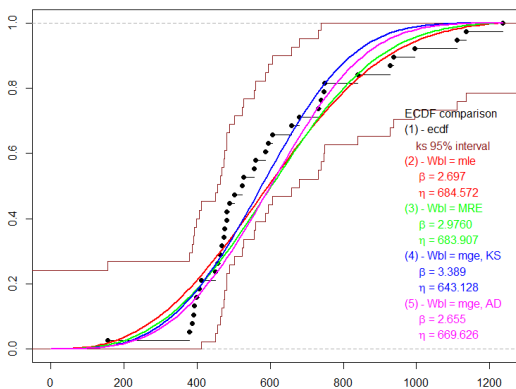


Fig.2. Comparison for algorithms fit with ECDF for D1

	MRE	mle	KS	AD
$\beta$	2.9760	2.6965	3.3891	2.6545
$\eta$	683.907	684.572	643.128	669.626
$R^2$	0.8595			
ks.test				
KS <sub>n</sub> (D)	0.1570	0.1571	0.1269	0.1715
KS <sub>p-value</sub>	0.276	0.275	0.532	0.191
cvm.test				
CM <sub>n</sub> ( $\omega^2$ )	0.254	0.228	0.184	0.196
CM <sub>p-value</sub>	0.184	0.220	0.302	0.275

Fig.3. Algorithms fit numerical values comparison for D1 (table view)

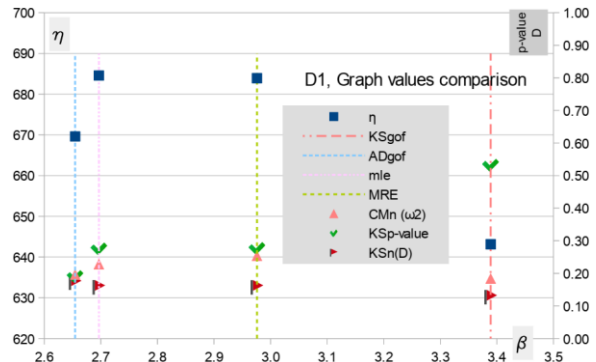


Fig.4. Algorithms fit values comparison for D1 (chart view)

Interpolation of distribution parameters with different algorithms is shown on fig. 1 and fig. 3 as it's noted. This particular data set fits quite well in Weibull model despite estimation method used. Kolmogorov-Smirnov and Cramer-Von Mises test are used after the fitting procedure within different computational function. This is shown in comparison table 1 and fig. 2. On figures 2, 5, and 8:

- flags - Kolmogorov-Smirnov estimated distance  $KS_n$  ;
- boxes - " $\eta$ " values;
- check tick - p-value as and;
- triangle - estimated  $CM_n$  distance. Which representation aims easy and distinctive comparison between estimation models.

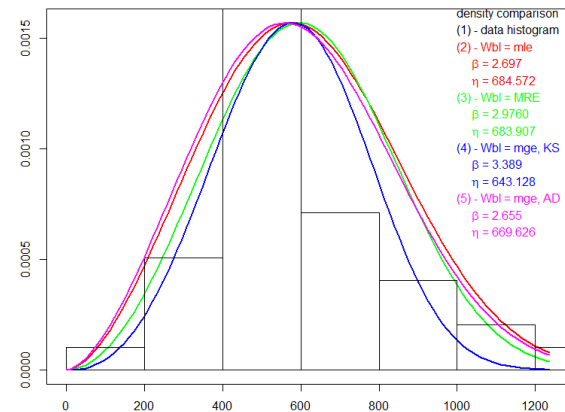


Fig.5. Density chart comparison for different interpolation algorithms - dataset D1

The same procedure is used, so following are the D2 processing results:

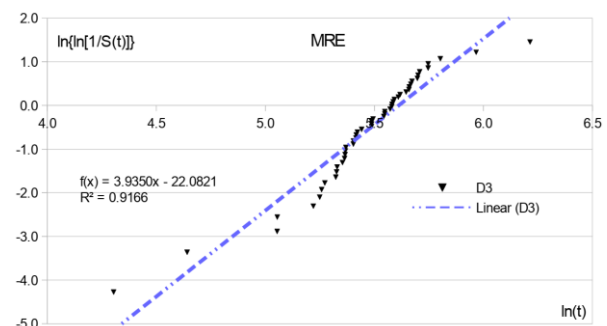


Fig.6. MRE regression for D2 with linear interpolation of MRE

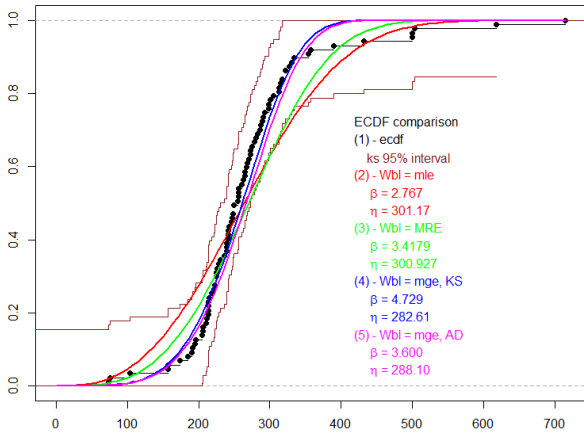


Fig.7. Comparison for algorithms fit with ECDF for D2

	MRE	mle	KS mge	AD mge
$\beta$	3.4179	2.7671	4.7286	3.6000
$\eta$	300.927	301.169	282.609	288.098
$R^2$	0.8809			
ks.test				
KS <sub>n</sub> (D)	0.1511	0.1654	0.0704	0.1282
KS p-value	0.038	0.017	0.781	0.115
cvm.test				
CMn ( $\omega^2$ )	0.678	0.877	0.134	0.368
CM p-value	0.014	0.005	0.442	0.087

Fig.8. Algorithms fit numerical values comparison for D2 (table view)

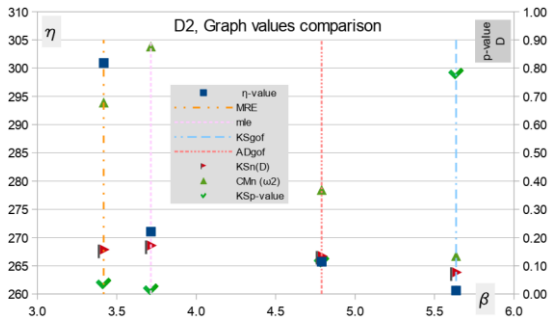


Fig.9. Algorithms fit values comparison for D2 (chart view)

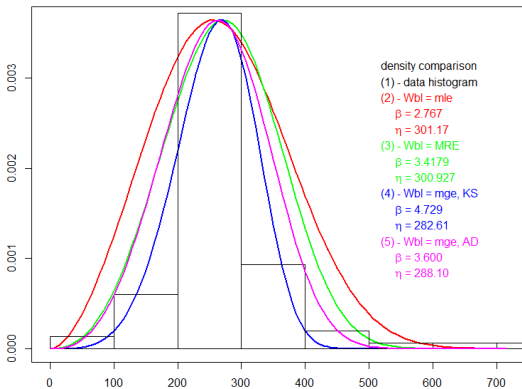


Fig.10. Density chart comparison for different interpolation algorithms - dataset D2

The improved procedure using goodness-of-fit procedure shows better results with both datasets, so it is supposed to be tested with some testing pieces, so following are the D3 processing results:

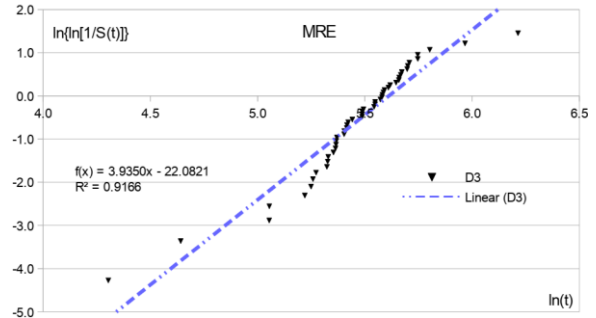


Fig.11. MRE regression for D3 with linear interpolation of MRE

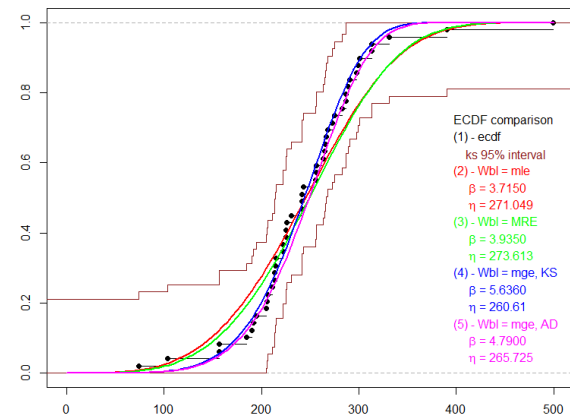


Fig.12. Comparison for algorithms fit with ECDF for D3

	MRE	mle	KS mge	AD mge
$\beta$	3.9350	3.7150	5.6360	4.7900
$\eta$	273.613	271.049	260.614	265.725
$R^2$	0.9166			
ks.test				
KS <sub>n</sub> (D)	0.338	0.135	0.065	0.088
KS p-value	0.131	0.304	0.978	0.816
cvm.test				
CMn ( $\omega^2$ )	0.209	0.230	0.049	0.058
CM p-value	0.251	0.216	0.887	0.830

Fig.13. Algorithms fit numerical values comparison for D3 (table view)

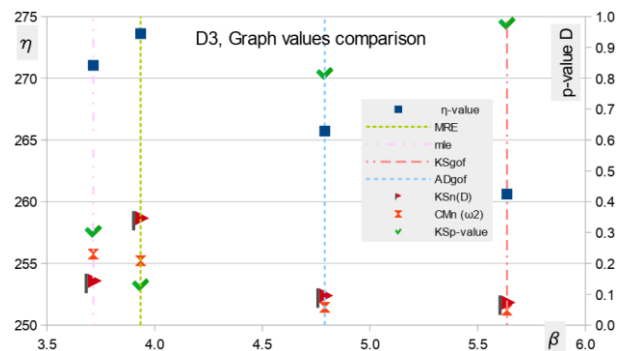


Fig.14. Algorithms fit values comparison for D3 (chart view)

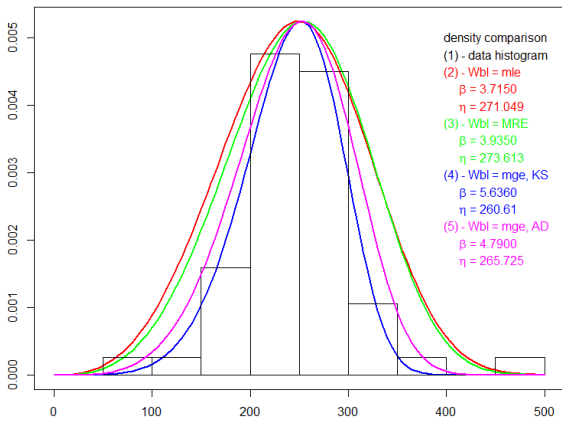


Fig.15. Density chart comparison for different interpolation algorithms - dataset D3

The acceptance of these models is controversial according to the graphical instruments. The better verification is comparison between numerical values from goodness-of-fit tests. Results from test verification are placed below interpolation values as shown in tables 1-3. Base researchers Stephens (1974) and O'Connor (2012) prefer Kolmogorov-Smirnov with critical asymptotical value calculated as:

$$KS_n < \frac{d_\alpha}{n^{1/2} + 0.12 + 0.11 \cdot n^{-1/2}} \quad (14)$$

, where  $d_\alpha$  - tabulated constant for Kolmogorov-Smirnov distance Stephens (1974) at significance level  $\alpha = 5\%$ , so  $d_{0.05} = 1.358$ , or for  $n > 40$  as:

$$KS_n < d_\alpha \cdot n^{-1/2} = 1.358 \cdot n^{-1/2} \quad (15)$$

For Cramer-Von Mises test critical values [Stephens (1974)] are asymptotically calculated as:

$$(CM_n - 0.4 \cdot n^{-1} + 0.6 \cdot n^{-2}) \cdot (1.0 + 1.0 \cdot n^{-1}) < CM_\alpha \quad (16)$$

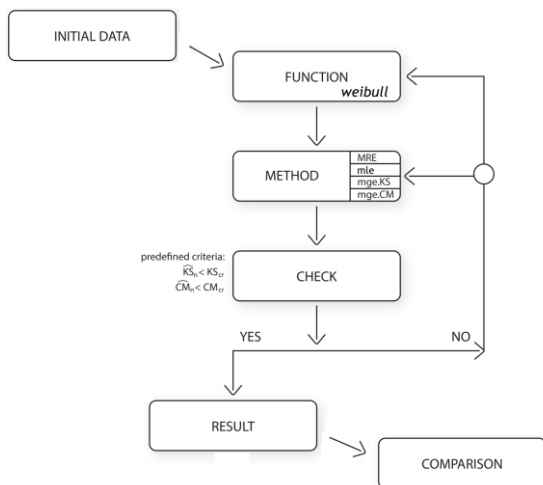


Fig.16. Function interpolation acceptance block scheme

## Conclusions

Initial data are being interpolated using chosen function (Weibull) and method (MRE, mle, mge.KS, mge.CM). Approved result (YES flow) comes after examination check following assigned criteria between initial data and fitted function. Approved results are being presented graphically and are used to draw the other reliability functions, for example: hazard and survival function. If the result is not approved (NO flow), new function or method iteration are conducted. The iteration process continues until the result match the assigned criteria.

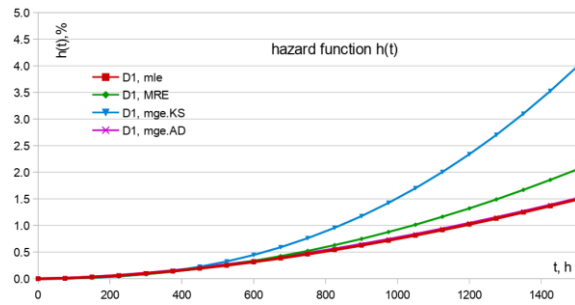


Fig.17. Hazard  $h(t)$  function based on estimated and accepted Weibull models for D1

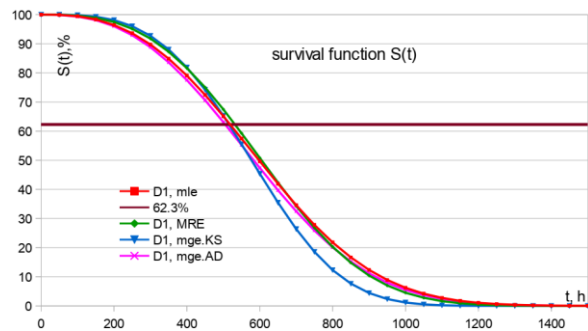


Fig.18. Survival  $S(t)$  function based on estimated and accepted Weibull models for D1

The result for hazard and survival functions shown in charts 17-18 match the assigned criteria for data set D1. Analogically for data set D2: in charts 19-20 are shown results for hazard and survival functions passing assigned criteria; and for data set D3: in charts 21-22 are shown results for hazard and survival functions passing assigned criteria.

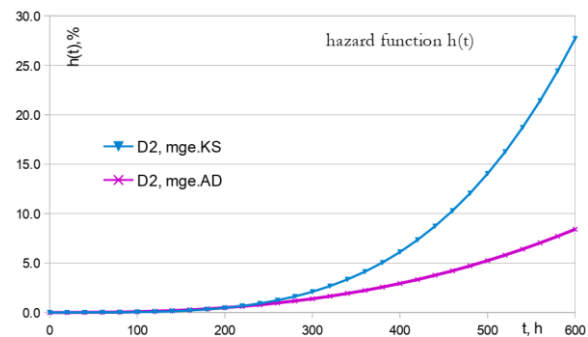


Fig.19. Hazard  $h(t)$  function based on estimated and accepted Weibull models for D3

Summary models have to be accepted at particular data set admit, with calculated value and author's preference for Kolmogorov-Smirnov method implementation of maximum goodness-of-fit estimation, so for D1 calculated  $MTTF_{1,KS} =$

577.7 h, and hazard function deviations is at interval of 0.5%. For D2 calculated  $MTTF_{2,KS} = 240.9$  h, which show hazard function deviations in interval of 0.1%. For D3 calculated  $MTTF_{2,KS} = 258.6$  h, hazard function deviations in interval of 0.3%. It is quite preferable to fit Weibull model using procedures of maximum goodness-of-fit with Kolmogorov-Smirnov or Anderson-Darling procedures. Related hazard function  $h(t)$  curves and survival function curves  $S(t)$  could be used in repair cycle analysis and reliability analysis for that particular machine.

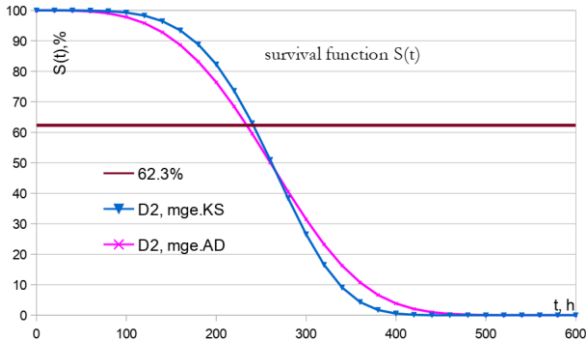


Fig.20. Survival  $S(t)$  function based on estimated and accepted Weibull models for D1

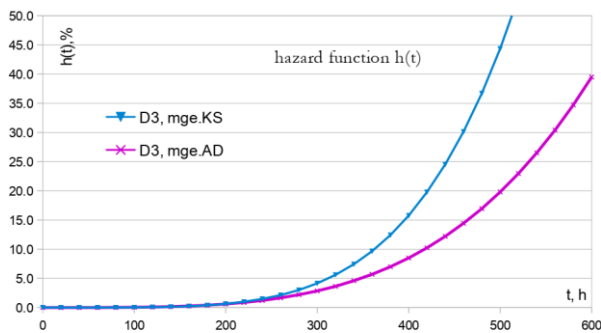


Fig.21. Hazard  $h(t)$  function based on estimated and accepted Weibull models for D3

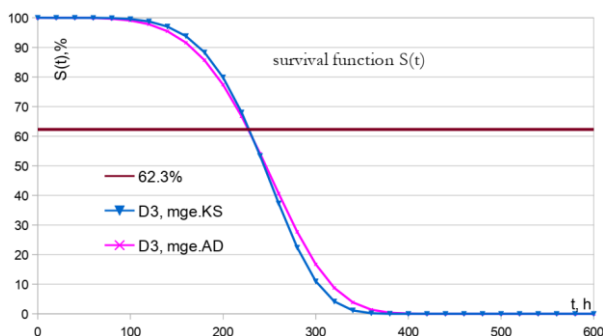


Fig.22. Survival  $S(t)$  function based on estimated and accepted Weibull models for D3

The particular fit procedure about distribution laws is in constant development, same the software instruments that achieve it. Many commercial software packages are widely used. In this research in development of program calculation as well as computational algorithms and procedures and graph presenting plots is used the iterative package for RStudio under GNU license in comparison with non iterative calculation made in spreadsheet.

Presented Weibull model fit is well fit to give an account of wearing process of jaw crusher liners with shown values in parameters interpolation. General view shows that using

maximum goodness-of-fit procedures gave narrow density distribution graph and narrow interval in ECDF comparison so it have to be proffered in more precise interpolation of reliability function analysis.

The reliability assessment for hazard and survival functions through goodness-of-fit procedures gave very smooth and close neighbour graphs as it is shown on fig. 17 till 21 (KS and AD charts) which is main achievement and condition to recommend GOF procedure despite the fact it is computationally expensive and quite complicated in understanding. It is clearly recommended in examination of reliability procedures for stochastically phenomena in mechanical wearing for mining and processing machines.

## References

- Weibull W. (1951), "A statistical distribution function of wide applicability", *Journal of Applied Mechanics*, 18, 293–296, 1951.
- Minin Iv. and D. Mitev (2017), "Determination of the function of reliability and the possibility of failure-free operation of a jaw crusher type CJ615:01", "St. Ivan Rilski" University of Mining and Geology - Sofia, *Journal of Mining and Geological Sciences*, ISSN:1312-1820, Vol. 60, Part III, pp. 11-17, 2017.
- Hristova T. (2016), "Approximate method for determination of engine power of jaw crusher for coarse crushing", "St. Ivan Rilski" University of Mining and Geology - Sofia, *Journal of Mining and Geological Sciences*, ISSN 1312-1820, Vol. 59, Part III, pp.80-83, 2016
- Lazov Lachezar (2014), "Simulation study of the wind turbine bearing loads", *Bulgarian Journal for Engineering Design*, ISSN: 1313-7530, Iss. 6 December 2010, pp. 33-38, Technical University of Sofia, Mechanical Engineering Faculty, 2010.
- Krit M. (2014), "Goodness-of-fit tests for the Weibull distribution based on the Laplace transform", *Journal de la Société Française de Statistique*, Vol. 153 No. 3, 135-151, ISSN: 2102-6238 (2014), Société Française de Statistique et Société Mathématique de France, 2014.
- Krit M., Ol. Gaudoin, M. Xie & E. Remy (2016), "Simplified Likelihood Based Goodness-of-fit Tests for the Weibull Distribution", doi: 10.1080/03610918.2013.879889, *Communications in Statistics - Simulation and Computation*, 45:3, 920-951, 2016.
- Delignete-Muller M. L. and Chr. Dutang (2014), "fitdistrplus: An R Package for Fitting Distributions", ISSN:1548-7660, Oct. 2014 (rev. July 2018), doi:10.18637/jss.v064.i04; <http://www.jstatsoft.org/article/view/v064i04>, 2014.
- Luceno Alb. (2006), "Fitting the generalized Pareto distribution to data using maximum goodness-of-fit estimators", *Computational Statistics & Data Analysis* 51 (2006) 904–917, doi:10.1016/j.csda.2005.09.011, 2006.
- O'Connor P. D. T. and A. Kleyner (2012), "Practical Reliability Engineering" Fifth Edition John Wiley & Sons, Ltd., App. 3, Kolmogorov-Smirnov tests, accessed [https://www.soest.hawaii.edu/GG/FACULTY/ITO/GG413/K\\_S\\_Table\\_one\\_Sample.pdf](https://www.soest.hawaii.edu/GG/FACULTY/ITO/GG413/K_S_Table_one_Sample.pdf), 2012
- Stephens M. A. (1974), "EDF Statistics for Goodness of Fit and Some Comparisons", *Journal of the American Statistical Association*, Vol. 69, No. 347 (Sep., 1974), pp. 730-737, 1974.
- Murthy, D. P., Xie, M., and Jiang, R. (2004), *Weibull Models*, John Wiley and Sons, Inc., 2004.

## ELECTRICITY EFFICIENCY OF A SEMI-AUTOGENOUS MILL INVESTIGATION

**Plamen Petrov, Rumen Istalianov, Salcho Manev**

University of Mining and Geology "St. Ivan Rilski", 1700 Sofia; ivanov@abv.bg, rgi@mgu.bg

**ABSTRACT** This paper discusses a semi-autogenous ore grinder. A software product is considered, which makes it possible to study data by using the polynomial model for interpolation. The input-output data related to the grinding process are collected, processed and analyzed. The purpose is to find the relationship between the power of the electric motor and the amount of ore at different openings of the grids of the unloading cover of the mill and to find the optimal mode of operation of the mill.

**Keywords:** Electricity efficiency, Semi-autogenous mills

### ИЗСЛЕДВАНЕ НА ЕЛЕКТРОЕНЕРГИЙНАТА ЕФЕКТИВНОСТ НА ПОЛУАВТОГЕННА МЕЛНИЦА

**Пламен Петров, Румен Исталиянов, Салчо Манев**

<sup>1</sup>Минно-геоложки университет „Св. Иван Рилски“, 1700 София

**РЕЗЮМЕ.** В тази статия е разгледана полу-автогенна мелница за смилане на руда. Разгледан е софтуерен продукт, който дава възможност, за изследване на данни, чрез използването на полиномния модел за интерполация. Събрани, обработени и анализирани са входно-изходните данни, свързани с процеса на смилане. Целта е да се намери връзка между мощността на електродвигателя и количеството руда при различни отвори на решетките на разтоварващия капак на мелницата и да се намери оптималният режим на работа на мелницата.

**Ключови думи:** електроенергийна ефективност, полуавтогенни мелници, решетки

### Introduction

In modern production conditions in the mining industry, in addition to ball mills, as the most used method for changing the particle size, grinding or mixing materials, semi-autogenous mills are widely used. Semi-autogenous mills grind the ore by rotating the drum of the mill, which raises the ore to a certain height. Lifters located in the inner surface of the mill help to lift. After lifting the material (ore), it goes into the mode of free flight, beginning to fall below its own weight. When falling, the material is crushed by parts grind. Semi-autogenous machines and the grinding medium, which is most often in a spherical shape (balls), which help grind (Tsvetkov, 1988, Minin, 2012).

Semi-autogenous grinding extends to many applications due to the range of available mill sizes. They can do the same job of reducing ore size as rod and ball mills in two or three stages of crushing and sieving. Semi-autogenous mills are also the optimal solution for wet grinding, as crushing and sieving can in some cases be difficult at other mills, if not impossible (Timm, 2011).

This article collects, processes and analyzes input-output data related to the grinding process, as well as the operation of the electric motor crushing mill. The aim is to study the ratio of energy consumption to process values in unloading lining of the mill with hole sizes of 23 mm and unloading lining with hole sizes of 25 mm. For this purpose, measurements performed on a mill type SAG 8.5 x 5.3 m are used (Minin, 2014).

### Description of the software

MatLab is a dialog program system for conducting scientific and technical calculations. It integrates the possibilities for analytical transformations, numerical calculations and graphical presentation of the obtained results. It is oriented to work with data arrays - vectors, matrices, multidimensional arrays, arrays of cells and arrays of records. Hence the name MatLab - Matrix LABoratory. This allows a single operator to perform simultaneous actions on all elements of the array, without the need to organize loops. The system has built-in functions that solve basic problems in linear algebra, numerical analysis, experimental data processing, two-dimensional and three-dimensional graphics, animation and more. The most used areas of application of MatLab are:

- Mathematical and computer calculations;
- Development of algorithms;
- Computational computer experiments;
- Simulation modulation;
- Computer data analysis;
- Research and visualization of data;
- Scientific and engineering graphics;

Development of applications including graphical user interface. As a tool for computer modeling, which provides research in virtually all known fields of science and technology.

Another feature of the software that is used is the input of data from Excel, which are downloaded from the monitoring and data collection system PI.

## Principles of the grinding process

The grinding process in semi-autogenous mills can be considered as a process of increasing the total particle area of the digestible material. This is done by reducing the particle size due to the collision with the grinding bodies and the subsequent crushing and grinding of the material. The kinetic energy of the grinding medium depends on the rotation speed of the mill and the mass of the grinding bodies, and in terms of rotation speed three main modes of operation are possible: cascade, waterfall, centrifugation. The effective operation of drum mills depends on the nature of the movement of the digestion medium.

**Cascading:** The charge is lifted to then roll to the toe of the charge. This occurs at lower speeds and results in mainly attrition and abrasion grinding regimes. When the mill operates in cascade mode, productivity is low, so this mode is rarely used.

**Catacting:** The charge is lifted and thrown to the toe of the charge. This occurs at higher speeds and results in predominantly impact breakage. Grinding is done mainly by impact and partly by grinding. This is the most common mode in practice.

In practice, the charge motion is a combination of cascading and catacting to achieve all three principle types of grinding. For variable speed drive mills, the shell speed can be adjusted to promote effective impact breakage at the toe of the charge. The optimum speed for a given mill load allows for direct contact between the catacting charge and toe of the charge. If the speed is too low, catacting conditions may not be created. If the speed is too high, the catacting grinding media may impinge directly onto the liners, potentially cracking balls and seriously damaging liners.

For grate discharge mills, the total charge level can be variable as compared to the constantly full nature of overflow mills. As such, measurement of the total charge is important and is achieved via the installation of load cells under one of the trun-nions.

As for mill speed, the total charge level must be optimized to promote effective impact breakage at the toe of the charge. Underloaded or overloaded mills behave similarly to mills operating at too fast or too slow shell speeds, respectively. Correct total charge conditions also expose sufficient grate area for slurry to be effectively pumped from the mill.

When the angular velocity of the mill becomes so high that it exceeds the critical one

and for the innermost layer of balls, the entire ball filling is distributed evenly over

the periphery of the drum and begins to move with it. This mode is called flywheel mode.

The semi-autogenous mills are unloaded through grids (fig. 1) with a certain size  $X$  and the ratio of the diameter and their length is medium to high. The grain size of the source material, the circulating load and the amount of feed ore to the mill depend on the grids.

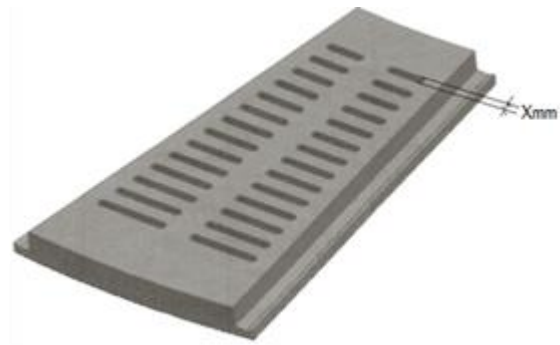


Fig. 1. Unloading grid

## Conducting the Experiment and Collecting Data

The data required for the present study were obtained from a monitoring and data collection system PI. They cover the period from 11.12.2019 to 24.07.2020. The measured parameters are shown schematically in (fig. 2).

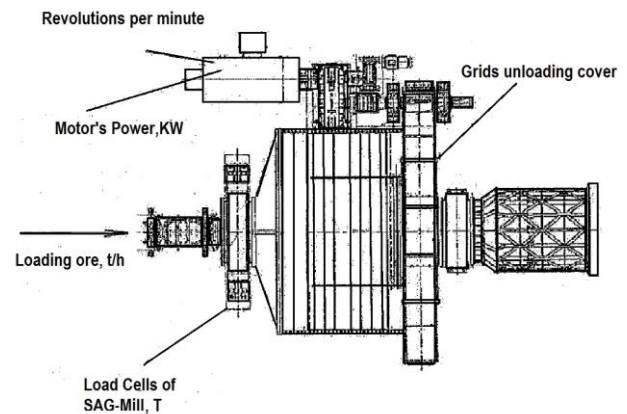


Fig. 2. Scheme of a semi-autogenous mill

## Results of measurements of the main parameters influencing the value of motor power

The obtained results from the measurements are averaged over one hour and are shown in (table 1), covering every day of the period - installation of a new lining of the cylinder and grids with holes' s size  $X = 23$  mm on 11.12.2019 - until the change of grids on 29.03. 2020 and (table 2), from the period-work with grids on the unloading cover with the size of the holes  $X = 25$  mm and installation of a new lining of the cylinder on 03.05.2020 to 24.07.2020

The first column of the table shows the day of the measurement; the second column is hour. The third column records the average hourly values of the motor power. The following columns record the average hourly values of the motor speed, the load cell of the mill and the amount of incoming ore.

Table 1. Measured during the operation of a semi-autogenous mill, I at dimensions X = 23mm for opening the grids of unloading cover.

Date	Time	Motor's stator	Revolution, (min-1)	Load Cells SAG Mill, (t)	Ore feed in SAG Mill ,(t)
12/11/2019	12:15:00 PM	4981.32854	1093.75948	75.8351524	0.05425353
12/14/2019	4:15:00 AM	1998.87227	372.499721	87.5192693	0.05425353
12/14/2019	5:15:00 AM	3755.25383	887.858583	88.3816083	0.05425353
12/14/2019	6:15:00 AM	4735.74578	995.390315	90.9309222	0.05425353
12/14/2019	7:15:00 AM	4641.80828	1000.36478	89.4022953	0.05425353
12/14/2019	8:15:00 AM	4235.3366	976.168898	88.5727039	0.05425353
12/14/2019	9:15:00 AM	4216.77156	962.011046	91.8758733	0.05425353
12/14/2019	10:15:00 AM	4691.09768	1000.00631	94.3464637	0.05425353
12/14/2019	11:15:00 AM	4679.81729	999.348534	93.5625713	0.05425353
12/14/2019	12:15:00 PM	4825.44993	999.608526	93.8173708	0.05425353
12/14/2019	1:15:00 PM	4612.44206	999.73862	94.7911541	0.05425353
12/14/2019	2:15:00 PM	4603.39886	1000.11188	93.6777951	0.05425353
12/14/2019	3:15:00 PM	4542.51509	1000.11331	92.6615897	0.05425353
12/14/2019	4:15:00 PM	4554.02466	999.517553	92.2629581	0.05425353
12/14/2019	5:15:00 PM	4518.17907	999.322721	93.2684463	0.05425353
12/14/2019	6:15:00 PM	4665.01727	999.387167	95.7261337	0.05425353
12/14/2019	7:15:00 PM	4378.21014	999.13111	93.9649615	0.05425353
12/14/2019	8:15:00 PM	4345.21203	999.302426	92.9054474	0.05425353
12/14/2019	9:15:00 PM	4315.38887	999.286543	91.8464863	0.05425353
12/14/2019	10:15:00 PM	4330.90401	999.366353	91.9721745	0.05425353
12/14/2019	11:15:00 PM	4431.30586	999.602915	92.8343761	0.05425353
12/15/2019	12:15:00 AM	4447.29388	999.35169	92.4329555	0.05425353
12/15/2019	1:15:00 AM	4424.84194	999.689235	92.7187536	0.05425353
12/15/2019	2:15:00 AM	4488.91668	999.226784	93.377018	0.05425353
12/15/2019	3:15:00 AM	4509.39188	999.706925	92.7109154	0.05425353
12/15/2019	4:15:00 AM	4540.50769	999.520069	93.2415222	0.05425353
12/15/2019	5:15:00 AM	4652.13123	998.751599	94.3883338	0.05425353
.....					
.....					
3/28/2020	3:15:00 PM	5035.82424	998.944933	83.718898	196.939333
3/28/2020	4:15:00 PM	4919.11997	998.670465	82.4335167	172.773774
3/28/2020	5:15:00 PM	4680.99048	987.72397	81.8188468	198.093953
3/28/2020	6:15:00 PM	4961.0612	974.15606	82.5039658	268.95435
3/28/2020	7:15:00 PM	5353.24226	999.102381	84.285327	233.253157
3/28/2020	8:15:00 PM	5284.3748	999.022975	83.7101525	250.713953
3/28/2020	9:15:00 PM	5343.40655	999.142292	83.9420467	240.252062
3/28/2020	10:15:00 PM	5304.588	999.016433	83.7130983	242.376537
3/28/2020	11:15:00 PM	5348.77576	998.741871	84.0893812	249.344618
3/29/2020	12:15:00 AM	4921.26015	986.373423	81.9527649	202.947724
3/29/2020	1:15:00 AM	4982.30901	992.034893	82.3423554	228.95965
3/29/2020	2:15:00 AM	5050.50219	998.97055	82.3614841	224.122808
3/29/2020	4:15:00 AM	4962.97676	995.364841	82.150314	225.189842
3/29/2020	5:15:00 AM	5119.51982	995.24346	82.7308403	195.355891
3/29/2020	6:15:00 AM	5148.65635	999.035425	83.0627596	189.746784
3/29/2020	7:15:00 AM	5185.45685	998.743416	82.9676871	251.319545
3/29/2020	8:15:00 AM	5068.1658	998.709547	84.020514	250.068831
3/29/2020	9:15:00 AM	5041.66659	998.627479	82.642305	261.765735
3/29/2020	10:15:00 AM	5311.47087	998.90686	83.5996484	259.473669
3/29/2020	11:15:00 AM	5307.27039	999.090831	84.595343	241.529223
3/29/2020	12:15:00 PM	5046.00434	998.840892	82.6369958	262.829804
3/29/2020	1:15:00 PM	4792.59863	998.731102	81.7334712	275.322305
3/29/2020	2:15:00 PM	5228.71355	998.853542	83.1570415	265.628276
3/29/2020	3:15:00 PM	5268.26931	998.848989	83.4777883	258.565337
3/29/2020	4:15:00 PM	5098.43237	999.011702	82.6326041	258.457278
3/29/2020	5:15:00 PM	5340.48781	998.964607	83.8909183	263.679383
3/29/2020	6:15:00 PM	5459.16937	998.84746	85.0418499	249.635751
3/29/2020	7:15:00 PM	4980.80273	998.471833	82.0938328	245.013521
3/29/2020	8:15:00 PM	4860.52185	992.692473	81.2301569	234.980913
3/29/2020	9:15:00 PM	4986.39967	998.809272	81.8433984	240.244693

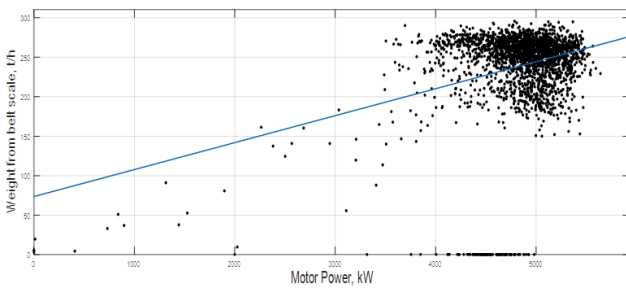
Table 2. Measured during the operation of a semi-autogenous mill, I at dimensions X = 25mm for opening the grids of unloading cover.

Data	Time	Motor's stator	Revolution, (min-1)	Load Cells SAG Mill, (t)	Ore feed in SAG Mill, (t)
4/10/2020	12:15:00 AM	5221.36535	1013.42233	82.0606701	177.260677
4/10/2020	1:15:00 AM	4916.69084	1010.32498	81.861611	182.219455
4/10/2020	2:15:00 AM	3950.32581	904.661892	78.8836192	219.56048
4/10/2020	3:15:00 AM	4943.91229	943.113882	84.5226746	240.473118
4/10/2020	4:15:00 AM	5255.97613	1013.73626	84.3407097	257.069658
4/10/2020	5:15:00 AM	5245.60167	1013.59319	83.8106956	268.728345
4/10/2020	6:15:00 AM	5101.36191	1013.71432	83.5491268	268.733561
4/10/2020	7:15:00 AM	3634.40281	762.8746	82.1471584	167.100927
4/12/2020	1:15:00 AM	624.313166	155.091078	79.9593529	35.276039
4/12/2020	2:15:00 AM	4038.31401	872.822353	81.2865226	291.510145
4/12/2020	3:15:00 AM	4818.67484	936.911757	83.1277503	251.635697
4/12/2020	4:15:00 AM	4548.96129	943.443172	81.2448139	271.107035
4/12/2020	5:15:00 AM	3986.05351	877.853505	80.8766088	276.167817
4/12/2020	6:15:00 AM	4371.63583	889.826995	83.1351383	257.613452
4/12/2020	7:15:00 AM	4976.75723	961.729795	82.8479638	259.273603
4/12/2020	8:15:00 AM	5058.53372	976.812153	82.0548901	235.733872
4/12/2020	9:15:00 AM	4956.73066	969.854999	81.2685204	173.008275
4/12/2020	10:15:00 AM	4672.43039	923.28552	81.7390312	158.360012
4/12/2020	11:15:00 AM	5110.31161	953.67778	83.1368479	156.316223
4/12/2020	12:15:00 PM	5403.5203	1007.71582	82.6006832	155.760099
4/12/2020	1:15:00 PM	5464.68382	1013.35359	82.4304799	154.278832
4/12/2020	2:15:00 PM	5323.45532	1009.98868	81.8300113	223.998773
4/12/2020	3:15:00 PM	5024.5378	975.383811	81.2393829	234.569044
4/12/2020	4:15:00 PM	5064.49905	962.744157	82.2983138	231.692266
4/12/2020	5:15:00 PM	5062.7518	979.586337	82.1648445	234.557167
4/12/2020	6:15:00 PM	4953.57394	968.444647	81.5620241	190.606345
...					
...					
7/23/2020	4:15:00 PM	4849.91774	928.19952	86.7339391	293.382214
7/23/2020	5:15:00 PM	4955.10159	965.352225	85.0732896	286.835014
7/23/2020	6:15:00 PM	4538.92611	940.853808	84.1431337	291.720608
7/23/2020	7:15:00 PM	3947.90157	889.007109	82.425296	216.470838
7/23/2020	8:15:00 PM	3822.95279	867.947049	81.6385381	298.305039
7/23/2020	9:15:00 PM	4431.27777	981.520427	85.4415935	291.392028
7/23/2020	10:15:00 PM	4574.42136	915.388489	85.1744899	292.375529
7/23/2020	11:15:00 PM	4651.62195	925.250635	85.133078	290.902096
7/24/2020	12:15:00 AM	4325.32688	894.772105	84.3612661	282.452611
7/24/2020	1:15:00 AM	4948.63187	938.617017	86.5583461	295.006411
7/24/2020	2:15:00 AM	4993.84176	975.285173	84.6544527	290.232079
7/24/2020	3:15:00 AM	4697.8022	941.525234	84.4780017	293.217976
7/24/2020	4:15:00 AM	4675.11886	931.8373	85.1847261	292.256413
7/24/2020	5:15:00 AM	5009.81323	956.592376	85.8235175	290.841973
7/24/2020	6:15:00 AM	5315.00258	996.966546	86.3018428	293.393837
7/24/2020	7:15:00 AM	5102.79698	997.490243	85.3109624	290.862992
7/24/2020	8:15:00 AM	5068.68374	982.917879	84.8697449	289.177754
7/24/2020	9:15:00 AM	4500.45274	965.371888	83.2967888	274.738602
7/24/2020	10:15:00 AM	3641.27444	869.07113	81.8928033	290.24497
7/24/2020	11:15:00 AM	4335.56098	875.884505	85.3955506	290.292388
7/24/2020	12:15:00 PM	5020.15294	949.141082	86.3285851	275.56469
7/24/2020	1:15:00 PM	5151.76474	982.88658	85.191256	290.623709
7/24/2020	2:15:00 PM	5045.71506	982.377445	84.7333025	291.471446
7/24/2020	3:15:00 PM	4993.96264	969.27835	84.7718216	294.313256
7/24/2020	4:15:00 PM	4847.64222	952.177783	84.7385717	291.052048
7/24/2020	5:15:00 PM	4695.63518	940.824656	84.7167837	294.353312
7/24/2020	6:15:00 PM	3957.49302	900.1514	83.2809808	242.001773
7/24/2020	7:15:00 PM	3830.83256	867.379109	81.8436054	199.762501
7/24/2020	8:15:00 PM	4023.194	867.250112	83.1192581	161.674442
7/24/2020	9:15:00 PM	4161.72057	867.219406	83.8872701	169.285251
7/24/2020	10:15:00 PM	4865.56104	916.593997	86.7520972	249.781302

### Analysis of the obtained results

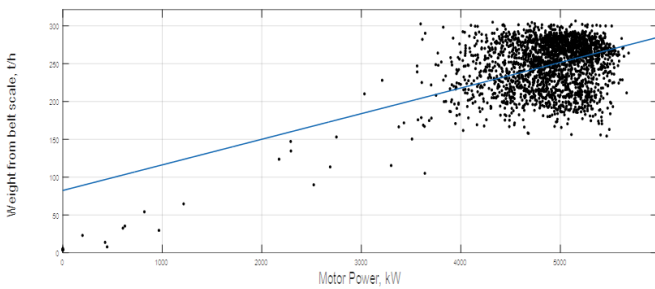
The analysis of the obtained results allows research, using the polynomial model for interpolation and quantitative measurement of dependence through the correlation coefficients and determination of the measured power of the electric motor to the productivity of the mill by the amount of incoming ore per unit time, motor speed, mill load cell during mill operation with two different sizes of gratings on the unloading cover.

After processing the input - output data from the software shown in (fig. 3a and b) there is a lower consumption for processing the amount of incoming ore per unit time when operating the mill with gratings with holes 25mm, but the total amount of energy consumed with gratings with holes 25mm is higher comparing the two reported periods, as the amount of processed ore is bigger. The correlation coefficient  $r$  of both scatter plots is  $0.3 \div 0.5$ , which makes the relationship moderate.



R-square: 0.09502

a) relationship on the sizes of holes of the gratings 23 mm

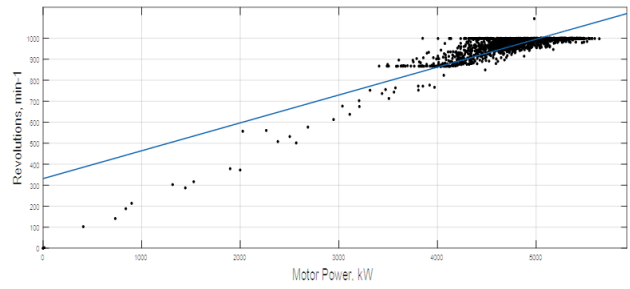


R-square: 0.2533

b) relationship on the sizes of the holes of the gratings 25 mm

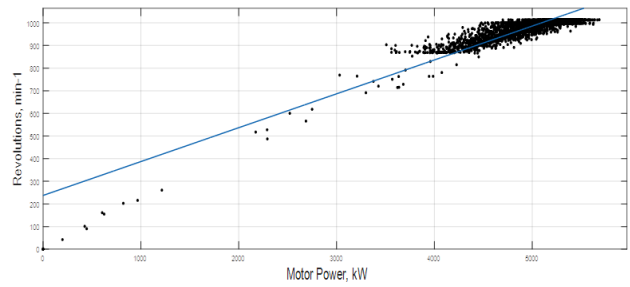
Fig. 3. Relationships between the measured power of the electric motor and the amount of ore entering the mill per unit time

On (fig. 4a and b) show the relationships between the motor power and the motor speed. The same energy consumption is observed at the same motor revolutions at the different holes of the grids. This is due to the automatic control of the motor speed by the load cell of the mill. The correlation coefficient  $r$  in both graphs is  $0.7 \div 0.9$ , which makes the relationship strong.



R-square: 0.754

a) relationship on the sizes of holes of the gratings 23 mm

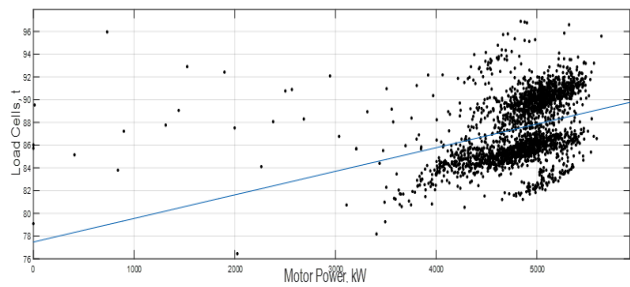


R-square: 0.843

a) relationship on the sizes of holes of the gratings 23 mm

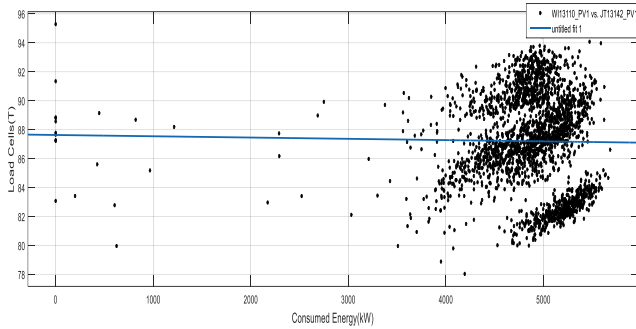
Fig. 4. Relationships between measured power and motor speed

From the scatter plots shown in (Fig. 5b), it can be seen that no correlation between the motor power and the load cell during the operation of the mill with unloading grids 25 mm. The correlation between the motor power of an ore mill with 23 mm unloading grids is positive. As the load cell increases, the energy consumed increases. The most optimal weight of the load cell is 92-94 t. The correlation coefficient of the scatter plots (Fig. 5a) is  $r = 0.34$ , which makes the relationship weak.



R-square: 0.1205

a) relationship on the sizes of holes of the gratings 23 mm

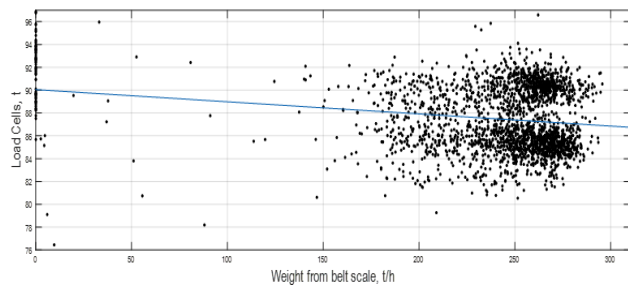


R-square: 0.0002272

b) relationship on the sizes of the holes of the gratings 25 mm

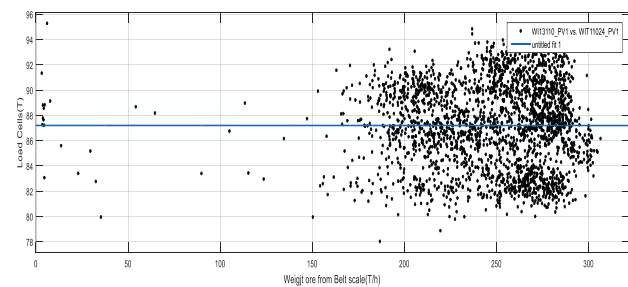
Fig. 5. Relationship between the measured power of the electric motor and the load cell of the mill

The relationship between the measurement results (Fig. 6a) is very weak. The relationship with the dimensions of the openings of the gratings 23 mm (Fig. 6b),  $r = -2.53e-04$ , which makes it negative and with very weak dependence. The reason is the large openings in the gratings of the unloading cover of the mill, which leads to a reduction in the time of passage of the ore in the mill.



R-square: 0.03895

a) relationship on the sizes of holes of the gratings 23 mm



R-square: 6.419e-08

b) dependence on the sizes of the holes of the gratings 25 mm

Fig. 6. Relationships between the measured amount of ore entering the mill and load cell of the mill

## Conclusion

In conclusion, the following conclusions can be drawn:

1. The power of the electric motor to the feed ore to the mill has 25 mm larger grid holes than the 23 mm grid sizes. This is due to the faster passage of the ore through the unloading cover, which allows higher processing.

2. With larger openings of the grids there is no relationship between the power of the electric motor and the load cell of the mill. With the grids with openings 23 mm we see a very weak connection, but still allows to use a correlation relationship.

3. No relationship is observed between the incoming ore in and the load cell of the mill in both types of grids.

4. The most cost-effective operation of the mill in terms of energy used in grinding the ore is setting a weight of more than 90 tons reported by the load cell of the mill. This is observed when operating the mill with both types of grids on the unloading cover

## References

- Minin I., Experimental study of the wear of the lifters of the drum linings of a mill type SAG 8.5 x 5.3 in order to determine their boundary wear, Sofia, MGU "St. Ivan Rilski", 2014, (in Bulgarian).
- Minin I., Techniques and technologies for mineral enrichment part I, Sofia, 2012, (in Bulgarian).
- Timm D., HIRSCHI N., Moir T., Ecoff B., "MILL LINNER FOR A GRINDING MILL" Pub. №WO2011 / 037600 A1, Pub. Date: March 31.2011, (English).
- Tsvetkov H., Concentrators, DI "Technique", Sofia, 1988. (in Bulgarian).

## TIGHTING THE PIECES OF MATERIAL IN CENTRIFUGAL ROLLER MILLS

**Stefan Pulev**

University of Mining and Geology "St. Ivan Rilski", 1700 Sofia; [st\\_pulev@yahoo.com](mailto:st_pulev@yahoo.com)

**ABSTRACT.** The grinding bodies in the centrifugal roller mills are cylindrical rollers that roll on the inner cylindrical surface of the mill drum. Trapped between the roll and the drum, the ore particles are crushed by the large centrifugal forces. In this work, a mathematical relation is obtained between the dimensions of the drum, the rollers and the particles entering for grinding, so that the angle of capture is optimal. This allows maximum reduction factor (ratio) and high productivity to be achieved. A numerical example is also provided.

**Keywords:** centrifugal roller mill, angle of capture

### ЗАХВАЩАНЕ НА МАТЕРИАЛА ПРИ ЦЕНТРОБЕЖНИТЕ РОЛКОВИ МЕЛНИЦИ

**Стефан Пулев**

Минно-геоложки университет „Св. Иван Рилски“, 1700 София

**РЕЗЮМЕ.** Мелещите тела в центробежните ролкови мелници са цилиндрични ролки, които обтъркават вътрешната цилиндрична повърхнина на барабана. Попаднали между ролката и барабана, частиците руда се натрошават благодарение на големите центробежни сили. В този труд е получена зависимост между размерите на барабана, ролките и постъпващите за смилане частици, така че ъгълът на захващане да е оптимален. Така може да се постигне максимална степен на смилане и висока производителност. Приложен е и числен пример.

**Ключови думи:** не центробежна ролкова мелница, ъгъл на захващане

### Introduction

The working bodies of the considered machines are the cylindrical steel rollers, which rotate at a high angular speed, press the ore pieces to the cylindrical drum and break them (Pulev 2013, Sezonov 2011, Chalashkanov 1978, Cvetkov 1988). Grinding is due to the large centrifugal forces. The main technological parameter is the gripping angle  $\alpha$ , which directly affects the grinding intensity. When the angle is too small, the grinding rate is very low. At a large angle, the grinding rate increases, but the productivity decreases. The aim of this work is to determine the optimal gripping angle taking into account the dimensions of the drum, the rollers and the particles entering for grinding.

### Analysis

The determination scheme is shown in Figure 1. The mill drum is represented by a circle of diameter  $D$  and center  $O$ . The roller with diameter  $d$  and center  $O_1$  rolls without sliding on the inner cylindrical surface of the drum. The centrifugal force presses the roller tightly against the housing and eliminates the possibility of detachment or slipping. The ore piece has a regular shape with a diameter  $x$  and center  $O_2$ . The gripping angle is formed between the tangents to the ore piece at the points of contact with the drum and the roller.

These tangents are perpendicular to the lines  $OO_2$  and  $O_1O_2$ .

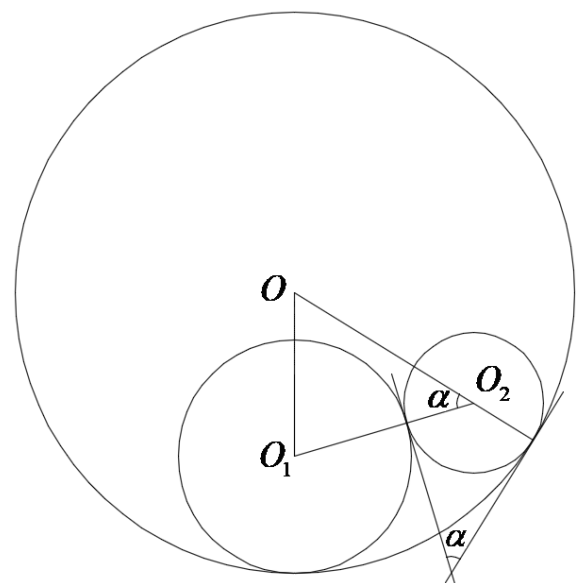


**Fig. 1. The determination scheme**

Therefore, the angle  $\angle O_1O_2O = \alpha$  can be determined by a triangle with sides

$$OO_1 = \frac{D-d}{2}$$

$$OO_2 = \frac{D-x}{2}$$

$$O_1O_2 = \frac{d+x}{2}$$

By the law of cosines in triangle  $O_1O_2O$

$$\cos\alpha = \frac{(D-x)^2 + (d+x)^2 - (D-d)^2}{2(D-x)(d+x)}. \quad (1)$$

With using trigonometric identity

$$\operatorname{tg} \frac{\alpha}{2} = \sqrt{\frac{1-\cos\alpha}{1+\cos\alpha}} \quad (2)$$

after transformation from (1) and (2) is obtained

$$\operatorname{tg} \frac{\alpha}{2} = \sqrt{\frac{-x^2 + (D-d)x}{Dd}}. \quad (3)$$

The condition for tighting the ore particle is

$$\alpha \leq 2\rho, \quad (4)$$

where  $\rho$  is the angle of friction, and  $\mu = \operatorname{tg}\rho$  is the coefficient of friction between the ore particle and the steel drum and roller. Condition (4) is equivalent to

$$\operatorname{tg} \frac{\alpha}{2} \leq \operatorname{tg}\rho = \mu \quad (5).$$

From (3) and (5) the inequality is obtained

$$\frac{-x^2 + (D-d)x}{Dd} \leq \mu^2$$

or

$$x^2 - (D-d)x + \mu^2 Dd \geq 0. \quad (6)$$

The roots of the quadratic equation corresponding to inequality (6) are

$$x_{1,2} = \frac{D-d \pm \sqrt{(D-d)^2 - 4\mu^2 Dd}}{2},$$

which after transformation acquire the species

$$x_{1,2} = \frac{(D-d) \left( 1 \pm \sqrt{1 - \frac{4\mu^2 Dd}{(D-d)^2}} \right)}{2}. \quad (7)$$

It is known that a function  $f(t) = \sqrt{1-t}$  can be described by a Taylor series and at small values of the argument  $|t| < 0,089$  can be represented as

$$\sqrt{1-t} \approx 1 - \frac{1}{2}t. \quad (8)$$

Taking into account (8), formula (7) is transformed into

$$x_{1,2} = \frac{(D-d) \left( 1 \pm \left( 1 - \frac{2\mu^2 Dd}{(D-d)^2} \right) \right)}{2}.$$

Thus for the roots of the quadratic equation is obtained

$$\begin{aligned} x_1 &= \frac{\mu^2 Dd}{D-d}, \\ x_2 &= \frac{(D-d)^2 - \mu^2 Dd}{D-d}. \end{aligned} \quad (9)$$

The solution of inequality (6) is

$$x \in (-\infty, x_1] \cup [x_2, +\infty) \quad (10)$$

The condition that the ore particle is smaller than the roll, ie.

$$x \in (0, d). \quad (11)$$

From (10) and (11) the final solution of inequality (6) is obtained

$$x \in (0, x_1]. \quad (12)$$

Therefore, optimal grip is obtained when the maximum size of the particles entering the grinding is determined by the formula

$$x_{\max} = \frac{\mu^2 Dd}{D-d}. \quad (13)$$

Therefore, the size of the ore particles depends on three circumstances

- the diameter of the drum, which cannot be substantially changed with a centrifugal roller mill operating;
- the coefficient of sliding friction, which depends on the material of the drum, rollers and ore particles;
- the diameter of the rollers.

The only way to ensure an optimal angle of capture is to select the dimensions of the rollers depending on the size of the ore particles. The diameter of the rollers can be determined by the formula

$$d = \frac{x_{\max} D}{x_{\max} + \mu^2 D},$$

obtained after transformation of (13).

## Numerical experiment and discussion

An example is a centrifugal roller mill with diameters of drum  $D = 1,2 \text{ m}$  and roller  $d = 0,2 \text{ m}$ . The coefficient of friction between the pieces of ore and steel is  $\mu = 0,3$ . For the discriminant of (6) is obtained  $(D-d)^2 - 4\mu^2 Dd = 0,9136 > 0$ . The roots of (6) have the following values:  $x_1 = 0,022$ ,  $x_2 = 0,978$ . The inequality  $x_1 < d < x_2$  is satisfied, which proves that the interval (12) is defined correctly. Applying the derived formula (13) to the diameter of the particles fed for grinding is obtained  $x_{\max} = 0,022 \text{ m} = 22 \text{ mm}$ .

Figure 2 shows the dependence of  $x$  on  $d$  with a drum diameter  $D = 1,2 \text{ m}$ . It is obtained according to (13) and can be used by technologists in the operation of centrifugal roller mills. With the aid of Fig. 2, the diameter of the rollers can be selected according to the size of the ground particles so that the gripping angle is optimal.

The productivity of centrifugal roller mills and the degree of grinding directly depends on the correct determination of the diameter of the rollers according to the size of the ore particles. Therefore, the dependence obtained in this study (13) may be useful in mineral processing.

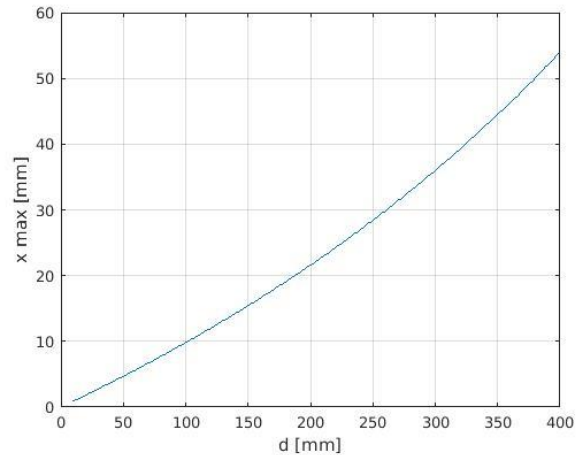


Fig. 2. Influence of the size of the ore particles on rollers diameter

## References

- Pulev, S., S. Sezonov. 2013. Opređelyane na centrobejnite sili pri edin ekstremen rejim na rabota na centrobejno rolkovite melnici. - Annual of the University of Mining and Geology "St. Ivan Rilski", 56, Part 2, 151-154 (in Bulgarian with English abstract).
- Sezonov S., M. Vulkov. 2011. Vuzmojnosti za usuvurshenstvane na centrobejno rolkovi melnici. Mashinostroene i mashinoznanie, 15, 25-28 (in Bulgarian)
- Chalashkanov, M. 1978. Izsledvane na funkcionalnata vruzka meĵdu osnovnite konstruktivno-tehnologichni parametric na centrobejno rolkova melnica pri smilane na polezni izkopaemi. Disertacia (in Bulgarian)
- Cvetkov, H., 1988. Obogatitelni mashini. Tehnika, Sofia, 413 p. (in Bulgarian)

## STORAGE OF THE GOODS UNDER THE OPERATION OF THE MINING DUMPER TRUCK

**Stefan Pulev**

University of Mining and Geology "St. Ivan Rilski", 1700 Sofia; [st\\_pulev@yahoo.com](mailto:st_pulev@yahoo.com)

**ABSTRACT.** Storage of the goods means the non-scattering of the transported bulk load outside the body of the mining dump truck during its operation. When overcoming unevenness and various obstacles along technological roads, inertia forces arise, which can cause some different size particles of load to bounce off and out of the body. This reduces productivity and creates conditions for production accidents. In this work, a dynamic model of a mining dumper truck is investigated, taking into account the arising vibrations due to road roughness. The formula for determining the maximum safe operating speed, adapted to the road conditions, has been analytically derived. A numerical experiment was also conducted.

**Keywords:** mining dump truck, storage of the goods

### СЪХРАНЯЕМОСТ НА ТОВАРА ПРИ ЕКСПЛОАТАЦИЯТА НА РУДНИЧЕН САМОСВАЛ

**Стефан Пулев**

Минно-геоложки университет „Св. Иван Рилски“, 1700 София

**РЕЗЮМЕ.** Под съхраняемост се разбира неразпиляването на транспортирания насипен товар извън каросерията на рудничния самосвал в процеса на неговата експлоатация. При преодоляването на неравности и различни препятствия по технологичните пътища възникват инерционни сили, които могат да предизвикат отскачане и излизане извън каросерията на частици от товара с различна големина. Това намалява производителността и създава условия за трудови злополуки и производствени аварии. В настоящия труд се изследва динамичен модел на рудничен самосвал с отчитане на възникващите трептения вследствие от пътните неравности. Аналитично е изведена формула за определяне на максималната безопасна експлоатационна скорост, съобразена с пътните условия. Проведен е и числен експеримент.

**Ключови думи:** рудничен самосвал, съхраняемост на товара.

### Introduction

An important requirement when transporting ore is to preserve the integrity of the cargo. The technological roads on which the mining dump truck travels are full of large single and also periodically recurring unevenness. In order to achieve high productivity, it is often allowed to overload the mining dump truck and move at high speed. Intense vibrations and large inertial forces occur, which also affect the transported load. Overcoming unevenness at high operating speeds causes pieces of ore to bounce and scatter outside the body. This endangers other vehicles and people nearby and degrades the quality of the technological road. Especially important is the role of the driver in choosing a safe operating speed, tailored to the characteristics of the road. The purpose of this work is to determine the maximum safe operating speed allowing storage of the transported bulk cargo.

### Dynamic model

Due to the large size of the mining dump truck, it can be assumed that the oscillations of the front and rear suspension are independent. Much of the load (about 70%) rests on the

rear axle and there is a risk of falling pieces of the body. The dynamic model for studying the oscillations of the rear suspension is presented in fig. 1. The following denotations are made:

$M$  – mass of the mine dump truck together with the load carried by the rear suspension;

$m$  - mass of one piece of the transported load, endangered by falling;

$y$  - vertical movement of the vibrating mass;

$c$  - reduced coefficient of elasticity of the rear suspension.

The cross-section of a horizontal path is considered as a sine wave with amplitude  $a$  and period  $l$ , which represent respectively the height and length of the predominant irregularities in a given road section. If the dump truck is moving at a constant speed on a straight horizontal section, the distance traveled by it will be  $s = v.t$ . The kinematic disturbance on the wheels is represented by the periodic

function  $q = a \cdot \sin \frac{2\pi vt}{l}$  (Pulev 2012).

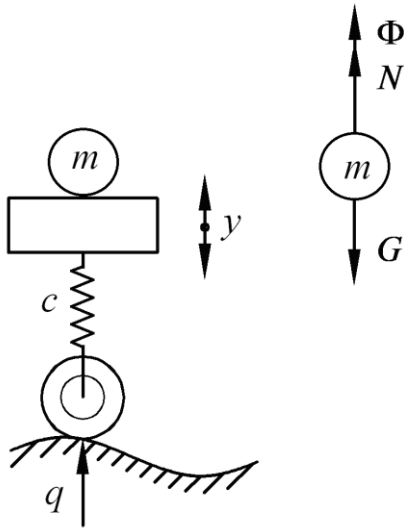


Fig. 1. Dynamic model

The differential equation describing the vertical vibrations of the dump truck is

$$m\ddot{y} + c(y - q) = 0.$$

After transformation it acquires the form

$$\ddot{y} + k^2 y = k^2 a \sin \frac{2\pi vt}{l}, \tag{1}$$

where  $k = \sqrt{\frac{c}{M}}$  is the circular frequency of the free

vibrations. This is an inhomogeneous second-order differential equation with constant coefficients. Due to the rapid attenuation of the free ones, the purely forced oscillations of the mining dumper truck are of interest. That is why we are looking for a private solution in the form:

$$y = C \sin \frac{2\pi vt}{l}. \tag{2}$$

After substituting (2) in (1) for the integration constant is obtained

$$C = \frac{k^2 a}{k^2 - \left(\frac{2\pi v}{l}\right)^2}.$$

Therefore, the law of motion is

$$y = \frac{k^2 a}{k^2 - \left(\frac{2\pi v}{l}\right)^2} \sin \frac{2\pi vt}{l}$$

and the acceleration of the oscillating mass has the form

$$\ddot{y} = -\frac{\left(\frac{2\pi v}{l}\right)^2 k^2 a}{k^2 - \left(\frac{2\pi v}{l}\right)^2} \sin \frac{2\pi vt}{l}.$$

Figure 1 presents the acting forces on a piece with a mass  $m$  of the transported load. These are the normal reaction  $N$  of the support, the inertial force  $\Phi$  and gravity  $G = mg$ . The inertial force is variable

$$\Phi = m\ddot{y} = -\frac{m\left(\frac{2\pi v}{l}\right)^2 k^2 a}{k^2 - \left(\frac{2\pi v}{l}\right)^2} \sin \frac{2\pi vt}{l}$$

and has an amplitude

$$\Phi_{\max} = \frac{m\left(\frac{2\pi v}{l}\right)^2 k^2 a}{k^2 - \left(\frac{2\pi v}{l}\right)^2}; \tag{3}$$

The friction forces between the particles of the transported bulk load are not taken into account because the pieces threatened by scattering have little contact with the others. In order for the particle in question to be in equilibrium, the following equation must be satisfied

$$N = G - \Phi.$$

In this work, it is considered that in order not to bounce out of the body, the particle in question should not lose contact with the support. This means

$$N \geq 0$$

or

$$\Phi_{\max} \leq G. \tag{4}$$

Taking into account (3), inequality (4) acquires the following form

$$\frac{\left(\frac{2\pi v}{l}\right)^2 k^2 a}{k^2 - \left(\frac{2\pi v}{l}\right)^2} \leq g. \tag{5}$$

The frequency of free vibrations is many times higher than the frequency of the disturbance, which means that the denominator of (5) can only accept positive values. This fact is also confirmed by the applied numerical experiment and is of

great importance in the analytical solution of the inequality (5). In view of the purpose of the study, it is important to decide (5) the operating speed of the mining dumper truck. Thus the following condition for storage of the transported cargo is obtained:

$$v \leq v_{\max} = \frac{l}{2\pi} \sqrt{\frac{g \cdot c}{a \cdot c + M \cdot g}} \quad (6)$$

This means that the operating speed must not exceed the maximum value  $v_{\max}$ , which depends to the greatest extent on the length and height of the irregularities and on the mass of the dump truck together with the load carried.

### Numerical experiment and discussion

The object of the experiment is a mine dump truck BELAZ-7555B with a mass without load 40250 kg, maximum load capacity 55000 kg and a total mass of 95250 kg, 67% of which rests on the rear axle. The values of the parameters are:

- $M = 63818$  kg,
- $c = 2.7 \cdot 10^6$  N / m,
- $a = 0.05$  m and
- $l = 10$  m.

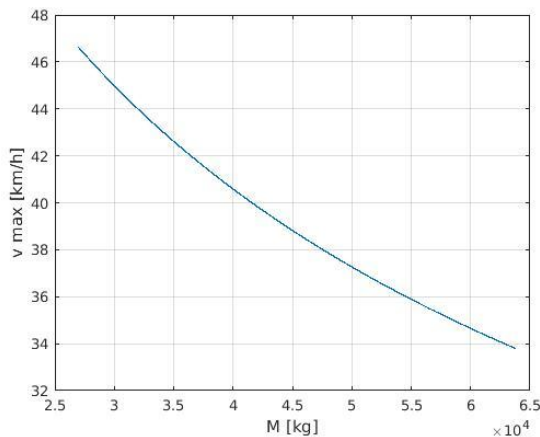


Fig. 2. Influence the mass on the speed

For the frequency of free vibrations we get

$$k = 6,5 \text{ s}^{-1},$$

and the maximum operating speed according to (6) is

$$v_{\max} = 9,4 \text{ m/s} = 33,8 \text{ km/h}.$$

The frequency of the disturbance is  $\frac{2\pi v}{l} = 5,9 \text{ s}^{-1}$ ,

which confirms the assumption of a positive denominator in inequality (5).

Formula (6) makes it possible to assess the influence of individual factors on the operating speed of the mining dump truck. Figures 2 and 3 show that the operating speed is low with large bumps and heavy load. Figure 2 shows that the larger the lengths of the irregularities, the higher the velocity.

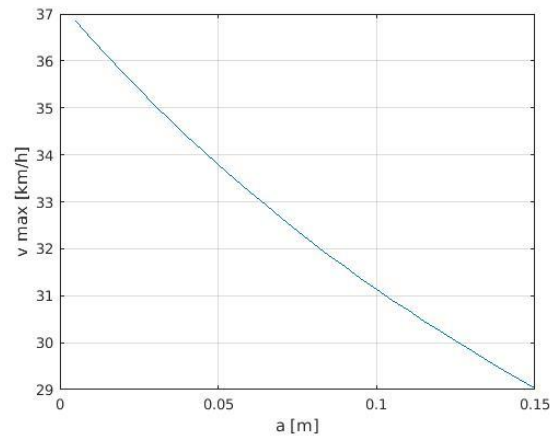


Fig. 3. Influence of irregularities height on the speed

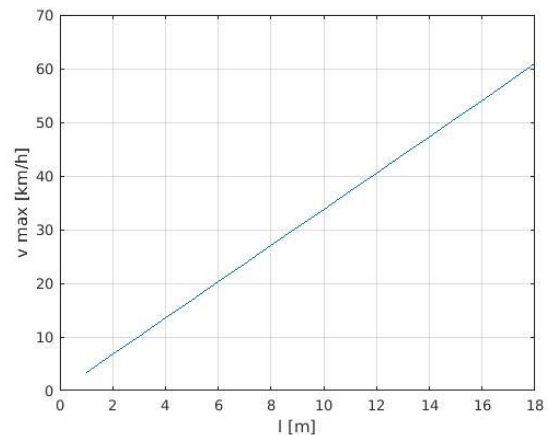


Fig. 4. Influence of irregularities length on the speed

Properly selected operating speed, ensuring that the load is not scattered outside the body, is an extremely important condition for high productivity and prevention of accidents at work. The obtained formula (6) makes it possible to calculate the maximum permissible safe speed, ensuring the storage of the transported bulk cargo, taking into account the heights and lengths of the irregularities characteristic for a given section of the road. The role of the driver of the mine dump truck is also very important in providing an appropriate speed, in accordance with the specific dimensions of the road irregularities and the weight of the transported cargo.

### References

Pulev S. N. 2012. Treptenia na rudnichen samosval. IK na MGU „Sv. Ivan Rilski”, Sofia, 116 p. (in Bulgarian)

## DETERMINATION OF KINEMATIC CHARACTERISTICS OF THE COMPLEX MOTION OF A PARTICLE BY MATHCAD

Asen Stoyanov<sup>1</sup>, Juliana Javorova<sup>2</sup>

<sup>1</sup> University of Mining and Geology "St. Ivan Rilski", 1700 Sofia; asen.stoyanov@mgu.bg

<sup>2</sup> University of Chemical Technology and Metallurgy, 1756 Sofia

**ABSTRACT:** The current problem considers the complex motion of a point M on the surface of a circular disk such as the latter performs a plane motion. The disc rolls without sliding on a horizontal straight line. The problem is solved graphically for a given time interval. The part of the trajectory of the point M is shown. The values of the transfer, relative and absolute velocities are graphically shown. The same is done for the transfer, relative, Coriolis and absolute accelerations, as well as for their components. The above mentioned kinematic characteristics are determined for the same time interval. The problem is solved using the MathCAD application. In this way the complexity of the graphical solution by hand is overcome.

**Keywords:** material particle, motion, velocity, acceleration, MathCAD

## ОПРЕДЕЛЯНЕ НА КИНЕМАТИЧНИТЕ ХАРАКТЕРИСТИКИ НА СЛОЖНОТО ДВИЖЕНИЕ НА ТОЧКА С MATHCAD Асен Стоянов<sup>1</sup>, Юлияна Яворова<sup>2</sup>

<sup>1</sup> Минно-геоложки университет „Св. Иван Рилски“, 1700 София

<sup>2</sup> Химикотехнологичен и металургичен университет, 1756 София

**РЕЗЮМЕ:** Задачата разглежда сложното движение на точка М върху повърхността на кръгъл диск, като последният извършва равнинно движение. Дискът се търкаля без плъзгане по хоризонтална права линия. Задачата се решава графично за даден интервал от време. Показана е частта от траекторията на точка М. Стойностите на преносната, относителната и абсолютната скорости са представени графично. Същото се прави за преносното, относителното, кориолисовото и абсолютното ускорения, както и за техните компоненти. По-горе споменатите кинематични характеристики се определят за същия времеви интервал. Задачата се решава с помощта на приложението MathCAD. По този начин се преодолява сложността на графичното решение на ръка.

**Ключови думи:** материална точка, движение, скорост, ускорение, MathCAD

### Introduction

It is well known that there are difficulties in the 'manual' determination of the 3D-temporal characteristics of a material particle performing complex motion for a certain time interval. They arise from the graphical nature of the solution itself, as well as from possible errors caused by the complexity of the resulting expressions due to the twofold differentiation. Similar results are published by different authors (Doev and Doronin, 2016; Bertyaev, 2005; Velichenko, 1988; Gurskiy, 2003; Horn and Johnson, 2012, Lucko and Kavalchuk, 2018; etc.). In the means of the above mentioned the present study improves and complements the solution of this problem.

### Formulation of the problem

The material particle  $M(x_{2M}(t), y_{2M}(t), z_{2M}(t))$  moves on the surface of a round disk "T" with a radius  $R = 25 \text{ cm}$  according to the law:

$$\begin{cases} x_{2M}(t) = \rho[\theta(t)] \cdot \cos[\theta(t)]; \\ y_{2M}(t) = \rho[\theta(t)] \cdot \sin[\theta(t)]; \\ z_{2M} = 0; \end{cases}$$

where  $\rho[\theta(t)] = 7 + 1,7 \cdot \sin(2,5 \cdot \theta(t))^2, \text{ cm}$ ;

$$\theta(t) = [\pi \cdot (1 + \cos(\pi \cdot t))], \text{ rad}.$$

The disk lies in the plane  $Ox_0y_0$  and rolls on a horizontal line without slipping (Fig. 1). The position of the disk center - point  $C(x_{0C}, y_{0C}, z_{0C})$  is determined according to the law:

$$\begin{cases} x_{0C} = s(t) = R \cdot \lambda, \text{ cm}; \\ y_{0C} = 0; \\ z_{0C} = 0; \end{cases}$$

where  $\lambda = 0,5 \cdot t^2 + t, \text{ rad}$ .

In the plane of the disc lie the following four reference (coordinate) systems -  $Ox_0y_0z_0$ ,  $Cxy$ ,  $Cx_1y_1$ ,  $Ax_2y_2$ :

1) The first of them  $Ox_0y_0z_0$  is global - conditionally motionless;

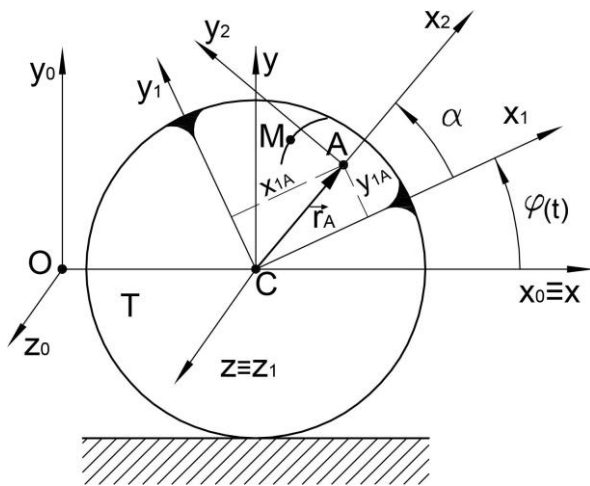


Fig. 1. Calculation scheme

2) The second  $Cxyz$  is local and it is connected to the disk in a point  $C$ . It moves translationally. Its coordinate axes are parallel to the axes  $Ox_0, y_0, z_0$ ;

3) The third coordinate system  $Cx_1y_1z_1$  is local and it is rigidly connected to the disk. It rotates around the axis  $Cz_1$  according to the law  $\varphi(t) = \frac{s(t)}{R}$ , rad. The angle  $\varphi(t)$  is accounted from an axis  $Cx$ ;

4) The fourth reference system  $Ax_2y_2z_2$  is local with an arbitrary point  $A$  ( $x_A = 8\text{ cm}, y_A = 4\text{ cm}, z_A = 0$ ). It is rotated

around the axis  $Az_2$  at an angle  $\alpha = \frac{\pi}{5}$ , rad counted by an axis  $Cx_1$  in counterclockwise direction.

In the global coordinate system it is necessary to determine the kinematical characteristics of the point  $M$ :

A) For the moment  $t_1 = 2\text{ s}$ :

- The transfer, relative and absolute point velocity;
- The transfer, relative, Coriolis and absolute point acceleration.

B) The trajectory of the point for the time interval  $[0, 6\text{ s}]$ ;

C) For the same time interval, in a graphical form - the components and modules of:

- The transfer, relative and absolute velocity of the point;
- The transfer, relative, Coriolis and absolute acceleration of the point.

### Solution of the problem by MathCAD package

The calculation and graphical visualization are performed by using the MathCAD package.

The angle  $\alpha$  is accounted in a positive direction, i.e. in counterclockwise direction.

At the rolling of the disc the angle  $\varphi(t)$  changes in the negative direction.

The analytical expressions for all velocities and accelerations are too long and they are not shown in Fig. 2.a. and Fig. 2.b.

All unknown quantities as well as their modules are determined for the time moment  $t_1 = 2\text{ s}$ .

$$\begin{aligned}
 R &:= 25 \quad \lambda(t) := .5 \cdot t^2 + t \quad s(t) := R \cdot \lambda(t) \quad x_{OC}(t) := s(t) \quad y_{OC}(t) := 0 \\
 \varphi(t) &:= \frac{-s(t)}{R} \quad \alpha := \frac{\pi}{5} \quad t_1 := 2 \quad t_2 := 6 \quad x_{1A} := 8 \quad y_{1A} := 4 \quad r_{OC}(t) := \begin{pmatrix} s(t) \\ 0 \end{pmatrix} \\
 r_{1A} &:= (x_{1A} \quad y_{1A})^T \quad \theta(t) := \pi \cdot (1 + \cos(\pi \cdot t)) \quad \rho(t) := 7 + 1.7 \cdot \sin(2.5 \cdot \theta(t))^2 \\
 x_{2M}(t) &:= \rho(t) \cdot \cos(\theta(t)) \quad y_{2M}(t) := \rho(t) \cdot \sin(\theta(t)) \quad r_{2M}(t) := (x_{2M}(t) \quad y_{2M}(t))^T \\
 Sz_1(\alpha) &:= \begin{pmatrix} \cos(\alpha) & \sin(\alpha) \\ -\sin(\alpha) & \cos(\alpha) \end{pmatrix} \quad r_{1M}(t) := r_{1A} + Sz_1(\alpha)^T \cdot r_{2M}(t) \quad r_{1Mx}(t) := r_{1M}(t)_0 \\
 r_{1My}(t) &:= r_{1M}(t)_1 \quad r_{1M}(t) := (r_{1Mx}(t) \quad r_{1My}(t))^T \quad Sz_\varphi(t) := \begin{pmatrix} \cos(\varphi(t)) & \sin(\varphi(t)) \\ -\sin(\varphi(t)) & \cos(\varphi(t)) \end{pmatrix} \\
 r_{OM}(t) &:= r_{OC}(t) + Sz_\varphi(t)^T \cdot r_{1M}(t) \quad x_{OM}(t) := r_{OM}(t)_0 \quad y_{OM}(t) := r_{OM}(t)_1 \\
 r_{OM}(t) &:= (x_{OM}(t) \quad y_{OM}(t))^T \quad v_{1M}(t) := \frac{d}{dt} r_{1M}(t) \quad v_{OC}(t) := \frac{d}{dt} r_{OC}(t) \\
 \omega_e(t) &:= \frac{d}{dt} (-\varphi(t)) \quad v_{OM}(t) := \frac{d}{dt} r_{OM}(t) \quad v_{1Mx}(t) := v_{1M}(t)_0 \quad v_{1My}(t) := v_{1M}(t)_1 \\
 v_{1M}(t) &:= (v_{1Mx}(t) \quad v_{1My}(t))^T \quad K := \begin{pmatrix} 0 & -1 \\ 1 & 0 \end{pmatrix} \quad v_{OMex}(t) := v_{OMe}(t)_0 \quad v_{OMey}(t) := v_{OMe}(t)_1 \\
 v_{OMe}(t) &:= v_{OC}(t) + \omega_e(t) \cdot K \cdot Sz_\varphi(t)^T \cdot r_{1M}(t) \quad v_{OMe}(t) := (v_{OMex}(t) \quad v_{OMey}(t))^T \\
 v_{OMr}(t) &:= Sz_\varphi(t)^T \cdot v_{1M}(t) \quad v_{OMrx}(t) := v_{OMr}(t)_0 \quad v_{OMry}(t) := v_{OMr}(t)_1 \\
 v_{OMr}(t) &:= (v_{OMrx}(t) \quad v_{OMry}(t))^T \quad v_{OMe}(t) := v_{OC}(t) + \frac{d}{dt} Sz_\varphi(t) \cdot r_{1M}(t) + Sz_\varphi(t)^T \cdot v_{1M}(t) \\
 v_{OM}(t) &:= v_{OMe}(t) + v_{OMr}(t) \quad v_{OMx}(t) := v_{OM}(t)_0 \quad v_{OMy}(t) := v_{OM}(t)_1
 \end{aligned}$$

Fig. 2.a. Analytical expressions for determining the kinematics characteristics of point  $M$

$$\begin{aligned}
 r2M(t1) &= \begin{pmatrix} 7 \\ -1.714 \times 10^{-15} \end{pmatrix} \quad |r2M(t1)| = 7 \quad rOM(t1) = \begin{pmatrix} 84.928 \\ 5.036 \end{pmatrix} \quad |rOM(t1)| = 85.077 \\
 r1M(t1) &= \begin{pmatrix} 13.663 \\ 8.114 \end{pmatrix} \quad |r1M(t1)| = 15.891 \quad \varphi(t1) = -4 \quad \omega e(t1) = 3 \quad vOMe(t1) = \begin{pmatrix} 59.891 \\ -45.216 \end{pmatrix} \\
 |vOMe(t1)| &= 75.043 \quad vOMr(t1) = \begin{pmatrix} -3.859 \times 10^{-15} \\ -1.648 \times 10^{-14} \end{pmatrix} \quad |vOMr(t1)| = 1.692 \times 10^{-14} \\
 vOM(t1) &= \begin{pmatrix} 59.891 \\ -45.216 \end{pmatrix} \quad |vOM(t1)| = 75.043 \\
 \varepsilon(t) &:= \frac{d}{dt} \omega e(t) \quad aOC(t) := \frac{d}{dt} vOC(t) \quad aOMe(t) := aOC(t) + [\varepsilon(t) \cdot K + (\omega e(t) \cdot K)^2] \cdot rOM(t) \\
 aOMex(t) &:= aOMe(t)_0 \quad aOMey(t) := aOMe(t)_1 \quad aOMe(t) := (aOMex(t) \quad aOMey(t))^T \\
 a1M(t) &:= \frac{d}{dt} v1M(t) \quad aOMr(t) := Sz\varphi(t)^T \cdot a1M(t) \quad aOMrx(t) := aOMr(t)_0 \quad aOMry(t) := aOMr(t)_1 \\
 aOMr(t) &:= (aOMr(t)_0 \quad aOMr(t)_1)^T \quad aOMC(t) := 2 \cdot \omega e(t) \cdot K \cdot Sz\varphi(t)^T \cdot v1M(t) \quad aOMCx(t) := aOMC(t)_0 \\
 aOMCy(t) &:= aOMC(t)_1 \quad aOMC(t) := (aOMCx(t) \quad aOMCy(t))^T \quad aOM(t) := aOMe(t) + aOMr(t) + aOMC(t) \\
 aOMx(t) &:= aOM(t)_0 \quad aOMy(t) := aOM(t)_1 \quad aOM(t) := (aOMx(t) \quad aOMy(t))^T \\
 \varepsilon(t1) &= 1 \quad aOMe(t1) = \begin{pmatrix} -744.389 \\ 39.601 \end{pmatrix} \quad aOMr(t1) = \begin{pmatrix} 49.5 \\ 211.324 \end{pmatrix} \quad aOMC(t1) = \begin{pmatrix} 9.885 \times 10^{-14} \\ -2.315 \times 10^{-14} \end{pmatrix} \quad aOM(t1) = \begin{pmatrix} -694.889 \\ 250.925 \end{pmatrix} \\
 |aOMe(t1)| &= 745.442 \quad |aOMr(t1)| = 217.044 \quad |aOMC(t1)| = 1.015 \times 10^{-13} \quad |aOM(t1)| = 738.806
 \end{aligned}$$

Fig. 2.b. Certain values for the positions and velocities of point *M* as well as analytical expressions for its accelerations and their values for the moment  $t_1 = 2\text{ s}$

The position of a particle *M* for the moment  $t_1 = 2\text{ s}$  in the space of the local coordinate system  $Ax_2y_2z_2$  is shown in Fig. 3.a. The trajectory of the point for its relative motion is also described.

The same figure shows also the position of the point *M* for the moment  $t_1 = 2\text{ s}$  on the trajectory described by it in the space of the global coordinate system  $Ox_0y_0z_0$ .

The dependences between the projections of velocities and accelerations on the global axes and time are graphically presented on Fig. 3.a., 3.b. and 3.c. In addition, on the same figures are shown also the changes of their respective modules.

The presented graphic visualization refers only to the specified time period  $[0, 6\text{ s}]$ .

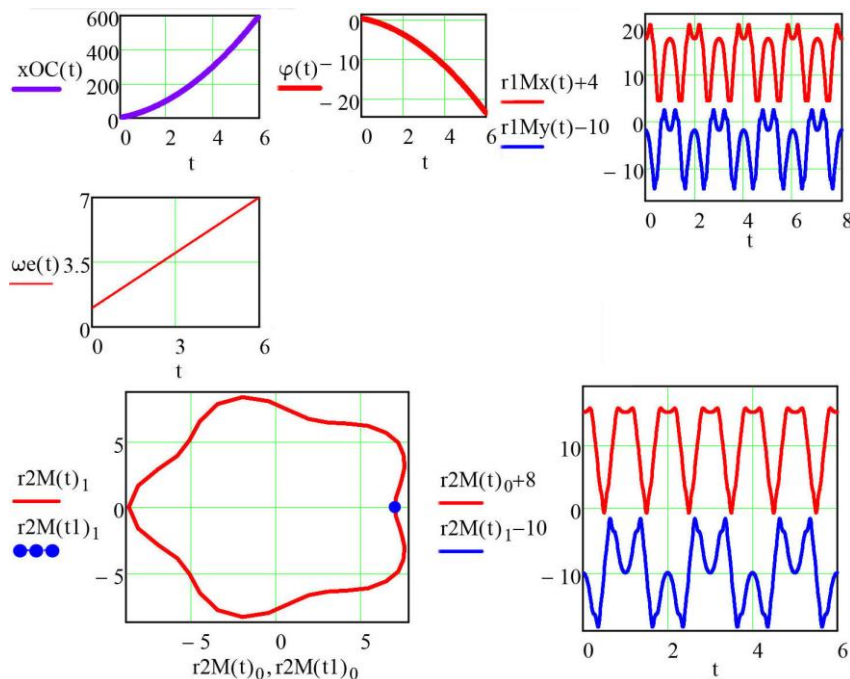


Fig. 3.a. Graphs expressing the dependence of the kinematics characteristics of the point *M* on time  $t(s)$

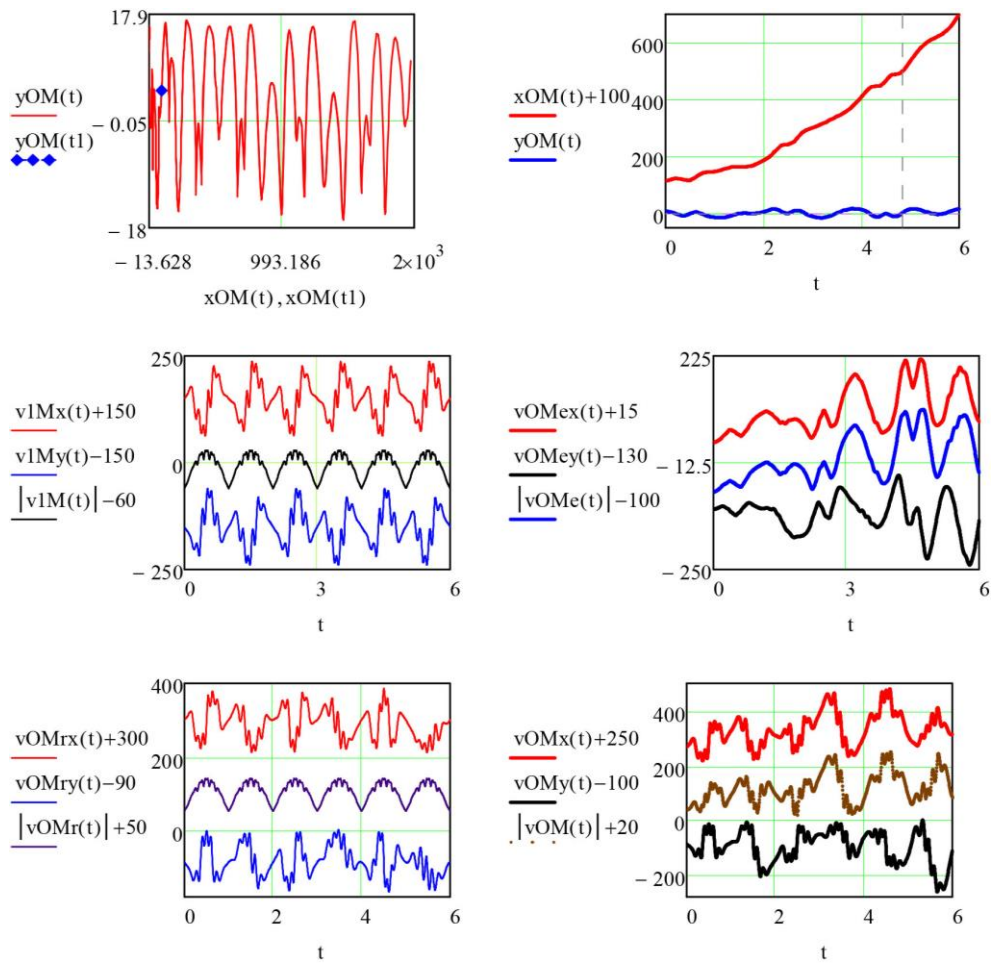


Fig. 3.b. Graphs expressing the dependence of the kinematics characteristics of the point  $M$  on time  $t$  (s)

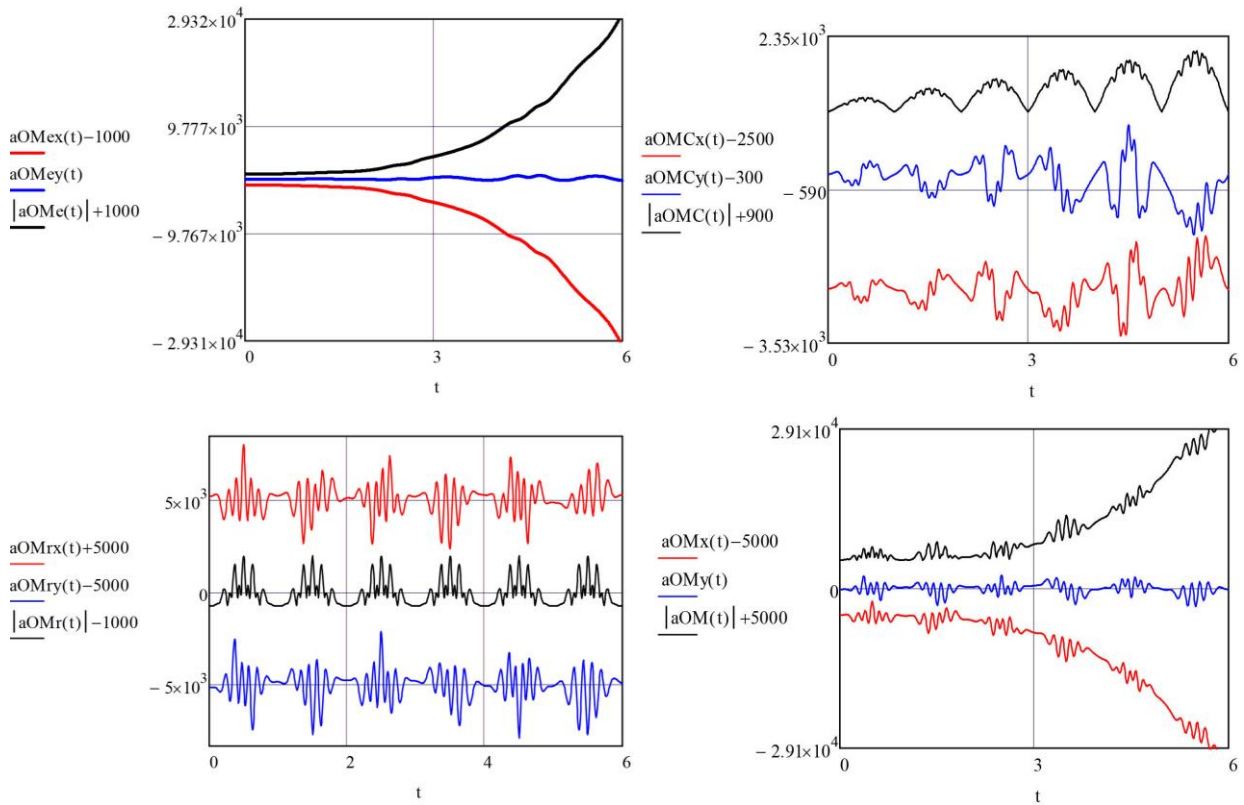


Fig. 3.c. Graphs expressing the dependence of the kinematics characteristics of the point  $M$  on time  $t$  (s)

## Conclusion

The conventional solution of the problem, solved in the current paper, is related to some difficulties.

These difficulties are easily overcome by using of the modern mathematical packages in dependences of the aim of the study. In the considered case, the program MathCAD package can be used to check the problem solved by the traditional way.

The automated solution and the graphical editor of MathCAD provide control and optimization on the obtained results.

Some adjustments in the initial data are possible in order to achieve certain values of specific kinematic quantities.

The contemporary teaching of all fields of mechanics at the universities is related to using the most advanced mathematical packages such as MatLab, MathCAD, Mathematica, MuPAD and others (Doev and Doronin, 2016; Bertyaev, 2005; Stoyanov, 2016; Ivanov, 2017; Stoyanov and Javorova, 2012; Pavlov et al., 2013; Lekova et al., 2013; Stoyanov, 2017; Pavlov and Evlogiev, 2015; Ivanov, 2018; Aleksandrov et al., 2012, Ivanov, 2019, Pavlov, 2018).

The presented study demonstrates a fast solution and excellent graphical visualization as can be seen for example from the last two figures of the paper. By this way the main advantages of the MathCAD package are confirmed.

## References

- Doev V.S., Doronin F.A., Collections of problems on theoretical mechanics based on MathCAD, Saint-Petersburg, M., Krasnodar, Lany, 2016, 585 p. (in Russian)
- Bertyaev V. Theoretical mechanics on the base of MathCAD practicum, Saint-Petersburg, BHV-Petersburg, 2005, 739 p. (in Russian)
- Velichenko V.V, Matrix-geometric methods in mechanics with applications to robot-engineering problems, Moscow, Nauka, 1988, 280 p. (in Russian)
- Gurskiy D.A., Calculations in MathCAD, Minsk, Novoe znanie, 2003, 814 p.
- Horn R., Johnson C., Matrix analysis, Cambridge University Press, NY, 2012.
- Lucko N., Kavalchuk O., Engineering calculations in MATHCAD, Belarusian National Technical University, Minsk, 2018. (in Russian)
- Stoyanov A., Matrix operations by MathCAD in theoretical mechanics – Statics, Kineziologij BG, Sofia, 2016, 165 p. (in Bulgarian)
- Ivanov A., Theoretical matrix study of rigid body general motion, Greener Journal of Physics and Natural Sciences, ISSN: 2384-6410, vol. 3 (2), October 2017, pp. 009-020.
- Stoyanov A., Javorova J., Determination of rod forces in a plane statically determinate truss, Annual of the University of Mining and Geology "St. Ivan Rilski", Sofia, 55, 2, 2012, 89–92. (in Bulgarian with English abstract).
- Pavlov P.D, Lilkova-Markova S., Nakov B., Kehajova J. A Geometric Oriented Approach in Drawing the Simulation Model of the Small Angular Vibrations of a Body, Miskolc Mathematical Notes, 2013, Volume 14, Issue: 2, p. 679-684.
- Lekova S., A. Aleksandrov, M. Milenova, T. Tzolov, Orthogonal dynamic model of viscoelastic deformation under variable concentration and loading. Journal of Theoretical and Applied Mechanics, Sofia, 2013, vol. 43, No. 3, pp. 51–58.
- Stoyanov A., Survey of the relationship between the efforts in the bars and geometrical parameter on three-dimensional truss, XVII International scientific conference VSU'2017, 8-9 June 2017, Sofia, Bulgaria.
- Pavlov P., Evlogiev D., Experimental determination of the elastic-viscous characteristics of elastic ropes, Procedia Engineering, 2015, Vol. 108, p. 488 – 495.
- Ivanov A.I., Theoretical matrix study of rigid body relative motion. International Journal of Advancement In Engineering Management and Applied Science (IJAETMAS), ISSN: 2349-3224, Volume 05, Issue 05, 2018, pp. 21-28.
- Aleksandrov A., Lekova S., Milenova M., Generalized Model of Viscoelastic Deformation. Int. J of Pure and Applied Mathematics, Vol.81, No 4, 2012, 635-646.
- Ivanov A.I., Theoretical Matrix Study of Rigid Body Absolute Motion, The International Journal of Engineering and Science (IJES), ISSN (e): 2319-1813, Volume 7, Issue 6, pp 01-08, 2019.
- Pavlov P., Nonlinear damped vibrations of planar discrete systems – numerical and experimental modeling, MATEC Web of Conferences 211, 02006 (2018), VETOMAC XIV, Lisbon, Portugal, 2018.

## TECHNICAL DIAGNOSTICS AND SERVICE OF GAS DISTRIBUTION NETWORKS

**Tony Slavkov<sup>1</sup>, Veselin Mitkov<sup>2</sup>**

<sup>1</sup> University of Mining and Geology "St. Ivan Rilski" 1700 Sofia; toni\_slavkov06@abv.bg

<sup>2</sup> University of Mining and Geology "St. Ivan Rilski" 1700 Sofia; veselin\_mitkov@abv.bg

**ABSTRACT.** The report examines and analyzes the main activities related to technical diagnostics and service of distribution networks. The main methods for detecting natural gas leaks from gas distribution networks are considered.

**Keywords:** gas pipelines, gas distribution networks, technical diagnostics

### ТЕХНИЧЕСКА ДИАГНОСТИКА И СЕРВИЗ НА ГАЗОРАЗПРЕДЕЛИТЕЛНИ МРЕЖИ

**Тони Славков, Веселин Митков**

Минно-геоложки университет „Св. Иван Рилски“, 1700 София

**РЕЗЮМЕ.** В доклада са разгледани и анализирани основните дейности свързани с техническа диагностика и сервиз на разпределителни мрежи. Разгледани са основните методи за откриване на утечки на природен газ от газоразпределителните мрежи.

**Ключови думи:** газопроводи, газоразпределителни мрежи, техническа диагностика

### Introduction

The operation of the gas distribution networks is a technical and technological complex of activities aimed at ensuring continuous, safe and trouble-free operation of the network, in order to supply consumers reliably with natural gas in compliance with the quality requirements according to the current regulations in the country, to protect environment and citizens' health, life and property (Nikolov, 2007).

Maintenance, diagnostics and service of the gas distribution networks is a combination of methodological and technical means for assessing the condition of the controlled parameters; accumulation of professional experience and storage of data about them; their systematization; processing and analysis of results; selection of organizational and technical measures aimed at the practical implementation of the most efficient and rational form of service.

Maintenance is control over the technical condition, cleaning, readjustment and other operations without disassembly regarding the maintenance of the functionality and serviceability of the equipment in automatic gas control stations, gas control points and switchboards and in gas control and measuring points and switchboards;

Disassembly audit is a set of operations with disassembly, cleaning, inspection and replacement of rapidly wearing parts of the equipment in the facilities, as well as establishing the need to repair units and parts and restore normal functional operating conditions for the next operational period.

Repair is a complex of operations with replacement of parts and assemblies, after the implementation of which the serviceability and trouble-free operation of the equipment is guaranteed during the next period of operation.

For proper functioning of the various pieces of equipment installed in gas control points and switchboards and in gas control and measuring points and switchboards, the operating staff systematically visit them with a frequency depending on the type of equipment (gas consumption, frequency of filter contamination, age, conditions and mode of operation). The periodicity of these inspections is determined by the annual plan for the activity of maintenance diagnostics and service of the gas distribution network.

If necessary, the periods for these inspections are shortened by conducting an emergency, unscheduled inspection, appointed and performed depending on local operating conditions or for specific gas control points and switchboards or gas control and measuring points and switchboards (Boyadzhiev, 2014). These inspections do not replace the periodic scheduled inspection.

### Maintenance of the gas distribution network

It is carried out in accordance with the specific operating conditions, gas pressure, duration of operation and condition of the gas distribution network, characteristics and corrosion activity of the soil, the presence of stray currents, the nature of the area and specific passages (through various obstacles), the organization and training of the service staff in the respective gas distribution company.

Inspecting the route of the gas pipelines is performed periodically as follows:

- the route of the newly built and put into operation gas pipelines - immediately on the day of their filling with gas and on the next day after the gasification;

- gas pipelines operated under normal conditions and in good technical condition are inspected on the following intervals:

- gas pipelines for pressure 0.4 MPa and higher on the territory of the settlement - not less than twice a month;
- the gas pipelines from GCS / AGCS to the settlement - not less than once a month;
- gas pipelines for pressure 0.1 (0.01) MPa - not less than once a month;
- gas pipelines located within a radius of 15 m from the place of construction works - daily, until the danger of damage is eliminated;

When inspecting the gas pipelines, the following is performed:

- inspection of the route and the linear crane units for gas leaks by external signs and instrumentation;
- checking the presence and condition of the benchmarks for marking the route;
- inspection of the area along the route of the gas pipeline in order to detect shrinkage, erosion;
- checking the presence and condition of the signs on the fence panels, cabinets, crane units, etc., the condition of the cabinet doors;
- inspection of the supports and obstacles on both sides of the above-ground sections of the gas pipelines;
- when crossing water obstacles - the erosion of the shores or the accumulation of materials;
- control of the activities over or near the gas pipelines by third parties without the written consent of the gas distribution company;
- inspection of the condition of the cast iron pots of the underground installed shut-off fittings made of polyethylene and cleaning of ice, snow, mud;
- checking the presence of clogging with mud, sand and other contaminants in the shafts of the underground cranes made of polyethylene, preventing the normal and trouble-free handling of the rotors and the leads to the shut-off fittings;
- immediate cleaning with appropriate shaft fittings if necessary;
- checking for gas contamination of the shaft in the siege pot with the help of a gas analyzer;
- checking the direction of the linear valve on the actuator cap, "open" and "closed", in relation to the direction of the axis of the gas pipeline (for ball valves, 1/4 revolution, type KHP);
- inspection (smoothly and carefully) of "closing" and "opening" of the shut-off valve once a year;
- The operating staff of the gas distribution company prepares numbered route maps (schemes) for inspecting the gas distribution network (GDN). The results of the performed inspections are recorded in the Operational Register of the GDN, and a report is prepared for the patrols (the detected faults and violations are entered) in the Register for the patrols - working document.

The checking of steel gas pipelines that are subject to scheduled repairs after technical inspection is carried out in accordance with the Instruction for control and diagnostics of the technical condition of the gas distribution network for natural gas leaks, as follows:

- in the built-up area of the settlement - not less than once a week;
- in the unbuilt area of the settlement - not less than twice a month.

- For the proper functioning of the equipment installed in the facilities, the operating staff of GDC systematically visits and monitors them with a frequency depending on the type of equipment and in accordance with the requirements of the Instruction for adjustment of gas control points and switchboards and Instruction for maintenance and repair.

- The results are entered in the Operational Register of the facility, and for the inspection of the facility an entry is made in the Operational Register of GDN.

- The control of the technological parameters of the gas in the GDN, equipped with remote control devices is carried out with the help of an automated SKADA system.

## **Maintenance of gas distribution network facilities**

### **Gas filters**

The contamination of the filter is checked with a differential manometer. If there is an indication of contamination, it is opened and cleaned or the filter element is replaced.

### **Stopcocks**

The entrance is checked (smooth opening and closing) and the closing tightness of the shut-off valves in the equipment, too.

### **Gas pressure regulators and pilots**

The setting of the regulators in the facility is carried out with a metrologically checked manometer and, if necessary, a readjustment is performed.

Periodic change of the main and reserve regulatory line.

The faults of the regulators causing an inadmissible increase or decrease of the working pressure above the limits of the pressure setting are eliminated immediately or the unit is replaced and the reasons for this are established.

The regulator, during operation, must not allow the outlet pressure to exceed the highest level of operating pressure (OP) according to BSS EN 12279 + A1: 2006.

The monitor must not allow the outlet pressure to exceed the temporary working pressure (TOP) according to BSS EN 12279 + A1: 2006.

### **Safety-discharge valves (SDV)**

With a checked manometer, the setting in the facility is checked and, if necessary, a readjustment is performed.

These valves, including those built into the pressure regulators, are set to operate when the pressure after the regulator /monitor/ exceeds the temporary operating pressure (TOP) according to BSS EN 12279 + A1: 2006.

### **Safety shut-off valves (SSV)**

With a checked manometer, the settings of the safety shut-off valves in the facility are checked and, if necessary, readjustments are made.

These valves are set to operate when the pressure after the regulator reaches the maximum accidental pressure (MAP) or falls by more than 30 percent of the maximum operating pressure (MOP) according to BSS EN 12279 + A1: 2006.

### **Manometers**

They are declared and submitted for inspection to the State Agency for Metrology and Technical Supervision (BIM).

### Flowmeters

They are declared and submitted for metrological inspection by an authorized laboratory. The frequency of inspections is determined by an order of the Chairman of the State Agency for Metrology and Technical Supervision (SAMTS).

### Diagnosis of the technical conditions of distributive gas pipelines for natural gas leaks

The devices for measuring the natural gas content and, accordingly, for detecting leaks and gas leaks must be in accordance with the current European norms and standards. The control of gas distribution networks (GDN) in relation to gas leaks can be performed by means of mobile devices for footinspection or to use specially equipped vehicles. These devices can be used in collective gas pipelines of gas fields and in collective oil pipelines through which gas-oil emulsion is transported (Boyadzhiev, 2008; Georgiev, 2014).

Depending on the specific cases, the devices for detection and localization of natural gas leak work on a different principle and are equipped with different types of sensors. In many respects it is appropriate to use combined devices capable of measuring the gas concentration in different ranges;

### Methods for search and localization of natural gas leak

#### Foot method

It is inspected by means of a mobile device equipped with a plain or bell-shaped probe, checking the air directly on the soil surface for the presence of gas. Care must be taken to place the probe tightly in order to maximally avoid influences, for example, from exhaust gases, wind, etc. Gas pipelines should be inspected as close as possible to the axis of their route, and if they are laid under a solid surface (asphalt, concrete, paving), the closest breaks or cracks should be checked. When using a plain probe, the test must be performed at a slow walking speed. The bell-shaped probe is placed along the route every 1-1.5 m, holding for sampling the soil air for about 5 seconds. The inspection of the building deviations is performed next to the wall of the house. Wet or frozen soil surfaces can become gas-tight. Therefore, routine control is not recommended in these circumstances. If unscheduled inspections cannot be avoided, the frozen cover should be ruptured and the soil air - checked.

The distribution of gas must be observed and taken into account, especially in the direction of buildings and cavities. All breakdown and leakage data are documented on drafts. The drafts are unambiguously marked with control numbers and documented. Note: the method of testing, the instruments used, the name of the inspector, the deep drillings and the number of breaches or leaks detected. The inspected sections, respectively routes are marked in the reports..

The equipment built in the road surface and sidewalks (shafts, canals, pots of underground cranes, etc.) is also checked for the presence of gas. When establishing the presence of gas, precautionary measures are taken

immediately and the companies operating the underground facilities are notified. Neighboring buildings should also be involved in the inspection and possible security work.

#### Acoustic method

This method is based on the detection of ultrasonic waves received from the movement of the gas in the pipeline. The waves are with a frequency of 40-45 kHz. In this method, the detection of leakage is based on the gas flow rate. The method is characterized by high sensitivity  $1 \times 10^{-2} \text{ cm}^2 / \text{sec}$  (Nikolov 2007). Main disadvantage of the method is disturbances in the research equipment as a result of background noise.

### Conclusion

The correct functioning of the various equipment installed in gas control points and switchboards and in gas control and measuring points and switchboards it is obligatory for the staff to inspect them regularly depending on the type of facilities (consumption of gas, frequency of filter contamination, age, conditions and mode of operation).

Devices for measuring the natural gas content and, accordingly, for detecting leaks and gas leaks from gas pipelines must be in accordance with the current European norms and standards. The control of the gas distribution networks (GDN) with regard to gas leaks is carried out on a large scale by means of mobile devices for inspection by foot method or by the use of specially equipped vehicles.

### References

- Boyadzhiev. M., L. Georgiev *Management of the gas infrastructure*. - Sofia: UMG, 2014 – p.100. (in Bulgarian)
- Boyadzhiev M., L. Georgiev, B. Dzhorov, G. Uzunov. *Possibilities for usage of gas from small gas fields and accumulations through new technologies and technical means. XIV Scientific and Technical Conference with International Participation "Transport, ecology - sustainable development", ECOVARNA 2008, p. 231-237. ISBN -954-20-00030 (in Bulgarian).*
- Georgiev L., R. Kulev, *Modes of multiphase movement of gas and oil emulsion in collective oil pipelines.*, *Collection of reports from the XII National Youth Scientific and Practical Conference, April 14-15, 2014, Sofia, Federation of NTS in Bulgaria, p. 85 -88. ISSN 1314-8931 (in Bulgarian).*
- Boyadzhiev M., L. Georgiev. *Model for determining the relation between environmental temperature and natural gas used in households in the Republic of Bulgaria. Yearbook of the University of Mining and Geology "St. Ivan Rilski", Volume 58, p. 1, Geology and Geophysics, 2015, p. 232-235. ISSN 1312-1820 (in Bulgarian with English abstract).*
- Nikolov G.K *"Distribution and usage of natural gas"*, Sofia, 2007, p.510. (in Bulgarian)
- Ordinance for the construction and safe operation of the portable and distributive gas pipelines and of the facilities, installations and appliances for natural gas.

## RESEARCH OF GROWTH AND DEVELOPMENT OF PLANTS UNDER ARTIFICIAL LIGHT

**Svetlana Velinova**

University of Mining and Geology "St. Ivan Rilski", Sofia 1700, Research Laboratory "Lighting Technology"; svetliv@mail.bg, <http://light-bg.eu/>

**ABSTRACT.** Growing plants with artificial light recently becomes quite relevant. Two specialized lighting systems were created in the Research Laboratory "Lighting Technology" at the University of Mining and Geology "St. Ivan Rilski" in order to study which part of the spectrum of visible light has the strongest influence on the growth and development of plants. The first one was set up in 2015 and the second one - in 2019. Cabins dimensions of the second system are suitable for growing plants to their full life cycle - not only measurement of quantitative indicators and the obtained biomass, but also qualitative indicators such as color, odor, taste and others. The influence of light with different wavelengths on photosynthesis efficiency was studied with the help of the newly created lighting system. This report presents some pilot experiments for the selection of plant species that would be suitable as indicators for research in their cultivation under artificial light. Some guidelines are also mentioned in determining the methods for evaluation of obtained results. More detailed examination in the recent experiments, showed in this paper, concerns cultivation of tomato plants (*Solanum lycopersicum*) with the application of newly created lighting system. Research will allow plants to be grown with artificial light with minimal energy consumption.

**Keywords:** LED, photosynthesis, photosynthetic active radiation (PAR), growing plants in artificial light, light spectrum

### ИЗСЛЕДВАНЕ НА РАСТЕЖА И РАЗВИТИЕТО НА РАСТЕНИЯ ПРИ ОТГЛЕЖДАНЕТО ИМ НА ИЗКУСТВЕНА СВЕТЛИНА

**Светлана Велинова**

Минно-геоложки университет „Св. Иван Рилски“, София 1700, НИЛ „Осветителна техника“, svetliv@mail.bg, <http://light-bg.eu/>

**РЕЗЮМЕ.** Отглеждането на растения при изкуствена светлина в последно време придоби особена актуалност. За да се изследва коя част от спектъра на видимата светлина влияе най-силно върху растежа и развитието на растенията, веднъж през 2015 и втори път през 2019 г. в НИЛ "Осветителна техника" към Минно-геоложки университет "Св. Иван Рилски" бяха създадени две специализирани осветителни уредби. Размерите на кабините на втората уредба са подходящи за отглеждане на растения и изследването на пълния им жизнен цикъл, което включва освен измерването на количествени показатели и получената биомаса, така и качествени показатели като цвят, мирис, вкусови качества и др. С помощта на новосъздадената осветителна уредба е изследвано влиянието на светлина с различна дължина на вълната върху ефективността на фотосинтезата. Този доклад представя някои пилотни експерименти за избор на растителни видове, които биха били подходящи като индикатори за изследвания при отглеждането им на изкуствена светлина. Споменати са също и някои насоки при определяне на методите за оценка на получените резултати. В доклада по-подробно са разгледани последно проведените експерименти с отглеждане на домати растения (*Solanum lycopersicum*) в новосъздадената осветителна уредба. Изследванията ще позволят да се отглеждат растения при изкуствена светлина с минимален разход на енергия.

**Ключови думи:** LED, фотосинтеза, фотосинтетична активна радиация (ФАР), отглеждане на растения на изкуствена светлина, спектъра на светлината

### Introduction

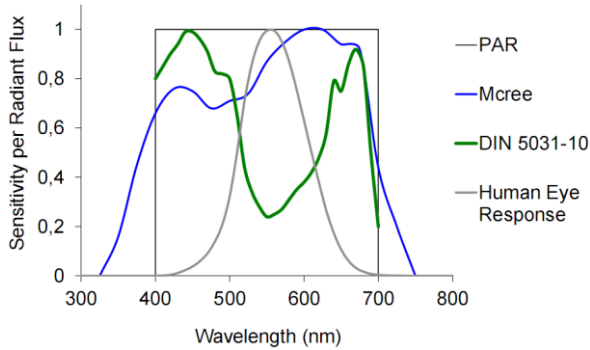
Cultivation of artificial light plants in recent years has gained special popularity. On one hand, it is economically advantageous for places with low sunshine during winter time or northern from 50th parallel. Even in the conditions of our country, in the winter months it is economically advantageous to grow some vegetables with artificial lighting. Plant growing in space is also of interest - for longer stays outside the Earth where, besides supplying oxygen, cosmonauts will need vegetation as a food and as a recreation area.

Critical level of illumination is required for photosynthesis. Photosynthesis in plants has maximum effect in irradiation with blue and red light. (For comparison, the human eye has a maximum sensitivity in the yellow-green range, about 555 nanometers.) (Figure 1).

Blue and red rays affect photosynthesis directly and indirectly. Blue rays (70 kcal / mole) have about 1.5 times more energy than red (40 kcal / mole). According to quantum theory, once a photon replaces only one electron of the pigment molecule, the blue is losing more unproductive energy. It was observed that in normal illumination with the same energy of blue and red light, photosynthesis is more effective with red rays. This can be explained by the fact that, with the same energy, more red quanta will fall on the leaves and therefore more pigment molecules will be excited.

At a high level of brightness, however, blue rays have the advantage because they activate protein synthesis and this has a stimulating effect on the carboxylating enzymes, while the red rays - enhance the formation of carbohydrates. The addition of blue light (about 20%) to the red, significantly enhances photosynthesis and can be used in greenhouse production.

The efficiency of conversion of light energy into chemical energy in plants is estimated to be between 3 and 6%. The actual effectiveness of photosynthesis varies greatly with changes in the light spectrum, intensity of light, temperature and carbon dioxide concentration. This part of the solar radiation spectrum (400-700 nm) is called photosynthetic active radiation (PAR) (Figure 1). In the process of photosynthesis, practically only 1-3% of PAR is used. Typically, PAR is expressed in  $\mu\text{mol photons m}^{-2}\text{s}^{-1}$ .



Фиг. 1. Different methods of weighting the light spectrum

McCree measured three physiological parameters: quantum yield of photosynthesis, action, and absorptance. Physiologically, it describes the maximum photosynthetic efficiency with which light can be converted into chemical energy at low light (Fig. 1).

It is also possible to calculate the effective spectrum of photosynthesis based on DIN 5031-10 (Fig. 1).

Due to the rapid development of technologies in the field of LED technology, specialized luminaires for photosynthesis are already available from many companies. Examples of emission spectra of such light sources are shown in Fig. 2

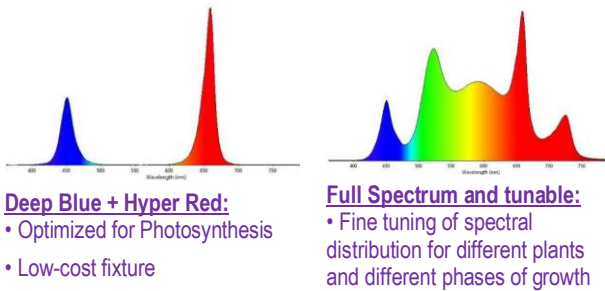


Fig. 2. Variants of emission spectra of specialized luminaires for photosynthesis

Advantages of LEDs in the field of plant cultivation are that a single-color LED emits light in a narrow spectral band, resulting in a saturated color. Reproduction of several spectra with single-color leds is also possible.

**Realization**

In order to study which part of the spectrum most strongly influences the photosynthesis in research laboratory "Lighting Technology" at the University of Mining and Geology "St. Ivan Rilski ", in 2015 a specialized lighting system was created. It

consists of 18 LED luminaires, each of which emits in a narrow area of the spectrum and the intensity of photosynthetic radiation of  $300 - 500 \mu\text{mol /s.m}^2$  (Velinova, 2015).

The purpose of this system is to study the influence of individual parts of the light spectrum on the quantitative and qualitative characteristics of photosynthesis in different plant species, while monitoring their growth and development.

The following species were selected for study: lettuce (*Lactuca sativa*), cloves (*Dianthus caryophyllus*), tagetes (*Tagetes patula*), tomato (*Solanum lycopersicum*). The following morphological indicators were studied: plant height; leaf mass development; number of developed leaves; stem length; leaf length and width; length and development of the root system.

Results of these studies are published in (Velinova, 2017a; 2017b; 2018).

In the above-discussed LED lighting system, the volume of the chambers and respectively the size of the studied plants is limited to dimensions of about 30x30x40 cm. Therefore, in 2019 in RL "Lighting Technology" was created another specialized lighting system (Fig. 3).



Fig. 3. Specialized lighting system 2 – 2019 year

It is an improved version and functional continuation of the one from 2015. It consists of 7 cabins with dimensions 60x60x125 cm, illuminated by LED modules, each emitting in a narrow area of the visible spectrum (Table 1, Fig.3 and Fig. 5).

Table 1

Chamber №	Luminaire	Length on wave $\lambda$ / nm	PAR / mmol	Power / W
1.	BLUE	467 +/-3	298	150
2.	GREEN	523 +/-3	219	150
3.	AMBER	601 +/-2	77	150
4.	RED	626 +/-2	237	150
5.	DEEP RED	658 +/-2	333	150
6.	BLUE / RED	447 / 650	333	160
7.	WHITE	4337 K	188	180

A specialized LED luminaire designed for photosynthesis is installed in chamber № 6.

In chamber № 7 is installed a LED luminaire emitting a neutral white light - 4337 K, which will be used as a cabin with control. measurement samples (Fig. 4).



Fig. 4. Chamber № 7 with neutral white LED light.

The dimensions of the cabins are suitable for growing plants and the study of their full life cycle, which includes not only the obtained biomass, but also quality indicators such as color, odor, taste and others. A more detailed description of this lighting system is given in (Velinova, 2019).

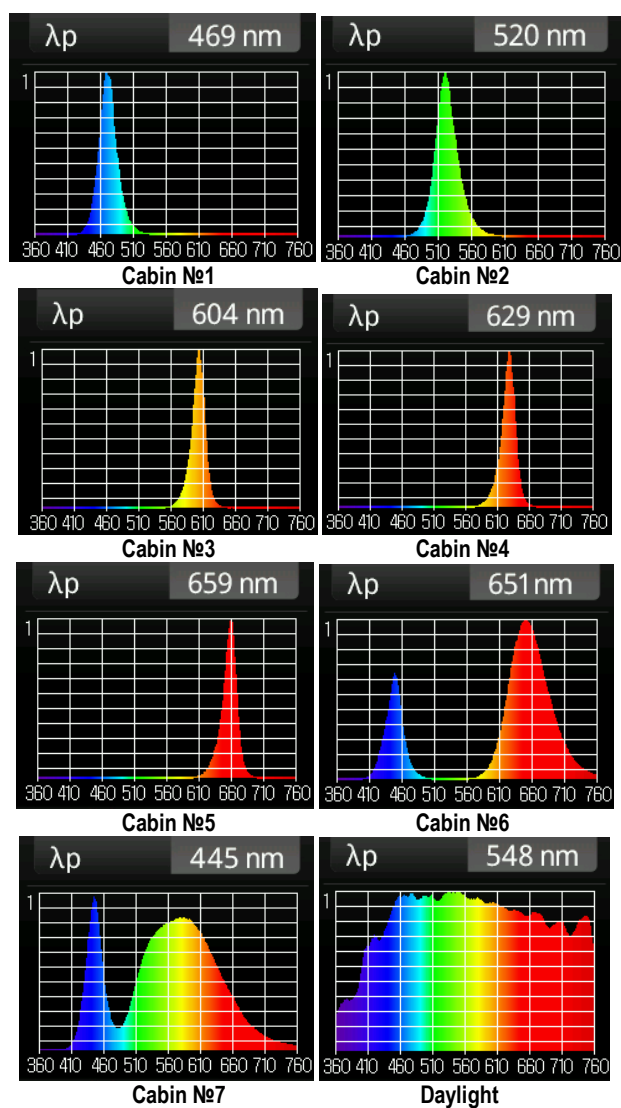


Fig. 5. Emission spectra cameras VS spectrum of daylight

The problems and questions that arise during such experiments are the following:

- Selection of suitable plant species: The aim is to use those that have a strong reaction to light as a factor; be suitable both for indicators and for growing in the conditions of the available cabins, if possible to be self-pollinating (or at least monoecious) and last but not least, those that are suitable for consumption;

- Providing appropriate conditions such as temperature, humidity, light regime and intensity, CO<sub>2</sub>, nutrients, pollination and retention of fruits, protection and control of pathogens and pests, etc. These parameters are kept constant and are the same for each cabin.

- Use of appropriate assessment methods at each stage of plant development: The light spectrum in nm and the PHAR intensity in  $\mu\text{mol} / \text{s.m}^2$  were measured in each cabin (Table 1) using a Specbos 1201 spectroradiometer. The evaluation of growth and development is performed by measuring certain qualitative and quantitative indicators (plant height, stem thickness, number of leaves, leaf size, number of stalks or stems, number of flowers, number of ties, number of fruits managed to ripen, qualitative evaluation of fruits, etc.); visually - by assessing the general habitus of the plants and assessing their health (relative visual assessment).

- Objective interpretation of the results of the experiment: The results are presented in tables and graphs, and it is still too early to draw definite conclusions due to insufficient statistical material and too many factors that influence the experiments, despite the desire to unify them.

#### Preliminary experiments carried out in 2019

In 2019, some preliminary (pilot) experiments were performed in the newly created lighting system. Tomatoes (*Solanum lycopersicum*) - variety "Milyana" (Fig. 6) and strawberries (*Fragaria sp.*) - self-pollinating variety were used as experimental species. (Fig. 7).



Fig. 6. Tomato plant from the experiments in 2019.

Feeding of the plants was hydroponic, using nutrient solutions according to recipes recommended by (Simidchiev Hr., V. Kanazirska, 2017). Such a feeding method is more suitable for constant circulation of the solution. Unfortunately, in our case there was no possibility for this and unicellular algae stuck to the walls and bottom of the containers, so for

the next experiments in 2020 the cultivation and feeding of the plants was in containers with soil-fertilizer mixture and liquid fertilizers.



Fig. 7. Strawberries fed hydroponically -experiments in 2019.

When growing strawberries in the cabins, it was found that the conditions there were not suitable for these crops: insufficient ventilation, relatively high temperatures and the appearance of mites greatly compromised the strawberry plants and the further conduct of the experiment with it. For future experiments with strawberries, it is necessary to provide better ventilation, carrying them out during the colder months of the year and last but not least - good sterilization of the room and the soil substrate.

On the other hand, tomato plants responded quite well to the same conditions in the cabins where strawberries were grown, so experiments with them were continued in 2020, but with a different variety (Rugby), which was considered more suitable as an object for research and evaluation.

**Experiments carried out in 2020.**

As experimental species were used tomatoes (*Solanum lycopersicum*) - variety "Rugby" (Fig. 12), onions (*Allium*) (Fig. 9), lettuce (*Lactuca sativa*) (Fig. 9), and tagetes (*Tagetes patula*) (Fig. 11).

The plants are moved under the lamps at a stage of development seedlings - after the growth of the first true leaf. They are selected so that they are relatively the same size. At certain intervals (two to three weeks) they are measured and photographed. During each measurement, the temperature and humidity of the air in the cabins are taken into account (the average temperature is maintained around 20-25° and the humidity 55-60%). The light regime in the cabins is 18 hours light / 6 hours dark, in order to bring the light conditions close to the natural ones for the plants.

**Growing Egyptian onions (*Allium cepa* var. *multiplicans*).**

Egyptian onions are grown mainly for their leaves similar to some other species of onions, with the difference that it withstands low temperatures and can overwinter outdoors. Instead of flowers, a group of bulbs is formed directly on the tops of the flowering stems, which weigh, bend the stem and when in contact with the ground put down roots, thus multiplying - hence the name "creeping onion".

On 24.01.20 the plants were placed under the lamps in the cabins – one bucket with 3 bulbs each. The following indicators were measured: plant height (the aboveground part) in centimeters; number of leaves; thickness of the stem in its thickest part in mm.

Results for height and relative visual assessment are presented in (Fig. 8) and (Fig. 10).

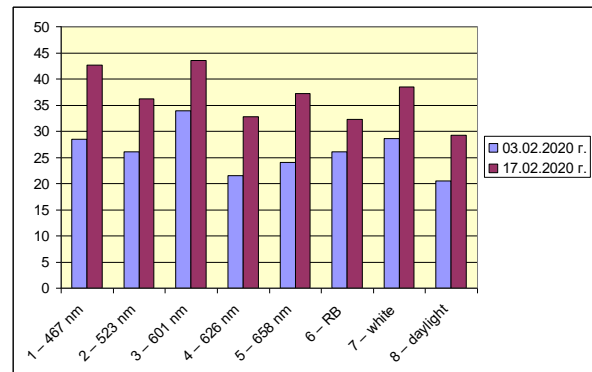


Fig. 8 Egyptian onion - plant height in cm - 03.02 and 17.02.20.

The plants formed edible leaves after about two weeks. Measurements were made, after which the leaves were cut, leaving one leaf at a time. After about a month, they grew back to approximately the previous level. The best growth was observed in the blue (1), combined RB (6) and white LED (7) spectrum.



Fig. 9 Leafy vegetables - 19.03.2020

**Growing lettuce (*Lactuca sativa*) - variety "Oak leaf".**

On 20.02.20 the plants were placed under the lamps. The following indicators were measured: height and width (diameter) of the aboveground part of the salad in cm and number of leaves. Results for relative visual assessment are presented in (Fig. 10).

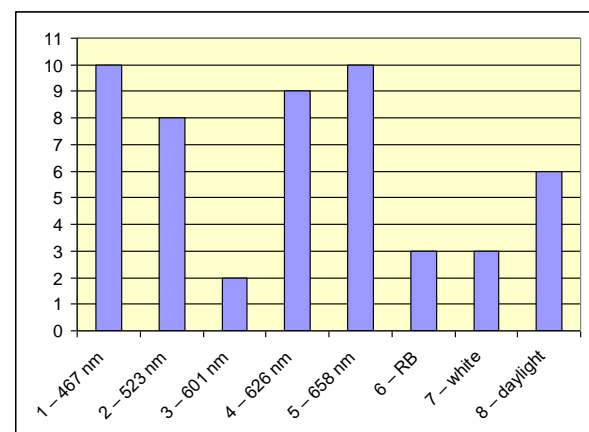


Fig. 10 Lettuce and leafy vegetables - relative visual assessment from 1 to 10 on 19.03.2020.

The salads reached an edible size after about a month. The most satisfactory results were in the blue (1), red (4 and 5) and somewhat green (2) spectrum.

**Growing tagetes (*Tagetes patula*)** On 17.06.20, 9 buckets were placed under the lamps in a cabin. (Fig. 11). After a month they were in the flowering stage. No visible differences in plant growth and development were observed in the different light spectra.



Fig. 11 Tagetes photographed on July 17, 2020

**Growing tomatoes (*Solanum lycopersicum*).** On 24.01.20 they were placed under the lamps – 4 plants in a cabin, each planted in a separate container (Fig. 12).



Fig. 12 Tomatoes photographed on March 6, 2020

The following indicators were measured: height of the plant (above-ground part) in cm. (Fig. 14); thickness of the stem in its thickest part in mm (Fig. 13); number of leaves (with stalks) (Fig. 16); length of the largest leaf in cm.; number of stalks; number of flowers (flower buds) (Fig. 13 и Fig. 17); number of ties (Fig. 13) and number of ripe fruits (Fig. 13). A relative visual assessment of 1 to 10 was also made (Fig. 15).



Fig. 13 Some of the measured indicators

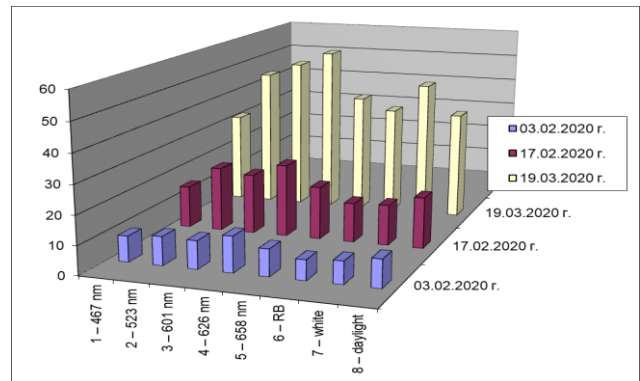


Fig. 14 Tomatoes - stem height in cm measured on 03.02, 17.02 and 19.03.20.

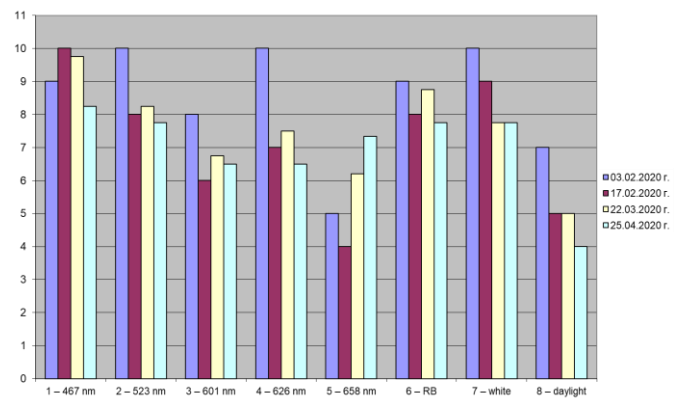


Fig. 15 Tomatoes - Relative visual assessment from 1 to 10 made on 03.02, 17.02, 22.03 and 25.04.20.

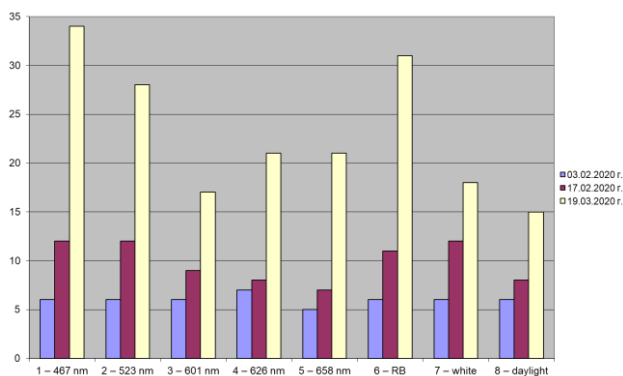


Fig. 16 Tomatoes - Number of leaves (with stalks) on 03.02, 17.02 and 19.03.20.

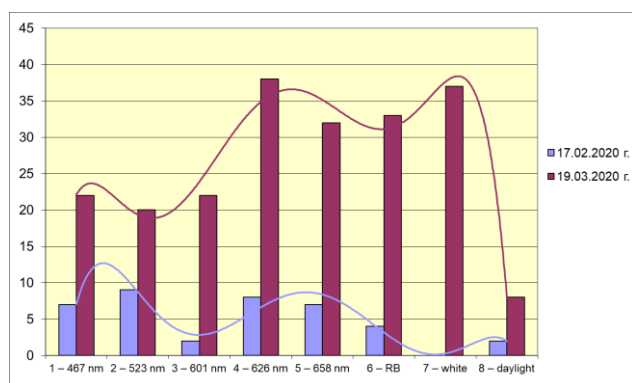


Fig. 17. Tomatoes - Number of flowers (flower buds) on 17.02 and on 19.03.20 the graph is for the total number in each cabin

**Number of tied fruits.** In the case of tomatoes as cross-pollinated plants, artificial pollination had to be carried out. The number of tied fruits as of 19.03.20 was the largest in cabins (1) - blue, (4 and 5) - red and (6) RB spectrum.



Fig. 18 Tomato plant photographed on April 21, 2020

A qualitative evaluation of the ripe fruits was made by tasting by three evaluators. There was no relationship between the

taste of the fruit and the spectrum of light under which it was grown.

### Conclusions and guidelines for future work

- The main observations so far are that during the different stages of plant development a somewhat different spectrum of light is required. It is recommended to add other spectra (blue, red and green) to the main white light.
- Growing plants in artificial light in the above lighting system is more suitable and effective for young plants up to the seedling stage (for about 1-2 months). Problems arise when growing adult plants for a long period of time: there is a depletion and weariness of plant resources after the first harvest, which slows down and stops later growth.
- It is desirable to carry out the experiments in the cooler months of the year in order to more easily provide appropriate temperature and humidity conditions. (the cooling of the lamps additionally heats the cabins). In this way, the danger of diseases and pests, which usually occur in warmer and drier environments, is avoided.
- Objective interpretation of the results of the experiment and drawing the appropriate conclusions are still a problem.

**Acknowledgements.** Research Laboratory "Lighting Equipment", Assoc. Prof. Dr. Eng. Krasimir Velinov, Prof. Dr. Veselina Ilieva, Prof. Dr. Hristo Simidchiev, Prof. Dr. Vasily Goltsev, Assoc. Prof. Dr. Eng. Svetlana Bratkova.

### References

Aleksandrov, N., 2012. Fundamental theory of colors ed. East-West, ISBN: 978-619-152-110-4, p. 255.

Angelov, V., Irradiator for growing plants without sunlight, 2018, VII Balkan conference on lighting - Balkanlight 2018, 04-06 June, Sofia, ISBN 978-954-353-347-3, 161-164.

Blankenship R., 2014. Molecular mechanisms of photosynthesis, WILEY Blackwell, Washington University in St. Louis, Missouri, USA, ISBN 978-1-4051-8975-0

DIN 5031-10, DEUTSCHE NORM, 2000., 03, 16-18.

Goltsev, V., M. Kaladzi, M. Kuzmanova, S. Allahverdiev. 2014. Chlorophyll fluorescence in studies of the physiological state of plants, Izhevsk Moscow, Institute for Computer studies, p. 197

Ilieva, M., V. Ilieva, 2014., LED Irradiation systems for plant growing, XV National conference with international participation Bullight / Bulgaria LIGHT 2014, 10 - 13 June, Sozopol, ISSN 1314-0787, 184-187

Ilieva, V., S. Velinova LED-technology in greenhouse horticulture, 2018, VII Balkan conference on lighting - Balkanlight 2018, 04-06 June, Sofia, ISBN 978-954-353-347-3, 157-160.

Poryazov I., V. Petkova, N. Tommekova. 2013. Vegetable production, Publishing House "DIMI 99" OOD, Sofia

Rossi, M., D. Casciani. 2018. Lighting design research for horticultural vegetables growing: A case study (in English), VII Balkan conference on lighting - Balkanlight 2018, 04-06 June, Sofia, ISBN 978-954-353-347-3, 145-149.

- Simidchiev H., V. Kanazirska, 2017. For hydroponics from A to Z, Kota publ., ISBN 13 9789543054381, p. 496
- Velinova, S., 2015. LED Lighting system for the study of the photosynthesis, 58th International Scientific Conference, October 20, Sofia, Yearbook of Mining and geological university "St. Ivan Rilski ", vol. 58, scroll III, ISSN 1312-1820, 105-109.
- Velinova, S., 2017. Possibilities for using of mining galleries for growing plants on artificial lighting, International Scientific Conference UNITECH 2017, November 17-18, Gabrovo, ISSN 1313-230X, vol. 1, 148-153.
- Velinova, S., Growing plants on artificial lighting. 2018. VII Balkan conference on lighting - Balkanlight 2018, 04-06 june, Sofia, ISBN 978-954-353-347-3, 150-156.
- Velinova, S., V. Ilieva, 2017. Influence of the spectrum of light on plant growth, XVI National conference with international participation Bullight / Bulgaria Light 2017 and BalkanlightJunior 2017, 25 - 27 may, Sozopol, ISSN 1314-0787, 55-61
- Velinova, S., 2019 Lighting system for studying plant growth, 62th International Scientific Conference, October 20, Sofia, Journal of Mining and geological sciences, vol. 62, scroll III, ISSN 2682-9525, 132-137.

## LIGHTING CONDITIONS IN PHOTOVOLTAIC GREENHOUSES

**Svetlana Velinova<sup>1</sup>, Veselina Ilieva<sup>2</sup>, Krasimir Velinov<sup>3</sup>**

<sup>1,3</sup> University of Mining and Geology "St. Ivan Rilski", 1700 Sofia; svetliv@mail.bg, <http://light-bg.eu/>

<sup>2</sup> Institute of Soil Science, Agrotechnology and Plant Protection "N. Pushkarov", Sofia

**ABSTRACT.** The cultivation of plants at extremely low temperatures is carried out in specialized greenhouses. They must provide very good thermal insulation with the environment, as heating costs will otherwise become disproportionately high. An example of such conditions is the climate of Mars or Antarctica. Unlike greenhouses built in temperate climates, where a polyethylene cover is sufficient to provide the necessary heat and transmit the necessary solar radiation to carry out photosynthesis, the greenhouses of the above type must be closed well-insulated rooms without windows. The required light will be generated by LED luminaires with a plant-optimized emission spectrum. The report analyzes the energy costs required for lighting. It is proposed to use photovoltaic panels to power the lighting. Options have been developed for powering greenhouses at different outdoor temperatures and levels of solar radiation.

**Keywords:** greenhouse, LED luminaires, photosynthesis, photovoltaic panels

### СВЕТЛИННИ УСЛОВИЯ ВЪВ ФОТОВОЛТАИЧНИ ОРАНЖЕРИИ

**Светлана Велинова<sup>1</sup>, Веселина Илиева<sup>2</sup>, Красимир Велинов<sup>3</sup>**

<sup>1,3</sup> Минно-геоложки университет „Св. Иван Рилски“, 1700 София

<sup>2</sup> Институт по почвознание, агротехнология и защита на растенията „Н. Пушкарров“, София

**РЕЗЮМЕ.** Отглеждането на растения при екстремно ниски температури се извършва в специализирани оранжерии. Те трябва да осигурят много добра топлоизолация с околната среда, тъй като разходите за отопление в противен случай ще станат несъразмерно високи. Пример за такива условия са климата на Марс или Антарктида. За разлика от оранжерии изградени в умерените климатични пояси, където полиетиленова покривка е достатъчна да осигури нужната топлина и да пропуска необходимата слънчева радиация за осъществяване на фотосинтезата, то оранжерии от горния тип трябва да представляват затворени добре топлоизолирани помещения без прозорци. Необходимата светлина ще се генерира от светодиодни осветители с оптимизиран за растенията спектър на излъчване.

В доклада се прави анализ на необходимите енергийни разходи за осветление. Предлага се да се използват фотоволтаични панели за захранване на осветлението. Разработени са варианти за захранване на оранжерии при различна външна температура и ниво на слънчевата радиация.

**Ключови думи:** оранжерии, светодиодни осветители, фотосинтеза, фотоволтаични панели

Growing plants in greenhouses is practiced in the following cases:

- Use of waste heat from other productions and growing vegetables during the winter season in temperate latitudes.
- Growing crops that require special conditions - gas composition of the atmosphere, special soil, diet, lighting.
- Use of a closed volume to store scarce moisture (in desert areas).
- Growing of varietal seeds, where they should not be mixed with other crops. (this can only be done indoors).
- Intensive production with multi-storey plant placement.
- Getting food in extreme conditions - lack of suitable soil, extremely low temperatures or lack of suitable atmosphere.
- In all cases, except for the third option, additional artificial lighting will be required. The required amount and spectrum of light has already been discussed in [Velinova, 2019 and 2015, Blankenship R., 2014].

In this report, the subject of consideration is the last category of greenhouses - those operating in extreme conditions. An example of such conditions is the climate of Mars or Antarctica. Unlike greenhouses built in temperate climates, where a polyethylene cover is sufficient to provide the necessary heat and transmit the necessary solar radiation to carry out photosynthesis, the greenhouses of the above type must be closed, well-insulated rooms without windows. They must provide very good thermal insulation with the environment, as heating costs will otherwise become disproportionately high. The required light will be obtained from LED luminaires with a plant-optimized emission spectrum. The energy needed for heating and lighting can be generated in two ways - from a nuclear reactor or from photovoltaic panels. Technical capability also now. For example, the US Department of Energy has announced a tender for the creation of a small nuclear power supply system. The reactor must give not less than 10 KW of power, which must not be interrupted and be stable. According to the terms of this contract, the weight of the reactor must be no more than 3500 kg and it must be able to work autonomously for 10 years [kalddata.com].

At the same time, as early as 1990, Hyperion Power Generation, Inc. built a portable reactor with a thermal capacity of 10MW, which has a volume of about 3 cubic meters and can produce energy for 10 years. This reactor or rather nuclear battery was developed for the needs of the US military, and can be transported by truck and it is assumed that all permits for use have been obtained.

Hyperion Power Generation, Inc. is an American energy company in Santa Fe, New Mexico, USA, created for the purpose of implementation, construction and sale of several types of relatively small modular nuclear reactors (70 MW thermal, 25 MW electric), which have innate protection against accidents and do not provide the opportunity for the development of nuclear weapons. The reactor is the size of an oil tank and a diameter of 1.50 meters. [bg.oclifescience.com]

Another possibility for obtaining energy is the use of a photovoltaic plant. Under normal conditions for average latitudes, the incident solar radiation on a horizontal surface is from 1100 to 1400 kWh / year per sq.m. In the extreme conditions in which we want our greenhouses to operate, we can count on a much lower level of solar radiation.

What is the current state of technology and what part of this energy can be converted into electricity? The mass production of solar panels is produced on the basis of pure silicon. The technology is similar to that for the production of integrated circuits and the price of solar panels has dropped significantly. Currently, the price for deliveries of quality panels is about 0.2 € / Wp. For the last 10 years, the average annual increase in global cumulative production of PV capacity is about 30%. Applying the law of SWANSON (doubling the cumulative production leads to a reduction of prices by 24%), the price of the panels will fall below 0.1 € / Wp. Over the last 40 years, the prices of PV panels have decreased by more than 150 times. In places where there is high solar radiation (these are mostly desert places), tenders are held en masse for the construction of photovoltaic power plants according to the criterion of the lowest price of energy sold. An example of this is the recently won tender in Abu Dhabi for an energy price of \$ 0.0135 per kWh or \$ 13.5 / MWh (~ BGN 23 / MWh. For comparison, the price of the stock exchange in Bulgaria these days was about BGN 85 / MWh). Chinese solar developer Jinko Power and French energy giant EDF this year announced a new record low price for solar energy, which will be generated on a 1.5 GW Al Dhafra solar project in Abu Dhabi at a tariff price of 0.0135. \$ / kWh. [pv-magazine.com].

In terms of solar energy utilization for silicon panels, there is still much to be desired. The efficiency of energy conversion is in the range of 13-15%. The latest panels with dimensions of 2x1m and power 500W, now have an efficiency of more than 20%. Is it possible to increase efficiency even more and is there a limit to this? According to the National Renewable Energy Laboratory of the USA, NREL in silicon cells without light concentration, results with 31% efficiency were obtained. Much higher efficiency results can be obtained with multilayer panels with light concentration. In this case, an efficiency of 47% is achieved for semiconductors with three or four P-N junctions. [nrel.gov]

In this report, an attempt is made to design a greenhouse for growing plants in extreme environmental conditions at a

level of solar radiation of a maximum of 400 - 500 W / sq.m. In this case, all the energy for heating and plant growth will be obtained from external solar radiation.

An example of such a place is the planet Mars

The atmosphere on Mars is about 100 times less dense than on Earth. But the Martian atmosphere is dense enough to have clouds and winds. Huge sandstorms engulf the entire planet. Mars is a much colder planet than Earth. The temperature of the Martian surface varies from -125 °C near the poles in winter and reaches 20 °C at noon near the equator. The average temperature on Mars is about -60 °C. The atmosphere on Mars contains significantly less oxygen (O<sub>2</sub>) than on Earth. The content of O<sub>2</sub> in the atmosphere of Mars is only 0.13%, while on Earth it is 21%. Carbon dioxide makes up 95.3% of the gases in Mars' atmosphere. The other gases are nitrogen (N<sub>2</sub>) 2.7%, argon (Ar) 1.6% and water vapor (H<sub>2</sub>O) 0.03%.

Winds on the surface of Mars are usually light, with a speed of about 10 km / h. Scientists have observed gusts of wind at a speed of 90 km / h. Martian winds have less strength due to the low density of the atmosphere.

Sandstorms

The biggest sandstorms can cover the entire surface of Mars. Storms of this size are rare, but can last for months. Such storms occurred in 1971 and 2001.

Sandstorms occur more often when Mars is closest to the sun. The reason for this is that the sun heats the atmosphere of Mars the most [solarsystem.valchev-bg.com].

The Insight spacecraft, which landed on Mars in November 2018, can count the time on Mars. [nationalgeographic.bg]

It is located near the Martian equator, 4 degrees north. According to the latest data, the temperature on Mars at five in the morning local time is minus 95 degrees Celsius. When the Sun warms the planet's surface, the maximum temperature reaches minus 5 degrees Celsius.

Another place with extreme conditions is Antarctica.

Antarctica is the coldest place on Earth. The Japanese station in Antarctica on December 8, 2013 reported -91.2 °C. Winter temperatures reach minimum values - between -80 °C and -90 °C in the interior of the continent and maximum between 5 °C and 15 °C around the coast in summer. The snow surface reflects almost all the ultraviolet rays that fall on it. Almost the entire continent is covered with ice with an average thickness of 2.5 km. Stormy winds often descend from the polar plateau on the periphery of the continent. Inside, the wind is usually moderate. During the clear days of summer, more solar radiation reaches the surface than at the equator, due to the 24-hour glow

Under these thermal and light conditions, an attempt will be made to design an enclosed space in which to grow plants, all energy being obtained from solar radiation. A room with approximate dimensions 20x20x20 m will be built. Only existing technologies and materials will be used. As a thermal insulation material for the construction of the walls can be used some of the following materials shown in Table 1 and having the following coefficients of thermal conductivity (thermal conductivity), W / (m.K).

Table 1.

Material	The coefficient of thermal conductivity, W/m <sup>2</sup> *K
Styrofoam	0,04
Polyurethane foam sheets	0,035
Polyurethane foam panels	0,025
Light foam	0,06
Perlite	0,05
Cotton wool mineral light	0,045
Mineral wool heavy	0,055
Expanded polystyrene - styrofoam	0,031
Mineral wool heavy	0,055

Most of these materials do not have good mechanical properties except for the foam glass, and you will need to build an external stable skeleton. Expanded polystyrene - styrofoam with a thermal conductivity coefficient of 0.031 W / mK will be used as thermal insulation material. If it is assumed that a temperature of 20 °C will be maintained inside the room and the outdoor temperature will be -80 °C, then the thermal difference will be  $\Delta T = 100$  °C

At a thickness of the thermal insulation panel of 20 cm, the power losses will be 15.5W / sq.m. Accordingly, with a wall thickness of 30 cm, power losses will be 10.3W / sq.m

With dimensions of the room 20x20x20 m, the outdoor area will be 6x20x20 = 2400 sq.m. The corresponding heat losses will be: 2400 sq.m x 15W / sq.m = 36kW. 864 kWh of electricity will be needed for one day to maintain the required temperature.

The effective area of the building for placement of PV panels is 1500 - 1800 sq.m. Panels with dimensions 2x1m and power 500 Wp will be used. It is assumed that the panels will be located only on the surface of the building. The average efficiency of using solar radiation for the months in spring, summer and autumn will be about 30%. With an effective number of panels - ~ 700 - 800 pcs. The peak power generated in the conditions of Antarctica for 30% efficiency of the system will reach - 700 pcs. x 0.5 kW x 0.3 = 105 kW. For the summer months, the effective operating time of the system will be about 16 hours, and for spring and autumn - an effective time of 8 hours. Respectively, in the summer 1680 kWh will be generated per day, and in the spring-autumn season - 840 kWh. This means that with modern technology, such a building can be heated by the energy received from the sun in the conditions of Antarctica for the months from September to April. As the solar radiation fluctuates around the clock during the transition months, it will be necessary to create a heat accumulator with a capacity of 1700 kWh (this provides heating power for two days). A water tank with a volume of 28-30 cubic meters can be used as such an accumulator. In fact, this is a cube with a wall size of 3 m. In hydroponic plant cultivation, such a tank will be needed to store the nutrient solution.

Is this power enough for plant photosynthesis? In this volume of the room - about 8000 cubic meters, shelves for hydroponic cultivation of plants with a total area of 4000 - 6000 sq.m can be located.

What luminous flux can be achieved at 105kW?

Modern LEDs have an efficiency of 180 - 200 lm / W. This means that with the available power a luminous flux of 19 to 21

million lm can be generated. With this luminous flux distributed over the effective area of 4000 to 6000 sq.m, irradiation from 3200 to 5200 lm / sq.m will be realized. This value is close to the lower limit for efficient photosynthesis, but is sufficient for the development of most plants.

The conditions on the planet Mars are similar to those in Antarctica. The advantage is the high content of carbon dioxide - 95%, which is useful for plants. The difference is that there the atmosphere is diluted and high-speed winds cannot cause the destruction of the structure. Sandstorms are dangerous. Due to their duration, there is a risk of the system shutting down. Nevertheless, building such an enclosed space is the only way for people on this planet to survive.

## Conclusions and recommendations

1. The construction of modular heat-insulated greenhouses with a volume of 8000 cubic meters is possible with the current technological possibilities. In them it will be possible to grow plants for human consumption, and the necessary energy for lighting and heating will be obtained from photovoltaic panels.

2. It is recommended that the thickness of the thermal insulation be not less than 30 cm.

## References

- Blankenship R., 2014. Molecular mechanisms of photosynthesis, WILEY Blackwell, Washington University.
- Ilieva, V., S. Velinova LED-technology in greenhouse horticulture, 2018, VII Balkan conference on lighting - Balkanlight 2018, 04-06 June, Sofia, ISBN 978-954-353-347-3, 157-160.
- Poryazov I., V. Petkova, N. Tommekova. 2013. Vegetable production, Publishing House "DIMI 99" OOD, Sofia. St. Louis, Missouri, USA, ISBN 978-1-4051-8975-0, p. 314.
- Velinova, S., 2019 Lighting system for studying plant growth, 62th International Scientific Conference, October 20, Sofia, Journal of Mining and geological sciences, vol. 62, scroll III, ISSN 2682-9525, 132-137.
- Velinova, S., 2015. LED Lighting system for the study of the photosynthesis, 58th International Scientific Conference, October 20, Sofia, Yearbook of Mining and geological university "St. Ivan Rilski ", vol. 58, scroll III, ISSN 1312-1820, 105-109.
- САЩ възнамерява да изпрати на Луната и Марс малки ядрени реактори с мощност 10 KW. <https://www.kaldata.com/>
- <https://bg.oclifescience.com/1516482-over-the-counter-miniature-nuclear-reactors>
- Exclusive interview – Jinko Power on how it offered the world's lowest solar power price, pv-magazine, [https://www.pv-magazine.com/2020/07/27/exclusive-interview-jinkopower-on-how-it-offered-the-worlds-lowest-solar-power-price/?utm\\_source=dvtr.it&utm\\_medium=facebook](https://www.pv-magazine.com/2020/07/27/exclusive-interview-jinkopower-on-how-it-offered-the-worlds-lowest-solar-power-price/?utm_source=dvtr.it&utm_medium=facebook)
- National Renewable Energy Laboratory <https://www.nrel.gov/pv/assets/pdfs/best-research-cell-efficiencies.20200708.pdf>
- <http://www.solarsystem.valchev-bg.com/mars.php>
- <https://www.nationalgeographic.bg/?cid=120&article=8447>

## IMPLEMENTATION OF REMOTE MONITORING SYSTEMS AND COMMERCIAL MEASUREMENT

**Viliyan Yanakiev**

*University of Mining and Geology "St. Ivan Rilski", 1700 Sofia; qnakiev91@abv.bg*

**ABSTRACT.** Intelligent energy metering systems in the gas industry are innovative solutions with many advantages. Smart meters and systems are a method of modernization and automation not only in the industrial but also in the domestic sector. The system monitors and enables control of all activities. It provides an efficient and reliable bidirectional flow of data and information between the company and consumers. The basic principle in building smart energy metering systems is to integrate the metering devices into a single remote transmission system into a common database. From the consumer's point of view, this means correct accounting of the energy used and access to real-time information on natural gas consumption, which allows for corrections in current consumption and behaviour, resulting in high energy efficiency of homes and buildings.

**Keywords:** natural gas, automated control, metering device, energy efficiency

### ИМПЛЕМЕНТАЦИЯТА НА СИСТЕМИ ЗА ДИСТАНЦИОННО НАБЛЮДЕНИЕ И УПРАВЛЕНИЕ НА СРЕДСТВА ЗА ТЪРГОВСКО ИЗМЕРВАНЕ

**Вилиян Янакиев**

*Минно-геоложки университет „Св. Иван Рилски“, 1700 София*

**РЕЗЮМЕ.** Интелигентните системи за измерване на енергия в газовата промишленост са иновативни решения с много предимства. „Умните“ измервателни устройства и системи са метод за модернизация и автоматизация не само в промишления, но и в битовия сектор. Системата следи и дава възможност за контрол на всички дейности. Тя осигурява ефикасен и надежден двупосочен поток от данни и информация между компанията и потребителите. Основният принцип при изграждането на интелигентни системи за измерване на енергия е обединяването на измервателните устройства в една единствена система за отдалечено предаване в обща база данни. От гледна точка на потребителя това означава коректно отчитане на използваната енергия и достъп до информация за консумацията на природен газ в реално време, което позволява корекции в текущото потребление и поведение, което води до висока енергийна ефективност на домовете и сградите.

**Ключови думи:** природен газ, автоматизирано управление, измервателно устройство, енергийна ефективност

### Introduction

The smart metering device is an electrical device that records consumption at intervals of one hour or less and transmits this information at least once a day back to the information system of the gas distribution company for monitoring and invoicing purposes.

The main feature of intelligent measurement is the ability to provide finite customers more information about their energy consumption. According to a study by implementing Smart metering, end users can save between 5% and 10% of their energy consumption when such information is provided. [1] [2] [5] [6] [3] [9]

Intelligent measurement has the following characteristics: automated processing, transfer, management and use of measurement data; automatic control of the measuring device; two-way data communication with the measuring device; provides meaningful and timely information to the relevant countries and their systems; support for services that improve the energy efficiency of energy consumption and the energy system (generation, transmission, distribution and especially final consumption).

All intelligent commercial metering devices purchased for invoicing purposes in Europe must comply with the Measuring Instruments Directive [MID 2004]. This sets out the minimum requirements for fiscal meters, including their accuracy, divided into several different classes suitable for different market applications. The MID standard specifies the quantities that the gas flow meter must measure: In Energy (if this is provided by the calorific value of the gas); instantaneous flow (for ultrasonic and similar gas flow meters); Maximum demand. Smoothed consumption data approximating to the steady heat output (where the boiler is modulated through a simple on / off control).

All these qualities can be used as a resource to build a smart measurement scheme. For energy use feedback purposes, it is possible to provide additional information based on those measured quantities: Anticipation of the next account; transmission interval - 60 min; detailed data on customer behaviour; closing and opening the gas shut-off valve; remote gas stop; manual release of gas from the point of view of safety; dynamic tariffs; up to eight registers are considered in intelligent accounting for the UK [SMOF] specification, with a tariff set for each register; Availability of configuration options

on the Smart flow meter or the device that connects to it. [2] [3] [4] [10]

Feedback from users to receive information from smart meters can be done in several ways: the use of the Internet as a communication environment and the construction of a WEB-based application in which each user will have access to track their consumption, to receive historical information for the past period, etc.; the use of specialized devices in the home, through which the consumer will be able to receive various information about his consumption; the transmission of data from the smart measuring device to a specialized device (display) in the home is a relatively new approach and will require the application of new technologies. This implies the need for a LAN (Local Area Network) to support this feedback, where the location of the meter is not suitable for direct customer feedback. This LAN can provide a number of other functions as well as display streaming data; providing connection to other utility measuring devices; providing connection to the home device (display); When using the devices described above, the following specifics must be taken into account: the quality of the display, what color range it will contain; the power supply of the displays; batteries for single use; rechargeable batteries; direct power supply from 220V network.

Some of the functions of the specialized device for the home are: information about the calorific value of the gas; sound signal when an alarm occurs; communication signal level information; information on the degree of discharge of the battery power supply; sending an alarm / event signal; overflow warning; tariff information; historical data for the past period; energy consumption and its price expression; The effectiveness of the final customer feedback includes a balance of price and quality. Data security and customer privacy.

- The first and most important condition for intelligent measurement systems is considered to be data security and preservation of customer integrity. The user must be able to decide individually how and by whom his personal data and consumption data (except for the minimum necessary for the implementation of regulatory requirements by the company) will be used and disseminated. Consent and full transparency in the collection of consumer information are required, and it is the company's obligation to provide this information (for a "reasonable" fee) upon request by the consumer.

- Taken out of context, it can be concluded that the provision of information on the consumption of household customers once a month is considered sufficient. The same must be free of charge and can be done through various channels (SMS, customer service center, Internet-based, etc.). For paper accounts, companies may require a "reasonable" fee. The information must be presented in detail and in an understandable form. It is explicitly mentioned that the interval of actual reporting and the period of summary data provided to users differ.

- Provision of reports on current consumption and the resulting financial costs at the request of the client must be carried out through various information channels (SMS, customer service center, Internet-based, etc.) without additional fees. The same goes for access to historical consumption data.

- Remote interval reading and archiving of information in registers should facilitate a change of provider or changes in contract terms.

- Remote consumption monitors the actual consumption in a timely manner and eliminates the forecast and "balancing" bills and "based" bills.

- Development of new tariff formulas, according to certain periods and taking into account the volatility of consumption, at least on a daily basis. For this purpose and to avoid the processing of a large number of reported periodic data (hourly for example), it is recommended to have at least 3 time (ToU - Time of Use) registers, according to the national specifics of consumption. These registers can store time-based consumption, divided into, for example, peak / peak, normal and minimum consumption, or seasonal.

### **Regulatory framework in Bulgaria in the implementation of systems for remote monitoring and control of commercial metering devices**

As part of the in-depth analysis of the current situation on the energy market, as well as the rules and frameworks for the activity of the gas distribution company, in the context of which this paper is prepared, a detailed analysis of the current state of regulations, current laws, decisions and standards was made. including: Energy Law, Promulgated, SG no. 107 of 9.12.2003, last ed. no. 56 of 24.07.2015 Ordinance on the essential requirements and conformity assessment of measuring instruments Ordinance on the essential requirements and conformity assessment for electromagnetic compatibility, adopted by Decree № 76 of the Council of Ministers of 2007 (promulgated, SG No. 32/2007, amended, SG No. 50/2014) The Technical Requirements for Products Act (LTRP).

Ordinance № 6 of 25 November 2004, amended, no. 1 of 2012 for technical rules and regulations for design, construction and use of sites and facilities for transmission, storage, distribution and supply of natural gas;

Ordinance № 4 of 5 November 2013 on connection to the gas transmission and distribution networks - issued by SEWRC, Prom. DV. issue 105 of December 6, 2013.

Ordinance №2 of March 19, 2013 on the regulation of natural gas prices - Prom. DV. issue 33 of April 5, 2013, supplement DV. issue 17 of 28 February 2014, amended DV. No. 65 of August 25, 2015, amended. and ext. DV. issue 94 of December 4, 2015.

Ordinance № 3 of March 21, 2013 on licensing of activities in the energy sector, prom. DV. issue 33 of April 5, 2013 Rules for trade in natural gas - issued by SEWRC, Prom. DV. issue 59 of August 4, 2015.

Rules for granting access to the gas transmission and / or gas distribution networks and for access to the natural gas storage facilities - adopted by protocol Decision № P-1 of 14.03.2013 of SEWRC, Prom. DV. issue 36 of 16 April 2013, amended And extra. DV. No. 59 of 4 August 2015.

Rules for management and technical rules of the gas transmission networks, adopted by the State Commission for Energy and Water Regulation on the grounds of Art. 170, para 3 in conjunction with art. 21, para. 1, item 9 of the Energy Act with Protocol Decision № 124 of 19.08.2013 under item 4.

Rules for management of the gas distribution networks - adopted by the State Commission for Energy and Water Regulation on the grounds of Art. 171, para. 2 in conjunction with Art. 21, para. 1, item 9 of the Energy Act with Protocol Decision № 124 of 19.08.2013 under item 5.

Methodology for determining the eligible amounts of technological costs for transmission, distribution and storage of natural gas - adopted by protocol Decision № 117 of 16.07.2012 under item 3 of SEWRC.

Internal rules of SEWRC for work on complaints and requests for voluntary settlement of disputes under the Energy Act Transposed requirements in the Bulgarian legislation of DIRECTIVE 2004/22 / EC of 31 March 2004 on measuring instruments. Project for energy strategy of the Republic of Bulgaria until 2020.

Ordinance on the essential requirements and conformity assessment of measuring instruments, which introduces into the Bulgarian legislation DIRECTIVE 2004/22 / EC of 31 March 2004 (MID) on measuring instruments defines the requirements that each measuring device or system must meet, to be placed on the market. The annexes accompanying the directive define the basic concepts and essential requirements for end measuring instruments such as accuracy class, tolerances, climatic conditions and environment, mechanical and electromagnetic classes, resolution and sensitivity, stability, reliability, suitability, protection, additional information, tests, trials, etc. It is important to note that the directive does not currently cite requirements for ultrasonic flow meters and an addition is forthcoming. [10] [11] [12] [13]

There is currently a new Ordinance on essential requirements and conformity assessment for electromagnetic compatibility, which aims to introduce the provisions of Directive 2014/30 / EU of the European Parliament and of the Council of 26 February 2014 on the harmonization of the laws of the Member States relating to electromagnetic compatibility (OJ L 96/79 of 29 March 2014). The new elements in Directive 2014/30 / EU, and respectively in an ordinance, are related to the introduction of more detailed provisions on the obligations of economic operators and the traceability of products throughout the supply chain to facilitate market surveillance.

The Ordinance on the essential requirements and conformity assessment of equipment and protection systems intended for operation in potentially explosive atmospheres, which introduces into Bulgarian legislation Directive 94/9 / EC (ATEX) defines parameters for equipment related to explosion and accident protection. Many of the smart flow meters offered and implemented in Europe meet the requirements of the regulation to varying degrees (Zone 0, Zone 1 and Zone 2).

In Bulgaria, the transition to systems for remote monitoring and control of commercial metering devices (JTI) from a regulatory point of view is left entirely to the competence of the State Commission for Energy and Water Regulation. One of the few actions of SEWRC in this direction is related to the consideration of feasibility studies provided in 2013 by each of the three major electricity distribution companies in the form of a detailed cost-benefit analysis, assessed on the basis of experience gained from pilot projects. In preparing these models, the companies considered 2 scenarios: the first follows the set European targets of 80% coverage with smart meters by 2024, in the second, each company follows its own investment program. The obtained results are grounds for decision №IS-1 from 31.07.2013 of SEWRC, in which the

regulator concludes that the introduction of intelligent systems for measuring electricity at the moment is economically unjustified.

Accordingly, given the lack of a positive assessment, SEWRC does not prepare a mandatory schedule for the introduction of smart metering systems in Bulgaria, but only recommends the introduction of smart metering systems up to 20%, but not less than 10% by 2021. As their introduction must be financed with public funds under European programs, which does not lead to an increase in the prices of end customers.

### Practical application and benefits of the implementation of systems for remote monitoring and control of commercial metering devices (Smart Metering)

Table 1. Practical application and use of the data obtained from systems for remote monitoring and control of commercial metering devices.

Temperature in Celsius °C	1 <sup>o</sup>	2 <sup>o</sup>	3 <sup>o</sup>	4 <sup>o</sup>
	2	3	4	5
	14.4.2020	15.4.2020	16.4.2020	17.4.2020
	20	20	0	20
8:00	14,2	1,3	1,6	5,9
9:00	13,9	1,6	4,8	8,8
10:00	15,7	2,3	8,0	12,9
11:00	19,3	3,4	10,2	16,8
12:00	19,5	4,4	12,3	19,1
13:00	18,6	4,8	13,7	20,6
14:00	18,9	5,0	15,2	21,8
15:00	19,6	4,8	16,0	22,6
16:00	19,1	4,8	16,9	23,0
17:00	17,4	5,3	17,1	23,2
18:00	15,3	5,6	16,7	22,7
19:00	13,9	4,9	15,5	21,5
20:00	12,5	3,6	12,4	17,7
21:00	11,1	2,6	9,7	15,0
22:00	10,3	1,4	8,5	12,5
23:00	8,7	1,2	7,3	11,1
0:00	3,5	1,2	7,0	15,5
1:00	5,2	0,7	6,9	12,8
2:00	4,6	0,7	6,1	11,9
3:00	3,9	0,6	6,0	11,6
4:00	3,1	0,4	5,9	11,4
5:00	2,1	0,1	5,9	10,9
6:00	1,6	-0,4	5,4	10,9
7:00	1,1	-0,5	5,2	10,1
<b>MAX 1<sup>o</sup></b>	<b>20</b>	<b>6</b>	<b>17</b>	<b>23</b>
<b>MIN 1<sup>o</sup></b>	<b>1</b>	<b>-1</b>	<b>2</b>	<b>6</b>
<b>Average 1<sup>o</sup></b>	<b>11</b>	<b>2</b>	<b>10</b>	<b>15</b>

sum t°	308	71	268	421
Total m3	135 340	186 624	138 869	105 392
Representative calorific	10,535	10,535	10,535	10,535
	Nm3	Nm3	Nm3	Nm3
	2	3	4	5
Consumption in Nm3	14.4.2020	15.4.2020	16.4.2020	17.4.2020
8:00	6 194	8 710	9 187	6 411
9:00	6 354	9 802	9 032	6 140
10:00	6 752	9 402	8 486	5 836
11:00	5 375	8 878	7 654	5 680
12:00	5 178	8 428	6 803	5 382
13:00	4 654	8 546	6 623	5 111
14:00	4 510	8 414	6 088	4 571
15:00	4 249	8 172	5 385	4 150
16:00	3 983	7 753	5 083	3 864
17:00	4 903	7 301	4 531	3 720
18:00	5 746	7 578	4 802	3 430
19:00	6 614	7 985	4 776	4 097
20:00	6 885	8 261	5 587	4 245
21:00	6 514	8 553	6 055	4 791
22:00	6 653	8 598	5 975	4 843
23:00	6 533	7 694	5 720	4 457
0:00	5 743	7 149	5 042	4 061
1:00	5 329	6 492	4 762	3 681
2:00	4 905	5 943	4 213	3 395
3:00	4 892	5 921	4 096	2 982
4:00	4 905	5 916	4 190	3 103
5:00	5 156	6 048	4 340	3 359
6:00	5 965	6 717	5 014	3 629
7:00	7 348	8 363	5 425	4 454
<b>Тотал</b>	<b>135 340</b>	<b>186 624</b>	<b>138 869</b>	<b>105 392</b>
<b>16:00</b>	<b>34 507</b>	<b>53 766</b>	<b>47 785</b>	<b>34 560</b>
<b>%</b>	<b>25,50%</b>	<b>28,81%</b>	<b>34,41%</b>	<b>32,79%</b>
<b>23:00</b>	<b>91 097</b>	<b>134 075</b>	<b>101 787</b>	<b>76 728</b>
<b>%</b>	<b>67,31%</b>	<b>71,84%</b>	<b>73,30%</b>	<b>72,80%</b>

In (Table 1.) the data obtained for four days from the "Smart" measuring devices and their use for balancing are considered. It is clearly visualized how the consumption of natural gas can be related to the ambient temperature and to predict the future consumption of a given consumer or gas distribution network.

## Conclusion and conclusions for the implementation of systems for remote monitoring and control of commercial metering devices (Smart Metering)

In summary of the existing regulatory framework, it should be noted that there are extremely specific and specific requirements for measuring devices (gas flow meters and correctors), including tolerances, climatic conditions and environment, mechanical and electromagnetic classes, resolution and sensitivity, stability, reliability, suitability, protection, additional information, tests, trials, etc. These specific limitations and recommendations should be an integral part of the metering infrastructure.

Apart from the detailed parameters of the field equipment, the regulatory framework lacks mandatory regulated characteristics concerning the transmission environment and infrastructure, methods for data processing and transmission, time intervals, requirements for second-level devices for data archiving and buffering.

The normative documents describe only abstract basic requirements for the methods of visualization and presentation of data, and do not specify real technical solutions - be it a local display, a device connected to HAN (Home Area Network), web-based application and others. There are no mandatory requirements for the Head-End system that manages the automated remote reading, the database, redundancy, security and data storage periods, scalability, etc.

The official institutions of the European Union make recommendations and best practices for the construction of smart metering systems in the member states, avoiding the imposition of mandatory requirements and leaving the policy to national regulators.

The preparation of the CBA is in the interest of each contracting authority and it is desirable to prepare a separate report covering the economic justification of the project based on the proposed technical work provides solutions to provide clarity to each contracting authority about the expected capital and operating costs for construction and maintenance. of systems for remote monitoring and management of commercial metering devices (STI) and the expected economic benefits for each company.

From a regulatory point of view, regulatory requirements related to electromagnetic compatibility, frequency distribution and standards should be considered as legal restrictions on the system, in cases where RF and GSM / GPRS data transmission protocols will be used as part of AMI.

**Acknowledgements.** I owe a lot for the constant work of Prof. Georgi Nikolov and Assoc. Prof. Martin Boyadzhiev, who did not stop and do not stop helping me to develop, I received a lot of valuable advice for which I am infinitely grateful.

## References

1. Laws and regulations in the field of oil and gas industries.
2. European regulations in the oil and gas industry.
3. Gas infrastructure management: Textbook for universities / Martin Boyadzhiev, Lachezar Georgiev. - Sofia: MGU St. Ivan Rilski, 2014.
4. Martin Boyadzhiev, G. Filkov, Research to determine the dependence between the environmental temperature and the temperature of natural gas used for the domestic sector as a consumption factor, p.79-83, Journal of mining and geological sciences, 2018. ISSN 2682-9525
5. Martin Boyadzhiev, L. Georgiev, „Model for the determination relationship between ambient temperature and the natural gas used by households in R. Bulgaria, p.232-235, Journal of mining and geological sciences 2015. ISSN 1312-1820
6. J. Radev, L. Georgiev, M. Boiyadzhiev. Sustainable development in the conditions of limited natural resources. Proceedings of scientific and technical conference with international participation “Oil and Gas prospectivity of the BALKAN-BLACK SEA REGION” Varna 2008, p.165-171 ISBN 978-954-92219-2-3.
7. Gas-regulating and measuring equipment: Textbook for universities / Martin Boyadzhiev, Sergey Andreev. - Sofia: MGU St. Ivan Rilski, 2014.
8. Oil & Gas Journal, International Petroleum News and Technology.
9. Pipeline & Gas Journal, International Pipeline & Gas Utility Operations, Design & Maintenance.
10. <https://www.etsi.org/technologies-clusters/technologies/internet-of-things/smart-metering>
11. <https://www.britishgas.co.uk/smart-home/smart-meters.html>
12. <https://www.elster-instromet.com/en/smart-metering#sbox5239=sbox52390>
13. [www.suntront.com](http://www.suntront.com)

**SECTION**

**GEOLOGY AND PROSPECTING OF MINERAL AND  
ENERGY RESOURCES**

## BIOMARKERS ASSEMBLAGE OF UNBURNED COAL PARTICLES IN FLY ASHES FROM BULGARIAN THERMOELECTRIC POWER PLANTS

**Denitsa Apostolova<sup>1</sup>, Achim Bechtel<sup>2</sup>, Irena Kostova<sup>1</sup>, Maya Stefanova<sup>3</sup>**

<sup>1</sup>Sofia University „St. Kliment Ohridski“, 1504 Sofia, Bulgaria; [dapostolova@gea.uni-sofia.bg](mailto:dapostolova@gea.uni-sofia.bg); [irenko@gea.uni-sofia.bg](mailto:irenko@gea.uni-sofia.bg)

<sup>2</sup>University of Leoben, A-8700 Leoben, Austria; [achim.bechtel@unileoben.ac.at](mailto:achim.bechtel@unileoben.ac.at)

<sup>3</sup>Institute of Organic Chemistry with Centre of Phytochemistry, Bulgarian Academy of Sciences, 1113 Sofia, Bulgaria; [maia@orgchm.bas.bg](mailto:maia@orgchm.bas.bg)

**ABSTRACT.** The study aimed to assess the occurrence and composition of biomarkers in fly ashes emitted during lignite, subbituminous and bituminous coal combustion in four Bulgarian thermoelectric power plants (TPPs). A protocol for isolation, fractionation and identification of organic components in extractable organic matter was applied. Gas chromatography–mass spectrometry was used to assess organic matter sources. Data for biomarkers were quantitatively interpreted and expressed in  $\mu\text{g/gTOC}$ . Several groups of organic compounds were identified, i.e. sesquiterpanes, diterpanes, triterpanes and hopanes. Only in fly ashes from TPPs feed by lignite and subbituminous coal hopanes were registered. Their patterns of distributions were characterized by the presence of  $\alpha\beta$  and  $\beta\beta$  hopane, from C27 to C31. The predominance of  $\alpha\beta$  hopanes has indicated geochemically mature organic matter. The diterpenoids were mainly represented by cyclic hydrocarbons with beyerane, abietane and phyllocladane skeleton. Triterpanes were represented by structures typical for terrestrial vegetation, i.e. oleanane, ursane, and lupane types. The cyclic aliphatic and aromatic compounds (biomarkers) in the extracts of fly ash represent a complex mixture of compounds of different origins: - from the feed coal (petrogenic source); and, compounds formed during combustion (pyrolytic source).

**Keywords:** fly ashes, gas-chromatography–mass spectrometry, biomarkers

### СЪСТАВ НА БИОМАРКЕРИТЕ ОТ НЕИЗГОРЕЛИ ВЪГЛИЩНИ ЧАСТИЦИ В ЛЕТЛИВИ ПЕПЕЛИ ОТ БЪЛГАРСКИ ТОПЛОЕЛЕКТРИЧЕСКИ ЦЕНТРАЛИ

**Деница Апостолова<sup>1</sup>, Ахим Бехтел<sup>2</sup>, Ирена Костова<sup>1</sup>, Мая Стефанова<sup>3</sup>**

<sup>1</sup>Софийски университет „Св. Климент Охридски“, 1504 София

<sup>2</sup>Минен университет, А-8700, Леобен, Австрия

<sup>3</sup>Институт по органична химия с център по фитохимия, Българска академия на науките, 1113 София

**АБСТРАКТ.** Цел на изследването е да се определи състава на биомаркерите в летливи пепели от изгарянето на лигнитите, кафяви и черни въглища в четири български топлоелектрически централи (ТЕЦ). Приложен е системен ход за изолиране, фракциониране и идентифициране на органични компоненти в екстрахируемото органично вещество /ЕОВ/. За оценка на състава на биомаркерите е приложен газхроматографски – масспектрален анализ (GC-MS). Данните са количествено интерпретирани и представени в  $\mu\text{g/gTOC}$ . Установени са следните групи органични съединения: сескитерпеноиди, дитерпеноиди, тритерпеноиди, хопаноиди и др. Хопаноиди присъстват само в пробите от ТЕЦ, изгарящи лигнити и кафяви въглища. Техните модели на разпределение се характеризират с присъствието на хопани в интервала от C<sub>27</sub> до C<sub>31</sub>  $\alpha\beta$  и  $\beta\beta$  конфигурация. Преобладаване на  $\alpha\beta$  хопани е типично за зряло органично вещество. Дитерпеноидите са представени главно от циклични въглеводороди с абиетанов, байеранов и филокладанов тип скелетна структура. Установени са тритерпеноиди съдържащи структури от олеананов, урсанов и лупанов тип, които са характерни биомаркери за сухоземна растителност. Регистрираните в ЕОВ от летливи пепели циклични, алифатни и ароматни съединения (биомаркери), представляват сложна смес от съединения с различен произход: от първичните въглища (петрогенен източник); и/или съединения, образувани по време на изгарянето им (пиролитичен източник).

**Ключови думи:** летливи пепели, газова хроматография-масспектрометрия, биомаркери

### Introduction

Coal is still the primary energy source in Bulgaria. It has been estimated that in the country production of coal ash from only coal fired power plants exceeds 10.4 Mt of solid combustion wastes and the storehouses hold more than 300 Mt ashes and slag. The huge part of coal mineral fraction is collected in cyclones (fly ash) to be stored in waste dumps or reused in building industry or landfilling. Because of this it is very important to know more details about their technological features and geochemical characteristics.

Coal ash can contain organic compounds deriving from parent coal or formed in burning process (Bailey,1992). There

are few studies reported for relatively low amounts of carbon in fly ash from coal-fired power plants (Goodarzi et al., 2002; 2005) while ash from domestic combustion contain higher amounts (Den Boer et al., 2010). Characterization of unburned carbon in fly ashes has been shown to contribute to the assessment of the possible impact of organic matter on human health and the environment.

Many compounds such as n-alkanes, acyclic isoprenoids, sesquiterpenoids, diterpenoids, steranes, tri- and pentacyclic triterpanes were established as markers of organic matter sources in coal fly ashes (Misz et al., 2007; Fabianska and Smolka-Danielowska, 2012; Ribeiro et al., 2014; Fabianska et al., 2017; Kostova et al., 2020).

The aim of the present study is to assess the occurrence and composition of biomarkers in fly ashes emitted during lignite, subbituminous and bituminous coal combustion in four Bulgarian thermoelectric power plants (TPPs).

## Materials and Methods

The fly ashes from four TPPs in Bulgaria burning coals of different rank were investigated: lignites from Maritza East-2 (ME-2) and Maritza East-3 (ME-3) TPPs, subbituminous coal for Republika TPP and bituminous coals from Russe TPP. Fly ash samples were collected at each row of the electrostatic precipitators (ESPs) of Republika, and Russe TPPs. From ME-2 and ME-3 TPPs bulk ("average") samples were studied.

The total organic carbon (TOC) determination was done by an Eltra Helios C/S analyzer on samples preliminary pretreated with H<sub>3</sub>PO<sub>4</sub>. Measurements were in duplicate, with analytical error < 5% for the respective concentrations.

The molecular compositions of feed coals and fly ashes hydrocarbons were determined by a protocol developed previously in the study of biomarker assemblages and PAHs in different rank Bulgarian coals (Apostolova et al., 2017). Briefly, ca: 5 g were extracted by dichloromethane, 1 h at 75°C and a pressure of 75 bar in a Dionex ASR 200 instrument. Asphaltenes were separated and hexane-soluble organic compounds (maltenes) were sub-divided into saturated (I fr.) and aromatic (II fr.) hydrocarbons and polar compounds using a Willsch MPLC (medium pressure liquid chromatography) instrument. Herein the saturated and aromatic hydrocarbon fractions were analyzed by a gas chromatography-mass spectrometer (GC-MS) Finnigan MAT GCQ, equipped with a DB-5MS silica

capillary column (30 m x 0.25 mm x 0.25µm), 70–300°C with steps of 4°C/min, followed by an isothermal period of 15 min. The device was set in EI mode with a scan rate of 50–650 Daltons (0.7 s/scan). The absolute concentrations were determined using deuterated tetracosane and 1,1'-binaphthyl as internal standards, respectively. Results were normalized to µg/gTOC.

## Results and Discussions

In a previous study n-alkanes present in industrial coal-derived fly ashes from the same set of samples were investigated (Kostova et al., 2020). In this study, changes in the distribution patterns of biomarker during combustion have been outlined. For lower rank coals the extraction yields of fly ashes (FAs) were high, all dominated by polar components. In fly ashes derived from the combustion of higher rank coals, extractable organic matter (EOM) were an order of magnitude lower with a considerable portion of neutral compounds (Table 1). A strong correlation ( $R^2=0.9991$ ) between TOC and C content was estimated (Kostova et al., 2020).

With the present study we complement the existing information on the composition of fly ash EOM. In all extracts aliphatic hydrocarbons strongly predominated over aromatic components. Beside n-alkanes, the dominant components in the neutral fractions, a broad range of biomarkers was found. The following compound groups, derived from feed coals lignite, subbituminous and bituminous coal, were identified in the EOM of the fly ashes (FAs): sesquiterpenoids (Sesqui-Ts), diterpenoids (DTs), triterpenoids (TTs) and hopanes (Hs) (Figure 1). Only in FAs from TPPs feed by lignite and subbituminous coals Hs were identified (Table 2).

Table 1. Characteristics of EOM of FAs (according Kostova et al., 2020)

TPP	ESP row	Yield		Fractional composition, %			
		mg/gTOC	wt.%	I fr.**	II fr***	III fr.****	Asph.
ME-2	avr. *	8.88	0.0121	7.8	1.0	83.4	7.8
ME-3	avr.	2.74	0.0103	35.7	11.9	51.2	1.2
Republika	I	7.27	0.0088	5.4	9.5	70.3	14.8
	II	15.05	0.0102	25.8	11.8	42.4	20.0
	III	19.87	0.0117	13.1	1.0	77.8	8.1
Russe	I	0.8	0.0145	21.8	1.8	59.8	16.6
	II	1.91	0.0308	37.9	1.5	45.7	14.9
	III	0.23	0.0154	28.0	0.6	55.0	16.4

\*average sample; \*\* neutral; \*\*\* aromatic; \*\*\*\* polar

Table 2. Biomarkers assemblage of EOM of fly ashes (µg/g TOC)

TPP	ESP row	Sesqui-Ts	DTs	TTs	Hs	H <sub>ββ</sub>	H <sub>αβ</sub>	Ratio H <sub>ββ</sub> / H <sub>αβ</sub>	Hop-(17,21)-en
ME-2	avr.	2.00	70.21	0.37	2.08	0.47	1.60	0.29	0.49
ME-3	avr.	2.76	104.93	3.25	4.99	1.82	3.17	0.57	1.93
Republika	I	0.30	14.98	-	1.71	0.70	1.01	0.69	0.00
	II	45.88	205.53	-	17.83	3.09	14.74	0.21	0.00
	III	5.78	273.82	-	13.62	1.99	11.64	0.17	1.12
Russe	I	0.70	2.40	0.23	-	-	-	-	-
	II	2.53	1.18	0.11	-	-	-	-	-
	III	0.06	0.40	0.03	-	-	-	-	-

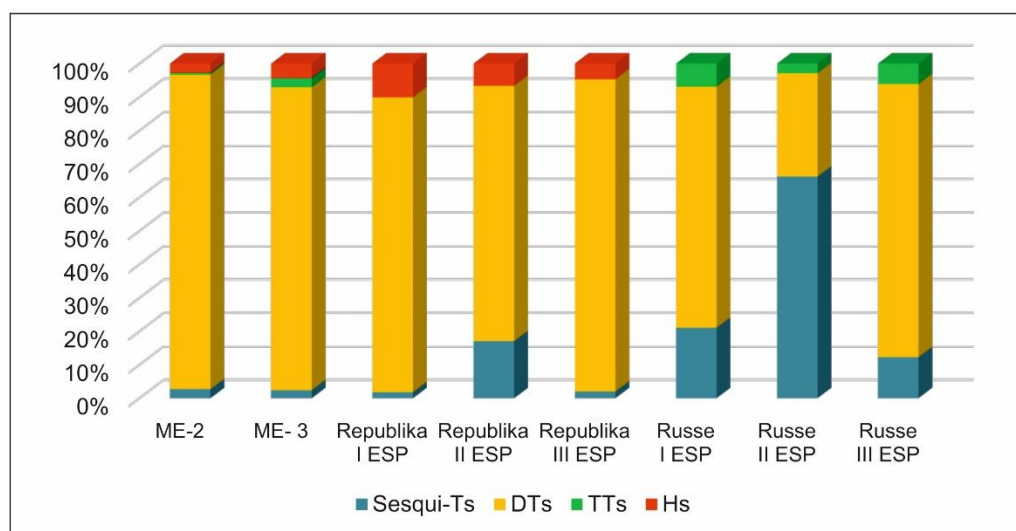


Figure 1. Distribution of the biomarkers in EOM of fly ashes, studied, in rel.%

Saturated and monounsaturated sesqui-Ts, including the C14 and C15 compounds, related to the cadinene, eudesmane and drimane types were identified. Aromatic sesqui-Ts were dominated by curcumene, cuparene, cadalene and isocadalene structures. In most samples cadalene, C15H18, predominate over the other aromatic sesqui-Ts.

Di-Ts in the samples were represented mainly by hydrocarbons with beyerane, abietane and phyllocladane type skeleton. Their amounts in EOM of FAs were found to be higher for subbituminous and lignite and lower for bituminous coal (Table 2). The following Di-Ts were identified in the non-aromatic hydrocarbon fractions of EOM: norpimarane, beyerane, pimarane,  $\alpha$ -phyllocladane, abietane and  $\beta$ -phyllocladane. The  $\alpha$ -phyllocladane has been usually found in conifers except of Pinaceae (ten Haven et al., 1992) and was regarded as a typical biomarker of Araucariaceae, Cupressaceae, and Taxodiaceae. In all samples studied, the aromatic tricyclic Di-Ts, i.e. norabietatriene, dehydroabietane, simonellite, retene and methyl retene were identified. Simonellite was the dominant aromatic Di-T in the FAs from TPPs feed by subbituminous coal.

Non-hopanoid TTs were found in very low amount only in FAs from TPPs feed by lignite and bituminous coals. TTs containing the structures typical of the oleanane, ursane, or the lupane type derivatives were considered as biomarkers for angiosperms (Karrer et al., 1977). Compounds of these series were identified in the saturated and aromatic hydrocarbon fractions. They included des-A degraded and pentacyclic TTs of oleanane-, ursane-, and lupane-types.

Only in FAs from TPPs feed by lignite and subbituminous coal hopanes were registered. Their patterns of distributions were characterized by the presence of  $\alpha\beta$  and  $\beta\beta$  hopane (H), in the range from C27 to C31. The predominance of  $\alpha\beta$ -H indicates geochemically mature organic matter. C28 was not detected. Hop-17(21)-ene was detected in high amounts in the EOM from ME-2 TPP, ME-3 TPP and Republika TPP, III ESP row, consistent with the low rank of the feed coal. In contrast to the ratio of  $17\beta$ (H), $21\beta$ (H)-hopanes to  $17\alpha$ (H), $21\beta$ (H)-hopanes ( $H\beta\beta/H\alpha\beta$ ) found in ME feed coal ( $\geq 1$ ), in FAs ratios  $\leq 1$  were obtained, a hint for serious modification in hopanes distributions induced by combustion.

$18\alpha$ (H)-22,29,30-trisnorhopane (Ts) and  $17\alpha$ (H)-22,29,30-trisnorhopane (Tm) were absent. In all samples studied moretanes were not registered. During maturation moretanes were transformed in  $\alpha\beta$ -hopanes and finely disappeared from coal extracts or oils (Peters et al., 2005; Misz et al., 2007).

The absence of steranes and high content of DTs in all EOM indicate that, most of the organic matter present in the fly ashes reflects their biogenic origin and depositional environment. DTs were indicators for conifer input into sedimentary organic matter (Noble et al., 1985; Otto and Simoneit, 2001). They were registered in feed coals from Maritza East and Pernik basins (Dodova-Angelova et al., 1985; Stefanova et al., 2002; Bechtel et al., 2005; Stefanova et al., 2016; Apostolova et al., 2016; Atanassova et al., 2017).

Geochemical features of the EOM studied have indicated a mixture of compounds derived from feed coals and combustion products (Fabianska and Danielowska, 2012). The biomarkers common in most humic coals and kerogen-type III (terrestrial organic matter), was described for coals from the Maritza East and Pernik coal basins. However, hopanes distributions were seriously altered by combustion. The strong dominance of  $\beta\beta$ -hopanes characteristic for the feed coals of Maritza East basin has disappeared and was replaced by considerable amounts of  $\alpha\beta$  stereoisomers.

## Conclusion

Several coal biomarkers were found to be well preserved in EOM of unburned coal in FAs from four Bulgarian TPPs. The study has demonstrated that the distributions of aliphatic components in FAs generated during combustion of lignite, subbituminous and bituminous coal show a significant similarity to feed coal. For compounds registered in the EOM of coal-derived fly ashes two origins were distinguished: compounds from the feed coal and components formed in combustion process or with thermal-induced changes in stereochemistry.

In conclusion, EOM biomarker assemblages kept the features of the feed coals. Thus, they could be successfully used in surveys for potential pollutants in the environment.

**Acknowledgements:** This study was supported by the Bulgarian National Science Fund in the framework of Project KP-06-H34 / 5. 12. 2019.

## References

- Apostolova D, A. Bechtel, K. Markova, I. Kostova. 2017. "Biomarker composition and PAHs characteristics of Bulgarian coals with different rank and origin", *C.R. Acad. Bulgare des Sciences*, 217, 243-252.
- Apostolova, D., A. Bechtel, K. Markova, I. Kostova. 2016. Geochemical characterization of organic matter in subbituminous coals from the Pernik basin, Bulgaria. – In: Proceedings of the National Conference of the Bulg. Geol. Soc., GEOSCIENCES 2016, 49-50.
- Atanassova I., B. Hristov, T. Shishkov. 2017. Lipid biomarkers and their environmental significance in mine soils from Eastern Europe. *Archives of Agronomy and Soil Science*, 63 (2), 1697-1710.
- Bailey J.G. 1992. The origin of unburnt combustibles in coal. The University of Newcastle, NSW, Unpublished Ph.D. Thesis.
- Bechtel A., R. F. Sachsenhofer, A. Zdravkov, I. Kostova, R. Gratzner. 2005. Influence of floral assemblage, facies and diagenesis on petrography and organic geochemistry of the Eocene Bourgas coal and the Miocene Maritza-East lignite (Bulgaria), *Organic Geochemistry*. 2005, (36), 1498–1522.
- Den Boer E, A. Jedrczak, Z. Kowalski, J. Kulczycka, R. Szpadt. 2010. A review municipal solid waste composition and quantities in Poland. *Waste Manage*, 30, 369–377.
- Dodova-Angelova, M. S., D. Roushev, S. Malovska. 1985. Content and composition of the alkanes and alk-1-enes isolated from various solid fuels. *Fuel*, 64, 313-315.
- Fabiańska, M.J., B. Kozielska, J. Koniecznyński. 2017. Differences in the Occurrence of Polycyclic Aromatic Hydrocarbons and Geochemical Markers in the Dust Emitted from Various Coal-Fired Boilers, *Energy & Fuels* 31, 2585-2595.
- Fabiańska, M.J and D. Smólka-Danielowska. 2012. "Biomarker compounds in ash from coal combustion in domestic furnaces", *Fuel*, 102, 333-344.
- Goodarzi F. 2005. Petrology of subbituminous feed coal as guide to capture of mercury by ESP –Influence of depositional environment. *Int J Coal Geol*, 61,1–12
- Goodarzi F, W.P. Peel, J. Brown, J.P Charland, F. Huggins, J. Percival. 2002. Elemental concentration and speciation, polyaromatic hydrocarbons and mineralogical characteristics of milled-coal and ashes from the Unit #5 at Battle River Station. *Bull Geol Surv Canada*, 57, pp 148.
- Karrer W., E. Cherbuliez, C.H. Eugster. 1977. Konstitution und Vorkommen der organischen Pflanzenstoffe, Ergänzungsband I., Basel, Stuttgart, Birkhäuser, pp. 1038.
- Kostova I, D. Apostolova. M. Stefanova. (in press). Geochemical features of unburned coal particles in fly ashes from thermal power plants in Bulgaria. 6<sup>th</sup> World Multidisciplinary Earth Sciences Symposium (WMESS 2020), 7-11 September 2020, Prague, Czech Republic.
- Misz M, M. Fabiańska M, Cmiel S. 2007. Organic components in thermally altered coal waste: preliminary petrographic and geochemical investigations. *International Journal of Coal Geology*, 71, 405–24.
- Noble, R.A., R.M. Alexander, R.I. Kagi, J. Knox, J. 1985. Tetracyclic diterpenoid hydrocarbons in some Australian coals, sediments and crude oils. *Geochimica et Cosmochimica Acta*, 49, 2141–2147.
- Otto, A., B. R. T. Simoneit. 2001. Chemosystematics and diagenesis of terpenoids in fossil conifer species and sediment from the Eocene Zeitz formation, Saxony, Germany. *Geochimica et Cosmochimica Acta* 65, 3505–3527.
- Peters, K.E., C.C Walters, J.M Moldowan 2005. The Biomarker Guide. Biomarkers and Isotopes in Petroleum Exploration and Earth History, 2nd ed. Cambridge University Press. pp 1155.
- Ribeiro J, T.F. Silva, J.G. Mendonça Filho, D. Flores. 2014. Fly ash from coal combustion – An environmental source of organic compounds. *Applied Geochemistry*, 44,103–110.
- Stefanova M, B.R.T.Simoneit, S. P. Marinov. A. Zdravkov, J. Kortenski. 2016. Novel polar biomarkers of the Miocene Maritza-East lignite, Bulgaria. *Organic Geochemistry*, 96,1-10
- Stefanova, M. 2005. Tetramethylammonium hydroxide (TMAH) thermochemolysis of some "Maritza-East" lignite lithotypes. *Bulgarian Chemical Communications*, 37, 93–99.
- Stefanova, M., D. R. Oros, A. Otto, B.R.T. Simoneit. 2002. Polar aromatic biomarkers in the Miocene Maritza-East lignite, Bulgaria. *Organic Geochemistry*, 33,1079–1091.
- Ten Haven H. L., T.M. Peakman, J. Rullkötter. 1992. Early diagenetic transformation of higher-plant triterpenoids in deep-sea sediments from Baffin Bay. *Geochimica et Cosmochimica Acta*, 56, 2001–2024.

## SYNTHESIS, BIOFUNCTIONALIZATION AND APPLICATION OF GOLD NANOPARTICLES

**Aleksandar Chanachev**

University of Mining and Geology "St. Ivan Rilski", 1700 Sofia; a.chanachev@mgu.bg

**ABSTRACT.** Gold nanoparticles (AuNPs) have specific chemical and physical properties, which make them suitable drug carriers and allow them to be used in various fields of biology, medicine, pharmacy and environment monitoring. In the last 30 years, with the rapid development of nanotechnologies, scientists have found an increasing number of applications of AuNPs and improved methods for their synthesis and characterization. The mechanisms of their formation and growth, as well as in their biofunctionalization, for example with proteins, are of increasing interest, which allows the study of various enzyme-catalytic processes.

**Key words:** gold nanoparticles, biofunctionalization, sensors

### СИНТЕЗ, БИОФУНКЦИОНАЛИЗИРАНЕ И ПРИЛОЖЕНИЕ НА ЗЛАТНИ НАНОЧАСТИЦИ

**Александър Чаначев**

Минно-геоложки университет „Св. Иван Рилски“, 1700 София

**РЕЗЮМЕ.** Златните наночастици имат специфични химични и физични свойства, които ги правят подходящи лекарствени носители и позволяват да бъдат използвани в редица области на биологията, медицината, фармацията и мониторинга на околната среда. През последните 30 години, с бързото развитие на нанотехнологиите, учените намират все по-голям брой приложения на златните наночастици и подобряват методите за тяхното получаване. Все по-голям интерес представляват и механизмите на тяхното формиране и растеж, както и в биофункционализирането им, например с протеини, което позволява изучаването на различни ензимо-каталитични процеси.

**Ключови думи:** златни наночастици, биофункционализиране, сензори

### Introduction

Gold nanoparticles have peculiar chemical and physical properties, that make them appropriate drug carriers and allows them to be used in diverse fields of biology, medicine and pharmacy, environment protection.

Gold nanoparticles can be functionalized with a large number of organic or biological ligands for selective binding and serve to determine the presence and concentration of small molecules and biological objects (R. Pool, 1990). The color of gold nanoparticles is very sensitive to the degree of their aggregation in suspension (H. Li, L. Rothberg, J, 2004).

Methods for the synthesis of gold nanoparticles make it possible to obtain nanosized objects of different sizes, which is essential for their further use in various fields of chemistry, biology, pharmacy, medicine and environment monitoring and protection. For example, AuNPs can be used at detection of phenolic compounds, which is important because they have extremely hazardous impact and poor environmental degradation (Nusiba Mohammed Modawe Alshik Edrisab, Yusran Sulaiman, 2020).

The characterization of gold nanoparticles is an essential issue for a better understanding of their properties and nature. Among the most commonly used methods for their characterization are UV-vis spectroscopy, Transmission electron microscopy (TEM) and Atomic force microscopy (AFM). They allow us to monitor both their specific properties such as surface plasmon resonance and to obtain sufficient information about the size of individual particles, their shape

and distribution. Due to the important relationship between particle size and their properties, methods for characterizing gold nanoparticles that have been synthesized are essential in conducting experiments with them.

The paper presents the most important and widely applied methods for AuNPs synthesis and analysis, as well as the AuNPs applications.

### Historic preparation of AuNPs

Gold nanoparticles have been known to humans since antiquity. They were obtained probably in a purely empirical way and this can be confirmed by the found and preserved objects from different historical periods.

Among the most famous and well-preserved objects from antiquity is probably the cup of a Lycurgus. It is an exquisite object of Roman art, which was made around the 4th century AD. During its manufacture in the glass small amounts of gold and silver nanoparticles were dispersed in a certain proportion, which created an interesting optical effect - if through the glass no light passes, the cup is green, but when a ray of light passes through it, it turns red.

The first scientifically documented production of colloidal gold belonged to the English physicist M. Faraday. In 1857 he conducted a series of experiments based on the use of gold hydrosols, which were prepared by reducing aqueous solutions of chloroauric acid (HAuCl<sub>4</sub>) with phosphorus dissolved in carbon disulfide (M. Faraday, 1857).

A large number of methods for the synthesis of colloidal gold have been developed - the Turkevich method, the Brust method, the Navarro method, etc., each of which allows to obtain particles with different stability. These methods can be conditionally - according to the time in which they were created, divided into classical and new (modern).

Turkevich created one of the most famous syntheses of gold nanoparticles. His method is based on citrate reduction of carbon tetrachloric acid in an aqueous medium (J. Turkevich et al., 1951). Citrate anions have both the role of reducing and stabilizing agent. This type of colloidal gold production was first developed by Hauser and Lynn and later modified by Turkevich (Hauser and Lynn, 1940). Figure 1 shows a scheme of citrate synthesis.

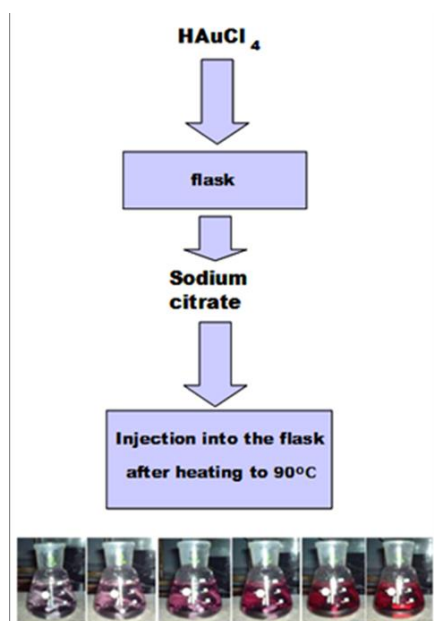


Fig. 1 Scheme of Au nanoparticle synthesis by the citrate method.

The Turkevich method is a relatively simple synthesis in which 10 ml of a  $\text{HAuCl}_4$  solution containing 5 mg of Au is carefully added to 85 ml of boiling distilled water ( $100^\circ\text{C}$ ). When the mixture is refluxed, 5 ml of 1% sodium citrate solution are added. The reaction mixture was stirred continuously with a magnetic stirrer. The synthesis is completed after about 30 min. It produces spherical nanoparticles of gold that have an average diameter of about 20 nm.

### Nowadays preparation of AuNPs

Due to the scientific interest in obtaining gold nanoparticles, the methods for their synthesis are numerous. These methods can differ both in the synthesis procedure itself and in the average size of the obtained gold nanoparticles, as well as in the possibilities of the method itself to obtain particles similar in size and shape in their entire volume. Many ideas for the synthesis of gold nanoparticles can be mentioned, and to illustrate the basic principles by which such suspensions are obtained, we can consider the following procedures:

#### Golden sol of Faraday

This method is based on the interaction between a solution of  $\text{HAuCl}_4$ , a saturated solution of white phosphorus in diethyl ether and a solution of KOH. The color of the solution changes, first to brown, then gray, purple and red. In this synthesis, the average diameter of the nanoparticles is 5 nm. (J. Perez-Juste et al, 2005).

#### Donau golden sol

This synthesis consists in passing gaseous  $\text{CO}_2$  through a solution of  $\text{HAuCl}_4$ . The solution turns purple. The diameter of the nanoparticles is about 20 nm. (J. Perez-Juste et al, 2005, 2005).

#### Acetylene gold sol

In this method, a solution of  $\text{HAuCl}_4$  is treated with an aqueous solution of acetylene. A pink color appears in about 20 seconds, and in 2 minutes the solution turns dark red. The diameter of the nanoparticles is about 29 nm. (J. Perez-Juste et al, 2005)

#### Golden sol with citric acid.

This approach consists of preparing a  $\text{HAuCl}_4$  solution and then heating it to boiling. A solution of citric acid is added to it, a dark blue to red color is observed. The diameter of the nanoparticles is about 50 nm.

#### The fungal gold nanoparticles synthesis

An excellent example of eco-friendly synthesis of gold nanoparticles is the fungal gold nanoparticles synthesis. Its essence is that AuNPs with 20 nm diameter were synthesized on the fungal surface and the cytoplasmic membrane of the fungal mycelium (Kalishwaralal Kalimuthu et al., 2020).

#### Marine alga synthesis

In this approach, the synthesis is carried out by algal cells with absorption at around 540 nm. The average size of gold nanoparticles is about 15 nm (Kalishwaralal Kalimuthu et al., 2020).

#### Bacteria synthesis

It is known that just a few groups of bacteria can selectively reduce metal ions. In this approach it is observed intracellular synthesis of AuNPs. Different morphologies – cubic, hexagonal, and spherical – with particles size in the range in the range of 5–200 nm were reported by using sulfate-reducing bacteria (Kalishwaralal Kalimuthu et al., 2020).

These methods make it possible to obtain particles of different sizes, and in the volume of the solution these particles can be both relatively similar in shape and not so homogeneous. Due to the search for solutions that have the largest possible number of identical particles in their volume (size and shape), the synthesis methods that are chosen to prepare AuNPs used as sensors for enzyme activity or in the development of drug carriers should be able to a large extent to ensure the production of homogeneous particles. This provides a good opportunity to study different biological systems, as well as to create good physicochemical models to explain the behavior and formation of gold nanoparticles, their behavior on different boundary surfaces or in the bulk phase.

#### AuNPs application

The advantages of nanoparticles that distinguish them from bulk materials are mainly in their specific chemical and

physical properties. For example, gold nanoparticles have a specific characteristic absorption maximum at 520 nm, which is due to their surface plasmon resonance, and this provides an excellent opportunity for them to be functionalized with proteins, such as antibodies, proteins attached to them, and the like. This facts are widely used in medicine as a therapeutic agent in targeted drug delivery systems.

The aggregation of Au nanoparticles with certain dimensions ( $d > 3.5$  nm) is a result of the interaction between the surface plasmons of individual nanoparticles, as a result of which a change in their color from red to blue is observed (S. Srivastava et al., 2005). This color change of Au nanoparticles leads to their successful application as absorption-based colorimetric sensors for an analyte that causes aggregation of Au nanoparticles (R. R. Liu et al., 2007). This type of use of gold nanoparticles as sensors starts a new and distinct scientific field in which they can find opportunities for research and be used to solve various biological, analytical, biochemical and medical problems.

Gold nanoparticles are objects that can be functionalized with a wide range of organic or biological ligands for selective binding and serve to determine the presence and concentration of small molecules and biological objects. They can be used as drug carriers or in monitoring the catalytic activity of enzyme-catalytic chemical reactions.

The preparation of stable suspensions of protein-modified gold nanoparticles is a prerequisite for their use as an analytical procedure for colorimetric analysis. In recent years, colorimetric studies based on surface plasmon resonance of metal nanoparticles have received special attention due to their simplicity, sensitivity and low cost. Spherical gold nanoparticles are used to detect biomolecules on the principle of aggregation-induced red to blue color change. The ability of gold nanoparticles to retain biomolecules is a major advantage for their use as biosensors.

In recent decades, the development of medicine has been directly linked to the search for new chemical approaches for the diagnosis and treatment of various diseases. Attaching molecules of a particular protein to the surface of various nanostructured materials, as well as nanosized objects (quantum dots, nanoparticles, etc.) is an efficient way to improve their stability and a good opportunity to create particles for targeted delivery of drug carriers, as well as other functional properties. Therefore, biofunctionalized protein nanomaterials are widely used in modern pharmaceutical technologies for the transport of dosage forms, as well as for biocatalysis.

Nanoscale objects that are close to the dimension of biological units, as well as their easy synthesis, relatively large surface area and easy functionalization make them particularly interesting for achieving various biological goals, such as tissue engineering and regenerative medicine.

Gold nanoparticles can be used effectively for environmental monitoring. Gold nanoparticles- Biphenyl-4,4'-dithiol and AuNPs- p-Terphenyl-4,4"-dithiol with size 6–8 nm were deposited onto quartz fibres and used as adsorbent materials for the detection of total gaseous mercury, both indoor for adsorption studies, at defined concentrations and outdoor, at the vapour mercury concentration of the environmental countryside (Andrea Bearzotta et al., 2018).

## Conclusion

Gold nanoparticles have been known to humans since ancient times and their specific properties have attracted their attention. With the development of chemistry, various methods for their synthesis gradually began to appear, and in the last three decades their study has become an increasingly interesting issue for science. This is due to their properties, which make them excellent drug carriers, allow them to be used in the diagnosis of various diseases, as well as various other applications in the natural sciences and the environment protection. Their biofunctionalization is an important step for the implementation of these tasks and is carried out by covering the surface of gold nanoparticles with various proteins.

This makes gold nanoparticles an increasingly evolving field of research that will be increasingly used mainly in pharmacy and medicine, but also in biology and the environmental monitoring.

## References

- Andrea Bearzotta, Paolo Papaab, Antonella Macagnanoa, Emiliano Zampettialole, Vendittid Raoul, Fioravantib, Laura Fontanab, Roberto Matassac, Giuseppe Familiaric, Ilaria Fratoddi. 2018. Environmental Hg vapours adsorption and detection by using functionalized gold nanoparticles network - *Journal of Environmental Chemical Engineering*, 6, 4, 4706-4713.
- Hauser and Lynn. 1940. Experiments in Colloid Chemistry - *McGraw Hill*, p. 18.
- H. Li, L. Rothberg, J.. 2004. Label-Free Colorimetric Detection of Specific Sequences in Genomic DNA Amplified by the Polymerase Chain Reaction - *Am. Chem. Soc.*, 126, 10958-10961
- J. Turkevich, P. Stevenson, J. Hillier. 1951. A study of the nucleation and growth processes in the synthesis of colloidal gold - *Discuss. Faraday Soc.*, 11, 55-75.
- Kalishwaralal Kalimuthu, Byung SeokCha, Seokjoon Kim, Ki SooPark. 2020. Eco-friendly synthesis and biomedical applications of gold nanoparticles: A review - *Microchemical Journal*, 152, 104296
- M. Faraday. 1857. Experimental relations of gold (and other metals) to light. - *Philos. Trans. R. Soc.*, London, 147-14.
- Nusiba Mohammed Modawe Alshik Edrisab, Yusran Sulaiman. 2020. Ultrasensitive voltammetric detection of benzenediol isomers using reduced graphene oxide-azo dye decorated with gold nanoparticles - *Ecotoxicology and Environmental Safety*, 203, 111026
- R. Pool. 1990. Clusters: Strange Morsels of Matter *Science*, 248 (4960), 1186-8
- R. R. Liu, R. S. Liew, H. Zhou, B. G. Xing. 2007. A simple and specific assay for real-time colorimetric visualization of beta-lactamase activity by using gold nanoparticles - *Angew. Chem.*, Int. Ed. 46, 8799.
- S. Srivastava, B. L. Frankamp, V. M. Rotello. 2005. Controlled Plasmon Resonance of Gold Nanoparticles Self-Assembled with PAMAM Dendrimers - *Chem. Mater.*, 17, 487.
- J. Perez-Juste, I. Pastoriza-Santos, L. M. Liz-Marzan, P. Mulvaney. 2005. Gold nanorods: Synthesis, characterization and applications -*Coord Chem. Rev.* 249, 1870.

## METHODOLOGY OF MAPPING AND DIGITALIZATION OF $V_{s\_30}$ FOR THE SEISMIC HAZARD ASSESSMENT IN BIG CITIES

**Bozhurka Georgieva<sup>1</sup>, Boyko Rangelov<sup>1</sup>, Dimo Solakov<sup>2</sup>, Stefan Dimovsky<sup>1</sup>, Atanas KisyoV<sup>1</sup>**

<sup>1</sup>University of Mining and Geology "St. Ivan Rilski", 1700 Sofia; bojurkageorgieva97@abv.bg

<sup>2</sup>National Institute of Geophysics, Geodesy and Geography, Bulgarian Academy of Sciences, 1113 Sofia; dimos@geophys.bas.bg

**ABSTRACT.** This publication presents the data sources, methodology, digitalization and mapping of the soil ground conditions reflected by the parameter  $V_{s\_30}$ . This parameter is an integral characteristic of the ground conditions used in almost all procedures of the seismic hazard mapping software. The  $V_{s\_30}$  means the velocity of the transverse seismic waves to the depths of 30 meters of the ground layers measured from the ground surface. It depends of many factors like density and type of rocks and sediments, ground waters level, the seismic wave's velocity propagation, etc. and modifying the influence of the seismic waves to the structures located on the surface. This influence is measured by observed intensity, registered seismic acceleration and other dynamic parameters affected the built structures located on earth's surface. The methodology used a lot of archive data, because in situ measurements are difficult, frequently impossible to be done due to the intensive build environment of the big cities. The digitalization of this parameter is the main task solved for several big cities of Bulgaria intended to the seismic hazard and risk assessment. Examples of the solutions are presented.

**Keywords:**  $V_{s\_30}$ , ground conditions, seismic hazard

## МЕТОДОЛОГИЯ ЗА КАРТИРАНЕ И ДИГИТАЛИЗАЦИЯ НА $V_{s\_30}$ ЗА ОЦЕНКА НА СЕИЗМИЧНАТА ОПАСНОСТ ЗА ГОЛЕМИ ГРАДОВЕ

**Божурка Георгиева<sup>1</sup>, Бойко Рангелов<sup>1</sup>, Димо Солаков<sup>2</sup>, Стефан Димовски<sup>1</sup>, Атанас Кисъов<sup>1</sup>**

<sup>1</sup>Минно-геоложки университет „Св. Иван Рилски“, 1700 София

<sup>2</sup>Национален институт по геофизика, геодезия и география, Българска академия на науките, 1113 София

**РЕЗЮМЕ.** Публикацията представя източниците на данни, методологията, дигитализацията и картирането на грунтовете повърхностни условия, отразени в параметъра  $V_{s\_30}$ . Този параметър представлява интегрална характеристика на повърхностния грунтов слой и се използва в почти всички софтуерни програми за оценка на сеизмичната опасност. С него се означава стойността на скоростта на вторичните сеизмични вълни до дълбочини 30 метра. Зависи от много фактори – вид на скалите и седиментите, здравина на земната основа, ниво на грунтовете води, и др. и демонстрира модифициращите свойства на грунта върху скоростта на разпространение на сеизмичните вълни и тяхното въздействие върху построеното на повърхността. Това влияние се отразява върху наблюдаваната сеизмична интензивност, регистрираното ускорение на вълните и други техни динамични параметри. Методологията използва много архивни данни, поради невъзможността да бъдат правени *in situ* измервания, което се дължи на интензивното застрояване в големите градски агломерации.

**Ключови думи:**  $V_{s\_30}$ , грунтови условия, сеизмична опасност

## Introduction

The mapping of the natural hazards and environmental threats, vulnerability of structures and risk assessment and management are important issues to the prevention of population and the infrastructure as presented in (Frantzova, 2016a; Frantzova, 2017). The assessment of the damages and losses is the most important task in case of huge catastrophes and frequently influencing the GDP of any country (Frantzova, 2016b). The most advanced techniques and technologies are extensively used for the research and assessment of the consequences of the natural and technological disasters such as space remote sensing, high effective communication systems, etc. (Frantzova, 2012a; Frantzova, 2012b).

The seismic hazard and risk assessment in the recent times are exploited and implemented using different technologies, the most popular of which are models for simulation and risk management. This study is focused to the  $V_{s\_30}$  determination and digitalization as the very important parameter to the seismic hazard modeling.

The  $V_{s\_30}$  means the average velocity of the transverse seismic waves (S-waves) to the depths of 30 meters. This important characteristic is responsible for the S wave's velocity changes in the most upper ground layer and is an essential element included in the most calculus software packages for seismic hazard and risk assessment (HAZUS, EMERCOM, etc.) (Frolova, et al., 2019). Increased difficulties appear when the  $V_{s\_30}$  determination is necessary to be done for the seismic microzonation, seismic hazard and risk assessment, vulnerability of structures in the populated zones, urban areas etc., and have to be performed in large scales (Muco et al., 2012). All methods described above are very difficult to perform, due to the complicated measurement conditions. It is absolutely impossible to make regular grid, to perform bore holing and/or to take samples. Due to these difficulties a lot of archive materials have to be extracted, collected, digitized and interpret (Rangelov et al., 2001), which is the main task in this work.

## Data and Materials

The used materials have mostly the archive origin (the archive information is useful, having in mind that the ground conditions are conservative and did not change a lot in the time domain). In the urban environment frequently this is the only way to obtain reliable primary data and information. The collected and exploited data and materials are as follows:

- Data and information about former direct measurements of  $V_s_{30}$  (seismic exploration data)
- Data and information about former direct measurements of  $V_p_{30}$  (obtained by different seismic methods) and the following calculation of  $V_s_{30}$  using well known relationships.
- Former borehole data extracted by borehole direct (seismic) and non-direct (densitometry) measurements
- Archive information about geology (maps of different scales, layers of petrology composition, age, time of origin, thickness, roughness of the layers overlapping boundaries, lateral inhomogeneity, etc.)
- Hydrogeology information including archive data about depth of the ground waters level, pore permeability, liquefaction potential, etc.
- Laboratory tests data about samples taken earlier (use of the petro physical properties relationships to determine  $V_s$  (when possible), granulometry data, penetration tests, loading tests, etc.)
- Seismological data about macro seismic field of former earthquakes, intensities observed in the area, local inhomogeneity, observed liquefaction, cracks, sand volcanoes, land sliding and subsidence, etc. [8].
- Recent DEM, river's network, water bodies.
- Other data about former earthquakes, the macro seismic maps, acceleration records, attenuation laws.
- Geophysical maps and data about active faults, block structures, regional geophysical fields, geophysical prospecting information, etc.

In-situ measurements are performed, when possible, including direct seismic methods ( $V_p$ ,  $V_s$  estimation), ground water level measurements, possible landslide surfaces determination, angle of slopes assessment.

To obtain the former data and information is necessary to discover, transform and use the archives, to transfer the searched information into recent measurement units and to present effectively analogue data collected in former times and not used until now. This is not an easy task. The transformation from analogue format to the digital one is performed using different software and processing platforms. For example, the short list of data and information sources about Sofia city is presented in Table 1. The advantages of the information digitalization are useful. The data are easy accessible and ready for computer processing.

Table 1. Sources of data and information for Sofia city

Source	Quantity	Referred to:
Geology maps	2	Published
Seismology maps	3	Published
Data from boreholes	8	Archive units
Lab tests	11	Archive units
In situ measurements	4	Field measurements
Geophysical maps	5	Archive units

## Methodology

The methodology used for the data processing and interpretations includes:

- Graphic presentation of the investigated site as a polygon. This gives a possibility to cover the whole area of the urban territory following the curvature of the city shape.
- Construction of the dense network of longitudinal and latitudinal lines (in different scales, if necessary) and formation of a grid.
  - Interpolation procedures and calculation of the investigated parameter as weighted average value ( $V_s_{30}$ ).
  - Performing the comparative analysis of all available data, processing the information and assessing the reliability of obtained values of  $V_s_{30}$  as input data introduced
  - Attribution to each cell of the grid the two obtained values of  $V_s_{30}$  (the minimal and the maximal value). This provides the conservative approach and the user can choose the minimum value, the maximum value or the average one. This gives the possibility of the multiparameter approach for selection of the different variants for further calculations (Paskaleva, Ranguelov, 2015).
  - Creation of the final map containing all geology units (simplified and presented like blocks for practical use), digital Excel table containing the presented on the map values of  $V_s_{30}$  (min and max), together with the geography coordinates (in preferred by the user coordination system) thus forming the digital data base for the users Muco et al., 2012).
  - Presentation of the explanatory notes considering the liquefaction potential, the landslide potential and the possible modification of the amplitudes and velocities of S waves due to the different hardness of the ground (Frolova, et al., 2019).
  - The data for former earthquakes and their influences are presented as well. It includes, intensities, macroseismic maps, observed secondary effects generated by strong earthquakes (liquefaction, surface cracks, triggered landslides and stone falls, subsidence, generated tsunamis, avalanches and other gravitational phenomena, etc. (Ranguelov, 2011).
- Similar approach gives the possibility of the interpreter to select the best fit of the data and information to the task and required elements thus providing flexibility and multi variances.
- The algorithms and models used consider the scale of the investigated area, the density of buildings and structures, the population distribution, etc., but need most accurate ground condition assessment. Frequently it is not possible to assure such accuracy due to the intensive variability of the ground conditions and needs to use different approximations and extrapolation.

## Example, Results and Discussion

The collected and processed data and information as well as the described methodology have been performed for a seismic vulnerable urban area of Sofia city. The presented maps illustrate the results obtained to the different modeled results and the reliability of the calculations. The grid selection (250x250 meters) is dominated by the practical consideration of convenient use and reliable input data to the seismic hazard maps generation. Two maps are presented to illustrate the obtained results.

Fig. 1 shows the digital map of  $V_{s30}$ . On it the boundaries of the city are presented as polygon enveloping the urban limits of Sofia. As background the geology unified (based on the parameter  $V_{s30}$ ) blocks are separated.

Each block represents the unit with similar values of  $V_{s30}$ . Two values are expressed:  $V_{s30min}$  and  $V_{s30max}$ . The consideration of this separation is practical. The user can vary in its calculations and use the minimum or maximum value according the main task and the purposes of the seismic hazard assessment, as well as to use average value as

integral characteristic. This variability is rather convenient especially in case of lateral changes of the ground conditions.

The main difficulties from methodological point of view was the separation of the sediments of Block 1 to three sub blocks – 1.1; 1.2 and 1.3. The sedimentary characteristics especially according the genesis of sediments are valuable from geological constrains, but the geophysical properties are very similar and thus influenced the urban environment under possible seismic loading. Another peculiarity is related to the petrophysical properties of Block 2 – the Neogene sediments.

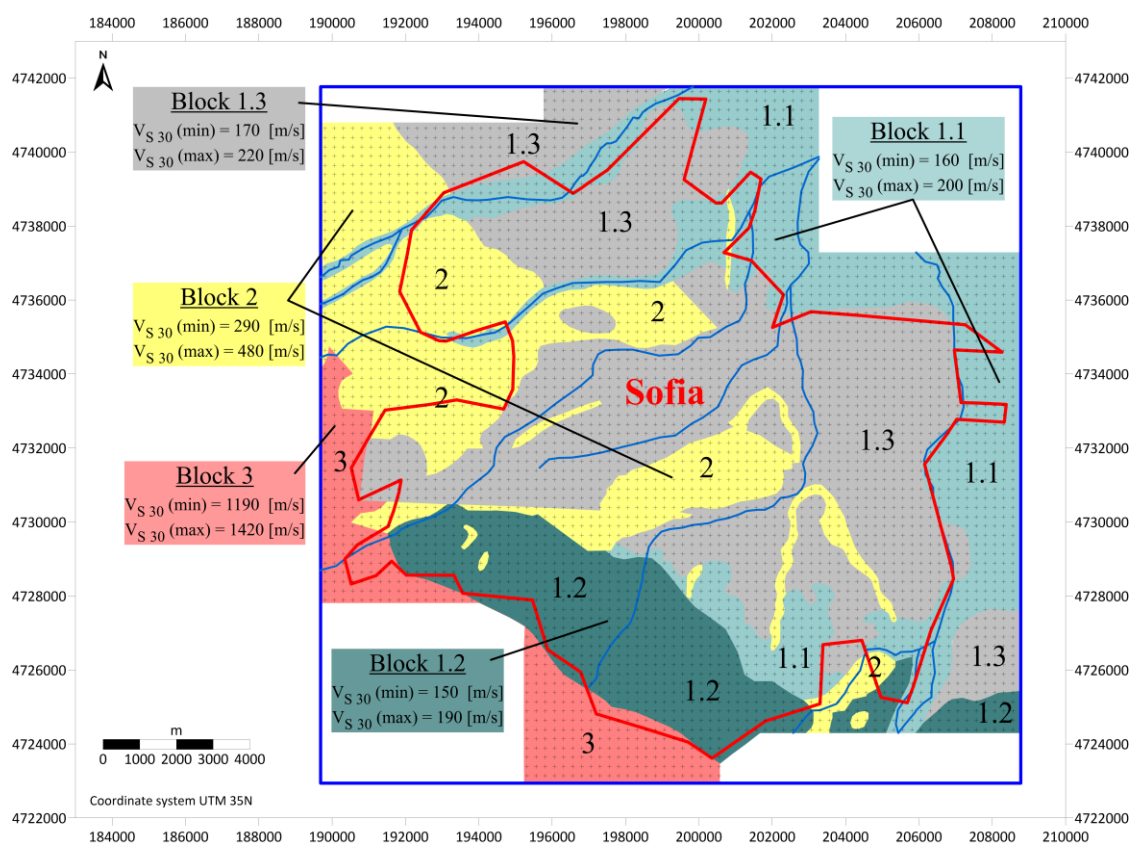


Fig. 1. Digital map of  $V_{s30}$  for Sofia city

They are very different and variable in their geophysical properties – mainly to  $V_{s30}$  values. That's why these variations attribute this block to two separate groups of ground properties (up to 280 m/s and between 280 and 360 m/s) according the international standards. The calculation homogenization procedures required to attribute this block to one of the two groups. To avoid this inconsistency two variants are suggested:

- To use the average value, which means to attribute the values of this block to the second standard group, or
- To calculate two variants – one with the minimum value (i.e. attribute to the first group) and one with the maximum value – assessment by second standard group.

It is well known that in Sofia region there are areas with landslides or other gravitational processes development. To get and asses the influence of the gravitational expected effects in case of strong earthquake, the DEM of the region is attached – Fig. 2. DEM or Digital Elevation Model is the

innovative presentation of the ground elevations covering wide range of scales. It is clear visible that the largest gradient is presented at the footnotes of Vitosha Mountain, where the most gravitational processes are strongly developed. From point of view of the seismic danger it is also important to mention the possibilities of activation of the snow avalanches during strong earthquake if it occurs in winter times. Such secondary activated phenomena are now incorporated in the seismic hazard assessment procedures and must be included in the calculations. Another part of Sofia valley is flat and no needs the DEM application.

The important part of the prepared map models include the digital data base of the parameter  $V_{s30}$ . It consists of coordinates of the grid points and values of  $V_{s30}$  for each point. In our case more than 4 300 values are calculated and ready for use just by import to the main software of the seismic hazard assessment procedure. The seismic hazard assessment of Sofia city itself is not the target to this

publication and will be developed in future research and applications.

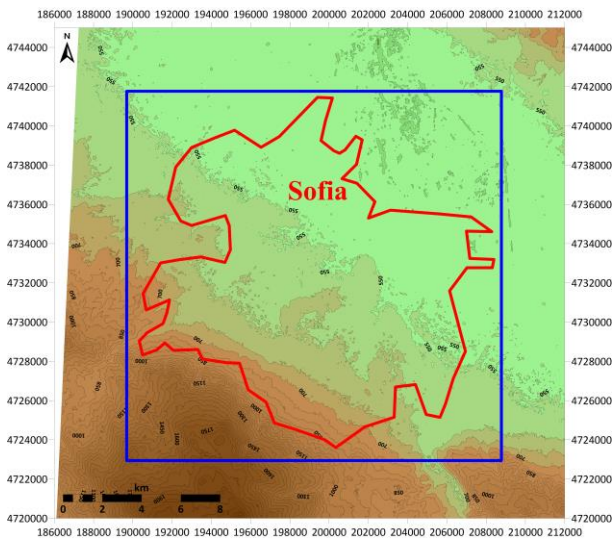


Fig. 2. DEM for Sofia city

## Conclusions

The updated digital methodology for assessment of the integral values of  $V_{s\_30}$  is developed for practical purposes. It is intended to be in use for the massive electronic calculations of the digital seismic hazards maps for big cities in Bulgaria. In total six cities are selected (Varna, Rousse, Plovdiv, Blagoevgrad, Veliko Tarnovo and Sofia, located in seismic prone areas), but for the illustration purposes only one sample is presented (Sofia). The performed methodology including mostly archive materials (but also some in-situ measurements) shows high effectiveness and reasonable results. The new element is the suggestion of the two values of the  $V_{s\_30}$  ( $V_{s\_30min}$  and  $V_{s\_30max}$ ). This provides the users of the newly calculated maps, wide diapason in variability of this parameter and gives the possibility for multi variant approach.

Sofia case is specific due to the peculiarities of the Neogene and Holocene sediments. The first are large variable in their seismic velocities properties. The second demonstrates variability which is due to their different genetics.

The performance of the model in different ground conditions in different case studies and seismic hazards calculations needs near future verification (Rangelov et al., 2010).

**Acknowledgements.** This work has been carried out in the framework of the National Science Program "Environmental Protection and Reduction of Risks of Adverse Events and Natural Disasters", approved by the Resolution of the Council of Ministers № 577/17.08.2018 and supported by the Ministry of Education and Science (MES) of Bulgaria (Agreement № Д01-322/18.12.2019).

## References

- Frantzova, A. 2016a. Risk mapping methodology for environmental hazards, *Proceedings, 6<sup>th</sup> Intl. Conf. on Cartography and GIS*, 13-17 June 2016, Albena, Bulgaria 314-321.
- Frantzova, A. 2017. *Risk mapping methodology and classification for environmental hazards*, Lambert Academic Publishing, 112 p.
- Frantzova, A. 2016b. Classifications and typology of the natural and triggered technological risks according to the GDP and probability of occurrence *Proceedings, 6<sup>th</sup> Intl. Conf. on Cartography and GIS*, 13-17 June 2016, Albena, Bulgaria.
- Frantzova, A. 2012a. Remote sensing data for snow cover monitoring and mapping. *South-Eastern European Journal of Earth Observation and Geomatics*, Vol 1, No 1 e-ISSN: 2241-1224
- Frantzova, A. 2012b. Detecting and monitoring of wildfires with remote sensing data, *South-Eastern European Journal of Earth Observation and Geomatics*, Vol 1 No 2 e-ISSN: 2241-1224
- Frolova, N., Larionov, V., Bonnin, J., Suchshev, S., Ugarov, A., Malaeva, N. 2019. Impact data bases application for natural and technological risk management. *Nat. Hazards Earth Syst. Sci. NHESS (2019)* 264-273
- Muco, B., Alexiev, G., Aliaj, S., Elezi, Z., Grecu, B., Mandrescu, N., Milutinovic, Z., Radulian, M., Rangelov, B., Shkupi, D. 2012. Geohazards assessment and mapping of some Balkan Countries., *Nat Hazards* 64 2 943-981
- Paskaleva, I., Rangelov, B. 2015. Lessons learned by recently happened natural disasters and future research needs. Engaging the Public to Fight the Consequences of Terrorism and Disasters. - In: *NATO Science for Peace and Security Series, E: Human and Societal Dynamics*, vol. 120 (Eds. Apostol, I., Mamasaklihsi, J., Subotta, D., Reimer, D., IOS Press, 257-268.
- Rangelov, B. 2011. *Natural Hazards – Nonlinearities and assessment*. Bulgarian Academy of Sciences Pres, Sofia, 327 p.
- Rangelov, B., Rizhikova, S., Toteva, T. 2001. *The earthquake (M7.8) source zone (South-West Bulgaria)*, Bulgarian Academy of Sciences Pres, Sofia, 279 p.
- Rangelov, B. 2013. Risk profiles and hazards for the Black Sea area. - In: *Landslide Science and Practice*, Vol. 7: *Social and Economic Impact and Policies* (Eds: Margottini, C., Canuti, P., Sassa, K.). Springer-Verlag, Berlin, Heidelberg, 3-9.
- Rangelov, B., Alexiev, G., Gospodinov, D., Scheer, S. 2010. Natural hazards and preventive measures in Bulgaria. - In: *Bulgaria and Bulgarians in Europe* (Ed. Petkov, P.), "Faber", V.Turnovo, 385-393.

## STRUCTURAL GEOLOGY OF THE CENTRAL PART OF KAMENITSA-RAKOVITSA FAULT ZONE

*Ianko Gerdjikov<sup>1</sup>, Yasen Dinev<sup>1</sup>, Dian Vangelov<sup>1</sup>*

*<sup>1</sup>Sofia University "St Kliment Ohridski", 15 Tsar Osvoboditel Blvd, 1504 Sofia, Bulgaria; janko@gea.uni-sofia.bg; paralelepipet1991@gmail.com*

**ABSTRACT.** Kamenitsa-Rakovitsa dislocation is well recognized as one of the most important structural elements in the Central Balkanides, yet, there is an obvious lack of structural studies and there are contrasting views on its kinematics. The presented here data are based on detailed mapping and structural studies of the central part of the zone, that is cropping out between the valley of Topolnitsa river and the area of the village of Kamenitsa. Here the hanging wall is built by Variscan metamorphic rocks and post-metamorphic granites, whereas the footwall includes Triassic dolomites and different Upper Cretaceous rocks. The trace of the fault zone in the strongly dissected relief indicate its steep dip (60-70°). With the help of small excavation the core of the fault zone was cropped out (west of the village of Kamenitsa). The core is composed of gauge and matrix-supported tectonic breccia with thickness 50-70 cm. A large number of meso-scale structures were documented in the strongly shortened immediate footwall that forms the overturned SW limb of Kayryaka syncline. Kinematic analyses of meso-scale imbrications, faults and folds, as well as cleavage-shear bands relations show consistent top N/NE shortening directions and allow interpretation of Kamenitsa-Rakovitsa dislocation as important Late Alpine compressional zone.

**Keywords:** Kamenitsa-Rakovitsa fault zone, Late Alpine tectonics, Upper Cretaceous rocks, tectonics, Central Balkanides

### СТРУКТУРНА ГЕОЛОГИЯ НА ЦЕНТРАЛНАТА ЧАСТ ОТ КАМЕНИШКО-РАКОВИШКАТА РАЗЛОМНА ЗОНА

*Янко Герджиков<sup>1</sup>, Ясен Динев<sup>1</sup>, Диан Вангелов<sup>1</sup>*

*<sup>1</sup>Софийски Университет „Св. Климент Охридски“ Бул. Цар Освободител 15, 1504 София, България*

**РЕЗЮМЕ.** Каменишко-Раковишката дислокация е отдавна разпозната като една от най-важните тектонски зони в Западното Средногорие. В литературата са изложени противоречиви данни за характера ѝ, като също така не са провеждани специализирани структурни изследвания. Изложените тук данни се основават на детайлно картиране и структурни изследвания на централната част на зоната, разкриваща се между долината на река Тополница и района на село Каменица. Тук висиящият блок е изграден от Херцински метаморфити и пост-метаморфни гранити, докато лежащият включва пластини от триаски доломити и пъстър горнокреден разрез. Хода на разломната зона в разчленения релеф индикира стръмния ѝ наклон (60-70°). С помощта на разчистка бе разкрита тектонска зона (западно от с. Каменица). Дебелината ѝ е 50-70 сантиметра и е изградена от сиво-зелена тектонска глина и матрикс-поддържана тектонска брекча. За кинематиката на сръзванията в зоната може да се съди по структурите в лежащия блок, който в съседство със зоната се характеризира с интензивно съкращаване на разреза. Тук горнокредните последователности за засегнати от мезомасщабни огъвания, сръзвания и оформят преобърнатото бедро на Кайряшката синклинала. Установените в този силно деформиран домен структури (мезомасщабни сръзвания, кинематика на второстепенни разломни зони, асиметрични гънки) индикират насочени на С/СИ движения. Тези данни насочват към интерпретирането на Каменишко-Раковишката дислокация като важна Късноалпийска компресионна зона.

**Ключови думи:** Каменишко-Раковишка разломна зона, Късноалпийска тектоника, Горнокредни скали, тектоника, Централни Балканиди

### Introduction

The Kamenitsa-Rakovitsa fault zone (KRFZ) has been recognized (Poushkarov (1927); Bončev (1940a); Karagyuleva et al. (1974); Ivanov (1998) as the most prominent tectonic feature in the western part of Central Srednogorie (Fig. 1). This is a NW-SE trending structure juxtaposing high-grade pre-Alpine basement with 4.5-9 km wide belt of deformed Upper Cretaceous sediments, volcanics and volcanoclastics of the Panagyurishte basin. Due to the lack of serious structural studies, at least two contradicting models for the kinematic and age of the fault zone have been proposed. Traditionally, the KRFZ has been regarded as a north, NE vergent, thrust (Boyadziev, 1940; Bončev, 1940; Karagyuleva et al., 1974). In the last twenty years another interpretation started to gain popularity. According to this new model the zone was reinterpreted as strike-slip fault (Ivanov, 1998)), where it was

suggested (Rieser et al., 2008) that the KRFZ is a splay of the Maritsa shear zone.

In this paper we address these problems as we present new evidence from field observation obtained during detailed mapping of the KRFZ in the area of Topolnitsa and Kamenitsa river valleys. Field studies were conducted for about three weeks in the period 2017-2020. The mapped territory is approximately 13 km<sup>2</sup> and covers the area around KRFZ, but mainly in its footwall from the hamlet of Srebrinovo to the area of Gorna Rakovitsa village. Outcrop conditions vary significantly, often limiting the possibility to document precisely the location of the contacts and collecting structural data. Much better outcropped are the area of Kamenishka river watershed and the area between Kamenitsa village and hamlet Kayryaka. Here, our detailed structural studies allowed us to construct several cross-sections along the well-outcropped traverses across KRFZ and Kayryaka syncline. Westward, in the watershed of Kalugritsa river and in the area of Gorna Rakovitsa village the

outcrop conditions allow only roughly to delineate the unit contacts.

## Local Stratigraphy

The complete stratigraphy of the study area is described in Katskov and Iliev (1993). For this study, most important is the stratigraphy of the Upper Cretaceous sequence that build up the footwall of KRFZ. A more recent stratigraphy overview of the Upper Cretaceous sequence is given in Vangelov et al. (2019).

The oldest rocks exposed in the study area are the rocks of the Central Srednogie High-grade Metamorphic complex. Here this Variscan basement consists mainly of migmatitic paragneisses, that contain from meter- to hundreds of meters bodies of leucocratic orthogneisses and metagabbros. The rocks are well foliated, as the foliation is striking NW-SE. The dips are mainly to SW, but due to the presence of large-scale folds with NW-SE axes, there are domains with NE dip. Thus, KRFZ is in fact running parallel to the Variscan penetrative fabric. Pre-Turonian Mesozoic rocks are rare in the area. They occur either as tectonic slices in the immediate footwall of the KRFZ, or in the hanging wall of another prominent fault zone - Petrich fault (Fig. 1). The lowermost part of the Upper Cretaceous sequence is represented by the basal terrigenous unit with Turonian age (Vangelov et al., 2019). This unit is cropping out only along the northern margin of the Panagyurishte basin, the hanging wall of Petrich fault or farther in the northernmost tip of the basin. The intermediate parts of the sedimentary sequence are represented by volcanics and various volcanoclastic deposits (terminology of McPhie et al., 1993). Several magmatic centers (see also Popov et al., 2012) are defined - Golyama Rakovitsa, Vran kamak, Smolsko, as only for the first center there are solid geochronological data ( $89.47 \pm 1.2$  Ma - Nedkova et al., 2012). While the older studies (Karagyuleva et al., 1974) interpreted the upper parts of the volcanic deposits as syn-eruptive products (pyroclastic deposits), in a recent re-evaluation they are described as epiclastic rocks (lower epiclastic unit - Vangelov et al., 2019). Most often these epiclastics underlie the regionally traceable unit in the Upper Cretaceous sequence - Mirkovo Formation of Santonian-Campanian age. This unit mark establishment of a stable marine basin with more or less unified carbonate sedimentation. The lateral consistency of this facies was recognized since first detailed studies (e.g. Boyadziev, 1940; Bončev, 1940) and since then these red beds are used as a marker to delineate large-scale folds in the Upper Cretaceous sequence. A turbiditic series of sandstones, siltstones, marls and rare limestones, denoted as Chugovitsa Formation (Moev and Antonov, 1978) is the youngest unit affected by Late Alpine tectonic overprint. For the area of Topolnitsa and Kamenishka river valleys, the Chugovitsa sequence is underlay by thick, up to tens of meters, siliciclastic rocks enriched in magmatic detritus. This subunit was denoted as Upper epiclastic (Vangelov et al., 2019).

## Geometry of KRFZ

Mapping of the KRFZ is relatively easy even if the direct contact is not cropping out, because it separates very different lithologies. Our mapping indicate that the trace of the zone as

delineated on the geological map (Iliev and Katskov, 1990; Katskov and Iliev, 1993) is rather precise. The zone strikes NW-SE as in several places is displaced by small-amplitude strike-slip faults. Our estimates of the dip of 50-70° - are based on detailed structural profiles, trench data as well as digital calculation of best fit plane for a set of points. A characteristic deviation from NW-SE trend is observed in the area of Gorna Rakovitsa village, where the presence of Turonian magmatic center strongly influenced local structural pattern. Despite our efforts to find outcrops of the fault (approx. 15 km along the KRFZ were checked in areas with deeply incised relief) no direct contact was found. At several places in the area of Kamenitsa village the hanging-wall (gneisses, Variscan granites) and the footwall (Triassic dolostones, Cretaceous sediments, volcanics and volcanoclastic) are separated by 1-5 m slope deposits. At one of these localities (E 23.9232, N 42.58751) the covered interval between the Variscan granites and Triassic dolostones is less than 1 m wide, so a small trench was excavated along the fault zone core. Both hanging-wall and footwall rocks are strongly brecciated, as in the proximity of the contact there are 0.2-0.5 m thick matrix-supported tectonic breccia. The core of the zone is represented by thick, up to 0.6 m gauge with colors varied from orange (next to the hanging-wall granites) to green (next to the dolostones). The gauge is often rich in survival grains with size up to several centimeters. No pronounced and consistent striations have been observed.

## KRFZ related deformation

While the trench data clearly indicate strong localization of deformation within the fault core, our field data indicate that there are structural features, more pronounced in the footwall, that can be related to the movements along KRFZ.

### KRFZ hanging wall

Deeply incised valleys of Redutin dol (SW of Kayryaka hamlet) and Golyamata reka (SW of Kamenitsa village) provide good possibility to study the structures within the hanging wall. The Variscan high-grade fabric is unevenly affected by brittle overprint, as no major fault zones can be defined. Well-defined kinematics was determined only for a set of shallow dipping to SW shear planes, bearing quartz fibers indicating top-to-the NE transport.

### KRFZ-related fabric in the footwall

Mandev (1940) was first to recognize the existence of syncline front of the KRFZ to which later Karagyuleva et al. (1974) gave the name Kayryaka syncline. This structure is well defined for approx. 18 km from the hamlet Srebrinovo (to the SE) to the area NE of Golyama Rakovitsa village (to the NW). The syncline trends NW-SE and only NE of Golyama Rakovitsa the trend changes to approx. E-W, following the strike of KRFZ (Fig. 1, 2). It represents a tight fold with overturned SW limb and shallowly dipping NE limb. Both limbs of the syncline show differences in the lithologies, their thickness, but most pronounced are structural differences (Fig. 3A). The normal limb, as observed, along the Kamenishka river valley is devoid of meso-scale folds and shear planes and provides one of the best sections of the Cretaceous sequence (Vangelov et al., 2019). On the contrary, the SW limb is strongly shortened and overturned and provides wealth of meso-scale structures

allowing to constrain the character of shearing along KRFZ and its structural evolution.

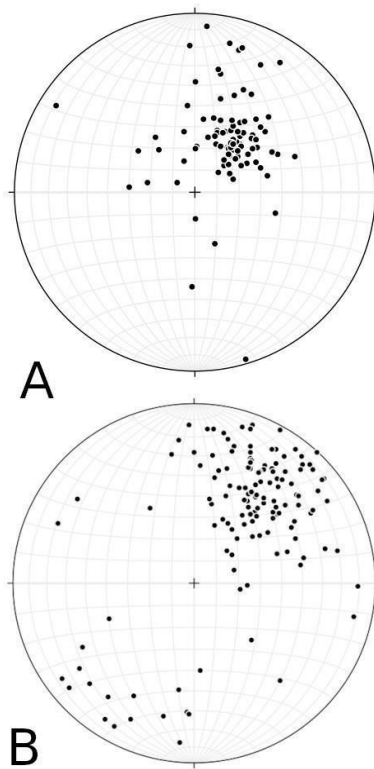


**Fig. 2. Bedding orientations for normal (A) and overturned (B) limb of Kayryaka syncline, displayed on equal-area lower-hemisphere stereoplots**

### **Geometry of the overturned limb**

An overturned sedimentary sequence, often displaying evidences for faulted contacts between different rock units is characteristic for the immediate KRFZ footwall. In the northern tip of the zone below the Variscan basement there is a discontinuous layer of dolostones (Iskar Carbonate Group, Fig. 1), occurring as thin lenses (up to 30-50 m width in map view, not shown on Fig. 1). Where present, they are underlying coherent magmatics or directly the limestones of Mirkovo Formation. These relations are clearly documented in the deeply incised relief W and SW of Kamenitsa village. In most of the cases the Variscan basement is in direct contact either with Cretaceous magmatics or with Mirkovo Formation. The magmatics crop out as areally extensive, elongated parallel to the KRFZ, strongly faulted and fractured rock volume or as rather thin (up to several meters, not shown on Fig. 1) strip. Neither in the dolostones nor in the magmatics clear primary fabric can be recognized. In a few cases a rough cataclastic foliation (formed by closely spaced joints) or marked by black ultracataclastic levels occurs, oriented sub-parallel to the main surface of KRFZ. Field data unambiguously indicate that the basement and the volcanics structurally overlie the upper most parts of the Cretaceous sequence (Fig. 3B, 3C).

NE and N of the KRFZ the Mirkovo Formation limestones are the best regionally traceable unit. Most often they are represented by vertical, strongly folded by upright folds and cleaved sequence of pinkish and grey limestones, sometimes containing intercalations of whitish wacke sandstones. Where observed, the lower structural contact of these limestones is

always faulted. They are juxtaposed with moderately SW dipping (50-40°), strongly faulted and altered thin (up to few tens of meters) fine-grained dark rocks, most probably representing Upper epiclastic sequence (Vangelov et al. (2019).

Structurally lowest position in the overturned limb occupies the turbiditic sequence of Chugovitsa Formation. There is no sharp break between the overturned and normal limb of Kayryaka syncline. The transition occurs within the monotonous turbidite intercalation of sandstones, silts, pelites, marls and clayey limestones. As criteria to delineate both limbs of Kayryaka syncline we used features as: lack of meter-scale folds and cleavage and syndimentary way-up structures indicating normal polarity - for the normal limb; and: strong meso-scale folding, cleavage development and inverted polarity, indicated by syndimentary fabric. Thus our data point to about 0.5 km wide in map view deformed rock volume, situated in the intermediate footwall of KRFZ. There are field data, as well as reasoning related to regional-scale tectonics are grounds to propose existence of thrust zone, more or less following the axial plane of Kayryaka fold (Fig. 3A).

### **Meso-scale features in the overturned limb**

Structurally below the rigid block made of Variscan basement and Turonian magmatics, the low-strength sediments of Mirkovo and Chugovitsa Formation are unevenly, but most often strongly deformed. A well-outcropped section along Dobri dol river valley (Fig. 3C) allows to document the style and sequence of the deformation, that we relate to the movements along KRFZ. A fault sets (minor fault arrays) are most widespread meso-scale features in this rock volume. Unfortunately in most of the cases indicators of the sense of relative movement (Petit, 1987) are missing. North of Kamenitsa village small-displacement thrust faults are rather common (Fig. 4A). Meter-scale folds are affecting the whole volume of Mirkovo Formation, and are also common in Chugovitsa Formation. They can be observed only in steep valley walls, while in cases of lack of vertical sections their presence is indicated by the steep attitude of bedding. These folds are not omnipresent; some decameter-scale domains are devoid of folds and dip monoclinaly to the NE (Fig. 3C). As previously documented by Boyadziev (1940), upright folds are typical (Fig. 4B). The folds are mostly similar with rounded and thickened hinge zones and often N-vergent.

Penetrative cleavage is unevenly present, and it is best documented along Dobri dol section (Fig. 3C). It is marked by closely spaced (several mm) fractures and it is most pronounced in marly lithologies. Except in the vicinity of the main faults, cleavage is associated with folds and shows divergent cleavage fan geometry. Within the strongly shortened by upright folds limestones and marls of Mirkovo Formation the steeply dipping cleavage is cut by subhorizontal to shallowly dipping to the SW shear planes (Fig. 4C). Sliken-fibre lineations on the shear surfaces (Fig. 4D) indicate top-to-the NE sense of shear. This sense of shear is also confirmed by the curvature of the cleavage toward shear planes (in section orthogonal to the cleavage/shear planes and parallel to the lineation).

### **Cross faults**

The main NW-SE structural grain is dissected by a set of sub-vertical faults, mainly with NE strike. Nowhere in the field

these faults are well outcropped, yet, the displacement of beds faults and contacts indicate their strike-slip kinematics.

## Conclusions

In the studied area KRFZ represents a NW-SE trending steep brittle fault zone along which Variscan metamorphic basement is emplaced over different levels of Upper Cretaceous sedimentary sequence. Within the fault zone, often meter- to decameter scale tectonic lenses of strongly brecciated Triassic dolostones were observed. When observed the main contact is marked by approx. 1 m thick gauge and matrix-supported tectonic breccia formed at the expense mainly of the Variscan metamorphics and granitoids.

Often along its immediate footwall, boudinaged layers of coherent volcanics with intermediate composition are cropping out. No particular structures were observed in both, dolostones and the magmatics which are generally affected by strong cataclasis. The Variscan metamorphic basement along with the competent dolostones and magmatics can be regarded as a buttress front of which the layered and less competent sequences of Mirkovo and Chugovitsa Formations were strongly deformed.

These units outline a strongly asymmetric footwall syncline with overturned SW limb. Based on detailed mapping the width of the overturned domain is about 0.5 km. Within this domain a number of features (upright folds, cleavage, meso-scale faulting) indicate significant shortening of the sequence.

Our data support the original ideas about the compressional character of KRFZ. Main arguments for this are: 1/ dip and stratigraphic offset across the fault zone; 2/ geometry and kinematics of small-scale faults in the vicinity of the zone; 3/ locally penetrative cleavage-shear bands associations; 4/ overall geometry of the deformed rocks from the footwall.

A single protracted compressional event can explain all the observed along the KRFZ structures. There are no data suggesting several contractional events (e.g. Pyrenean as suggested) or significant strike-slip reactivation.

The studied area represents one of the best outcropped sections along the inverted Upper Cretaceous basin. Our data indicate rather uneven distribution of the Late Alpine shortening within the Cretaceous belt: compression-related structures are localized in the footwalls of the main fault zones: KRFZ, Petrich fault and Negushevo dislocation.

**Acknowledgements.** The study was realized within the frame of the project funded by the Sofia University scientific foundation "Spatial and temporal distribution of the peri-Thethys CORB facies (Cretaceous Oceanic Red Beds) in parts of Central and Western Srednogie tectonic zone", Grant 2570/2019.

## References

- Bončev, E. 1940. Über Die Geologie Des Bajlovo Teiles Der Panagjuriste-Zone Der Srednogorie Unter Berücksichtigung Der Tektonik Dieser Zone. - *Review of the Bulgarian Geological Society* 11, 205–38 (in Bulgarian with German abstract).
- Boyadziev, N. 1940. Beitrag Zur Geologie in Der Gegend Des Dorfes Smolsko. - *Review of the Bulgarian Geological Society* 11, 181–93 (in Bulgarian with German abstract).
- Iliev, K., N. Katskov. 1990. *Geological Map of the Republic of Bulgaria 1:100 000. Panagyurishte Map Sheet*. Committee of Geology.
- Ivanov, Ž. 1998. "Tectonics of Bulgaria." Professorship thesis, Sofia University "St Kliment Ohridski" (in Bulgarian).
- Karagyuleva, J., V. Kostadinov, T. Tsankov, and P. Gochev. 1974. Composition of the Pangyuriste Strip East of the Topolnitsa River. - *Bulletin of the Geological Institute, Bulgarian Academy of Sciences ser. Geotectonic*, 23, 231–301 (in Bulgarian with English abstract).
- Katskov, N., K. Iliev. 1993. *Geological Map of the Republic of Bulgaria 1:100 000. Ihtiman Map Sheet*. Committee of Geology.
- Mandev, P. 1940. Geologische Skizze Des Gebietes Westlich von Topolnica Zwischen Den Dörfen, Poibrene, Petrič, Benkowski Und Kamenica. - *Review of the Bulgarian Geological Society*, 11, 169–180 (in Bulgarian with German abstract).
- McPhie, J. M. Doyle, R. Allen. 1993. *Volcanic Textures: A Guide to the Interpretation of Textures in Volcanic Rocks*. Centre for Ore Deposit and Exploration Studies, University of Tasmania, 196 p.
- Moev, M., M. Antonov. 1978. Stratigraphy of the Upper Cretaceous in the Eastern Part of the Sturguel-Chelopech Strip. - *Annual of the University of Mining and Geology, Geology and Geophysics*, 28 2, 7–30 (in Bulgarian with English abstract).
- Petit, J. P. 1987. Criteria for the Sense of Movement on Fault Surfaces in Brittle Rocks. - *Journal of Structural Geology*, 9, 5, 597–608.
- Popov, P., S. Strashimirov, K. Popov, M. Kanazirski, K. Bogdanov, R. Radichev, S. Dimovski, S. Stoykov. 2012. *Geology and Metallogeny of the Panagyurishte Ore Region*.
- Poushkarov, N. 1927. Study of the Geological Structure of the Western Link Between the Balkan and Sredna Gora Mountain. - *Contr. Bulg. Sci. Agricultural Institute*, 14, 1–44 (in Bulgarian).
- Rieser, B. A., F. Neubauer, R. Handler, S. Velichkova, Z. Ivanov. 2008. New 40 Ar/ 39 Ar Age Constraints on the Timing of Magmatic Events in the Panagyurishte Region, Bulgaria. - *Swiss Journal of Geosciences*, 101, 107–23.
- Vangelov, D., I. Gerdjikov, D. Dochev, Z. Dotseva, S. Velev, Y. Dinev, D. Trayanova, J. Dancheva. 2019. Upper Cretaceous lithostratigraphy of the Panagyurishte strip (Central Bulgaria) – part of the Late Cretaceous Apuseni -Banat-Timok- Srednogorie magmatic belt. - *Geologica Balcanica*, 48 (3), 11–33.

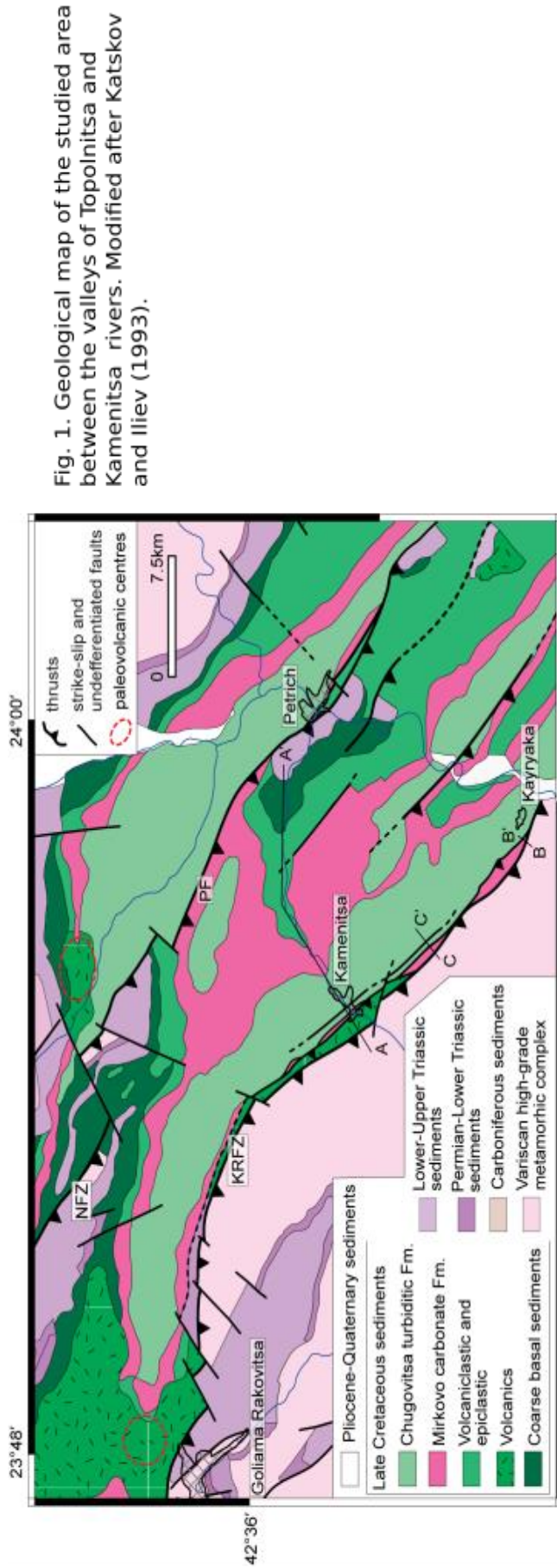


Fig. 1. Geological map of the studied area between the valleys of Topolnitsa and Kamenitsa rivers. Modified after Katskov and Iliev (1993).

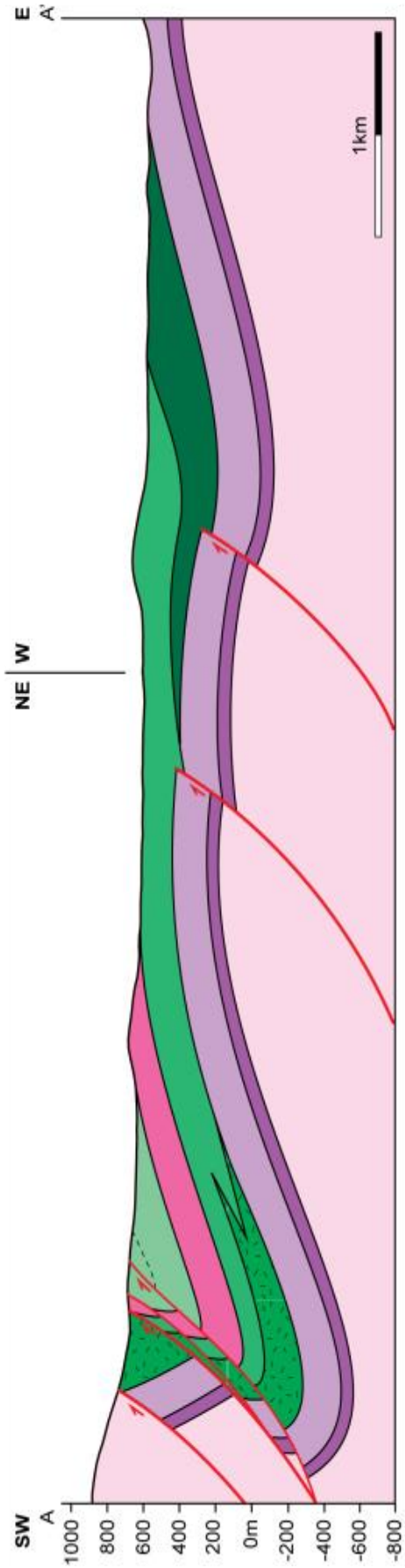


Fig. 3. Geological cross-sections. A. Kamenitsa river valley.

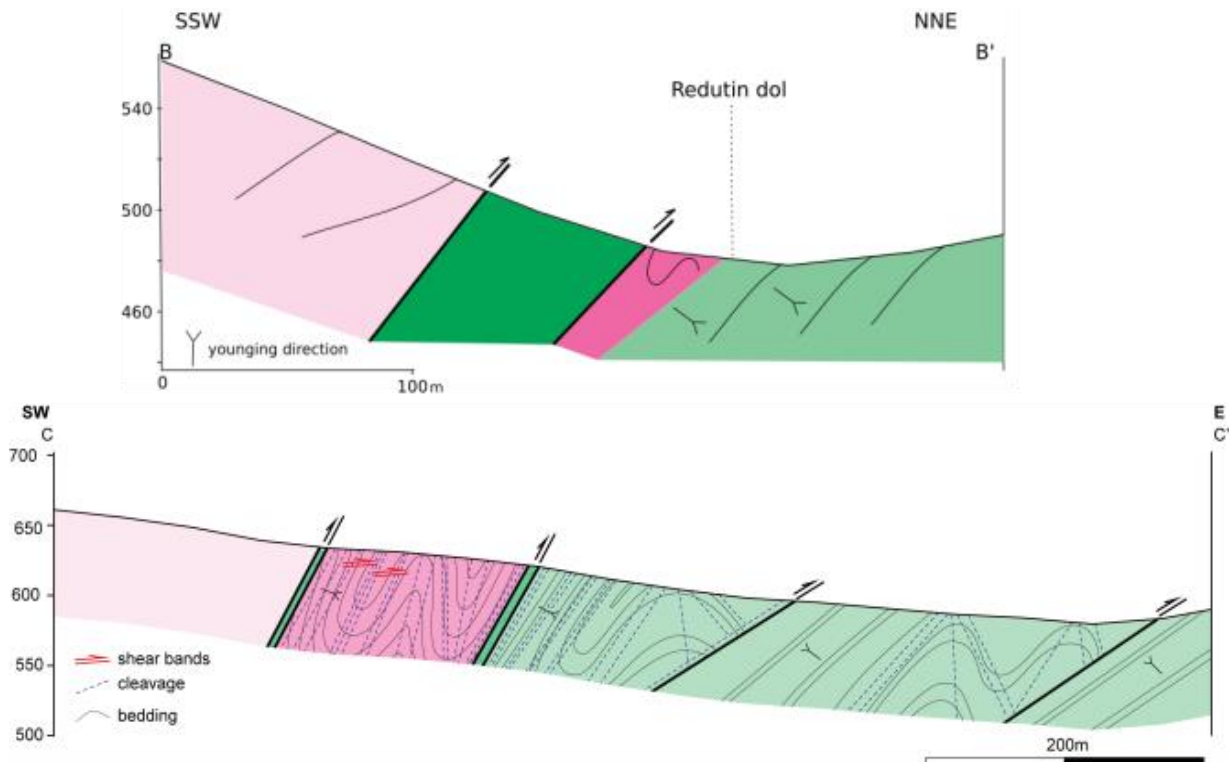


Fig. 3. Geological cross-sections. B. Kayryaka (Center: E 23.97805; N 42.55083) C. Dobri dol (SW: E 23.94886; N 42.56629; NE: E 23.95573 N 42.57191). Unit colors are the same as Fig. 1.



Fig. 4. A. Small-scale N vergent thrust, Chugovitsa Formation, North of Kamenitsa village ( E 23,9113; N 42,6041). B. Upright anticline-syncline pair. Chugovitsa Formation, Dobri dol section (E 23,9530; N 42,5690). Width of the photo - 6 m. C. Vertical bedding and cleavage are dissected by a set of low-angle shear bands (arrows). Mirkovo Formation, Eastern cliff of Gradishteto peak (E 23,9477; N 42,5702). D. Calcite fibres with steps on the shear band surface indicate top-to-the NE shear sense. Same location as C.

## STRENGTH AND DEFORMATION PROPERTIES OF THE INTACT GNEISS ROCK FROM ZHELEZNITSA TUNNEL OF STRUMA HIGHWAY (BULGARIA)

**Antonio Lakov<sup>1</sup>, Stefcho Stoynev<sup>2</sup>, Alexander Hristov<sup>3</sup>**

<sup>1</sup>University of Mining and Geology "St. Ivan Rilski", 1700 Sofia; antoniolakov@gmail.com

<sup>2</sup>University of Mining and Geology "St. Ivan Rilski", 1700 Sofia; stoynev@mail.bg

<sup>3</sup>University of Mining and Geology "St. Ivan Rilski", 1700 Sofia; aleksanderigrp@abv.bg

**ABSTRACT.** The article presents the laboratory test results from the intact gneiss rock from Zheleznitsa Tunnel of Struma Highway (Bulgaria). The following parameters were determined: uniaxial compression strength from direct loading and Point load test, the tensile strength from Brazilian test, as well as the elastic modulus and the Poisson's ratio. Correlation analyses between the parameters were carried out and the relevant equations and their correlation strength were determined. Cross-calculation were performed to complete the populations with correlated values. The statistical distributions of the parameters populations were estimated and the characteristic values were determined.

**Keywords:** intact rock, strength parameters, elastic modulus, cross-correlations, characteristic values

### ЯКОСТНО-ДЕФОРМАЦИОННИ СВОЙСТВА НА НЕНАРУШЕНАТА СКАЛА ОТ ТУНЕЛ „ЖЕЛЕЗНИЦА“ НА АМ „СТРУМА“

**Антонио Лаков, Стефчо Стойнев, Александър Христов**

Минно-геоложки университет „Св. Иван Рилски“, 1700 София

**РЕЗЮМЕ.** В настоящата статия са обобщени резултатите от лабораторните изследвания на ненарушената скала (гнайси), изградящи масива, през който преминава Тунел „Железница“ на АМ „Струма“. Определени са якостта на едноосов натиск чрез преки изпитвания и чрез точково (поасоново) натоварване, якостта на опън по Бразилския метод, както и модулът на еластичност и коефициентът на Поасон. Изследвани са корелационните зависимости между тях и са определени съответните зависимости и тяхната значимост. Извършено е допълване на пряко определените съвкупности от данни със са изчисления по тях стойности. Направени са оценки на статистическото разпределение на стойностите за отделните показатели на ненарушената скала, като са определени съответните характеристични стойности.

**Ключови думи:** ненарушена скала, якостни свойства, еластичен модул, корелационни връзки, характеристични стойности

### Introduction

Zheleznitsa Tunnel is a part of a newly constructed section from Struma Highway between Blagoevgrad and Simitli towns (South-west Bulgaria). It is with total length of 2,280m, comprises two parallel tubes with maximum top cover of about 110m.

The tunnel passes through a rock-mass of amphibolites and amphibolitic gneisses with Neo-Proterozoic age, from the Troskovski Metamorphic Complex. The region is characterized by intensive contemporary tectonic and seismic activity (Dobrev et al., 2000; 2015). The various tectonic and seismic stages had superimposed each other to produce numerous adjacent blocks in the rock-mass with quick transitions to extreme degrees and spatial orientation of fracturing, jointing and foliation (Fig. 1).

An extensive drilling campaign was carried out including 16 boreholes up to 135m deep. More than 150 nos. of HQ and NQ rock-core samples with were collected for laboratory testing.

As the project approach for evaluating the rock-mass properties was based on Hoek-Bray strength and deformation models the following major mechanical parameters of the intact rock were determined: uniaxial compression strength (UCS - ASTM D7012-14) from direct loading, tensile strength from

Brazilian test (BTS-ISRM, 2007), as well as the elastic modulus  $E_{el}$  and the Poisson's ratio  $\mu$  (ASTM D7012-14), determined as average from the central linear portion of the stress-strain curves. To evaluate the compression strength of rock from the disturbed and crushed intervals point load tests (PLT - ASTM D5731) were carried out by loading in axial (vertical) and diametral (horizontal) directions of dry core specimens.



**Fig. 1. Typical sequence of intact and crushed core intervals (depth interval 37m-47m).**

The UCS's and the BTS's were tested out on air dry specimens and water saturated to constant weight specimens. Complete degradation during saturation from about one third to half of the tested specimens was observed.

The scope of the current study is to present the applied correlation analysis and cross-calculations between the parameters in order to enrich the direct testing data matrix, as well as the calculation of their characteristic values, based on the estimated statistical distributions. All calculations were carried out with MS EXCEL.

**Relationships between parameters**

A vast quantity of studies dealing with empirical correlations between the rock physical and mechanical parameters can be enlisted, but none of them, no matter of their simplicity or complexity none are universally verified. If they are recommended for common engineering practice, important applicability cautions and/or wide variational ranges regarding rock types, their structures, weathering etc. are assigned, so their application for a specific site may generate more ambiguity rather than confidence. In studying such relationships it is strategically important to define the type of approximation functions to be estimated. In many cases they include a free member that makes them physically inadmissible as for '0' values of the argument parameters a non-zero value are produced if no functions' validity truncation is mentioned.

In this regard the current study is aimed but to establish basic and strictly local relationships aimed to enlarge and improve the statistical quality the data samples.

Two major relationships were studied: between UCS and PLT and between UCS and  $E_{61}$ .

**Relationship between UCS and PLTs' results**

The PLT is standardized by both in ASTM and ISRM for indirect estimation of the USC of rocks by the equation:

$$UCS = kI_{C(50)}, \tag{1}$$

where 'k' is a linear conversion factor and  $I_{S(50)}$  is the Point Load Stress Index normalized to core specimen's diameter 50 mm (NQ). The values of 'k' usually are recommended as 20÷25 (mean 24) (Bieniawski, 1975; Broch and Franklin, 1972). ASTM 5731-05 (referring to ISRM, 1985) recommends the k-factors varying from 20 to 60 for 20mm to 60mm specimen diameters. In ISRM (2007) no such values are not presented but is mentioned that the k-factor for the different rock types may vary from 15 to 50, that is up to ±100% from the previous value of 24.

For defining a correct k-factor value for the gneiss rock, paired UCS tests and PLTs' were carried out on specimens from the same or adjacent rock samples (Table 1). The individual  $I_{S(50)}$  values and k-factor values for each PLT were calculated. Further the integral k-factor values for the rock were defined both by averaging (Table 1) and by linear correlations between the paired values of USC and  $I_{S(50)(II)} / I_{S(50)(L)}$  – Fig. 2.

Table 1. Results from paired USC tests and PLTs'.

UCS	$I_{S(50)(II)}$	$I_{S(50)(L)}$	$k_{(II)}$	$k_{(L)}$
MPa	MPa	MPa	-	-
11.60	0.37	0.22	31.35	52.73
	0.25	-	46.40	-
18.10	0.88	0.44	20.57	41.14
	-	0.30	-	60.33
	-	0.58	-	31.21
0.31	0.04	0.04	7.75	7.75
10.10	0.17	0.18	59.41	56.11
	-	0.13	-	77.69
	-	0.09	-	112.22
19.70*	1.74*	3.02*	11.32*	6.52*
	4.04*	1.40*	4.88*	14.07*
57.90*	2.34	2.97*	24.74*	19.49*
	4.24*	3.08*	13.66*	18.80*
17.80	-	1.86*	-	9.57*
1.40	0.20	0.12	7.00	11.67
	0.14	-	10.00	-
2.92	0.28	0.07	10.43	41.71
4.07	0.07	0.04	58.14	101.75
11.59	0.47	0.37	24.66	31.32
	0.41	-	28.27	-
<b>Average (all values)</b>				
<b>17.48</b>	<b>1.04</b>	<b>0.88</b>	<b>23.91</b>	<b>40.83</b>
<b>Average (without excluded values)*</b>				
<b>8.65</b>	<b>0.30</b>	<b>0.22</b>	<b>27.63</b>	<b>52.14</b>

(\*) The values were excluded from the data processing.

As the values show considerable scatter around the average a certain estimation for outliers of the data set was carried out. An initial Grubb's test (Grubb, 1950 - not presented here) showed not any like, but the graphical presentation (Fig. 2) revealed that for specimens with UCS values above 20 MPa the points were considerably shifted from the expected linear relationships. In this regard the k-factors values were averaged in Table 2 and correlated on Fig. 2 both for the complete set and the reduced set excluding the 'outliers' values (marked with '\*' in Table 1 and with cross-hair marker on Fig. 2). The correlated values (Fig. 2), give  $k_{(II)} = 12.0$  and  $k_{(L)} = 15.0$  for all values sets and  $k_{(II)} = 23.8$  and  $k_{(L)} = 39.9$  for the reduced sets.

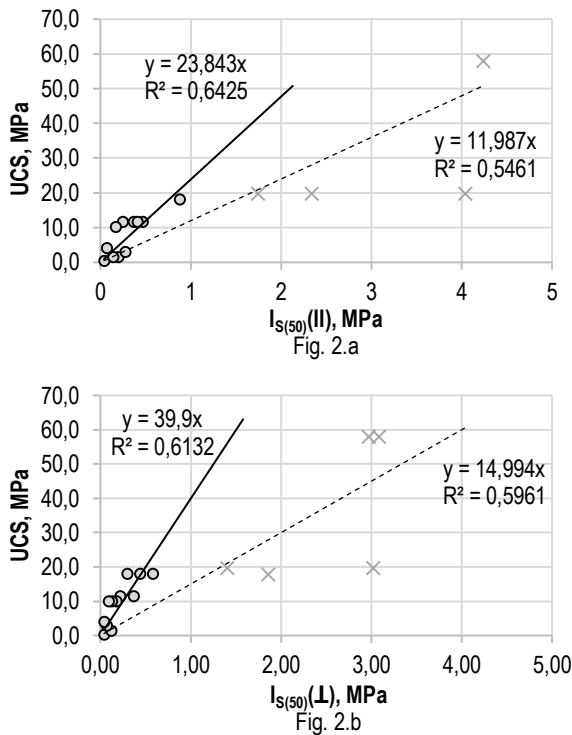


Fig. 2. Relationships USC and a)  $I_{s(50)(II)}$  and b)  $I_{s(50)(L)}$ .

Comparing the above results it can be concluded that the average calculations can considerably smooth up the scattered values while the linear correlation distinctly differentiates between them. As the reduced data sets correlations present much higher regression coefficients and as the majority of the unpaired PLTs' are with values of  $I_{s(50)}$  less than 1.0-1.5 they are considered representative for the study. Further, the  $k$ -values from the reduced data sets are as twice as higher that these from the total data sets, that will result in higher estimated UCS that seems more reasonable for the project. The results revealed a marked anisotropy of the  $k$ -values in vertical to horizontal directions with anisotropy index  $I_{a(I_{s(50)})} = 1.25-1.60$ , that was recommended to be used in the tunnel's design.

**Relationship between  $E_{el}$  and UCS**

The most popular relationship between  $E_{el}$  and UCS is the Modulus Ratio  $MR = E_{el}/UCS$ . Hoek et al. (2006) recommend values for gneiss are in the range of 300-750, that was attributed to attributed to the high anisotropy of the rock. Depending on the degree of weathering of gneisses Ekanayake et al. (2015) report even larger spreads of MR limits. Chang et al. (2006), Palchik (2011) and Alnuaim (2019) present some more complicated polynomial or power relationships but still with considerable scatter of the results.

In the current study the relationship between the  $E_{el}$  and UCS was estimated on 29 paired samples tested for both parameters (Table 2).

Table 2. Results from paired USC and  $E_{el}$  tests.

<b>UCS</b>	MPa	0.20	0.59	1.25	2.34	2.34	2.98	3.08
<b><math>E_{el}</math></b>	GPa	0.36	0.95	0.36	1.67	0.95	1.67	0.70
<b>UCS</b>	MPa	5.76	10.10	10.60	11.00	11.70	12.36	13.30
<b><math>E_{el}</math></b>	GPa	1.12	3.89	6.06	3.46	4.48	13.77	11.40
<b>UCS</b>	MPa	13.70	13.90	14.61	16.84	17.82	27.30	31.98

<b><math>E_{el}</math></b>	GPa	10.53	3.77	4.66	7.07	20.85	14.30	19.04
<b>UCS</b>	MPa	36.80	38.68	53.00	53.10	54.70	57.90	263.24
<b><math>E_{el}</math></b>	GPa	24.78	23.25	22.56	25.18	41.43	39.09	84.15

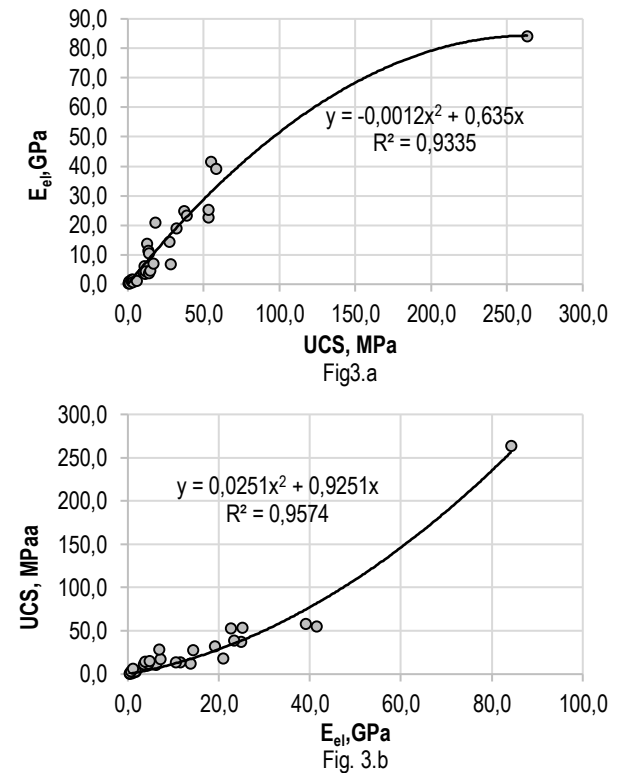


Fig. 3. Relationships between a)  $E_{el}$  and USC and b) USC and  $E_{el}$ .

The obtained relationships (Fig. 3.a and b) are with very good strongness (correlation coefficients are above 0.95). The estimated curve functions are:

$$E_{el} = - 0.0012UCS^2 + 0.635UCS \tag{2}$$

$$UCS = 0.0251E_{el}^2 + 0.925E_{el} \tag{3}$$

It should be mentioned that equations (2) and (3) are not mathematically reciprocal as the curves are forced to pass through the axes' origin.

The 'raw' laboratory dataset for USC was filled up with new values calculated with eq. (1) from the unpaired values of  $I_{s(50)(II)}$  and  $I_{s(50)(L)}$  applying the relevant  $k$ -factors  $k_{(II)}$  and  $k_{(L)}$  as well as with values calculated from the unpaired  $E_{el}$  values using eq. (3). The same was carried out for  $E_{el}$  values where eq. (2) was applied to the unpaired USC values, incl. these calculated from the PLT's.

**Characteristic values**

The concept of the characteristic values was introduced in Eurocode 7, that on statistical grounds (clause 2.4.5.2(1)) should be derived at probability levels not greater than 5% of the worse parameter value (lower or upper) that governs the occurrence of the limit state. For a given parameter values probability distribution that is equivalent to the lower confidence

limit (LCL) and the upper confidence limit (UCL) to the population mean at 90% two-tailed probability.

Two types of distributions were tested towards the intact rock properties – normal and log-normal. The simplest way to check the distribution type is visually inspection of histograms. As the sample populations for the different parameters vary in size and shape this may not be enough. So the normality of the data distributions was also checked with Q-Q plots in the form of a Normal Quantile Plots relating the test values and the corresponding Z-score values based on the estimated quantiles  $Q$  of each test value with  $i$ -th rank in the sample:

$$Q = \frac{i-0.5}{n} \quad (4)$$

As theoretically for a normal distribution the Q-Q plot is a straight line the visual linear appearance of the trend should be the initial criteria for the normality of the distribution. Further the correlation coefficient  $R$  was used to establish the stronger correlation, especially for similarly looking trends.

Both Q-Q plots were created for the actual and log-values of the parameters, the criterion for best fitting being the better value of the correlation coefficient  $R$ .

The UCL and LCL for a normal distribution were calculated as:

$$\frac{UCL}{LCL} = AVE \pm t_{\alpha/2} \frac{SD}{\sqrt{N}} \quad (5)$$

where  $\alpha$  is 0.1 for two-tailed probability of non-exceedance.

The issue for the efficient CLs' calculation of log-normal distribution can be solved based on different approaches (Olsson, 2005). The so called 'naïve' approach applies equation (5) to the normal log-values distribution parameters and antilogging the CL values. This approach is usually rejected due to unacceptable shifting the confidence interval towards the average value and even excluding it, what was observed in the study as well (not presented here). So, a modified Cox solution (Olsson, 2005) was applied where the UCL and LCL are calculated for the estimated log-values ( $\ln$ ) normal distribution parameters:

$$\frac{(\ln)UCL}{(\ln)LCL} = AVE(\ln) \pm t_{\alpha/2} \sqrt{\frac{SD(\ln)^2}{N} + \frac{SD(\ln)^4}{2(N-1)}} \quad (6)$$

Further they are back-transferred to normal values by antilogging.

### UCL and LCL calculations results

The calculation results for the UCL and LCL values corresponding to the upper and lower characteristic values of the main properties for the intact rock are presented in Table 3. It includes the statistics that are incorporated in eq. (5) and (6) both for normal and log-normal data distribution. The USC and  $E_{el}$  dataset values that were considerably extended with the inter-parametric calculations with 50 nos. and 30 nos. accordingly. The data histogram plots with the estimated normal and log-normal probability distribution curves as well as the corresponding Q-Q plots for the studied rock parameters are presented in the Appendix of this article.

## Discussions

The presented study reveals that practically all parameters are characterized with log-normal distribution that can be visually estimated from most of the data histograms and is strongly supported by the Q-Q plots linear correlation coefficients  $R$ . An exception is observed for the UCS (dry) and  $E_{el}$  datasets where the correlations coefficient for normal and log-normal plots are high quite (above 0.94) but the normal Q-Q plots are with unacceptable curvature. The bulk density data distribution can be described with equal probability both as normal and lognormal distribution curves are practically identical with very good trends of the Q-Q plots. This results in practically identical upper and lower characteristic values.

As general tendency the log-normal distributions produce slightly higher confidence limits corresponding to higher characteristic values thus decreasing the conservativity in their estimation. For some parameters (saturated UCS) the normal distributions extend the lower confidence values within the negative scores that is physically inadmissible.

The cross-parameters data extension resulted in slight – about 10% - increase of the average value for dry UCS and more significant – about 35% - increase of the average value for  $E_{el}$ . However, the data variances increase as well, that is considered more relevant to the natural structure and properties variation in the rockmass.

Important issue is that not only the LCL's should be considered as characteristic values that govern the instability limit states in the rockmass. Depending on the stress state and limit state origin the bulk density through overburden weight can play both favourable and unfavourable role. As noted in Eurocode 7 clause 11.5.1(12) for overall slope stability the limit state should be tested for both lower and upper characteristic values. This consideration is appropriate to extend in the underground structures design as well. A specific aspect of the applicability of UCL's and LCL's is their effect on mathematically related parameters. Let consider the parameter 'm' from Hoek-Brown failure criterion. According to Cai (2000)  $m \approx USC/BTS$  if this ratio is above 8. Calculated from the log-normal UCL and LCL 'm' equals to 8.0 and 11.8. This is an example where the UCL's values produce more unfavourable parameter value, so for the  $m$ -value so they should be considered as characteristic.

## Conclusions

The intact gneiss rock from Zheleznița tunnel exhibits generally vary quite irregularly in the rockmass that can be explained with intensive tectonic and seismic background, fracturing and jointing. The parameters variation magnitudes is from 10 to 1000 that are not typical for this rock type. Another unfavorable factor for the rockmass behaviour is the UCS degradation of the saturated rock from 400% to 600%, up to complete material degradation.

To overcome the shortage of good quality undisturbed samples for laboratory testing for the structurally disturbed drilling core intervals, indirect PLT's were carried out and representative correlative relationships with UCS and  $E_{el}$  were established.

Basic statistical methods including interpretation of histograms and Normal distribution Q-Q plots were applied to establish predominantly log-normal distribution of the mechanical parameters. Relative to the normal distribution the log-normal distribution amplifies the relative weight of the lower range values that reflects in considerably lower mean but results

in more narrow confidence intervals with higher confidence limits values. It is demonstrated that both LCL's or/and UCL's can be assigned as characteristic values depending on their effect or that of related to them parameters on the rockmass limit states.

Table 3. Calculation results for the LCL and UCL values.

STATISTICS		NORMAL DISTRIBUTION								LOG-NORMAL DISTRIBUTION				
		N	R	AVE	SD	min	max	LCL	UCL	R	AVE (ln)	SD(ln)	LCL	UCL
Bulk Density	g/cm <sup>3</sup>	92	0.99	<b>2.61</b>	0.23	1.89	3.13	2.56	2.66	0.99	0.96	0.09	<b>2.57</b>	<b>2.65</b>
UCS (dry)	MPa	102	0.94	<b>16.44</b>	28.96	0.2	207.72	10.75	22.13	0.99	1.97	1.35	<b>13.15</b>	<b>24.37</b>
UCS (sat.)	MPa	21	0.65	<b>7.13</b>	16.73	0.13	75.78	-0.48	14.75	0.97	0.61	1.58	<b>2.6</b>	<b>15.76</b>
BTS (dry)	MPa	56	0.83	<b>1.54</b>	2.17	0.02	11.06	0.96	2.13	0.99	-0.53	1.51	<b>1.12</b>	<b>3.03</b>
BTS (sat.)	MPa	8	0.88	<b>2.78</b>	3.41	0.17	10.25	-0.08	5.63	0.99	0.29	1.4	<b>0.91</b>	<b>14.01</b>
E <sub>el</sub>	GPa	103	0.94	<b>9.21</b>	13.06	0.13	74.39	6.65	11.76	0.99	1.47	1.33	<b>7.79</b>	<b>14.17</b>
μ	-	30	0.93	<b>0.12</b>	0.07	0.01	0.37	0.09	0.14	0.97	-2.34	0.67	<b>0.10</b>	<b>0.15</b>

References

Alnuaim, A.,W. Hamid, A. Alshenawy. 2019. Unconfined Compressive Strength and Young's Modulus of Riyadh Limestone. - *Electronic Journal of Geotechnical Engineering*, 2019 (24.03), 707-717. (available at ejege.com)

ASTM D5731-16. Standard Test Method for Determination of the Point Load Strength Index of Rock and Application to Rock Strength Classifications.

ASTM D7012-14. Standard Test Methods for Compressive Strength and Elastic Moduli of Intact Rock Core Specimens under Varying States of Stress and Temperatures.

Bieniawski, Z. 1975. Point load test in geotechnical practice - *Engineering Geology* 9, 1-11

Cai, M. 2010. Practical Estimates of Tensile Strength and Hoek-Brown Strength Parameter m<sub>i</sub> of Brittle Rocks. - *Rock Mechanics and Rock Engineering* 43, 167-184.

Chang, C., M. Zoback, A. Khaksar. 2006. Empirical Relations between Rock Strength and Physical Properties in Sedimentary Rocks. - *Journal of Petroleum Science and Engineering*, v. 51/3, 223-237.

Dobrev, N., B.Kostak. 2000. Monitoring tectonic movements in the Simitli Graben, SW Bulgaria. - *Engineering Geology* 57, 179-192.

Dobrev, N., E. Botev, V. Protopopova, I. Georgiev, D. Dimitrov. 2005. Seismicity and nowadays movements along some active faults in SW Bulgaria - *Chemical Communications*, v. 42, 1-10.

Eberhardt, E. 2012. The Hoek-Brown Failure Criterion. - *Rock Mech Rock Eng* 45, 981-988.

Ekanayake, E. M., H. M. Herath, A. Virajh Dias. 2015. Empirical Relationships of Elastic Modules and Uniaxial Strength of Intact Metamorphic Rocks of Sri Lanka - in ICGE Colombo - 2015.

Eurocode 7. Geotechnical design. Part 1, General rules.

Grubbs, F. 1950. Sample criteria for testing outlying observations. - *Annals of Mathematical Statistics* 21(1), 27-58.

Hoek, E., Diederichs, M. 2006. Empirical estimation of rock mass modulus. - *International Journal of Rock Mechanics and Mining Sciences*. v. 43(2), 203-215.

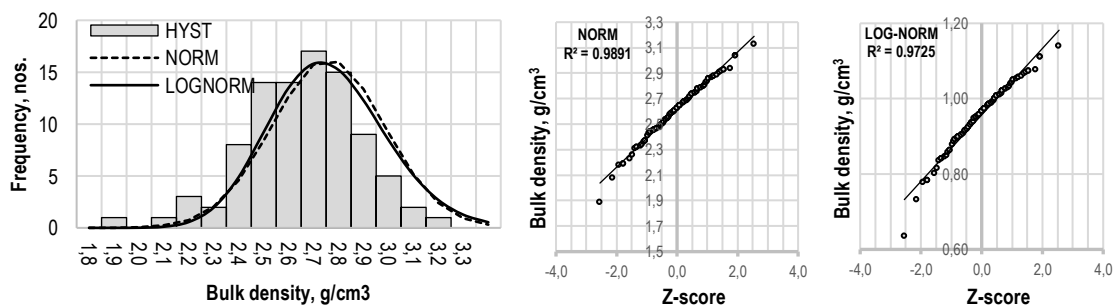
ISRM. 2006. The Complete Suggested Methods for Rock Characterization, Testing and Monitoring:1974-2006 (Ed. R. Ulusay and J.A. Hudson).

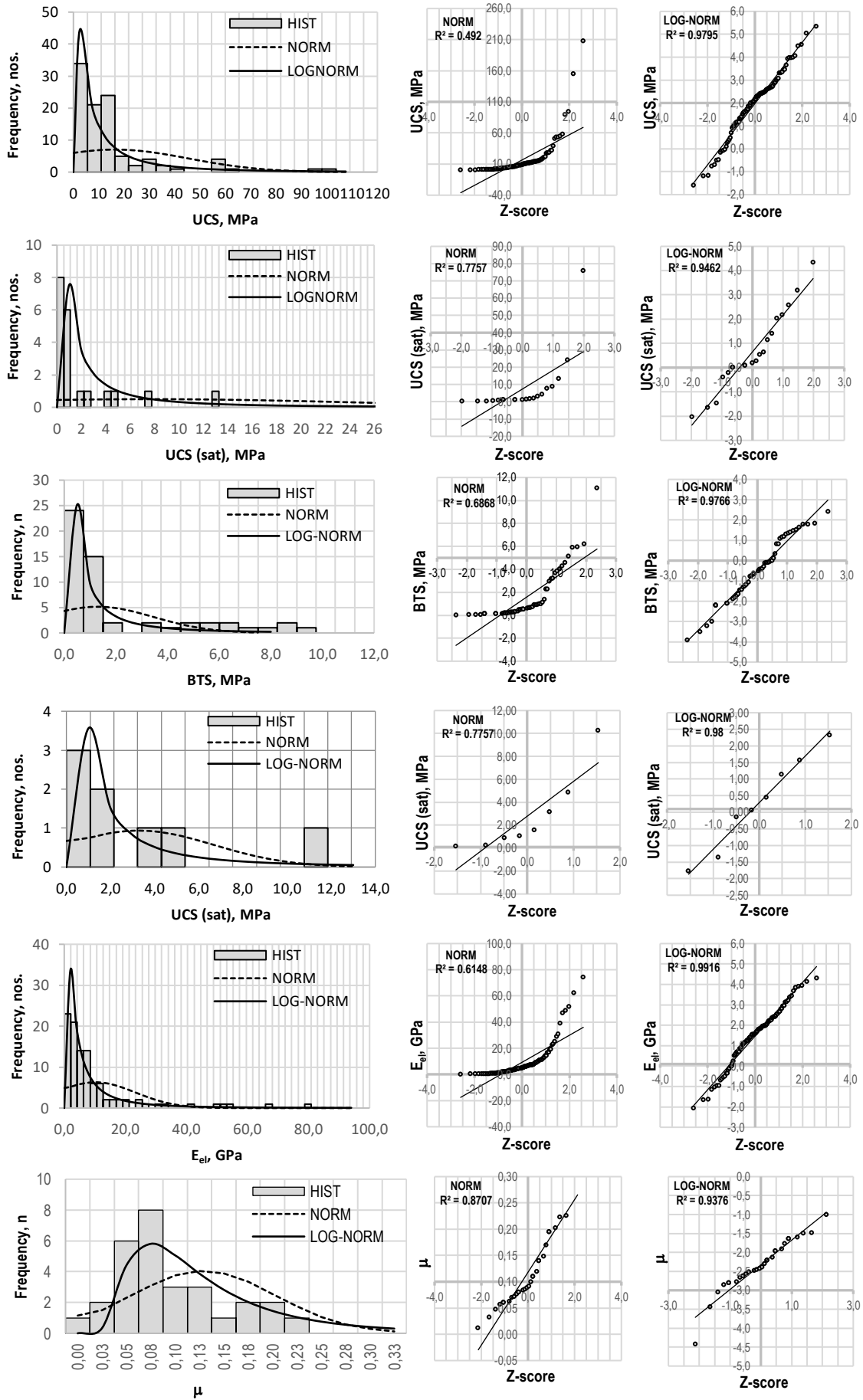
Olsson, U. 2005. Confidence Intervals for the Mean of a Log-Normal Distribution. - *Journal of Statistics Education*, 13:1

Palchik, V. 2011. On the Ratios between Elastic Modulus and Uniaxial Compressive Strength of Heterogeneous Carbonate Rocks. - *Rock Mechanics and Rock Engineering* 44, 121-128.

APPENDIX

Histograms with normal and log-normal distribution curves and Q-Q plots for the intact rock parameters





## 3D IMPLICIT MODELLING OF ALTERATION ROCKS AND LITHOLOGICAL UNITS IN THE MILIN KAMAK AU-AG DEPOSIT: RESULTS AND APPLICATIONS

*Ivan Marinov, Kalin Ruskov, Kamen Popov, Nenko Temelakiev*

*University of Mining and Geology "St. Ivan Rilski", 1700 Sofia; E-mails: imarrinov@gmail.com, rouskov@mgu.bg kpopov@mgu.bg, nenkotemelakiev@outlook.com*

**ABSTRACT.** The present study is focused on the interpretation of outcomes received from implicit 3D geological modelling. The analysis and technical possibilities allow the extraction and interpretation of the main geological characteristics and spatial distributions of the alteration rocks and lithological units. Advanced radial basic function (RBF) interpolation technique have been used in order to define the geological boundaries and provide more accurate representation of 3D isosurfaces. The implicit model is generated by non-numerical lithological data. According to the results, the distribution of dykes and later sericitic and argillic alterations emphasize strictly their common alignment in the space. This show also that dykes and alteration rocks share common hosting structures and are formed by the prior magmatic activity and subsequent ore hydrothermal fluids. The structural analysis based on lineament extraction and 3D building of fault surfaces shows three systems with NW-SE, NE-SW and E-W directions. The faults with NE-SW and E-W direction can be marked out as main hosting structures for magmatic products and hydrothermal fluids. The integration of structural data and body geometry analysis allows better understanding and more accurate definition of the local structural trend and spatial distribution of the alteration rocks and dykes.

**Key words:** 3D implicit modelling, faults, body geometry, Western Srednogie

### 3D ИМПЛИЦИТНО МОДЕЛИРАНЕ НА ХИДРОТЕРМАЛНИ ПРОМЕНИ И ЛИТОЛОЖКИ ТЕЛА В ЗЛАТНО-СРЕБЪРНО НАХОДИЩЕ „МИЛИН КАМЪК“: ИЗВОДИ И ПРИЛОЖЕНИЯ

*Иван Маринов, Калин Русков, Камен Попов, Ненко Темелакиев*

*Минно-геоложки университет Св. Иван Рилски 1700 София*

**РЕЗЮМЕ.** Предмет на настоящето изследване са резултатите получени от 3D имплицитно моделиране. Анализът и техническите възможности в триизмерното моделиране позволяват извличане и интерпретация на пространствената ориентация и геоложките особености на главните литоложки единици и хидротермални промени, разкриващи се около златно-сребърно находище „Милин камък“, Брезник. С цел по-точно дефиниране на геоложките граници и предоставяне на по-акуратен облик на генерираните 3D изоповърхнини е използвана RBF (Radial Basic Function) интерполационна техника. За имплицитното моделиране са използвани символни (номинални) литоложки данни. Според резултатите, пространственото разпределение на дайките и по-късните хидротермални промени, като серицитизация и аргилизация, са с подчертано съвместно разпределение в пространството. Това показва, че дайките и хидротермалните промени споделят общи рудовместващи структури и са формирани при придвижването на по-ранни магматични продукти и по-късни хидротермални флуиди. Структурният анализ, базиран на линеаментното картиране и построяване на 3D повърхнини на разломните нарушения, показва три разломни системи с посоки СЗ-ЮЕ, СЕ-ЮЗ и И-З. Разломните нарушения със СЕ-ЮЗ и И-З посоки се маркират като главни вместващи структури за магматичните продукти и рудоносните хидротермални разтвори. Интеграцията на структурните данни и анализът на пространствената ориентация на геоложките тела позволяват по-добро разбиране и по-акуратно дефиниране на локалния структурен тренд и пространственото разпределение на дайките и хидротермалните промени.

**Ключови думи:** 3D имплицитно моделиране, разломи, Западно Средногорие

### Introduction

This work is address on the results received from 3D geological implicit modelling applied on the main lithological units and rock alterations exposed around the Milin Kamak Au-Ag deposit. The study area is situated in the Western Bulgaria, southern from the town of Breznik. The 3D modelling is considered as precise and valuable instrument, basis for geological exploration projects and mining works. The received results serve as a suitable footing for taking geological decisions and groundwork for future prospecting and investigation works. The purpose and requirements of three-dimensional modelling can broadly differ depending mainly on the geological settings, structures framework, spatial resolution and available geological information and knowledge. To be

accepted geological modelling as accurate, every volume models that consist of lithological units or alteration rocks should be combined with 3D surface data involving faults, brittle or ductile zones and topography as boundary surface. At present, the geological modelling can integrate two-dimensional (2D) GIS data, various statistical methods, database and 3D software technologies with powerful three-dimensional visualization modules (Wang and Huang, 2012). 3D modelling can be applied to build three-dimensional structural objects involving various structures, stratum, rock body, ore body, geochemical anomaly and geophysical anomaly (Kaufmann and Martin, 2008; Xiao, 2009; Wang and Huang, 2012; Pears and Chalke, 2016). Therefore, three-dimensional modelling can be used as a powerful instrument to

explain the genesis of constructed geological objects through spatial analysis (Pouliot et al., 2008; Wang and Huang, 2012).

The main goals in this study are: 1) Construction of 3D implicit model based on the spatial relationship of regional lithological units; 2) Building of 3D implicit model based on the spatial distribution of the local alteration rocks and dykes in the Milin Kamak deposit; 3) Incorporating three-dimensional model with a distribution of 3D fault surfaces, extracted from lineament structures; 4) Integration of structural data and body geometry analysis for accurate definition of a local structural trend.

## Geological settings

In regional tectonic position aspect, the study area belongs to the Apuseni-Banat-Timok-Srednogorie magmatic and metallogenic belt, which is considered as formed in an extensional geodynamic regime and widespread development of Late Cretaceous magmatic activities with numerous submarine volcanoes (Popov et al., 2002). During the Laramian phase of Alpine orogeny, the area in Western Srednogorie was an arena for widespread thrust-nappe deformations. This regional tectonic event has a significant effect, which leads to the formation of the slight South-West vergent Krasava syncline (Marinova et al., 2010) (Fig.1).

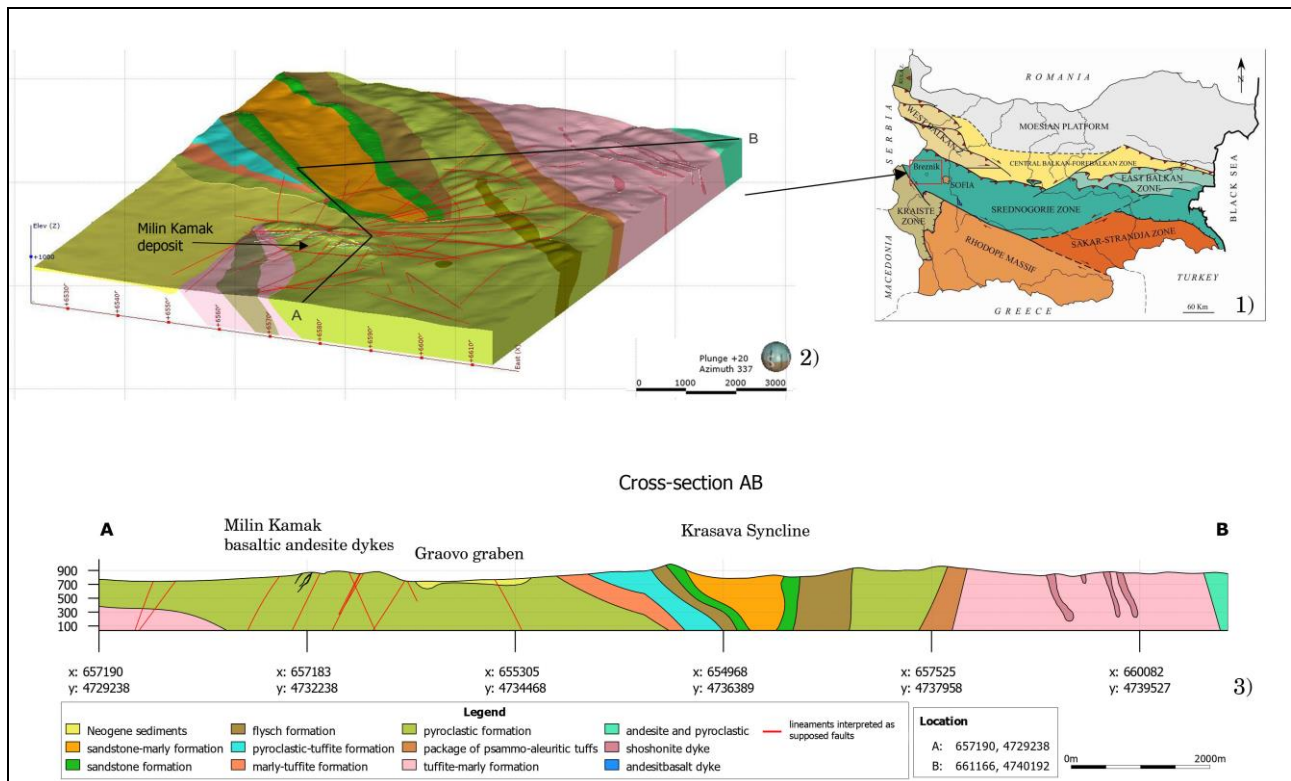


**Fig. 1. Three-dimensional lithological model of regional rock units around Milin Kamak deposit**

1) simplified tectonic map of Bulgaria (Ivanov J, 1998); 2) three-dimensional model of regional rock units around Milin Kamak deposit with attached lineament structures (based on Marinova et al., 2010); 3) cross-section on A-B line based on the 3D lithological model

The Laramian orogenic processes lead to the formation of regional structures with directions of 140-160°. During the Illyrian phase of Alpine orogeny, the second tectonic event arose and leads to the formation of strike-slip and normal faults with N-S directions. Prior to the main phases of Alpine orogeny, the region around Breznik was the arena of intensive volcanic activities

These events lead to the formation of numerous radial and concentric structures that contribute to the development of a ring morphostructure. This structure is considered as a reflection of Late Cretaceous Breznik paleo-volcano (Marinov et al., 2019). The volcanic activities begin through the Coniacian and ends during the Campanian (Bairactarov, 1989). The volcanics are represented by high potassium calc-alkaline, calc-alkaline and shoshonitic series rocks (Dabovski, 2009; Velev, 2012). The rock formations around Milin Kamak deposit and the town of Breznik contain an up to 1400 m thick

succession of shoshonites, potassium trachybasalts, various ash, psephtic, lapilli and bomb tuffs. This succession belongs mainly to Breznik paleo-volcano (Marinov and Bairactarov, 1980). Further, away to the North-West direction the later volcanic succession of Vidrica paleo-volcano overlay the volcanic deposit of Breznik paleo-volcano (Dabovski, 2009). In a local tectonic setting, the rocks belong to the Srednogorie Tectonic Zone that is divided into two main units in the study area – Sofia and Lubash units (Marinova et al., 2010). The Lubash Unit is considered as a Late Alpine monoclinal structure (Zagorchev, 1995). The main feature of the unit is the distinct absence of volcanic products and the corresponding ore deposits associated with Upper Cretaceous magmatic activities. The Sofia Unit involves itself numerous and various volcanic products. This magmatic presence is regarded as the main important feature to distinguishing both zones.

The basement rocks in the work area consist of various Paleozoic, Mesozoic and Lower Cretaceous sedimentary successions outcropped mainly in the southern parts. The Paleozoic and Mesozoic rocks are developed mainly in the Lubash unit. In the Sofia unit, the Mesozoic sedimentary rocks are outcropped only as tectonically confined blocks in northeastern parts. This succession includes mainly different terrigenous-carbonate rocks. Various Upper Cretaceous sedimentary formations overlies the volcanic products of Breznik and Vidrica paleo-volcanoes and consequently builds up the core of Krasava syncline.

The rocks that form the cover belong to Neogene sediments. They are considered as sedimentary fill in graben systems and partially covers the southwestern part of the studied area. To the south-west, the Neogene succession fills the Graovo graben that is considered as the latest tectonic event aroused in the study area.

## Data used

There are two main approaches in geological modelling – explicit (controlled by hand drawing) and implicit (automated). Three-dimensional implicit modelling has been applied for the extraction and interpretation of outcomes received by the spatial distribution of the lithological units and alteration rocks. The necessary technical background is provided by using Leapfrog GEO 5.0 (Seequent Limited), specialized software with powerful instruments for 3D implicit modelling. To ensure a more accurate representation of the 3D surfaces and geological boundaries an advanced radial basic function (RBF) interpolation techniques have been used. The concept of compiling the 3D models are different depending on different geology, spatial resolution, different data and access sources of data. The 2D surface data represent faults and geological boundaries. The volume data describe in 3D the lithological units and alteration rocks. Two 3D models of the studied area where prepared in this paper – one regional (in lower resolution and one local (around the Milin Kamak deposit, in higher resolution). The sources data for compiling the main regional lithological units were obtained from the geological map in scale 1:50000. The first stage of compiling the 3D models is drawing the polylines that follow strictly the geological boundaries of lithological units drawn on the geological map. The next step is to generate a 3D surface boundaries. The three-dimensional distribution and the slopes of these surfaces are based on structural elements taken from the geological map. Afterwards, with respect on previously created the 3D surface, the volume data are generated as wireframes. The modeling of these geological units was done in lower spatial resolution due to the limited data, large volume and the widespread distribution of the units.

The concept of compiling the local detail 3D model around Milin Kamak deposit is based on modelling of the lithological units and alteration rocks. The local model differs in methodology in comparison to the modeling of regional lithological units. The implicit modelling can use both types of data – numerical and non-numerical categorical data. In this work, the implicit modelling is generated by non-numerical data such as rock codes. Significant amount of data from various exploration works were used for the creation of the models. The geological information is obtained from surface mapping,

trenches, drill holes and underground works. The data integration of more than 450 drills and 160 trenches have been used for three-dimensional modelling.

In order to generate a three-dimensional structural model, remote sensing method and surface mapping have been used to help the lineaments extraction (Marinov et al., 2019). In respect to this, it was possible to created 3D fault surfaces and to be integrated into the model of lithological units and alteration rocks.

## Interpretation and Results

The results obtained from three-dimensional implicit modelling represent the spatial distributions of alteration rocks and lithological units exposed around Milin Kamak deposit located near the town of Breznik. This data allows a body geometry analysis of the main ore veins and therefore better understanding of the local structural trend. The traditional 3D modelling techniques use explicit modelling approach for wireframe models. This technique is available in many of the mining software. One of the gains of the explicit modelling are possibilities for hand (explicitly) drawn geological interpretations by polylines and can be useful instruments for simplified representation of geological units and wireframe building.

For the modelling of lithological units, ore body or other geological structures, the explicit modelling uses vertical cross-sections, elevation or inclined planes within a predefined corridor in the viewed space. Inside this space, 3D wireframes are generated manually by hand drawing in 2D sections that are manually linked through triangles (Vollgger et al., 2012). These manually linked sections lead to a design of wireframes with more straight-line nature that is unlikely to define accurate nature boundaries of the lithological units or structures (Fig. 2 e, f). The triangle intersections and open triangles are common problems in explicit 3D modelling and must be cleaned before further operation such as volume evaluation.

The implicit modelling is regarded as an alternative option for wireframes building. This modelling technique use data directly received from various exploration works like drillhls, trenches or point data derived from underground works without any manually linked polylines in the 2D section. From these measured numerical or non-numerical categorical data, computer algorithms calculate spatial interpolation between the samples and build mesh structures as 3D isosurfaces (Vollgger et al., 2012). As an automated operation the implicit modelling allows faster building of the wireframes and provides an accurate representation of the geological boundaries. This modelling is accurate, flexible and efficient compared to the explicit methodology (Knight et al., 2007; Silveira Braga et al., 2019). The 3D model is automatically updated every time when a new data is received. The results of three-dimensional implicit modelling application can be used surefire to comprehend the distribution of the alteration rocks and lithological units in the space according to regional and local structural patterns.

During the modelling process, stereo images obtained by ASTER optical instrument on TERRA satellite has been integrated into the 3D models to compute the structural trend surfaces. This information was subsequently combined with the data received from fieldworks. The lineament structures

extracted in this way allowed to distinguish a distinct ring morphostructure located around the town of Breznik (Marinov et al., 2019; Popov, 2011). One distinctive feature relating to the movement of magmatic products and hydrothermal fluids are the presence of permeable settings. The early magmatic products are most often represent by layered intrusions concordant to the beds. They are formed before the most intensive activity of the Breznik paleo-volcano. Such layered sill bodies were localized SW and NE parts of the ring morphostructure. Numerous radial and concentric faults were formed in the latest stages of volcano-tectonic evolution. The

dykes in Milin Kamak deposit are associated with these later stress phases. These faults most likely served as channels and hosting structures for later ore-body fluids and dykes (Marinov et al., 2019). During the modelling process, the distribution of the argillic and sericitic alteration and dykes show that there is strict common alignment in the space with EW and NE-SW direction (Fig. 2). This emphasizes that they share common hosting fault structures. The structural data obtained by the geological exploration in Milin Kamak deposit show three main fault systems with NW-SE, NE-SW and E-W direction, which defined local structural trend (Fig. 3).

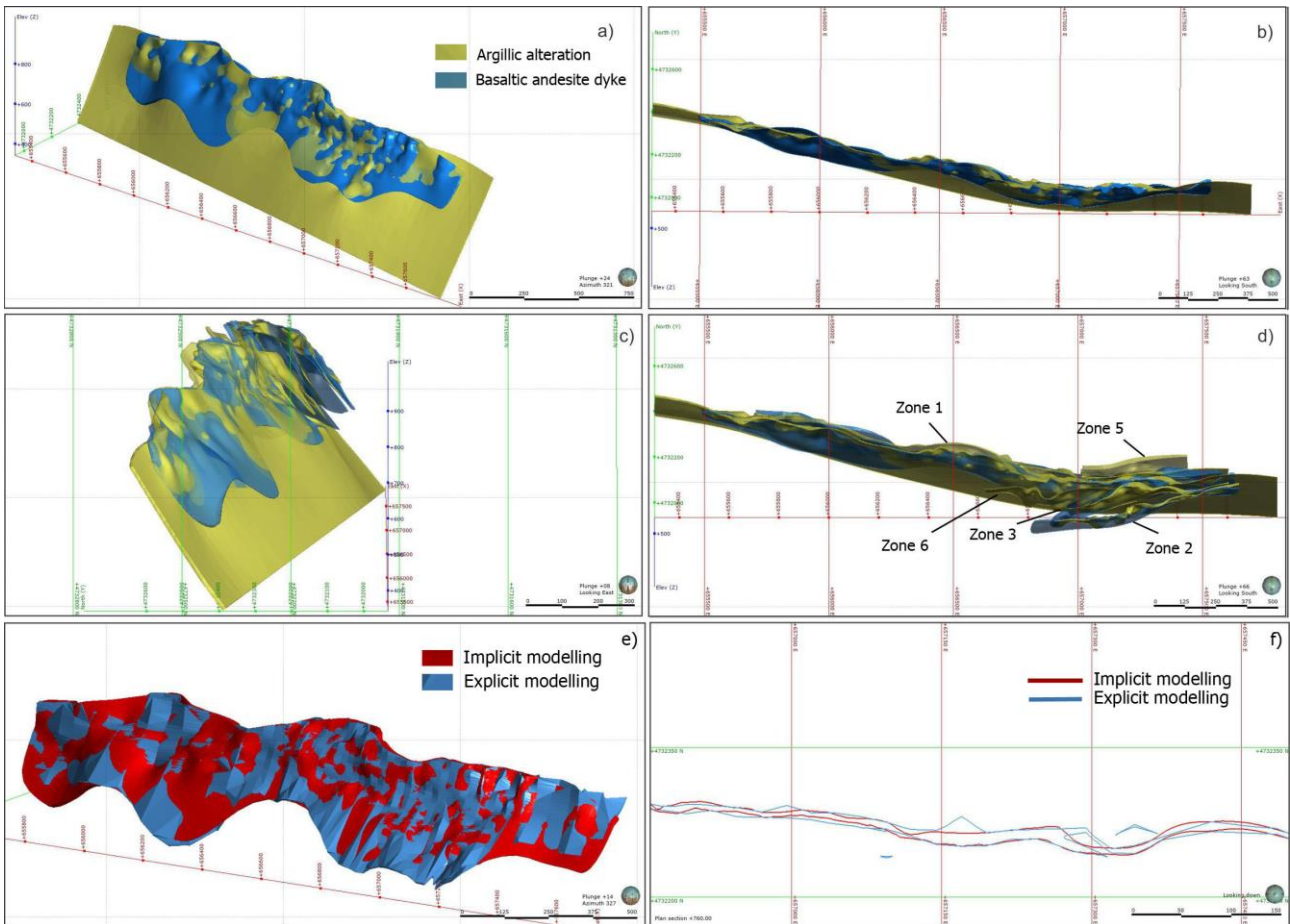


**Fig. 2 Comparison of three-dimensional model of the spatial distribution of argillic alteration and basaltic andesite dykes and comparison between results of implicit and explicit modelling of the dyke**

a) spatial distribution of argillic alteration around zone 1 and basaltic andesite dyke; b) in plan view; c) spatial distribution of argillic alteration around all zones and all basaltic andesite dykes; d) in plan view; e) comparison between implicit and explicit modelling of the basaltic andesite dyke; f) comparison in plan view with straight-line nature

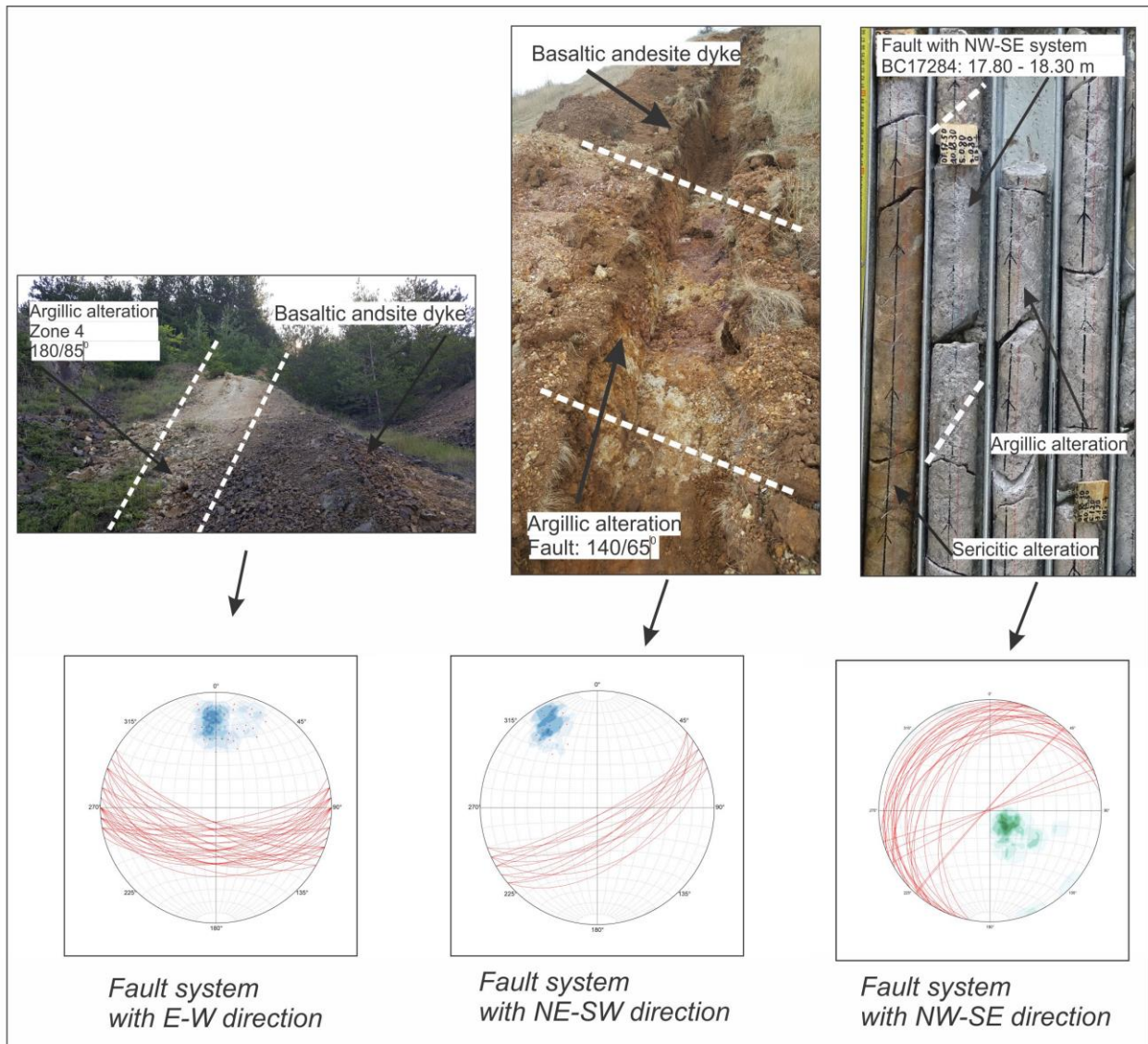


Fig. 3. Outcrops around the Milin Kamak deposit with argillic alteration and basaltic andesite dykes showing main structure systems

This trend fully coincides with the spatial distribution of lineaments defined by stereo-images. Geological structures observed in the well logs and point data obtained from underground works in Milin Kamak deposit allows to define more accurate the spatial position and dip of direction for the observed lineament structures observed on ASTER stereo images. The spatial position of the lineaments could be considered with higher confidence in the southern parts of the ring morphostructure. Whereas, due to the lack of outcrops and exploration works in the north part the 3D space orientation of the lineaments are indistinct and under discussion.

## Conclusion

3D implicit modelling is used as automatic tool for building three-dimensional models for alteration rocks and main lithological unit exposes around Milin Kamak Au-Ag deposit. This automatic modelling is considered as a precise and useful instrument that allows the processing of huge amount of

information in a short time. Respectively, the ability to build the model quickly allows more time to be engaged to further geological interpretation. Based on the methodology and results described in this study the following conclusion has been done:

- 1.) The completed 3D implicit model provides an accurate representation of 3D isosurfaces and precise construction of the geological boundary and spatial distribution of the alteration rocks and lithological units in the studied area.
- 2.) The results from the remote sensing methods allow to build the 3D fault surfaces based on lineament drawing. The three-dimensional fault surfaces show distinctive radial and concentric pattern that marks the volcanic cone.
- 3.) The local structural trend with fault systems with NW-SE, NE-SW and E-W direction defined by underground works in Milin Kamak deposit coincides with spatial position of the lineament structures in the southern part of the ring morphostructures.

- 4.) The spatial distribution of the dykes and later sericitic and argillic alterations emphasize strictly their common alignment in space.
- 5.) In the 3D geological model, the direction and dip of the dykes and alteration rocks show the same structural trend as the defined fault systems with NE-SW and E-W direction. This emphasizes that the faults with this trend serve as permeable and hosting structures for the ore-bearing fluids and dykes. The creation of these structures probably arises during the development of local stress during the final stages of the volcanic activity.

**Acknowledgements.** The authors are grateful to the Seequent Limited for the providing of Leapfrog Geo academic license and to the Trace Resources LTD for the providing of drillhole core data.

## References

- Bairactarov, I. 1989. *Upper Cretaceous metallogeny of Western Srednogie and Plana Mountain*. Phd thesis, Research Institute for Mineral Resources, Sofia, 197 p. (in Bulgarian).
- Dabovski, H., B. Kamenov, D. Sinnyovsky, E. Vasilev, E. Dimitrova, I. Bairactarov. 2009. Upper Cretaceous geology. – In: Zagorchev, I., H. Dabovski, T. Nikolov (Eds.). *Geology of Bulgaria. Part II, Mesozoic Geology*. Sofia, Marin Drinov Acad. Publ. House, 305–638.
- Ivanov, Ž. 1998. *Tectonics of Bulgaria*. Unpublished Professorship Thesis, Sofia University “St. Kliment Ohridski”, 579 p. (in Bulgarian).
- Kaufmann, O., T. Martin. 2008. 3D geological modelling from boreholes, cross-sections and geological maps, application over former natural gas storage in coal mines. *Computers and Geosciences* 34 (3), 278-290.
- Knight, H., R. Lane, H. Ross, A. Abraham, J. Cowan. 2007. Implicit ore delineation. In: Fifth Decennial. Mineral. Exploration Conference on Mineral Exploration. Annals Toronto: Mine Site Exploration and Ore Delineation & Ore Deposits and Exploration Technology, 2007, v. 1, p. 1165-1169.
- Marinov, T., I. Bairactarov. 1980. Alkaline Basalts in the Western Srednogie. – *C. R. Acad. Bulg. Sci.*, 33, 4, 529–532.
- Marinov, I., K. Popov N. Temelakiev. 2019. Volcanic ring morphostructures in the Western Srednogie, Bulgaria. – *Ann. Univ. Mining and. Geol* 62, 5–10.
- Marinova, P., V. Grozdev, D. Ivanova, D. Sinnyovsky, I. Petrov, P. Milovanov, A. Popov. 2010. *Explanatory Note to the Geological Map of the Republic of Bulgaria. Scale 1:50 000. Map Sheet Breznik K-34-46-G (Breznik)*. Sofia, Ministry of Environment and Water, Bulgarian Geological Survey, 63 p.
- Pears, G., T. Chalke. 2016. Geological and geophysical integrated interpretation and modelling techniques. *ASEG Extended Abstracts 2016*, 4 p.
- Popov, P., T. Berza, A. Grubich, I. Dimitru. 2002. Late Cretaceous Apuseni-Banat-Timok-Srednogie (ABTS) Magmatic and Metallogenic Belt in the Carpathian-Balkan orogen. – *Geologica Balc.*, 32, 2-4, 145–163.
- Popov, K. 2011. Recognition of the Panagyurishte Ring Morphostructure by satellite stereo-images. – *Ann. Univ. Min. Geol.*, 54, Part. I, Geol. and Geophys., 81–88.
- Pouliot, J., K. Bedrad, D. Kirkwood, B. Lachance. 2008. Reasoning about geological space: coupling 3D GeoModels and topological queries as an aid to spatial data selection. *Computers and Geosciences* 34, 529-541.
- Silveira Braga, F., C. Rosiere, J. Santos, S. Hagemann, P. Salles. 2019. Depicting the 3D geometry of ore bodies using implicit lithological modeling: An example from The Horto-Baratinha iron deposit, Guanhães block, MG. *Revista Escola de Minas*, 72(3), 435-443.
- Velev, S., R. Nedialkov, I. Peycheva, A. von Quadt. 2012. Geological and petrological characteristics of the volcanic centres from the upper volcanogenic–sedimentary unit from the Western Srednogie. – *Geologica Macedonica*, 3, 7–12.
- Vollgger, S., A. Cruden, J. Cowan. 2012. Structural Geology Meets 3D Implicit Deposit Modelling, Proceedings of Structural Geology and Resources. Abstract from Structural Geology and Resources, Kalgoorlie, Australia.
- Wang, G., L. Huang. 2012. 3D geological modeling for mineral resource assessment of the Tongshan Cu deposit, Heilongjiang Province, China. – *Geoscience Frontiers*, Volume 3, Issue 4, 483-491.
- Xiao, K. 2009. Computer simulation of three-dimensional geologic map and resource evaluation. In: The 9<sup>th</sup> National Deposit Congress, pp.742-743 (English abstract)
- Zagorchev, I., V. Kostadinov, D. Chounev, R. Dimitrova. I. Sapunov, P. Chumachenko, S. Yanev. 1995. *Explanatory Note to the Geological Map of Bulgaria on Scale 1:100 000, Vlasotince and Breznik Map Sheets*. Sofia, Committee of Geology and Mineral Resources, Geology and Geophysics Ltd, 60 p. (in Bulgarian with English abstract).

## MODELLING AND ASSESSMENT OF DEBRIS FLOW EROSION AND DEPOSITION USING GEOINFORMATION TECHNOLOGIES

*Valentina Nikolova, Asparuh Kamburov, Radostina Rizova*

*University of Mining and Geology "St. Ivan Rilski", 1700 Sofia; v.nikolova@mgu.bg; asparuh.kamburov@mgu.bg; r.rizova@mgu.bg*

**ABSTRACT.** Debris flows are one of the most destructive geological-geomorphological hazards in mountain areas. Although the frequency of their occurrence is low, their sudden character increase the risk and requires preventative measures as well as increased preparedness for action in case of the event propagation. Studying the dynamic of debris flows can contribute to better understanding the process and to mitigate the risk. The aim of the current research is to analyse the geomorphic change due to debris flow occurrence and to assess erosion and deposition. The study is carried out on a gully induced debris flow located in a low mountain area of the Eastern Rhodopes (Bulgaria). The methodology of the research includes making of digital elevation models (DEMs) generated of two point clouds acquired in two terrestrial laser scanning (TLS) field campaign and deriving of surfaces of slope and curvature. The spatio-temporal changes in erosion and deposition are assessed in GIS environment by analyses of the changes in slope and topographic curvature of the debris fan and low part of the transport channel for the period October 2019 – June 2020. The results show that although increasing the convex areas at the debris fan, the volume of the deposits is decreased with 0.58 m<sup>3</sup>, which can be explained by mass movement to the lower erosion basis. The results of the GIS analysis are interpreted having regard the grain-size analysis of sediments from the channel and debris fan, and confirm the activity of the process in the studied period.

**Keywords:** debris flow, erosion, modelling, DEM, TLS

### МОДЕЛИРАНЕ И ОЦЕНКА НА ЕРОЗИЯ И АКУМУЛАЦИЯ ОТ КАЛНО-КАМЕНЕН ПОРОЙ С ИЗПОЛЗВАНЕ НА ГЕОИНФОРМАЦИОННИ ТЕХНОЛОГИИ

*Валентина Николова, Аспарух Камбуров, Радостина Ризова*

*Минно-геоложки университет „Св. Иван Рилски“, 1700 София*

**РЕЗЮМЕ.** Кално-каменните порои са едни от най-разрушителните геолого-геоморфоложки процеси в планинските територии. Въпреки ниската честота на проява, внезапният им характер увеличава риска и изисква превантивни мерки, както и повишаване на подготвеността в случай на проява на тези явления. Изучаването на динамиката на кално-каменните порои ще допринесе за по-добро разбиране на процеса и намаляване на риска. Целта на настоящото изследване е да се анализира промяната на топографската повърхнина, предизвикана от проява на кално-каменен порой и да се направи оценка на ерозията и акумулацията. Изследвана е промяната от кално-каменен порой, проявен в овраг, в нископланинския релеф на Източните Родопи (България). Методологията на проучването включва съставяне на цифрови модели на релефа (ЦМР) от два облака от точки, получени при две наземни лазерни сканирания (НЛС) и генериране на повърхнини на наклоните и на топографската кривина. Пространствено-временните промени в ерозията и акумулацията са оценени в ГИС среда чрез анализ на промените в наклоните и кривината при наносния конус и долната част на ерозионния канал за периода октомври 2019–юни 2020 г. Резултатите показват, че въпреки увеличаване на изпъкналите площи в наносния конус, обемът на наслагите е намалал с 0,58 m<sup>3</sup>, което може да се обясни с движението на материала към по-ниския ерозионен базис. Резултатите от ГИС анализа са интерпретирани във връзка с резултатите от гранулометричния анализ на седименти от ерозионния канал и наносния конус на кално-каменния порой и потвърждават активността на процеса в изследвания период.

**Ключови думи:** кално-каменен порой, ерозия, моделиране, цифров модел на релефа, наземно лазерно сканиране

### Introduction

Erosion and deposition are the processes that provide information about the spatio-temporal dynamic of debris flows. These processes are closely related to intensive rainfall and occurrence of torrential flows but in many cases debris flows occur in ungauged basins and then modelling of debris flow susceptibility based on geomorphological parameters is of great importance for planning of mitigation measures. The review of publication about modelling of debris flow geomorphic changes shows two main approaches. The first one is direct use of digital elevation models (DEMs) and calculation the elevation difference between old and new surfaces (Lane et al., 2003; Wheaton et al., 2010; Schürch et al., 2011, Theule et al., 2012; Cavalli et al., 2017). The second approach is based on spatial analyses of DEMs derivatives like as slope, topographic curvature, roughness and other

morphometric parameters (Cavalli et al., 2017; Grelle et al., 2019). Terrain variables slope gradient and curvature are used for determining terrain based erosion reference units for erosion modelling and deriving potential erosion areas (Flügel and Märker, 2001; Tcherkezova and Sarafov, 2015). Cavalli et al. (2017) analyse the relation between geomorphometry and geomorphic changes and conclude that erosion prevails on positive values of planform curvature, which correspond to concave features, while the majority deposition areas occur on convex features. Many researchers analyse morphometric parameters of debris flows areas and different indices calculated on the basis of catchment morphometry (Melton index, topographic wetness index, stream power index) to determine debris flows source, erosion channel and deposition areas and to evaluate the dynamic of the processes (Wilford et al., 2004; Rowbotham et al., 2005; Chen and Yu, 2011; Zhou et al., 2016). For this purpose high resolution DEMs of debris

flows areas are used which shows the growing application of geoinformation technologies in debris flows research. Monitoring of debris flows through multi-temporal LiDAR data is becoming a common practice (Loye et al., 2016; Cavalli et al., 2017; Morino et al., 2018). Although the growing use of remote sensing in debris flow research it is still a challenge to determine the most effective DEM resolution for the particular area of research and to generate the model of the terrain when it is covered by forest and shrubs vegetation.

Considering the recent trends in studying debris flow erosion and deposition, the aim of the current study is to analyse the geomorphic change of a debris flow by using terrestrial laser scanning (TLS) and GIS analyses. This is a part of wider research of debris flow in the Eastern Rhodopes which is the first one in this area applying geoinformation technologies and particularly TLS data. It will contribute meaningfully to the organizing the monitoring of debris flows and mitigating the negative impacts of this hazardous event.

## Study area

The current study is done on the example of a gully located in the Eastern Rhodopes, Bulgaria (Fig. 1). The area is characterized by often occurrence of debris flows due to the intensive rainfall, deforested slopes and rocks highly susceptible to weathering and erosion. The sampling area is the lower part of a gully incised in a steep slope, located near to the village of Golyama Bara.

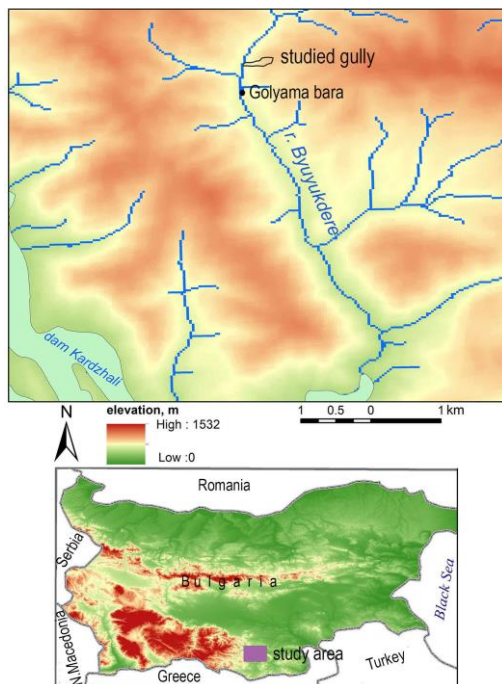


**Fig. 1. Study area**

The catchment of the gully reaches an altitude of about 600 m and is covered by low deciduous vegetation and shrubs. The transport channel is very steep with a width from 0.40–0.60 m in its narrowest sections, to 2–3 m in the widest. It ends with a well-defined debris fan, built of boulders and pebbles (Fig. 2). The gully is a left tributary of the river Byuyukdere that flows in the dam Kardzhali. In the lower course, the river valley is conditioned by a fault, which explains the high slope gradients of the left tributaries in this section.

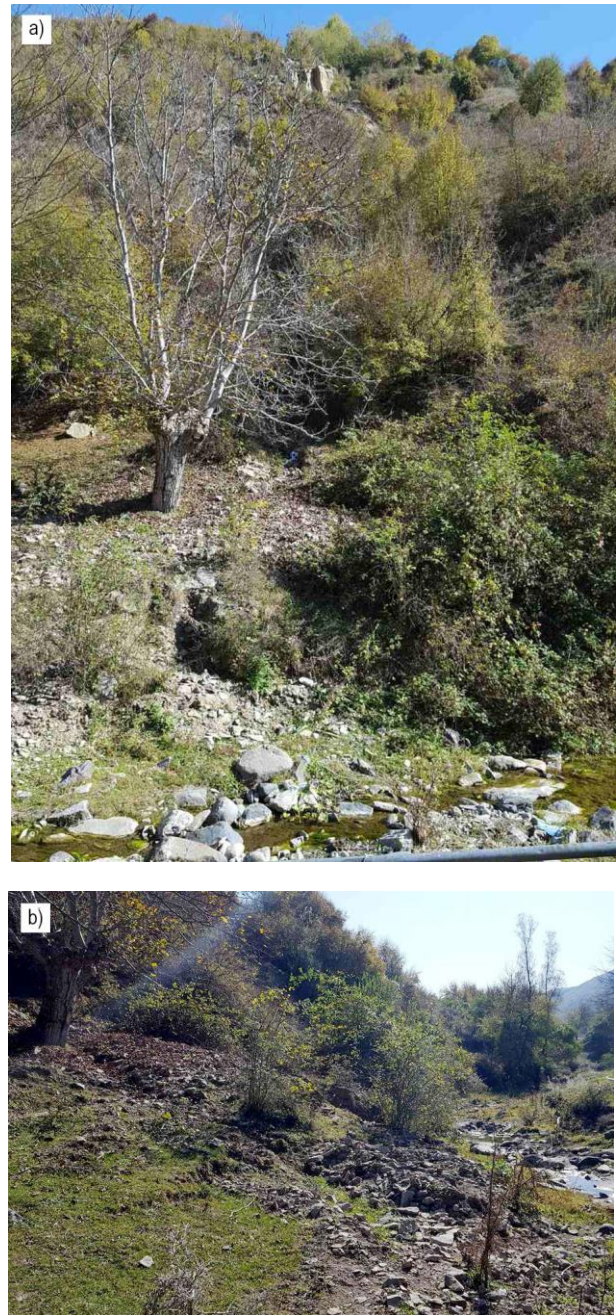


**Fig. 2. Debris flow area:** a) the watershed with debris source area in the upper part of the photo; b) debris fan.

The rocks in which the gully is cut are of Paleogene age (Jordanov et al., 2008). They are represented by medium acid volcanics – latites to andesites, tuffs, tuffites and epiclastites. These rocks build the contemporary debris fan. The large size of the clasts can be explained by the rocks susceptibility to weathering and erosion as well as by the high slope gradient and are an indicator of high kinetic energy of the slope processes during intense rainfall.

The often occurrence of debris flows in this part of the Eastern Rhodopes impacts on the sediment regime in the rivers and retention capacity of the dam Kardzhali. This increase the flood risk and requires consistent monitoring of the debris flows and mitigation measures.

## Data and methods

The analyses of erosion and debris deposition are done on the basis of field surveying and high resolution DEMs. Two consecutive terrestrial laser scanning (TLS) campaigns were performed in order to derive DEMs of the low part of debris flow area and to analyse geomorphic change. The first campaign was organized in October 2019, and the second one – in June 2020. During the first campaign 2 scans were carried out, from which a set of 2 point clouds were obtained. The second campaign was performed with more terrain details via 4 scans. The TLS data was derived using Stonex X300 laser scanner – a mid-range (1.6–300 m) device with two cameras and Wi-Fi web interface. All scans were performed in 360° panoramic mode. Standard resolution was deemed appropriate for the required terrain details. All the data was processed via the Stonex 3D Reconstructor software. The following workflow was followed during the data processing stage:

1. Data pre-processing – during this step noise and outliers were removed from the point clouds via median and range-reflectance filter;
2. Computation of normals of the point cloud;
3. Confidence coefficient was computed, based on the incident angle between the laser beam and the tangent plane of the target, the distance to the target and the material of the object;
4. Registration of the point clouds via identical points and features;
5. Vegetation removal via manual selection and cropping. It has to be noted that the first campaign required much less vegetation cleaning than the second, due to seasonal vegetation changes.
6. Georeferencing of the point clouds.

An example of point cloud before and after vegetation removal is given in Fig. 3.

The cleaned data was subsequently exported in ASCII point cloud format (X, Y, Z) was further processed in GIS environment. As a result DEMs with a horizontal resolution 0.1 m are derived. Taking into account the characteristics of the studied area and the size of the debris deposits, the models are smoothed in using ArcGIS Spatial Analyst Tools – Neighborhood – Focal Statistics with neighborhood type (moving window) 5 x 5 cells, statistics type "Mean". On the basis of the smoothed DEMs and analyses of the slope and topographic curvature the low part of the debris flow transport channel and deposition area are delineated. The changes in profile and planform curvature are considered as an indicators for erosion and deposition. For this purpose curvature rasters are calculated on the DEMs, derived of the data of October 2019 and June 2020. Profile curvature is the curvature parallel to the maximum slope. Positive values of the profile curvature indicate that the surface is concave which can be related to mass wasting and erosion, and negative values indicate convex surface and can be related to accumulation of the deposits. Planform curvature is perpendicular to the direction of the maximum slope and allows to determine ridges and valleys. When the planform curvature is positive the surface is convex and flow lines divergent, while the negative values of the planform curvature indicate that the surface is concave and flow lines convergent.

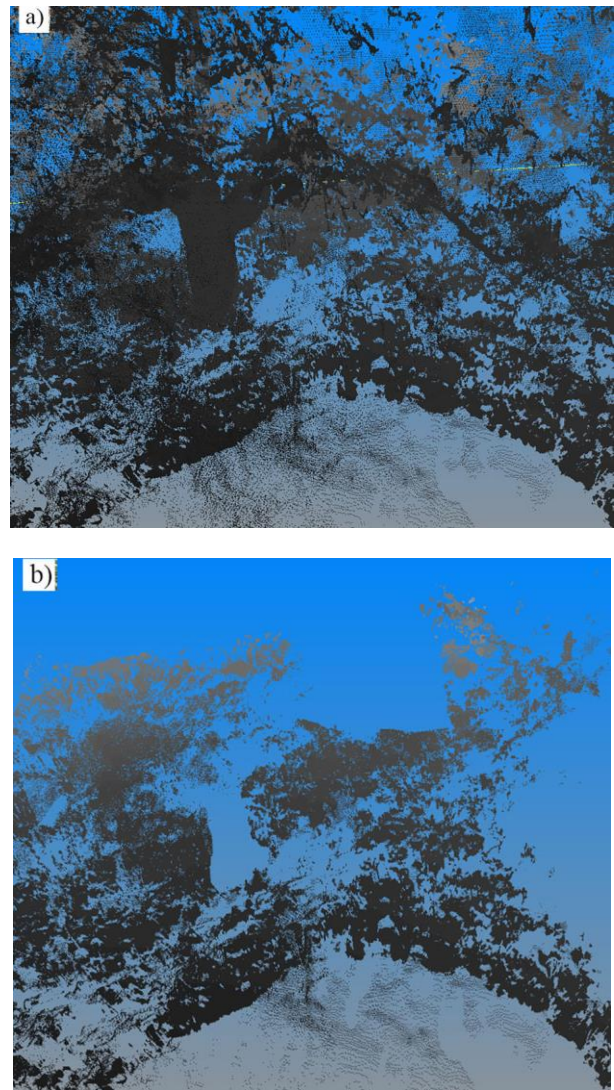


Fig. 3. Point clouds: a) before vegetation removal; b) cleaned data.

The volume of the contemporary deposits on the debris fan is calculated using Cut Fill tool of ArcGIS 3D Analyst Tools, which calculates the volume between two surfaces: the surface of the debris fan (unsmoothed DEM) and a straight surface, modeled between the base of the fan and the fan apex (Fig. 4).



Fig. 4. Debris deposits above the flat surface

The observed geomorphic changes estimated by morphometric analysis are considered in relation of the results of morphoscopic and grain-size analyses of the debris deposits. The form of the boulders and pebbles is determined by coefficient of elongation ( $C_e$ ) and coefficient of flattening ( $C_f$ ), Serebryanniy (1980), calculated as a ratio between the axis "a", "b" and "c" of the measured clasts as follow:  $C_e = b/a$ , and  $C_f = c/b$ . Conclusions about the conditions of the transport

and deposition are done on the basis of the degree of sorting (standard deviation) calculated on the grain size cumulative curves (Folk and Ward, 1957) as:

$$\sigma_1 = (\varphi_{84} - \varphi_{16})/4 + (\varphi_{95} - \varphi_5)/6.6, \text{ where } \varphi \text{ is grain size diameter in a logarithmic scale.}$$

**Results**

As a result of the TLS, detailed DEMs of the contemporary debris fan and the low part of the transport channel have been compiled as it written above. Two main morphometric parameters – curvature of the topographic surface and slope, derived of DEMs are analysed as indicators of the geomorphic change. The outputs of the analysis are given in Table 1.

Table 1. Morphometric parameters

	debris fan			
	October 2019		June 2020	
	concave, %	convex, %	concave, %	convex, %
profile curvature	48.07	51.93	45.16	54.84
planform curvature	46.83	53.14	43.38	56.58
average	47.45	52.54	44.27	55.71
	transport channel			
	October 2019		June 2020	
	concave, %	convex, %	concave, %	convex, %
profile curvature	55.74	44.26	51.55	48.45
planform curvature	52.54	47.46	51.16	48.84
average	52.54	47.46	51.36	48.64
mean slope, degrees	debris fan			
	October 2019		June 2020	
	15.28		19.36	
	transport channel			
	October 2019		June 2020	
	30.12		42.31	

The values of the curvature show that the area of convex parts of the debris fan is larger than the area of concave ones. This confirm the model of accumulation of the deposits. The comparison between October 2019 and June 2020 indicates increasing the convex areas in the debris fan which is related to changes in the spatial distribution of the deposits, where the accumulated mass in the upper and middle part of the debris fan were moved to the lower part (Fig. 5).

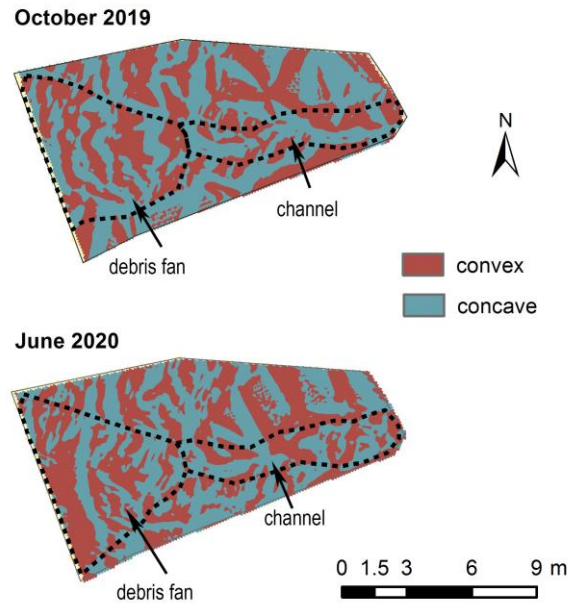


Fig. 5. Profile curvature

Planform curvature shows the changes in the convergence and divergence of the flows lines and in this regard allow to determinate the debris transport channel and deposition area (Fig. 6).

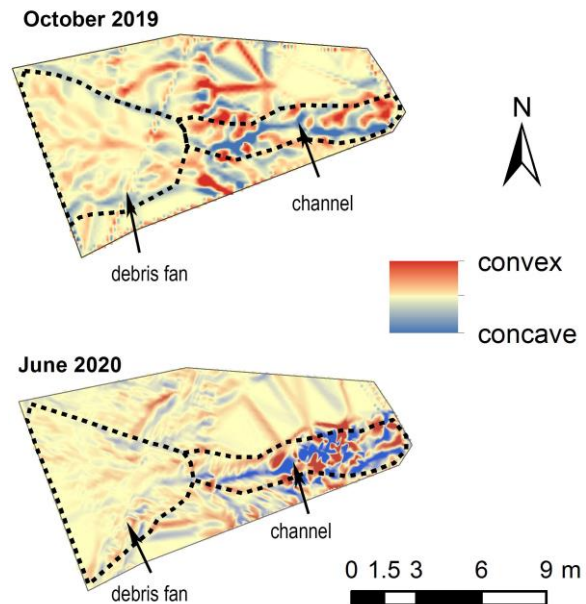


Fig. 6. Planform curvature

The changes in the curvature of the surface at the transport channel in the observed period are less expressed (Table 1). Although the concave parts are predominant the analysis show slight decrease of their areas and increasing of the convex parts. This can be explained by erosion and movement of debris deposits from the source area to the upper and middle part of the channel, and temporary stationing of the deposits due to lower flow energy or retaining role of vegetation. Increasing of the slope also indicate mass wasting to the local erosion basis from October 2019 to June 2020 (Fig. 7). The images in Fig. 7 are of the low part of the transport

channel and correspond well to the models of profile curvature (Fig. 5), where convex parts are visible at the low part of the channel in October 2019, and are replaced by concave ones at the model of June 2020.



**Fig. 7. Debris flow transport channel:** a) October 2019; b) June 2020.

The volume of the contemporary debris deposits on the fan, calculated relative to the reference slope surface, is  $5.99 \text{ m}^3$  in October 2019 and decreased to  $5.41 \text{ m}^3$  in June 2020. This indicates that  $0.58 \text{ m}^3$  rock and earth masses are removed to the direction of the erosion basis. Having regard the relatively small area of the gully and contemporary debris fan (nearly  $25 \text{ m}^2$  of the fan) we can conclude that the area is subject to intensive erosion. The results of the geospatial modelling of the low part of the transport channel and the contemporary debris fan correspond well to the sampling of the deposits and to the results of the carried out morphoscopic and grain-size analyses.

The morphoscopic analysis of the clasts and calculated coefficients of elongation and flattening show that the disk-shaped and flat-drawn shape of the deposits predominates. This, on the one hand, suggests that they are moved along the slope by dragging, and on the other hand, it is related to the way the pyroclastic rocks weather. All fragments have a low degree of smoothness (0 and I), which indicates a short transport. The analyses of the size of the debris deposit at "a" and "b" axis show the largest size of the clasts at sampling in October 2019 (average "a" = 28 cm, average "b" = 17.7 cm) while in July 2019 the sampling shows average "a" = 21.7 cm

and average "b" = 13.5 cm, and in June 2020 the average size of the sampled clasts is 22.9 cm along the axis "a" and 12.9 cm along the axis "b". This suggests that debris flow occurred between the first 2 sampling periods (July 2019 – October 2019), which was confirmed by local people who spoke about the event in the end of July. The decreasing of the size of the rock fragments at sampling in June 2020 can be explained by activation of the process and gravitational or water-gravitational movement of boulders and earth masses to the lower erosion basis of the gully – the river Byuyukdere, that reflect on the volume of the debris fan.

The grain size analysis of samples taken in October 2019 shows extremely poorly sorted materials. Sorting coefficient varies between 5.89 and 8.15 and increase from the transport channel to the basis of the debris fan, which is an indicator for turbulent nature of the flow, combined with gravitational movement of material and dynamic environment of deposition. Comparison of the values of sorting with the results of previous sampling in July 2019, when the sorting coefficient of the deposits in the flow channel is calculated at 3.73 show poorer sorted materials in October 2019 and indicate a process of torrential nature occurred between the two observation periods.

## Conclusion

Erosion and deposition of gully induced debris flow are estimated in the current study on the basis of the detailed DEMs derived from TLS in two consecutive campaigns. The results show that the considered gully is a subject of intensive erosion and mass movement triggered by intensive rainfall causing torrential flows.

The analyses of the terrain and derived models of slope and curvature show that although increasing the area of convex parts of the contemporary debris fan in comparison with their extent eight months before, the volume of the deposits decreases. This indicates that the models of curvature of the topographic surface and particularly profile curvature give reliable information about the character of the geomorphological processes and the spatial distribution of the erosion, mass wasting and deposition, but give only relative quantitative information about the processes. Although the relative character of the models of curvature the information of them can meaningfully contribute to the erosion susceptibility assessment.

Detailed information about the intensity of erosion and deposition can be received of high resolution DEMs. Beside the DEM resolution and the chosen methodology, the results depend also on the way of data processing. In cases when the slopes of the gully are covered with trees and shrubs, as in the current study, and in applying manual removal of vegetation from the point cloud it is a challenge to achieve maximum accuracy of the result due to differences in vegetation removal. The season of data acquisition and vegetation state also impact on the quality of the results.

Though some uncertainties in the models the interpretation of the results according to the results of field sampling and grain size analysis shows the reliability of the applied methodology for debris flow investigation and for assessment of the geomorphic change.

**Acknowledgements.** This work has been carried out in the framework of the National Science Program “Environmental Protection and Reduction of Risks of Adverse Events and Natural Disasters”, approved by the Resolution of the Council of Ministers № 577/17.08.2018 and supported by the Ministry of Education and Science (MES) of Bulgaria (Agreement № Д01-322/18.12.2019).

Authors express also their acknowledgement to the project Contract No MTF-170/2019, financed by the UMG “St. Ivan Rilski”.

## References

- Cavalli, M., B. Goldin, F. Comiti, F. Brardinoni, L. Marchi. 2017. Assessment of erosion and deposition in steep mountain basins by differencing sequential digital terrain models. *Geomorphology*, 291, 4–16; <http://dx.doi.org/10.1016/j.geomorph.2016.04.009>.
- Chen, Ch.-Y., F.-Ch. Yu. 2011. Morphometric analysis of debris flows and their source areas using GIS. *Geomorphology*, 129, 387–397; DOI: 10.1016/j.geomorph.2011.03.002.
- Flügel, W.-A., M. Märker. 2001. The response units concept and its application for the assessment of hydrologically related erosion processes in semiarid catchments of Southern Africa, spatial methods for solution of environmental and hydrologic problems – science, policy, and standardization, ASTM STP 1420. – In: A. B. Smith, C. D. Jones (Eds), American Society for Testing and Materials, Conshohocken, PA.
- Folk, R. L., W. C. Ward. 1957. Brazos river bar: A study in the significance of grain size parameters. – *Journal of Sedimentary Petrology*, 27, 1, 3–26.
- Grelle, G., A. Rossi, P. Revellino, L. Guerriero, F. M. Guadagno, G. Sappa. 2019. Assessment of debris-flow erosion and deposit areas by morphometric analysis and a GIS-based simplified procedure: a case study of Paupisi in the Southern Apennines. – *Sustainability*, 11, 2382; DOI:10.3390/su11082382
- Jordanov B., S. Sarov, S. Georgiev, G. Dobrev, L. Moskovska, V. Grozdev, E. Balkanska, 2008. Geolozhka karta na Balgaria, 1: 50 000, karten list K-35-75-G (Nikolovo)
- Lane, S. N., R. M. Westaway, D. M. Hicks. 2003. Estimation of erosion and deposition volumes in a large, gravel-bed, braided river using synoptic remote sensing. – *Earth Surface Processes and Landforms*, 28, 249–271; DOI: 10.1002/esp.483.
- Loye, A., M. Jaboyedoff, J. I. Theule, F. Liébault. 2016. Headwater sediment dynamics in a debris flow catchment constrained by high-resolution topographic surveys. – *Earth Surface Dynamics*, 4, 489–513; DOI:10.5194/esurf-4-489-2016.
- Morino, C., S. Conway, M. Balme, J. Hillier, C. Jordan, Colm, Th. Saemundsson, T. Argles. 2018. Debris-flow release processes investigated through the analysis of multi-temporal LiDAR datasets in north-western Iceland. – *Earth Surface Processes and Landforms*; DOI:10.1002/esp.4488.
- Rowbotham, D., F. de Scally, J. Louis. 2005: The identification of debris torrent basins using morphometric measures derived within a GIS. – *Geogr. Ann.*, 87 A(4), 527–537.
- Schürch, P., A. L. Densmore, N. J. Rosser, B. W. McArdeil, 2011. Dynamic controls on erosion and deposition on debris-flow fans. – *Geology*, 39, 9, 827–830; DOI:10.1130/G32103.1.
- Serebryaniy, L. R., 1980. Laboratorniy analiz v geomorfologii, M., pages In Russian.
- Tcherkezova, E., A. Sarafov. 2015. Applying GIS and Erosion Response Units to derive erosion processes in the Tsaparevska river watershed, Bulgaria. – *Compt. rend. Acad. bulg. Sci.*, 68, 12.
- Theule, J. I., F. Liébault, A. Loye, D. Laigle, M. Jaboyedoff. 2012. Sediment budget monitoring of debris-flow and bedload transport in the Manival Torrent, SE France. – *Natural Hazards and Earth System Science*, 12, 731–749.
- Wheaton, J. M., J. Brasington, S. E. Darby, D. A. Sear. 2010. Accounting for uncertainty in DEMs from repeat topographic surveys: improved sediment budgets. – *Earth Surface Processes and Landforms*, 35, 136–156; DOI: 10.1002/esp.1886
- Wilford, D. J., M. E. Sakals, J. L. Innes, R. C. Sidle, W. A. Bergerud. 2004. Recognition of debris flow, debris flood and flood hazard through watershed morphometrics. – *Landslides*, 1, 61–66; DOI: 10.1007/s10346-003-0002-0.
- Zhou, W., Ch. Tang, Th. W. J. Van Asch, M. Chang. 2016. A rapid method to identify the potential of debris flow development induced by rainfall in the catchments of the Wenchuan earthquake area. – *Landslides*, 13, 1243; <https://doi.org/10.1007/s10346-015-0631-0>, pp. 1243-1259.

## HYDROTHERMAL ALTERATION AND ORE MINERALIZATION OF THE NUNATAK DE CASTILLO, LIVINGSTON ISLAND, ANTARCTICA

**Ralica Sabeva<sup>1</sup>, Stefan Velev<sup>2</sup>, Hristiana Georgieva<sup>1</sup>, Tsveta Stanimirova<sup>1</sup>**

<sup>1</sup>Sofia University St. Kliment Ohridski, 1504 Sofia; E-mail: rsabeva@gea.uni-sofia.bg;

<sup>2</sup>National Center for Polar Studies, Sofia University St. Kliment Ohridski, 1504 Sofia; E-mail: velev.stefan83@gmail.com

**ABSTRACT.** Nunatak de Castillo is situated in the most northeastern part of Hurd Peninsula, Livingston Island, Antarctica. In this area of the island some well exposed small plutonic bodies are cropped out. They are emplaced into the volcanic sequence, known as Mount Bowles Formation. Nunatak de Castillo is a remnant volcanic structure (volcanic plug) with typical textures - autoclastic breccias and poorly developed columnar jointing. Macroscopically the rocks are hydrothermally altered diorite porphyries. The style of alteration is propylitic. The alteration mineralogy is based on investigations using optical microscopy and XRD analyses. Epidote and potassium feldspar veins with several cm width and lenses are observed in the propylites. At the Nunatak de Castillo an ore zone is established. It is a vein structure with thickness of about 1 m. The mineral composition of the zone is represented by copper-containing minerals like chalcopyrite, chalcocite, bornite, and covellite. The supergene alteration consists of malachite and azurite.

**Keywords:** Antarctica, Nunatak de Castillo, hydrothermal alteration, ore mineralization

### ХИДРОТЕРМАЛНО ПРОМЕНЕНИ СКАЛИ И РУДНА МИНЕРАЛИЗАЦИЯ ОТ НУНАТАК ДЕ КАСТИЙО, ОСТРОВ ЛИВИНГСТЪН, АНТАРКТИКА

**Ралица Събева<sup>1</sup>, Стефан Велев<sup>2</sup>, Християна Георгиева<sup>1</sup>, Цвета Станимирова<sup>1</sup>**

<sup>1</sup>Софийски университет „Св. Климент Охридски“, 1504 София

<sup>2</sup>Национален център за поларни изследвания, Софийски университет „Св. Климент Охридски“, 1504 София

**РЕЗЮМЕ.** Нунатак де Кастийо се намира в най-североизточната част на полуостров Хърд, остров Ливингстън, Антарктика. В този район се разкриват няколко малки плутонични тела. Те са вместили в скалите от вулканската група, известна като формация Маунт Боулес. Нунатак де Кастийо е древна вулканска структура (вулкански нег). Типични за скалите, изграждащи постройката, са автокластичните брекчиране и слабо проявената призматична напуканост. Макроскопски скалите са представени от хидротермално променени диоритови порфирити. Хидротермалната промяна на скалите е представена от пропилитизация. Минералният състав е определен на базата на оптична микроскопия и рентгенова дифракция. Сред пропилитите се наблюдават жили с няколко cm дебелина и лещи, изградени от епидот и калиев фелдшпат. В скалите на Нунатак де Кастийо се установява рудна зона, която представлява жилна структура с дебелина около 1 m. Зоната е изградена от медсъдържащи рудни минерали – халкопирит, халкоцит, борнит и ковелит. Супергенната минерализация е представена от малахит и азурит.

**Ключови думи:** Антарктика, Нунатак де Кастийо, хидротермално променени скали, рудна минерализация

### Introduction

Nunatak de Castillo is situated in the most northeastern part of Hurd Peninsula, Livingston Island, Antarctica. The island is one of the South Shetland Islands, an archipelago in the Southern Ocean. It extends in a W-SW to E-NE direction to the NW coast of the Antarctic Peninsula (Fig. 1).

Previous studies of the rocks and mineralization at Nunatak de Castillo are limited and dealt with preliminary data of the petrographical characteristics of plutonic rocks (Kamenov, 1997).

The aim of this study is to present new data of the host rocks, hydrothermal alteration and ore mineralization. The results will be of great significance for the Antarctic science.

### Regional settings

The South Shetland Block represents a continental fragment situated between the South Shetland Trench zone to the NW and Bransfield Back-arc Basin to the SE. There is a broad consensus that since Early Mesozoic the South Shetland Block represents a magmatic arc related to the subduction of the oceanic lithosphere of Phoenix Plate (Smelie et al., 1984).

The South Shetland Islands together with Antarctic Peninsula are part of the Andean Metallogenic Province which is the most economically important province in the world with giant Cu-Au porphyry, epithermal, Fe oxide-Cu-Au and manto-type Cu deposits (Sillitoe and Perello, 2005).

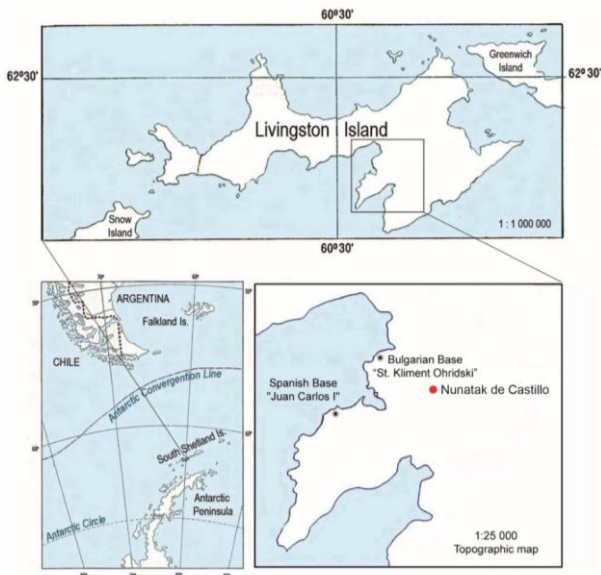


**Fig. 1.** Simplified map of Livingston Island as part of South Shetland archipelago. Nunatak de Castillo is situated in Hurd Peninsula SW from Bulgarian Antarctic Base.

## Geology of Hurd Peninsula

The Hurd Peninsula is mainly built of the sedimentary sequence of Miers Bluff Formation (Dalziel, 1972). The successions are represented by terrigenous and aleuro-pelitic mixed rocks (mudstones) formed at different depositional environments – from turbiditic to delta and alluvial fans (Pimpirev, 2015; Stefanov, 2015). The sedimentary complex is intruded by a number of dykes. Their various ages indicate several stages of magmatic activity. The NE part of the peninsula is occupied by the rocks of the Hesperides Pluton and related diorite-porphyrific mid- to shallow-crustal sill-like bodies. Smaller quartz-dioritic bodies with island-arc affinity are emplaced within the Mount Bowles volcanic rocks in the eastern part of the peninsula near to Moores Peak (Kamenov, 1997).

Hurd Peninsula contains some well exposed small plutonic outcrops with presumed Eocene age. All these small stocks are interpreted as apophyses of the larger Barnard Point Batholith (Smellie et al., 1996; Kamenov, 1997), but weighty arguments in favor of this idea are not advanced up to know. All of the hypabyssal stocks are intruded in the rocks of the Miers Bluff Formation and the Bowles Formation.

## Geology of Nunatak de Castillo

Nunatak de Castillo is heterogeneous subvolcanic body. Coherent (massive) and autoclastic textures are the most common. Autobreccias form as the cooling crust of a lava or subvolcanic intrusion fragments during continued flow of the unit. These breccias comprise jigsaw-fit and rotated clasts of the same composition as the associated coherent unit (fig. 2).

Macroscopically the rocks are grey, altered, porphyroidal, fine-grained diorite porphyries.

The ore zone is about 1 m wide and is a vein structure hosted by NW-SE-striking fault. The mineralization is represented of predominantly copper- and iron-containing minerals (Fig. 2b).

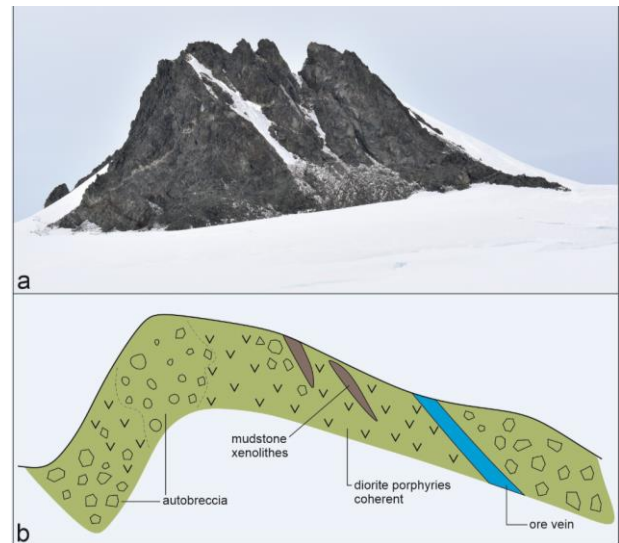


**Fig. 2.** (a) Nunatak de Castillo volcanic body (b) Simplified geological cross section of Nunatak de Castillo and the location of the ore zone (after Pimpirev (2001), unpublished data, with additions and modifications).

## Sampling and analytical techniques

The samples from Nunatak de Castillo are collected from the host and altered rocks, and also from the ore zone.

To identify the alteration and ore mineral assemblages and to define their paragenetic relationships, polished sections and polished thin sections were prepared.

X-ray powder diffraction (XRD) analyses were done at Sofia University "St. Kliment Ohridski", Sofia, Bulgaria. TUR M62 diffractometer use filtered Co-K $\alpha$  radiation in the 2 $\theta$  range 4-80°, step size 1.5°.

## Host rocks and hydrothermal alteration

The rocks from Nunatak de Castillo are determine as diorite porphyries with rare, small porphyries of plagioclase and amphibole with individual crystals of porphyry quartz. A lot of xenoliths (mainly from mudstones and granitoids) are found in the rocks.

The primary mineral assemblages include plagioclase, amphibole, quartz, potassium feldspar and single zircons. The ground mass is fine to medium-grained.

The plagioclase forms subhedral to euhedral crystals usually moderately altered to sericite (fig.3). Amphiboles are subordinate to plagioclase; they form subhedral crystals and are usually altered to carbonate, epidote and chlorite (fig. 4). Quartz porphyries are only observed as single anhedral crystals in the ground mass. Potassium feldspars are rare.

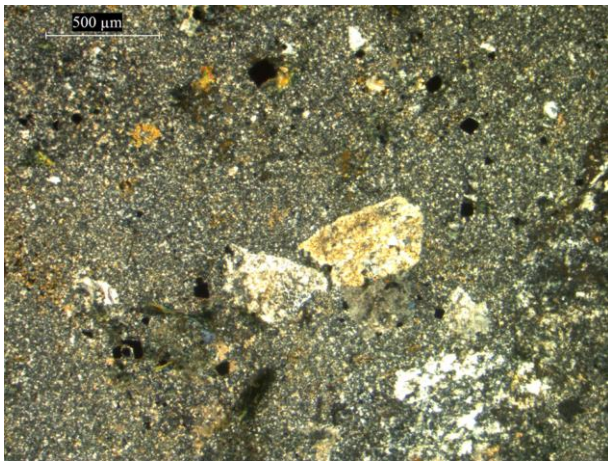


Fig. 3. Altered plagioclase crystals and occurring of secondary minerals in the ground mass (CPL).



Fig. 4. Altered amphibole crystals with carbonate and chlorite (CPL).

The secondary mineral assemblages include epidote, chlorite, amphiboles, albite, carbonates, sericite, pyrite, quartz, potassium feldspar, with small quantity of apatite and zircons. Part of the minerals are also affirmed by XRD analyses (fig. 5). The alteration is unevenly distributed into the host rock. It is intensive around veins and veins with chlorite and epidote. In the host-rock away from the veins the alteration is uniformly distributed and the new-formed minerals occur in the ground mass or replacing primary minerals. The type of alteration of the host rocks in Nunatak de Castillo strongly resembles propylitic alteration.

Epidote and chlorite are the main minerals in the alterations. Epidote usually forms subhedral to anhedral crystals (fig 6), mainly occurs in veins and veinlets or is distributed into the host rock forming clusters in the ground mass with chlorite, ore minerals, and carbonates or replacing primary minerals. Chlorite occurs as anhedral and/or radial aggregates (fig 6). Amphiboles occur as fine-grained crystals with intense green color in veins or are distributed into the host rock. Carbonates and sericite are found in the ground mass or forming aggregates on plagioclase and primary amphiboles. Small subhedral crystals of albite occur in the ground mass or form thin veins with quartz. On the basis of the distribution hydrothermal zircons are determined.

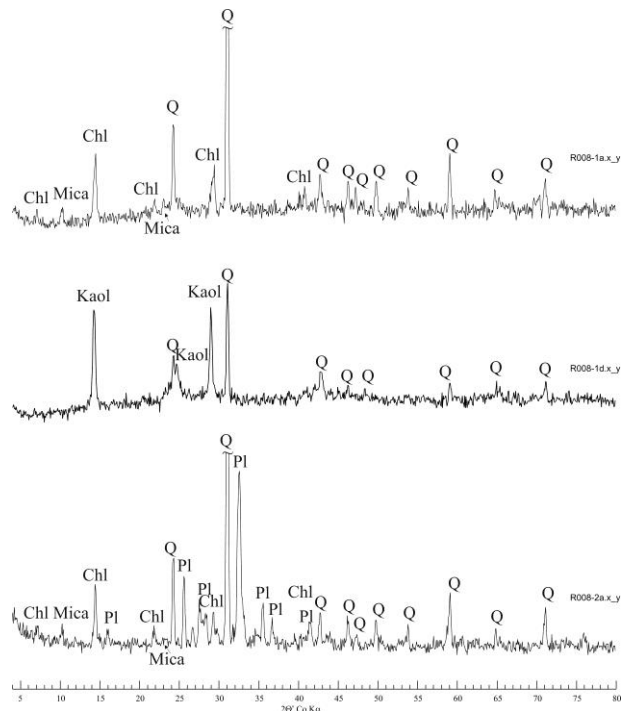


Fig. 5. X-ray diffractograms (XRD) of the alteration minerals. Chl – chlorite; Q – quartz; Mica (sericite); Kaol – kaolinite; Pl – plagioclase.

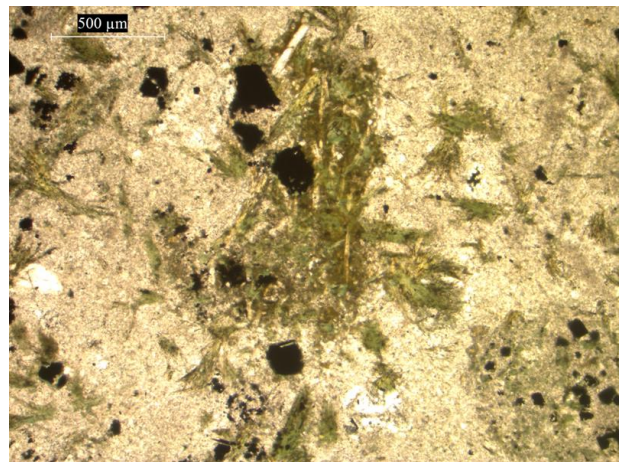


Fig. 6. Chlorite and epidote replacing primary igneous minerals (PPL).

Different veins are determined in the rocks of Nunatak de Castillo: epidote-chlorite veins; amphibole veins with quartz and chlorite; quartz veins with sericite, chlorite, kaolinite, and small quantity of epidote and carbonates; quartz veins with potassium feldspar (fig. 7.); and thin albite veins.

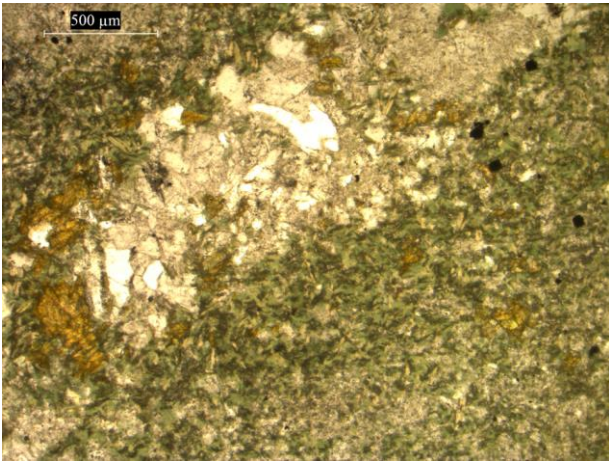


Fig. 7. Quartz-feldspar veins with intense alteration of epidote and chlorite (PPL).

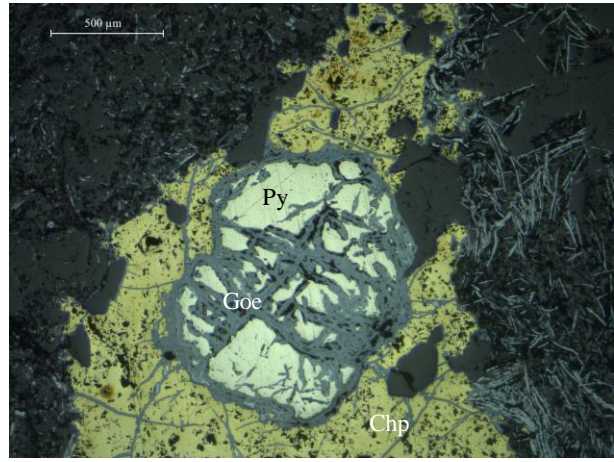


Fig. 9. Chalcopyrite (Chp) encloses single pyrite (Py) crystal. Goethite (Goe) and other iron oxide-hydroxides replaces pyrite and chalcopyrite.

### Ore mineralogy

Two stages of mineralization are identified on the basis of mineral assemblages and depositional sequence.

The first stage is copper-iron bearing and is represented by primary pyrite and chalcopyrite.

Pyrite occurs as porous and fractured subhedral to anhedral single crystals and aggregates and forms nests and thin veinlets up to 100 μm (fig. 8). Rare euhedral crystals with cubic and octahedral forms can be observed. Predominantly it is replaced by iron oxide-hydroxides.

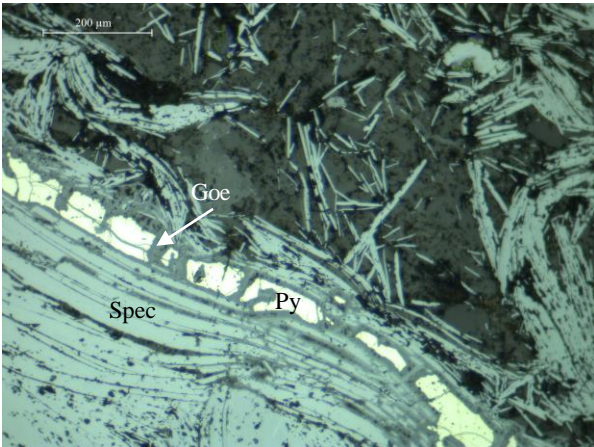


Fig. 8. Pyrite (Py) veinlet replaced by goethite (Goe) and other iron oxide-hydroxides, enclosed by specularite (Spec).

Chalcopyrite is observed as irregular grains, disseminated in the altered rock, also forms nests and rare veinlets. It encloses pyrite and probably is deposited later (fig. 9). In the most samples chalcopyrite is replaced by supergene copper sulfides (bornite, covellite, rarely chalcocite) and carbonates (malachite and azurite).

The second stage is supergene and is formed under oxidizing conditions. Hematite (specularite), goethite and other iron oxide-hydroxides replace pyrite. Bornite, covellite, chalcocite, malachite and azurite are supergene alteration minerals of chalcopyrite.

Specularite is micaceous hematite and is the most abundant in supergene stage. Forms mainly veins up to 4-5 cm. Under microscope a lot of disseminated blade crystals can be observed in the groundmass (fig. 8). X-Ray analyses also affirm the presence of hematite in the samples (fig. 10).

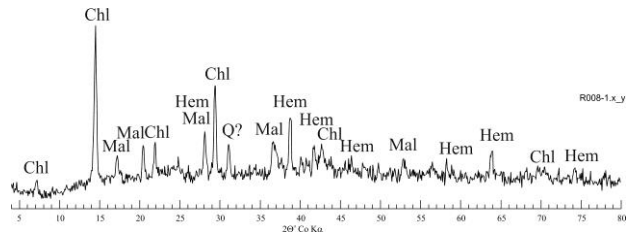


Fig. 10. X-ray diffractogram (XRD) of minerals from supergene stage. Hem – hematite (specularite); Mal – malachite; Chl – chlorite; Q – quartz.

Goethite and the other iron oxide-hydroxides replace pyrite and chalcopyrite. In some sample pyrite is completely replaced. They form net-mesh-like microstructures in both primary sulfides (fig. 9). Colloform texture is also typical.

Bornite occurs with covellite and together they form rims and infill cracks in chalcopyrite aggregates (fig. 11). Chalcocite is observed in the samples but is rare.

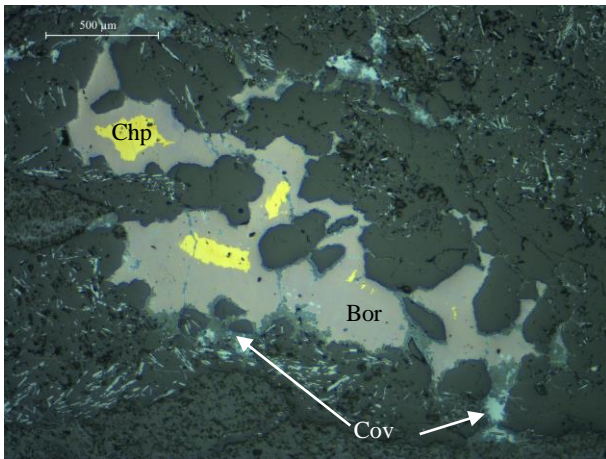


Fig. 11. Bornite (Bor) and covellite (Cov) replace chalcopyrite (Chp).

Malachite is more abundant than azurite. On the field malachite indicates the most abundant part with sulfides in the ore zone.

## Discussion and conclusions

Nunatak de Castillo is located at the Hurd Peninsula, Livingston Island, Antarctica. This investigation represents a thesis that the subvolcanic body is a remnant volcanic structure (volcanic plug) with unknown age. It crosscuts the rocks of Myers Bluff formation (Upper Cretaceous). More data are needed to determine the origin of the outcrop and the volcanic facies.

The alteration mineral assemblages consist mainly of epidote, chlorite, amphiboles, albite, carbonates, sericite, pyrite, quartz, potassium feldspar and probably corresponds with propylites.

The mineralization occurs within altered diorite porphyries and is hosted by NW-SE-striking fault.

The ore minerals are Cu- and Fe-containing and their presence corresponds with the mineralization in the Andean Metallogenic Province. Chalcopyrite and pyrite together with the secondary copper sulfides (bornite, covellite, chalcocite?), copper carbonates (malachite, azurite) and iron oxide-hydroxides (specularite, goetite and others) are identified for the first time.

There is a moratorium for the prospecting and exploration of ore deposits at the Antarctic territories but the world demand for metals will continue to grow and the area could show economic potential for the future.

**Acknowledgements.** Sincere thanks to Prof. Christo Pimpirev for the opportunity to do researches on Livingston Island. This work has been carried out in the framework of the National Program of Polar Research supported by Ministry of Education and Science of Bulgaria (Agreement No 70.25-176 FROM 22.11.2019). Thanks to the logistic team for the support and our safe arrival and stay in Antarctica.

## References

- Dalziel, I. W. D. 1972. Large-scale folding in the Scotia arc. – In: *Antarctic Geology and Geophysics* (Eds. Adie, R. D.). Universitetsforlaget, Oslo, 47-55.
- Kamenov, B. K. 1997. Geochemistry and petrology of the Hesperides point intrusion, Hurd Peninsula, Livingston Island. – In: *The Antarctic Region: Geological Evolution and Processes* (Eds. Ricci, C.). Terra Antarc., Siena, Italy, 341-352.
- Pimpirev, C., M. Ivanov, K. Stoykova. 2015. Lithostratigraphy of the Miers Bluff Formation, Hurd Peninsula, Livingston Island. – In: *Bulgarian Antarctic Research. A Synthesis*. (Eds. Pimpirev, C., N. Chipev). St. Kliment Ohridski University Press, 33-39.
- Sillitoe, R. H., J. Perello. 2005. Andean Copper Province: Tectonomagmatic Settings, Deposit Types, Metallogeny, Exploration, and Discovery. – *Economic Geology 100th Anniversary*, 845-890.
- Smellie, J. L., R. J. Pankhurst, M. R. Thomson, R. E. Davies. 1984. The geology of the South Shetland Island: IV. Stratigraphy, geochemistry and evolution. *British Antarctic Survey Scientific Reports*, 87, 85 p.
- Smellie, J. L., R. Pallas, F. Sabat, X. Zheng. 1996. Age and correlation of volcanism in central Livingston Island, South Shetland Islands: K-Ar and geochemical constraints. – In: *Journal of South American Earth Science*, 9, 265–272.
- Stefanov, Y., C. Pimpirev. 2015. Deep-water facies and facies associations in the siliciclastic rocks of the Miers Bluff Formation. – In: *Bulgarian Antarctic Research. A Synthesis*. (Eds. Pimpirev, C., N. Chipev). St. Kliment Ohridski University Press, 49-59.

## HOLOCENE TRANSGRESSIONS IN THE AREA OF THE BURGAS LAKES COMPLEX – MANIFESTATION OF GLOBAL CLIMATIC FLUCTUATIONS

**Dimitar Sinnyovsky**

*University of Mining and Geology “St. Ivan Rilski”, 1700 Sofia; sinsky@mgu.bg*

**ABSTRACT.** Modern climate changes, heavily overexposed by the media and unscrupulous scientists, have led to understandable panic among much of the world's population. It has been taken seriously not only by ordinary citizens but also by the governments of advanced countries. However, geologists know that global warming is not measured in degrees, but in millimeters due to the melting of ice caps at the poles that cause rising of the global sea level. Cyclically repeated glacial and interglacial ages, known as Milankovitch cycles, have an astronomical forcing. They can really cause global sea level fluctuations of tens of meters, however, not in a few tens of years, but in tens of thousands of years. Against the background of these cycles, there are also short-term (from a geological point of view) stages of warming and cooling, which have no unambiguous explanation. Similar trend has been observed since 1850, without it being associated with any human activity. The main Holocene warming events that led to the last transgressions in the Earth's history – the Flandrean (Novochernomorian) and Nymphaean transgressions, are well expressed on the Black Sea coast in the form of old marine terraces. The Novochernomorian (New Black Sea) terrace is at ~4 m above the modern sea level. On this surface is the town of Pomorie and some neighborhoods of the town of Burgas. The Nymphaean terrace, disposed ~2 m above sea level, is well defined on the shores of the Burgas Lakes which are protected from abrasion acting on the open Black Sea coast. Transgressions played an important role in antiquity by providing a navigation access to the ancient Deultum (now Debelt) inside the Mandra Liman, thanks to which this important Roman polis became a flourishing port for 2–3 centuries.

**Keywords:** Burgas Lakes complex, Novochernomorian terrace, Nymphaean terrace

### ХОЛОЦЕНСКИТЕ ТРАНСГРЕСИИ В БУРГАСКИЯ ЕЗЕРЕН КОМПЛЕКС – ПРОЯВА НА ГЛОБАЛНИ КЛИМАТИЧНИ КОЛЕБАНИЯ

**Димитър Синьовски**

*Минно-геоложки университет „Св. Иван Рилски“, 1700 София*

**РЕЗЮМЕ.** Съвременните климатични промени, силно преекспонирани от медии и безскрупулни учени, доведоха до разбираема паника сред голяма част от населението на Земята. Те се възприемат сериозно не само от обикновените граждани, но и от правителствата на развитите страни. Геолозите обаче знаят, че глобалното затопляне не се измерва в градуси, а в милиметри, поради топенето на ледените шапки на полюсите и покачването на глобалното морско ниво. Циклично повтарящите се ледникови и междуледникови епохи, известни като цикли на Миланкович, имат астрономичен произход. Те наистина могат да причинят колебания на глобалното морско ниво от порядъка на десетки метри, но не за няколко десетки години, а за десетки хиляди години. На фона на тези цикли има и краткотрайни (от геоложка гледна точка) периоди на затопляне и захладяване, които нямат еднозначно обяснение. Подобна тенденция се наблюдава от 1850 г. насам, без тя да е свързана с каквато и да е човешка дейност. Главните холоценски събития на затопляне, предизвикали последните трансгресии в историята на Земята – Фландърската (Новочерноморската) и Нимфейската, са добре изразени по Черноморието под формата на стари морски тераси. Новочерноморската тераса е на ~4 m над съвременното морско ниво. Върху тази повърхност е град Поморие и някои квартали на Бургас. Нимфейската тераса, разположена на ~2 m над морското ниво, е добре изразена по бреговете на Бургаските езера, които са защитени от абразията на откритото крайбрежие. Трансгресиите са играли важна роля в древността, осигурявайки достъп до античния Деултум (днес Дебелт) в Мандренския лиман, благодарение на който този важен римски полис се превръща в процъфтяващо пристанище в продължение на 2–3 века.

**Ключови думи:** Бургаски езерен комплекс, Новочерноморска тераса, Нимфейска тераса

### Introduction

The term “climate change” is used for significant and long-standing global climate change. The geological meaning of “significant and long-standing” is quite different from the generally accepted notions of time. In geology it is usually millions of years. However, when we talk about global climate changes, we most often mean Quaternary glacial and interglacial stages, known as Milankovitch cycles that last for tens and hundreds of thousands of years. The term “global warming” is formulated as a slow increase in the average temperature of the atmosphere due to the heat coming from the sun, which is retained in it and is not radiated into space. Like any theory, the concept of global warming has both supporters and opponents. The former consider global warming to be an indisputable fact that is directly related to human activity, in

particular the increase in carbon emissions. Opponents believe that there is no global warming or climate change. There is a third category of scientists who believe that global warming is a natural cyclic process which is not caused by human activity. Firmly convinced of the latter statement, the author of this paper belongs to a fourth category of scientists considering that the present global warming belongs to small-scale non cyclic climatic change of complex origin superimposed on the interglacial Milankovitch astronomical cycle that began after the end of the last ice age 11.7 ka ago.

### Holocene climate fluctuations

There are several proven examples in the Holocene history of the Earth for interruptions to the gradual warming of the climate after the severe Last Glacial Maximum (LGM), about 27

to 24 ka BP. The most recent large-scale event of cooling since the LGM, the Younger Dryas stadial (YD), occurred between 12.9 and 11.5 ka ago (Fig. 1). It is characterized by very low temperatures for the most part of the YD, rapidly rising afterwards to reach the warm Holocene temperatures. The YD is one of the three major abrupt cold events that interrupted the warming during the last deglaciation, recognizable in a variety of tracers in terrestrial, marine and ice records across the

Northern Hemisphere (Meissner, 2007). The first explanation of this event belongs to Johnson and McClure (1976) postulating that an increased freshwater influx of the St. Lawrence River triggered the YD cold event by causing an increase in North Atlantic sea ice. Against the background of these minor (compared to the Milankovitch cycles) climatic changes, smaller sea level fluctuations could be also recognized by investigation of the ancient shorelines and archeological artifacts.

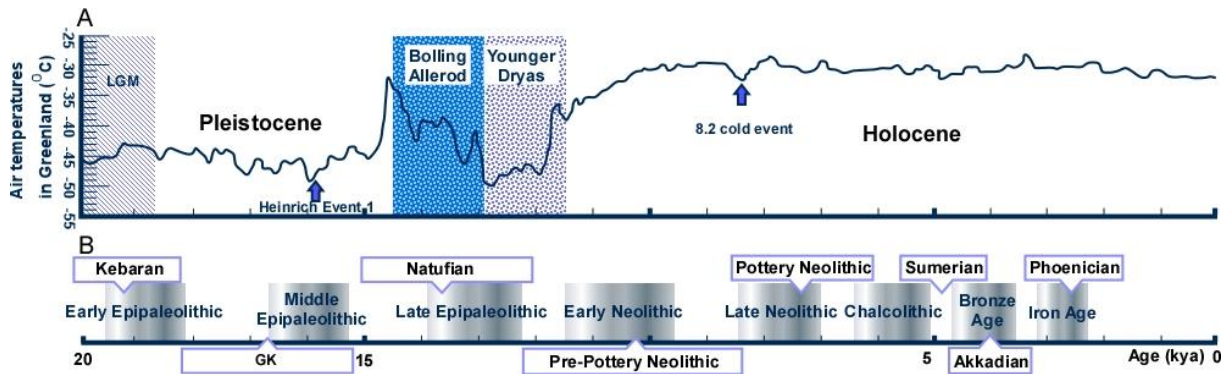


**Fig.1. Curve of air temperature variation in the latest Pleistocene and Holocene (after Platt et al., 2017):** (A) Reconstructed air temperatures from the GISP 2 Ice core in Greenland; (B) Chronology of cultural entities in the Levant

## Modern climate changes

Modern climate changes, heavily overexposed by the media and unscrupulous scientists, have caused a wide response among much of the world's population. The world is flooded daily with statistics showing high average annual temperatures in the late 20th and early 21st centuries. As a result, the idea of global warming is being taken more and more seriously not only by common people, but also by the governments of advanced countries, which have begun to allocate funds to "fight global warming". The apocalyptic predictions were joined by influential figures from the fields of culture, politics and business, who in fact have no idea what it is all about. The escalation of this global hysteria has left behind the real problems of the humanity – hunger, environmental pollution and overpopulation of the planet.

It is widely known that the best lie is the half-told truth. Based on mass measurements of temperatures in different parts of the world, "scientific" models are constantly being created that predict an apocalyptic picture until the end of the century: glacier shortening, powerful cyclones, prolonged droughts, submerged cities, destroyed crops, fires, floods, deforestation, misery and famine. Speculating on strictly scientific facts, such as the greenhouse gases ratio in the atmosphere, most of these models do not involve important natural processes, such as the absorption of CO<sub>2</sub> from the oceans, but involve human activity, such as the industrial release of heat-trapping greenhouse gases into the atmosphere. Ordinary people are not experts and find it difficult to orient in this avalanche of information. They accept these apocalyptic predictions for granted and believe that they should participate in the "salvation of future generations", according to the principle of sustainable development,

formulated in the report of the UN "Brundtland" Commission entitled "Our Common Future" (UN World Commission on Environment and Development, 1987). The truth is that we cannot influence such global processes and even if there is global warming, we can in no way fight it. We all remember the ozone hole that made us feel guilty about using deodorants. What happened with it?

Now many scientists tend to exaggerate human participation in global processes, as is the case with global warming and the ozone hole. However, many facts are ignored simply because they are not in line with the "global trend" in science. Robinson et al. (2007) provided data that refute the main arguments for the anthropogenic causes of global warming, which gives the United States a reason not to sign the global climate accords. They apply an example from Sargasso Sea, suggesting that the Earth's temperature today is essentially at the 3000-year average global temperature (Fig. 2A), and glacier shortening started about 1850, 25 years before the start of intensive fossil fuel use (Fig. 2B). Respectively, at the same time started the sea-level increase with 7 inches per century. The "medieval climate optimum" with temperature 24°C higher than the average global temperature corresponds to the high sea level at the maximum of the Nymphaean transgression during 10–11th century. Historically the pick of the Nymphaean warming coincides with the Viking Age (793–1066 AD). During this time, the Norsemen conquered Greenland and called it "Grœnland" because of its green shores. This simply means that very recently, in historical times, the southern shores of Greenland were grassed. This has led neither to the sinking of medieval civilizations nor to the halting of the Gulf Stream, as speculated by proponents of global warming, widely popularized in Al Gore's documentary "An Inconvenient Truth" winning the Academy Award for best documentary feature in 2007.

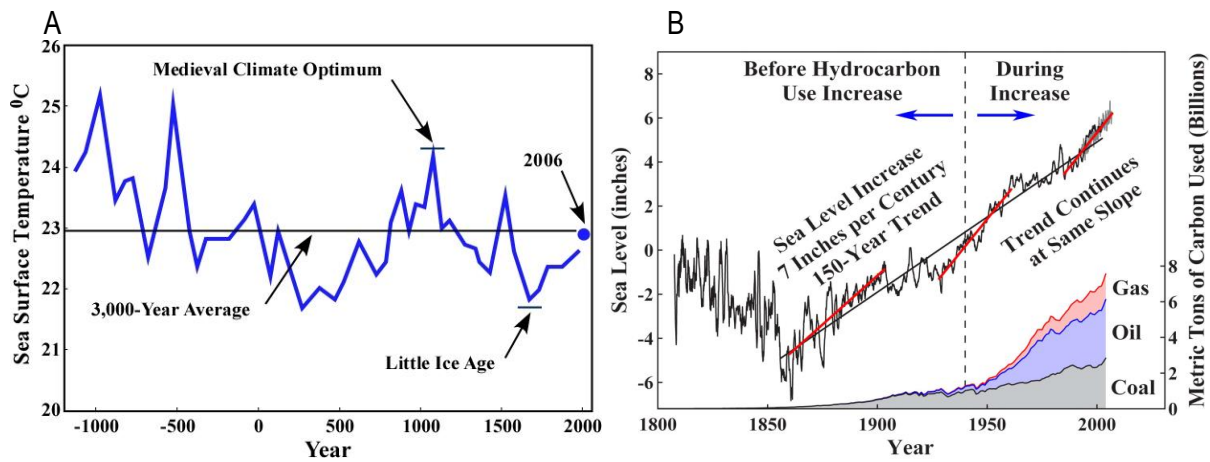


**Fig. 2. Climatic and sea-level fluctuations in historic time (after Robinson et al., 2007):** (A) Surface temperatures in the Sargasso Sea, the horizontal line is the average temperature for this 3,000-year period corresponding to the present one, the Little Ice Age and Medieval Climate Optimum were naturally occurring, extended intervals of climate departures from the mean. (B) Global sea-level measured by surface gauges between 1807 and 2002, and by satellite between 1993 and 2006; this trend lags the temperature increase, so it predates the increase in hydrocarbon use, and it is unaffected by the very large increase in hydrocarbon use

### The Black Sea level fluctuations in the post-glacial period

The continuous alternation of warming and cooling in the Earth history, which is repeated in 20 ka, 43 ka, and 100 ka, known as Milankovitch climatic cyclicity, is of astronomical origin. Every geologist or geomorphologist is acquainted with these cycles and knows that global warming is not measured in degrees, but in millimeters due to the melting and freezing of the ice caps at the poles, causing global sea-level fluctuations of tens of meters. Today, the Black Sea is a continental marine basin, but it has been oscillating between lacustrine and marine stages following, respectively, glacial and interglacial global sea-level changes. The Black sea level fluctuations during the post-glacial period are synchronous and unambiguous with the global sea-level fluctuations (Fedorov, 1959). In the end of the last glacial stage about 10–12 ka ago, the Black Sea inherited the Late Neoeuxinian sea-lake which level was tens of meters below the present one. The melting of the ice shield covering the northern part of the continent led to a high fresh water influx into the Neoeuxinian basin and its level started to rise. The first penetration of saltwater and reconnection with the Mediterranean Sea, recently dated to 8400 years BP on strontium isotopes and  $^{14}\text{C}$  (Major et al., 2006; Marret et al., 2009 and others) led to stratification of the marine water due to different salinity (Fedorov, 1983).

There are two hypotheses about the transition between Neoeuxinian and Black Sea basins. According to the so called “Noah’s Flood” hypothesis (Ryan et al., 1997a, b; Ryan, Pitman, 1998; Ryan, 2007, and other authors) an abrupt Mediterranean saltwater flooding of the Black Sea’s ice-age freshwater lake occurred 8400 years ago. Due to this catastrophic inundation, the sea level increased from -90 to -30 m in the frame of one year. As an alternative to this hypotheses, Aksu et al. (2002), Yanko-Hombach and Tchepaliga (2003), Yanko-Hombach et al. (2004), Yanko-Hombach (2007), Sorokin and Kuprin (2007), Kuprin and Sorokin (2007) and many others argue that the sea-level rise was gradual. This is based on abundant scientific data recovered directly from the Black Sea by USSR and Former Eastern Bloc scientists, which have unfortunately been largely

ignored in the global scientific debate, apparently due to language barriers and the lack of west-east scientific dialogue (Yanko-Hombach, 2007).

Since then there have been several minor fluctuations of the Black Sea level, the most remarkable of which is the Novochernomorian (New Black Sea) Holocene transgression (Fedorov, 1956) which reached the maximum sea level of 4–5 m higher than today’s level during the Chalcolithic and Bronze Ages (~6000–3000 years BP). It corresponds to the Nice transgression in the Mediterranean, Flandrean transgression of the Atlantic coast and Littorina transgression in Baltic Sea (Fedorov, 1959). The Novochernomorian transgression is followed by a small regression called “Phanagorian regression” (Fedorov, 1956), that resulted in 2–3 m fall of the Black Sea level compared to the present sea-level between 3000 and 2000 years ago. The last transgression in the Earth’s history is the so called “Nymphaean transgression” (Fedorov, 1959) that caused 1.5–2 m sea-level rise above the present sea-level in the Middle Ages between 6th and 12th century. The short-term warmings and coolings, such as the Nymphaean transgression, have no unambiguous explanation. It is established in many places on the Black Sea coast in the form of a marine terrace located 1.5–2 m above the modern sea level.

### Novochernomorian and Nymphaean transgressions in the Burgas Lakes area

The Burgas Lakes complex includes four separate basins: three estuaries (limans) – Burgas (Vaya), Atanasovsko and Mandra Lakes, and one lagoon – Pomorie Lake. Novochernomorian and Nymphaean transgressions are well expressed on the shores of the lakes, which are protected from the active abrasion of the open coast and have preserved flat surfaces, formed during the periods of high sea level. The Holocene terraces along the Bulgarian Black Sea coast were established by Fedorov et al. (1962) and Fedorov (1963) shortly after Fedorov (1959) introduced the Nymphaean transgression into literature. These authors described Novochernomorian terrace as an abrasive-accumulative surface 5 m above the

present sea-level east of the town of Balchik, and as abrasive flat surfaces 5–6 m above the present sea level along the southern Black Sea coast (Strandzha) incised in Upper Cretaceous tuffs (Fig. 3). The Nymphaean terrace characterized as “younger terrace disposed 2 m above sea level” is established near Batova River (west of Balchik town), Varna estuary, Kamchia River estuary, between cape Emine and Burgas, and south of Burgas till the town of Michurin (now Tzarevo). The authors noted that the Sunny Beach resort is located on this terrace, which corresponds also to the coastal accumulative forms such as the Pomorie tombolo, connecting the Sarmatian carbonate island (old town of Pomorie) with the beach. Christov (1967) mentioned the presence of the Nymphaean terrace in the vicinities of Burgas and Pomorie. Mishev et al. (1970) noted that the Holocene terraces – the Novochernomorian and probably the Nymphaean one, form a narrow beach strip as well as the adjacent estuary and lagoon lowlands. Popov and Mishev (1974) especially noted that Pomorie town is disposed on the Novochernomorian terrace and the Nymphaean terrace is present around the Burgas Lakes. Our recent investigations confirm the presence of the Nymphaean terrace along the shoreline of the Burgas Lakes (Sinnyovskiy et al., 2018) and fossil humus deposits 1 m above the present sea level (Sinnyovskiy et al., 2019).



**Fig. 3. The Novochernomorian terrace at Foros Cape, south of Burgas, incised in Upper Cretaceous tuffs**

As mentioned above, most of the authors believe in a gradual transgression between Neoeuxinian and Black Sea basins, with the average rate of sea-level rise ~3 mm/yr. According to Larchenkov and Kadurin (2011) the late Pleistocene and Holocene transgressions occurred in pulsing, transgressive-regressive stages. The highest Holocene global sea level was reached 5000–6000 years ago during the Flandrean transgression, known in the Black Sea as Novochernomorian. At that time the Pomorie lagoon did not yet exist, but the Burgas Lakes were wide bays of the Black Sea, as evidenced by archaeological artifacts of the ancient Roman ports Deultum and Skafida, located at the Gulf of Mandra. At this time the higher part of Pomorie town, built of Sarmatian limestones of the Odartsi Formation, was an island. Such coastal islands are often connected to the beach with a sandbar, called “tombolo”. Sometimes the sandbars may appear on both sides of the island forming a “double tombolo” which may form an enclosed lake (lagoon). In the course of the high sea level during the Late Chernomorian transgressive interval, submarine barrier

bars were formed on both sides of the Pomorie Island connecting it with the mainland. After the retreat of the sea these sandbars (double tombolo after Popov and Mishev, 1974), emerged above the surface and formed the Pomorie lagoon (Fig. 4).



**Fig. 4. The northern sandbar of the Pomorie tombolo separating the Black Sea (left) from the Pomorie lagoon (right)**

At the same time, the three limans, known as Burgas Lakes, have undergone a maritime regime. During the Early Chernomorian transgressive interval (Vityazevian Stage, 8.9–7.1 ka BP) the Black Sea waters invaded the land and many limans were established along the southern Black Sea coast. For several thousands of years they have existed as open marine embayments with marine sedimentation. After the Novochernomorian transgression to the end of the Kalamitian stage (until 4 ka BP) the sea level dropped to its present position and the Burgas Lakes regain the appearance of limans. Probably during the Phanagorian regression they became closed lakes without direct connection with the sea. However, the connection was carried out by infiltrating the seawater through the barrier sandbar as is now the case with the Pomorie lagoon.



**Fig. 5. Novochernomorian terrace west of Manrda Liman on the left bank of Sredetska River south of Debelt: the wave-cut surface 4 m above the lake level (the arable land) extends to the paleo-shoreline of the Mandra Bay composed of Upper Cretaceous tuffs**

The genesis of these terraces is still the subject of controversy. The Novochernomorian terrace is well developed at the Black sea capes, where it is an erosional surface 4–5 m above today’s sea level. Popov and Mishev (1974) referred to the same terrace the wide flat surfaces at the lower reaches of Sredetska and Rusokastrenska Rivers elevated 4 m above the

lake-level and reaching to the ancient liman's shoreline of Upper Cretaceous tuffs (Fig. 5). However, the formation of accumulative terraces along the shoreline of the Burgas Lakes during the Middle Ages is indisputable. This flat surface, surrounding the lakes, is 1–2 m above water level. In the bays, where the shore is nearly flat, the Nymphaean terrace is overgrown with reeds but on the steep shores it reaches the rocky outcrops of the paleo-shoreline, composed of Upper Cretaceous tuffs (Fig. 6).



Fig. 6. Nymphaean terrace near Ezerovo village: a flat surface around the Vaya Lake (left), overgrown with reeds reaching the paleo-shoreline of Upper Cretaceous tuffs (right)

## Archeological aspects

The unification of geological and archaeological data is difficult because of the different methodology used for recognizing ancient events. Paleogeographic reconstructions may serve as a basis for locating submerged ancient settlements during the past 7000 years. Historically, the Novochemomorian transgression is too far back in time to be used for comparing with events in ancient human history of the area. During this time one of the oldest Bulgarian towns – Sozopol was founded, known in the antiquity under the name Apolonia (Greek colony Apolonia Pontica). Submarine investigations of the shelf near Sozopol revealed relics of dwellings, ceramic pottery, stone and bone tools from the Bronze Age when the sea-level was still higher than today's.

Many artifacts obtained during the investigation of the roman settlements Skafida and Deultum support the assumption that in the Middle Ages the sea level was higher than today. Deultum was founded in 70 AD by the Emperor Vespasian who granted the veterans of Legio VIII Augusta the right to rule a large area near the estuaries of the rivers Sredetska, Rusokastrenska, Fakiyska and Izvorska, as well as Vaya and Mandra Lakes. The border stone between Deultum and Anchialo, which was found in 19th century near the old Burgas station, marks the northern border of the colony. Over the next three centuries, the city has grown and became one of the most important centers in the province of Thrace that acquired the right to mint own bronze coins between I and III century. According to a Hellenistic source of the Roman geographer Plinius, who characterized it as "stagnum" (open basin), the fairway navigation penetrated to the western coast of Mandra Lake, where the port of the ancient Deultum was found during the recent archeological excavations. These artifacts suggest that 1) the sea level during I–III century was higher and Mandra liman was connected to the sea before

the beginning of the Nymphaean transgression at about 6th century, or 2) the transgression began earlier.

## Conclusions

The last 11 500 years have been filled with important events in geological history on which many events of the human civilization history are superimposed. Geological data about the Holocene climate changes are obtained through interpretation of the global sea level changes, as evidenced by the youngest marine terraces in the area of the Burgas Lakes complex. They carry a huge amount of information about both the paleoenvironment and the ancient civilizations on the coast of Pontus Euxinos. The archaeological artifacts obtained from the ancient Roman ports of Deultum near the village of Debelt and Skafida north of the village of Dimchevo, indicate a higher level of the Mandra liman at the beginning of the new era, ensuring a wide connection with the Black Sea. This proves that the sea level was higher many years before the beginning of the Nymphaean transgression in the Middle Ages. Traces of higher sea level in the Middle Ages are well recorded on the shores of the Burgas Lakes. This area is a wonderful place to demonstrate this geological event, which happened very recently in the human history, but long before the industrial revolution during the 18th century. This is a natural process that humanity cannot and does not need to fight.

**Acknowledgements.** This investigation is performed with the support of the National Science Program "Environmental Protection and Reduction of Risks of Adverse Events and Natural Disasters", approved by the Resolution of the Council of Ministers № 577/17.08.2018 and supported by the Ministry of Education and Science (MES) of Bulgaria (Agreement № D01-230/06.12.2018).

## References

- Aksu, A. E., R. N. Hiscott, D. Yaşar, F. I. İşler, S. Marsh. 2002. Seismic stratigraphy of Late Quaternary deposits from the southwestern Black Sea shelf: evidence for non-catastrophic variations in sea-level during the last ~10000 years. – *Marine Geology*, 190, 61–94.
- Christov, R. 1967. Des terrasses littorales de la Mer Noire au nord de Bourgas. – *Ann. de l'Ecole Supérieure des Mines et de Géologie*, 12 (1965–1966), 2–géol. et géophys, 75–88 (In Bulgarian with French abstract).
- Fedorov, P. V. 1956. About the Modern Epoch in the geological history of the Black Sea. – *Proc. Acad. Sci. USSR, ser. geol.*, 110, 5, 839–841 (In Russian).
- Fedorov, P. V. 1959. About the Black Sea level fluctuations in the post-glacial time. – *Proc. Acad. Sci. USSR, ser. geol.*, 124, 5, 1127–1129 (In Russian).
- Fedorov, P. V. 1963. Stratigraphy of Quaternary deposits on the Crimean-Caucasian coast and certain problems in the geological history of the Black Sea. – *Transactions Geol. Inst. Acad. Sci. USSR*, 88, 1–157. (In Russian)
- Fedorov, P. V., D. A. Lilienberg, V. I. Popov. 1962. New data about the terraces along the Black Sea coast. – *Proc. Acad. Sci. USSR, ser. geol.*, 144, 2, 431–434 (In Russian).
- Johnson, R. G., B. T. McClure. 1976. A model for Northern Hemisphere continental ice sheet variation. – *Quaternary Research*, 6, 325–353.

- Kuprin, P. N., V. M. Sorokin. 2007. On the post-glacial changes in the level of the Black Sea. – In: Yanko-Hombach, V., A. S. Gilbert, N. Panin, P. M. Dolukhanov (Eds). *The Black Sea Flood Question: Changes in Coastline, Climate and Human Settlement*. Dordrecht, Springer, 205–220.
- Larchenkov, E., S. Kadurin. 2011. Paleogeography of the Pontic Lowland and northwestern Black Sea shelf for the past 25 k.y. – In: Buynevich, I. V., V. Yanko-Hombach, A. S. Gilbert, R. E. Martin (Eds). *Geology and Geoarcheology of the Black Sea Region*, 71–84.
- Major, C. O., S. L. Goldstein, W. B. F. Ryan, G. Lericolais, A. M. Piotrowski, I. Hajdas. 2006. The co-evolution of Black Sea level and composition through the last deglaciation and its paleoclimatic significance. – *Quaternary Sci. Rev.*, 25, 2031–2047.
- Marret, F., P. Mudie, A. Akşu, R. N. Hiscott. 2009. A Holocene dinocyst record of a two-step transformation of the Neoeuxinian brackish water lake into the Black Sea. – *Quaternary International*, 197, 72–86.
- Meissner, K. 2007. Younger Dryas: A data to model comparison to constrain the strength of the overturning circulation. – *Geophys. Res. Lett.*, 34, L21705, DOI:10.1029/2007GL031304.
- Michev, K., V. Popov, D. Lilienberg. 1970. Résultats obtenue par de récentes investigation géomorphologiques du littoral Bulgare de la Mer Noire. – *Bull. Soc. Bulg. de géographie*, 9, 19, 37–55 (In Bulgarian with French abstract).
- Robinson, A. B., N. E. Robinson, W. Soon. 2007. Environmental effects of increased atmospheric carbon Dioxide. – *J. of American Physicians and Surgeons*, 12, 79–90.
- UN World Commission on Environment and Development. 1987. *Our Common Future*. Oxford University Press, Business and Economics, 400 pp.
- Platt, E., M. Haber, M. Bou Dagher-Kharrat, B. Douaihy, G. Khazen, M. A. Bonab, A. Salloum, F. Mouzaya, D. Luiselli, C. Tyler-Smith, C. Renfrew, E. Matisoo-Smith, P. A. Zalloua. 2017. Mapping Post-Glacial expansions: The Peopling of Southwest Asia. – *Sci. Rep.*, 7, 40338; DOI: 10.1038/srep40338.
- Popov, V., K. Mishev. 1974. *Geomorphology of the Bulgarian Black Sea Coast and Shelf*. Sofia, Publ. House of the Bulgarian Academy of Sciences, 267 pp. (In Bulgarian with English abstract).
- Ryan, W. B. F. 2007. Status of the Black Sea flood hypothesis. – In: Yanko-Hombach, V., A. S. Gilbert, N. Panin, P. M. Dolukhanov (Eds). *The Black Sea Flood Question: Changes in Coastline, Climate and Human Settlement*. Dordrecht, Springer, 63–88.
- Ryan, W. B. F., W. C. Pitman III. 1998. *Noah's Flood: The New Scientific Discoveries about the Event that Changed History*. New York, Simon & Schuster, 320 pp.
- Ryan, W. B. F., W. C. Pitman III, C. O. Major, K. Shimkus, V. Moskalenko, G. A. Jones, P. Dimitrov, N. Görür, M. Sakiç, H. Yüce. 1997a. An abrupt drowning of the Black Sea shelf. – *Marine Geol.*, 138, 119–126.
- Ryan, W. B. F., W. C. Pitman III, C. O. Major, K. Shimkus, V. Moskalenko, G. A. Jones, P. Dimitrov, N. Görür, M. Sakiç, H. Yüce. 1997b. An abrupt drowning of the Black Sea shelf at 7.5 k yr BP. – *Geo-Eco-Marina*, 2, 115–126.
- Sinnyovsky, D., N. Kalutskova, N. Dronin, D. Sinnyovska. 2018. Nymphaean terrace in the area of the Burgas Lakes. – *Rev. Bulg. geol. soc.*, 79, 3, 115–116.
- Sinnyovsky, D., D. Sinnyovska, N. Kalutskova, N. Dronin, A. Medvedev, N. Telnova. 2019. Fossil humus mad and its Novochemomorian base at the Atanasovsko Lake, Burgas Lakes Complex. – *J. Mining and Geol. Sci.*, 61, 1-Geol. and Geophys., 62–65.
- Sorokin, V. M., P. N. Kuprin. 2007. On the character of Black Sea level rise during the Holocene. – *Moscow Univ. Geol. Bull.*, 62, 5, 334–341.
- Yanko-Hombach, V. 2007. Controversy over Noah's flood in the Black sea: geological and foraminiferal evidence from the shelf. – In: Yanko-Hombach, V., A. S. Gilbert, N. Panin, P. M. Dolukhanov (Eds). *The Black Sea Flood Question: Changes in Coastline, Climate and Human Settlement*. Dordrecht, Springer, 149–203.
- Yanko-Hombach, V., A. Tschepaliga. 2003. Geology of a catastrophe—the when and where of the Black Sea Flood. – *Abstracts XVI INQUA Congress (23–30 July 2003, Reno, Nevada)*, Session 84, p. 224.
- Yanko-Hombach, V., E. Meriç, N. Aşar, E. Kerey, M. Görmüş. 2004. Micropaleontological evidence of the Black Sea–Marmara Sea connection for the last 800 ka BP. – In: Yanko-Hombach, V., M. Görmüş, A. Ertunç, M. McGann, R. Martin, J. Jacob, S. Ishman (Eds). *Extended Abstracts of the Fourth International Congress on Environmental Micropalaeontology, Microbiology and Meiobenthology (13–18 September 2004, Isparta, Turkey)*, 228–230.

## HOLOCENE DEPOSITS OF VARNA LAKE

**Dimitar Sinnyovsky**

University of Mining and Geology "St. Ivan Rilski", 1700 Sofia; [sinsky@mgu.bg](mailto:sinsky@mgu.bg)

**ABSTRACT.** This article is an overview of the existing data on lithology and relationships of the bottom sediments and their significance for the reconstruction of the Holocene history of Varna estuary. With the end of the cold Younger Dryas stadial 11.5 ka ago comes the end of the last glacial stage and the Neoeuxinian basin, also called "ice-age fresh water lake". The saltwater flooding through Bosphorus during the Early Chemomorian transgressive phase caused flooding of the river mouths and formation of limans. Probably then started the accumulation of the Holocene deposits of the newly formed Varna liman. Previous studies of these deposits are based on data obtained from hundreds of boreholes drilled for the construction and maintenance of the navigation channels ensuring connection of the Varna Lakes with the Black Sea. New drilling has recently been carried out for the deepening of the channels, which provided more information about the Holocene deposits. Novochemomorian and Nymphaean terraces, marking the high sea level during the Holocene history of the Black Sea, are well exposed on the lake shores. The section of the Holocene deposits at Nalbanka bay shows well traceable subsurface terraces marking sea level lowstands. The sea-level fluctuations have had an important influence on the ancient civilizations inhabiting Pontus Euxinus coast. The archaeological artifacts provide evidence of these fluctuations and important facts for the restoration of the Black Sea coastline in antiquity and Middle Ages.

**Keywords:** Varna Lake, marine terraces, estuary deposits

### ХОЛОЦЕНСКИТЕ НАСЛАГИ НА ВАРНЕНСКОТО ЕЗЕРО

**Димитър Синьовски**

Минно-геоложки университет „Св. Иван Рилски“, 1700 София

**РЕЗЮМЕ.** Тази статия е преглед на съществуващите данни за литологията и взаимоотношенията на дънните утайки и тяхното значение за възстановяването на холоценската история на Варненския лиман. С края на студения Късен Дриас преди 11,5 ka идва краят на последния ледников период и Новоевксинския басейн, наричан още „пресноводно ледниково езеро“. Нахлуването на солени води през Босфора по време на ранночерноморската трансгресивна фаза предизвиква наводняване на речните устия и образуване на лимани. Вероятно тогава е започнало натрупването на холоценските утайки в новообразувания Варненски лиман. Предишните проучвания на тези седименти се основават на стотици сондажи, прокарани за изграждането и поддържането на навигационните канали, осигуряващи връзка на Варненските езера с Черно море. Наскоро бе проведено ново сондиране за удълбочаване на каналите, което предостави още информация за холоценските утайки. Новочерноморската и Нимфейската тераса, индикиращи високи морски нива през холоценската история на Черно море, са добре експонирани по бреговете на езерото. Разрезът на холоценските отложения в залива Налбанка показва добре проследими подповърхностни тераси, маркиращи ниски морски нива. Флукуациите на морското ниво са оказвали важно влияние върху древните цивилизации, обитаващи брега на древния Понтос Евксинос. Археологическите артефакти предоставят доказателства за тези колебания и важни факти за възстановяването на бреговата ивица на Черно море в древността и Средновековието.

**Ключови думи:** Варненско езеро, морски тераси, лиманни отложения

### Introduction

Limans and lagoons are typical nearshore basins along the Bulgarian Black Sea coast. They are Holocene water bodies formed during the sea level rise after the last glacial period. During the Vityazevian Stage of the Early Chemomorian transgressive interval (9–7 ka ago) the sea invaded the land and many limans were established along the Black Sea coast. Varna and Beloslav Lakes are among the largest limans along the Bulgarian coast formed in drowned river valley of the Provadia River. During the seventies of the last century Varna Lake was connected to the sea via navigation Channel 1 and to Beloslav Lake via navigation Channel 2 (Fig. 1). Hundreds of boreholes have been drilled for the construction and maintenance of these channels. Recently, more drillings were made by "Transport Construction and Reconstruction" Corp. in seven profiles across Channel 1 which is of total length 6 695 m, average design depth 12.50 m and maximum navigation width – 310 m (Fig. 2). The new boreholes provided valuable information about the structure and composition of the estuary deposits and subsurface Holocene terraces. For the deepening of navigation Channels 1 and 2, connecting the Black Sea with

Varna and Beloslav Lakes, new engineer-geological investigations were made. The present paper is a review of the previous results obtained during the construction of Channel 1 in the seventies of the 20th century, and during its reconstruction for navigation purposes made in 2019 and 2020.



**Fig. 1. Situation map with the location of the channels connecting the Beloslav and Varna Lakes with the Black Sea**

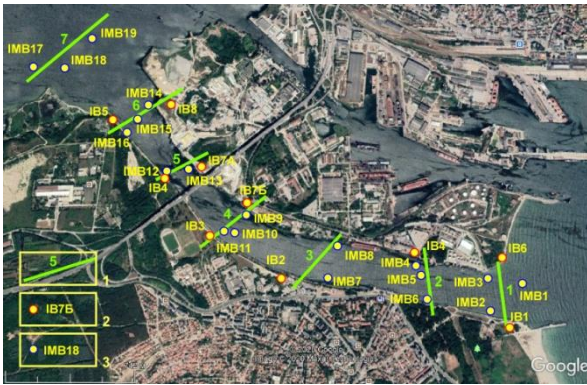


Fig. 2. Satellite map of the borehole profiles across Channel 1: 1, profile; 2, onshore borehole; 3, marine borehole

## Geological setting

Varna Lake is situated in the Varna depression, also known as Varna monocline with layers dipping 5–10° to the east. It is part of the Moesian Platform, which builds the post-Jurassic structural plan. The area is characterized by good outcrops of geological formations. A number of faults buried by the Quaternary sediments have been identified. The geological foundation of the Varna Lake is represented by several Paleogene and Neogene units, cropping out on the slopes of Varna and Avren Plateaus. They belong to the Avren, Ruslar and Galata Formations. In the higher parts sediments of the Frangja, Evksinograd, Odarci and Karvuna Formations are also exposed (Fig. 3).

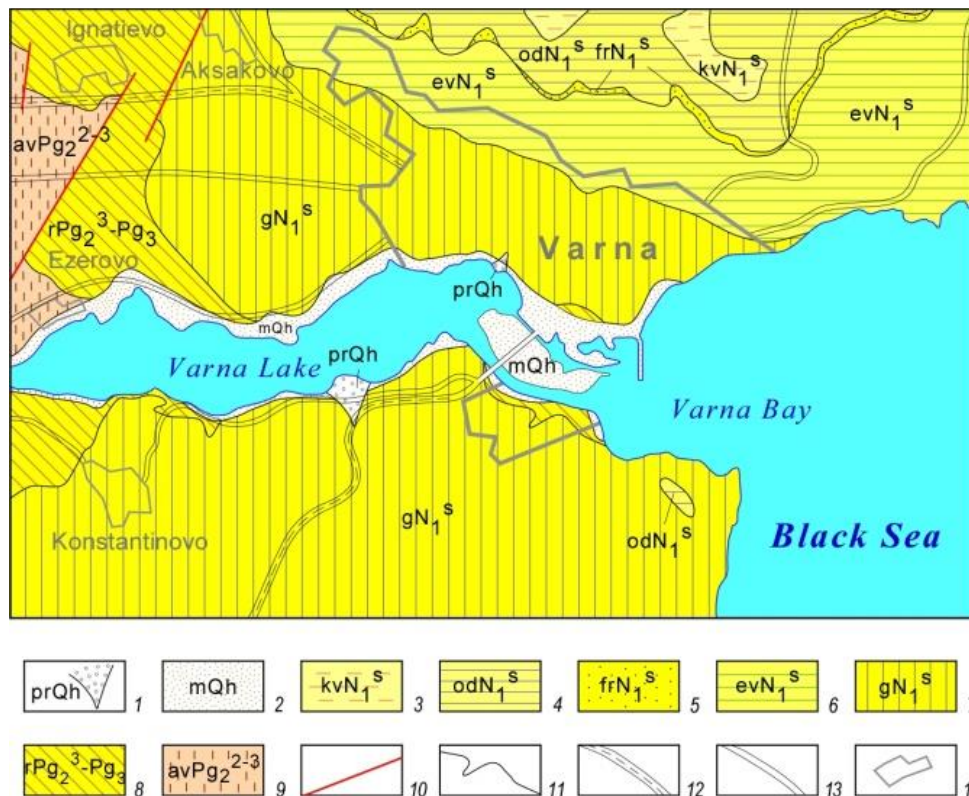


Fig. 3. Geological map of the area (after Cheshitev et al., 1992, with additional data): 1, proluvial fans: boulders, gravel and sand (Holocene); 2, modern sediments of the Novochernomorlian and Nymphaean terraces: beach sands with shell clusters (Holocene); 3, Mactra limestone – Karvuna Fm., Miocene, Sarmatian (Khersonian); 4, detrital shelly and oolite limestone with clay and sand layers – Odarci Fm., Miocene, Sarmatian (Upper Bessarabian); 5, oligomictic sands with thin sandstone layers and lenses – Frangja Fm., Miocene, Sarmatian (Volhynian); 6, clays – Evksinograd Fm., Miocene, Sarmatian (Volhynian–Bessarabian); 7, sands with layers of clays, sandstones and rarely conglomerates – Galata Fm., Miocene (Tarkhanian–Konkian); 8, clays, sands and clayey sandstones with manganese ore – Ruslar Fm., Upper Eocene–Oligocene; 9, marls with thin sandstone layers – Avren Fm., Middle–Upper Eocene; 10, fault; 11, lithostratigraphic boundary; 12, highway; 13, road; 14, settlement

## Geomorphological notes

Morphologically, Varna valley is located in the easternmost part of the Danube plain. The valley is surrounded by low uplands: Varna Plateau from the north with a height up to 370 m, and Avren Plateau from the south with a height of 180 m. These uplands are composed of Paleogene and Neogene rocks. The valley is formed by Provadia River, whose mouth was turned into an estuary during the Holocene transgression after the last ice age. The study area is part of the modern Black Sea coast, which has been subject to repeated flooding and drainage for the last 2 million years due to sea level

fluctuations caused by the Quaternary glacial and interglacial stages. As a result, marine terraces have been formed, located above the modern sea level and below it. Above the modern water level of the Varna Lake several terrace surfaces at different altitudes are established by Koyumdzhieva (1962), Popov and Mishev (1974), and Evstatiev and Manov (1988).

### Chaudinian terrace

Popov and Mishev (1974) correlate the flattened surfaces at an altitude of 90–100 m south of Asparuhovo neighborhood with the Chaudinian terrace. They are situated west of Galata Cape at an altitude of 90–100 m, and in Sakam dere – at 90 m.

### Euxinian-Uzunliarian terrace

The presence of this terrace in the area is noted by Popov and Mishev (1974) at Cape Galata at an altitude of 35–40 m.

According to them it is proven by fossil fauna. Evstatiev and Manov (1988) also noted a terrace level at an altitude of 41–42 m recognized during geological engineering studies for the chemical plants on the northern shore of the Beloslav Lake. In the eastern part of the Varna Lake a terrace level at an altitude of 38–40 m is established in several places.

### Old Karangatian terrace

The presence of this terrace level is established by Popov and Mishev (1974) within the city of Varna at an altitude of 18–25 m. They noted that no fauna was found and the age was determined by analogy with other parts of the coast. Evstatiev and Manov (1988) also described a wide terrace level at an altitude of 20–22 m near soda plants. They consider as its continuation the terrace surface on the northern shore of the Varna Lake at an altitude of 15–20 m.

### Young Karangatian terrace

The sediments of this terrace in the area are first established on the northern shore of Varna Lake by Kojumdgieva (1962, 1964), 1 km west of Varna at “Yanko Kostov” cannery. It is described as a “second marine terrace” of Middle Pleistocene age in the explanatory note to the geological map of Bulgaria at a scale 1:100 000, map sheet Varna and Golden Sands (Cheshitev et al., 1994). The 50 cm thick basal layer of small to medium-sized conglomerate is followed by 8–12 m medium to coarse-grained sands. Popov and Mishev (1974) determined typical Karangatian fauna in the conglomerate layer proving the presence of a shallow bay in the Karangatian Sea.

### Novochernomorian terrace

The presence of the Holocene terraces along the Bulgarian Black Sea coast is first noted by Fedorov et al. (1962) and Fedorov (1963). The Novochernomorian terrace near Varna Lake was established by Kojumdgieva (1962) at the same place where the Young Karangatian terrace is described. It contains bluish sands and silts with rich fauna, similar to the modern one, on the basis of which is determined Early Holocene age (Novochernomorian). Its presence was confirmed by a large number of boreholes during the geological surveys at the construction of the soda plants and the chemical plant “Varna”. The foundation of this terrace is 3–5 m above sea level. Gravel, covered with gray-yellow fine-grained sand, silt and clay are deposited on this surface. According to Evstatiev and Manov (1988), the width of this terrace reaches 300–400 m and its boundaries with the higher Young Karangatian terrace and the lower modern lake terrace are often unclear.

### Nymphaean terrace

The Nymphaean terrace is not well characterized along the Bulgarian coast. It is briefly mentioned in the works of Christov (1967) and Popov and Mishev (1974), but recently it was noted in several outcrops along the shoreline of the Burgas Lakes (Sinnyovsky et al., 2018, 2019). The youngest terrace in the studied area is very well defined at 1.5–2 m above sea level. Popov and Mishev (1974) described a wide “liman-marine terrace” 1–2 m above sea level, surrounding the lake from north, east and south reaching 2.8 km width between the lake

and the sea. Evstatiev and Manov (1988) described it as a “modern lake terrace”, which is represented by a variety of sediments – from coarse-grained sands with shell mussels to swamp clays and peat. It could be identified with the Nymphaean terrace of Fedorov (1959), although in the Middle Ages the lake was probably a closed estuary. According to Shkorpil and Shkorpil (1921), initially the sea was widely connected with the lake that formed a sea bay. Although the historical sources are not reliable in terms of geological data, Shkorpil (1923) noted that during the battle between Vladislav Varnenchik and the Turks in 1444, the area between the lake and the sea was swamped, so it is possible that they were really connected.

Along the northern shore of the lake near the village of Kazashko, the sediments of the terrace are represented by sands with mussel shells. If the shells are of marine origin, then surely this surface can be identified with the Nymphaean terrace. It is also possible that these deposits contain mixed or brackish-water fauna. Morphologically the younger Holocene terrace is well expressed along the entire shore of the lake and is covered with reeds everywhere (Fig. 4).

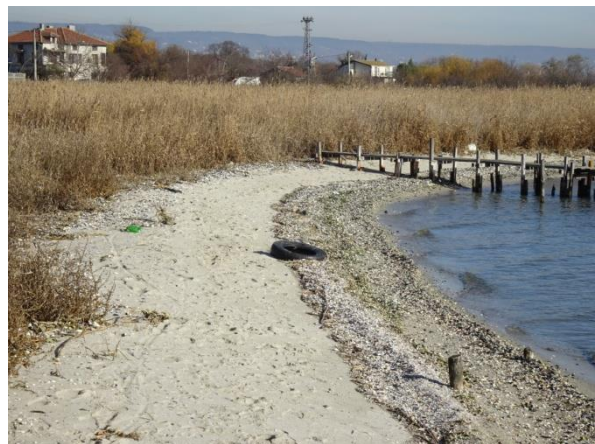


Fig. 4. The Nymphaean terrace near the village of Kazashko with the coastal deposits of sands and shells

### Sub-bottom terraces

Evstatiev and Manov (1988) summarized data from over 250 boreholes drilled along 15 km long and 0.5–1 km wide strip in connection with the port construction on the northern shore of the Varna Lake and compiled a map of the lake basement on which alluvial gravels marking sub-level terrace surfaces have been deposited. There are two well correlatable terrace levels. Against the background of these well expressed terraces some sublevels with a displacement of several meters were also recognized.

The lowest terrace recognized in the bottom deposits is at a depth of -28 to -35 m, but near the Asparuhovo Bridge it reaches -40 m. The base of the second, higher terrace in the lake deposits, which is very well expressed, from west to east sinks from -19 to -27 m. In the western part near the village of Ezerovo it is a flat surface with elevation between -19 and -20 m, but in the eastern part it is between -20 and -24 m (Fig. 5). Between the villages of Ezerovo and Kazashko, the terrace is cut by the Beglik valley, which flows into Varna Lake from the north. To the east towards the village of Kazashko the terrace surface is inclined from -20 m to -24 m. At the village of Kazashko this surface is crossed by parallel to the shore depression with a length of five to six hundred meters and a

depth up to 5 m formed by the valley flowing into the lake immediately east of the village. Another flattened area of the second terrace follows to the east at a depth of about -26, -27 m, in which the Nalbanka valley is incised (Fig. 4). Gravel layers with a thickness of 1 to 5–6 m are located on the terrace socles of both terraces. The map of the surface of the second terrace (Evstatiev, Manov, 1988) shows that it follows the surface of the Holocene basement. It is represented by flat areas in which small ravines descending from the north are incised (Figs 5, 6). There are slight elevations and funnel-shaped depressions east of the village of Kazashko, where the thickness of the gravel layer covering the second terrace vary in the frame of 1–2 m. The surface of this gravel layer is inclined to the south and merges with the surface of the terrace socle at the transition between the two subsurface terraces.

### Holocene deposits at the bottom of the lake

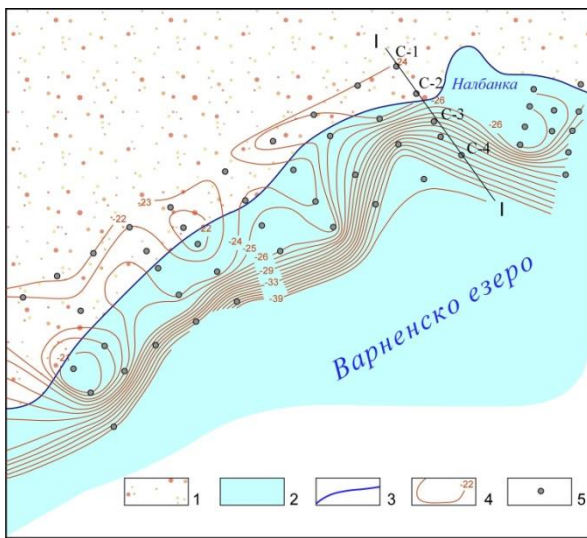


**Fig. 5. Contours on the surface of the alluvial gravel layer of the second terrace, following the underlying Oligocene terrace socle (after Evstatiev and Manov, 1988, with additional data):** 1 - land; 2 - water area of Varna Lake; 3 - shoreline; 4 - contours of the alluvial gravel on the second underwater terrace; 5 - drillings; I-I profile across the Holocene sediments illustrated on Fig. 5

After the Drevnechernomorion transgressive phase at 9 ka (Larchenkov and Kadurin, 2011) the Black Sea level rose to about -20 m. The saltwater flooding through Bosphorus caused drowning of the river mouths and formation of limans. Probably then started the accumulation of the Holocene deposits of the newly formed Varna liman. The sediments at the bottom of the northern shore of the lake have been studied in great details based on the information of more than 250 boreholes, drilled during Transproekt's engineering-geological survey for the port construction.

A cross-section of the Holocene sediments deposited on the bottom of the lake is shown in Fig. 6, along the profile I-I from Fig. 5 (after Evstatiev and Manov, 1988). On the Nymphaean terrace, surrounding the shoreline, there is a thin peat layer, which is formed in the Middle Ages during the high sea level (Nymphaean transgression) and continues its formation to these days (Fig. 6, unit 1). In the coastal zone, sands with accumulations of mussel shells are formed (Fig. 4; 6, unit 2). The youngest sediments, which are currently formed

at the bottom of the Varna Lake, are the water-saturated silts (Fig. 6, unit 3) and sandy water-saturated silts (Fig. 6, unit 4). They correspond to the lithological Type 1 – sandy and clayey silts to sandy-silty clays with rare small gravels, established during the engineering-geological study conducted by “Transport Construction and Reconstruction” Enterprise in the upper part of all exploratory shore drillings with thickness from 0.50 to over 3.00 m.

Under these deposits there are sands with mussel shells, whose thickness under the peat is up to 1 m, but under the shallow part of the lake it reaches 5 m (Fig. 6, unit 5). They correspond to lithological Type 2 – fine-grained sand, in places clayey, with small to medium-sized gravels and crushed mussel shells, established during the engineering-geological study of “Transport Construction and Reconstruction” Corp. along the entire length of Channel 1 and at the beginning of Channel 2. In Nalbanka bay, these sands continue until the sharp deepening of the lake bottom due to the fault structure marking the northern shoreline. Below these deposits sandy clays with sand layers are penetrated (Fig. 6, unit 6). This unit pinches out in the direction of the lake. Below are limestone deposits (so-called “lake chalk”), whose thickness increases from 2–3 m below the Nymphaean terrace to 5–6 m below the coastal zone (Fig 6, unit 7). Inside the carbonate deposits there is a lens of organogenic limestone up to 2 m thick (Fig. 6, unit 8). Below these carbonate deposits follow 3 m of consolidated mussel shells (Fig. 6, unit 9), 2 m of terrace deposits (Fig. 6, unit 10), 4 m of gray sandy clays (Fig. 6, unit 11), thin alluvial gravels (Fig. 6, unit 12), again thin clays (Fig. 6, unit 13), 3–4 m of sands (Fig. 6, unit 14) and alluvial clays (Fig. 6, unit 13) with a layer of sand and peat, underlying directly by the Oligocene socle (Ruslar Formation) to the land and gray sandy clays to the lake.

Further to the lake, laterally analogous of the sequence of units 11–14, the carbonate sediments are underlain by 5–6 m thick gray-green clay with mussel shells (Fig. 6, unit 15). In turn, this unit is underlain by 10 m alluvial clays and sandy clays with sandy layers (Fig 6, units 11, 13) at the base of which are the mentioned alluvial sands and gravels overlying the second river terrace. East of the village of Kazashko to the Nalbanka bay they cover directly the Oligocene socle (Ruslar Formation) at a depth of -20 to -26 m (Fig. 5). These clays can be compared with the lithological Type 3 – sandy-silty clay to clayey sand with clayey-sandy interbeds and crushed mussel shells, established during the engineering-geological study by “Transport Construction and Reconstruction” Enterprise in the marine drillings on the bottom of Channel 1. In the deep zone of the lake, south of the fault, under the modern water-saturated muds, a thick series of over 15 m clay muds with thin shell layers is disposed with a peat layer in the lower part which can be correlated also with the lithological Type 3. This unit covers sandy alluvial clays and river gravels. On the gravels of the second terrace there are up to 5–6 m thick sands of various particle size with fine-grained river gravels and yellowish sandstones. The deposits of the second terrace end with gray sandy clays, on which in many places a thin 0.5–1 m layer of buried peat is preserved, which at the railway near Nalbanka Bay is at a depth of -20 m (Figs 5, 6). Identical sequence is described by Popov and Mishev (1974) in a borehole drilled on the beach strip between Varna Lake and Black Sea, in which the second terrace level is established at a depth of 45.2 m. It is covered by 3 m gravel with sandy matrix.

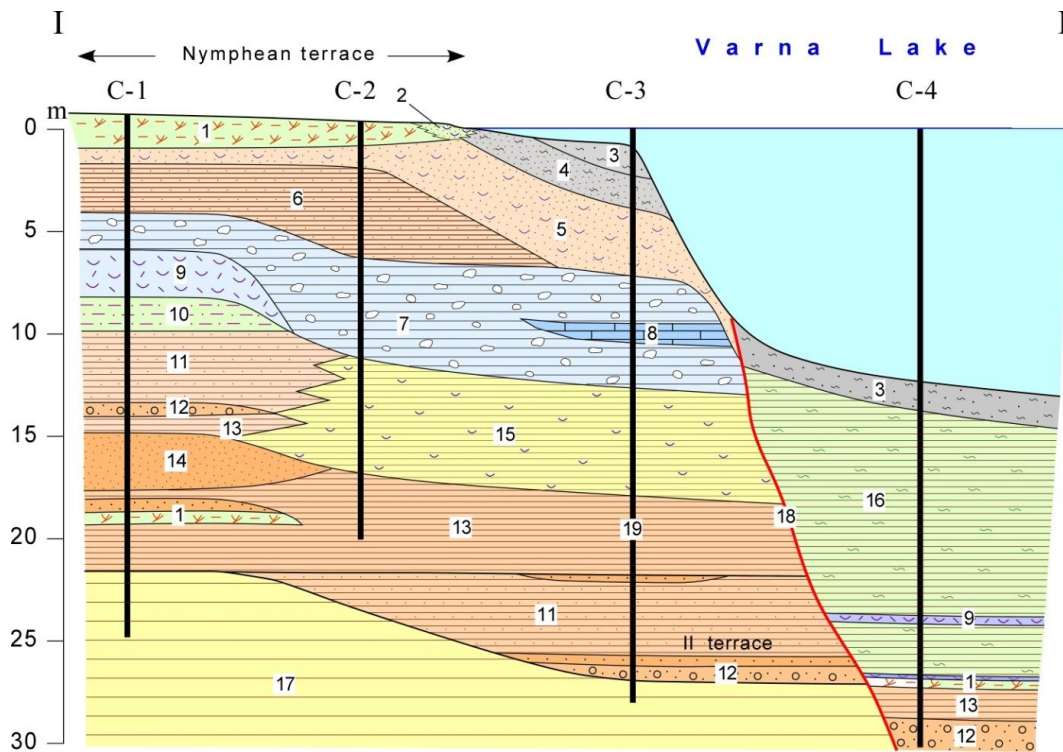


**Fig. 6. Geological section along profile I-I in Fig. 5 west of Nalbanka bay on the northern shore of Varna Lake (according to Evstatiev and Manov, 1988, with additional data):** 1, peat; 2, modern coastal deposits – sand and shell accumulations; 3, water-saturated silt; 4, sandy water-saturated silt; 5, sands with mussel shells; 6, sandy clay with sand layers; 7, calcareous deposits (lake chalk); 8, organogynvn limestone; 9, welded mussel shells; 10, terrace deposits; 11, gray sandy clays; 12, alluvial gravel; 13, alluvial clays; 14, sands; 15, gray-green clay with mussel shells; 16, clay mud; 17, Oligocene plinth (Ruslar Formation): clays, sands and clayey sandstones; 18, fault; 19, drilling

At a depth of 40 m is situated 60 cm thick peat layer covered by 3.5 m gray-bluish clay and 18 m marine mud – an evidence of swamp marine sedimentation. The rest of the section is represented by 1.5 m sand and 14 m sand with mussel shells, covered by 1 m thick peat layer and 2 m beach sands. The last investigations showed that Type 1 (water saturated sandy-silty clays) and Type 2 (fine-grained sand with crushed mussel shells) are prevailing to the depths of 14–15 m in all of the boreholes drilled for the deepening of the navigation Channel 1. In profile 3 it is very thin and is underlain by the sediments belonging to Type 3 (sandy-silty clay to clayey sand with crushed mussel shells) which is characteristic for the depths below 14 m. In profile 5 this interval between 6 and 15 m depth is represented by fine-grained sand.

### Historical and archeological aspects

Until 1906, before digging the first chanel to the sea, Devnya Lake (Varna Lake) flowed down along the Devnya River (Shkorpil and Shkorpil, 1921) through which there was a stone bridge called “Tash Kyupryu” (Fig. 7). After the construction of the channel it became unnecessary and was destroyed in 1908. Thus, the waters of the lake were salted and its level, which was 1.4 m higher, is equalized with the sea level. The existence of a higher sea level in the Middle Ages is confirmed by historical sources. Shkorpil and Shkorpil (1921) noted that the lake was initially connected directly to the sea and was a sea bay. Then a barrier gradually begins to form from the sediments of the beach sand. The famous Asparuhov shaft was originally built on the beach, while now it is 600 m

away from it. This is characteristic feature of the limans, indicating the sea level rise during the Middle Ages. According to Shkorpil (1923) during the famous battle in 1444 between the armies of Vladislav Varnenchik and the Turks, the area between Varna and the Asparuhovo district was swampy and the horses sank along with the heavily armed knights.



**Fig. 7. Photograph of the stone bridge “Tash Kyupryu” over the Devnya River in front of the city gate of Varna, destroyed in 1908**

On the other hand, the ancient pile dwellings, fortifications, breakwater walls and others, discovered at different depths in the Holocene deposits during the widening of the channel and other construction works, testify to a low sea level (3–4 m lower than it is today), which can be compared with the Phanagorian regression (Fedorov, 1956) proved by the remains of the ancient Greek colony of Khersones in Crimea, which are 3–4 m underwater. All these analogies show the

great importance of the archaeological artifacts for restoration of the Holocene geological history.

## Conclusions

The available lithological data about the Holocene deposits of the Varna Lake, obtained during the construction and maintenance of the navigation channels ensuring the connection with the Black Sea, provide excellent possibilities for interpretation of the Holocene history of this unique water basin, as evidenced by surface and subbottom lake terraces. The archeological artifacts, testifying for low lake level before the Odesos foundation, correspond to the geological evidence of low sea level in many places of the Black Sea coast. The question is whether the Varna estuary was closed during the Nymphaean transgression in the Middle Ages or the sand barrier appeared after the Nymphaean transgression. It should be resolved by investigation of the Nymphaean fauna of the youngest liman-marine terrace.

**Acknowledgements.** This investigation is performed with the support of the National Science Program "Environmental Protection and Reduction of Risks of Adverse Events and Natural Disasters", approved by the Resolution of the Council of Ministers № 577/17.08.2018 and supported by the Ministry of Education and Science (MES) of Bulgaria (Agreement № D01-230/06.12.2018).

## References

- Cheshitev, G., V. Milanova, N. Popov, E. Kojumdjieva. 1992. *Geological Map of Bulgaria Scale 1:100 000, Map Sheet Varna and Resort Zlatni Pyassatsi*. Sofia, Committee of Geology and Mineral Resources, Dept. of Geophys. Prosp. and Geol. Mapping.
- Cheshitev, G., V. Milanova, N. Popov, E. Kojumdjieva. 1994. *Explanatory Note to a Geological Map of Bulgaria Scale 1:100 000, Map Sheet Varna and Zlatni Pyassatsi*. Sofia, Committee of Geology and Mineral Resources, Geology and Geophysics Corp, 75 pp. (In Bulgarian with English abstract).
- Kojumdjieva, E. 1961. Sur le presence de faune Quaternaire marine pres du Lac Varna (Bulgarie de nord-est). – *Ann. Dir. General Rech. Geol.*, 12, 225–227.
- Kojumdjieva, E. 1964. Le faune Pleistocene marine (Karangatienne) des environs de Varna (Bulgarie de nord-est). – *Requeil en l'honneur de l'académicien Jovtcho Smilov Jovtchev*, 519–529.
- Fedorov, P. V. 1956. About the Modern Epoch in the geological history of the Black Sea. – *Proc. Acad. Sci. USSR, ser. geol.*, 110, 5, 839–841 (In Russian).
- Fedorov, P. V. 1959. About the Black Sea level fluctuations in the post-glacial time. – *Proc. Acad. Sci. USSR, ser. geol.*, 124, 5, 1127–1129 (In Russian).
- Fedorov, P. V. 1963. Stratigraphy of Quaternary deposits on the Crimean-Caucasian coast and certain problems in the geological history of the Black Sea. – *Transactions Geol. Inst. Acad. Sci. USSR*, 88, 1–157 (In Russian).
- Fedorov, P. V., D. A. Lilienberg, V. I. Popov. 1962. New data about the terraces along the Black Sea coast. – *Proc. Acad. Sci. USSR, ser. geol.*, 144, 2, 431–434 (In Russian).
- Larchenkov, E., S. Kadurin. 2011. Paleogeography of the Pontic Lowland and northwestern Black Sea shelf for the past 25 k.y. – In: Buynevich, I. V., V. Yanko-Hombach, A. S. Gilbert, R. E. Martin (Eds). *Geology and geoarcheology of the Black Sea Region*, 71–84.
- Popov, V., K. Mishev. 1974. *Geomorphology of the Bulgarian Black Sea Coast and Shelf*. Sofia, Publ. House of the Bulgarian Academy of Sciences, 267 pp. (In Bulgarian with English abstract)
- Sinnyovsky, D., N. Kalutskova, N. Dronin, D. Sinnyovska. 2018. Nymphaean terrace in the area of the Burgas Lakes. – *Rev. Bulg. geol. soc.*, 79, 3, 115–116.
- Sinnyovsky, D., D. Sinnyovska, N. Kalutskova, N. Dronin, A. Medvedev, N. Telnova. 2019. Fossil humus mad and its Novochemomorion base at the Atanasovsko Lake, Burgas Lakes Complex. – *J. Mining and Geol. Sci.*, 61, 1-Geol. and Geophys., 62–65.
- Shkorpil, H., K. Shkorpil. 1921. Twenty years activity of the Varna Archaeological Society, 1901–1921. – *Proc. Varna Arhaeol. Soc.*, 7, 3–84 (In Bulgarian).
- Shkorpil, H. K. 1923. *Vladislav Varnenchik 1444–1923*. Varna Arhaeol. Soc., Prosveshtenie Publ. House, 67 pp. (In Bulgarian).

## PROGNOSTICATION OF GROUNDWATER CONTAMINATION CAUSED BY OLD SANITARY LANDFILLS – PART I. MODELS OF THE MASS TRANSPORT OF POLLUTANTS THROUGH THE UNSATURATED ZONE

*Nikolay Stoyanov<sup>1</sup>, Stefan Dimovski<sup>1</sup>*

<sup>1</sup> *University of Mining and Geology “St. Ivan Rilski”, 1700 Sofia; nts@mgu.bg; dimovski@mgu.bg*

**ABSTRACT.** Sanitary landfills are one of the most common sources of environmental contamination that have accompanied humans from ancient times to the present day. An important task in the complex assessment of their impact is to acquire long-term prognostications of groundwater contamination by landfill leachate. A general approach is proposed to resolve it, involving the consecutive development of mathematical models of the mass transport of pollutants in the unsaturated and saturated zones. Its applicability is illustrated by a specific example for the region of the old sanitary landfill near Haskovo, Bulgaria. The VS2DI computer program was applied in order to develop two-dimensional models of the conditions for passage of liquid emissions from the landfill body through the bottom isolating layer and the unsaturated zone. These models were used for investigating the behavior of highly mobile and less mobile pollutants on the example of chloride and ammonium ions ( $\text{Cl}^-$  and  $\text{NH}_4^+$ ). The scheme of convective-diffusion mass transport is employed, taking into account reversible elimination (sorption-desorption), mechanical dispersion and mixing. Based on the obtained model solutions, the impact during the period of operation of the landfill was reconstructed. In addition, a medium-term forecast of the extent and degree of contamination in the unsaturated zone is developed and the concentration of pollutants in the percolation flux towards the saturated zone is estimated.

**Keywords:** groundwater contamination, unsaturated zone, sanitary landfills, solute transport models

### ПРОГНОЗИРАНЕ НА ЗАМЪРСЯВАНЕТО НА ПОДЗЕМНИТЕ ВОДИ ОТ СТАРИ ДЕПА ЗА БИТОВИ ОТПАДЪЦИ – ЧАСТ I. МОДЕЛИ НА ДВИЖЕНИЕТО НА ЗАМЪРСИТЕЛИ ПРЕЗ НЕНАСИТЕНАТА ЗОНА

*Николай Стоянов, Стефан Димовски*

*Минно-геоложки университет “Св. Иван Рилски”, 1700 София*

**РЕЗЮМЕ.** Депата за битови отпадъци са едни от най-разпространените източници на замърсяване на околната среда, които съпътстват човека от древността до наши дни. Важна задача при комплексната оценка на тяхното въздействие е изготвянето на дългосрочни прогнози за възможно замърсяване на подземните води със сметищен инфилтрат. За нейното решаване е предложен общ подход, включващ последователно разработване на математически модели на движението на замърсители в ненаситена и водонаситена среда. Неговата приложимост е илюстрирана с конкретен пример за района на старото депо за отпадъци на гр. Хасково, България. Посредством компютърна програма VS2DI са съставени двумерни модели на условията за преминаване на течни емисии от сметищното тяло през защитния екран и зоната на аерация, с които е изследвано поведението на силно подвижни и слабо подвижни замърсители по примера на хлоридните и амониеви йони ( $\text{Cl}^-$  и  $\text{NH}_4^+$ ). Използвана е схемата на конвективно-дифузионен пренос на вещество, с отчитане на обратимото елиминиране (сорбция-десорбция), механичната дисперсия и смесването. На базата на моделните решения е направена реконструкция на въздействието в периода на експлоатация на депото, а след неговото закриване и средносрочна прогноза за обхвата и степента на замърсяване в ненаситената зона и концентрацията на замърсители в подхранващия подземните води инфилтрационен поток.

**Ключови думи:** замърсяване на подземните води, ненаситена зона, депа за битови отпадъци, миграционни модели

### Introduction

Sanitary landfills as a major source of contamination are an important and very relevant topic in the discussions on the protection of global water resources. The study and the search for solutions to reduce their harmful effects is a worldwide problem considering their wide distribution, enduring action and the serious damage they cause to all elements of the environment – air, water and soil (Christensen et al., 1989; Montgomery, 2019; Vaverková, 2019). Part of the complex assessment of the problem is the development of long-term prognostications for the extent, degree and period of groundwater contamination caused by old sanitary landfills. Our experience in this sphere shows that the most effective

tools for making these forecasts are the mathematical models of the mass transport of pollutants in the unsaturated and saturated zones. The applicability of the proposed general approach will be demonstrated by an example for the region of the old sanitary landfill near Haskovo, Southern Bulgaria. The two-dimensional models of the conditions for passage of liquid emissions from the landfill body through the bottom isolation layer and the unsaturated zone, presented in this first part of the article, are developed using the computer program VS2DI (Healy, 1990). The acquired model solutions were used for investigating the fate and transport of highly mobile and less mobile pollutants on the example of chloride and ammonium ions ( $\text{Cl}^-$  and  $\text{NH}_4^+$ ) during the operation of the landfill and in the period after its closure.

## General approach for modeling of groundwater contamination caused by sanitary landfills

### Selection of key pollutants

The contamination models usually do not include all the pollutants contained in the landfill leachate, as this is usually not necessary and the additional costs required cannot be compensated by a higher quality of the end result. For that reason, from the many pollutants in the contamination source (emitter), two or more key pollutants are selected, with which different conservative (critical) scenarios are reproduced in the models. The main selection criteria are the pollutant concentration in the emitter; the pollutant mobility in the unsaturated and saturated zones; the pollutant ability to affect the geochemical barriers; its harmful effects on human health and the environment. The key pollutants must represent the maximum extent of subsurface contamination and the most intense (toxic) pollution around the source. From this point of view, highly mobile, with low sorption potential, pollutants (chlorides, sulphates, some organic compounds such as TCE, PCE, etc.) and less mobile, with high sorption potential, contaminants (ammonium ions, heavy metals, etc.) are an adequate selection (Fatta et al., 1999; Kjeldsen et al., 2002; Christensen et al., 1989).

### Contaminant migration field and its components

The contaminant migration field by definition includes this part of the subsurface in which the pollutants from the landfill advance to the first recipient – the nearest river or surface water body (Stoyanov, 2019). Pollution models should cover the three main components of this field: (1) engineering barriers at the landfill bottom – isolating layers; (2) unsaturated zone – from the last engineering barrier to the groundwater level; (3) saturated zone – potentially endangered aquifers or aquifer complexes. Formally, the engineering barriers are part of the unsaturated zone.

### Modelling techniques

The starting positions in the proposed general concept for modeling of groundwater contamination caused by old sanitary landfills are: (1) The mass-transport of key pollutants through the unsaturated zone and the engineering barriers (if any) is simulated with 2D models, and their subsequent spreading in groundwater – with 3D models. The obtained two-dimensional solutions are used as input data in the 3D models. (*Remark: The development of complex 3D models, including all components of the contaminant migration field, is difficult to apply due to the fact that computer simulation in case of long-term predictions an extremely time-consuming process. At the same time, the separate simulation of the processes in the unsaturated and saturated zones does not a priori reduce the solutions accuracy, on the contrary – it improves the stability of the mathematical models and makes the prognostications more detailed.*) (2) The 2D model area covers sections along lines passing through the central part of the landfill body in the direction of the underground flow, and the 3D one – the subsurface from the emitter to the first recipient. (3) The models are deterministic. The hydrogeological units and the engineering barriers are simulated as two-dimensional or three-dimensional objects according to their main characteristics: geometric (thickness, length, extension), physical (density, porosity), hydrodynamic (hydraulic

conductivity) and mass transport ones (distribution, dispersion and molecular diffusion coefficients). In the 2D models are additionally set parameters specific for the unsaturated zone: natural moisture content, coefficient of moisture conductivity, etc. (4) The groundwater recharge by infiltration and percolation is set in accordance with the climatic, geologic and technogenic conditions. (5) The mechanism of the mass transport of key pollutants is in its full form: convective and diffusion transport, accompanied by mechanical dispersion, reversible elimination (sorption-desorption), irreversible elimination (radioactive decay and biodegradation) and mixing. (6) The flow through the engineering barriers and the input concentrations of the studied key pollutants are set as variables taking into account the specific technogenic conditions. (7) The models simulate the fate and transport of selected key pollutants (chlorides, sulfates, ammonium ions, heavy metals, etc.) and the target is to achieve long-term predictions – forecast period of up to 100 years. (8) The results of the model studies are presented as vertical and horizontal sections of the concentration field at different points in time.

### Modelling tools

Standard computer programs are used, in whose algorithms are implemented numerical solutions of the equations of moisture and mass transport in the unsaturated zone and the flow and mass transport equations in a water-saturated environment. The two-dimensional models of contaminant transport across the engineering barriers and the unsaturated zone are compiled using the VS2DTI package from the computer program VS2DI (Healy, 1990, Hsieh et al., 2000). The three-dimensional models of the pollutant fate and transport in the saturated zone are developed using the computer programs Modflow and MT3D-MS (Anderson et al., 2015; McDonald and Harbaugh, 1988; Stoyanov, 2019; Zheng and Bennet, 2002).

### Characteristics of the study area

The applicability of the presented general approach will be illustrated with models of groundwater contamination caused by the old sanitary landfill near the town of Haskovo (Fig. 1). The studied region is situated in the northern periphery of the Haskovo valley in the catchment area of the Gidikli dere River, a right tributary of the Banska River. The geological section is dominated by Paleogene volcano-sedimentary rocks (latites and pyroclastic rocks), partially covered by a 1-2 m thick clay layer. Down to a depth of 60-70 m the rocks are fractured, differently weathered, in places decomposed to clay.



Fig. 1. Location of study area

The main hydrogeological unit in the region is the Paleogene aquifer complex, which is very heterogeneous and is characterized by relatively low water permeability. Based on the degree of secondary alteration, several hydrogeological units of lower rank are separated in it. The hydraulic conductivity most often varies between 0,005 and 1,5 m/d. The aquifer complex is unconfined and vulnerable to surface pollutants. The groundwater recharge occurs chiefly from infiltration of rainfall and snowmelt. The general direction of groundwater flow is to the southeast – towards Gidikli dere River. The average hydraulic gradient is 0,02, about 0,012 in the sanitary landfill area. The modulus of groundwater discharge is less than 0,1 (l/s)/km<sup>2</sup>, i.e. the groundwater resources are insignificant. The sanitary landfill is located in the upper part of a ravine, which in the period 1997/2015 was gradually filled with waste materials. The engineering barrier designed to provide leachate control is a layer of compacted clay laid down under landfill cell.

Key pollutants for the study area are chloride and ammonium ions (Cl<sup>-</sup> and NH<sub>4</sub><sup>+</sup>). They are selected on the basis of continuous monitoring of landfill leachate and groundwater chemical composition.

### Methodology. Development of models of pollutant transport in the unsaturated zone

The two-dimensional models M2D-CL and M2D-NH<sub>4</sub>, designed for studying the behavior of the key pollutants Cl<sup>-</sup> and NH<sub>4</sub><sup>+</sup> in the unsaturated zone, were compiled with the program VS2DI. The model area covers the section underneath the landfill cell along profile I-I, passing lengthwise the axis of the ravine (Fig. 2).

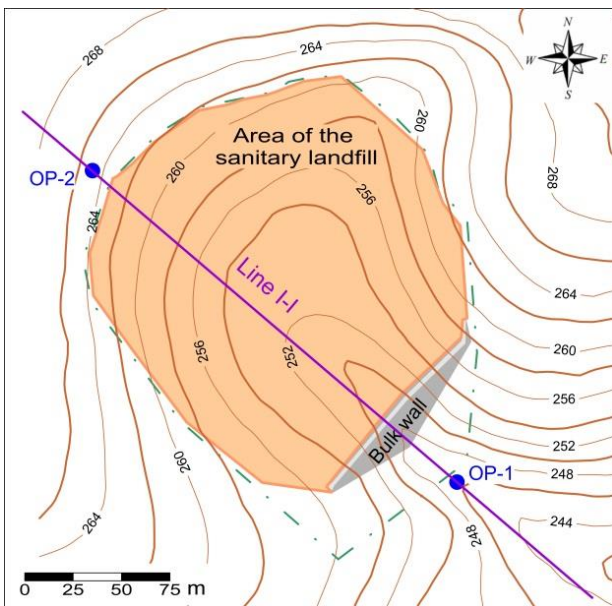


Fig. 2. Boundaries of the landfill as of 2015. Topographic map of the landfill area

In the section, down to a depth of 90 m, are separated two hydrogeological units, which together with the engineering barrier (Table 1) are set in the models as zones with corresponding hydrogeological parameters - total porosity  $n$ ,

bulk density  $\rho_d$ , hydraulic conductivity  $k$ , longitudinal dispersion  $\alpha_L$ , diffusion coefficient  $D_M$  and distribution (partition) coefficient  $K_D$  (Fig. 3 and Table 2). The van Genuchten function is used to model the relations between pressure head, moisture content, and relative hydraulic conductivity. The time of the computer simulation, including the period of landfill operation 1998/2015 and the period after its cessation until 2025, is divided into 27 stress periods, each lasting 1 year.

Table 1. Mass transport field components, low-rank hydrogeological units and model zones

Component	Hydrogeological unit	Model zone
Engineering barrier	Layer of compacted clay	MZ 1
Unsaturated zone	Layer of low permeability (diluvial clay)	MZ 2
	Zone of low permeability (rock complex)	MZ 3

Table 2. Hydrogeological parameters for the model zones

Hydrogeological parameter	Model zone		
	MZ 1	MZ 2	MZ 3
$n$ , dimensionless	0,32	0,35	0,36
$\rho_d$ , g/cm <sup>3</sup>	1,61	1,74	1,78
$k$ , m/d	$2,6 \cdot 10^{-5}$	0,05	0,25
$\alpha_L$ , m	0,55	2,50	10,00
$D_M$ , m <sup>2</sup> /d	$5,0 \cdot 10^{-4}$	$4,5 \cdot 10^{-4}$	$4,0 \cdot 10^{-4}$
$K_D$ for Cl <sup>-</sup> , cm <sup>3</sup> /g	0,70	0,50	0,20
$K_D$ for NH <sub>4</sub> <sup>+</sup> , cm <sup>3</sup> /g	4,50	1,50	1,10

Remark: The values of  $n$ ,  $\rho_d$ ,  $k$ ,  $\alpha_L$ , as well as the values of  $K_D$  for Cl<sup>-</sup> are determined according to data from slug tests and tracer tests conducted by the authors (Stoyanov et al., 2010; Stoyanov, 2010), and the values of  $D_M$  and  $K_D$  for NH<sub>4</sub><sup>+</sup> are determined from literature data for a similar soils (Spitz and Moreno, 1996).

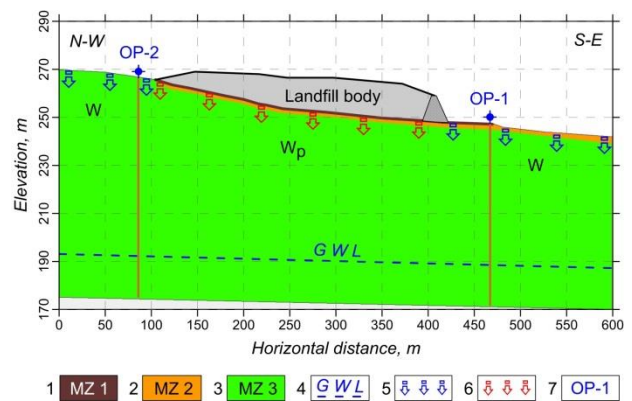


Fig. 3. Conceptual framework of the two-dimensional models 1, 2 and 3 – Boundaries of the model zones, 4 – Groundwater level; 5 – Rainfall infiltration; 6 – Leachate infiltration; 7 – Monitoring observation points.

The groundwater level is set as specified total head at a depth of 65-80 m (Fig. 3). The landfill body is set as a line source of pollution, the length of which increases according to the rate of its expansion (Fig. 4). The leachate is simulated as specified flux characterized by the calculated for each stress period average values of the infiltration rate  $W_p$  and the concentrations of Cl<sup>-</sup> and NH<sub>4</sub><sup>+</sup> in them –  $C_{Cl}$  and  $C_{NH_4}$  (Table 3). The values of  $W_p$  are presumed on the basis of the landfill

water balances for the respective time intervals, determined by the average annual values of precipitation, air temperature and evaporation provided by Hydro-meteorological observation station Haskovo (Table 4), taking into account the water permeability of the surface layer (Brendenkamp, 1990).

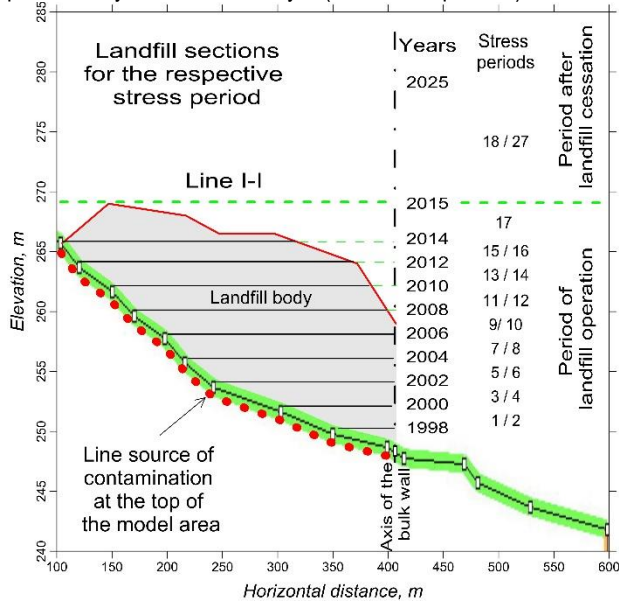


Fig. 4. Scheme of waste disposal along profile I-I. Length of the line source of contamination at the top boundary of the two-dimensional models in the different stress periods.

Table 3. Average values of  $W_p$ ,  $C_{Cl}$  u  $C_{NH4}$  for the landfill leachate

Time interval	Stress period	$W_p$ , m/d	$C_{Cl}$ mg/l	$C_{NH4}$ mg/l
1998-2006	1/8	$4,6 \cdot 10^{-4}$	1850	700
2007	9	$5,9 \cdot 10^{-4}$	1850	700
2008	10	$6,3 \cdot 10^{-5}$	1850	700
2009	11	$3,5 \cdot 10^{-4}$	1850	515
2010	12	$6,2 \cdot 10^{-4}$	1850	460
2011	13	$3,2 \cdot 10^{-4}$	2000	350
2012	14	$8,3 \cdot 10^{-4}$	1300	85
2013	15	$3,0 \cdot 10^{-4}$	1860	700
2014	16	$1,2 \cdot 10^{-3}$	1820	85
2015	17	$3,7 \cdot 10^{-4}$	600	450
2016-2025	18/27	$5,0 \cdot 10^{-4}$	1400	120

Table 4. Average annual values of precipitation  $P$ , air temperature  $T$  and evaporation  $E$

Observation period	Precipitation $P$ , mm	Air temperature $T$ , °C	Evaporation $E$ , mm
1956-2006	668,0	12,5	501,0
2007	790,1	14,1	574,1
2008	372,1	13,6	349,0
2009	621,1	13,2	491,7
2010	785,1	13,4	557,8
2011	580,4	12,4	462,0
2012	892,0	13,4	588,8
2013	597,4	13,6	486,4
2014	1059,9	13,7	634,6
2015	647,0	14,1	517,0
2007-2015	724,0	13,5	538,7

Remark: Data provided by Hydro-meteorological observation station Haskovo

The values of  $C_{Cl}$  and  $C_{NH4}$  are deduced according to data from the monitoring of landfill leachate chemical composition. The groundwater recharge from rainfall is set along the entire length of the profile with an average for the period infiltration rate  $W = 2,0 \cdot 10^{-5}$  m/d and zero concentrations of  $Cl^-$  and  $NH_4^+$ . The models are calibrated to the registered concentration values in the monitoring points by varying the values of  $k$ ,  $D_M$ ,  $\alpha_L$  and  $W_p$ .

## Results and discussion

The results of the computer simulations of the mass transport of highly mobile and less mobile pollutants through the unsaturated zone and their subsequent passage into the saturated zone are illustrated with the model solutions presented in Fig. 5 and Fig. 6. They display the extent and degree of subsurface and groundwater contamination in different periods of the landfill operation (2005, 2010 and 2015) and demonstrate the acquired forecast for the development of these negative processes by 2025.

During landfill operation, the following more important patterns in the behavior of the key pollutants used in the simulations are observed: *Chloride ions* are highly mobile, so the boundaries of the region, contaminated by them, are dynamic and quickly cover large subsurface areas. By 2012 they reach the groundwater level beneath the oldest part of the sanitary landfill. Here the unsaturated zone is the most polluted, and the  $Cl^-$  concentration down to a depth of 25-30 m is around and above 1000 mg/l. These high values are an indirect sign for the presence of some non-sorbent organic compounds (TCE, PCE, phenol, etc.) part of which are very toxic. The  $Cl^-$  concentration in the contaminated infiltration flux that enters groundwater is in the range of 200-250 mg/l. At the end of the operation period, the highly mobile pollutants spread out over a distance of 130-150 m from landfill's southeastern border. *Ammonium ions* have high sorption potential and are principally retained by the engineering barrier and the diluvial clays. They migrate very slowly and contaminate more limited subsurface parts. The most polluted by them areas in the unsaturated zone are down to a depth of 20-25 m beneath the old part of the landfill and down to 10-15 m under the new parts. In these zones the  $NH_4^+$  concentration is 150-200 mg/l, and in depth it decreases very rapidly. At the end of the operation period, the front of the zone of  $NH_4^+$  contamination reaches a depth of 45-50 m underneath the old part of the landfill and laterally spreads out over a distance of 10 m from its southeastern border. In a very limited area, small quantities of ammonium ions infiltrate to the groundwater level, affecting a minor part of the saturated zone, where their concentration is not more than 2-3 mg/l. Due to their very low mobility,  $NH_4^+$  ions have only indicative value for localizing the most intensive pollution. Their presence in the already contaminated areas is associated with the manifestation of many other pollutants including heavy metals, organic compounds, etc.

After the cessation of the sanitary landfill operation, the medium-term forecast for the fate and transport of pollutants in the unsaturated zone and groundwater, based on the model solutions – Fig. 5-D and Fig. 6-D, in short is the following. The concentrations of the various components in the composition of the leachate generated by the old landfill will gradually decrease. The concentration of key pollutants in the liquid emissions infiltrating beneath the landfill will also decrease.

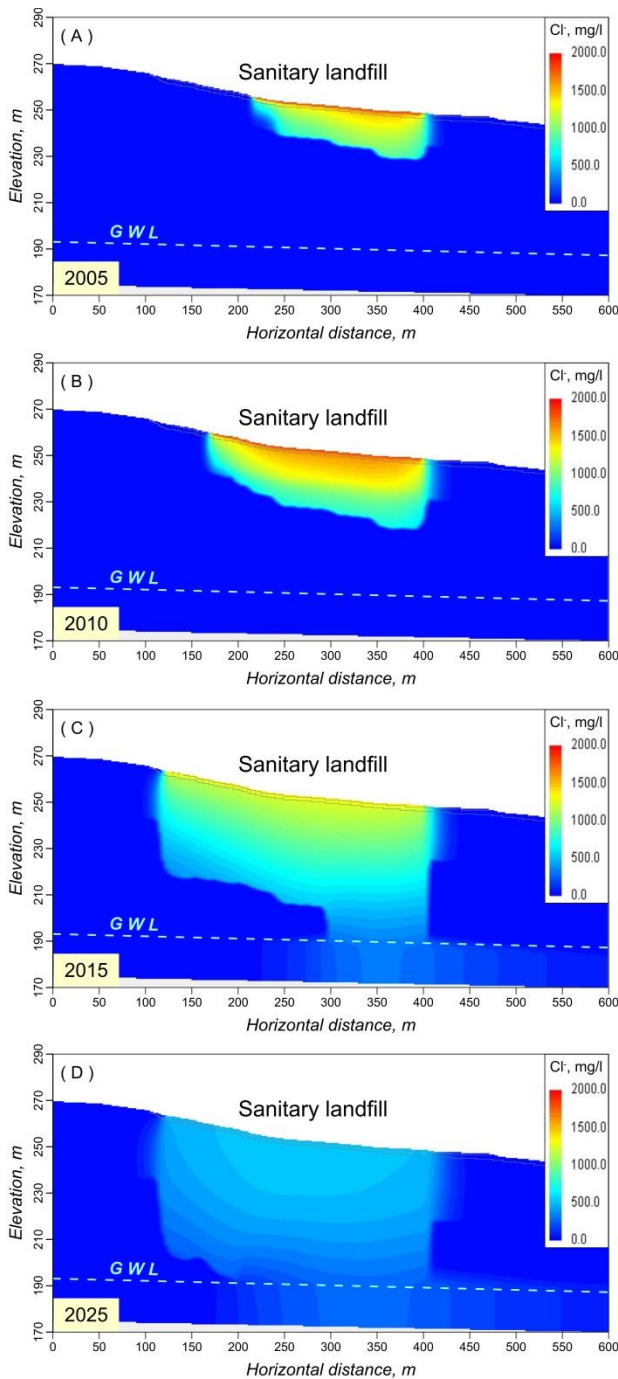


**Fig. 5. Model M2D-CL. Distribution of highly mobile pollutants on the example of Cl<sup>-</sup>.**  
 (A), (B) and (C) – model solutions for different periods of landfill operation, respectively at 2005, 2010 and 2015, (D) – model solution after landfill cessation, prognosis for 2025.

The spatial boundaries of the polluted zones, although slower, will continue to expand, while the concentrations in the most contaminated parts of these areas will progressively decline. At the end of the forecast period by 2025, the Cl<sup>-</sup> concentration in the most polluted parts of the unsaturated zone will be between 350 and 650 mg/l, and the NH<sub>4</sub><sup>+</sup> concentration will not be higher than 100-180 mg/l. At the same time, the contaminated infiltration flux will continue to enter groundwater through larger areas. The Cl<sup>-</sup> concentration in it will be between 200 and 350 mg/l, and the NH<sub>4</sub><sup>+</sup> concentration will not exceed 7-8 mg/l. The groundwater

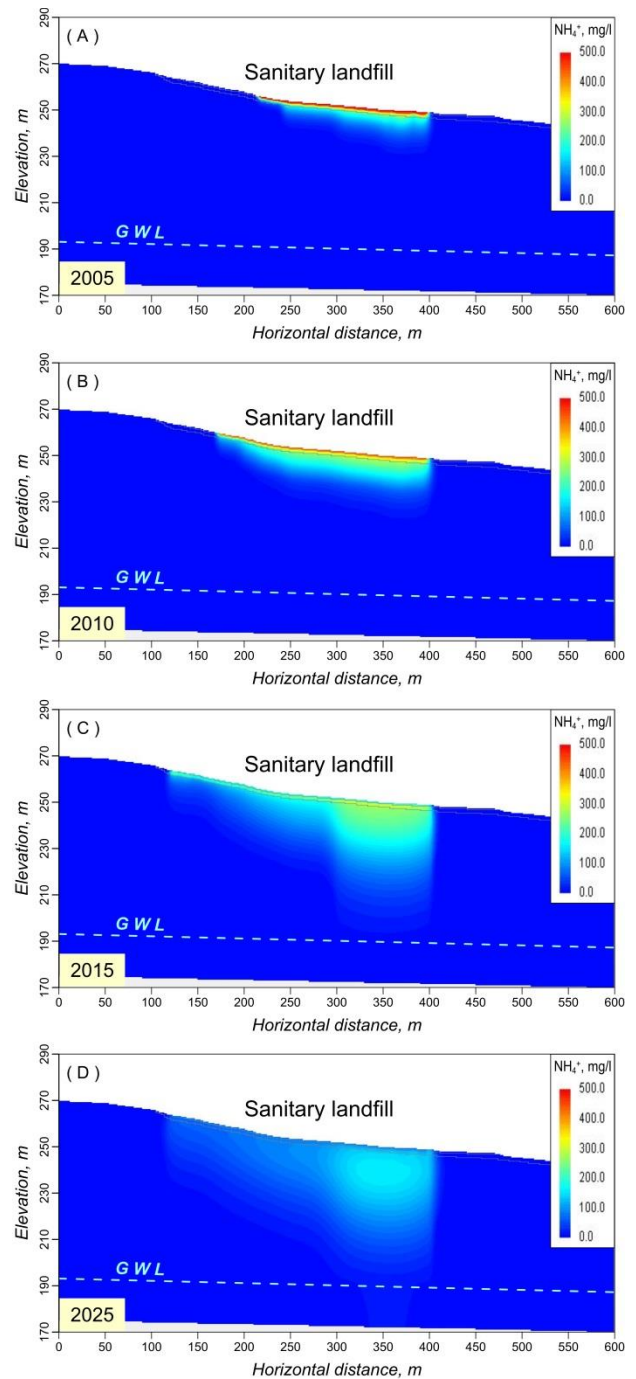


**Fig. 6. Model M2D-NH4. Distribution of less mobile pollutants on the example of NH<sub>4</sub><sup>+</sup>.**  
 (A), (B) and (C) – model solutions for different periods of landfill operation, respectively at 2005, 2010 and 2015, (D) – model solution after landfill cessation, prognosis for 2025.

contamination by highly mobile pollutants will expand to about 150-200 m southeast of the landfill, and the contamination by less mobile pollutants – to no more than 50-60 m.

The performed model studies of the fate and transport of pollutants in the unsaturated zone show that the low water permeability characteristics of the rock massif and the covering diluvial clays are a good natural barrier that minimize the leachate infiltration beneath the bottom of the sanitary landfill. The layer of compacted clay (the engineering barrier) laid down under landfill cell further limits the possibilities for environmental pollution.

## Conclusion

Using two-dimensional models, a computer simulation of the mass transport of selected key pollutants through the unsaturated zone is performed for the region of the old sanitary landfill near Haskovo. The concentrations of contaminants in the percolation flux towards the saturated zone are estimated for the period of operation, as well as for ten years after landfill cessation. The obtained solutions show that the landfill operation is accompanied by a local and low level subsurface contamination caused by the leachate passage through the compacted clay layer laid down under landfill cell. According to the developed prognostic models, assuming that the old sanitary landfill continues to emit pollutants, although with lower concentrations, the polluted zones will continue to expand their spread with gradually declining concentrations in the most contaminated parts of these areas. The obtained solutions for the transit time of pollutants to groundwater level and their concentration in the contaminated percolation flux towards the saturated zone are presented in the second part of the article, where they are used as input data in the three-dimensional models.

The developed two-dimensional models provide an opportunity to quantify the effectiveness of engineering barriers that restrict the free flow of leachate from old landfills, as well as to identify measures for improving their performance. The obtained results are of practical importance as they provide a prognostic evaluation of the possible ecological consequences in the studied area. The presented methodological approach can be successfully implemented in solving other similar hydrogeological problems.

**Acknowledgements.** This work has been carried out in the framework of the National Science Program "Environmental Protection and Reduction of Risks of Adverse Events and Natural Disasters", approved by the Resolution of the Council of Ministers № 577/17.08.2018 and supported by the Ministry of Education and Science (MES) of Bulgaria (Agreement № DO-230/06-12-2018). The presented models are based on unpublished author's works for the project "Soil and water pollution monitoring, protection and remediation in the area of the regional landfill for non-hazardous waste, Haskovo" - 2009/16.

## References

- Anderson, M., W. Woessner, R. J. Hunt. 2015. *Applied groundwater modeling: simulation of flow and advective transport*. Elsevier, Academic press, 720 p.
- Bredenkamp, D. 1990. Quantitative estimation of groundwater recharge by means of a simple rainfall-recharge relationship. – In: *Groundwater recharge. IAH Memoir, Vol 8*. (Eds. Lerner, D., A. Issar, I. Simmers). Heise, 247–256.
- Christensen, T., R. Cossu, R. Stegmann. (Eds.) 1989. *Sanitary Landfilling: Process, Technology and Environmental Impact*. Elsevier, Academic Press, 602 p.
- Fatta, D., A. Papadopoulos, M. Loizidou. 1999. A study on the landfill leachate and its impact on the groundwater quality of the greater area. – *Environmental Geochemistry and Health* 21, 175–190.
- Healy, R. W. 1990. Simulation of solute transport in variably saturated porous media with supplemental information on modifications to the US Geological Survey's computer program VS2D. – *USGS Numb. Ser., Water-Resour. Inv. Rep. 90-4025*, 125 p.
- Hsieh, P., W. Wingle, R. W. Healy. 2000. VS2DI - A graphical software package for simulating fluid flow and solute or energy transport in variably saturated porous media. – *USGS Numb. Ser., Water-Resour. Inv. Rep. 99-4130*, 16 p.
- Kjeldsen, P., Barlaz, M., Rooker, A., Baun, A., Ledin, A., Christensen, T. 2002. Present and long-term composition of MSW landfill leachate: A review. – *Critical Reviews in Environmental Science and Technology*, 32 (4), 297-336.
- McDonald, M., A. Harbaugh. 1988. A modular three-dimensional finite-difference groundwater flow model. - *Techn. of Water Res. Inv. of the USGS, Book 6-A1*, 586 p.
- Montgomery, C. W. 2019. *Environmental geology*. McGraw-Hill, NY, 576 p.
- Spitz, K., J. Moreno. 1996. *A practical guide to groundwater and solute modeling*. JW&S, NY, 460 p.
- Stoyanov, N., B. Banushev, S. Dimovski, S. Nedelcheva. 2010. Uslovia za migratsia na nesorbiruemi zamarsiteli v nevodonasitenata zona na paleogenskite vulkaniti v raiona na gr. Haskovo. Chast 1. Determinirane na niskorangovi hidrogeolozhki edinitsi. – *Annual of the University of Mining and Geology "St. Ivan Rilski"*, 53, Part 1, 163-168 (in Bulgarian with English abstract).
- Stoyanov, N. 2010. Uslovia za migratsia na nesorbiruemi zamarsiteli v nevodonasitenata zona na paleogenskite vulkaniti v raiona na gr. Haskovo. Chast 2. Matematicheski Model. – *Annual of the University of Mining and Geology "St. Ivan Rilski"*, 53, Part 1, 169-173 (in Bulgarian with English abstract).
- Stoyanov, N. 2019. *Matematicheskoto modelirane v hidrogeologiyata. Chisleni 3D modeli po metoda na krainite razliki*. Vanio Nedkov, Sofia, 246 p. (in Bulgarian)
- Vaverková, M.D. 2019. Landfill impacts on the environment - review. – *Geosciences*. 9, 431
- Zheng, C., G. Bennet. 2002. *Applied contaminant transport modeling: Theory and practice*. J&WS, NY, 440 p.

## PROGNOSTICATION OF GROUNDWATER CONTAMINATION CAUSED BY OLD SANITARY LANDFILLS – PART II. MODELS OF THE MASS TRANSPORT OF POLLUTANTS IN THE SATURATED ZONE

*Nikolay Stoyanov<sup>1</sup>, Stefan Dimovski<sup>1</sup>*

<sup>1</sup> *University of Mining and Geology “St. Ivan Rilski”, 1700 Sofia; nts@mgu.bg; dimovski@mgu.bg*

**ABSTRACT.** In Part I were described a general approach for prognostications of groundwater contamination caused by old sanitary landfills, as well as the developed models of the contamination in the unsaturated zone on the example of the old landfill in Haskovo, Bulgaria. Part II presents the composed, according to general approach, three-dimensional models of the conditions for mass transport of pollutants in the saturated zone through which a long-term prediction of groundwater contamination for a period of 100 years is acquired. A numerical three-dimensional flow model for the vulnerable to pollution aquifer complex was compiled using the Modflow computer program. Based on the flow model and taking into account the two-dimensional model solutions, applying computer program MT3D-MS, two 3D mass transport models were developed, which simulate the behavior of highly mobile and less mobile pollutants on the example of Cl<sup>-</sup> and NH<sub>4</sub><sup>+</sup>. For the modeling of mass transport in the three-dimensional models, as in the two-dimensional models, the convective-diffusion scheme and the accompanying processes of reversible elimination, mechanical dispersion and mixing were used. The first mass transport model estimates the maximum spread of the groundwater contaminated area, and the second model determines the boundaries of the critical high contamination area, in which many and often toxic pollutants are expected to be present.

**Keywords:** groundwater contamination, saturated zone, sanitary landfills, flow models, mass transport models

### ПРОГНОЗИРАНЕ НА ЗАМЪРСЯВАНЕТО НА ПОДЗЕМНИТЕ ВОДИ ОТ СТАРИ ДЕПА ЗА БИТОВИ ОТПАДЪЦИ – ЧАСТ II. МОДЕЛИ НА РАЗПРОСТРАНЕНИЕТО НА ЗАМЪРСИТЕЛИТЕ ВЪВ ВОДОНАСИТЕНАТА ЗОНА

*Николай Стоянов, Стефан Димовски*

*Минно-геоложки университет “Св. Иван Рилски”, 1700 София*

**РЕЗЮМЕ.** В Част I бяха описани един общ подход за прогнозиране замърсяването на подземните води от стари депа за отпадъци и модели на замърсяването в ненаситената зона по примера на старото депо на гр. Хасково, България. Част II представя съставените по общ подход тримерни модели на условията за движение на замърсители във водонаситената зона, посредством които е направена дългосрочна прогноза за замърсяването на подземните води за период от 100 години. Посредством компютърна програма Modflow е съставен филтрационен тримерен модел на застрашения от замърсяване водоносен комплекс. На базата на филтрационния модел и при отчитане на двумерните моделни решения с компютърна програма MT3D-MS са съставени два миграционни тримерни модела, с които е симулирано поведението на силно подвижните и слабоподвижните замърсители по примера на Cl<sup>-</sup> и NH<sub>4</sub><sup>+</sup>. За моделиране на миграцията в тримерните модели, както в двумерните, е използвана конвективно-дифузионна схема и съпътстващите я процеси на обратимо елиминиране, механична дисперсия и смесване. С първия миграционен модел е направена прогноза за максималния обхват на зоната със замърсени подземни води, а с втория модел са определени границите на зоната с критично високо замърсяване, в която се очаква да присъстват много на брой и често токсични замърсители.

**Ключови думи:** замърсяване на подземните води, водонаситена зона, депа за битови отпадъци, филтрационни модели, миграционни модели

### Introduction

Following global trends, various software products are used in Bulgaria to model the fate and transport of various pollutants in the saturated zone – Modflow, MT3D-MS, Feflow, Hidrus, etc. (Benderev et al., 2015; Gerginov et al., 2017; Stoyanov and Dimovski, 2004; Stoyanov, 2007, 2012; Stoyanov et al., 2015, 2018, 2019). In the first part is presented the concept of one very effective approach for quantitative assessment and prediction of groundwater contamination caused by old sanitary landfills. A computer simulation of the mass transport of leachate pollutants through the engineering barriers and the unsaturated zone for the period of operation, as well as for ten years after the cessation of the sanitary landfill nearby Haskovo is performed implementing 2D models. These models are used for studying the behavior of highly mobile and less mobile pollutants on the example of chloride

and ammonium ions. On this basis, an evaluation and a medium-term forecast for the transit time of pollutants to groundwater level and their concentration in the contaminated percolation flux towards the saturated zone are made. Three-dimensional flow and mass transport models of the fate and behavior of pollutants in the Paleogene aquifer are developed in order to predict the following development of the processes of groundwater contamination for a longer period (100 years) after the landfill cessation. The three-dimensional models are compiled using computer programs Modflow and MT3D-MS. The obtained solutions from the 2D models are employed as input data. Applying 3D mass transport models, a computer simulation of the distribution of Cl<sup>-</sup> and NH<sub>4</sub><sup>+</sup> is developed. Subsequently, a long-term forecast for the size and degree of groundwater contamination in the Paleogene aquifer complex, caused by the old sanitary landfill near Haskovo, is acquired.

## Methodology. Development of models of pollutant transport in the saturated zone

The mathematical model studies for assessment and prognostication of contamination processes in the saturated zone include two main problems – the hydrodynamic field and the mass transport one (Anderson et al., 2015; Stoyanov, 2019). Standard hydrogeological software is used to develop 3D numerical models. To solve the first problem, a flow model (FM3D) of the Paleogene aquifer in the area of the studied site is compiled using the computer program Modflow (McDonald and Harbaugh, 1988). The second problem is solved with mass transport models (M3D-CL M3D-NH4) of the conditions for distribution of Cl<sup>-</sup> and NH<sub>4</sub><sup>+</sup>. These models are developed implementing the basic flow model and applying the computer program MT3D-MS (Zheng and Bennet, 2002).

### Conceptual model of the pollution source

The source of contamination in the saturated zone is the percolation flux entering through the entire area of the projection of the landfill on the groundwater table, marking the boundary between the unsaturated and the saturated zone. The conservative scenario accepts the simplified assumption that the infiltration rate over the entire source area is constant and equal to the rate set in the two-dimensional models for the leachate coming from the landfill. The pollutants concentration in the source, in this case in the percolation flux, depends on the age of the deposited waste materials, the leachate infiltration rate beneath landfill, the depth towards groundwater table, the water permeability and the retention capacity of the unsaturated zone. According to monitoring data, the Cl<sup>-</sup> concentration in the “fresh” leachate varies from 1300 to 2000 mg/l, having an average value of 1700 mg/l, and the NH<sub>4</sub><sup>+</sup> concentration – from 85 to 700 mg/l, having an average value of 450 mg/l. For a short period, however, these values decrease exponentially by one or two orders of magnitude and remain relatively constant for decades. At the same time, the leachate infiltration rate is high (1.10<sup>-4</sup> m/d), the depth towards groundwater table is great (65-80 m), and the conditions for mass transport of pollutants beneath the old and the new sectors of the sanitary landfill are different. Under these conditions and based on the results of the 2D models in the source range, three zones with different recharge mode and intensity of the percolation flux are separated. Their areas coincide with the projections of the landfill’s oldest sector – Zone 1, old sector – Zone 2 and new sector – Zone 3. The recharge mode and the concentrations of Cl<sup>-</sup> and NH<sub>4</sub><sup>+</sup> in the percolation flux in each zone are presented by the functions  $C_{Cl} = f(t)$  and  $C_{NH4} = f(t)$  – Fig. 1 and Fig. 2.

### Basic flow model

The basic flow model FM3D is a three-dimensional simulation of the hydrodynamic field structure. The model area covers part of the Paleogene aquifer to a depth of 100-150 m, falling within the boundaries of a catchment area of 2,4 km<sup>2</sup> that includes the old landfill region and the potential recipients. Two low-rank hydrogeological units are separated in the section (Table 1), which are set as model layers with their corresponding geometry and values of hydraulic conductivity k (Fig. 3 and Table 2). The relief of their bottom and top surfaces is in accordance with the terrain and the extension of the hydrogeological low-rank units. The regional flow is modeled

according to the General Head Boundary (GHB) scheme, with the general direction of groundwater being southeast at a mean hydraulic gradient of 0,02. The recharge from infiltration and percolation is set with the Recharge software package, as the accepted initial value for the rate of recharge from infiltration is 2.10<sup>-5</sup> m/d, and for the rate of contaminated percolation flux – 1.10<sup>-4</sup> m/d. The basic flow model FM3D is calibrated to the water levels at the monitoring observation points by varying the values of the heads set at the external boundaries, the infiltration rate and the hydraulic conductivity in model layer ML 1.

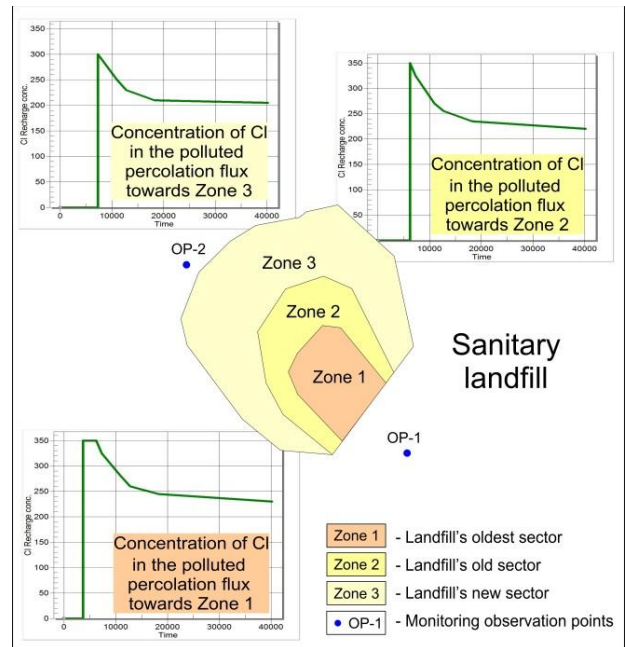


Fig. 1. Concentration of Cl<sup>-</sup> in the pollution source

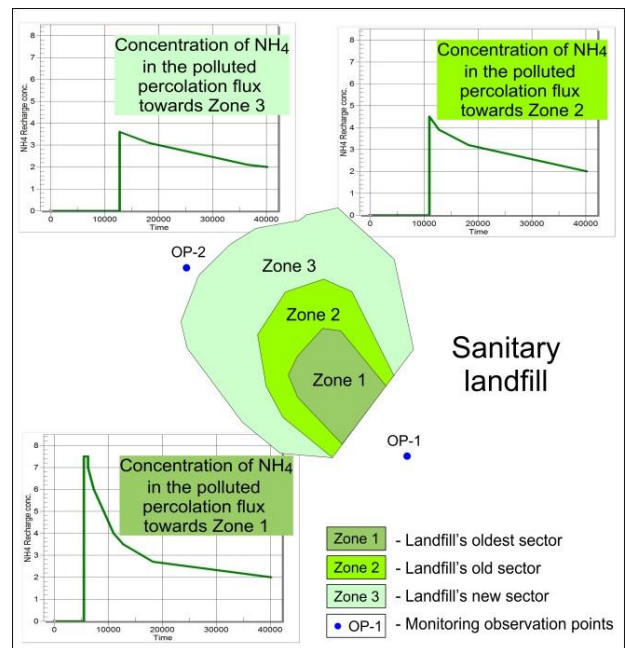
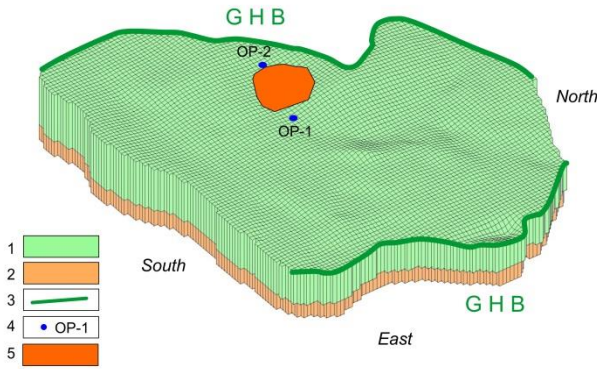


Fig. 2. Concentration of NH<sub>4</sub><sup>+</sup> in the pollution source



**Fig. 3. Grid frame, model layers and boundary conditions**  
 1 – Model layer ML 1; 2 – Model layer ML 2; 3 – General Head Boundary (GHB); 4 – Pollution source; 5 – Monitoring observation points.

**Table 1. Hydrogeological units. Model layers.**

Hydrogeological unit		Model layers
Paleogene aquifer complex	Upper zone of low permeability	ML 1
	Bottom zone of very low permeability	ML 2

**Table 2. Hydrogeological parameters for the model layers – total porosity  $n$ , bulk density  $\rho_d$ , hydraulic conductivity  $k$ , longitudinal dispersivity  $\alpha_L$ , diffusion coefficient  $D_M$  and distribution (partition) coefficient  $K_D$  for  $Cl^-$  and  $NH_4^+$**

Hydrogeological parameter	Model layer	
	ML 1	ML 2
$n$ , dimensionless	0,31	0,26
$\rho_d$ , g/cm <sup>3</sup>	1,80	2,07
$k$ , m/d	0,10	0,03
$\alpha_L$ , m	12,00	5,50
$D_M$ , m <sup>2</sup> /d	$4,0 \cdot 10^{-4}$	$2,5 \cdot 10^{-4}$
$K_D$ $3a$ $Cl^-$ , cm <sup>3</sup> /g	0,20	1,10
$K_D$ $3a$ $NH_4^+$ , cm <sup>3</sup> /g	0,50	2,30

Remark: The values of  $n$ ,  $\rho_d$ ,  $k$ ,  $\alpha_L$ , and  $K_D$  for  $Cl^-$  in model layer ML 1 are determined according to data from slug tests and tracer tests conducted by the authors (Stoyanov et al., 2010; Stoyanov, 2010), and the values of  $n$ ,  $\rho_d$ ,  $k$ ,  $\alpha_L$ , and  $K_D$  for  $Cl^-$  in ML 2, as well as the values of  $D_M$  and  $K_D$  for  $NH_4^+$  in both model layers are determined from literature data for a similar soils (Spitz and Moreno, 1996).

**Mass transport models**

The mass transport models M3D-CL and M3D-NH4 are three-dimensional computer simulations of the fate and transport of the key pollutants  $Cl^-$  and  $NH_4^+$ . Both models are based on the spatial distribution of hydraulic heads, gradients and groundwater flow velocities obtained with the FM3D model. The calculation scheme includes the processes of convective transport, molecular diffusion, mechanical dispersion, reversible elimination and mixing. The accepted for the respective model layers values of the hydrogeological parameters total porosity  $n$ , bulk density  $\rho_d$ , hydraulic conductivity  $k$ , longitudinal dispersivity  $\alpha_L$ , diffusion coefficient  $D_M$  and distribution (partition) coefficient  $K_D$  for  $Cl^-$  and  $NH_4^+$  are presented in Table 2. The horizontal and vertical components of transverse dispersivity are determined by the

ratio  $\alpha_L = 10\alpha_{TH} = 100\alpha_{TV}$ . The initial concentrations of  $Cl^-$  and  $NH_4^+$  in the groundwater, in the precipitation, and in the groundwater inflow along the NW boundary, are set as zero in both models. The source of pollution is simulated with three model zones, delineating the boundaries of the separated three sectors characterized by different recharge mode and intensity of the percolation flux. In the Recharge software package, the concentrations of  $Cl^-$  and  $NH_4^+$  in the percolation flux in each zone are set as variables by the pre-defined functions for all sectors  $C_{CL} = f(t)$  and  $C_{NH4} = f(t)$ . The mass transport models are calibrated to the concentrations of  $Cl^-$  and  $NH_4^+$  at the monitoring observation points OP-1 and OP-2 by varying the values of  $D_M$  and  $\alpha_L$ .

**Results and discussion**

**Structure of the hydrodynamic field**

The hydrodynamic field structure, obtained with the basic flow model FM3D, is illustrated in Fig. 4. The correspondence achieved during the calibration between the registered water levels in the monitoring boreholes and the model piezometry guarantees the reliability of the model and the stability of the predictive solutions.

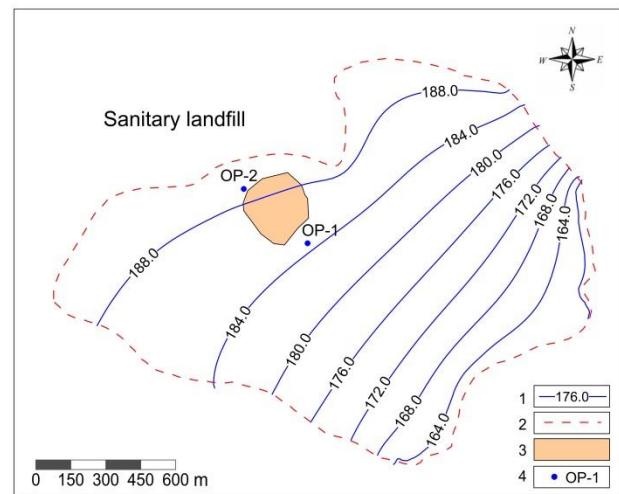


**Fig. 4. Model FM3D. Structure of the hydrodynamic field**  
 1 – Piezometric line; 2 – Limits of the model area (surface catchment area); 3 – Pollution source; 4 – Monitoring observation points.

The general direction of groundwater flow is to the southeast and the average hydraulic gradient in the region of the sanitary landfill and its adjacent areas is around 0.015. Such a structure of the hydrodynamic field, in combination with the low water permeability of the Paleogene complex, suggests that the pollutants that have entered the saturated zone will move slowly, following the direction of the simulated groundwater flow.

**Groundwater budget**

The groundwater budget for the studied part of the Paleogene aquifer complex (Table 3), composed with the FM3D model, shows that the landfill area has poor groundwater resources (about 150 m<sup>3</sup>/d) that are practically of no economic importance. The main ingredient in these resources (over 62%) is the groundwater inflow along the NW

boundary of the model, and the other significant element (about 34%) is the precipitation that percolates through the unsaturated zone to the water table. The landfill leachate contributes the remaining 4% of the inflow part of the groundwater budget. The outflow segment of the budget has only one ingredient and it is the groundwater outflow along the SE boundary of the model. The modulus of groundwater discharge is 0,7 (l/s)/km<sup>2</sup>.

Table 3. Model FM3D. Groundwater budget.

INFLOW $Q_{in}$ , m <sup>3</sup> /d	
Groundwater inflow along the NW boundary of the model	92,45
Recharge from precipitation that percolates through the unsaturated zone to the water table	50,11
Landfill leachate	6,05
Total:	148,61
OUTFLOW $Q_{out}$ , m <sup>3</sup> /d	
Groundwater outflow along the SE boundary of the model	148,87
Total:	148,87
Overall error in the budget 0.2 %	

### Pollutants transport in the saturated zone

The results of the computer simulations of pollutants fate and transport in the saturated zone, performed with model M3D-CL and model M3D-NH<sub>4</sub>, are illustrated with a series of maps of the distribution of chloride ions and ammonium ions presented in Fig. 5 and Fig. 6. They exhibit the prognostic impact of the old sanitary landfill on the Paleogene aquifer for 1, 5, 10, 50, and 100 year computational (forecast) periods after the start of the computer simulation, i.e. after the first "portions" of polluted percolation flux have reached the saturated zone. This moment is preceded by a period of 10-15 years during which the leachate that has passed through the engineering barrier percolates through the unsaturated zone to the water table.

The following conclusions can be drawn as a result of the analysis of the presented model solutions:

(1) The chief mechanism for movement of contaminants in the saturated zone is convective transport. The direction and rate of mass transport processes are controlled by the hydrodynamic field structure, respectively by the spatial distribution of hydraulic heads and gradients. The pollution front is moving to the southeast following the general direction of groundwater flow.

(2) The pollutant transport in groundwater is not only in lateral direction, but also in depth. The vertical mass transport is determined by the density differences between the contaminated waters and the fresh groundwater lying below them, i.e. by the concentration gradients. Reaching in depth to the undisturbed and practically impermeable parts of the rock massif, the pollutants move in the direction of underground flow, forming a characteristic "plume".

(3) Within the delineated boundaries of the contaminated area, the distinct types of pollutants show significant differences in their behavior (Fig. 5 and Fig. 6).

*Chloride ions* are conservative, characterized by a very low sorption potential, and move at a pace close to the flow rate of

groundwater. They mark the maximum range of possible groundwater contamination. The plume will extend to the southeast with an average rate of 3 m/a. Long-term prognosis shows that in 100 years the pollution front will reach to no more than 300-350 m from the old landfill (Fig. 5). The most intensive contamination will be limited in the space beneath the sanitary landfill and in a narrow strip 70-80 m southeast of it, where the expected Cl<sup>-</sup> concentration will be between 200 and 350 mg/l. Outside these limits, the level of pollution will be much lower. Chloride concentration in groundwater will most often be in the range of 30 to 200 mg/l, i.e. will not exceed the permissible limits of drinking water in Bulgaria, established by Ordinance No. 9/16.03.2001. This Regulation sets out the requirements for the quality of water intended for drinking and household purposes in order to protect human health against the negative impact of drinking water pollution.

*Ammonium ions* have high sorption potential, which is the reason for their very low mass transfer ability. Their movement in the Paleogene aquifer complex is slow, so the groundwater polluted by them is expected to occupy small areas. Calculations made with the M3D-NH<sub>4</sub> model show that NH<sub>4</sub><sup>+</sup> transport in groundwater flow direction has an average rate of 1 m/a. Long-term prognosis shows that in 100 years the less mobile pollutants will reach to no more than 100-120 m from the old landfill (Fig. 6). The prevailing concentrations of ammonium ions will be low, most often in the range of 0,01 to 0,25 mg/l. Only beneath the landfill and in the strip 20-25 m from its borders the concentration will be higher, but will not exceed 2 mg/l.

The prognostic solutions show that as time progresses, within the expanding boundaries of the already contaminated zone and in the groundwater flow direction, there is a gradual decrease in the concentrations of Cl<sup>-</sup> and NH<sub>4</sub><sup>+</sup>. This is due to the decreasing concentration of pollutants in the leachate produced by the old sanitary landfill, as well as due to the processes of reversible elimination (sorption-desorption), hydrodynamic dispersion and mixing that are accompanying the convective transport. The low water permeability of the Paleogene rock massif in combination with the high sorption characteristics of the medium are the reasons for its very good self-purification abilities.

### Conclusion

Using three-dimensional models, a computer simulation of the mass transport of selected key pollutants in the saturated zone is performed. The obtained prognostic solutions show that the groundwater contamination caused by the old sanitary landfill near the town of Haskovo, from a long-term point of view (100 years), will be quite limited in size and of very low intensity. It will affect only a minor part of the characterized by low water permeability Paleogene aquifer complex, whose groundwater resources are poor and of no economic importance.

The methodological approach, implemented in the both parts of the presented study, includes the complex application of standard software for development of 2D and 3D models of fate and transport of pollutants in the unsaturated and saturated zones. This general approach is very effective for acquiring quantitative assessments and long-term predictions about groundwater contamination caused by surface sources.

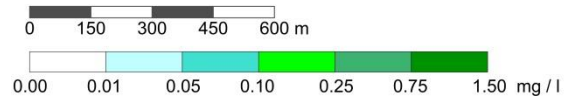
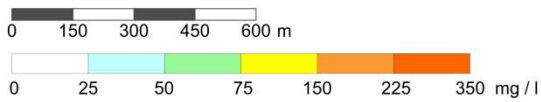
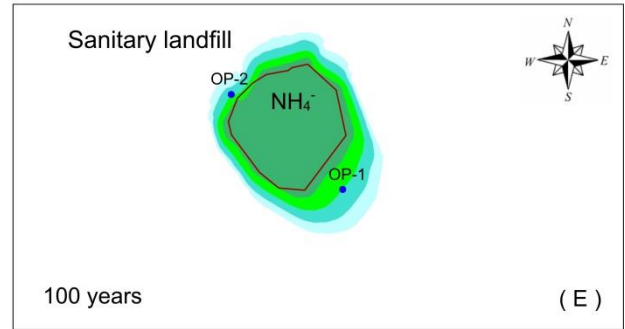
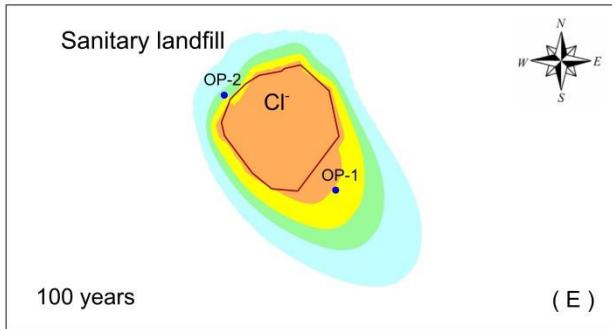
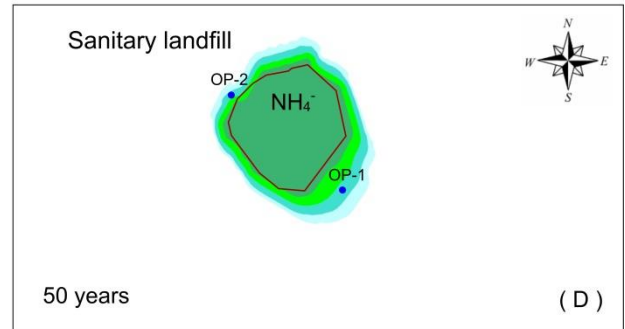
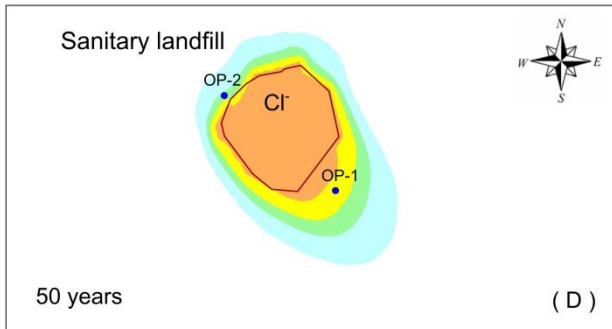
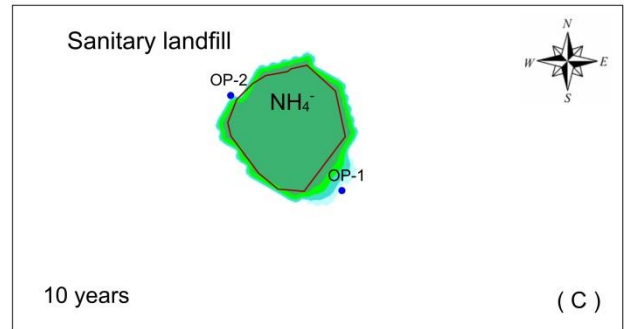
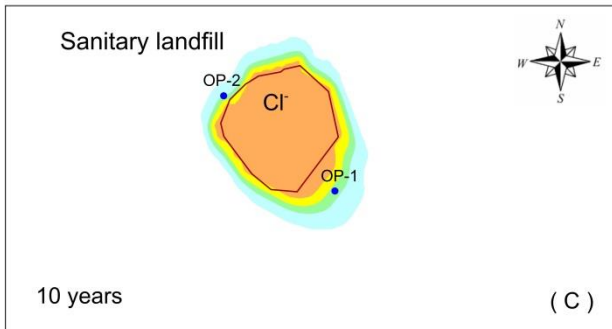
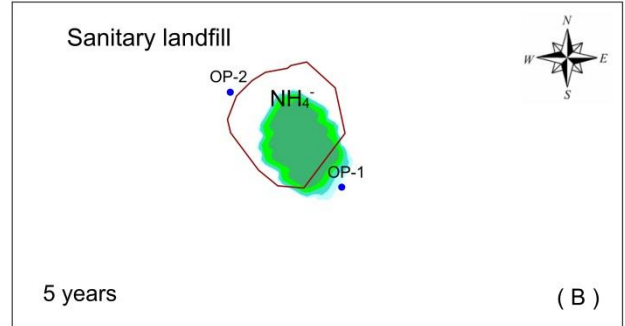
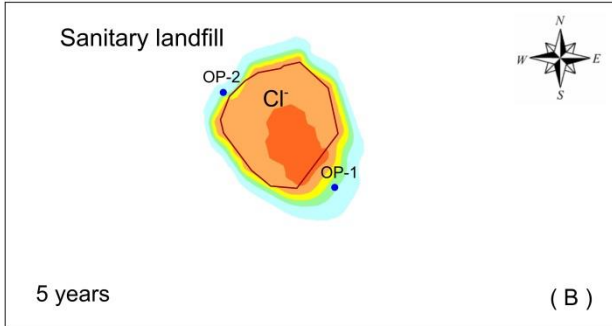
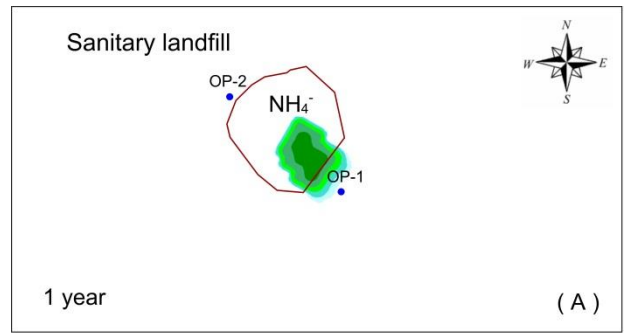
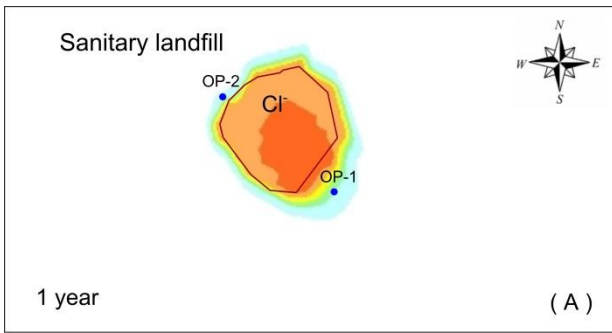


Fig. 5. Model M3D-CL. Distribution of highly mobile pollutants on the example of Cl<sup>-</sup>. Model solutions for 1, 5, 10, 50, and 100 year forecast periods after the start of the computer simulation.

Fig. 6. Model M3D-NH4. Distribution of less mobile pollutants on the example of NH<sub>4</sub><sup>+</sup>. Model solutions for 1, 5, 10, 50, and 100 year forecast periods after the start of the computer simulation.

Our experience shows that this methodology can be successfully applied in solving many similar environmental problems related to the evaluation of the impact on groundwater caused by of different technogenic sources of pollution. These are disposal facilities for different types of waste materials, tailings dams, chemical warehouses, hazardous industries, such as oil and gas production, hydrocarbon refining, nuclear power, manufacture of chemicals and pharmaceuticals, etc.

**Acknowledgements.** This work has been carried out in the framework of the National Science Program "Environmental Protection and Reduction of Risks of Adverse Events and Natural Disasters", approved by the Resolution of the Council of Ministers № 577/17.08.2018 and supported by the Ministry of Education and Science (MES) of Bulgaria (Agreement № DO-230/06-12-2018). The presented models are based on unpublished author's works for the project "Soil and water pollution monitoring, protection and remediation in the area of the regional landfill for non-hazardous waste, Haskovo" - 2009/16.

## References

- Anderson, M., W. Woessner, R. J. Hunt. 2015. *Applied groundwater modeling: simulation of flow and advective transport*. Elsevier, Academic press, 720 p.
- Benderev, A., P. Gerginov, D. Antonov, N. Van Meir, R. Kretschmar. 2015. Conceptual hydrogeological model of the Ogosta river floodplain (Western Balkan, Bulgaria) and its application for predicting of groundwater contamination with arsenic – *Proceedings of the 15th international multidisciplinary scientific geoconference SGEM 2015*, Book 1, Vol. 2, 195-202.
- Gerginov, P., A. Benderev, D. Antonov, Ts. Kotsev, V. Asenova. 2017. Dinamika na podzemnite vodi i migratsia na arsen v nasitenata zona na terasata na r. Ogotsta. – *Engineering geology and hydrogeology*, 31, 53-64 (in Bulgarian with English abstract).
- McDonald, M., A. Harbaugh. 1988. A modular three-dimensional finite-difference groundwater flow model. - *Techn. of Water Res. Inv. of the USGS, Book 6-A1*, 586 p.
- Spitz, K., J. Moreno. 1996. *A practical guide to groundwater and solute modeling*. JW&S, NY, 460 p.
- Stoyanov, N., S. Dimovski. 2004. A simplified approach for modeling of groundwater pollution caused by the sanitary landfill of the city of Plovdiv, Bulgaria. – *Lucrările științifice ale simpozionului "Univesitaria Ropet 2004"*, Editura Universitas, Petroșani, Romania, 104-109.
- Stoyanov, N. 2007. Matematičeski model na zamarsivaneto na podzemnite vodi v raiona na DBO Asenovgrad – *BULAQUA*, 1, 32-40 (in Bulgarian with English abstract)
- Stoyanov, N., B. Banushev, S. Dimovski, S. Nedelcheva. 2010. Uslovia za migratsia na nesorbiruemi zamarsiteli v nevodonasitenata zona na paleogenskite vulkaniti v raiona na gr. Haskovo. Chast 1. Determinirane na niskorangovi hidrogeolozhki edinitsi. – *Annual of the University of Mining and Geology "St. Ivan Rilski"*, 53, Part 1, 163-168 (in Bulgarian with English abstract).
- Stoyanov, N. 2010. Uslovia za migratsia na nesorbiruemi zamarsiteli v nevodonasitenata zona na paleogenskite vulkaniti v raiona na gr. Haskovo. Chast 2. Matematičeski Model. – *Annual of the University of Mining and Geology "St. Ivan Rilski"*, 53, Part 1, 169-173 (in Bulgarian with English abstract).
- Stoyanov, N. 2012. Modelni izsledvania na riska ot zamarsivane na geolozhkata osnova i podzemnite vodi ot proektiranoto Natsionalno hraniliste za radioaktivni otpadatsi kraii AEZ "Kozlodui" – *Annual of the University of Mining and Geology "St. Ivan Rilski"*, 55, Part 1, 140-145 (in Bulgarian with English abstract)
- Stoyanov, N., P. Gerginov, A. Benderev, K. Boyadjieva, V. Hristov, V. Vesselinov. 2015. Otsenka i prognoziranje na vazmozhnoto zamarsivane na podzemnite vodi pri prouchvane i dobiv na neft i gaz – *Review of the Bulgarian geological society*, 76, 2, 79-88. (in Bulgarian with English abstract)
- Stoyanov, N., S. Kolev, V. Petrov. 2018. Prognosis of contaminants mass transport in groundwater after cessation of uranium mining in Momino deposit (South Bulgaria) – *Proceedings of the 18th international multidisciplinary scientific geoconference SGEM 2018*, Vol. 18, Issue 12, 593-600.
- Stoyanov, N., S. Bratkova, S. Dimovski. 2019. Mathematical models of contamination with heavy metals from the abandoned mines in the Madjarovo ore field, Eastern Rhodopes – *Journal of Mining and Geological Sciences*, 62, 1, 83-88.
- Stoyanov, N. 2019. *Matematičesko modelirane v hidrogeologiyata. Chisleni 3D modeli po metoda na krainite razliki*. Vanio Nedkov, Sofia, 246 p. (in Bulgarian)
- Zheng, C., G. Bennet. 2002. *Applied contaminant transport modeling: Theory and practice*. J&WS, NY, 440 p.

## MINERALOGICAL STUDY OF ARCHAEOLOGICAL COPPER SLAGS FOUND IN THE AREA OF THE BOYADZHİK VILLAGE, YAMBOL REGION, SOUTHEAST BULGARIA

**Nikoleta Tzankova<sup>1</sup>, Dobrinka Stavrakeva<sup>2</sup>**

<sup>1</sup>University of Mining and Geology "St Ivan Rilski", 1700 Sofia; niktzankova@abv.bg

<sup>2</sup>University of Chemical Technology and Metallurgy, Sofia 1756; dobrinka@uctm.edu

**ABSTRACT.** In this paper, we present the results from a phase-chemical and structural study of metallurgical slags, found in an archaeological site near the village of Boyadzhik, Yambol region. The studied samples are mainly composed of SiO<sub>2</sub> (37.22 – 37.45%), Fe<sub>2</sub>O<sub>3</sub> (36.26 – 36.71%), CaO (11.11 – 11.66%) and Al<sub>2</sub>O<sub>3</sub> (6.03 – 6.15). The dominant phase is fayalite, followed by magnetite and maghemite, augite, and augite-type pyroxene closest to esseneite. These minerals were observed microscopically in transmitted and reflected light and were established by XRD study and SEM CDD-EDS microanalyses. The copper in the studied slags goes up to 2.46 % indicating low process efficiency of copper extraction from the raw material. The copper was presented by metallic droplets as well as copper-oxide and copper-iron-oxide phases. No relics of sulfide minerals and sulfur-containing phases were found in the analyzed samples. The mineral composition of the studied samples, as well as their structural and phase characteristics, allow us to define these materials as by-products (slags) from copper containing oxidic ore smelting.

**Keywords:** Archaeological copper slags, SEM CDD-EDS, XRD, old copper mining, SE Bulgaria

### МИНЕРАЛОЖКО ИЗСЛЕДВАНЕ НА АРХЕОЛОГИЧЕСКИ МЕДНИ ШЛАКИ, НАМЕРЕНИ КРАЙ СЕЛО БОЯДЖИК, ЯМБОЛСКО, ЮГОИЗТОЧНА БЪЛГАРИЯ

**Николета Цанкова<sup>1</sup>, Добринка Ставракева<sup>2</sup>**

<sup>1</sup>Минно-геоложки университет „Св. Иван Рилски“, 1700 София

<sup>2</sup>Химикотехнологичен и металургичен университет, София 1756

**РЕЗЮМЕ.** В статията са представени резултати от фазово-химични и структурни характеристики на металургични шлаки, открити в археологически обект край с. Бояджик, Ямболско. Химичният състав на изследваните образци е представен главно от SiO<sub>2</sub> (37.22 – 37.45%), Fe<sub>2</sub>O<sub>3</sub> (36.26 – 36.71%), CaO (11.11 – 11.66%) and Al<sub>2</sub>O<sub>3</sub> (6.03 – 6.15). Фаялитът е доминираща кристална фаза. Освен него в образците са определени магнетит и магхемит, авгит и пироксен от авгитов тип, най-близък до есенеит. Тези минерали са установени микроскопски в преминаваща и в отразена светлина, и са доказани с рентгенофазов анализ и SEM CDD-EDS микроанализи. Съдържанието на мед в шлаките е до 2,46 %, което свидетелства за ниска ефективност на медодобивния процес. Медта в образците е под формата на метални капки, медно-оксидни и медно-желязооксидни фази. В анализирания образци не са установени сулфидни минерали и сяросъдържащи фази. Минералният състав на изследваните образци, както и техните структурни и фазови характеристики ни позволиха да определим тези материали като отпадни продукти (шлаки), получени от топене на медсъдържаща оксидна руда.

**Ключови думи:** археологически медни шлаки, SEM CDD-EDS, XRD, древен добив на мед, ЮИ България

### Introduction

The studied metallurgical by-products were found at an archaeological site near Boyadzhik village. The archeological site of the slag finding falls into arable plowed fields (Fig. 1). It is located about 4 km northeast of the Prohorovo porphyry-copper deposit with three phased ore formation processes – skarn, hydrothermal and supergene (Bogdanov, 1987; Bogdanov & Bogdanova, 1984). Many other smaller copper mineralizations outcrop in this area also. The slags, object of this study, based on their external characteristics, was conditionally referred by the archaeologists to Antiquity or the Middle Ages (Leshtakov & Dimitrov, 2016; Leshtakov et al, 2018). A ceramic fragment with traces of strong temperature impact was found in the same archeological site also. It was identified as a part of an ore-smelting furnace and was dated to the Chalcolithic (Leshtakov et al, 2018).

The aim of this study is to present data about phase-chemical and structural characteristics of the archaeological

slags found in the region of Boyadzhik village. These data will provide information about the ore raw material mined in this region in the past and about the type of metal extracted.



**Fig. 1.** The archeological site of slag finding and its location on the map marked with number 1

The obtained data will enrich our knowledge about the mineral composition and phase-structural characteristics of the old metallurgical by-products. This study is a part of a complex investigation on the archeological slags from Burgas and Yambol ore regions (Stavrakeva & Tzankova, 2016a, 2016 b; Tzankova et al., 2016).

## Material and methods

The studied slag is dark gray with many pores inside. Their surface alteration has proceeded with the formation of secondary minerals such as green carbonates (mainly malachite), chrysocolla, iron oxides, and hydroxides. Two samples of the slag were analyzed (Fig. 2).



Fig. 2. Macroscopic photographs of the slags selected for this study: a) sample 1; b) sample 2

The powdered and homogenized in an agate mortar slag samples were prepared for Powder X-ray diffraction and subsequent ICP-OES analyses. XRD patterns for the selected samples were obtained using a Bruker D2 Phaser X-ray diffractometer (at 30 kV and 10 mA, with CuK $\alpha$  radiation, 2 $\theta$  range from 4° to 70°, 0.2/0.5 s). The JCPDS PDF database (International Centre for Diffraction Data, 1997) was used for data interpretation. The bulk chemical composition of the slags was examined with inductively coupled plasma – optical emission spectrometry 720-ICP-OES, Agilent Technologies. The preliminary optical studies on the polished samples and thin sections were carried out using optical microscopes Meiji MT9200 and MT9430 in transmitted and reflected light mode. The microstructure of the samples and chemical composition of the slag phases were studied with JOEL JSM 6010 Plus/LA InTouchScope™ Scanning Electron Microscope (SEM) equipped with a silicon drift detector energy dispersive X-ray spectrometer (SDD-EDS) with a resolution of 128 eV. The device is equipped with a software platform that ensures accuracy and precision of measurements, and produces useful concentration values of the measured elements (Newbury & Ritchie, 2013). SEM CDD-EDS microanalyses were performed on highly polished flat specimens with graphite coating, 20 kV accelerating voltage. All analyses were conducted at the University of Mining and Geology „St. Ivan Rilski“ – Sofia. The content ratio of basic oxides (CaO and MgO) to acidic oxides (SiO<sub>2</sub> and Al<sub>2</sub>O<sub>3</sub>) was used for assessment of the basicity of slag. The calculation of the valence of transitional elements in the composition of crystal phases is according to the methodology proposed by Stavrakeva (1990).

## Results

### Bulk composition

The analyzed samples contain SiO<sub>2</sub> (37.22 – 37.45 %), Fe<sub>2</sub>O<sub>3</sub> (36.26 – 36.71 %), high levels of CaO (11.11 – 11.66%), and Al<sub>2</sub>O<sub>3</sub> (6.03 – 6.15 %). The copper is in the range of 1.73 to 2.46 %. In addition, the studied slags also contain minute amount of TiO<sub>2</sub>, MgO, MnO, K<sub>2</sub>O, P<sub>2</sub>O<sub>5</sub>, and very low SO<sub>3</sub> content (Table 1). The basicity value for both of the studied samples is smaller than one, and it referred slags to as acidic. The basicity for sample 1 is 0.31, and for sample 2 is 0.32. The basicity of the slag can affect its viscosity and melting temperature. Viscosity plays an important role in the area of mass transfer at chemical reactions in metallurgical processes (Schlesinger et al., 2011.).

Table 1. Bulk chemical composition of the studied slags – OES-ICP analyses

Oxides/ mass%	SiO <sub>2</sub>	TiO <sub>2</sub>	Al <sub>2</sub> O <sub>3</sub>	Fe <sub>2</sub> O <sub>3</sub>	CaO	MgO	MnO	K <sub>2</sub> O	Na <sub>2</sub> O	P <sub>2</sub> O <sub>5</sub>	SO <sub>3</sub>	Cu	Σ
Samp. 1	37.45	0.40	6.15	36.71	11.11	2.26	0.29	0.67	<0.05	0.32	0.33	2.46	98.20
Samp. 2	37.22	0.38	6.03	36.26	11.66	2.16	0.31	0.74	<0.05	0.31	0.38	1.73	97.23

### Mineralogy and phase composition

#### Powder XRD study

The dominant crystalline phase in the slag composition, as indicated by XRD analysis, is fayalite Fe<sub>2</sub>SiO<sub>4</sub> (Fa) followed by magnetite Fe<sup>2+</sup>Fe<sup>3+</sup><sub>2</sub>O<sub>4</sub> (Mag), augite Ca(Mg,Fe<sup>3+</sup>,Al)(Si,Al)<sub>2</sub>O<sub>6</sub> (Aug), and augite-type pyroxene closest to esseneite (Ess) (Fig. 3).

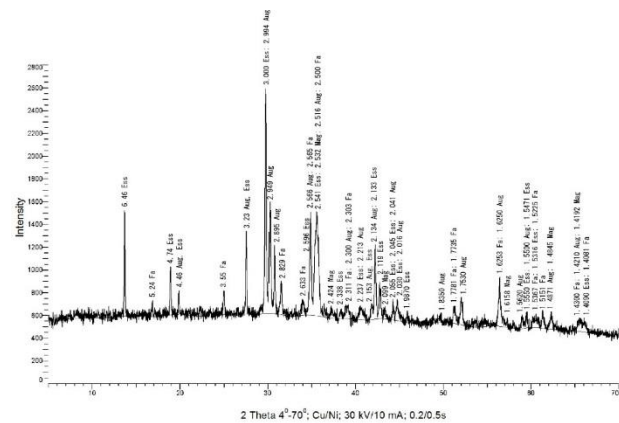


Fig. 3. XRD graph of the slag: fayalite (Fa); augite (Aug); esseneite (Ess); magnetite (Mag).

#### Light optical microscopy

Representative slag microstructure and phase assemblages, observed microscopically in transmitted and reflected light, are given in Figs 4, 5. The material is even-grained (Fig. 4a, b). Fayalite is the dominant crystal phase. It occurs as needle-like or prismatic skeletal crystals, indicating rapid crystallization (Fig. 4a-c; Fig. 5a-e). These individuals are either randomly distributed in the glass matrix or form sub-radiating aggregates. Fayalite is followed by magnetite/maghemite with white color in reflected light (Fig. 4d-f; Fig. 5f-h). Magnetite/maghemite shows isometric not fully formed skeletal crystals or dendritic aggregates also. They are

situated separately in the hosted glass matrix or are arranged one after the other in one direction. The copper droplets are irregular in their shape. They are inhomogeneous. In the larger ones, two phases with different color and reflectivity were observed (Fig. 4a, c; Fig. 5e, f). Microscopically, no relics of sulfide minerals were detected in these droplets.

According to their chemical composition, the minerals and phases found in the slags were grouped as follows: silicate phases, iron oxide phases, copper droplets and hosted glass mass.

**Silicate phases**

The crystalline silicate phases are mainly presented by the crystals from fayalite group  $Fe_2SiO_4$  and pyroxene group  $Ca(Mg,Fe^{3+},Al)(Si,Al)_2O_6$ . Their chemical compositions according to the conducted elemental microanalyses (SEM CDD-EDS) data, are shown in Table 2. Fayalite and augite-type pyroxene were detected by Powder XRD analysis with their characteristic set of d-spacings (Fig. 3). Pyroxene crystals are small and needle-shaped (Fig. 6c), while the fayalite crystals are well-developed elongated prismatic ones (Fig. 6e).

Table 2. Chemical composition of fayalite (Fa) and pyroxene (Py), SEM CDD-EDS microanalyses

Oxides	Content, mass. %			
	An. field 5-4 (Fig. 6e)		An. field 5-2 (Fig. 6c)	
	Point 1 (Fa)	Point 2 (Fa)	Point 1 (Py)	Point 2 (Py)
SiO <sub>2</sub>	30.27	31.20	41.68	40.61
FeO	61.87	63.28	42.41	40.60
MgO	4.93	–	–	–
CaO	2.93	3.24	7.49	6.63
Al <sub>2</sub> O <sub>3</sub>	–	2.28	8.42	9.68
K <sub>2</sub> O	3.02	–	–	2.48

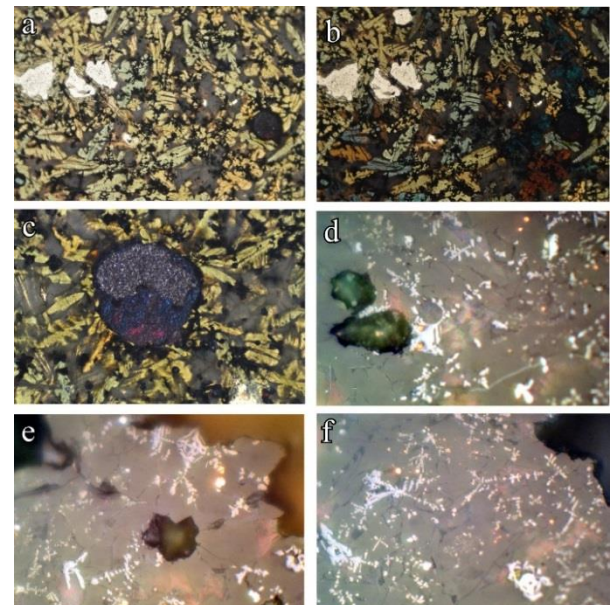


Fig. 4. Microstructure of slag samples: a) elongated fayalite crystals, x10, plane-polarized, transm. light; b) fayalite, x10, cross-polarized, transm. light; c) copper droplet and fayalite, x20, plane-polarized, transm. light; d) magnetite/maghemite crystals and copper droplets, x40, plane-polarized, refl. light; e) isometric and skeletal magnetite/maghemite crystals, x40, plane-polarized, refl. light; f) magnetite/maghemite crystals and copper droplets, x40, plane-polarized, refl. light.

Crystal-chemical formulas of the fayalite individuals in the analyzed field 5-4 (Fig. 6e):

- Point 1:  $Fe_{1.76} Mg_{0.22} Ca_{0.10} Si_{1.03} O_4$  – fayalite;
- Point 2:  $Fe_{1.87} Ca_{0.12} Al_{0.09} Si_{1.11} O_4$  – fayalite.

Crystal-chemical formulas of pyroxene crystals in the analyzed field 5-2 (Fig. 6c):

- Point 1:  $(Fe_{0.77} Ca_{0.17} Al_{0.06})_{1.00} (Si_{0.92} Al_{0.15})_{1.07} O_3$  – pyroxene;
- Point 2:  $(Fe_{0.73} Ca_{0.15} Al_{0.02} K_{0.06})_{1.00} (Si_{0.88} Al_{0.19})_{1.07} O_3$  – pyroxene.

Fayalite composition indicates that calcium-, magnesium- and aluminum-containing minerals were included in the ore used. These chemical elements are inserted in the fayalite crystals as impurities.

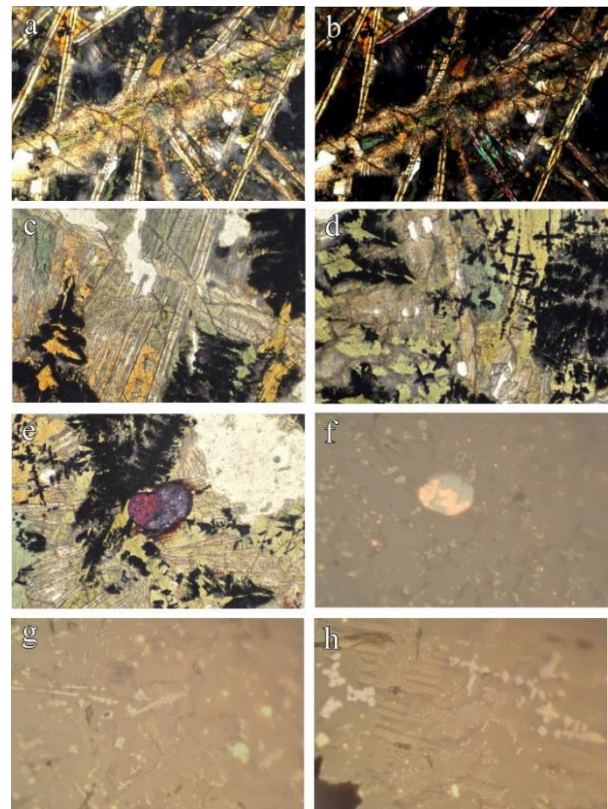


Fig. 5. Microstructure of slag samples: a) fayalite, x10, plane-polarized, transm. light; b) fayalite, x10, cross-polarized, transm. light; c) aggregate of fayalite crystals, x20, plane-polarized, transm. light; d) fayalite, plane-polarized, transm. light; e) fayalite, copper droplet, x20, plane-polarized, transm. light; f) copper droplet, magnetite/maghemite, x40, plane-polarized, refl. light; g) magnetite/maghemite, copper droplets, x40, plane-polarized, refl. light; h) magnetite/maghemite, copper droplets, x40, plane-polarized, refl. light.

**Iron oxide phases**

Microscopically in reflected light magnetite/maghemite crystals were observed in the slag (Fig. 4d-f; Fig. 5f-h). Their chemical composition is shown in Table 3. The XRD study confirmed the presence of magnetite in the samples (Fig. 3).

Table 3. Chemical composition of magnetite (Mag) and maghemite (Mgh), SEM CDD-EDS microanalyses

El.	Content, mass. %						
	An. field 5-1 (Fig. 6a)		A. f. 5-2 (Fig.6c)	An. field 5-3 (Fig. 6d)		An. field 5-5 (Fig. 6f)	
	Point 1 (Mag)	Point 2 (Mag)	Point 4 (Mag)	Point 1 (Mag)	Point 6 (Mag)	Point 1 (Mag)	Point 2 (Mgh)
Fe	68.40	68.77	72.49	72.92	68.26	72.18	69.87
Ti	1.39	1.23	—	—	2.66	—	—
Al	2.14	2.02	—	—	1.59	—	—
O	28.07	27.96	27.51	27.08	27.49	27.82	30.13

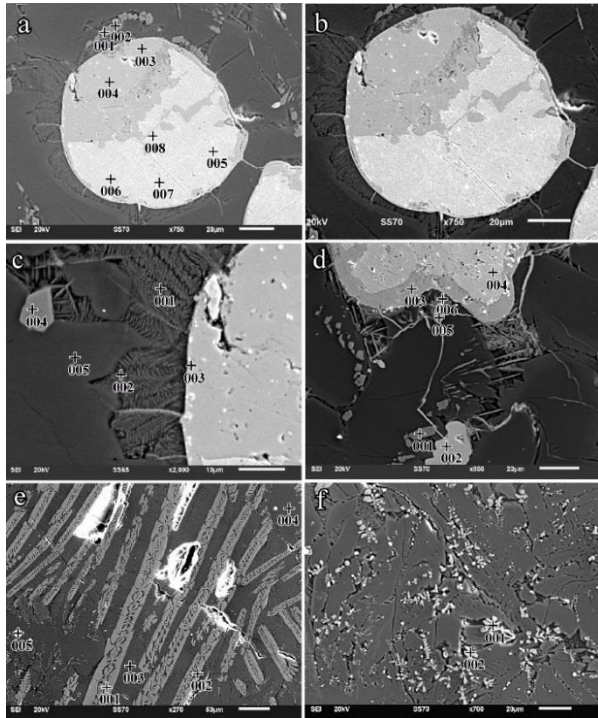


Fig. 6. Scanning electron microscope images of the phases identified in slag samples: a) analyzed field 5-1 with points: 1 and 2 (magnetite), from 3 to 6 (copper oxide phase, cuprite), 7 and 8 (copper); b) analyzed field 5-1 close-up; c) analyzed field 5-2 with points: 1 and 2 (pyroxene), 3 (copper iron oxide phase), 4 (magnetite), 5 (slag glass); d) analyzed field 5-3 with points: 1 (magnetite), 2 (copper iron oxide phase), 3 (copper oxide phase, cuprite), 4 (copper), 5 (copper iron oxide phase), 6 (magnetite); e) analyzed field 5-4 with points: 1 and 2 (fayalite), 3 and 4 (slag glass), 5 (copper iron oxide phase); f) analyzed field 5-5 with points: 1 (magnetite) and 2 (maghemite).

The crystal-chemical formulas of the iron oxide phases presented in Table 3 are as follows:

In analyzed field 5-1 (Fig. 6a):

- Point 1:  $Fe^{+2}_{1.00} (Fe^{+3}_{1.72} Ti_{0.06} Al_{0.18})_{2.05} O_4$  – magnetite;
- Point 2:  $Fe^{+2}_{1.00} (Fe^{+3}_{1.81} Ti_{0.05} Al_{0.17})_{2.03} O_4$  – magnetite.

In analyzed field 5-2 (Fig. 6c):

- Point 4:  $Fe^{+2}_{1.00} Fe^{+3}_{2.05} O_4$  – magnetite.

In analyzed field 5-3 (Fig. 6d):

- Point 1:  $Fe^{+2}_{1.00} Fe^{+3}_{2.08} O_4$  – magnetite;
- Point 6:  $Fe^{+2}_{1.00} (Fe^{+3}_{1.84} Ti_{0.12} Al_{0.13})_{2.09} O_4$  – magnetite.

In analyzed field 5-5 (Fig. 6f):

- Point 1:  $Fe^{+2}_{1.00} Fe^{+3}_{1.97} O_4$  – magnetite;
- Point 2:  $Fe^{+3}_{1.995} O_3$  – maghemite.

### Copper droplets

The chemical composition of the copper droplets is presented in Table 4.

Table 4. Chemical composition of copper droplets, SEM CDD-EDS microanalyses

El.	Content, mass. %											
	An. field 5-1 (Fig. 6a)					5-2 (F.6c)	An. field 5-3 (Fig. 6d)					
	P. 3	P. 4	P. 5	P. 6	P. 7	P. 8	P. 3	P. 2	P. 3	P. 4	P. 5	P. 5
Cu	90.10	90.14	98.89	98.55	100	100	87.89	88.56	90.97	100	87.40	92.20
Fe	—	—	—	—	—	—	2.46	2.05	—	—	3.21	4.07
O	9.90	9.86	1.11	1.15	—	—	9.65	9.39	9.03	—	9.03	3.75

Many spherical droplets of unbound (free) copper, copper-oxide and copper-iron-oxide phases were established during the microscopic study of the slag samples in reflected light (Fig. 4d-f; Fig. 5f-h). The composition of the copper oxide phase corresponds to cuprite ( $Cu_2O$ ) –  $Cu_{2.26}O$ . The copper iron oxide phase is a solid solution of  $Fe_2O_3$  in cuprite. Its stoichiometry is close to  $Cu_{2.29}Fe_{0.04}O$ .

### Slag glass

No sulfur content was recorded in the chemical composition of the hosted glass matrix in the studied slag samples (Table 5).

Table 5. Chemical composition of the glass mass, SEM CDD-EDS microanalyses

Oxides	Content, mass %		
	An. field 5-2 (Fig. 6c)	An. field 5-4 (Fig. 6e)	
	Point 5	Point 3	Point 4
$SiO_2$	46.84	43.18	44.29
$Al_2O_3$	2.35	7.57	5.48
FeO	32.66	27.94	28.43
CaO	15.60	20.34	18.31
MgO	2.56	0.97	3.49

### Discussion

The chemical compositions of the slag glass and the copper-containing inclusions are very informative about the ore used for copper extraction. The following phases were established with complex methods of investigation: silicate phases – fayalite, pyroxenes of the augite-type and amorphous hosted glass; iron-oxide phases – magnetite and maghemite; copper-containing phases. Among the minerals found in ancient, as well as in modern, slags are fayalite, pyroxene, magnetite and maghemite (Ivanov *et al.*, 1967; Mihailova, 2009; Mihailova and Mehandrejiev, 2010; Stavrakeva and Stoytseva, 1966).

The performed analyses on the copper-containing inclusions in the slag show no sulfur in their composition (Table 4). This indicates that either the melting process was at a sufficiently high temperature to achieve an oxidizing atmosphere and complete desulfurization of the sulfide copper feedstock, or that the copper-containing ore used was not of sulfide minerals. The second assumption is supported by the higher amount of copper oxide phases in the slag. Slags from smelting oxidic ores differ from those of sulfide smelting slags with the lack of sulfide

inclusions like matte, relics of primary ore particles, often in a state of decomposition (Bachmann, 1982).

The copper content in the studied slags goes up to 2.46 % (Table 1), indicating low process efficiency of the copper extraction from the raw material. The results from the chemical analyses of the copper droplets showed: pure copper in 3 points, copper oxide phase in 5 points, and copper-iron oxide phase in the other 4 analyzed points (Table 4).

The slag samples from the area of the Boyadzhik village, Yambol region, differ from the previously studied from us slags found in Burgas ore region (Stavrakeva and Tzankova, 2016a; Stavrakeva and Tzankova, 2016b; Tzankova *et al.*, 2016) in the lack of sulfur in the hosted glass matrix and sulfur-containing secondary or relics minerals. This leads to the assumption that the studied slags from both regions are products from different raw materials used and ore smelting methodology.

## Conclusion

The microstructural characteristics of the studied slag samples, as well as their mineralogical composition, indicate that they are technogenic materials – by-products from metallurgical copper production. The absence of sulfur-containing inclusions in the copper droplets and the lack of sulfur content in the hosted glass matrix suggests that the raw material used was not of sulfide minerals. Probably the raw material used was mined from an oxidizing zone of copper deposit with malachite and azurite. This conclusion also explains the high content of CaO in the slag, which reaches up to 11,66 % (Table 1). Based on their chemical and mineralogical peculiarities, we assume that these samples are one of the oldest studied slags found in our lands.

**Acknowledgements.** The authors sincerely thank the reviewers for their comments and suggestions.

## References

- Bachmann, H. G. 1982. *The identification of slags from archaeological sites.* – Un. Coll. London Inst. Arch. Publ, Vol. 28, 6, 80 pp., <https://doi.org/10.4324/9781315418216>
- Bogdanov, B. 1987. *The copper ore deposits in Bulgaria.* – Technika, S., 388 p. (in Bulgarian).
- Bogdanov, B., R. Bogdanova. 1984. Mineral paragenetic associations and genetic characteristics of the Prohorovo porphyry copper deposit, Yambol district. – In: *Proceedings of the Research Institute of Mineral Resources*, 1, 175-184 (in Bulgarian with English abstract).
- Ivanov, I., P. Bakardzhiev, I. Grozdanov. 1967. Phase composition and structure of the waste copper slags from CMP “G. Damyanov” – Pirdop. – *Mining and metallurgy*, 9 (in Bulgarian).
- International Centre for Diffraction Data. 1997. PCPDFWIN software, Version 1.30
- Leshtakov, P., V. Ignatov, Kr. Nikov, Kr. Velkov, N. Gospodinov, J. Ilieva. 2018. Field searches in the Prohorovo and Gorno Alexandrovo ore deposits. – In: *Archaeological discoveries and excavations in 2017*, BAS-NAIM, Sofia, 665-668 (in Bulgarian).
- Leshtakov, P., K. Dimitrov. 2016. Archaeological survey on sites in the Prohorovo ore field. – In: *Archaeological discoveries and excavations in 2015*, BAS-NAIM, Sofia, 872-875 (in Bulgarian).
- Mihailova, I. 2009. Investigation of the phase composition and structure of furnace metallurgical slags from copper production. – *Ann. Univ. Min. Geol.*, vol. 52, 73-78 (in Bulgarian with English abstract).
- Mihailova I., Mehandrejiev, D. 2010. Characterization of fayalite from copper slags. *Journal of the University of Chemical Technology and Metallurgy* 45, 317–326.
- Newbury, D. E., N. W. M. Ritchie. 2013. Is Scanning Electron Microscopy / Energy Dispersive X-ray Spectrometry (SEM/EDS) Quantitative? – *Scanning*, Vol. 35, 141-168.
- Schlesinger, M. E., M. J. King, K. C. Sole, W. G. Davenport. 2011. *Extractive Metallurgy of Copper.* – Elsevier, Oxford, 5th edition, 472 p.
- Stavrakeva, D. 1990. Method for calculation of the valence of transitional elements in the composition of crystal phases. – *C. R. Acad. Bulg. Sci.*, 43, 11, 57-60.
- Stavrakeva, D., N. Tzankova. 2016a. Chemico-mineralogical characterization of ancient slags from Rosen Ore Field. Part 1 – Propadnala voda deposit. – *Ann. Univ. Min. Geol.*, 59, 1, Geol., 55-60 (in Bulgarian with English abstract).
- Stavrakeva, D., N. Tzankova. 2016b. Ancient metallurgical slags from the Rosen Ore Region – a potential raw material for the production of copper and lanthanides. – *Geology and mineral resources*, 6, 36-40 (in Bulgarian with English abstract).
- Stavrakeva, D., R. Stoytseva. 1966. Chemical-petrographic characteristics of the waste slags from SMME “G. Dimitrov”, Eliseina station. – *Mining and metallurgy*, Metallurgy, vol. 2, 15–18 (in Bulgarian).
- Tzankova, N., D. Stavrakeva, P. Leshtakov, K. Dimitrov. 2016. Chemico-mineralogical characterization of ancient slags from Rosen Ore Field. Part 2 – Korucheshme and Rosen deposits, metallurgical center „Atiya“ – *Ann. Univ. Min. Geol.*, 59, 1, Geol., 61-66 (in Bulgarian with English abstract).

## NEW DATA ABOUT VOLCANO-SEDIMENTARY SUCCESSIONS ON BYERS PENINSULA AND HANNAH POINT, LIVINGSTON ISLAND, ANTARCTICA

**Stefan Velev<sup>1</sup>, Cristine Trevisan<sup>2</sup>, Docho Dochev<sup>3</sup>, Janko Gerdjikov<sup>3</sup>, Kamen Bonev<sup>4</sup>**

<sup>1</sup>National Center for Polar Studies, Sofia University "St. Kliment Ohridski" 1504 Sofia; velev.stefan83@gmail.com

<sup>2</sup>Chilean Antarctic Institute (INACH), Punta Arenas; ctrevisan@inach.cl

<sup>3</sup>Sofia University "St Kliment Ohridski" 1504 Sofia, FGG, dochev@gea.uni-sofia.bg, janko@gea.uni-sofia.bg

<sup>4</sup>Bulgarian Antarctic Institute, Sofia; bonev.kamen@gmail.com

**ABSTRACT.** Livingston is the second largest of the South Shetland Islands, which are separated from the Antarctic Peninsula by the Bransfield Strait. Some ice-free areas, such as Byers Peninsula and Hannah Point provide a perfect opportunities for studying the outcropping rocks. The thick Upper Jurassic-Lower Cretaceous sedimentary sequences exposed on Byers Peninsula are dominated by mudstones, sandstones, and rare levels of conglomerates and breccias. Igneous rocks are presented by subvolcanic, hypabyssal shallow intrusions, effusive, explosive and volcanoclastic varieties. Several basaltic cryptodomes are intruded into unconsolidated sediment rocks. The penetration of the basalts into the wet sediments results in quench fragmentation and generation of in situ hyaloclastites (peperites). The rock sequences on Hannah Point are composed of different volcanic and volcanoclastic rocks with Upper Cretaceous age. Volcanic products include lava flows, pyroclastics, epiclastics, volcanic plugs and dykes. The magmatism on Livingston Island come to be younger from west to east: Lower Cretaceous at Byers Peninsula and Upper Cretaceous at the central part (Hannah Point). Along with this, the paleovolcanic setting changes from subaqueous at the most western part (Byers Peninsula) to subaerial at the central parts of the island (Hannah Point).

**Keywords:** Antarctica, Livingston Island, volcanic rocks, Lower-Upper Cretaceous

### НОВИ ДАННИ ЗА ВУЛКАНОГЕННО-СЕДИМЕНТНИТЕ ПОСЛЕДОВАТЕЛНОСТИ ОТ П-В БАЙЕРС И НОС ХАНА, О-В ЛИВИНГСТЪН, АНТАРКТИКА

**Стефан Велев<sup>1</sup>, Кристин Тревисан<sup>2</sup>, Дочо Дочев<sup>3</sup>, Янко Герджиков<sup>3</sup>, Камен Бонев<sup>4</sup>**

<sup>1</sup>Национален Център за Полярни Изследвания, СУ „Св. Климент Охридски“ 1504 София

<sup>2</sup>Чилийски Антарктически Институт, Пунта Арена

<sup>3</sup>СУ „Св. Климент Охридски“ ГГФ, 1504 София

<sup>4</sup>Български Антарктически Институт, София

**РЕЗЮМЕ.** Ливингстън е вторият по големина остров от архипелага на Южно Шетландските острови, които са отделени от Антарктическият полуостров посредством пролива Брансфийлд. Някои свободни от лед и сняг райони предоставят перфектни възможности за изследване на разкриващите се скали, именно такива са п-в Байерс и нос Хана. Горноюрско-долнокредните седиментни последователности на п-в Байерс са изградени от алевроитово-глинести скали, пясъчници и редки нива от конгломерати и брекчи. Магмените скали са представени от субвулкански, хипоабисални плиткови интрузии (щокове), ефузивни, експлозивни и вулканокластични разновидности. Няколко плитко заложени базалтови щока са внедрени във все още неконсолидираните седименти. Проникването на базалтовата магма сред влажните седименти води до тяхната фрагментация и бързо охлаждане, като това генерира хиалокластити (пеперити). Скалните последователности на нос Хана са съставени от различни вулкански и вулканокластични скали с горнокредна възраст. Вулканските продукти включват лавови потоци, пирокластити, епикластити, вулкански некове и дайки. Магматизмът на о-в Ливингстън се подмладява от запад на изток: Долна Креда на п-в Байерс и Горна Креда на нос Хана. Паралелно с това се променя и палеовулканската обстановка от субаквална в западните части на острова (п-в Байерс) до субаерална в централните части (нос Хана).

**Ключови думи:** Антарктика, о-в Ливингстън, вулкански скали, Долна-Горна Креда

### Introduction

Livingston is the second largest of the South Shetland Islands, which are separated from the Antarctic Peninsula by the Bransfield Strait (Fig. 1). On the island there are some places with excellent exposures of volcano-sedimentary successions such as Byers Peninsula and Hannah Point.

The aim of this research is a field characteristic of the volcanic and volcano-sedimentary rocks from these localities and correlation between them.

The focus of present study is on a volcanic rock types. The main reason for this is lower knowledge about them.

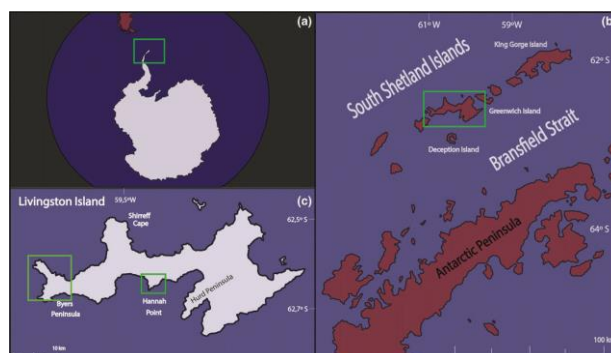


**Fig.1. General location of studied areas. (a) Antarctic Peninsula. (b) Antarctic Peninsula and South Shetland Islands. (c) Livingston Island, in a green square Hannah Point and Byers Peninsula**

## Methods

For the purposes of the present investigation were carried out field works aiming a detailed characteristic of volcanic and volcanoclastic sequences and rock sampling. Fieldwork was carried out by a Bulgarian geological expedition in 2017 and 2018.

## Geological overview

The South Shetland Island arc is the most conspicuous geological feature present in the archipelago. It was formed as response to the subduction of the Pacific oceanic crust in a southeast direction under the continental crust of the Antarctic Peninsula. Its volcanic activity record ranges between 135 and 47 Ma (Smellie et al., 1984; Haase et al., 2012). The volcanic rocks mainly consist of lavas and associated volcanoclastic products (Smellie et al., 1984) of calc-alkaline to tholeiitic affinities.

The late Jurassic to early Cretaceous Byers Group crops out on Byers Peninsula and records deposition in a marine to continental forearc basin (Smellie et al., 1980; Crame et al., 1993; Pimpirev et al., 1998). According to Crame et al. (1993) sedimentary and volcanic successions are grouped into 4 formations as follows: Anchorage Formation (Kimmeridgian–Tithonian), Devils Point Formation (Berriasian), President Beaches Formation (Berriasian) and Chester Cone Formation (Valanginian). Afterward Hathaway and Lomas (1998) revised the lithostratigraphical scheme of Crame et al. (1993) and proposed some new formal lithostratigraphic units: Anchorage Formation (Kimmeridgian–Tithonian), President Beaches Formation and Start Hill Formation (Berriasian), Chester Cone Formation (with Devils Point Member and Sealer Hill Member) (?Upper Berriasian to Valanginian) and Cerro Negro Formation (Aptian). On Byers Peninsula there are a lot of perfect examples of interaction between magma and wet unconsolidated sediments (Velev et al., 2018).

Hannah Point is part of the widespread occurrence of volcanic rocks from Livingston Island.

According to Hobbs (1968) the basal 43 m of the succession consist of andesites interbedded with agglomerates, amygdaloidal lavas and tuffs. The following 110 m are composed of friable agglomerates, ashes and lavas, while the top 195 m are composed of massive andesite layers interbedded with amygdaloidal lavas.

The rocks from Hannah Point were considered by Smellie et al. (1984) to be part of the volcanic succession cropping out on Byers Peninsula (Lower Cretaceous). Later K-Ar analyses of two basaltic andesite samples corresponding to the mid and upper part of the succession, gave  $87.9 \pm 2.6$  and  $67.5 \pm 2.5$  Ma, indicating they are Upper Cretaceous in age (Smellie et al., 1996).

Pallas et al. (1999) recognized five members from base to top: (a) 120 m of polymictic volcanoclastic breccias, (b) 70 m of volcanoclastic breccias, (c) 65 m of basaltic lavas, (d) 65 m of volcanoclastic breccias and (e) 150 m of andesitic lavas, suggesting that the rocks of this succession were emplaced as pyroclastic flows associated with explosive volcanic activity in a subaerial environment.

On the base of leaf imprints and fossil trunk Leppe et al. (2007) suggested a Late Cretaceous age. This was confirmed

by Haase et al. (2012) based on  $40\text{Ar}/39\text{Ar}$  whole rock data giving an age of 97.5 Ma.

## Results and discussion

### Byers Peninsula

On the Byers Peninsula igneous rocks are very widespread. The volcanic facies is represented by lava flows, sills, dykes, volcanic plugs and some hypabissal rocks with lower Cretaceous age (Fig. 2).

The lavas are characterized by well developed colonnade and entablature structures (Fig. 3). In most of the cases lava flows are stratified, separated each other by levels of lava breccias and volcanoclastic rocks.

Several volcanic plugs cropped out at Sealer Hill, Cerro Negro and Lair Point. Very characteristic for these structures is columnar jointing. They indicate different monogenetic volcanic centers.

Sill-like bodies have a much bigger distribution than dykes. Impressive structures of these type cropped out on Devils Point and Punta Campamento. Their thickness is up to about 45 m.

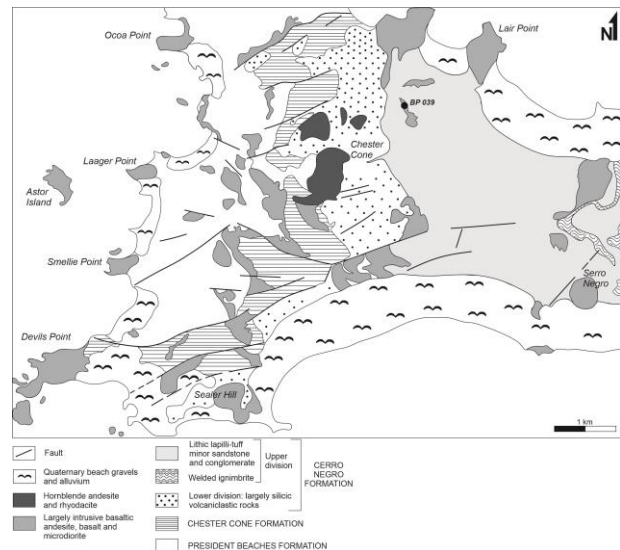


Fig. 2. Geological map of Byers Peninsula (after Hathaway and Lomas, 1997)

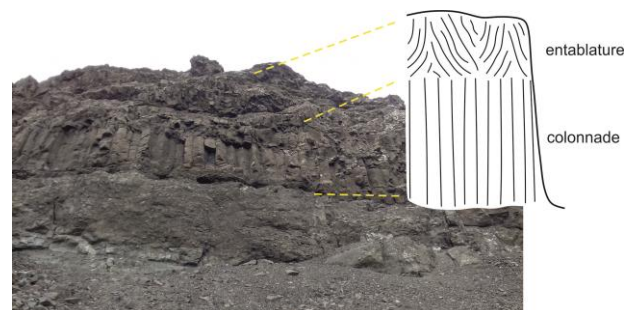


Fig. 3. Lava flow with colonnade and entablature

On Byers Peninsula there are a lot of evidences of interaction of magma and wet unconsolidated sediments.

The basaltic cryptodomes crop out in several places on the Byers Peninsula. They are intruded in unconsolidated sediment rocks (alternation of sandstones and siltstones). The

cryptodomes have irregular fingershaped contacts (Fig. 4a). The penetration of the basalts in the wet unconsolidated sediments results in quench fragmentation and generation of in situ hyaloclastite. The low viscosity magma is influxed in the sediments and peperites (White et al., 2000) are formed due to temperature differences and the fluidization effect. In peperitic facies, sandstones or siltstones fill joints and fractures that define pseudo-pillows (Fig. 4b), lobe-like bodies (Fig. 4e), polyhedral joint blocks and closely packed fabric (Fig. 4c) or sediment, matrix-rich breccia (Fig. 4d), contains fragments and apophyses of basalts (dispersed fabric). Often the basalt fragments show jigsaw-fit texture and some of the direct contacts with the sediments have chilled margins. Along some contacts, peperite with dispersed fabric passes through a zone of closely packed peperite into coherent facies. Alternatively, closely packed peperite passes directly into coherent facies. Examples of peperite with more than one clast type (globular, blocky and platy), and involving sedimentary matrix are common (Doyle, 2000).

The thick Upper Jurassic-Lower Cretaceous sedimentary and volcano-sedimentary sequences exposed on the Byers Peninsula are dominated by mudstones, sandstones, and rare levels of conglomerates and breccias. The sedimentary sequences are well dated based on ammonites, belemnites, palynomorphs, and fossil flora. Igneous rocks are present by almost magmatic facies – subvolcanic, hypabyssal shallow intrusion, effusive, explosive and volcanoclastic. Several basaltic cryptodomes are intruded into unconsolidated sediment rocks. The penetration of the basalts into wet sediments results in quench fragmentation and generation of in situ hyaloclastite. These textures are evidence for subaqueous setting of volcanism in this part of Livingston Island.

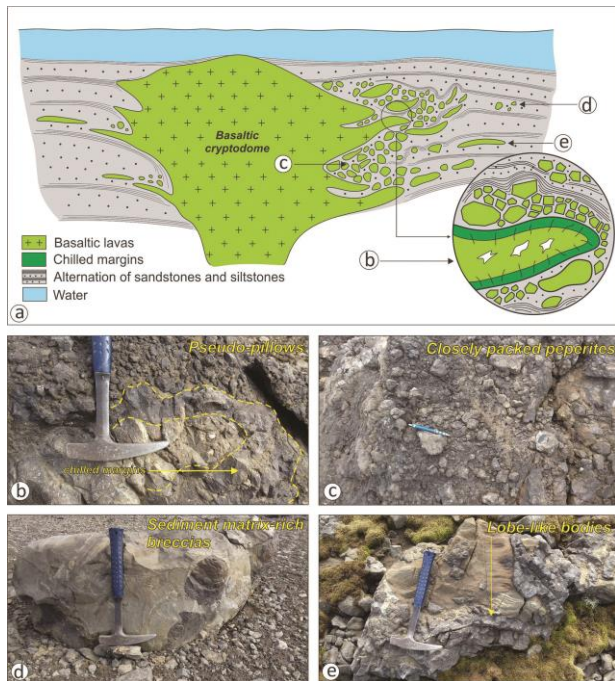


Fig. 4. Intrusions of cryptodomes in nonconsolidated sediments. (a) idealized scheme. (b) pseudo-pillows. (c) closely packed peperites. (d) sediment matrix-rich breccias. (e) lobe-like platy body

### Hannah Point

The upper Cretaceous volcano-sedimentary succession on Hannah Point is composed of lava flows, dykes, volcanic plugs, pyroclastic and epiclastic rocks and rare, thin levels of sediments.

In the lower parts of the cross section there are two lava flows separated each other by autobrecciated levels (lava breccias) (Fig. 5).

Typical for the flows are colonnade and entablature structures.

Other two lava flows are established in the middle parts of the succession.

Volcaniclastic rocks are the most common on Hannah Point. These include pyroclastic and epiclastic varieties.

There are two types of pyroclastic rocks-agglomerate tuffs and ignimbrites.

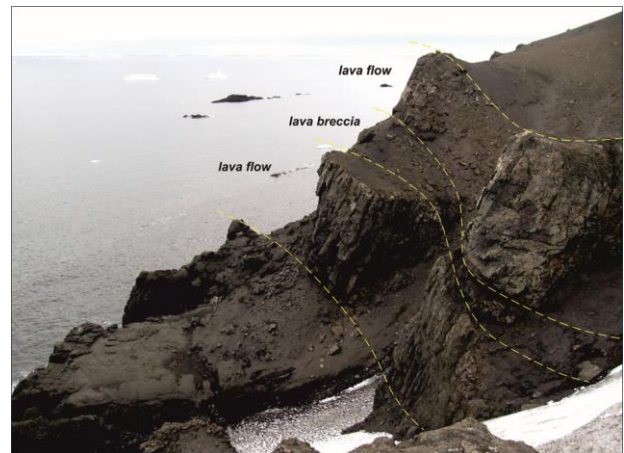


Fig. 5. Lava flows in the lower parts of the cross section on Hannah Point

One volcanic plug is intruded in volcano-sedimentary layers. It is located in the northern part of the cross section and represent typical remnant volcanic structure.

Perfectly developed is columnar jointing. In the lower and middle parts of the body columnar joints are vertical, which is an indication of the vertical movement of the lava. In the upper levels of the structure the lava begins to flow in different directions (Fig. 6).

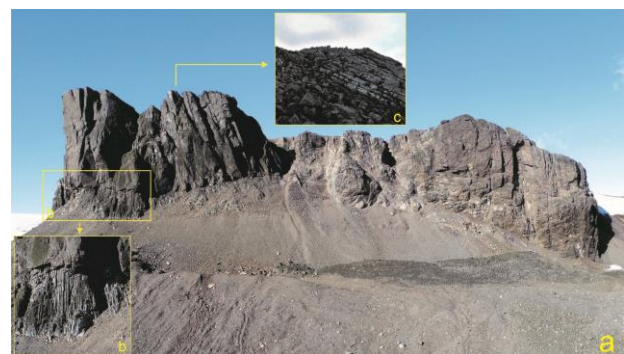
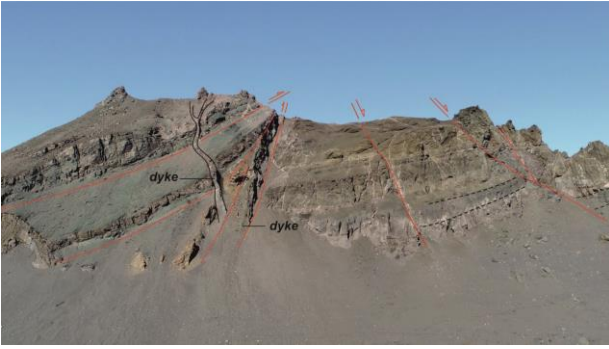


Fig. 6. (a) general view of volcanic plug. (b) vertical prismatic joints. (c) tilted prismatic joints

Two dikes are established with thickness ranging from 1 to 2.5 m (Fig. 7).



**Fig. 7. Subvertical dyke bodies**

The field works allowed to collect detailed data about the rocks from Hannah Point.

The studied area is dominated by volcanic and volcanoclastic rocks. Sediments are poorly represented.

All volcanic products (lava flows, pyroclastic and epiclastic rocks, volcanic plugs) are result of the activity of one subaerial volcanic center. The observed dikes are the the last magmatic phase.

The volcano-sedimentary succession can be considered as a monogenetic, stratified volcanic structure, formed by alternation of effusive, pyroclastic and epiclastic sequences.

## Conclusions

The magmatism on Livingston Island come to be younger from west to east: Upper Jurassic to Lower Cretaceous at Byers Peninsula, Upper Cretaceous at the central part (Hannah Point) and Eocene at Hurd Peninsula and Barnard Point. Along with this, the paleovolcanic setting changes from subaqueous at the most western part (Byers Peninsula) to subaerial at the central parts of the island (Hannah Point).

The deposition conditions for the sediments on the island are various. At the western part of the Byers Peninsula the gently dipping ?Kimmeridgian-Berriasian sediments are deposited in deep-marine paleoenvironments, while in the central part of the peninsula ?Berriasian-Valanginian sediments are shallow marine. In the eastern part of the Byers Peninsula sedimentary rocks Valanginian – Aptian in aged are deposited in non-marine conditions. The sedimentary beds exposed in the central part of the island (Hannah Point) are non-marine too and much younger (Coniacian-Maastrichtian). At the eastern part of the Island (Hurd Peninsula) lower and middle part of the anchimetamprphosed sedimentary sequences of Miers Bluff Formation (Campanian-Maastrichtian) are also formed in deep-marine paleoenvironments, while upper parts of the formation (Maastrichtian-?Paleocene) demonstrated the final regressive stage with coarse sedimentation.

**Acknowledgements.** Sincere thanks to Prof. Christo Pimpirev for the opportunity to work on Livingston Island.

This work has been carried out in the framework of the National Program of Polar Research supported by Ministry of Education and Science of Bulgaria (Agreement No 80-10-242)

Thanks to everyone from the logistic team who secured our safe arrival and stay in Antarctica.

## References

- Crame, J. A., D. Pirrie, J. S. Crampton, A. M. Duane. 1993. Stratigraphy and regional significance of the Upper Jurassic–Lower Cretaceous Byers Group, Livingston Island, Antarctica. – *J. Geol. Soc. London*, 150, 1075–1087.
- Doyle, M. G. 2000. Clast shape and textural associations in peperite as a guide to hydromagmatic interactions: Upper Permian basaltic and basaltic andesite examples from Kiama, Australia. – *Australian J. of Earth Sci.*, 47, 167–177.
- Haase, K. M., C. Beier, S. Fretzdorff, J. L. Smellie. Garbeschönberg. 2012. Magmatic evolution of the South Shetland Island, Antarctica, and implications for continental crust formation. *Contrib. Mineral. Petrol.* 163 (6), 1103–1119.
- Hathaway B., S. A. Lomas(1998) The Upper Jurassic-Lower Cretaceous By-ers Group, South Shetland Islands, Antarctica: revised stratigraphy and regional correlations, *Cret. Res.*,19, 43–67.
- Hobbs, G.J., 1968. The geology of the South Shetland Islands. IV . The Geology of Livingston Island. British Antarctic Survey Scientific Reports, 47, 34 pp.
- Leppe M., W. Michea, C. Muñoz, S. Palma-Heldt, and F. Fernandoy. 2007. Paleobotany of Livingston Island: The first report of a Cretaceous fossil flora from Hannah Point. U.S. Geological Survey and The National Academies; USGS OF-2007-1047, Short Research Paper 081; doi:10.3133/of2007-1047.srp081.
- Pallàs. R., C. Soriano., X. Zheng, F. Sabat, J.M. Casas. 1999. Volcanic stratigraphy of Hannah Point, Livingston Island, South Shetland Island, Antarctica. – *Acta Geologica Hispanica*, 34, 4, 323-328.
- Pimpirev Ch., D. Vangelov (1998) Ancient subaqueous mouth bar type system, Byers Group, Livingston Island, Antarctica, *Ann. Univ. Sofia "St. Kliment Ohridski", Fac. Geol. Geog.*, 90(1), 29–43.
- Smellie, J.L., R.E.S Davies, and M.R.A Thomson. 1980. Geology of a Mesozoic intra-arc sequence on Byers Peninsula, Livingston Island, South Shetland Islands. *British Antarctic Survey Bulletin*, No. 50, 55-76
- Smellie, J.L., R.J. Pankhurst, M.R. Thomson, R.E. Davies. 1984. The geology of the South Shetland Island: IV. Stratigraphy, geochemistry and evolution. *Br. Antarct. Surv.* 87 (85 pp.).
- Smellie, J.L., R. Pallas, F. Sabat, X. Zheng. 1996. Age and correlation of volcanism in central Livingston Island, South Shetland Islands: K-Ar and geochemical constraints. *J.S.Am. Earth Sci.* 9, 265–272.
- Velev, S., D. Dochev, and K. Bonev. 2018. Interaction of magma and wet unconsolidated sediments: case study from Byers Peninsula, Livingston Island, Antarctica. *REVIEW OF THE BULGARIAN GEOLOGICAL SOCIETY*, vol. 79, part 3, 2018, p. 63–64
- White, J. D. L., J. McPhie, I. Skilling. 2000. Peperite: a useful genetic term. – *Bull. Volcanol.*, 62, 65–66.

**SECTION**

**SUSTAINABLE DEVELOPMENT OF THE MINERAL  
RESOURCES INDUSTRY**

## REGIONAL CONFLICTS FOR NATURAL RESOURCES

**Erol Buyukliev**

*"G. S. Rakovski" National Defence College, Bulgaria, 1504 Sofia; e.buyukliev@mdc.bg*

**ABSTRACT.** The report analyzes the geostrategic rivalries that relate to natural resources and determine the regional balances of power. The report presents the influence of regional forces that clash their interests in rich in natural resources areas. In addition, natural resources are cited a reason for existing conflicts and wars. The focus is on certain aspects of the conflicts in the Middle East and South Asia, trying to bring out the key factors of the conflicts. The report analyzes the conflicts over natural resources and the genesis of the conflicting relationships between regional players and actors. The study seeks to bring out the main trends in the development of the regional security environment, which is determined by rivalry and the struggle for natural resources.

**Keywords:** conflicts, natural resources, Middle East, South Asia

### РЕГИОНАЛНИ КОНФЛИКТИ ЗА ПРИРОДНИ РЕСУРСИ

**Ерол Буюклиев**

*Военна Академия „Г. С. Раковски“, 1504 София*

**РЕЗЮМЕ.** В доклада се анализират геостратегическите съперничества, които са свързани с природни ресурси и определят регионалните баланси на силите. Докладът представя влиянието на регионалните сили, които сблъскват своите интереси в районите богати на природните ресурси. Освен това, природните източници са отбелязани като причини за съществуващи за конфликти и войни. На фокус се поставят определени аспекти на конфликтите в Близкия изток и Южна Азия, като се прави опит да се изведат ключовите фактори на конфликтните отношения. Докладът анализира конфликтите за природни ресурси и генезисът на конфликтните взаимоотношения между регионалните играчи и актори. Изследването се стреми към извеждането на основните тенденции в развитието на регионалната среда за сигурност, която се определя от съперничеството и борбата за природни ресурси.

**Ключови думи:** конфликти, природни ресурси, Близък Изток, Южна Азия

### Introduction

Natural resources retain their importance for human life. Their extraction, processing, supply and consumption depend on the needs of the growing population of the Earth. The Covid-19 pandemic has led to negative oil prices. These are fundamentally different contextual parameters that seem incomprehensible and confusing. Changing the value of oil is a factor that increases conflicts. As of August 1, 2020, 1:55 p.m., Humanity numbers 7,801,969,500 people. Vital to humanity is water, for which disputes, conflicts and wars are fought. About 70% of the Earth is covered with water, but only 2.5% of the "blue gold", as it is called, is freshwater and fresh water in rivers, lakes and dams is about 0.02%. Water, along with air, is one of the most valuable resources and sources of life for humans. The human body contains 60-75% water. As of August 1, 2020, 799,083,518 people do not have access to safe drinking water, since the beginning of the year 493,402 people have lost their lives due to water-related diseases. From the beginning of the year to the already mentioned date more than 2,560,170,000 liters of water have been used. . 140 liters of water are needed to make a cup of coffee with which we all wake up. Declining freshwater resources is a growing global trend that affects us all, but it is particularly significant for ¼ of the humanity. (The Global Risk Report 2020, p. 31) (World Economic Forum, 22 March 2019) Oil is another source of energy, which has defined the development of countries since it has been entering people's

daily lives at an intensive pace since 1950 as the main means of production, transport and energy. In one of his books, Professor Velichka Milina presents the "New Paradigm of Energy Security", which is determined mainly by three factors: the shale revolution, the crisis of the first decade of the XXI century and the increased vulnerability of critical energy infrastructure. Although the thesis of the "depletion" of fossil fuels seems hopelessly outdated, fueled by strategic shocks in new energy technologies that push the boundaries of what is possible and affordable. The new paradigm does not completely rule out the fact that oil and increasingly natural gas are the blood of the modern economy. The old paradigm determined the tendency towards increasing conflict for control over the last deposits of natural energy sources. (worldometer, 01.08.2020; Milina, 2013; Milina, 2007) Here comes the question, Does declining natural resources, such as drinking water and oil, continue to be the cause of conflicts?

Two mutually exclusive hypotheses are formed. The first identifies a reduction in the conflict caused by the desire to control natural resources, in relation to the Middle East, for example, based on the changing paradigm of energy security. It implies a diminishing interest of strong global and regional players, such as the global hegemon USA, in oil-rich countries, made possible by shale and technological revolutions that make it possible to search for alternative energy sources. The second one creates expectations for growing conflict over natural resources. It is based on the growing needs of the growing

number of people on Earth and the need for more energy, which, along with declining resources for vital drinking water and limited, hard to reach oil reserves, implies increasing competition and conflict for control over key region, transit corridors and resource - rich areas.

The rapidly changing security environment is part of the global trends for change in all aspects of life. The relevance of this study is determined by the ongoing conflict over natural resources, which retains importance for the survival and development of mankind. The **object** of study are the conflicts over natural resources as a key process in the global security environment. The subject of research are the conflicting relations between individual actors, which are motivated by the desire to control natural resources. The research topic imposes certain restrictions. The study focuses on certain manifestations of the oil conflicts in the Middle East and the water conflicts in South Asia: Afghanistan, Bangladesh, Bhutan, India, Nepal, Maldives, Pakistan, Sri Lanka. The aim of the study is to identify the importance of oil in the Middle East and water in South Asia to identify the specific manifestations of the conflict caused by the desire to control vital natural resources. The analysis is based on the hypothesis that, despite the changing realities caused by new technologies, natural resources in these regions remain the leading reason for conflicts. The research is based on a diverse set of scientific methodology: holistic approach, geopolitical analysis, multidisciplinary and historical approach, inductive and deductive analysis. Current analyzes, books on selected topics, scientific literature in the field of security, international relations, analyzes of think-tanks are used. The analysis is aimed at a wide range of users with interests in natural resources, international and regional security. Its significance is determined by the derivation of some of the modern conflict relations, which are caused by the competition for vital natural resources.

## **Oil as a mainspring for conflicts in the Middle East**

In his book, "Petro-aggression. When oil provokes war," Jeff Colgan (2013) identifies oil as the most valuable commodity traded on international markets. Iraq's wars with Iran, the invasion of Kuwait, and the subsequent wars of 1990 and 2003 can be described as affected by oil. The revolutionary period from 1958 to 1968, led by Saddam Hussein, and oil resources created the conditions for an aggressive policy, with a tendency to achieve geopolitical ambitions by means of war. The availability, production and sale of oil determine the agenda of the Middle East countries and their relations with the outside world, in particular with the United States, India and China. A leading problem identified by both Velichka Milina and Jeff Colgan is the "curse of resources" and the principle for energy nationalism typical of hydrocarbon-rich exporting countries. In the period of the "ruling" old paradigm of energy security, energy nationalism determines the behavior of the main participants in the international energy market. In this way, oil is used as a geopolitical weapon. The fierce race for energy resources determines the growing demand and consumption that shape the energy policy of the countries. Thus, energy geopolitics and geoeconomics become the most essential part of the global and foreign policy of the major players in the energy market (Milina,

2013). For his part, Jeff Colgan describes the emergence of conflicts as a failure of the state to act rationally. In certain cases, the emergence of conflicts is dictated by the reduction of the cost of conflict and the growing tolerance of the "risk state", ie. in the emerging global, postmodern, networked, risky society, the modern "risk state" is being formed, which tends to tolerate more and more risks and uncertainties. It turns out that oil has been the leading motive for almost half of the international conflicts since 1973. The shale revolution did not change this trend, despite the change in the oil and gas sector in the United States. The country is unlikely to be able to isolate itself from international markets and events, despite the many indications of this and America's withdrawal from many international agreements and commitments after the coming to power of Donald Trump. In addition, the need for energy resources of the US allies remains leading, which determines their interests in an open and accessible global oil market. To this, Kolgan adds unexpected causes of conflict: competition for the transportation of oil by ship and pipeline, the growing threat of terrorism related to oil fields and transit routes, and the lack of resources in consumer countries are a potential source of international conflict.

International oil conflicts are determined by eight different mechanisms: Resource wars, in which countries try to acquire oil reserves by force; isolation from the influence of the opposition leaders of oil states such as Saddam Hussein and Ayatollah Khomeini, who pursue risky foreign policies; the transformation of internal conflicts into international ones by countries that have oil reserves; financing insurgent actions, similar to Iran, which supports Hezbollah, with oil funds; conflicts caused by the prospect of a regional power dominating oil fields in a particular territory, the first Gulf War against Iraq for control of Kuwait in 1991; collisions along the pipelines and on the territory of the transit routes; activity of organizations such as Al Qaeda (and more recently Islamic State) on oil production; barriers related to oil in terms of multilateral cooperation and security. In addition, oil conflicts are complicating their dynamics due to three key global transformations: the shale revolution is displacing production centers from the Middle East to North America; about 16 developing countries in Africa have ambitions for conventional oil production and exports; the declining hegemony of the United States is related to the declining role of the country in providing security for the transportation of oil by ship and on transit routes and regions (Jeff Colgan, 2013).

As for the wars in Iraq, dictated by Saddam Hussein's ambitions in the late 20st century and early 21st century, it can be determined that the sole power in the country, the monopoly on natural resources, the resources accumulated by them lead to increased military capabilities. In addition, the inability of opposition forces to balance the concentration of power in a single center created the conditions for the expansionist ambitions of a traditionally militant elite. At the beginning for the 21st century, in 2001, Michael Claire's book "Resource Wars: The New Face of the World Conflict" was published, stating that one of the leading causes of the terrorist attack of September 11, 2001 in the United States from Al Qaeda is the desire to dethrone the pro-Western government in Saudi Arabia and replace it with Islamist fundamentalists to control ¼ from oil supplies to the world (Clare, 2001).

It is with this act of violence that it confirms the tendency towards the privatization of violence in the global era and the

transformation of the power of many power, legitimate and increasingly illegitimate, centers. In addition to the growing energy needs and ambitions to control the Middle East and the complex relationships between the various actors, identity policies and revolutionary changes with the security environment emerging, where the focus of state security is shifting to individual security. More and more people are demanding respect for their identity security. Under the pressure of global transformations, many totalitarian regimes have been bent by the pressure of networking and rapidly mobilizing self-organizing systems. It turns out that the system that manages to adapt and build a hybrid structure and manages to use the technological advances of our time will gain a strategic advantage. The main conflict is between hierarchies and networks. Asymmetry in the conflict turned out to be an advantage, flexibility, the swarming of the individual elements won over the solid force. The paradigm of war had to be changed quickly. Temenuga Rakadzhyska appears to be right that the nature of wars is radically changing, in the 21st century they will be fought between artificial and human intelligence. The validity of this thesis is questionable, a significant part of humanity has not passed into the new technological age, until it happens many of the wars to occur according to the laws of the twentieth century, and the main motive for them are territorial disputes and the struggle for resources (Rakadziiska, 2018 ). Thus, for the last 20 years, about 40% of the world's wars have been fought for natural resources. More and more conflicts are being fought over freshwater reserves in South Asia (Yuruk, B., Aynur Asgarli. 2018)

## **Water as a leading motive for conflicts in South Asia**

The growing population of the Earth also determines the growing need of water. Freshwater reserves are a limited natural resource that is causing more and more conflicts between countries. Water is the cause of wars and conflicts between species from the dawn of life. According to Michael Claire, there are four major rivers that determine development and relationships in the Middle East and Southwest Asia: the Jordan, the Tigris and Euphrates, and the Indus River. Our particular interest in this part of the analysis is the Indus River. Its waters serve Afghanistan, China, India, Pakistan and Kashmir. An additional factor for tension and conflicts are identity divisions based on political, religious, cultural, ideological differences (Clare, 2001). Hank Pellissier brings out 225 drinking water conflicts and pays special attention to nine danger zones: North vs. South Yemen; Egypt v. Ethiopia; India v. China (under their influence are Afghanistan and Bangladesh); Burkina Faso v. Ghana; Thailand v. Laos, Vietnam, Cambodia and China; India v. Pakistan for Kashmir water resources; Turkey against Syria, Iraq and Iran; Central Asia - Kazakhstan, Turkmenistan, Uzbekistan, Kyrgyzstan and Tajikistan; Israel v. Palestine (Pellissier, 2013) Kashmir's water resources are a mainspring for conflicts between India and Pakistan, two nuclear powers that often lead to clashes and create the preconditions for nuclear war. In 1960, a treaty was signed covering six rivers: the Indus, the Jhelum and the Chenab (ceded to Pakistan), the Sutlej, the Beas and the Ravi are Indian. However, Pakistan accuses India of diverting the Indus River through a dam system and canals, and 92% of Pakistan's territory depends on the

Indus water resources. The other line of tension in South Asia is the dispute between China and India over the waters of the Brahmaputra River. China is building a system of dams, with catastrophic consequences for India and Bangladesh. China plans to block about 10 major rivers that spring from the Tibetan Plateau. The reason for this is China's urgent need for water, which will increase in the coming years, more than 6,000 lakes have already dried up. For these reasons, the near future is full of uncertainty and appears to be potential for future conflicts.

The distribution of water resources in South Asia is a security issue, ie. securitized problem. The genesis of the conflicts in the region takes us back in centuries, but the problem worsened after World War II, during the withdrawal of the British Empire, when the new sovereign states were formed in 1947. India's central position determines its key role in water resources. The country borders the rest of the region, except Afghanistan, with which it is historically bound. The conflict between India and Pakistan is fueled, as mentioned, by control over the canals along the rivers that flow through the two countries. Authorities in the Eastern Punjab (India) periodically restrict and cut off water to the Western Punjab (Pakistan). The interests of three regional nuclear powers: India, Pakistan and China are the main problem in South Asia. The China-Pakistan partnership forces India to seek support from outside regional powers. The complexity of relations in the region escalated into a military clash in 1999, when India and Pakistan were on the cusp of nuclear war.

Pakistan's goal, with regard to the Indus River, is to control the entire course of the river, which flows from China through Indian territory, and the construction of dams exacerbates the conflict between the two countries. Examples are the Baglihar and Mangla dams (Keetelaar, 2007). Unresolved water issues in South Asia are potential conflicting source. The Tibetan Plateau is the largest water reservoir in the world, the lives of more than 1.3 billion people depend on water resources in the Himalayas, the countries directly affected are China, Nepal, India, Afghanistan, Bhutan and Pakistan (Dutt, S., Bansal, A., 2012) India and Bangladesh are arguing over 54 rivers, including the Ganges, Brahmaputra and Megna. One of the problem points is the construction of the Farakka dam, started before establishment of Bangladesh. In the past Bangladesh was part of Pakistan, East Pakistan, and Bangladesh was established in 1971 (Salman, M.A., 2002). India is also setting up a river connection project that harms Bangladesh.

India and Nepal have disputes over Nepal's energy supply potential and India's growing need. The energy used is only 1% of Nepal's capacity. A more significant problem remains the distribution of water between India and China. The two countries share 4 large rivers that flow through other countries. The Indus River also flows through Pakistan, the Brahmaputra River crosses India, China, Bhutan and Bangladesh, the Kosi and Gahara Rivers flow through India, China and Nepal, and the Sutley River crosses China, India and Pakistan. The disputed issues around the waters of the Brahmaputra River have a huge potential for conflict. The upper tributary of the river passes through China or 50% of the river basin. The waters of the river are vital for life in India and China. For India, the Brahmaputra River provides 30% of the country's fresh water and 40% of its water energy potential. The river is extremely important for Tibet. Added to this are the border disputes between the two

countries for the Eastern Himalayas, where Bhutan also intervenes (Hongzhou, Z. 2016). The forecasts for the growing population of India and China are not encouraging in terms of the conflict potential motivated by limited water resources. In the near future, water deficits may cause conflicts and wars between nuclear states, which not only threatens regional and energy security, but calls into question the survival of humanity as a whole (Uttam, S., 2016).

## Conclusions

1. The study found that despite the global transformations and the changing nature of wars, natural resources retain their importance and impact on human life. The race for them continues in the context of the Fourth World War, which is already underway;

2. The analysis focused on two of the main resources for modern life: water and oil. The relocation of the oil and gas production center to North America and the withdrawal of the United States from the Middle East is a prerequisite for the struggle for resources that is typical for in the past twentieth century. This process is fueled by the privatization of force and the means of violence, which enables legitimate and illegitimate actors to assert their political and economic aspirations through the means of war;

3. The study identified risks of a water conflict in South Asia between nuclear powers question the survival of humanity in the event of a nuclear war;

4. The nature of wars is changing. The introduction of new technologies is changing the forms of warfare. Contactless wars with the use of UAVs (drones) transformed the idea of participating in a war that became a game. The drone pilots intervene thousands of kilometers from the potential attack zone, destroy the targets and return home to their families after work. On the other hand, the current analysis shows that natural resources retain their impact on people's lives, and their depletion will lead to new conflicts. The dehumanization of war poses new challenges that will determine the future of the human race. The struggle will be between the representatives of the new age and those who are far behind in the old age, and as we saw on September 11, 2001, the asymmetry of the conflict does not mean victory for the more powerful ones.

## References

- Clare, M. 2001. Resource Wars: The New Landscape of Global Conflict. *Henry Holt and Company, New York*, pp. 7-13, 88-132, 258-302.
- Colgan, Jeff D. 2013. *Petro-Aggression: When Oil Causes War*. New York: Cambridge University Press, 1-37.
- Colgan, Jeff D. 2013. Oil, Conflict, and U.S. National Interests. *Harvard Kennedy School, Belfer Center for Science and International Affairs, Quarterly Journal: International Security*
- Dutt, S., Bansal, A. 2012. *South Asian Security – 21<sup>st</sup> Century Discourses*. Routledge Abingdon, pp. 7-8.
- Hongzhou, Z. 2016. Sino-Indian water disputes: the coming water wars?. *WIREs Water* 2016, 3:155-166. Doi: 10.1002/wat2.1123
- Keetelar, J. 2007. *Transboundary Water Issues in South Asia*. Erasmus University Rotterdam, pp. 31-33.
- Milina, V. 2013. The New Paradigm of Energy Security. "G. S. Rakovski" *National Defence College*, 5-24 (in Bulgarian).
- Milina, V. Energy Security and Geopolitics. In: *Connections, the Quarterly journal, PfP Consortium, Volume VI, № 4, Winter 2007*.
- Pellisier, H. 2013. Water Wars – Nine Thirsty Regions where H2O Conflict is Threatening. *Geopolitics* (In Bulgarian). 03.08.2020, <https://geopolitica.eu/more/drugi-statii/1832-devet-vazmozhni-boyni-poleta-na-badeshtite-vodni-voyni>
- Rakadjiiska, T. 2018. Our Obsolete European Mentality. *BISFRIM, Sofia. European Union, Bulgaria and The Conflicts of XXI Century*. Pp. 91-104.
- Salman, M. A. 2002. *Conflict and Cooperation in South Asia's International Rivers, A Legal Perspective*. Washington D. C.: The World Bank, pp. 135-136.
- Uttam, S. 2016. *Riverine Neighborhood: Hydro-politics in South Asia*. Pentagon Press, pp. 117-118.
- Worldometer, Current World Population 01.08.2020, 13:55 ч, <https://www.worldometers.info/world-population/>
- World Economic Forum, Your morning cup of coffee contains 140 litres of water, 22 Mart 2019, 03.08.2020, <https://www.weforum.org/agenda/2019/03/hidd-en-water-in-your-cup-of-coffee/>
- World Economic Forum. *The Global Risk Report 2020*, p. 31.
- Yuruk, B., Aynur Asgarli. 2018. About 40% of The Wars in The World were fought over natural resources. *Anadolu Agency* (In Russian), 03.08.2020, <https://www.aa.com>

## A MODEL FOR BUILDING A MOBILE APPLICATION FOR INDOOR NAVIGATION

**Dimitrina Deliyaska<sup>1</sup>, Nikolay Yanev<sup>2</sup>, Mariana Trifonova-Draganova<sup>3</sup>**

<sup>1</sup> University of Mining and Geology "St. Ivan Rilski", 1700 Sofia; dimitrina.deliyska@mgu.bg

<sup>2</sup> University of Mining and Geology "St. Ivan Rilski", 1700 Sofia; nikolay.yanev@mgu.bg

<sup>3</sup> University of Mining and Geology "St. Ivan Rilski", 1700 Sofia; trifonova.m@mgu.bg

**ABSTRACT.** In today's fast-moving world, people's ability to navigate quickly and effectively in an unfamiliar environment is essential. Using wireless technologies such as Wi-Fi or Bluetooth, moving objects can be traced as well as navigated. The current report offers a brief analysis of modern technologies and methods for determining location. It also provides algorithms that are used for navigation and location. The work includes a model for creating a mobile application for indoor navigation where GPS signals are hard to detect. A graph is used to describe the object, and a QR code is employed to locate the user. The research is aimed at the Laboratory Unit at the University of Mining and Geology "St. Ivan Rilski", but it can be applied to any type of building.

**Keywords:** navigation, location, Wi-Fi, QR code

### МОДЕЛ ЗА ИЗГРАЖДАНЕ НА МОБИЛНО ПРИЛОЖЕНИЕ ЗА НАВИГАЦИЯ В ЗАКРИТА СРЕДА

**Димитрина Делийска<sup>1</sup>, Николай Янев<sup>2</sup>, Мариана Трифонова-Драганова<sup>3</sup>**

<sup>1,2,3</sup> Минно-геоложки университет „Св. Иван Рилски“, 1700 София

**РЕЗЮМЕ.** От съществено значение в днешният забързан свят е възможността хората да се ориентират бързо и ефективно в непозната среда. Използвайки безжични технологии като Wi-Fi или Bluetooth могат да бъдат проследявани движещи се обекти, както и да бъдат навигирани. В настоящият доклад ще бъде направен кратък анализ на съвременните технологии и методи за определяне на местоположение, както и алгоритми прилагани се за навигиране и локализиране. Разработката включва модел за създаване на мобилно приложение за навигация в закрыта среда, където GPS сигналите са трудно доловими. За описание на обекта ще се използва граф, а за локализация на потребителя QR код. Изследването е насочено към Лабораторен блок към Минно-геоложки университет „Св. Иван Рилски“, но може да бъде приложено за всеки тип сгради.

**Ключови думи:** навигация, локализиране, Wi-Fi, QR код

### Introduction

Nowadays, with the evolution of intelligent technologies and when the need arises to determine the location of objects, it has become necessary to employ navigation systems. As the methodology of means to safely and effectively get from one place to another, navigation has been in use since ancient times. The first ideas for navigation information systems (NIS) date back to the middle of the 20<sup>th</sup> century, but the first practical implementations are from the late 1990s. The development of NIS has been directly related to that of the Internet and network technologies.

Selecting the proper methodology is of extreme importance for building a NIS. A universal methodology to suit all types of project has not been developed yet. Very often, a particular process necessitates a new methodology based on a specific technology and the related organisational, design, and other considerations.

In the age of information technology, locating an object and determining the shortest path from point to point is easy. Object tracking or route determination can be performed with the help of various software products that employ maps from which user

location information and mathematical calculations are derived. These are the so-called location-based services (LBS). They include all satellite navigation systems such as the Global Positioning System (GPS) and the Indoor Positioning Systems (IPS). But these are systems that work either only in an external or only in an internal environment, the latter being more complicated. Yet a more serious challenge is how to track the location of a moving object shifting from external to internal environment and/or vice versa.

In the age of information technology, locating an object and determining the shortest point-to-point path is easy. With the help of various software products using maps, from which user location information and mathematical calculations are derived, object tracking or route determination can be performed. These are the so-called location-based services (LBS). These include all satellite navigation systems such as: Global Positioning System (GPS) and Indoor Positioning Systems (IPS). But these are systems that work only in an external or only in an internal environment, which is more complicated. An even more serious challenge is how to track the location of a moving object, moving from external to internal environment and / or vice versa.

## Navigation systems

Global navigation systems are satellites positioned in Earth orbit that transmit signals from various receivers on land. Depending on the satellite system used, the signal strength varies.

The Global Navigation System (GPS) is the navigation system which is used most commonly. When it comes to locating an object or route in an unfamiliar internal environment, this system is unable to operate because the signal emitted by its satellites is lost.

To overcome GPS positioning defects and to achieve accurate positioning in a complex indoor environment, many practical indoor location schemes are introduced, such as infrared connection, WI-FI, Bluetooth, ZigBee, ultrasound, radio frequency identification (RFID), and ultra-wideband (UWB) connection (Cai, X.,2018).

Such systems are called Indoor Positioning Systems (IPs). With the help of the above technologies based on wireless internet, IPs detect the current location of an object and in real time determine its coordinates indoors. Typically, such systems are created to facilitate the movement of people in multi-floor buildings or in those with a more irregular structure design, as well as to track objects or people.

Many features exist that make indoor positioning different from outdoor positioning. Compared to the external environment, internal environments seem more complicated because there are many objects (such as pieces of equipment, walls and people) that reflect signals and bring about problems with too many paths and about delays (Alarifi A, 2016).

The technologies which are used to determine location fall into categories concurrently: they are active, as well as passive. Indoor positioning technologies via radio signal or WI-FI fall into the category of "active technologies", since they require for the object to move and to have some sort of a connecting device. Besides, the devices should be able to collect and process the transmitted information. Examples of systems that employ some of the above active technologies are Ekahau real time location system (RTLS), Microsoft research radar, Intel Place Lab, and others. But only the ultra-wideband (UWB) technology can be used as a passive system as well.

With passive systems, a physical device attached to the moving object should not necessarily be present. An example of such a system is the Device-free Passive (DfP) system. The concept with it is to use an available wireless network for data exchange, to detect changes in the environment, and to track the location of objects passively without requiring additional equipment.

Table 1 presents the criteria wherein wireless technologies can be compared (Brena, Ramon F.,2017, Zheliakov, G.,2013, Kucarov, St.,2005).

The following conclusions can be drawn from Table 1:

- Each of the technologies presented in the table is standardised;
- Various protocols for data transmission over the network are supported;
- The data transmission rate across the network is about 30Mbps on the average;
- The frequency of the transmitted information is about 2GHz;

- The range of the technologies under consideration is about 100m;
- The deviation yielded by technologies when calculating location is minimum, but it depends on various factors such as visibility between receivers and transmitters, density of access points, etc.;
- The price for implementation and maintenance of the systems is the lowest with WI-FI and BLUETOOTH.

Table 1. *Wireless technologies*

	Standard	Protocols supported	Speed	Frequency band	Range (meter)	Deviation (meter)	Type system	Mean equipment cost	Average maintenance cost	Network
RFID	ISO/IEC 18000-63	ISO 18000-6A/B	Between 27 and 128 Kbps	from 300 kHz to 1 GHz	>100	1-5	active	low	high	mesh
WI-FI	IEEE 802.11	Wi-Fi - Access Protocols	54Mbps	2.4 GHz or 5 GHz	Depending on the number AP	<1	active	high	low	WLAN
BLUETOOTH	IEEE 802.15.1	UDP/TCP, IPv6, 6LoWPAN	1Mbps up to 2Mbps	2.4 GHz	10-100	0.3-1	active	low	low	WPAN
UWB	IEEE 802.15.3a	MAC	100Mbps	150 kHz up to 48 GHz	30	0.15	active / passive	low	high	WPAN
ZigBee	IEEE 802.15.4	6LoWPAN, IPv6, PANA, RPL, TOP, TLS, and UDP	2500bps	up to 2.4 GHz	10-100	0.25	active	low	high	WLAN

## Commercial solutions for indoor positioning

Due to the need to quickly navigate in an unfamiliar environment, many companies around the world offer different solutions for the purposes of saving resources.

*Ekahau RTLS* (Denis, T. et al.,2006): provides real-time indoor positioning tools developed by the American company Ekahau, Inc. It functions on the principle of the radio signal. The patented software developments are compatible with the various platforms on which the Java language runs, therefore it is possible to develop your own application using the Ekahau Engine.

*AT&T Cambridge* (Gu, Y. et al.,2009): the technology on which this company's positioning systems of are developed is UWB. It provides 3-D information on the position orientation and on the orientation of the tracking markers. Users and objects are marked by ultrasonic tags identified as "bats" or active badges.

*SpotON* (Hightower, J.,2000, Liu, H. et al.,2007): this company's main concept is to create indoor positioning systems using the power of the radio signal. The focus is more on hardware components (markers, or tags) attached to the object whose location needs to be determined. The objects are located by homogeneous sensor nodes without central control, i.e. Ad-Hoc. SpotON tags use the resulting RSS value as a sensor measurement to assess the distance between the tags.

According to studies, *Microsoft Radar* (Deak, G, 2012) is considered the world's first positioning system based on WI-FI wireless connection. The "fingerprint" method is used to detect the location. This is an offline method which involves recording a radio map of the environment. The *Radar* system calculates the location by monitoring the signal strength of the monitored devices and comparing the values with the records in the database which are employed to create a radio map.

*SmartSpace* is a modular, open-source location tracking software platform. It has been developed by the UbiSense company. The development makes it possible to interact between the state of people and things in the physical world in

real time in order to make the most complex processes visible and controllable.

The Cisco company offers an overall solution for object locating via WI-FI through the Cisco Prime Infrastructure system. It allows real-time tracking of objects and detection of their current location with a precision of up to a few metres. This depends on the number of APs. Determining clients' location on the network is calculated by the RSSI and TdoA methods. Cisco Prime Infrastructure works entirely with Cisco hardware components which cost a lot.

#### Mobile applications for internal positioning:

*Navizon* is indoor navigation for devices with iOS and Android operating systems. *Navizon Indoors* is designed to provide location technology with an accuracy of less than one meter. An initial on-site study builds a database of fingerprint signals from the nearby WI-FIs or iBeacons. The mobile applications can then use the created SDK to obtain a high-precision location by combining the fingerprints of the surrounding signal and the output data of all sensors (accelerometer, compass, gyroscope, etc.)

*HERE Indoor Radio Mapper* is an indoor radio cartographer, an application available on Google Play for Android. It is designed to determine the object location in real time only indoors. It requires a WI-FI and Bluetooth connection with the necessary base access points and a map of the building pre-entered into the device. There are also specific requirements for the installation and use of the application itself.

An application is being developed by scientists from China using the *ZigBee* (Chen, J, 2018) wireless network to determine the location of a classroom. The purpose of this application is to reduce the time it takes students to search for classrooms, as well as for their seats in these rooms. The system uses wireless sensor networks to monitor vacant seats in the classroom. It consists of a monitoring system in the classroom and an information transmission system. The functions of the available seat monitoring system are to calculate the number of people and to transmit this information to the coordinator (the ZIGBEE system, in this case) to process; then it is displayed on an LCD screen

*MapsIndoors* is a SaaS cloud platform consisting of several components: virtual space (cloud) whose function is to provide input information from the user about the card to be used; *MapsIndoors Data AP* which makes it possible to retrieve maps from other applications as well; and the SDK application - *MapsIndoors app*. A card can be embedded in the application by the developers, for consideration, or used for tests. It functions under the Android and iOS operating systems.

A team from the University of National and World Economy in Bulgaria has been developing a static navigation system on the territory of the university. The system works using two numbers written: a hall number for the starting point and a hall number for the terminal station. The path from point A to point B is drawn in the form of an animation on pre-entered maps of the campus with the hall distribution in each building. The system requires initial knowledge of the distribution of university buildings. The application is attached to the university website as a webpage.

Each of the navigation systems under consideration has its own advantages and disadvantages. In general, we can say that currently the GPS is the most popular and developed Global

Navigation System. It is used by the majority of the navigation devices of motor vehicles. Regardless of what operating system they are designed for, mobile applications also use GPS navigation to guide objects in an unfamiliar environment. Since this is a satellite system whose signal is transmitted by on-land receivers, any unforeseen obstacle, such as tall buildings and trees, can lead to a route deviation.

Based on the considered technologies for indoor positioning of objects, the following assessment can be made in terms of efficiency, price, and information transmission speed:

- Price: analysis has been made of the most popular technologies for wireless exchange of information for determining the location of objects in an unfamiliar environment. With no infrastructure built, WI-FI ranks the highest in terms of equipment costs. However, with a network already in place, WI-FI technology is the most affordable option to build applications for determining location.

- Speed - the information exchange rate depends on the distance that will be measured from the base point to the desired location. Regardless of the fact that UWB supports the highest data transmission rate, the BLUETOOTH technology has the highest close-range speed.

- Efficiency - UWB technology is with the highest accuracy when determining an object location at short distances indoors. The use of W-I-FI technology is appropriate for routes at a greater distance.

An analysis of the existing indoor positioning systems in Bulgaria has been made. It has revealed scarce information about a single company engaged in this activity, but without any details. One of the largest companies in the mining industry with a branch in Bulgaria, *Dundee Precious Metals*, Chelopech, uses special-purpose software products operating with complex mathematical formulae in order to determine the object location via WI-FI connection. Those are expensive programs which the average user would hardly be able to afford.

#### Methods for object positioning

Each of the technologies listed uses specific methods for calculating the distance between objects or for localising the current location. A number of methods exist that can be applied to static or moving objects in- or outdoors. In general, they can be classified as follows:

- **Classical methods for determining the location of objects:**

- Odometry
- Absolute and relative localisation
- Triangulation
- Trilateration
- Inertial navigation

- **Methods for determining the distance of objects based on radio signals** - Other methods for object locating exist that employ the received signal strength (RSS), the angle of arrival (AoA) or the direction of arrival (DoA), as well as the time-of-arrival (TOA) measurements. They are all used to measure the location of objects over a wireless network.

A major problem in determining the route is the movement of the object from point to point, determining its current location, as well as finding the optimum path to the final destination by

avoiding probable obstacles along the route. This problem is related to the location of objects and ways to navigate them.

Depending on the chosen technology for locating or navigating objects, it is necessary to carefully consider the methods that will be used. Very often, a technology allows the application of more than one method, especially in wireless networks.

Having considered methods for object localisation via radio signals, it can be claimed that the combination between RSSI and TDoA is more common for greater localisation accuracy. In cases when there is no direct visibility between customer (tag, marker) and transmitters, it is possible to place an additional adapter for the purposes of amplifying the signal.

Each of the considered methods for localisation by means of radio signals works through the joint application of classical methods for determining location as well. The choice of combination between them depends on the environment whereby they will be applied.

In order to obtain higher localisation accuracy and to calculate deviations, as well as influences from various sources of unfavorable signal interferences in the transmission of data over wireless networks, it is necessary to apply familiar mathematical algorithms.

## Computer application for navigation in a complex of buildings

### Development of methodology

In order to localise an object, its position relative to the surrounding objects needs to be found. If the object is positioned in an outdoor environment, cartographic maps of the area in which it is located can be used. For indoor objects, a map similar to the Fire Evacuation Plans can also be constructed. Such maps are drawn in order to create reference points for finding the position of the object.

Various factors have to be taken into account in the process of developing computer applications for navigating people in an unfamiliar environment. The appropriate navigation technology must be selected according the building. Then, in relation to this technology, the methods must be taken into account that are used by it to calculate the distance and the algorithms for determining the path.

Various computer developments exist that are employed in indoor localisation and are commercial solutions; however, the methodology by which they have been developed is not specified.

The following methodology (Fig. 1) is suggested in Eng. Deliyska's dissertation (Deliyska, D., 2020).



Fig. 1. Methodology for building a computer application for navigation within a complex of buildings

### Digitisation of the map of the building

The object of the current study are the 1<sup>st</sup> and 2<sup>nd</sup> floors of the Laboratory Block at the University of Mining and Geology "St. Ivan Rilski". The available fire evacuation map has been used as a basis and it was updated with the current hall numeration and the refurbishment of some halls.

In order to determine the route along which the objects will move, a map of the building needs to be created.

Each hall visited by students and guests of the building, is considered as an object and is assigned a unique number. Fig. 2 shows a diagram of the 1<sup>st</sup> and 2<sup>nd</sup> floors. The starting point for the building is marked in black, the corridors are in yellow, the stairs leading to the groundfloor and the 2<sup>nd</sup> floor are in orange, and the entrances to the halls and the lecturers' offices are marked in green.

For a clearer view, the height between the floors on the scheme is extended. Such a map could be applied to any type of building.

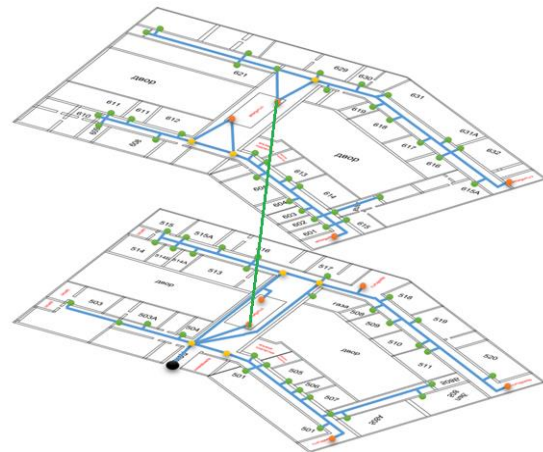


Fig. 2. Schematic presentation of the 1<sup>st</sup> and 2<sup>nd</sup> floors of the Laboratory Block at the University of Mining and Geology "St. Ivan Rilski"



## References

- Alarifi A, Al-Salman A, Alsaleh M, et al. *Ultra Wideband Indoor Positioning Technologies: Analysis and Recent Advances. Sensors (Basel)*. 2016;16(5):707. Published 2016 May 16. doi:10.3390/s16050707
- Brena, Ramon F., García-Vázquez, Juan Pablo, et al. *Evolution of Indoor Positioning Technologies: A Survey. Journal of Sensors (Hindawi)*. 2017;29(3):21. <https://doi.org/10.1155/2017/2630413>
- Cai, X., Ye, L. & Zhang, Q. *Ensemble learning particle swarm optimization for real-time UWB indoor localization. J Wireless Com Network* 2018, 125 (2018)
- Chen, J, C. Megxuan - *Design of Seat Search System in the Classroom Based on Wireless Sensor Networks*. January 2018, *International Journal of Online Engineering (iJOE)* 14(01):119, DOI: 10.3991/ijoe.v14i01.7986
- Deak, G., K. Curran, J. Condell - *A survey of active and passive indoor localisation systems. Computer Communications* Volume 35, Issue 16, 15 September 2012, Pages 1939-1954
- Deliyska, D. - *METHODOLOGY FOR BUILDING COMPUTER APPLICATIONS FOR NAVIGATION IN A COMPLEX OF BUILDINGS – chapter 3 into dissertation, 2020*
- Denis, T. et al. - *Real Time Location System using WiFi. Researchgate, 2006*
- Gu, Y. et al. - *A Survey of Indoor Positioning Systems for Wireless Personal Networks. IEEE COMMUNICATIONS SURVEYS & TUTORIALS, VOL. 11, NO. 1, FIRST QUARTER 2009*
- Hightower, J., G. Borriello - *SpotON: An Indoor 3D Location Sensing Technology Based on RF Signal Strength. UW CSE Technical Report #2000-02-02 February 18, 2000*
- Kucarov, St., - *ZigBee wireless communication networks. Engineering Review Magazine, issue 6,2005 (in Bulgarian)*
- Liu, H. et al. - *Survey of Wireless Indoor Positioning Techniques and Systems. IEEE TRANSACTIONS ON SYSTEMS, MAN, AND CYBERNETICS—PART C: APPLICATIONS AND REVIEWS, VOL. 37, NO. 6, NOVEMBER 2007, 1067 p*
- Nakov, Pr., P. Dobrikov - *Programming = ++ algorithms, books 2012, Chapter 5 Graph Theory, press: Software University (in Bulgarian)*
- Zheliazkov, G., D. Ivanov – *Methods and Technologies for Localization of Dynamic and Static Object. Institute of Information and Communication Technologies – BAS. W O R K S H O P I C T F O R N E W M A T E R I A L S A N D N A N O T E C H N O L O G I E S - N e w N a n o I N T E R N A T I O N A L C O N F E R E N C E R O B O T I C S , A U T O M A T I O N A N D M E C H A T R O N I O S 0 ' 1 3 - R A M 2 0 1 3 O c t o b e r 8 - 1 0 , 2 0 1 3 , B a n k y a , B u l g a r i a ( i n B u l g a r i a n ) .*

## THE MINING INDUSTRY AND THE RECYCLING OF RAW MATERIALS AS AN IMPORTANT ELEMENT OF THE BULGARIAN ECONOMY

**Emil Dimov<sup>1</sup>, Radostina Bakardjieva<sup>2</sup>, Nikola Stratiev<sup>3</sup>**

<sup>1</sup> University of Mining and Geology "St. Ivan Rilski", 1700 Sofia, [emil\\_dimov@abv.bg](mailto:emil_dimov@abv.bg)

<sup>2</sup> Economic Research Institute at BAS, 1700 Sofia, [r.bakardjieva@iki.bas.bg](mailto:r.bakardjieva@iki.bas.bg)

<sup>3</sup> University of Mining and Geology "St. Ivan Rilski", 1700 Sofia, [n.d.stratiev@gmail.com](mailto:n.d.stratiev@gmail.com)

**ABSTRACT.** This publication examines and summarizes the significance of mining industry for the national economy. Here are presented the strengths and weaknesses of the mining industry in the country. The recycling of raw materials and industrial wastes is considered as a possible alternative and an important element of the mining industry and the economy of Bulgaria. Some conclusions about the recycling of raw materials and future development of the mining industry in the country are summarized.

**Keywords:** mining industry; recycling; alternatives; economy; future

### ДОБИВНАТА ПРОМИШЛЕНОСТ И РЕЦИКЛИРАНЕТО НА СУРОВИНИ И МАТЕРИАЛИ КАТО ВАЖЕН ЕЛЕМЕНТ ОТ ИКОНОМИКАТА НА БЪЛГАРИЯ

**Емил Димов<sup>1</sup>, Радостина Бакърджиева<sup>2</sup>, Никола Стратиев<sup>3</sup>**

<sup>1</sup> Минно-геоложки университет „Св. Иван Рилски“, 1700 София

<sup>2</sup> Институт за икономически изследвания към БАН, 1700 София

<sup>3</sup> Минно-геоложки университет „Св. Иван Рилски“, 1700 София

**РЕЗЮМЕ.** Настоящата публикация разглежда и обобщава значимостта на добивната промишленост за националната икономика. Представени са силните и слабите страни на минната индустрия в страната. Рециклирането на суровини, материали и минни отпадъци е разгледано като възможна алтернатива и като важен елемент от добивната промишленост и икономиката на България. Обобщени са някои изводи за бъдещото развитие на добивната промишленост и на рециклирането на суровини и материали в България.

**Ключови думи:** добивна промишленост; рециклиране отпадъци; алтернативи; икономика; бъдеще

### Introduction

The mining industry is one of the oldest ones, it provides many of the constructive elements of the modern way of life in the developed countries. The ongoing demographic growth, the urbanization and the development of the global average class will continue to stimulate the demand of more metals and minerals. The demand will be stimulated additionally by the movement towards the production of low-carbon energy and electro mobility preventing the negative environmental impacts and the social activities of the mining and metallurgy industries is one of the most important sustainability problems, that have to be addressed worldwide (Christman, 2020).

### The mining industry in Bulgaria

The resources and raw materials generated by mining are widely used in areas such as industry, energetics, construction, medicine, electronics and others. Ore and non-ore minerals, as well as fuels, are an important and integral part of the normal functioning of the national and world economy.

After 1991, with the end of communism and newly accepted constitution, it became possible to lease mineral deposits on

state-owned concessions to private investors. The rise in prices of metals (Pb, Cu, Fe) on the market after 2009 makes the development of old and new deposits in the country profitable. The mining industry has given a strong impulse to the socio-economic development in Bulgaria and well-being of the municipalities on whose territory mineral resources have been discovered and mined, for example: Radnevo, Panagyurishte, Etropole, Mirkovo, Chelopech, Kardzhali, Smolyan, Madan and many others. Most mining companies annually donate significant funds for implementation of infrastructure projects and stimulate healthcare, education, culture, sport and social activities in the municipalities where they operate (Ministry of the Bulgarian economy, 2020).

The non-renewable natural resources (mineral raw materials) are base for development of the world economy and human well-being. The continuous growth of demand and consumption of natural resources is directly dependent on the aim to improve quality of life. The process of utilizing huge quantities of non-renewable and renewable resources, subject to anthropogenic impact, leads to their depletion and disturbs the ecological balance. That raises the question of how to apply the complex and the seemingly at first glance unclear concept of sustainable development in the mineral sector. The most

popular definition of sustainable development is formulated in report of the World Commission on Environment and Development (Brundtland, 1987), describing: sustainable development, as one "which meets the needs of the present without compromising the ability of future generations to meet their needs." The most important idea is consideration (and limitation) of human needs with the limit of resources, as well as equality between present and future generations (Denev et al., 2010).

An important and economically interesting aspect of the mining activity in the country are industrial wastes. Currently, the areas occupied by existing landfills for industrial waste in Bulgaria amount to about 70,000 decares. According to a preliminary estimate, the funds needed for closure and reclamation of these areas will exceed 1.2 billion BGN (Pavlov, 2018). Industrial wastes can be considered as a negative side of the extractive industry, reflecting on the environment, as well as a significant "loss" of useful components and maintenance costs for industrial waste landfills or tailings. On the other hand, with the development of technology in recent years, industrial wastes have become an effective way to extract useful components, to recycle and use ores previously considered "loss" or waste.

## **Strengths of the mining industry**

Without the extraction of mineral resources, the life of mankind is impossible. The mining industry is at the centre of all other industries and is an important factor for the economic stability and energy independence of any country with mineral resources. Constantly during its development, humanity has always sought access to subterranean resources and has had the need to extract them. Metallurgy, chemical industry, machine building, construction, transport, higher class technology and others are impossible without raw materials - the products of the mining industry. In Europe, industries dependent on access to mineral resources, annually generate € 1,324 billion in added value and provide employment to approximately 30 million people (Ministry of the Bulgarian Economy, 2020).

### **GDP and employment**

About 5% of our country's GDP is due to the mining industry. Most of the people - nearly 25,000 - are directly linked with this industry, 120,000 are indirectly connected, and those related to the supply of materials and others are about 800,000 workers operating in this sector. The mining industry of the past, now and in the future is the backbone of our economy, because without extraction of raw materials, coal, etc., we cannot exist. In addition, the mining industry provides both premises for investments in the country and also high salaries for its employees, as well as preservation of the population of small settlements and development of these regions. In general, the successful development of the mining sector in the country creates conditions and premises for the stay of young qualified personnel in Bulgaria.

### **Investments, new technologies, quality**

Companies extracting minerals and raw materials are among the few aiming towards and working on the application of various innovative practices, methods and models. They lead to increasing the competitiveness of their products and achieving better financial and economical results. Among them

are: innovations of processes related to environmental protection; innovations of processes related to improvement of work organization; innovations related to increasing the efficiency in the utilization of natural resources (Galabova, Trifonova, 2018). Bulgaria is among the leading European countries in terms of the share of value added created by those employed in the mining industry in the national economy. The share of the value added of the extractive sector from the value added of the entire industry of Bulgaria in the period 2000-2017 fluctuates between 6% and 12%, which confirms its significant contribution for the country (Galabova, Nestorov, 2019). Mining companies in Bulgaria distinguish themselves with relatively high productivity, which is nearly 2.5 times higher than the average industry in the country. Compared to European ones, for the most part the Bulgarian companies are proven to be profitable and competitive, offering quality and convertible products on international markets (Galabova, Nestorov, 2019). This is due to significant investments in tangible fixed assets, as for the last 18 years the leading mining companies have invested over 4 billion BGN in technological renewal, which provides improved economic and environmental outcomes, as well as improved performance in terms of health and safety. Innovative leaders in these aspects are Assarel-Medet AD, Ellatzite-Med AD, Dundee Precious-Chelopech AD, Gorubso-Madan, Maritza-East Mines EAD and others. They have implemented international standards for quality management, environmental protection and occupational safety.

### **Corporate social responsibility**

There is an increase of attention to corporate social responsibility (CSR) by more and more mining companies in Bulgaria understanding its importance and benefits. This results in them taking responsibility for development of their employees, as well as for their impact on environment and society. Social responsibility includes both economic and environmental responsibilities. Stakeholders are not only within the company, but also outside of it. The broader goal of corporate social responsibility is to create a higher standard of living for people inside and outside the company, while maintaining its profitability. In time, this concept has become a successful business strategy for sustainable development, which helps companies not only to increase their influence on the market, but also to create a positive public image. People today are tolerant to companies that participate in charitable initiatives and support cultural and social events. Also respected are the efforts to protect the environment through the recycling of unnecessary consumables (toners, paper, glass, plastic packaging, etc.), the introduction of energy efficiency measures and treatment or disposal of hazardous industrial waste. On the other hand, employees are looking for employers who offer them not only good pay, but also a suitable social benefits for them and their family members. Thus, with slow steps and regardless of its various forms and manifestations, corporate social responsibility is gradually taking over companies around the world (Petrova et al., 2012). The tendency of responsibility continues to develop towards employees, nature and society. This is a positive aspect of the mining industry and an important part for the future success of this business. Moreover, among the challenges, the industry faces are the wide range of administrative procedures and the large number of permits related to the so-called "work license" obligation documents for the trust of the community

towards companies to do mining extraction activities (Petrova, 2019).

## **Weaknesses of the mining industry**

### **Risk (high risk - high reward; Investment, exploitation and time-bond)**

Long investment process term from the exploration to realization of mining projects, i.e. extremely long economic life of investment projects with a long investment period (Mitev, 2004; 2014). High market risk, especially for exchange products. Natural risk associated with difficult predictability of quantitative and qualitative indicators of geological supplies and mining and technological indicators of deposits (Mitev, 2004; 2014), as well as risk of natural disasters. There is also a risk of lack of market balance (supply / demand) for construction materials due to unbalanced processes for demand and exploration of these materials. Social risk, which is associated with significant investments to ensure healthy and safe working conditions for employees. Significant investments in environmental protection and reclamation. Significant risk of unfair competition in the form of illegal extraction activities. It is important to note the risk of lack of a clear and transparent regulatory framework related to various aspects of natural resource management (Ministry of Economy of Bulgaria, 2020). For the mining industry, risk is based on large initial investments in localization and preparation for operation of a certain deposit. The long time period before the exploitation of the deposit and the return of the investments, predetermines the high market risk in the branch. Generally, the mining business is high risk and accordingly, very profitable (with justified risk).

### **Ecology**

In a global aspect, the humanity existence is based on the development of mining. While, this activity causes demolitions, subsidence, erosion processes, reversible and irreversible pollution of top earth layers. It generates huge amounts of waste. Parts of mining areas in our country are occupied by such polluted and impaired terrains (Pavlov, 2018). Extractive industry has a negative impact on the environment, for reducing the damage, adequate environmental measures must be applied by the companies developing mining activity in Bulgaria. Economically, this means damage to the environment as well as a loss of time and money in order to limit and reduce the negative anthropogenic impact through mining processes and after its completion.

### **Recultivation**

Generally, recultivation is a system of engineering-ecological, ameliorative, agro-technical, forest management, planting and other activities aimed towards restoring of damaged terrains, soil cover and fertility to create locations with different purposes: agricultural, forestry, sanitation, recreational and others. A number of technological solutions have been developed and are being implemented for restoration and recultivation of terrains and soils impaired or polluted due to ore extraction and processing. The preservation of lands exposed to anthropogenic impacts is controlled with a number of laws and regulations in line with European directives (Pavlov, 2018). The ecological mark and the costs of recultivation are among the weaknesses of the mining industry. The damage to nature and the consequences that we are trying to limit are the most

significant weaknesses of mining industry in Bulgaria and around the world. From an economic point of view - these are necessary and major financial and time costs in order to reduce the anthropogenic impact on nature. Mining companies in the country comply with a number of laws and requirements and are making all the necessary efforts to reduce the negative impact of extraction activities on nature.

## **Future perspectives and tendencies of improvements for the mining industry as a part of the economy**

Recycling of mineral resources should be considered as a process, which increases global supplies and offers significant potential in certain conditions. This is evident from a number of well-known facts. In modern mining methods and technologies - millions of tons of gaseous, vaporous, liquid and solid waste pollute the environment. In some types of raw materials, only 2% become useful products, and the remaining 98% remain as technogenic accumulations. Generally, from the annual production of about 25 billion tons of various mineral raw materials results in no more than 1.5 billion tons of effective production. Approximately two thirds of the extracted from earth's depths mass, accumulates for long periods of time in various landfills. Recycling technologies are being developed at a rapid pace and are becoming a mandatory part of mining companies's development programs. If the appropriate technologies are available, secondary production may mean that irrelevant and uneconomical to use low class raw materials that were impossible to use in the past will be available for recovery in the future. This helps to delay the inevitable depletion of resources and confirms the arguments of the paradigm for sustainable development. Aside from the problem of environmental damage, associated with mining should be noted the fact, that lower class of resources can also become a major argument in fulfilling the demand and aspiration to retain the economic and social standard of living.

Recycling of the mining industry wastes becomes possible due to improvement of technologies. For example: 1 tons of steel can be extracted from 2.5 - 4 tons of ore, the same amount can be extracted from 1.1 tons of ore wastes. Another appropriate example is that 1 tons of purified copper can be obtained from 300-500 tons of ore, or from 1.2 tons of ore wastes containing copper. The examples indicate significantly higher efficiency and lower energy consumption in the extraction of raw materials by recycling mining waste compared to standard extraction and processing of ore (Grigorova, Nishkov, 2015). The differences in efficiency and energy consumption vary for respective raw materials and the results are not always as impressive as in the given examples. It should be noted that the recycling of mining waste and raw materials is a great alternative for the mining branch. A number of countries (such as China) are considering and are taking advantage of this opportunity for efficient use of waste to generate profits and to reduce the environmental damage. Annually China purchases and recycles large amounts of mining waste. Recycling of resources, raw materials, as well as industrial and household wastes is an alternative, which may ensure the normal future existence of humanity.

## Conclusion

Society and technologies should strive to develop new rational alternatives that ensure equality between current and future generations in terms of non-renewable natural resources (Denev et al., 2010). The extractive industry, with its strengths and weaknesses, remains a significant element of the national and global economies.

The focus of extractive industry should be not only on exploration and exploitation of new deposits, but also on the opportunities for enrichment and recycling of raw materials, as well as on the efficient use of wastes. Investments in the construction of new factories for recycling of raw materials and for processing of industrial wastes are a necessary alternative and may prove to be an important strategic move for the future economic development of Bulgaria.

## References

- Brundtland, 1987. Our Common Future - Call for Action. – *Environmental Conservation*, Vol. 14, No. 4 (Winter 1987), pp. 291-294.
- Christman, P. 2020. Mining Industry. – *Encyclopaedia of Renewable and Sustainable Materials*, vol. 5, p. 433-443.
- Denev, B., I. Grigorova, V. Velevev, I. Nishkov. 2010. Model of the Fixed Stock for Sustainable Development in the Mining Industry. – *Annual of the University of Mining and Geology „St. Ivan Rilski“*, 53, Part 4, 39-52 (in Bulgarian with English abstract)
- Grigorova I., I. Nishkov. 2015. *Prerabotka i Reciklirane na Tehnogenni Surovini*. Publishing House „St. Ivan Rilski“, Sofia, 279 p. (in Bulgarian)
- Galabova, B, N. Nestorov. 2019. Role of the Extractive Industry for the Bulgarian Economy. – *Minno delo i Geologia Journal*, vol. 5, 18 – 24 (in Bulgarian with English abstract)
- Galabova, B, B. Trifonova. 2018. Innovation and Technological Development as Strategic Advantages of the Mining Company. – *Sbornik s Dokladi ot Meždunarodna Naučno-priložna Konferencija „Industrialen Biznes i Predpriemačestvo – Inovacii v Naukata i Praktikata“*, Ikonomičeski Universitet - Varna, 247-260. (in Bulgarian with English abstract).
- Mitev, V. 2004. Type of Risk and Methods for Risk Evaluation in Investment Projects for a Mining Industry. – *Annual of the University of Mining and Geology „St. Ivan Rilski“*, 47, Part 4, 49-53 (in Bulgarian with English abstract).
- Mitev, V. 2014. *Upravljenie na inovaciite i investiciite*. Avangard Prima, Sofia, 159 p. (in Bulgarian)
- Pavlov, P. 2018. Impact of the Mineral Sector on Lands and Soils. Subsequent Sustainable Management. – *Minno delo i Geologia Journal*, vol. 3, 19-23 (in Bulgarian with English abstract)
- Petrova, V., D. Kostova, V. Velevev. 2012. Corporate Social Responsibility – Factor for Sustainable Development. – *Annual of the University of Mining and Geology „St. Ivan Rilski“*, 55, Part 4, 49-53 (in Bulgarian with English abstract).
- Petrova, V., 2019, Research and analysis of the state of socially responsible policies of mining companies through the eyes of local communities. – *Journal of Mining and Geological Sciences, University of Mining and Geology „St. Ivan Rilski“*, 62, 4, 21-26 (in Bulgarian with English abstract)
- Ministerstvo na Ikonomikata na Bălgarija. 2020. *Osnovni Principi na Nacionalnata Strategija za Podzemnite Bogatstva i Ustojčivoto Razvitie na Bălgarskata Minna Industrija*, Ministerstvo na Ikonomikata na Bălgarija. (in Bulgarian) - [www.mi.government.bg](http://www.mi.government.bg).

## DECISION MAKING PROCESS IN PEACE TIME WITH REAL RISKS AND THREATS FOR SECURITY

**Georgi D. Dimov**

*"G. S. Rakovski" National Defence College, Bulgaria, 1504 Sofia*

**ABSTRACT.** In a state of emergency it is reasonable to raise the question of using the Armed Forces. The answer is directed towards actions requiring the use of weapons; however, those partially reflect the available military resources. The commanding structures of the military undoubtedly have the capability to apply all the necessary management procedures, and perform them in a non-military setting. These capabilities are part of the managerial capacity of the state and are appropriate to be used in a state of emergency. The report defends the possibility of increasing the effectiveness of managerial decisions in an active state of emergency through the process of planning in the Armed Forces.

**Keywords:** State of emergency, decisions, features, assess, efficiency

### ВЗЕМАНЕ НА РЕШЕНИЯ В МИРНО ВРЕМЕ ПРИ РЕАЛНИ РИСКОВЕ И ЗАПЛАХИ ЗА СИГУРНОСТТА

**Георги Д. Димов**

*Военна академия „Г. С. Раковски“, 1504 София*

**РЕЗЮМЕ.** При извънредно положение е резонно да се повдигне въпроса за използване на въоръжените сили. Отговорите се насочват към действия, изискващи употребата на оръжие, което частично отразява същността на ресурса, с който те разполагат. Органите за управление на въоръжените сили притежават несъмнени способности за прилагане на разнообразни управленски процедури и много бързо биха могли да ги изпълнят със съдържание от невоенно естество. Тези способности са част от управленския капацитет на държавата и затова е целесъобразно да бъдат използвани в трудните за страната условия. В доклада се обосновава възможността за повишаване ефективността на управленските решения при въведено извънредно положение чрез процеса на планиране във въоръжените сили.

**Ключови думи:** извънредно положение, решение, оценка, ефективност

### Introduction

The state of emergency imposed in our country due to the epidemic situation caused by the spread of COVID-19 has created conditions for wide debates on the decisions of the Government and the work of the newly established National Operations Staff. Many of these measures have been identified as extreme and incompatible with the peaceful living and working conditions of society. There were doubts about the legitimacy of the governing bodies and the effectiveness of the actions taken. The government used various principles and models to justify one or another of its decisions, which ranged from purely peacetime practices known to all citizens, to alleged wartime ones, instilling fear and insecurity among the people. Urgent measures had to be implemented, requiring special legislation balancing consent and coercion.

It is necessary to understand the essence of the state of emergency, as it forms an intermediate legal space in the legal world, where a number of contradictory principles for decision-making and management of the country's resources overlap. There is a difference between governance principles in peacetime and in times of emergency, martial law or state of war. And mixing the guiding principles for decision-making distances the decisions from the objective conditions of the situation, increases subjectivism and therefore can lead to extremely large losses of people, raw materials and financial resources, even endangering national security, which can slow

down or stop the development of the country. It can be argued that the rationale behind the state of emergency is rooted in the governance model rather than in the circumstances and reasons for its imposition. In this context, modern military planning models offer good practices for assessing the effectiveness of decisions taken, which should not be overlooked.

The purpose of this report is to propose good practices from military decision-making models to increase the effectiveness of governance in the face of real risks and threats to the country's security in peacetime.

Crises, conflicts and disasters usually create atypical, extraordinary conditions for decision-makers, especially given the great dynamics of change in the environment. Limited time and unpredictability impose serious difficulties on the government, which can be overcome only with unpopular measures close to wartime conditions.

Extraordinary conditions are generally accompanied by the effect of many subjective factors, which can both favor the management process and create additional difficulties. Different ambitions of the representatives of the governing bodies are manifested, formed mostly by the idea of changing the prerogative powers. Moreover, decisions sometimes have to be taken without a clearly defined hierarchy of management structures and a lack of competence with regard to exceptional circumstances. In such conditions, opportunities for realization of personal passions are revealed against the background of socially significant goals, which hides additional risk. To reduce

the problems of a subjective nature, we can again take advantage of the experience in the system of command and control of the armed forces. Military procedures, especially after the introduction in our country of NATO practices for planning operations, provided a decision-making environment with guaranteed competence and active position of the participants in the management process. More importantly, the decisions follow a clear logic and ensure transparency and trust in the management system.

The state of emergency is perceived as a safeguard against security threats and risks. Emergency has different faces given the nature of the threats that create it and the suitability of the management system to deal with specific threats. Under normal conditions of social development, there are risks and threats, but in principle it can be argued that the state maintains resources and capabilities with which it could systematically neutralize them. When the country's security guarantees are assessed as insufficient for a specific threat to national interests or for the functioning of the national security protection system, the available resources are used by priority and the management system creates conditions for acquiring new, necessary resources to deal with the existing problems. In fact, the situation calls for concrete, new capabilities based on a solution that, due to the obvious link to the national security system, may require the imposition of emergency measures. Therefore, the decision concerns both the executive and the legislature in the state, because it is in principle associated with threat to society or weakness of the management system.

Extraordinary circumstances exacerbate the sensitivity of citizens, political parties and government bodies in the country. It should be noted that each specific threat creates conditions for a number of accompanying negative phenomena that cannot be ignored by decision makers. The following can be specified:

- aggravation of political relations between the ruling party and the opposition;
- increase in crime;
- increasing attempts to influence the society by external organizations on ethnic and religious grounds;
- decline in economic growth or economic crisis;
- increase in corruption;
- outbreaks of infections, epidemics and pandemics, etc.,

which, together with the main threat as a whole or in combination with each other, can lead to significant social changes. Therefore, in a state of emergency, the state is allowed to take unconventional or unpopular actions, including with its law enforcement agencies. It is possible to create new structural elements with special prerogatives to manage and carry out tasks in the interest of the national security system.

Under exceptional conditions, all sources of aid are used to compensate for the lack of resources, either from donations or by provoking the economic entities in the country to transform their production towards the necessary material resources. In an emergency, it is important to unite the efforts of the whole society for a common understanding of the problems and reaching the desired state. That is, the decisions for management of public processes under extraordinary circumstances concern both the resources of the country and many organizational issues in a very short time (as a rule, decisions are made in short time). Therefore, an action may not be justified from all sides, but in any case the division of

responsibilities for its implementation and the means to achieve the common goal must be clear. In this context, a key issue in emergency decision-making is compliance with the principle of efficiency and compromise on divergent objectives in the name of common national interests or priorities. That is, a decision-making mechanism is needed in the event of a state of emergency.

The analysis of the military decision-making models shows that the requirements for efficiency can be combined with diverse sources of resources and services. These models support an ongoing process of review and feedback on results, which assesses the effectiveness of actions and provides an opportunity to adapt (change) to extraordinary circumstances. Procedures are proposed for evaluating the results in many unknown parameters of the existing situation. Trends for changing the conditions at a certain desired end state are formulated, which assess the various effects of the actions taken.

A strength of military models is the implementation of a "Comprehensive Approach" to operation planning. This approach is widely applied in NATO and takes into account both the extraordinary conditions in military operations and the political consensus of the Allied members to achieve a common goal. A number of researchers have demonstrated the leading role of the NATO decision-making model in terms of "its ability to join forces and determination to act" (Nedyalkov, 2019). The systemic characteristics of the NATO decision-making model overlap with many conditions and factors in the analysis of the changing environment, which is why it can be argued that it is applicable in an emergency situation. Moreover, this model offers opportunities to study new, unknown circumstances in order to create a common and unified understanding of the situation in its political, military, economic, social, informational and infrastructural domains.

Modern models for decision-making in the military sphere are not isolated from the social life. In terms of military policy, information and infrastructure, they are quite flexible and applicable to various crisis or emergency circumstances. Therefore, the system of management of the armed forces and the available resources can be used for the purposes of governance not only under martial law or in war, but also under peaceful conditions with a high degree of risk, which usually causes the imposition of a state of emergency. Thus, the idea of applying military models for decision-making under a state of emergency has its logical justification. Possible fears that the military models are oriented mainly towards the achievement of the set goals, regardless of the funds spent, i.e. inefficient, are unfounded. In the context of military planning, the process of evaluating the effectiveness of actions has a certain place. The general management process sets several reference, control and end states, which mark the unacceptable and acceptable conditions, goals and effects of the actions taken. In this process, the evaluation of effectiveness is continuous and determines both the objectives and the cost-risk analysis in terms of results.

Diagram 1 clearly shows the links in the evaluation process that can be used to determine the effectiveness of the actions taken. In fact, measuring change through the results achieved allows informed decisions to be made. The principle is that "what can be measured can be managed" (NATO operations assessment handbook, 2015).

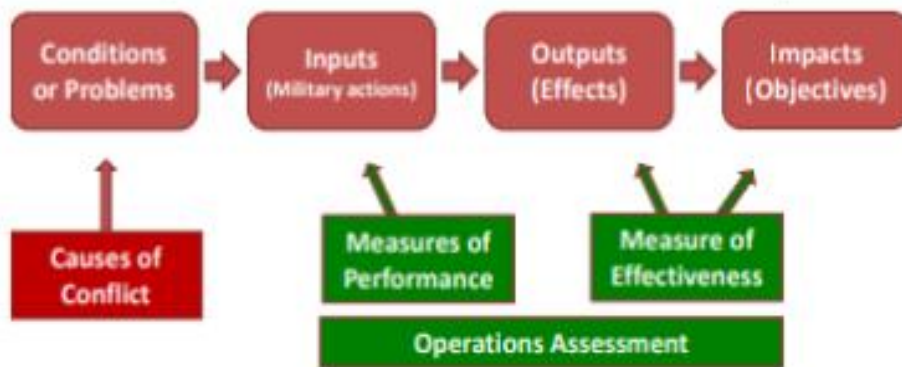


Diagram 1. Place of assessment in the NATO operational planning process

Military practice proves the applicability of NATO decision-making model for control of targeted cyclical and continuous actions (measures), which are related to studying changes, adapting plans and making recommendations for building new capabilities. In other words, it is logical that under a state of emergency a previously designed plan will be used or a new plan will be worked out in a short time. This practice does not necessarily have to be borrowed from one of the models of armed forces management, but it is applicable when it comes to assessing the effectiveness of measures in the vague and rapidly changing emergency situation.

The above considerations fully support the creation of the National Operations Staff in connection with the state of emergency in our country, introduced to limit the spread of COVID-19. The structure itself, called "staff", is of military origin and is oriented towards decision-making and planning of targeted actions to achieve the desired end state. It is logically headed by a military given the extraordinary conditions for making a decision. The information processed by the National Operations Staff is indicative of the functions assigned to it as a top-level governing body, namely:

- organizes all actions of the institutions in the country related to the health dimensions of the COVID-19 pandemic;
- collects, summarizes and analyzes data on the current health of Bulgarian citizens and data from other countries in their fight against the coronavirus;
- coordinates the actions of the institutions and allocates the available resources related to the causes of the emergency situation;
  - controls the results achieved;
  - assesses the changes and prepares forecasts for the health condition of the nation;
  - informs the media and the public about the decisions taken and their effects.

Other functions may be imposed on the National Operations Staff as well. But it must be clear that the work model of the staff is invisible to the public and must remain so. Of course, any requested information is provided in full and with accurate data. Many of the activities follow the operational nature of the changes in the emergency situation and cannot be discussed in the general public. However, the results of these activities are subject to verification and comparison.

These clarifications are in view of the criticism in the media of the National Operations Staff regarding their way of decision-making and especially the doubts about the correctness of the distribution of resources (available and necessary) between the various subjects in the public space. There is always room for

criticism, but for the purposes of the state of emergency and the level of governance that the Staff embodies, the results are undoubtedly timely action, fair treatment of the public representation, purposefulness and legality of the measures and, last but not least, effectiveness.

The problems are mostly in organizational terms. By analogy with the staffs of the armed forces and the NATO model for planning joint actions, certain management procedures and algorithms can be applied to facilitate the work of the National Operations Staff. So far so good, but the extension of the state of emergency will inevitably lead to exhaustion of the experts, and any exhaustion leads to mistakes. Given the high level of governance, errors can be irreversible, i.e. the benefits will be eliminated from the losses to the public. In this regard, the Staff may form a working group to assess measures and actions during the state of emergency, which will implement the procedures of the "Comprehensive Approach" to NATO planning. The idea is to facilitate the work of the Staff with a systematic analysis of the conditions during the state of emergency, the actions of the institutions and their effects. A number of the algorithms used can be optimized, mostly by analyzing the critical conditions and creating a matrix for the interaction between the different actors.

Of course, such a proposal is accompanied by some trade-offs in the operation of the country's governance system. Heavy (large) and therefore cumbersome management structures claim greater accuracy of decision-making information, but this does not mean that the decisions themselves automatically become more effective. For example, a number of publications (Slavov, P.) dispute the legitimacy of the National Operations Staff or argue the idea of organizing the fight against COVID-19 from the bottom up of the health system in our country (Todorov, G.). That is, the state should consult epidemiologists and infectious disease specialists from the "first line" of contact with the infection, given the greater accuracy of information for decision-making. However, this is unacceptable for the governance process, because even the most accurate information in the health domain is not enough to make decisions taking into account the future of society. The country needs a large picture of the state of emergency in its political, economic, social, informational and infrastructural aspects, along with health information about the coronavirus, which can only be seen in a top-down management system. Public administration is a collective image of governance in all social systems and it is not acceptable to eliminate important functions of public life at the expense of one of them. The National

Operations Staff is a hierarchically positioned body of government solely for the purposes of the state of emergency.

Planning is the more important issue. We need a plan for the work of the institutions under the conditions of the state of emergency, which is mainly a product of the Staff. Once the measures and actions during the state of emergency are determined by law, i.e. the decision has been made, the Staff is obliged to develop a plan for synchronizing the actions of the institutions and assessing their effectiveness.

Information is generally collected through the usual channels, but the plan should regulate the way of reporting the measures and actions. Relying on journalistic questions to evaluate results is highly questionable. Professional arguments are needed for each of the tools used with performance and effectiveness measures. Example parameters such as:

- measuring units;
- scale of variation;
- categorization of the nominal and interval data;
- upper and lower limits;
- sources of information;
- method of data collection;
- responsible individuals for the information;
- frequency of reports, etc.

The plan provides measurability in quantitative and qualitative terms and can favor evaluations with subsequent review and introduction of additional metrics. It reduces the conflict in public discussions and provides peace in governance, because there are insurmountable contradictions regarding the desired and achieved states of the managed social system.

It is clear that not everything can be measured or that the effort to obtain certain information may outweigh the benefits, making it unsuitable. In this regard, the plan disciplines the management by extracting the practical information, which justifies the measures and activities taken.

Planning organizes the information and reduces the possibility of its misuse. It is one thing to collect data from enforcement agencies, it is another thing to evaluate effectiveness. Most comments concern the objectivity of the data, which concern specific sources (actors), the method of processing and the order of provision. The beginning, intermediate changes and the end state are taken into account. It is more difficult to analyze data in processes and functions, where they are not a mechanical sum, but are systematically linked. Moreover, modern management is committed to analyses of complex systems that are built of systems and evaluations are never unambiguous. In this context, without a general plan of measures and actions under emergency decision-making circumstances, contradictions are inevitable.

The plan allows for the governance to be disciplined. Specific methods for collecting information are adopted and the risk of provocations is reduced. It is important where the source of information is located, when the data is analyzed, who makes the conclusions and assessments, how the results of the analysis can be included in the control signals, orders, directives, etc. It is extremely important to maintain the well-known among the military circles "synchronization matrix", with the help of which in the name of common goals and objectives it is possible to allocate efforts and resources and organize interaction.

It is not a question of resorting entirely to wartime planning in an emergency situation, but in the presence of a resource for

staff work in the armed forces, it is prudent to use it to support the activities of the National Operations Staff. Moreover, military experts in operational planning use unclassified software products for data processing. They have experience working with various civil organizations in the context of peacekeeping operations and the implementation of the Comprehensive Approach. Such assistance would certainly increase the efficiency of governance. Because planning is a demonstration of the governance capacity that is needed, including in time of emergency caused by health problems among the population.

In the case of COVID-19 the main connection is between the medical expertise and the governance capacity in the country. The pandemic has proved its negative impact on vital systems that ensure the security of citizens. The main effects of the spread of the infection turned out to be subject to many factors, in addition to those shaping the country's health system. The economic, social and even psychological effects altogether are no less important. On the contrary, some of them have lasting consequences for the development of society. That is why decisions at the highest level are difficult. In an emergency, they are even more difficult given the fact that the goals of governance are related to assessing the opinion of people from different groups, living standards, religious affiliation and culture, in a situation fraught with dangers for society as a whole.

## Conclusion

Modern military planning models are a proven source of situational awareness, which is the basis for effective decision-making. The methods used to evaluate the actions offer a good basis for qualitative analysis of the information. Most importantly, the personnel of the control bodies of the armed forces is trained, capable of applying a variety of management procedures, even of a non-military nature. These management capabilities are part of the governance capacity of the state and therefore it is appropriate to use them in time of emergency situations. It is good for the whole society to know that the armed forces are not only an expensive instrument of violence. They have a streamlined, flexible and effective management system for critical social conditions. During a state of emergency, this system must be seen as a national asset and a source of resources.

## References

- Nedyalkov, N. Strategic Deterrence in the Context of the Contemporary Security Environment. Rakovski National Defense College, Military Journal, issue 1-2, 2019. p. 44.
- NATO OPERATIONS ASSESSMENT HANDBOOK. 2015, p. 0-2.
- Slavov, P. The paradoxical National Operations Staff - a mega-organ or a planned scapegoat? [https://m.offnews.bg/news/Analizi-i-Komentari\\_65/Paradoksalniiat-shtab-NOSht-megaorgan-ili-planirana-izkupitelna-zh\\_727392.html](https://m.offnews.bg/news/Analizi-i-Komentari_65/Paradoksalniiat-shtab-NOSht-megaorgan-ili-planirana-izkupitelna-zh_727392.html)
- Todorov, G. Why don't we prove coronavirus in our country? <https://czpz.org/>

## HYBRID DISTANCE LEARNING DURING COVID-19 IN BULGARIA

*Hristina N. Dobreva*

"G.S.Rakovski" Military Academy, 1504 Sofia; h.dobreva@mdc.bg

**ABSTRACT.** COVID-19 is a time of challenge for the educational system. System's adaptation is due to already built platforms but a single approach of the universities is missing. The created apparent chaos however proves that it can respond to the requirements of the Ministry of Education and the speed of adaptation of teachers and students depends on their technical knowledge and access to Internet. The paper follows the recommendations for hybrid or mixed learning from the book and practice of Martha Cleveland-Innes of the University of Athabasca (Guide to Blended Learning), and is, as well, a result of my participation in a distance course on the subject, aimed towards improving the education of teachers from all over the world and mostly towards developing countries. The thesis is that the hybrid or mixed learning in the version of completely applying a distance model of education is most suitable for the time of the pandemic. Universities in Bulgaria have been examined as well as the systems that they apply. A concrete model of mixed education after the example of the Military Academy has been offered. Different educational platforms used in Bulgaria have been compared.

**Keywords:** educational system, hybrid learning, Bulgaria

### ХИБРИДНО ДИСТАНЦИОННО ОБУЧЕНИЕ ПО ВРЕМЕ НА COVID-19 В БЪЛГАРИЯ

*Христина Н. Добрева*

Военна академия „Г.С.Раковски“, 1504 София

**РЕЗЮМЕ.** COVID-19 е време на предизвикателство за образователната система, но това не означава, че е време на криза, защото самата система се пригоди достатъчно бързо. Адапцията и се дължи на изградени вече платформи, но липсва единство в подхода на университетите. Така получилият се привиден хаос обаче доказва, че може да отговори на изискванията на министерството на образованието, а скоростта с която преподаватели и студенти трябва да се адаптират зависи от техническата им грамотност и достъпа до интернет. Темата следва препоръките за хибридно или смесено обучение от книгата и практиката на Марта Кливланд Инес от Университет Атабаска (Guide to Blended Learning), както и е резултат от индивидуалното ми участие в дистанционен курс по предмета, целящ подобряване обучението на преподаватели от цял свят и най-вече насочен към развиващите се страни. Тезата е, че най-пригодно за времето на пандемията се оказва хибридно или смесено обучение във версията на напълно дистанционен модел. Разгледани са университети в България и системите, които те прилагат. Предлага се и конкретен модел на смесено обучение по примера на Военна академия. Сравнени са различните платформи за обучение, използвани в България.

**Ключови думи:** образователна система, хибридно обучение, България

### Introduction

The aim of the paper is to prove the viability of the hybrid distance education during COVID-19 in Bulgaria. Such a design of education has been offered in the example of the Military Academy in Bulgaria as a combination of synchronous and asynchronous activities.

The analysis shows that a variety of platforms have been used at the universities in Bulgaria and these platforms have been compared. Despite the apparent chaos, the importance of the paper is in coming to the conclusion that first, the educational system in Bulgaria has successfully adapted to the COVID-19 challenge and second, that the choice of LMS or computer apps depends on the individual choice and needs of the university.

### A sample design for hybrid education

#### Design Parameters

The resources that are required include classrooms at the Academy, as well as the system of academic communication of the Academy (based on a Content Management System),

composed of internet (site of the Academy), extranet (MS Office 365, BlackBoard, student accounts, shared documents) and intranet<sup>1</sup> (internal communication).

#### Design Plan

Table 1: Design plan of hybrid education

Activity description	Technology requirements/OER	Teaching/facilitation requirements
Online, asynchronous activity	BlackBoard LMS	-materials for Blackboard accessible in extranet -coordination with administrator to deal with account issues -uploaded summaries of lectures -weekly discussion board -quizzes using MS Forms

<sup>1</sup> It is not used for teaching/learning purposes.

Synchronous online and face-to-face activity	MS Teams-Office 365	-videos and digital bulletin posted in extranet about work with MS Office - coordination with administrator to deal with account issues and group membership issues for MS Teams -conducting guided discussions both online and in class
--	---------------------	--

### Blend structure and activity integration

There are **two versions of the blend**: one is when the course is fully online and the other uses both online and face-to-face classes. In the first case-the fully online model, there is a combination of both synchronous (online guided discussions in the form of tutorials) and asynchronous (reflexive reading of lecture materials followed by quizzes as well as a weekly discussion board) activities. In the second case-that resembles a blended block model, there is a combination of both online study and face-to-face discussion. The difference from the traditional blended block model is that lectures are online and tutorials are face-to-face. The intention is to use the Community of Inquiry (CoI) theoretical framework during the discussion sessions through: 1) asking questions to suggested readings or phase of active inquiry to find relationships between concepts and variables, 2) finding answers themselves through guided discussions, 3) discussion of a topic where learners identify questions, methods, problems and answers. The structure resembles that of a blended online class model and a flipped classroom<sup>2</sup> as a version of it. It can easily transform in blended MOOC (massive open online course) if the course starts to be offered for other institutions as well. Depending on the access of technology of students a SAMR (substitution, augmentation, modification, redefinition to describe how technology can be progressively integrated into the classroom<sup>3</sup>) model may be applied for the online form for example as a final paper requirement of the course. Wikis (or collaborative writing spaces constructed around interlinked webpages<sup>4</sup>) could also be part of this final course requirement.

### Design Rationale

The design could be applied both during pandemics/natural disasters that require strictly a distance type of education and as a supplement of the normal face-to-face discussions in class. This flexibility of the design makes it adaptable to different teaching requirements. In addition, it encourages both thoughtful reflection activities and interaction through discussions where competition and collaboration are stimulated. The design uses a student centered approach.

<sup>2</sup> The flipped classroom reverses the traditional class structure of listening to a lecture in class and completing homework activities at home. Students instead have a video lecture online and come to class to work as a group. p.16 Guide to...

<sup>3</sup> p.18 Guide to...

<sup>4</sup> p.41 Guide to...

## Results for the Universities in Bulgaria

In the sphere of higher education, for the purposes of the current paper, the decisions of more than 20 universities in Bulgaria have been examined. The starting point is the list of higher education institutions on the website of the National Agency for Assessment and Accreditation. As a result, it has been established that all of them have been conducting distance or online education but there is not a uniform criteria for efficiency assessment as the reliance is upon different virtual platforms and instruments. Several main platforms stand out: Zoom, Moodle, Microsoft Teams, Classroom Google, Meet Google, BigBlueButton, Skype, Blackboard, E-learning.

Among the first that have introduced such a learning by means of an Order of March 9, 2020 are the Georgi Rakovski Military Academy and the American University in Blagoevgrad, on March 13-the St. Kliment Ohridski Sofia University and the Todor Kableshkov Higher Transportation School, on March 16-the Nikola Yonkov Vaptzarov Naval Academy, Varna and the University of National and World Economy, on March 19-Technical University Varna, on March 20-the Varna Free University and the Stara Zagora Trakia University, on March 25-the Paisii Hilendarski Plovdiv University, on March 30-the Luben Karavelov Higher Construction School, Sofia[9].

With a letter № 9104-47/14.04.2020 to all universities, the Minister of education and science recommends the exams and councils of the collective bodies to be conducted via electronically based platforms BigBlueButtons and Microsoft Office 365 with a videoconference connection option. Despite that, a big part of the universities have introduced different systems for online application and submitting exam applications.

- Zoom has been used by the Agrarian University. Moodle has been used by: the Burgas Free University [10], the Todor Kableshkov Higher Transportation School [11], the New Bulgarian University, the St. Kliment Ohridski Sofia University [12], the Stara Zagora Trakia University and others.

- Microsoft Teams has been used by the Georgi Rakovski Military Academy, the Burgas Free University, the Angel Kanchev Ruse University in a combination with BigBlueButton as well as by the University of National and World Economy [13].

- Classroom Google, Meet Google have been used by: the Chernorizetz Hrabar Varna Free University[14], the Nikola Yonkov Vaptzarov Naval Academy, Varna.

- The Paisii Hilendarski Plovdiv University uses Google G Suite for Education [15].

- Blackboard has been used by: Georgi Rakovski Military Academy-Sofia, and Neofit Rilski Southwest University, Blagoevgrad. [16]

- E-learning has been used by: Technical University Varna, [17] and the University of Architecture, Construction and Geodesy [18].

Broadly, the platforms may be divided in two types: for distance education and for online learning.

**The distance education** usually works best with older students that have a constant access to technology at home and will work responsively alone with themselves. It however needs a resource prepared in advance before the crisis as well as preliminary provision of all educational materials. That is why the online learning perfectly complements it and they should be both conducted together as a mix.

The online learning has been built by systems for educational management called Learning management systems as both types of online learning: synchronous (happening at the same time for the teacher and the trained) and asynchronous (happening at any time and not necessarily in a group but with the feedback of a teacher) must complement each other. The online and the hybrid education present an opportunity for a more independent work, creativity and innovation.

Table 2: Differences between online and distance education

Differences	Online	Distance
1.location	Together in a virtual class-room	Independent work online
2.interaction	Regular, mixed education	LMS-learning management system
3. method of teaching	Face-to-face	Provision of teaching materials

In universities that have officially introduced only a distance education system of the type of Moodle, Blackboard, E-learning, the teachers start using the different online communication systems as Microsoft Teams and Zoom at their own discretion which hinders the students.

### The Case of the Military Academy

That is why at the Georgi Rakovski Military Academy we have run an experiment of creating a system for academic communication that integrates in itself a content management system of the website of Military Academy, Blackboard Learn for distance education and the applications of Microsoft Office 365 Education including the classrooms of Microsoft Teams for online education and other valuable resources as the academic library.

The content management system is based on WordPress CMS with an open source and serves for generating, organizing, publishing and editing digital content. That is the public site of the Military Academy with RNDG.BG domain, based on the PHP language and works with MySQL database that give the necessary freedom for an easy modification and refinement of the system in case of a need.

On the other hand, Wordpress has been chosen also because of the fact that there is a large society of volunteers and many plug-ins created around it, that make it very easy for work. From a functional point of view the content in the site of the Military Academy is structurally organized as every faculty, institute and department receives its own blog where to publish their content according to their rights and needs.

On the one hand the system for academic communication (SAC) of the Georgi Rakovski Military Academy is a system of people, software and procedures and on the other hand, it is a system of sub-systems: Internet, Extranet and Intranet:

- The RNDG.BG web site is visible for the public in **Internet** and is accessible from all over the world.
- The role of **Extranet** is played by a page built on SharePoint, also accessible from all over the world but only for employers, lecturers and students of the Military Academy that have an account certified by a business email ending with the rndg.bg domain and a private password. With the help of this account they can access all Microsoft applications, the

academic library, the data bases of Scopus and Web of Science, Blackboard Learn, a bulletin with COVID-19 helpful materials and the different documents gathered in a common cloud space.

- The **Intranet** is a private infrastructure and a network, accessible only from work devices located in the area of the Military Academy (for example the quality management system where orders and protocols are uploaded and so on).

The result of the experiment shows that the system for academic communication has been used very intensively during the peak of the crisis but its usage continues even after that.

Every day, information related to COVID-19 has been uploaded in the content management system and main communication with the director of the Military Academy Major-general doctor Grudi Angelov has been performed through the uploaded information under the "News" section.

By an Order, the Military Academy, transitions to a mixed-distance and online education happen on March 9, 2020, i.e. only a day after the face-to-face classes stop and the latter do not have an interruption in practice.

The educational materials have been mostly uploaded in the Blackboard distance education system while the online lectures, faculty and academic councils have been held in Microsoft Teams.

Besides that, a general group for group messaging has been used in the business mail for sending emails via Outlook of Office 365, and the digital bulletins with work advices have been sent in it.

### Comparison between the Educational Platforms Used in Bulgarian Universities

Some of the platforms are LMSs, others are computer apps for chats and calls. LMSs are technologies that still have not reached their potential in the Information Age. They are defined as systemic infrastructures or a framework, managing the learning process of an organization.<sup>5</sup> They provide the transition from the Industrial to the Information Age by the use of new approaches to instruction. The potential of the LMSs is in the application of computers to education. They use computer applications that are responsible not only for delivering instructional content but also for individual and organizational assessment, progress tracking and supervision. The LMS encompasses everything from course registration to course administration, tracking of performance and reporting of lessons learned.

#### Computer apps for chats/calls: MS Teams vs. Zoom

Table 3: Comparison between Zoom and MS Teams

	Zoom	MS Teams
1.type of collaboration	Internal+external	Internal-only Office 365 subscribers
2. audience of video chats	Up to 1,000 participants	Up to 250 people

<sup>5</sup> An argument for clarity: what are learning management systems, what are they not, and what should they become? William R. Watson, Sunnie Lee Watson, *ech Trends*, Springer Verlag, 2007, 51(2), pp.28-34., <https://hal.archives-ouvertes.fr/file/index/docid/692067/filename/Watson-2007.pdf>

3.charge	Paid for unlimited calls	Free of charge for MS Office users
4. pros	High participation outside of work	Secure internal collaboration, smooth integration
5. cons	Security concerns	Restriction of users' participation in video calls, only internal users

Zoom and MS Teams are the two most widely used for chats, audio and video calls.<sup>6</sup> MS Teams has the initial advantage because of the fact that it was recommended for use during the pandemic by an official letter from the Bulgarian minister of education. As the comparison shows MS Teams has the advantage as well of being more secure and allowing the smooth integration with calendars and email accounts, Office apps such as Word, Excel and Powerpoint, seamless file searches, backups and collaboration. In terms of security, Zoom has the most drawbacks, both because of the increase in security vulnerabilities and the so called “Zoombombers” (entering private video conferences by default).<sup>7</sup> Zoom’s advantage is mostly its ability to handle large events outside of work, especially when it comes to videoconferencing. Its screen supports up to 49 videos. In terms of meetings while MS Teams allows scheduling of meetings, accessing past meeting notes/recordings, inviting external guests to an active meeting and sharing meeting agendas before a meeting Zoom allows transcript generation, recording of meetings, co-annotation as a collaboration tool and simultaneous screen sharing.

The general conclusion is that usually companies use Teams internally and Zoom for communication outside the company. So they both complement each other.

**LMS Comparison: Google Classroom vs. Moodle**

Table 4: Comparison between Google Classroom and Moodle

	Google Classroom	Moodle
1.pros	Collaboration, easiness, integration	Flexibility, mobile app
2.cons	Not available for business	Ads in free accounts, restricted number of users, weaknesses of the interface
3.conclusion	Mostly intended for schools	Intended for teachers

Google Classroom focuses mostly on collaboration and it is very easy to set up classes and assignments. It also integrates not only with other Google products but with educational apps as well. However, it is not available for business and does not

<sup>6</sup>Microsoft Teams VS. Zoom, <https://velocitmsp.com/blog/>  
<sup>7</sup>MICROSOFT TEAMS VS. ZOOM, WHICH IS BETTER FOR MY TEAM?, [https://7n7.b66.myftpupload.com/wp-content/uploads/2020/05/VelocIT\\_WP\\_052120\\_v2.pdf](https://7n7.b66.myftpupload.com/wp-content/uploads/2020/05/VelocIT_WP_052120_v2.pdf)

offer accounts for parents. Generally, it is a learning management solution intended for schools and used for both online and classroom courses.<sup>8</sup> Moodle has lots of options where teachers can choose their content/activities. However, the ads in free accounts could be distracting and its plans for schools accommodate only up to 500 users and the interface is not always intuitive. Generally, it is an open source platform designed for teachers to build their curriculum.

Both are LMS but designed for different purposes, with different approach to online learning. Google Classroom is designed for users not familiar to LMS and can accommodate more than 500 students while Moodle requires more technical knowledge but has more restricted number of users. Google Classroom’s advantage as part of Google’s suite of applications for education is that it is free and easy to use, collaboration friendly, with more integration options. It is a cloud-based software but has limited tech support for users. Moodle on the other hand is modular which means that teachers can build their curriculum and customize interface. It is both cloud-based and with on-premise deployment and has a mobile application.<sup>9</sup> Another advantage is that it offers unlimited course and activities. Its drawbacks are that it is paid for more students, has small storage limit and smaller list of integrations, one of which is BigBlueButton.

**LMS Comparison Continued: BigBlueButton vs. Microsoft 365**

BigBlueButton is a web conferencing system designed for online learning as a virtual classroom. BigBlueButton provides real-time sharing of audio, video, slides, chat, and screen. Students are engaged through the sharing of emoji icons, polling, and breakout rooms.<sup>10</sup> Synchronous learning tools should feel like part of the management system (LMS). And BigBlueButton is learning tools interoperability (LTI) 1.0 compliant for widest adoption. Some of its software features are the LMS integration, the student portal and the virtual whiteboard.

The overview<sup>11</sup> shows that Microsoft 365, formerly Office 365, provides web, desktop, and mobile apps for Outlook, Word, Excel, PowerPoint, OneNote, Publisher, Skype, OneDrive, Exchange Online, and more. BigBlueButton is an open-source web conferencing and social collaboration software utilized by educational institutions for providing e-learning facilities. They support different platforms. While Microsoft 365 is supporting more platforms, BigBlueButton is supporting just the web-based platform. Also Microsoft 365 has more customer support including phone and online support and BigBlueButton has only knowledge base and video tutorials. Microsoft 365 can have 9 screenshots at a time and BigBlueButton-3 screenshots at a time. In terms of pricing,

<sup>8</sup>Google Classroom vs. Moodle: Key Features and Services Comparison, Melissa Pardo-Bunte, April 25, 2017, <https://www.betterbuys.com/lms/google-classroom-vs-moodle/>  
<sup>9</sup>GOOGLE CLASSROOM VS. MOODLE COMPARISON 2020, Arthur Zuckerman, April 1, 2020, <https://comparecamp.com/google-classroom-vs-moodle-comparison/>  
<sup>10</sup>BigBlueButton, ENGAGE YOUR ONLINE STUDENTS, <https://www.saasworthy.com/product/bigbluebutton>  
<sup>11</sup>Microsoft 365 vs BigBlueButton Comparison, <https://www.getapp.com/collaboration-software/a/microsoft-office-365/compare/bigbluebutton/>

Microsoft 365 is subscription based and BigBlueButton is free of charge.

According to the user reviews of Microsoft 365: 98% would recommend this app while 80% would recommend BigBlueButton. The latter is less recommended in the categories Ease of use, Features and Customer support. With Microsoft 365 it is especially easy to share documents and folders with coworkers or links with a document to anyone. Among some of the negative features of Microsoft 365 is the poor audio quality during calls, inability to pin important posts, problems with customer service. The total key features are 70 with Microsoft 365 and 20 with BigBlueButton. The total integrations are 709 with Microsoft 365 and 18 with BigBlueButton.

**Blackboard vs. Moodle**

The Blackboard (WebCT) is an open source LMS like Moodle. Both serve as three types of tools: communication, productivity and student involvement. Blackboard is a comprehensive and flexible platform which is more popular than Moodle, i.e. with more users.<sup>12</sup> Moodle is an open source (free) course management system (CMS) that can build a LMS. As a communication tool both can serve as discussion forums (using posts), notification dashboards for courses, and can exchange files. However Blackboard has no email notification. As productivity tool both have a calendar/progress review option, searching within course and a module page. As student involvement tool, both can organize groups, perform community networking, access the course menu, submit assignments, and customize grading options.

Table 5: Comparison between Moodle and Blackboard

	<b>Moodle</b>	<b>Blackboard</b>
<b>1.Admin</b>	Open source, free integration with Google, modular	Paid, e-Commerce integration, limited users
<b>2.Teacher</b>	Teachers can create courses and track performance	Teachers set goals for students, Blended learning option
<b>3.Student</b>	Old interface, interactive courses, good architecture	Interactive courses, offline activity

These are probably the two most widely used and both have different useful features. Moodle’s advantage is that it is free and supports student-centered learning based on enhanced user experience. It allows a large number of users and has a modular framework. Blackboard’s advantage is the in-house eCommerce integration when it comes to selling courses and has a Blended learning option (allowing online and offline mixing of training). Both allow sharing and uploading interactive courses.<sup>13</sup>

<sup>12</sup>A Study of Comparison between Moodle and Blackboard based on Case Studies for Better LMS, P.Subramanian,N. Zainuddin, S.Alatawi, T.Javabdeh and Ab Razak Hussin, JOURNAL OF INFORMATION SYSTEMS RESEARCH AND INNOVATION, [https://www.moodlebites.com/pluginfile.php/26295/mod\\_resource/content/1/Pub4\\_ComparisonBetweenMoodleAndBlackboard.pdf](https://www.moodlebites.com/pluginfile.php/26295/mod_resource/content/1/Pub4_ComparisonBetweenMoodleAndBlackboard.pdf)

<sup>13</sup>Which LMS is Better For You- Moodle or Blackboard?, October 16, 2017, <https://edwiser.org/blog/moodle-versus-blackboard/>

**Conclusion**

LMS provide successful online learning. The simplest definition of LMS is “a software application that automates the administration, tracking, and reporting of training events”<sup>14</sup>. In other words LMS is a framework, a type of integrated information system whose main problem is that of the feedback with the students. The choice of a LMS depends on the individual preference.

Each of the LMS or app listed in the paper has its advantages and drawbacks. All of them complement each other and serve different purposes. They mostly provide the adaptation of the universities to the distance type of education during COVID-19. A future task however is the unification of the platforms used, more in-depth analysis of the feedback of students and recommendations for improvement of possible weaknesses. Despite the weaknesses however, the hybrid form of education will continue to be in use as the most appropriate answer during times of crises that impede the face-to-face classes.

**References**

BigBlueButton, ENGAGE YOUR ONLINE STUDENTS, <https://www.saasworthy.com/product/bigbluebutton>

Cleveland-Innes, M. with Dan Wilton. Guide to BLENDED LEARNING, Athabasca University, Canada, Commonwealth of Learning, 2018, [http://oasis.col.org/bitstream/handle/11599/3095/2018\\_Cleveland-Innes-Wilton\\_Guide-to-Blended-Learning.pdf?sequence=1&isAllowed=y](http://oasis.col.org/bitstream/handle/11599/3095/2018_Cleveland-Innes-Wilton_Guide-to-Blended-Learning.pdf?sequence=1&isAllowed=y)

Microsoft 365 vs. BigBlueButton Comparison, <https://www.getapp.com/collaboration-software/a/microsoft-office-365/compare/bigbluebutton/>

Microsoft Teams VS. Zoom, <https://velocitmsp.com/blog/microsoft-teams-vs-zoom-which-is-better-for-my-team/>, [https://7n7.b66.myftpupload.com/wp-content/uploads/2020/05/VelocIT\\_WP\\_052120\\_v2.pdf](https://7n7.b66.myftpupload.com/wp-content/uploads/2020/05/VelocIT_WP_052120_v2.pdf)

Pardo-Bunte, M. Google Classroom vs. Moodle: Key Features and Services Comparison, April 25, 2017, <https://www.betterbuys.com/lms/google-classroom-vs-moodle/>

Subramanian, P, N. Zainuddin, S.Alatawi, T.Javabdeh and Ab Razak Hussin. A Study of Comparison between Moodle and Blackboard based on Case Studies for Better LMS, JOURNAL OF INFORMATION SYSTEMS RESEARCH AND INNOVATION, [https://www.moodlebites.com/pluginfile.php/26295/mod\\_resource/content/1/Pub4\\_ComparisonBetweenMoodleAndBlackboard.pdf](https://www.moodlebites.com/pluginfile.php/26295/mod_resource/content/1/Pub4_ComparisonBetweenMoodleAndBlackboard.pdf)

Watson, W., and Sunnie Lee Watson. An argument for clarity: what are learning management systems, what are they not, and what should they become?, *ech Trends*, Springer Verlag, 2007, 51(2),pp.28-34., <https://hal.archives-ouvertes.fr/file/index/docid/692067/filename/Watson-2007.pdf>

Which LMS is Better For You-Moodle or Blackboard? October 16, 2017, <https://edwiser.org/blog/moodle-versus-blackboard/>

Websites of Universities in Bulgaria (in Bulgarian)

Zuckerman, A. GOOGLE CLASSROOM VS. MOODLE COMPARISON 2020, April 1, 2020, <https://comparecamp.com/google-classroom-vs-moodle-comparison/>

<sup>14</sup> p.27, *ibid*

# ASSESSMENT OF DEBRIS FLOWS-PRONE WATERSHEDS IN SOUTHERN SLOPES OF STARA PLANINA MOUNTAIN BY COMBINED RASTER AND MORPHOMETRIC ANALYSIS

**Zornitsa Dotseva, Janko Gerdjikov**

*Sofia University "St. Kliment Ohridski", 1504 Sofia; janko@gea.uni-sofia.bg*

**ABSTRACT.** The southern slopes of Stara Planina Mountain are one of the well-defined areas in Bulgaria in terms of debris flows hazard. For the present study, we choose five watersheds located north and northwest of the village of Anton (Zlatitsa region) to make a preliminary hazard assessment for debris flows. Used methods include field observations, GIS and morphometric analysis of the relief, raster analysis and modeling of certain parameters. We determine and characterize the source, transition and deposition zones, and areas prone to erosion in river channels, thus giving an idea where in the studied watersheds could be formed areas with an accumulation of material with the potential to be mobilized and involved in debris flows during extreme meteorological events. To the obtained data we take into account the influence of lithology and tectonic conditions in the area, which affect the distribution of material on the slopes. Obtained results could be used for regional hazard estimations and mapping, and assess if the used approach is applicable for other areas in the country.

**Keywords:** natural hazard, debris flows, erosion, GIS, morphometry

## ОЦЕНКА НА ВОДОСБОРИ С ПРОЯВА НА КАЛНО-КАМЕННИ ПОТОЦИ В ЮЖНИТЕ СКЛОНОВЕ НА СТАРА ПЛАНИНА, ЧРЕЗ КОМБИНИРАН РАСТЕРЕН И МОРФОМЕТРИЧЕН АНАЛИЗ

**Зорница Доцева, Янко Герджиков**

*Софийски университет „Св. Климент Охридски“, 1504 София*

**РЕЗЮМЕ.** Южните склонове на Стара планина се очертават като една от добре изразените области в България по отношение на опасността от кално-каменни потоци. За настоящето изследване избрахме пет водосбора, разположени северно и североизточно от с.Антон (Златишко) за да бъде направена предварителна оценка на опасността от възникване на кално-каменни потоци. Използваните методи включват теренни наблюдения, ГИС и морфометричен анализ на релефа, растерен анализ и моделиране на определени параметри. Определени и характеризирани бяха зоните на подхранване, транспорт и отлагане, както и районите, склонни към ерозия в речните канали, които биха ни дали представа къде в изследваните водосбори могат да се формират зони с натрупване на материал с възможност да бъде мобилизиран и въвлечен в кално-каменни потоци при екстремни метеороложки явления. Към получените данни отчитаме и влиянието на литологията и тектонската обстановка в района, които оказват влияние при разпределението на материал по склоновете. Получените резултати биха могли да бъдат използвани при регионална оценка на опасността от кално-каменни потоци и тяхното картиране, а също и да се прецени дали използваният подход е приложим за други области на страната.

**Ключови думи:** природна опасност, кално-каменни потоци, ерозия, ГИС, морфометрия

## Introduction

Debris flows are often seen event in mountain areas and cause significant damage to infrastructure, property, and citizens because of the high mobility and energy, which also have an impact and cause changes in river channels and slope morphology. Debris flows are described as “turbulent flowing mixtures of sediment and liquid in nearly equal proportions” (Iverson, 1997), quickly formed and fast-moving mass that flows on slopes with high angles (Hungar, 2005). The assessment of debris flows hazard is important in mountain areas worldwide because of their high-damage possibilities. Debris flows are triggered by factors like erosion, geological characteristics, slope, climate conditions and their intensive activity in recent years could be explained in some cases with climate changes (Chen, 2016; Uzielli et al., 2018; Nikolova et al., 2018; etc.).

In Bulgaria, debris flows are still not so well-studied as impact and distribution, but instead of these last few years, different research groups work on hazard evaluation of their

regional occurrence in Bulgaria. Most of the studies are based on geomorphological analysis for the assessment of catchments suspected for debris flows. Few well-described examples for debris-flow activity are from Stara Planina Mountain (Gerdjikov et al., 2012; Kenderova, Baltakova, 2013; Dotseva et al., 2014; 2019a), Pirin and Rila Mountains (Baltakova et al., 2018; Dotseva et al., 2019b), Kresna Gorge and Struma River valley (Dobrev, Georgieva, 2010; Kenderova et al., 2013a,b; 2014; Nikolova et al., 2018), etc. Some of these areas were mapped by Iliev (1994) in Map of Geological Hazard in Bulgaria and noted in works of Kamenov, Iliev (1963) and Iliev, Bruchev (1994).

The determination of the source, transition, and deposition zones is one of the main steps for hazard assessment of watersheds prone to debris flows. For this purpose are used different methods like analysis of remote sensing data, spatial GIS analysis, dynamic and physical-based models, etc. In the present study, we characterise the main zones related to debris flow hazard in five watersheds from the southern slopes of Stara Planina Mountain, near Anton Village. The research

area is chosen generally because of field observations and data about torrential events in the past (Mishev et al., 1962; Kerenski et al., 1977), confirmed also by recent field and tectonic-geomorphological data (Gerdjikov et al., 2012; Glabadanidu et al., 2012).

Debris flow potential of the watersheds will be assessed by analysis and evaluation of geometrical and slope conditions in the watersheds and morphometric parameters, sensitive to flow type and erodible potential – Form Factor, Elevation Relief Ratio, Drainage Density, and Melton Ruggedness Number. Also, we apply simple GIS procedures as raster analysis and binary masks as proposed by Grelle et al. (2019), which were used for identification of areas in channels that are erosion-prone and could act like debris flows source areas. This type of approach has some limits - it does not consider specific debris flow factors like rainfall rates, flow velocity, energy, rheological characteristics, volume and thickness of sediment material in the channels, etc. Instead of this, it is a very useful step for hazard pre-assessment and easy for application in contrast with more complex physical-based models for debris flow development and evolution.

Along with GIS analysis field work was carried out for evaluation of the influence of lithology and tectonic conditions in the area, which affect the distribution of material on the slopes and its involvement in the flows.

## Geological and Geomorphological Setting

The study area is located to the north and northeast of the village of Anton, on the southern slope of Stara Planina Mountain, where the topography is characterized by steep slopes and deeply incised river channels (Fig. 1).

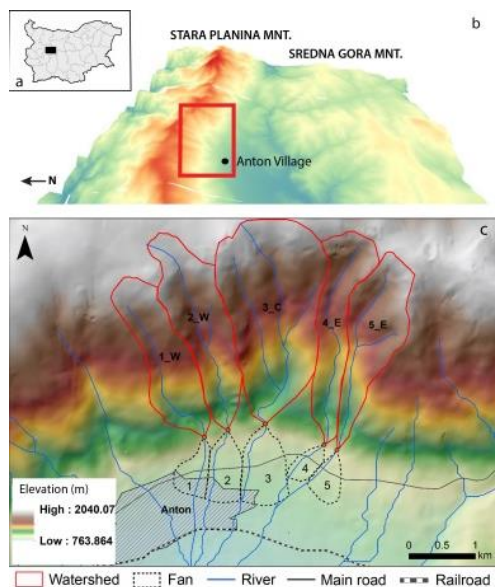


Fig. 1. a,b- Location of the studied area; c- Hillshaded DEM with delineated watersheds and associated fans

The area above 1500-1600 m is covered by grass and shrub vegetation, exposed to intensive erosion and weathering, and with a high chance to form slope-induced processes. Lower parts of the watersheds were occupied by forests. The climate is characterized by mean annual

temperatures of 9.3°C and mean precipitation ratio of 615 mm/y (up to 700 mm/y in upper parts of the Mountain). Extremely high rates of precipitation and snowmelt in the spring often leads to water drain over steep slopes, thus forming floods.

Rock types play a key role in the formation and accumulation of sediment cover which could be eroded and involved in debris flows. The geology of the area is represented by granodiorites of Vezhen Pluton, metasediments of a low-grade metamorphic complex with lenses of metabasitic rocks, and gneisses of the high-grade metamorphic complex (Antonov et al., 2010) (Fig. 2). All rocks are with Paleozoic age. Zlatitsa basin fill is represented by Quaternary alluvial, colluvial, and deluvial sediments, which formed coalescing fans at the slope base. Quaternary loose accumulations were distributed like screes on slopes in upper parts of the watersheds, in riverbanks, and on riverbeds, but due to their small size, they are not shown on the map.

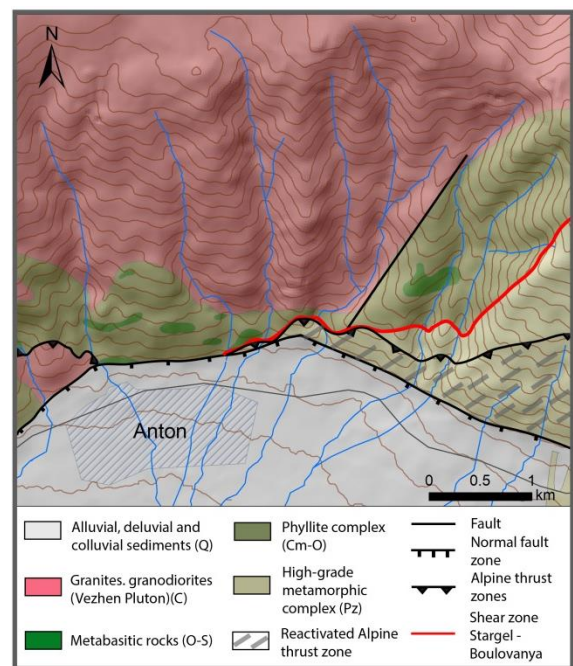


Fig. 2. Geological map of the studied area (modified after Antonov et al., 2010)

According to the classification proposed by Attewell and Farmer (1976) for rock hardness, rocks in watersheds fall into a range of very high strength (> 60 Mpa) for granodiorites and gneisses to medium to weak (< 5 to 5 – 30 Mpa) for low-grade metamorphic rocks (phyllites) in middle and lower parts of the watersheds.

One of the main tectonic features in the study area is the Quaternary normal fault zone traced along the southern slopes of the Stara Planina Mountain. Gerdjikov et al. (2017) described it as a “long-living tectonic zone with reactivation of older Alpine compressional structures”. The zone has well-pronounced geomorphological expression, strong impact on watersheds shape, size, channel length, incision, erosion and deposition (Gerdjikov et al., 2012; Glabadanidu et al., 2012).

Another tectonic zone that influences the area is the shear zone Sturgel-Bolouvanya which is the boundary between high- and low-grade metamorphic rocks (Gerdjikov et al., 2007). The zone is with Variscan age, at which the lower parts of the

earth's crust (high-grade metamorphic rocks) are exhumed. As a result of the Variscan orogeny, in both complexes was formed a foliation parallel to the zone and dipping to the SW with an angle of 30-50°. Polyphase Variscan and Alpine tectonics having a strong effect on the rock strength, so in the vicinities of the fault zones, the rocks are often rather weak.

## Materials and Methods

For the analysis purposes, EU-DEM v.1.1. (25 m) was interpolated by the bilinear interpolation method to grid resolution of 10 m. According to previous studies 10 m cell size is an appropriate resolution for the determination of slope gradient and debris flow areas (Tarolli and Tarboton, 2006; Carrara et al. 2008; etc.). Generated DEM was hydrologically adjusted, and the extracted river network was further corrected. Based on the topographic map of the scale of 1:50 000, remote sensing data, and DEM watershed areas, adjacent fans and watersheds closing sections were mapped. The pre-processed DEM was used for the extraction of Slope and Curvature maps, basin geometry, and morphometric parameters.

Morphometric analysis is based on calculations of four indices – Form Factor, Elevation Relief Ratio, Drainage Density, and Melton Ruggedness Number (MRN). Form Factor (HSF) (Horton, 1932) represents the shape of the watershed and influences the run-off distance, time, and peak discharge, where the higher the value of Form Factor more circular is the shape. Elevation Relief Ratio (ERR) (Pike et al., 1971) is related to the erosional evolution of the watershed and indicates the stages of youth, mature or old. Low values of the Elevation Relief Ratio indicate hard rocks and a small degree of the slope. Melton Ruggedness Number (Melton, 1965) is a slope index used for recognition of a type of the sediment transport – waterflood/bedload, mixed/debris flood, or debris flow and represents the relief ruggedness within the watersheds. Drainage Density (DD - 1 km/km<sup>2</sup>) (Horton, 1932) reflect the erosion activity and the permeability of the soils and rocks in watersheds.

For the definition of the erosion-prone areas in the main channels was used the spatial distribution of three parameters - Slope Ratio (SR) and Area of the watershed in square kilometers (A), obtained by DEM, and Trigger Ratio (TR) calculated in the Raster Calculator as a ratio between SR and ST (Slope Threshold) (Grelle et al., 2019). ST is equal to:

$$ST = k.A \quad (1)$$

where A is the watershed area in km<sup>2</sup>; and coefficient k - express the erosion proneness, related to soil properties, water saturation, vegetation, etc.

Different values of k and ST respectively were used to model the possible trigger conditions in the watersheds. For a visual representation of TR and delineation of erodible zones in river channels were used binary mask values (1 = yes; 0 = no).

Field data and observations were used for confirmation of the obtained results, characterization of source, transitional and depositional zones, and geological conditions in watersheds.

## Results

### DEM analysis, field observations and historical data

The average altitude in studied watersheds is from 1450 to 1570 m. The slope angle is one of the main triggering factors for debris flows and range between 21.10 and 24.96 degrees. These values correspond to the initiation slope ratio for debris flows (Hung, 2005) (Fig. 3). The slope exceeds 40 degrees in some places in the upper parts of the watersheds.

The source areas are located at an altitude above 1600 m, in the upstream area of watersheds. The channels characterized by V-shape and steep slopes with sparse vegetation on both sides, and also seasonally covered by snow (which leads to frost weathering). Gully and rill erosion is observed at the channels heads. Intense erosional processes form scree and loose material accumulations consisted of eroded Vezhen Pluton granitoid. The area is thus a potential source of initiation of debris flows in conditions of appropriate hydrodynamic conditions and inducing material in debris flows down to the slope.

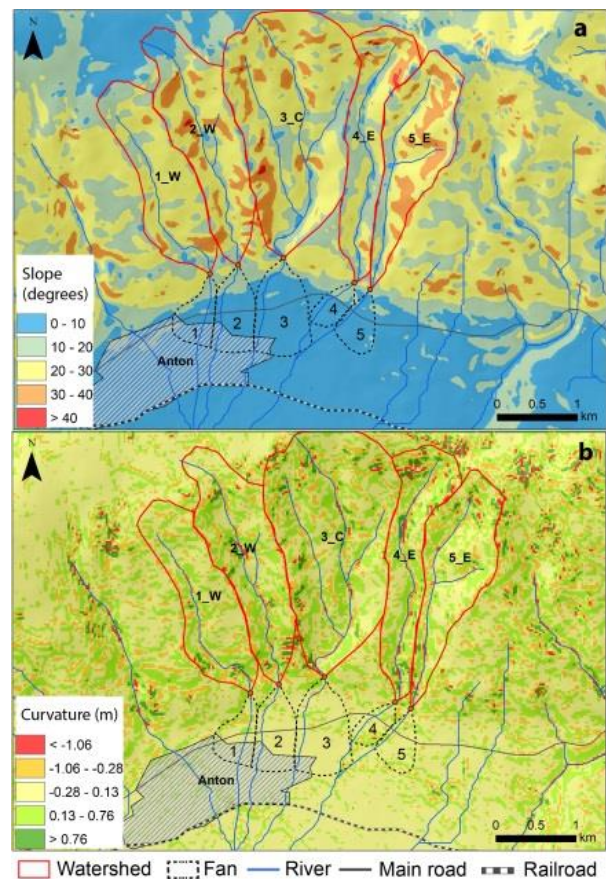
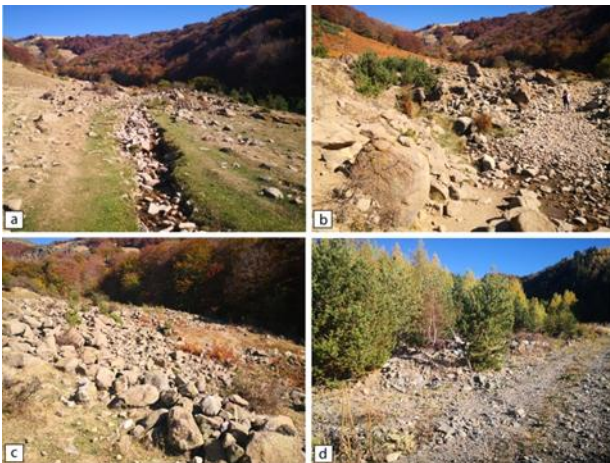


Fig. 3. a- Slope computed as a gradient of the DEM surface; b- Curvature, computed as a gradient of the slope surface

The transition zones are located in altitude between 1600 and 950 m in the middle and downstream reaches of watersheds and represents the main transport part of the channels. The slopes are steep and the movement of the formed flow can acquire high speed. Field observations show that both sides of the channels are vegetated with forests but there are unstable areas that could generate loose material. The almost entire transition zone in Watersheds 4\_E and 5\_E was occupied by weak and easy erodible low-grade

metamorphic rocks, likely to produce sediment material that could be included in the flows. The main processes in this zone are downward erosion and incising of the river valleys.

Torrential depositions in the study area are represented by very poorly to poorly sorted material, with a pebble to boulder size of the angular to sub-rounded clasts. There are indications for modern accumulations but with small intensity and inability to form large fans. Depositions form lateral levees and on areas with low-slope gradient in river valleys, near the confluence of river tributaries and on the margins of the active river channels (Fig. 4). The presence of well-preserved depositions related to debris flow activity observed on the river banks in Fans 4 and 5 (Fig. 4 d) could confirm the occurrence of at least one event in the last 100 years. This could be verified by historical data found in Kerenski et al. (1977) which speak for high-intensity torrent events in watersheds near Anton village in 1927, leading to widespread sediment depositions covering the area with size more than 20000 m<sup>2</sup>. According to Mishev et al. (1962) which characterized in detail the fans in Zlatitsa graben, torrential depositions are typical for the area east of Anton Village as a result of torrential events at the end of XIX Century and beginning of XX Century.



**Fig. 4. a,b,c – Debris flow deposits and morphology of the active channel in lower parts of Watershed 3\_C (a – 42.74726 N, 24.28382 E; b- 42.74756 N, 24.28412 E; c - 42.75018 N, 24.28660 E); d – Debris flow deposits accumulated on eastern river bank of Fan 4 (42.73907 N, 24.29021 E). The deposits have been cleared, but they can still be distinguished on field**

### Morphometric and raster analysis

Studied watersheds have typical area size and shape for debris flow prone watersheds. They occupy area from 1.52 to 3.76 km<sup>2</sup> and elongated shape according to Form Factor values between 0.14 and 0.37.

The values of the Drainage Density index are between 1.57 and 2.12 km/km<sup>2</sup>, indicating moderate permeability and moderate soil erosion.

Elevation Relief Ratio ranging from 0.37 to 0.46 and shows that watersheds are subject of medium to high erosion processes, which collaborates well with features as steep slopes, but also with the presence of erodible metamorphic rocks in lower parts of the watersheds. The relief can be classified as youthful. The results for Melton Ruggedness Number (0.54 – 0.73), Elevation Relief Ratio and watersheds

geometry indicate active and intensive erosional processes and high susceptibility to debris flows.

For identification of potential erosion areas in the main channels were used different values of coefficient  $k$  and Slope Threshold (ST). They control the TR which, in turn, affects the distribution of erosion. After the applied sensitive analysis for coefficient  $k$  and ST, and according to field observations, values of  $k$  between 0.26 and 0.30 were considered as appropriate for modeling the erosion probability (Fig. 5). The spatial distribution of triggering values (TR) is a result of binary masks obtained by  $TR \geq 1$  (1 (yes) to cells with slope angles greater than or equal to the slope threshold ST and 0 (no) to cells that have an ST less than one - Grelle et al., 2019).

Results delineate zones in channels from the watersheds upstream area and transition zone that are prone to erosion and able to produce sediment bedload involved in the flows.

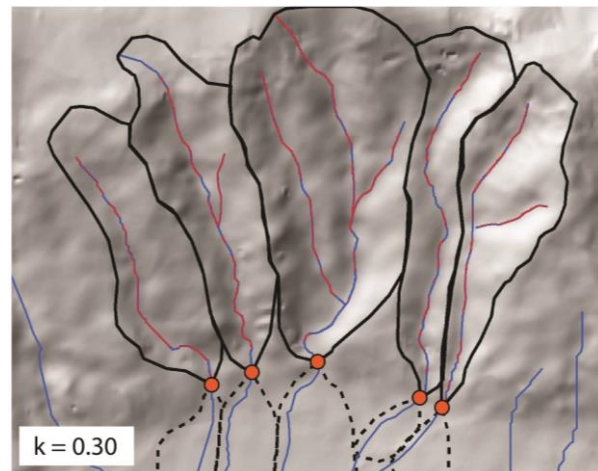


**Fig. 5. Erosion-prone areas in river channels, modeled with coefficient  $k = 0.30$  (red lines)**

### Specific features of Watershed 3\_C

Watershed 3\_C have more specific characteristics than the other four studied watersheds. Typical are low slope angles in downward parts of the watershed where we observe a large volume of eroded material, and gully erosion at the same time (Fig. 4 a, b, c). Also, Form Factor (0.37) shows that this watershed has a more circular shape and occupies a bigger area in contrast with the other four watersheds.

The main clast source and respectively accumulated material in the almost entire watershed is represented by the granite rocks of Vezhen Pluton. Erosion and denudation in the source zone are effective enough to disintegrate rocks, which are transported in gullies and rills or form unconsolidated colluvial cover on the steep slopes. This scenario also applies in source zones to the other watersheds but here is well field observed (drone footage and remote sensing data).

Erosive proneness in this watershed is supported by results from the morphometric analysis of ERR (0.46) and DD (2.12 km/km<sup>2</sup>). The widest erosion could be connected to the weak rocks from the low-grade metamorphic complex and tectonic features in addition to geomorphological conditions of the watershed.

In lower parts of this watershed were formed areas with a low slope angle that could prevent debris flows to reach the alluvial fan. These areas, covered by alluvial and colluvial-alluvial sediments could also act as temporal accumulation

zones. In some places active channels or parallel to them gulleys cut deep into the sediments, fulfilled with the accumulated material. One of this places could be seen on the modeled erosion-prone areas in channels where the main river makes a turn (Fig. 5).

The value of MRN (0.54) corresponds to low ruggedness areas located on the valley floor and according to an obtained result, the watershed falls in the category of mixed/debris flood, but close to values for debris flows ( $> 0.60$ ) (Wilford et al., 2004). In this watershed are more likely to occur debris flow events accompanied by debris flood phases downstream where the channels slope is more gentle.

## Conclusions

It is well-known that the southern slopes of Stara Planina Mountain are one of the debris-prone areas in Bulgaria as a result of specific geomorphological, geological, and climate conditions, sparse vegetation, etc. Depositions from past debris flow events were observed in most of the fans located in the Mountain Range slope base where the Quaternary normal fault zone has a major impact on the watersheds evolution, debris flow activity, and sedimentation. Field and historical data, as well as certain characteristics of the area, made us investigate in detail five watersheds which can be defined as debris-prone in the area of Anton Village.

The estimation of zones prone to erosion in main channels as one of the key parameters to consider when analyzing the dynamic process of debris flows was performed by the simple GIS-based proposed by Grelle et al. (2019) approach. Delineated erosion zones that could be a source for debris flows in the channels are located not only in the upstream area of the watersheds but also in their lower parts.

The results of morphometric analysis predict debris flow activity for five studied watersheds with possible debris flood transition downstream in Watershed 3\_C, medium to high erosion activity, and youthful stage of watersheds evolution. From characteristics of the source and transition zones, as well as the geological specifications and recent debris deposits over the fans and river banks, studied watersheds could be described as susceptible to debris flow initiation and transportation.

The obtained data could be used for regional hazard pre-assessment and susceptibility mapping. Further analysis of volume and grain-size distribution of the recent sediments need to be carried out for evaluation of deposition zones and their possible extent as well as a more detailed analysis of Watershed 3\_C which have slightly unusual characteristics in contrast with other four watersheds. Obtained results could be supported by analysis of hydrological and meteorological conditions, faults influence over the erosional processes as well as evaluation of physical properties of the flows for completed debris flow hazard and risk assessment of the area.

**Acknowledgements.** This work is funded by the National Program "Young Scientists and Postdoctoral candidates 2020" of the Ministry of Education and Science.

## References

- Antonov, M., S. Gerdzhikov, L. Metodiev, Ch. Kiselinov, V. Sirakov, V. Valev. 2010. Geological Map of the Republic of Bulgaria in Scale 1:50 000. Map Sheet K-35-37-G (Klisura). Sofia, Geocomplex
- Attewell, P.B. and I.W. Farmer. 1976. *Principles of engineering geology*. John Wiley & Sons Inc., New York, 182 -184 pp
- Baltakova, A., V. Nikolova, R.Kenderova, N.Hristova. 2018. Analysis of debris flows by application of GIS and remote sensing: case study of western foothills of Pirin Mountain (Bulgaria). – In: *Debris Flows: Disasters, Risk, Forecast, Protection. Proceedings of the 5<sup>th</sup> International Conference. Tbilisi, Georgia, 2018*. Publishing House "Universal", 22-32 (in English with Russian abstract)
- Carrara, A., and R. Pike. 2008. GIS technology and models for assessing landslide hazard and risk: Editorial. *Geomorphology*, 94, 257-260
- Chen, C.Y. 2016. Landslide and debris flow initiated characteristics after typhoon Morakot in Taiwan. *Landslides*, 13, 153–164.
- Dobrev, N., M. Georgieva. 2010. The debris flow in the northern part of Kresna Gorge: Characterization of the source zone and material properties. *Review of the Bulgarian Geological Society*, 71 (1–3), 113–121 (in Bulgarian with English abstract)
- Dotseva, Z., I. Gerdjikov, D. Vangelov. 2014. Case study of debris flows triggered by heavy rainfall – Etropole area, 2014. *Proceedings of National Conference "Geosciences 2014", Sofia, 2014*, 85-86.
- Dotseva, Z., I. Gerdjikov, N. Dobrev, D. Vangelov. 2019a. Recognizing debris flow hazard in heavily forested watersheds: an example from Etropole area, Central Bulgaria. – *Annual of the University of Mining and Geology "St.Ivan Rilski"*. 62, Part 1, 42-47
- Dotseva, Z., D. Vangelov, I.Gerdjikov, I. 2019b. Modern debris flow activity in southern slopes of Rila Mountains, with an example from the area of Cherna Mesta village. *Review of the Bulgarian Geological Society*, 80 (3), 227-229
- Gerdjikov, I., N. Georgiev, D. Dimov, A. Lazarova. 2007. The different faces of supposedly single thrust: a reevaluation of the Vezhen thrust, Central Balkanides. *Proceedings of the Bulgarian Geological Society*, 24-26
- Gerdjikov, I., D. Vangelov, I. Glabadanidu. 2012. One underestimated geological hazard: the debris flows. *Review of the Bulgarian Geological Society*, 73 (1–3), 85–104 (in Bulgarian with English abstract)
- Gerdjikov, I., Z. Dotseva, D. Vangelov. 2018. Extensional reactivation of a former compressional fault zone: an example from the eastern Zlatitsa graben. *Journal of Mining and Geological sciences*, 60, 1, 122-127
- Glabadanidu, I., I. Gerdzhikov, D. Vangelov, 2012. Structural and tectonic geomorphological studies in Zlatitsa graben, Central Bulgaria. *Proceedings of National Conference "Geosciences 2012", Sofia, 2012*, 107-108.
- Grelle, G., A. Rossi, P. Revellino, L. Guerriero, F.M. Guadagno, G. Sappa. 2019. Assessment of Debris-Flow Erosion and Deposition Areas by Morphometric Analysis and a GIS-Based Simplified Procedure: A Case Study of Paupisi in the Southern Apennines. –*Sustainability*, 11, 2382

- Kerenski, S., S.Dimitrov, M. Milchev. 1977. Borba s eroziyata v gorskia fond na Bulgaria. Zemizdat. Sofia, 161 p. (in Bulgarian)
- Iliev-Broutchev, I., ed. 1994. Geological hazards in Bulgaria – map in scale 1:500 000 and explanatory text.. House of BAS, Sofia, 143 p. (in Bulgarian with English abstract)
- Iverson R.M. 1997. The physics of debris flows. *Reviews of Geophysics*, 35, 3, 245-296
- Horton, R.E. 1932. Drainage-basin characteristics. *Trans. Am. Geophys. Union*. 13, 350–361.
- Hungr, O. 2005. Classification and terminology. – In: *Debris-flow Hazards and Related Phenomena* (Ed: Jakob, M., O. Hungr). Chichester, Springer, 739 p.
- Kamenov, B., I. Iliev. 1963. Engineering geological subdivision of the Republic of Bulgaria. – In: *Works on the Geology of Bulgaria, Ser. Engineer. Geology and Hydrogeology*, 2, 5–123 (in Bulgarian with Russian and English abstracts).
- Kenderova, R., A. Baltakova. 2013. Debris flows in Kazanlak Valley, south slopes of the Balkan Mountain Range, Bulgaria. *Journal of the Geographical Institute Jovan Cvijic SASA*, 63, 3, 361-370
- Kenderova R., G. Rachev, A. Baltakova. 2013a. Forming and activity of debris flow in Middle Struma Valley [3–5 December 2010]. – *Annual of Sofia University, Book 2 - Geography*, 105, 15–32 (in Bulgarian with English and Russian abstract).
- Kenderova R., A. Baltakova, G. Rachev. 2013b. Debris flows in the Middle Struma Valley, Southwest Bulgaria. – In: *Geomorphological impact of extreme weather: Case studies from central and eastern Europe* (Ed: D.Loczy) Springer Geography. 281-297
- Kenderova R., G. Rachev, A. Baltakova. 2014. Debris Flow in Middle Struma Valley. – *Annual of Sofia University, Book 2 - Geography*, 106, 13-40. (in Bulgarian with English abstract)
- Melton, M. 1965. The Geomorphic and Palaeoclimatic Significance of Alluvial Deposits in Southern Arizona. – *Journal of Geology*, 73, 1-38.
- Mishev, K., V. Popov, Tz. Mihaylov. 1962. Morphologie et Neo-Tectonique du pied de la Stara-Planina entre les seuils de Galabec et Koznica. *Reviews de Institute Geographique, BAS*, 6, 43-61 (in Bulgarian with French abstract)
- Nikolova, N., G. Rachev, R. Kenderova. 2018. Possible impact of climate and weather condition on debris flows occurrence (on the example of Kresna gorge, Bulgaria). – In: *Debris Flows: Disasters, Risk, Forecast, Protection. Proceedings of the 5<sup>th</sup> International Conference. Tbilisi, Georgia, 2018*. Publishing House “Universal”, 166-175 (in English with Russian abstract)
- Panagos, P., K. Meusburger, C. Ballabio, P. Borrelli, C. Alewell. 2014. Soil erodibility in Europe: A high-resolution dataset based on LUCAS. *Science of Total Environment*, 479–480, 189–200.
- Pike, R.J., S.E. Wilson. 1971. Elevation-Relief Ratio, Hypsometric Integral and Geomorphic Area—Altitude Analysis. *Geological Society of America Bulletin*, 82, 1079–1084.
- Renard, K.G, G.R. Foster, G.A. Weessies, D.K. McCool. 1997. Predicting soil erosion by water: a guide to conservation planning with the Revised Universal Soil Loss Equation (RUSLE). – In: *Agriculture Handbook (Ed: Yoder D.C.)*, U.S. Department of Agriculture, 703.
- Tarolli, P. and D.G. Tarboton. 2006. A new method for determination of most likely landslide initiation points and the evaluation of digital terrain model scale in terrain stability mapping. *Hydrology and Earth System Science*, 10, 663–677
- Uzielli, M.; Rianna, G.; Ciervo, F.; Mercogliano, P.; Eidsvig, U.K..2018. Temporal evolution of flow-like landslide hazard for a road infrastructure in the municipality of Nocera Inferiore (Southern Italy) under the effect of climate change. *Natural Hazards and Earth System Science*.18:3019–3035.
- Wilford, D.J, M.E. Sakals, J.L.Innes, R.C.Sidle, W.A. Bergerud. 2004. Recognition of debris flow, debris flood and flood hazard through watershed morphometrics. *Landslides*, 1, 61–66

## BLOCKCHAIN NODE MANAGEMENT IN SMART GRID

*Mila Ilieva-Obretenova*

*University of Mining and Geology "St. Ivan Rilski", 1700 Sofia; mila.ilieva@mgu.bg*

**ABSTRACT.** Blockchain is an open, distributed ledger that can record transactions between two parties efficiently and in a verifiable and permanent way. It is typically managed by a peer-to-peer network collectively adhering to a protocol for inter-node communication and validating new blocks. In Bulgaria were represented: the idea for application of blockchain in business environment, the blockchain technology – as a linked list with different key on every step, the structure of a node and the information models for a node management with a large granularity. The paper represents the second stage of project Blockchain (permissioned) in Smart Grid: representing of main classes managed objects; managed objects classes for blockchain network installation with accent on security and performance; detail the models for node management with accent on configuration. The models are designed for user interface developers, professors, and students. On the base of management functions managed objects classes are defined by the usage of UML (Unified Modelling Language). From the structure diagrams class diagrams are used. Class diagram describes objects types in the system and different types of static relationships among them. Represented are specific attributes of selected objects classes. The refined information model with more precise granularity of managed objects classes represents a step forward to development of user interface.

**Keywords:** Blockchain, distributed ledger, linked list, peer-to-peer network, transaction

### УПРАВЛЕНИЕ НА БЛОКЧЕЙН ВЪЗЕЛ В SMART GRID

*Мила Илиева-Обретенова*

*Минно-геоложки университет „Св. Иван Рилски“, 1700 София*

**РЕЗЮМЕ.** Блокчейн представлява отворено разпределено счетоводство, което може да записва транзакции между две страни ефективно, доказуемо и по постоянен начин. Блокчейн се управлява чрез мрежа „от точка до точка“, колективно придържаща се към протокол за междувъзлова комуникация и валидираща нови блокове. В България бяха представени: идеята за прилагане на блокчейн в бизнес среда, технологията на блокчейн – като свързан списък с нов ключ на всяка стъпка; структурата на възел и информационните модели за управление на възел с едра гранулност. Статията представлява втори етап на проект Блокчейн (фирмена) в smart grid: представяне на общи класове управлявани обекти; на класове управлявани обекти за инсталиране на блокчейн мрежа с акценти върху сигурността и техническите характеристики; детайлизиране на моделите за управление на възлите с акцент върху конфигурацията. Моделите са предназначени за разработчици на потребителски интерфейс, преподаватели и студенти. На базата на функциите за управление се дефинират класове управлявани обекти, като се прилага унифициран език за моделиране (UML). От диаграмите на структура се използват диаграми на класове. Диаграмата на класове описва типовете обекти в системата и различните видове статични взаимоотношения между тях. Представени са специфични атрибути на избрани класове обекти. Усъвършенстваният информационен модел с прецизирана гранулност на класовете управлявани обекти представлява стъпка напред към разработване на потребителския интерфейс.

**Ключови думи:** Блокчейн, мрежа от точка до точка, разпределено счетоводство, свързан списък, транзакция

### Introduction

Blockchain is an open, distributed ledger that can record transactions between two parties efficiently and in a verifiable and permanent way (Iansiti, Lakhani, 2017). It is typically managed by a peer-to-peer network collectively adhering to a protocol for inter-node communication and validating new blocks (Raval, 2016). China suggests blockchain to become one of the first like networks, build and maintained from government (Stockton, 2020). Europe walks slowly as it creates international blockchain association with the aim regulatory clarity for the early participants (Chandler, 2019). In smart grid blockchain could guarantee effective energy distribution, keep low losses, high quality, and security of power supply. Therefore, node and network management of

blockchain is timely and necessary. The international scientific community suggests different conceptual frameworks. For example, Ullah et al. (2019) suggest model for bidirectional communication in smart grid with blockchain, but without considering the life cycle of the network and its functional areas. Chren et al. (2018), Ge et al. (2019), Hrabovska et al. (2019), and Schwarcbacher et al. (2018) show different aspects of smart grid, but without blockchain. Krishna et al. (2020) represents blockchain application for analysis, but with no realization's suggestions in different business environments. Nedyalkova (2014) represents methodical basics for assessment for internal audit, also in smart grid, but without blockchain. Agung (2020) suggests architecture of smart grid with blockchain nodes – Fig.1.

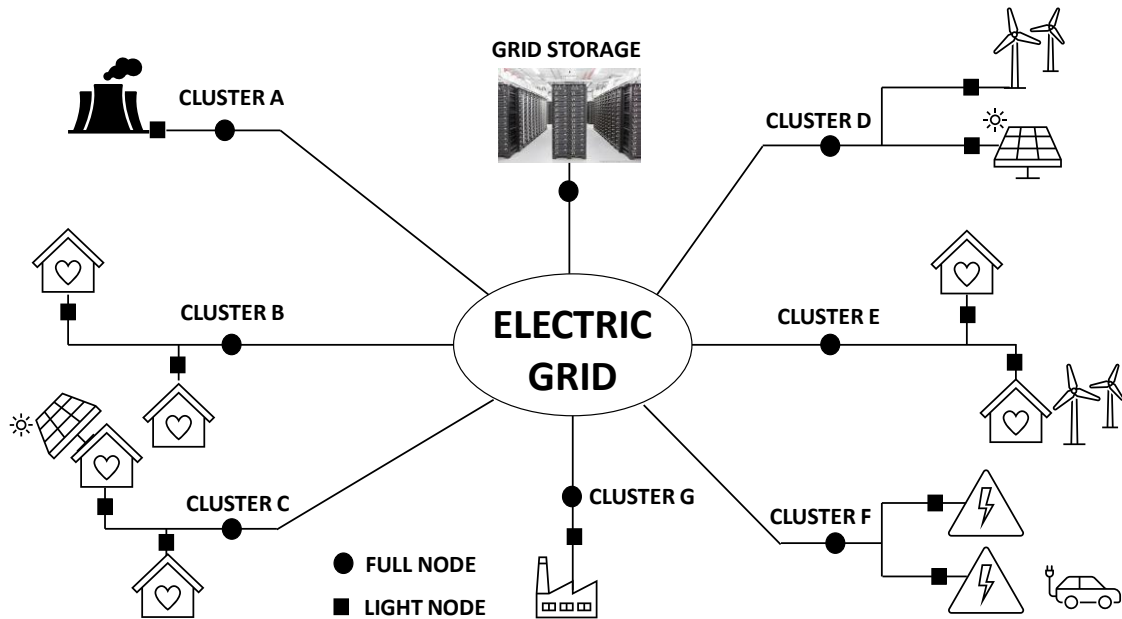


Fig. 1. Architecture of smart grid with blockchain nodes

Cluster A consists of government power plants, cluster B consists of residential buildings, clusters C and E consist of residential buildings too, but some can generate own electricity. Cluster D consists of private power plants, cluster F consists of public electric outlets and cluster G consists of manufacturing enterprise. Each cluster has own full node, and each subscriber (user/producer) has own light node. The grid storage doesn't have light node because it doesn't initiate transaction. Full nodes consist of blockchain copy and their basic functions include confirmation of transactions and consensus support with other full nodes. Full nodes are added to existing distribution points as step-down transformers at distribution lines to users. Light nodes are used in everyday transactions. They apply Simple Payment Verification (SPV) for transactions validation. They don't consist of the full copy of blockchain, so they depend of full nodes. Light nodes are connected to or substitute the existing electricity meters. Management data for both nodes are missing in this model. In Bulgaria were represented: the idea for blockchain application in business environment (Dimov, Stratiev, 2018), blockchain technology – as a linked list with a new key on every step; node structure and information models for node management with a large granularity. The paper represents the second stage of project Blockchain (permissioned) in smart grid: representing of main classes managed objects; representing of managed objects classes for installation of blockchain network with accent on security and performance and detail of models for node management with accent on configuration. Models are purposed for user interface developers, professors, and students.

## Methodology

On the base of management functions are defined classes managed objects applying Unified Modeling Language – UML (Fowler, 2004). From the structure diagrams are used class

diagrams. A class diagram describes objects types in the system and the different types static relationships among them. Diagrams show also features and operations of classes and limitations for the way connecting objects. Features are one term, but they are represented with two quite different notations: attributes and associations. The notation for the attribute describes a distinct feature as text line (second row) in the rectangle, symbolizing the class. Association is a directed line between two classes and its direction is from class-source to class-aim. The name of the feature is set on the aimed end of the association with its majority. The aimed end of the association is connected to the class which is the feature type. The majority of a feature is a note for how many objects could complete the feature. Operations are actions which a class could realize. The "Part-of"-relationship between objects is shown with a rhombus and a line. In the paper are represented specific attributes of selected objects classes. Operations are not represented.

## Results

### 1. Main managed objects classes

In this section are defined managed objects (MO) classes for the actors, the object of management and the way of management. The actors are: Network Operator – MO Operator, Transaction Provider (Network Subscriber) – MO NetworkSubscriber, Transaction Subscriber (Network User) – MO NetworkUser. Objects of management are: Blockchain Network – BCNetwork, Transaction Provider and Transaction Subscriber. Objects of management are managed by profile – MO Profile. Management elements are explained by functional areas on Open Systems Interconnection: MO NConfiguration, MO NMaintenance, MO NSecurity, MO NAccounting, and MO NPerformance. Managed objects for network are represented on Fig.2. In the next sections are identified the managed objects for network installation and for network nodes.

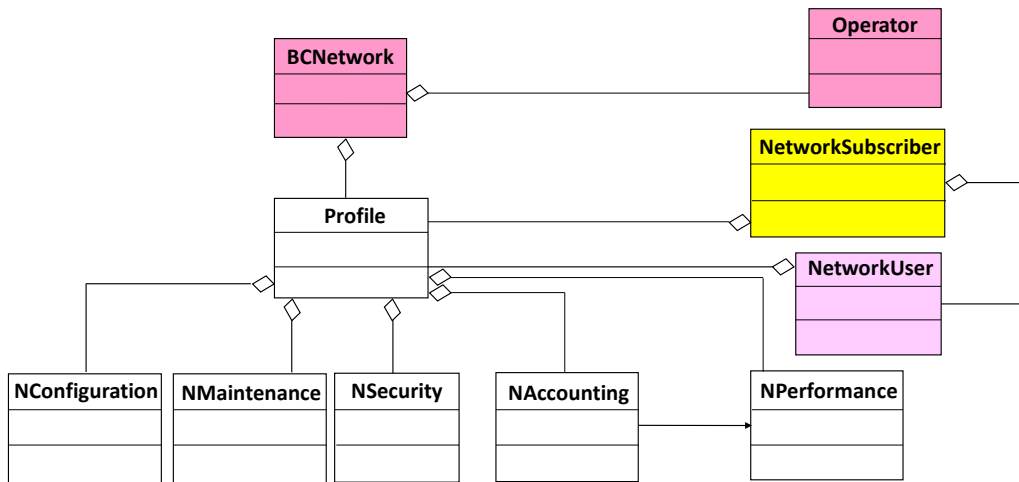


Fig. 2. UML diagram of main managed objects classes for blockchain network

**2. Main managed objects classes for blockchain network installation**

MO Operator represents the information for a person or usually organization, providing the network. MO BCNetwork represents a set of interconnected managed objects (logical and physical), able to transfer information. These objects have one or more general characteristics. In example they could be delegated to single user, producer or provider, and could relate to specific transaction network. A blockchain network could be embedded in another one. MO NetworkProfile consists of the whole information for a management of a blockchain network. MO BCNConfiguration represents the main configuration of blockchain. It consists of all available network elements. Attribute FullNode represents the full nodes in blockchain network. Attribute LightNode represents the light nodes in blockchain network. MO BCNMaintenance represents management information for network maintenance. MO BCNSecurity represents the rights on network security and the

corresponding data. This object must consist of a root key, which enables the monitoring of all transactions in the platform. MO BCNAccounting represents the management data, connected to the financial aspect of network provision. MO BCNPerformance represents the storage and generalization of managed data of performance and usage of specific network. So, it is reached separation of users' identity e.g. separation of transactions and identities. Important attribute is network speed e.g. 15 transactions/sec, hard coded in the protocol. Or 1 transaction is completed for 67 milliseconds. For comparison SCADA sends information every 2-3 sec. MO CoopNetwork represents data for the network, with which is cooperated blockchain. MO SNetwork represents signaling network, used for communication between full and light nodes. MO BNetwork represents the network serving the energy transport (bearer network). MO Configuration represents the configuration of bearer network. Fig.3 shows UML diagram of managed objects classes for Network Installation.

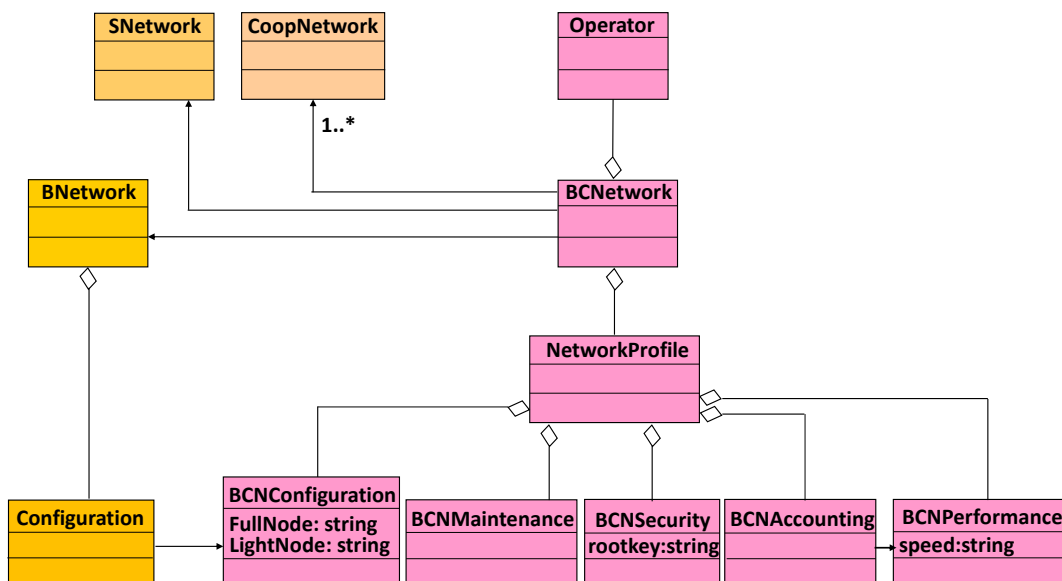


Fig. 3. UML diagram of managed objects classes for Network Installation

### 3. Managed Objects classes for network nodes

#### 3.1. Managed objects classes for light node Transaction Switching Point (TSP)

Aim of this node is continuously balancing of generation and load and keeping the microgrid's connection to the main grid stable. MO Switch represents information for switch in bearer network. MO SCF represents information about Supply Control Function, completed from switch in bearer network. MO BAccounting consists of data for accounting of bearer network. MO SCFConfig represents the configuration of specific SCF. MO RoutingTable represents the routing information of incoming requests in SCF. MO TSP represents management of a light node. MO TSF represents management information for a Transaction Switching Function. MO TSFConfig represents the configuration of specific TSF. MO TSFMainten represents the maintenance conditions of a TSF. MO TSFSecurity represents the security rules of TSF. MO TSFPerform represents performance parameters of TSF and their management. Attribute PowerTurn represents the ramp turn of wind generator when the wind power changes. The speed of turning is 1MW/min. Attribute NPeriods shows the number of periods, during which the node checks for output changes of wind power. One transaction execution is 67 milliseconds, the period by frequency 50 Hz is 20 milliseconds. So, the number of periods is  $67/20 = 3.35 \sim 4$ . This node also creates its own forecasts of load and generation based on weather forecasts and intelligent processing of statistical load data. The forecasting models are updated in real time to compute the optimal settings for power end energy storage in the system. The TSFAccounting represents management information for accounting of TSF. MO TriggerTable represents information for all transactions' triggers in blockchain. Attribute PowerCh shows threshold of charge on renewable output, by which it is necessary to turn on or off, e.g. 1 MW. MO TriggerInfo represents the routing information, connected with possible directions for network access for specific subscriber. This object is also necessary for transactions, allowing

subscriber several sources of power supply e.g. routing depending on time and weather. If the wind stops blowing, the system instantly compensates by discharging the batteries to the grid, as power from the main grid gradually increases to match demand. When the wind starts blowing again, the batteries immediately respond by absorbing a portion of the generated wind power. As they charge, the network turns off and the power supply is meted only from wind generator. The same is valid for solar parks. Attribute Manufacturer shows that in a specific moment the subscriber is turned on as a manufacturer. Attribute TSubscriber shows that in a specific moment the subscriber is turned on as a user. Attribute Renewable shows that in a specific moment the subscriber (could) receive energy from renewable. Attribute GridStorage shows that in a specific moment the subscriber (could) receive energy from grid storage. Attribute Network shows that in a specific moment the subscriber (could) receive energy from the network. This object belongs to the area Transactions management too. MO FSManager represents supporting mechanism for competitive realizations of blockchain transactions and transactions out of blockchain in a request. MO BCSManager represents interaction mechanism with TCF for transactions provision. It discovers events which might be reported to active transaction realization, and manage TSF resources, which must support transactions realizations. MO FEAManager represents mechanism for information transfer with other functional element (or node) by notifications. MO TCF will be represented in next section. MO BSManager represents a mechanism for return in requests, after the transaction have been completed (confirmed). MO NBCFManager represents requesting mechanism of transaction feature out of blockchain. MO TSFUsageLog represents the collected usage entries of TSF. MO TSFAccountingLog represents the collected accounting entries of TSF for transaction execution. Fig.4 shows UML diagram of managed objects classes for light node TSF.

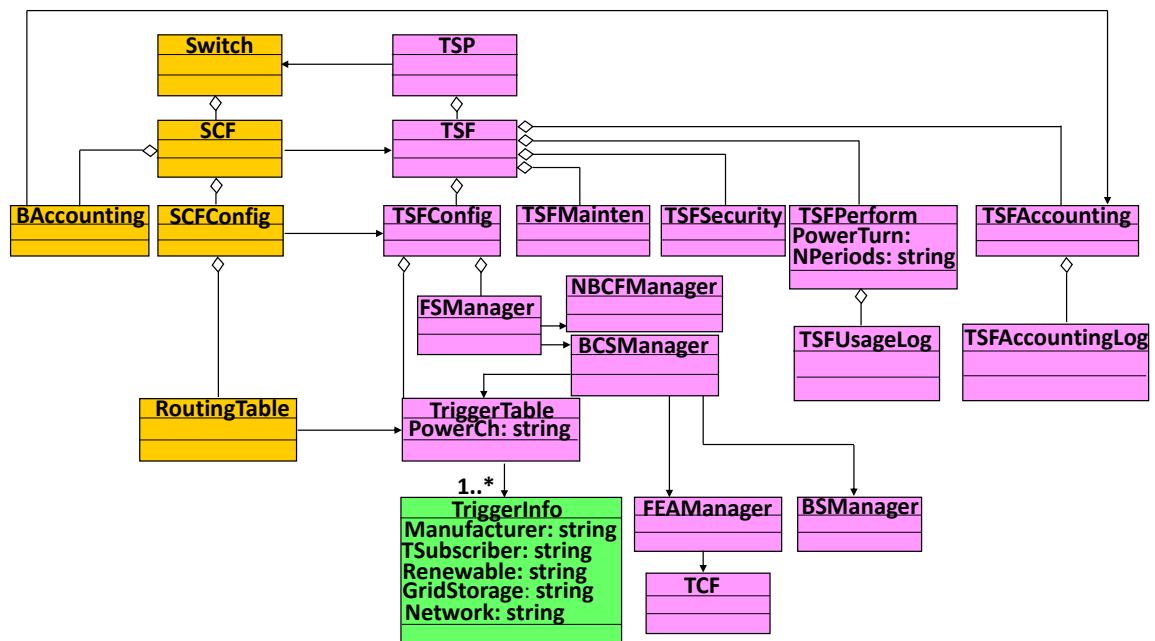


Fig. 4. UML diagram of managed objects classes for light node TSP

**3.2. Managed objects classes for full node Transaction Control Point (TCP)**

MO TCP represents information for node TCP. This node consists of three functions: TCF (Transaction Control Function), TDF (Transaction Data Function) and TRF (Transaction Resource Function).

**3.2.1. Managed Objects Classes for function TCF.** MO TCF represents information for control management over a transaction. MO TCFMaintenance represents maintenance conditions of TCF. MO TCFSecurity represents the security rules of TCF. MO TCFConfiguration represents the configuration of TCF. MO TCFPerformance represents the performance parameters of TCF and their management. MO TCFAccounting represents the management information for accounting of TCF. MO TCFPreventiveFunction represents the testing programs of TCF in normal working conditions. MO LogicExecutionEnvironment represents environment for execution of transaction logic with all included managers, programs, and data, e.g. Hyperledger. MO LogicExecutionManager represents information for

functionality, processing and controlling of transaction execution. MO ProgramLibrary represents resource for storage of different programs in TCF. MO Program represents the description of a program with transaction logic (consensus), e.g. PoW (Proof of Work), PoSt (Proof of Stake), PoSe (Proof of Service) and Pol (Proof of Importance). This object belongs to area Transactions Management too. MO DataAccessManager represents information for storage, management, and access to shared information in TCF and for access to remote information in other nodes and functional elements by MO FEAccessManager. MO FEAccessManager and MO TSF were represented in section 3.1. Managed Objects Classes for light node Transaction Switching Point (TSP). MO TRF (Transaction Resource Function) and MO TDF (Transaction Data Function) will be represented in next sections. MO TCFUsageLog represents the collected entries for usage of TCF. MO TCFAccountingLog represents the collected entries for accounting of TCF for transaction execution. Fig.5 shows UML diagram of managed objects classes for full node TCP.

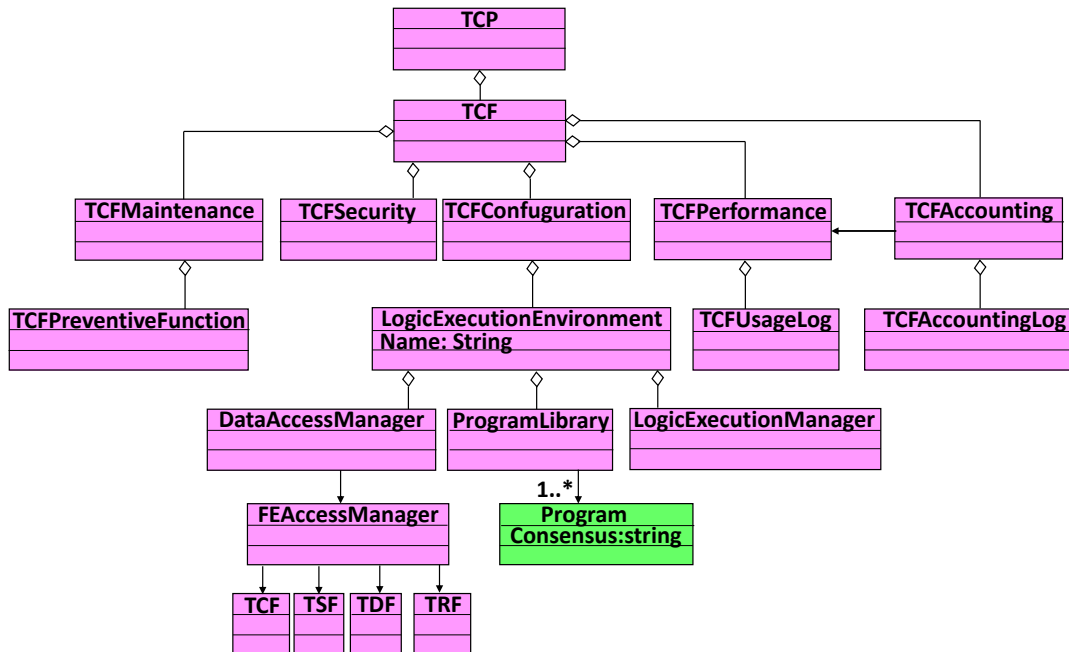


Fig. 5. UML diagram of managed objects classes for full node TCP

**3.2.2. Managed Objects Classes for function TDF.** MO TDF represents management information of data for transactions users. MO TDFConfiguration represents the configuration of a specific TDF. MO TDFPerformance represents the parameters for quality work of TDF and their management. MO TDFAccounting represents management information for accounting of TDF. MO TDFMaintenance represents maintenance conditions for TDF. MO TDFSecurity represents the security rules of TDF. MO TDFDataManager represents information for storage, management, and access to data in

TDF. MO TDFDataBase represents information for the data base in TDF. MO FEAccessManager was represented in section 3.1. Managed Objects Classes for light node Transaction Switching Point (TSP). MO TDFData represents an entry in functional element TDF for specific transactions user, e.g. Received/Consumed/Rest/Sold Energy. MO Template represents the description of entry format for each transaction in blockchain. The last two objects belong to the area Transactions Management too. MO TCF was represented in the previous section. Fig.6 shows UML diagram of managed objects classes for function TDF.

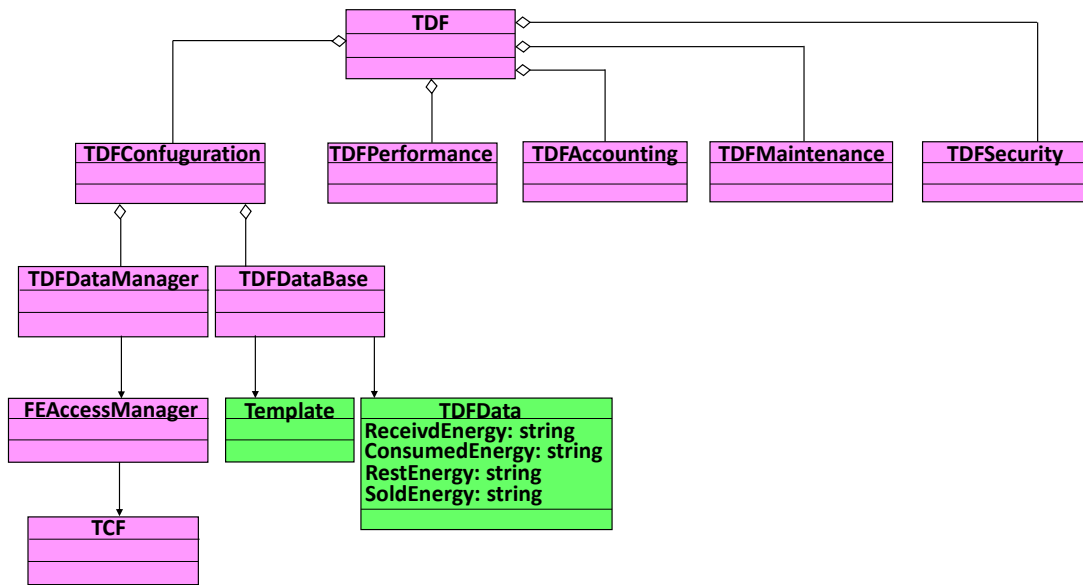


Fig. 6. UML diagram of managed objects classes for function TDF

**3.2.3. Managed Objects Classes for function TRF.** MO TRF represents management information for producer in transactions. MO TRFConfiguration represents the configuration of a specific TRF. MO TRFPerformance represents performance values of TRF and their management. MO TRFAccounting represents the management information of accounting in TRF. MO TRFMaintenance represents maintenance conditions for TRF. MO TRFSecurity represents the security rules of TRF. MO FEAccessManager was represented in previous sections. MO ResourceManager represents information for resources, managed from TRF. MO TRFUsageLog represents collected entries for usage of TRF.

MO Resource represents description of specialized resource, used in a transaction. MO PowerPlant describes the data for the used power plants, e.g. thermal and nuclear. MO Renewables describes the data of used renewables, e.g. hydroelectric powerplants, solar parks, wind generators, generators with biomass etc. MO GridStorage describes the data of used electricity storages, e.g. pumped and battery storages. The last four objects belong to the area Transactions Management too. MO TCF was represented in section 3.2.1. Managed Objects classes for function TCF. Fig. 7 shows UML diagram of managed objects classes for function TRF.

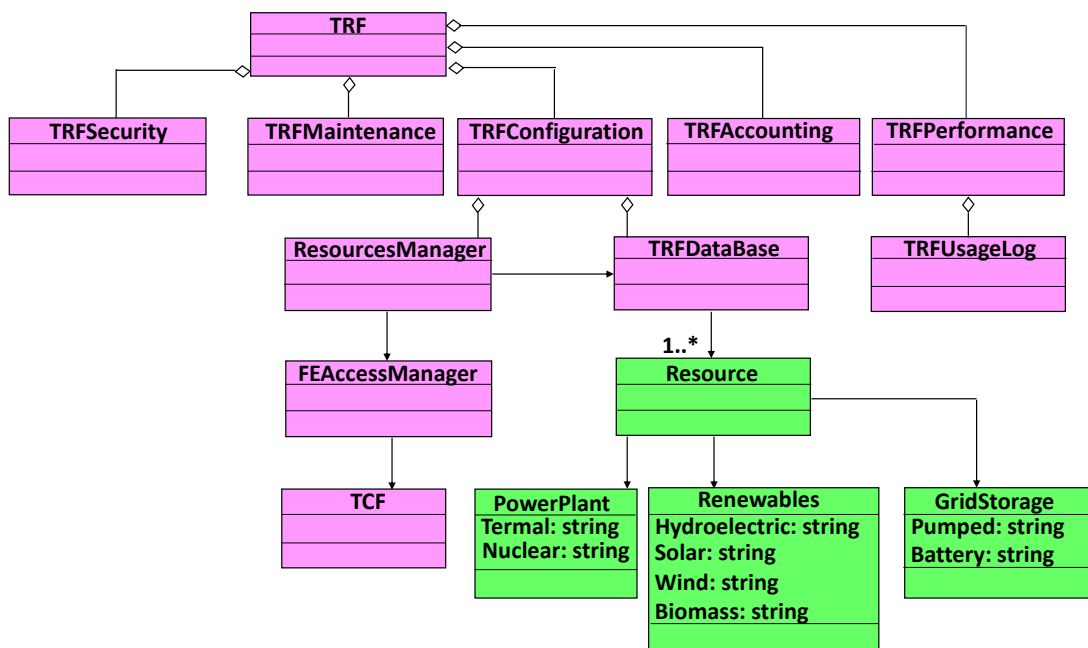


Fig. 7. UML diagram of managed objects classes for full node TRF

## Conclusion

Deployment of blockchain is still in testing stage. Although the paper shows its advantage – specialized (permissioned) networks could be easily scaled because all confirmations happen in network. Considered is the question about separation of transactions and identity of users. A detail information model represents refined granularity of managed objects classes about Blockchain Network Configuration, Blockchain Network Security, Blockchain Network Performance, Performance of Transaction Switching Function, Trigger Table, Trigger Information, Logic Execution Environment, Program, User data and Resources - Power Plants, Renewables and Grid Storage. With these improvements the model represents a good base for user interface development. The permissioned blockchain has its disadvantages, but the long-term perspective forecasts deployment in the next line: business platforms, local, national, and international networks.

**Acknowledgements.** This research was supported by the Bulgarian projects under contract: "Study of the possibilities for application of DLT using blockchain in data sharing in mining activities and electricity production from biogas "MEMF-164.

## References

Agung, A. A. G., Rini Handayani, 2020, "Blockchain in Smart Grid", *Journal of King Saud University – Computer and Information Sciences*, DOI: 10.1016/j.jcsuci.2020.01.002

Chandler, S., 2019, "EU launches International blockchain association bringing crypto one step closer to mainstream adoption", *Cointelegraph*, <https://cointelegraph.com/news/eu-launches-international-blockchain-association-bringing-crypto-one-step-closer-to-mainstream-adoption>

Chren, S. et al., 2018, "Reliability Data for Smart Grids: Where the real Data can be found", *Smart City Symposium Prague (SCSP)*

Dimov, E., Stratiev., N., 2018, "The Investment of Cryptocurrencies: A QUES for Earnings Lost", *University of Mining and Geology, Journal of Mining and Geological Sciences, Volume 61, Part IV: Humanitarian Sciences and Economics, Sofia, ISSN 2535-1206*, pp.33-36

Fowler, M., 2004, "UML Distilled: A Brief Guide to the Standard Object Modeling Language". 3<sup>rd</sup> ed. Addison-Wesley Professional

Ge, M. et al., 2019, "Data Quality Management Framework for Smart Grid Systems", *International Conference on Business Information Systems BIS 2019: Business Information Systems*, pp. 299-310, DOI: 10.1007/978-3-030-20482-2\_24

Hrabovska, K. et al., 2019, "Smart Grid and Software Testing Process Models", *Smart Cities Symposium Prague (SCSP) lansity, Marco; Lakhani, Karim R. (January 2017). "The Thorough about Blockchain". Harvard Business Review. Harvard University.*

Krishna, G. J. et al., 2020, "Smart Blockchain: A Formidable Combination of Analytics and Blockchain – A Survey", *In book: Smart Systems Design, Applications, and Challenges*, DOI: 10.4018/978-1-7998-2112-0.ch003

Nedyalkova, P., 2014, "Methodological Foundations of the Assessment of Internal Audit", *Izvestia Journal of Economics, Varna, 2014, No.1*, pp. 65-80

Raval, Saraj (2016). "What is a Decentralized Application?". *Decentralized Applications: Harnessing Bitcoin's Blockchain Technology*. O'Railly Media, Inc. pp. 1-2. ISBN 978-1-4919-2452-5. OCLC. 968277125

Schvarcbacher, M. et al., 2018, "Smart Grid Testing Management Platform" (SGTMP), *Applied Sciences* 8(11):2278, DOI: 10.3390/app8112278

Stockton, N., 2020, "China launches national Blockchain Network in 100 Cities", <https://spectrum.ieee.org/computing/software/china-launches-national-blockchain-in-100-cities>

Ullah, Z. et al., 2019, "Smart Grid Blockchain (BC) Conceptual Framework: Bi-Directional Models for Renewable Energy District and Utility", *15<sup>th</sup> International Conference on Emerging Technologies*

## SUBSTANTIATION OF THE EFFICIENCY OF CONTAINER TECHNOLOGIES APPLICATION FOR THE TRANSPORTATION OF ROCK IN DEEP PITS

**Kuzmin Sergey, Turbit Andrey, Salko Oksana**

*Rudny Industrial Institute, 111500 Rudny, Republic of Kazakhstan; info@rii.kz*

**ABSTRACT.** In the article a new technology of container carriage of rocks without construction of transport communications in an open-pit mine and with technological and energy-saving advantages is proposed. These advantages are: simultaneous excavation of rocks, transportation of rocks by the shortest distance, small mass of a container and mobility of a complex of hoists which will reduce energy expenses and the cost of transportation of the mined rock. One of the principal advantages of the developed technology is decrease in environmental emissions into the atmosphere of the open-pit mine thanks to the reduction of the vehicle fleet. This technology will enable significant improvement of the environmental situation in the area of mining operations. The main feature of the proposed technology is that all types of equipment for container transportation are simple to manufacture and can be created directly in the conditions of mining sites.

**Keywords:** pit, container, transport, economic and environmental efficiency

## ОБОСНОВАНИЕ ЭФФЕКТИВНОСТИ ПРИМЕНЕНИЯ НА ГЛУБОКИХ КАРЬЕРАХ КОНТЕЙНЕРНОЙ ТЕХНОЛОГИИ ТРАНСПОРТИРОВАНИЯ ГОРНОЙ МАССЫ

**Кузьмин Сергей, Турбит Андрей, Салько Оксана**

*Рудненский индустриальный институт, 111500 Рудный, Республика Казахстан*

**РЕЗЮМЕ.** В статье предлагается новая технология контейнерной перевозки горных пород без строительства транспортных коммуникаций в карьере и обладающей технологическими и энергосберегающими преимуществами. Этими преимуществами являются: одновременная выемка горных пород, транспортировка горных пород на кратчайшие расстояния, небольшая масса контейнера и подвижность комплекса подъемников, что позволит снизить энергозатраты и стоимость транспортировки добываемой породы. Одним из основных преимуществ разработанной технологии является снижение выбросов в атмосферу карьера, благодаря сокращению парка транспортных средств. Данная технология позволит значительно улучшить экологическую ситуацию в районе добычи полезных ископаемых. Главная особенность предлагаемой технологии заключается в том, что все виды оборудования для контейнерных перевозок просты в производстве и могут быть созданы непосредственно в условиях горных предприятий.

**Ключевые слова:** карьер, контейнер, транспорт, экономическая и экологическая эффективность

### Introduction

In the modern conditions the need for efficient and environmentally safe development and management of subsurface resources is becoming ever more relevant. As a result of the scientific and technological revolution the adverse effect on the environment has increased many times. The opencast mining – one of the principal sources of the environment pollution – plays a leading role in this.

In terms of power, conveyance of the mined rock along the edge of the open-pit mine by motor transport increases the rate of fuel consumption 2–3 times. Accordingly, harmful emissions into the atmosphere of the open-pit mine increase as well. Significant costs of conveying the rocks by motor transport limit the cost-efficient height of mine dumps, which leads to the increase of their occupied area and additional environmental losses.

The environmental issues of the use of motor transport at open-pit mines have several directions:

- First of all, pollution of the atmosphere of the open-pit mines as a result of diesel engine emissions. It was found that the biggest rate of fuel consumption takes place during conveyance of the mined rock from the open-pit mines. Excavating-motor transport hubs have one fundamental disadvantage in the form of additional inefficient diesel fuel

consumption during the down time in the process of loading a dump truck;

- Secondly, dust emission in the process of blow-off from the surface of the mined rock in the truck body and from the wheel-road surface interaction. The high level of the dust blow-off from the dump truck surface results from a significant area of the rock surface, which is related to the geometric parameters of the truck body. During interaction of the wheels with the road surface the level of dust emission depends on the speed of dump trucks and road surface. Additional road irrigation and surface improvement costs are required in order to fight dust emission;

- Third, dust emission from the surface of external mine dumps of waste rock. As mentioned above, the external motor dumping sites are characterised by a large area of dump operations and a long-term running order. This results in a high level of dust blow-off from the surface of mine dumps and environmental damage for the surrounding land;

- Fourthly, increase of the land area of external mine dumps and withdrawal of these areas from agriculture for long terms. The area of external mine dumps depends on their height, which in turn is determined by the cost-efficient height of rock hoisting by motor transport. High unit cost of motor transportation limits the height of mine dumps (usually up to 20–40 metres) and increases its area.

Delivery of mined rock to mine dumps or bunkers of concentrating factories accounts for the principal share of energy consumption in mining. The issue of transport support of the bottom levels of deep open-pit mines has no ultimate technological solution, while the principal share of transport costs falls on the cycle of hoisting the mined rock.

Enterprises developing deposits in the unconsolidated and water-flooded rock face significant transportation problems. A low load bearing capacity of rock, complicated road conditions lead to the fact that the prime cost of transportation works is double compared to the average values in other open-pit mines. Given the combination of the identified rock and technological issues in the conditions of critically increased man-caused pressure on the environment and intense competition in the external market, creation of an energy-saving and environmentally safe technology of opencast mining becomes very relevant.

The selection of technological equipment of open-pit mines is the most complicated issue in the technology of the existing open-pit mines. This shows that they have a range of contradictions requiring new solutions. With the lowering of mining in open-pit mines the distance of motor transportation increases therefore higher capacity dump trucks are required. Increase of the capacity of dump trucks disrupts the optimal ratio of the capacity of a shovel size of a face shovel to the dump truck's body capacity. In order to decrease the down time of expensive dump trucks it is required to increase the shovel power and standard dimensions of a face shovel. The increased dimensions of dump trucks require the extension of highways, manoeuvring platforms, etc., which significantly decreases the volumes of ore mining. This facilitates the increase in a number of internal open-pit mine loading points used in combined transportation.

### Technology Improvement

It is proposed to introduce a container technology of mined rock transportation in the opencast mining, which will allow increasing the opencast mining indicators in the area of saving energy resources and environment conservation at a totally new level.

It will include:

- One-off rock fragmentation in the process of loading a container, which reduces energy consumption;
- Delivery of mined rock by transportation of a container's assembly to the place of hoisting is performed at minimum horizontal road distances, which leads to reducing the required vehicle fleet, the rate of consumption of fuel, tires and emissions of harmful gases;
- The coefficient of dead load of a transport container (0.25–0.30) is significantly lower than the coefficient of a truck body (0.70–0.80) or of railway transport (0.80–0.82) therefore, the unit cost of energy for transportation of the rock mass in a container is reduced 1.4 times;
- The container hoisting hub is mobile, which allows moving to a new place during blasting operations or another bench in an open-pit mine with subsequent mining of the open-pit mines. Opportunities for regulation and maintenance of the optimum mining regime increase;
- The need for additional energy-intensive fragmentation of the mined rock is eliminated as opposed to the process schemes with the use of conveyer lifts;
- Container delivery of the overburden rock with the

use of an open-pit mine hoist during liquidation of the open-pit mine will reduce the required land and form a compact height with minimum rock hoisting.

The key aspect of the proposed technology is in the fact that the entire equipment for container carriage is not difficult to produce and can be produced at mining enterprises. Walking mining excavators may be used as hoists.

In accordance with the basic process scheme of the open-pit mine hoisting containers are installed on the benches of the open-pit mine for hoisting containers from the lower benches up (according to Fig. 1). On the intermediate platforms loaded and empty containers are cleared up. Following hoisting to benches, where the railway transport operates, containers are loaded directly into carriages.

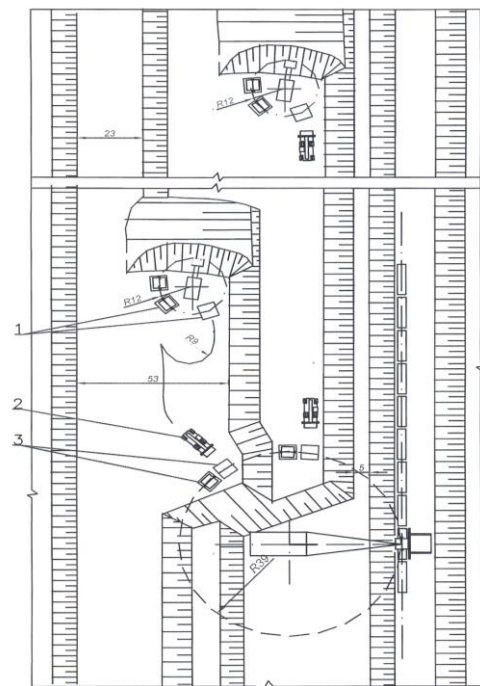


**Fig. 1. Plan of energy-saving container technology in opencast mining. 1 – containers under loading, 2 – container carriers; 3 – containers on the platform at the hoist**

One hoist serves two benches during the hoisting. The hoist is located at the platform of the lower bench beyond the possible caving area. The container is delivered by a container carrier to the bottom edge of the lower bench, the hoist moves the container to the upper bench platform from where a container is delivered to the next hoist through the interchange point.

The new technology may be applied within the existing combined transportation patterns, for example, within a motor-railway transportation pattern as an interagent – a hoisting-reloading point.

The container hoisting hub may become an alternative solution for a major problem of modern open-pit mines in tapping of new horizons, though it may be used at any mining stage in the open-pit mine.

Abandoning the hoisting of mined rock by motor transport provides an opportunity to increase the grade limit of ramps, as they will be used for traffic of empty cars only. A possible transition from the grades 8 % to the grades 15 % will reduce the area for positioning of ramps in the open-pit mine.

The efficiency of the new technology is expressed in reducing, in terms of cost savings, of the specific energy

consumption for transportation of the mined rock compared to the most common technology with the use of motor-railway transport with reloading at the internal open-pit mine warehouses: for hoisting the mined rock by an electric drive hoist in containers with the minimum dead load coefficient; from reducing the coefficient of overburden removal by reducing the area of the reloading point, which organisation in this case loses its meaning.

The hoist capacity is justified by the required productivity of the open-pit mine. The productivity of the hoist  $Q_{year}$ , thous. t/year will be determined depending on the time of its operating cycle  $T_c$  according to the equation:

$$Q_{year} = \frac{3600 \cdot T_c \cdot K_{eu} \cdot Q_{cont} \cdot K_{cu}}{T_{cycle}}, \quad (1)$$

where

- $T_c$  Calendar annual fund of time,  $T_c = 8760$  hours;
- $K_{eu}$  Coefficient of equipment use,  $K_{eu} = 0.75$ ;
- $Q_{cont}$  Container capacity, t;
- $K_{cu}$  Coefficient of the capacity use,  $K_{cu} = 0.95$ ;
- $T_{cycle}$  Time of cycle, sec.

We shall assess the impact of the container's capacity complex on the productivity, accepting the time of cycle according to the passport speed of hoisting of a walking excavator 1 m/s. The time of hoisting to the height of 80 m will be 80 seconds and taking the coupling into account the total time of the hoist's cycle is 220 seconds.

During movement of a dump truck the ascent time to the height of  $H = 80$  metres under the grade of  $i = 80 \text{ ‰}$  and average speed  $V = 15 \text{ km/h}$  will be:

$$t = H / (1000 \cdot i \cdot V) = 80 / (0.08 \cdot 15 \cdot 1000) = 0.067 \text{ hours.}$$

Consequently, during movement of a dump truck, only the time of the truck ascent will be 240 seconds.

The impact of the container capacity (G) on the productivity of hoisting devices (Q) is given in Fig. 2.

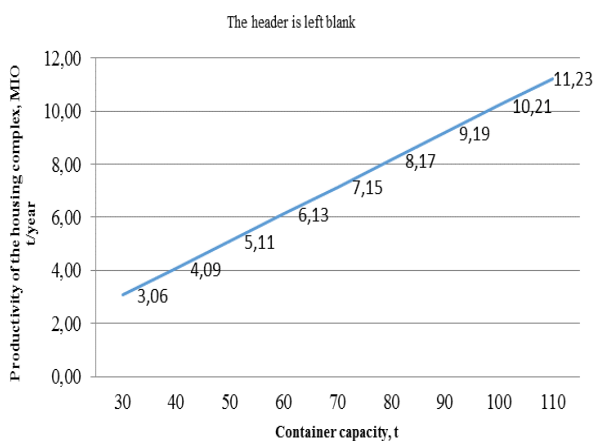


Fig. 2. Impact of the container capacity on the productivity of the hoisting complex

By analysing the graph it can be seen that one complex of hoisting devices with containers with the carrying capacity of 80 tons may secure productivity around 9 million tons/year but if higher productivity is required, it is necessary to increase the number of hoisting complexes.

## Results

The efficiency of container hoisting in the container technology of the opencast mining is in the reduction of energy and economic losses due to the down time of vehicles under loading and in the productivity increase of an excavator. The cycle path of a container carrier does not include down time during loading as opposed to dump trucks and railway trains.

The process scheme with the use of hoisting devices of the open-pit mine is sufficiently reliable, flexible and diverse. This allows gradual increasing of the height of hoist, positioning the systems of hoisting devices on the open pit benches, distributing or combining the cargo traffic according to the types of mined rock.

In this case the means for increasing the efficiency of the transport system will be the application of container equipment in the motor transport working area based on the increase of capacity of container carriers with the help of traction engines with an electric drive. If the hoisting height by one hoisting mechanism is insufficient, two- or three-stage hoisting is possible. This will allow reducing or excluding the container conveyance by container carriers, which deliver loaded containers from excavators to the hoisting locations. In the container technology the mined rock according to Fig. 1 is loaded to containers by excavators. Two-three containers are set up in the area of excavator's operations. The exchange of loaded containers to empty ones is performed by automatic loaders – container carriers. They deliver loaded containers to short distances on the container platform in the area of works of the next hoisting device. Container carriers also perform descent of empty containers into the open-pit mine.

In the container technology within the opencast mining the mined rock is loaded by face shovels into containers, which are delivered by hoisting-transport vehicles to the reloading point. Then containers are hoisted to surface by hoists and are delivered to concentrating factories or mine dumps by container carriers. There, a hoist carries out its automatic reloading by gripping it (Fig. 3).

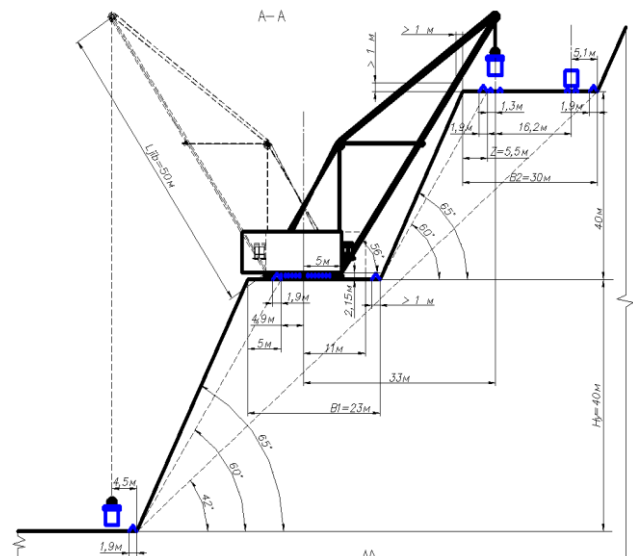


Fig. 3. Passport of setting up a hoist on a bench

Based on the analysis of existing containers that are used in the industry for the transportation of goods, it was found that none of the container designs suits us. Basically, containers are used to transport loose fine goods, and for the

transportation of lumpy abrasive rock, the patent search conducted has not given positive results. For transportation of rocks in a deep quarry, a container was designed that has no analogues (Fig. 4). The design of the container is protected by the patent of the Republic of Kazakhstan No. 33091.

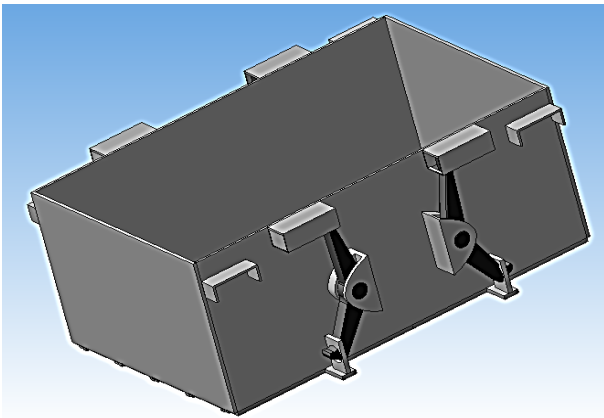


Fig. 4. General view of the container

Structurally, the container is welded, with a drop-down bottom. The opening of the bottom is controlled by the operator of the lifting machine due to the system of mechanical levers. All container assembly elements are tested for mechanical strength using computer simulation methods. The bottom section is attached to the walls on five hinges. When loading, the container is installed on the ground, and the bottom sections are fixed with a locking element – a knee. The container is lifted by the side fittings located on the side walls. In this case, the stops of the load gripping device come into contact with the fittings and keep the container in the closed state. During the unloading process, the stops are released from contact with the fittings, and due to their own weight, the rock is poured out of the container. The bottom closure occurs when the container is installed on the stand, which causes the bottom sections to move upwards until they are completely in contact with the knee. The bottom of the container is one of the most loaded parts and directly perceives the load of the weight of the transported rock, as well as the dynamic load from lifting, transporting and lowering to the surface. In addition, this part of the container perceives the main load from the impact of the loaded rock mass. For the manufacture of the bottom of the container, steel St60 is used. The most labour-intensive operations in the production of loading and unloading operations with large cargoes are their slinging and detaching. Performing these operations manually requires large expenditures of inefficient and unsafe labour of loaders and prevents the introduction of complex mechanised and automated technological processes for loading and unloading. In our case, the usual lifting device is not suitable and, therefore, it is advisable to use a spreader. The following requirements are imposed on the designed spreader: high reliability coefficient and reliability, economical operation, which allows increasing the service life and largely avoiding container deformation, automating container pickup, the possibility of unloading the container and the simplicity of the design. Known constructions of spreaders do not meet the requirements of open pit mining; therefore, the design of the spreader was developed to lift containers in a quarry (in accordance with Fig. 5).

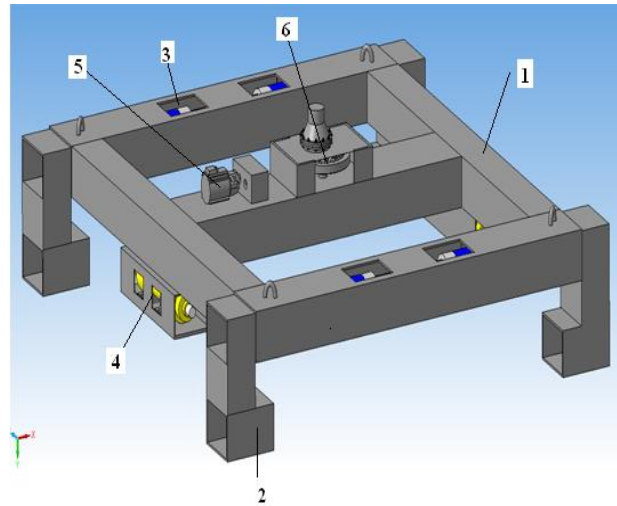


Fig. 5. General view of the gripping device

When transporting containers, the pickup device consists of a supporting beam 1, which is equipped with rectangular grippers 2. The length of the beam increases, and both sides are extended with the help of hydraulic cylinders 3. The grippers move to clamp the container. The beam is equipped with hydraulic cylinders 4, providing unloading of the container. The control hydraulic station 5 is located on the support beam and includes: engine, pumps and control valves. A gear that is rotated by a hydraulic motor located on the spreader 6 is used to centre the container. The beam of the traverse is made of steel grade 10HSND. The material of the bracket for unloading on the container is steel St10. The calculation of the hydraulic system of the unloading device was carried out. The hydraulic drive uses standard assembly items and parts. Hydraulic oil VMGZ (TU 101479-74) is used as a working fluid. The container with the spreader is shown in Fig. 6.

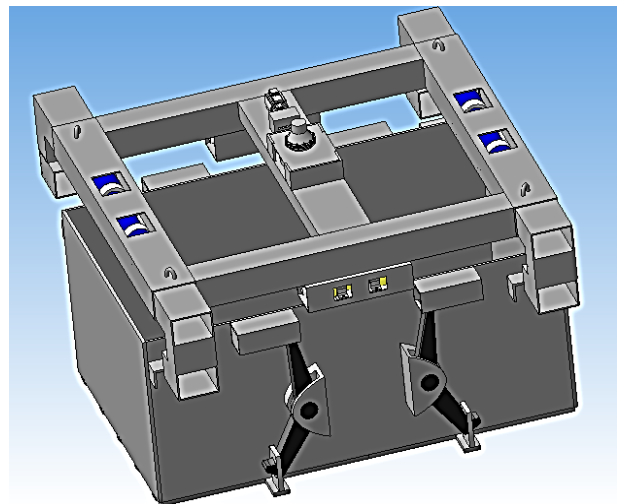


Fig. 6. View of the container with the spreader

The efficiency of the new technology will be reflected in the reduction of the specific energy consumption for transportation of the rock mass compared to the most common technology using road and rail transport with overloading into intra-warehouse warehouses due to cost savings: to lift the rock mass due to lifting it with electric powered hoppers in containers having minimum tare coefficient; from reducing the overburden by reducing the area of the transshipment point, the device of which in this case loses its significance.

## Discussion

Calculations of the use of container technologies in deep open-pit mines showed that compared to traditional options of transportation of the mined rock by motor transport or combined motor-railway transport, the energy efficiency of the new technology is obvious and the level of its advantage increases with the increasing hoisting height of the mined rock.

The graph of growth of the economic efficiency of the container technology depending on the depth of an open-pit mine is presented in Fig. 7.

Having analysed the graph it can be concluded that the economic efficiency from the introduction of a container hoisting in the open-pit mine increases with the growing depth of mining. It happens due to the reducing of operating costs, such as diesel fuel consumption, amortised values and decreasing the costs for equipment repairs and reducing the down time of the equipment due to environmental damages.

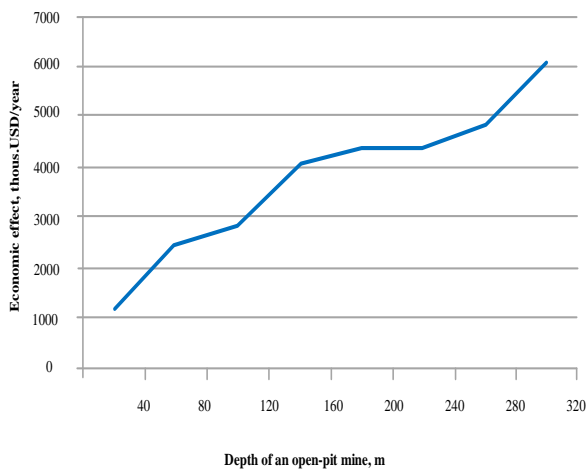


**Fig. 7. Dependence of the economic efficiency of the introduction of the container technology on the depth of an open-pit mine**

## Conclusions

The container technology allows solving the entire set of objectives of the principal technological processes of the opencast mining – from the extracting of rock in the front to loading into vehicles at the reloading warehouse. The use of exchangeable containers in the fronts will significantly change the organisational principles of the excavation-transport hubs, will increase their productivity and a coefficient of the use of excavators within principal operations. Replacement of the obsolete extraction-and-loading equipment with the advanced one and increase of the transport provision of the fronts will increase the level of used area of mining and productive capacity of the open-pit mine.

The major advantage of the container technology is an automation outlook of a range of operations of the transport process in the open-pit mine and on the daylight area. The performed assessment of the economic indicators of the container technology shows its economic advantages over the current methods of mined rock delivery. In the process of technical and economic justification of the introduction of the container technology a detailed comparison of the two technologies of deep horizon development was carried out – with the help of the motor transport and containers. As a result, at all depths of the open-pit mine the economic effect within the range from 1 to 6 million dollars a year was obtained.

## References

- Yudin, A.V., 2011. Theory and technical solutions of transport and cargo handling systems in quarries. Scientific monograph. Ekaterinburg: USMU. (in Russian)
- Sheshko, E.E., 2006. Mining transportation machines and equipment for open pit mining. Moscow: MISIS. (in Russian)
- Bitimbaev, M.Z., Kuzmin, S.L., Maulyanbaev, T.I., Osadchyi, V.I., Oryngozhin, E.S., 2015. The use of container-type transportation system in open pit mining: monograph. Almaty: ALESHAN. (in Russian)
- Rzevsky, V.V., 2014. Open pit mining. Technology and overall mechanization. Moscow: LIBROKOM Publishing House. (in Russian)

# PUBLIC-PRIVATE PARTNERSHIP IN DECLARED STATE OF EMERGENCY – A COMPARATIVE STUDY OF THE USA FEDERAL DEFENSE PRIORITIES AND ALLOCATIONS SYSTEM

**Irina Mindova**

*“G.S.Rakovski” National Defense College, Sofia, 82 bul. “Evlogi and Hristo Georgiev”, irina\_mindova@abv.bg*

**ABSTRACT.** The aim of the report is by means of comparative study of the US federal priorities and allocation system to introduce the possibility for constructing a public-private partnership mechanism, based on a system of priority contracts which is meant to guarantee security of supply in emergency.

**Keywords:** public-private partnership, scarce resources, security of supply

## ПУБЛИЧНО-ЧАСТНО ПАРТНЬОРСТВО ПРИ ИЗВЪНРЕДНИ РЕЖИМИ НА ДЪРЖАВНО УПРАВЛЕНИЕ – СРАВНИТЕЛНО ИЗСЛЕДВАНЕ НА ФЕДЕРАЛНАТА СИСТЕМА НА САЩ ЗА ПРИОРИТЕТНОСТ И РАЗПРЕДЕЛЕНИЕ

**Irina Mindova**

*Военна академия „Г.С.Раковски”, гр. София, бул. „Евлоги и Христо Георгиеви” №82, irina\_mindova@abv.bg*

**РЕЗЮМЕ.** Основната цел на доклада е посредством сравнително изследване на федералната система за приоритетност и разпределение на ресурсите в САЩ, да представи възможностите за създаване на механизъм, основан на публично-частно партньорство, за гарантиране сигурността на доставките в условията на извънредни режими на държавно управление, чрез система от приоритизирани договори.

**Ключови думи:** публично-частно партньорство, оскъдни ресурси, сигурност на доставките

## Introduction

The global pandemic caused by COVID-19 has become a global test for the adequacy of the emergency management legislation and system – both national and at regional level of cooperation. The current situation is unique for some reasons: the unprecedented scale of people affected all over the world and global scarcity of certain critical products like face masks, ethyl alcohol and breathing and respiratory equipment.

Bulgarian emergency management legislation provides the following decisions for security of supply in emergencies: the use of state reserves under the State Reserves and Wartime Stockpiles Act (SG 9/ 2003, last amend SG 65/ 2020) and the use of private resources and products under a signed agreement for assistance in emergency with private entities under the Disaster Protection Act (SG102/ 2006, last amend SG 60/ 2020). State reserves are intended to be used in state of war or emergency and crisis situations and they have to supply the population and national market. The main problem – they are calculated for a certain period of time and have a limited amount and there is always the risk it is unavailable, inadequate, of poor quality or just missing. The legal regulation for agreements of assistance is scarce at legislative level and it only gives the plea for signing such kind of agreements. There is no legal regulation for the content of the agreements and types of assistance – all these questions are decided at the level of emergency planning – which means no imperative provision for the content and no guarantee about the quality and availability of the assistance, also no transparency, no

strict and stable rules for the public-private partnership. The lack of legal regulation harms the principle of public-private partnership and shared responsibility for emergency preparedness. Security of supply is managed only by a standardization document<sup>1</sup> but it does not have a legal binding force.

That is why a comparative study of other national models is a good starting point for discussion.

Comparative study includes the concept for priorities and allocation system and the legal reglamentation of the thematic in order to point out the main idea that a special legislation development is needed to improve our national model.

## A special form of public-private partnership

A special form of public-private partnership that helps the government and the state to share the responsibility of emergency supply with scarce items, materials and resources is the Defense Priorities and Allocation System (DPAS). It is based on the Title I of the Defense Production Act 1950 which is used also for emergency preparedness activities pursuant to Title VI of the Robert T. Stafford Disaster Relief and Emergency Assistance Act and the priorities authority of the selective service act. The system is administered by the Bureau of Industry and Security<sup>2</sup>, Department of Commerce.

<sup>1</sup> BDS ISO 28 000:2012 Specification for Security Management Systems for the Supply Chain, Bulgarian Institute for Standardization.

<sup>2</sup> The Bureau of Industry and Security administers this authority through the Code of Federal Regulation, §700.

There is a clear legislative regulation for the functioning and administering the system which includes Defense Production Act, The National Defense Resources Preparedness Executive Order 13603 (which delegates the authority to various agencies and addresses national defense resources programs and policies) and Defense Priorities and Allocation System (DPAS) Regulation 15 Code of Federal Regulation, §700 with respect to industrial priorities.

## Key features

The main aim of the USA federal defense priorities and allocation system is to ensure **expeditious** availability of products, materials and services by means of prioritized national contracts throughout the USA supply chain in order to support **certain approved programs of a broad scope**. These programs relate to defense, energy, homeland security, emergency preparedness and critical infrastructure, and also to provision of military or critical infrastructure assistance to foreign nations<sup>3</sup>.

The Defense priorities and allocation system gives an alternative approach to overcome lack of or scarce resources and items needed in emergency and to supplement the available stockpile resources – by means of rated orders certain scarce resources and items can be produced with priority. It is very important that the system of priority and rated orders includes not only the main contractor but also all the sub-contractors or participants at the supply chain. In terms of rated orders they are complied with priority to all other orders and this priority follows the sub-producers. The activation of the priority is also a plea for other not rated orders to wait without penalties to be due.

This system has special purpose in national security public - private partnership relations – from one hand it is aimed to minimize disruption in normal commercial activities, but on the other – it meets national security requirements. It is aimed to provide authority to USA government agencies to order priority performance of contracts and allocate materials and also to support rapid industrial response in a national emergency.

The authority to place priority ratings to government contracts is delegated by the Department of Commerce to the following competent federal departments: Department of Defense, Department of Energy, Department of Homeland Security and General Services Administration. Department of Defense applies its own manual. Also on a case by case base this authority might be delegated to other national agencies or foreign governments and also to national or foreign contractors, subcontractors, suppliers or owners or operators of critical infrastructure. But this second option is under condition – it is possible to delegate authority to other persons if the request is considered to be necessary or appropriate to promote the national defense.

## Who is obliged under DPAS

The spectrum of the obliged persons is very broad – DPAS concerns all person and legal entities in the USA, there is an imperative obligation for all of them to comply with the provisions of the regulation and to accept rated orders and to wait performance of unrated orders in case of a rated order.

## Special priorities assistance

The regulations provide the option of special priorities assistance for persons and companies. Department of Commerce and other delegated authority agencies are competent to assist. Special priorities assistance is given if the request is timely and the applicant has made a reasonable effort to resolve the problem by oneself. Although the regulations provide that assistance is given for “any reason” it should be clear that assistance is refused in situations that are unconscientiously or unfair (like attempting to secure a price advantage, gain competitive advantage, disrupt an industry apportionment program in a manner designed to provide a person with a unwarranted share of scarce items, overcome a supplier’s regularly established terms of sale or conditions of doing business). There are certain types of situations concerned as usual for provision of assistance – in case of difficulties in obtaining delivery for items for rated orders, if a person cannot locate a supplier for an item for a rated order, if it is necessary to ensure that the rated orders will be treated preferentially, if there is a need to resolve a conflict of production or delivery of various rated orders, verification of urgency of rated orders and determination of the validity of the rated orders.

## Application of DPAS in COVID-19 pandemic

DPAS has proved its effectiveness in COVID-19 pandemic and gave the possibility for reasonable public-private partnership in order to preserve public interest.

After the declaration of state of national emergency on 13 March 2020 and invocation of the Defense Production Act by the US president Donald Trump, DPAS regulations has been activated several times in order to supplement the need for scarce products and items. On 27 March 2020 the Secretary of Health and Human Services has required from General Motors Company to accept, perform and prioritize federal contracts for medical ventilators. On 2 April 2020 there was a second invocation of Defense Production Act by the president of the country in order to clear supply chain issues in production of ventilators and N95 face masks. On 3 April 2020 there was a third invocation in order to compel a US manufacturer of N95 face masks to send them in factories overseas and to stop exportation of currently produced ones. The application of DPAS has encountered a problem with the Buy American Act (BAA) 41 U.S.C. chapter 83, the Trade Agreement Act (TAA) 19 U.S.C. 2501. That is why many government contractors have become subject of lawsuit under the False Claims Act.

The BAA requires that federal government purchases only products manufactured in the USA and that these products will be used in the USA. The act applies to orders that amount to \$20 000 or more. The federal government may use foreign products only under certain conditions – if the domestic price is unreasonable. That is why rated orders should be accomplished with product manufactured in the USA. There is a possibility under the Trade Agreement Act that the president can waive the BAA and allow foreign products to be used but this is possible to happen only for products originating in countries which have signed an international trade agreement with the USA or meets other criteria like least developed country. And again the value of the rated order is the most important one. If the value of the rated order is \$182 000 or more than the Federal Acquisition Regulation apply and the recipient provides only products manufactured in Trade

<sup>3</sup> The full list of approved programs is published at Schedule I, §700 Code of Federal Regulation-2016-title 15

agreement countries. The problem is that many products are manufactured in China, Malaysia, India and other countries that have not signed a trade agreement with USA and there is an urgent need for verification of the supply chain in order to avoid liability<sup>4</sup>.

In conclusion DPAS is an example of supplementary support in situations of severe need to keep the balance between preserving public interest and not to disrupt normal trade relations. That is why it is reasonable to improve Bulgarian approach for public-private partnership in emergency situations with supplementary models that are clearly and fully regulated, the rules for partnership and the obligations of the private contractors are explicit and legally introduced and the most important – these rules encourage conscientious partnership.

## References

1. DPAS Defense Priorities and Allocation System, 15 CFR 700, Office of Strategic Industries and Economic Security Roth, H. Mok, Fr. Creig, L. COVID-19 and the rated order: must you change manufacturing locations, sources for PPE? <https://www.law.com/corpcounsel/2020/04/09/covid-19-and-the-rated-order-must-you-change-manufacturing-locations-sources-for-ppe/>
2. BDS ISO 28 000:2012 Specification for Security Management Systems for the Supply Chain, Bulgarian Institute for Standardization.
3. Defense Production Act 1950
4. US Code of Federal Regulation, 2016, title 15, vol 2, part 700
5. The National Defense Resources Preparedness Executive Order 13603
6. DoD44001-M Department of Defense Priorities and Allocation Manual, Feb 21, 2002

---

<sup>4</sup> Roth, H. Mok, Fr. Creig, L. COVID-19 and the rated order: must you change manufacturing locations, sources for PPE? <https://www.law.com/corpcounsel/2020/04/09/covid-19-and-the-rated-order-must-you-change-manufacturing-locations-sources-for-ppe/>

## PRACTICAL WORK WITH THE LANGUAGE OF MATHEMATICS IN THE MODULE IN ENGLISH FOR SPECIAL PURPOSES AT THE UNIVERSITY OF MINING AND GEOLOGY “ST. IVAN RILSKI”

**Milena Purvanova, Velislava Panichkova, Beatris Dimitrova**

University of Mining and Geology “St. Ivan Rilski”, 1700 Sofia; Purvanova@mgu.bg; velislava75@abv.bg

**ABSTRACT.** The article presents practical work on the issue of *The Language of Mathematics* on the curriculum for the module in English for Special Purposes (ESP) offered to students in different courses of studies at the University of Mining and Geology “St. Ivan Rilski”: those trained in English in the second level within the “streamed” language groups and those “out of the stream” within the course of studies in *Computer Technology in Engineering*. The objective of the activities offered in class is for students to produce and lay out training translation of sentences with the variants of the measurement units from the imperial and metric (SI) systems, using the opportunities that are provided by the embedded tools within the higher versions of Word (Word 10 and above). The focus is on tasks on forward and back translation, term production, word processing, multiple variants. Work is targeted at translation stylistics and visualisation. The implementation of the tasks includes preparatory work in the Internet environment, independent work with a general English dictionary and a dictionary of terms, conversion of mathematical units of measurement. Errors, difficulties and achievements in the student work on the issue are analysed. The results of the activity are discussed.

**Keywords:** ESP, multiple variants, terms, language of mathematics, translation

### ПРАКТИЧЕСКА РАБОТА С ЕЗИКА НА МАТЕМАТИКАТА В МОДУЛА ПО СПЕЦИАЛИЗИРАН АНГЛИЙСКИ ЕЗИК ЗА СТУДЕНТИ ОТ МГУ „СВ. ИВАН РИЛСКИ“

**Милена Първанова, Велислава Паничкова, Беатрис Димитрова**

Минно-геоложки университет „Св. Иван Рилски“, 1700 София

**РЕЗЮМЕ.** Статията представя практическа работа по темата „Езикът на математиката“, включена в учебната програма за модула по „Специализиран английски език“ за студенти от различни специалности в МГУ „Св. Иван Рилски“, обучавани във второ ниво поток и в специалност „Компютърни технологии в инженерната дейност“ извън потока. Целта на предложените на занятията дейности е студентите да оформят учебни преводи на изречения с вариантите на мерните единици от имперската и от метричната (SI) система, използвайки възможностите, предоставени от вградения инструментариум във високите версии на Word (Word 10 и нагоре). Акцентът е върху задачи по прав и обратен превод, производство на термини, текстообработка, даване на варианти. Работи се за стилистика на превода и визуализация. Изпълнението на задачите включва подготвителна работа в среда Интернет, самостоятелна работа с речник по общ английски и терминологичен речник, конвертиране на математически единици. Анализират се грешки, затруднения и постижения при работата по темата. Обсъждат се резултатите от дейността по задачите.

**Ключови думи:** специализиран английски език, многовариантност, терминология, езикът на математиката, превод

### Introduction

Our research work touches on two fields of foreign language training: the methods of ESP training and the theory and practice of term translation.

The study of technical terminology at the University of Mining and Geology “St. Ivan Rilski” is part of the overall tuition hours for foreign language teaching and is included in the curriculum for all courses of studies. Gaining skills in working with technical terminology is crucial because of the fact that the materials which are used by the students in the process of their university education followed by their occupational fulfilment contain a high percentage of terms, and terminology is a means of conveying scientific facts and knowledge in the engineering courses of studies. Using the right terms increases the accuracy of speech and eliminates ambiguity. Therefore, the quality of work with terminology guarantees the quality of communication among specialists in various fields of engineering. We have covered this topic from different

perspectives in a number of our works, e.g. in Purvanova et al. (2011, 2014, 2017).

We have entered a period of physical social distancing and isolation which have brought about a prolonged spell of distance training of students. As lecturers, we have been faced with the need to plan different types of educational activities in foreign language teaching. The lack of auditory classes has transformed our outlook on the offered training materials and activities associated with them under the conditions of no direct, face-to-face contact with students.

### Methods

In this article, we share our experience from practical activities in the module in ESP. We present practical work on the issue of “The Language of Mathematics” which is on the curriculum offered to students in various engineering courses of studies at the University of Mining and Geology “St. Ivan Rilski”. We give examples of how to plan and apply

pedagogical and methodical criteria during preparation of training materials, as well as of how to give freedom or impose restraints when working with the training terminological materials.

### Objective

The objective of the activities offered for class work is for students to produce properly laid-out training translation of sentences with the variants of the measurement units from the imperial and the metric (SI) systems. The focus is on tasks on forward and back translation, term production, word processing, multiple variants. Work is targeted at translation stylistics and visualisation.

### Target group

The activities are directed to students trained in English in the second level within the “streamed” language groups and to those trained in the second, third and fourth year within the course of studies in *Computer Technology in Engineering*.

### Tools

The opportunities provided by the embedded tools within the higher versions of Word (Word 10) are offered to use for the implementation of the educational tasks.

### Algorithm of work

To fulfil the training activities, the following steps are followed that comprise:

- preparatory work within the Internet medium;
- independent work with a general English dictionary and a dictionary of terms;
- conversion of mathematical units of measurement.

During and after the performance of tasks, we have also considered including an analysis of errors, difficulties and achievements in student work on the issue.

### Scope

Students from the three faculties at the University of Mining and Geology “St. Ivan Rilski” are included in the training activity. They are distributed as follows:

- 9 first-year students trained in English in the second level within the “streamed” language groups; their distribution in faculties is the following:

- from the Faculty of Mining Electromechanics - 2 students
- from the Faculty of Mining Technology – 5 students;
- from the Faculty of Geology and Exploration – 2 students;

- and 43 students from the Faculty of Mining Electromechanics trained in English “off-stream” within the course of studies in *Computer Technology in Engineering*; their classification in courses follows:

- second-year students – a total of 14 colleagues:
  - 8 from the low level subgroup
  - 6 from low level subgroup
- third-year students – a total of 14 colleagues who are:
  - 8 from the low level subgroup
  - 6 from the high level subgroup
- fourth-year students – 15 colleagues.

### Activities

**Preparation.** The activities were offered to students taking the course of studies in *Computer Technology in Engineering* on the first class within a series of online classes intended to complete the work started in the second semester of the 2019-2020 academic year. The students trained in English in the second level within the “streamed” language groups did the training activities at the end of the series of distance learning classes.

Since we are in an unconventional health situation which influences all educational aspects, we have transformed the educational process in good time. We prepared the classes offered by putting an accent on the **activity “Work in the Internet medium”** and practicing two of the skills in foreign language teaching: reading and writing. The basic **source for reading** has been an article published in the Annual of the University of Mining and Geology for 2016. We have also offered steps for locating the article and the way to the source is indicated to every student who has taken part in the activities, namely:

Website of the UMG → Research activity → Сборник с научни доклади → Annual of the University of Mining and Geology → Part IV: Humanitarian Sciences and Economics → article “A Computer Approach to the Issue of Multiple Variants in Foreign Language Teaching” written by a team of authors well-known to students within the course of studies in *Computer Technology in Engineering* (Purvanova et al., 2016)

The students have been encouraged to read in detail the mentioned article whereby the advantages and disadvantages of each of the computer decisions is traced and illustrated. It has been explicitly stated that the text attached is for reading and comprehension, in the same manner as a lecture material or a manual is read. Within the context of considerable computer load in the virtual classroom, when a lecture and a seminar material are sometimes delivered to students by different lecturers remotely and frequently at the same time, students’ motivation to read all materials offered is of particular importance. Therefore, during classes, we aim at giving the trainees confidence that the conscientious reading and consideration of the material offered, along with the implementation of tasks, is not going to take longer than a regular class will take, and that students’ work on the course unit in *English language* will not be at the expense of the duration of work on other course units. From this point of view, we have guaranteed the tasks implementation. However, we presume that occasionally some students may be overburdened with on-line tasks and, therefore, busier with work on other subjects; that’s why we have also attached just the excerpt of the quoted article in our material assigned (ibid., 135, col.1, lines 33-136, col.1, line 48).

**The stage of initial explanations.** Students have been offered explanations about the objectives of the task. The focus hereby is that we outline the students’ practical skills, too, that are based on their knowledge acquired in the module in computer literacy. The task is connected with **giving lexical and syntactic variants** in the training translation from and into a foreign language.

Layout is a problem with multiple variants in written exercises, homework assignments, etc. A number of computer solutions to this problem are offered that are in conformity with the team of authors’ current knowledge and command of word

processing. Our activities are based on the word processing resources of the Microsoft® Word 10 programme. The examples given are from texts for translation from and into English that are employed within the module in English for Special Purposes at the University of Mining and Geology "St. Ivan Rilski". We have used the possibilities for inserting mathematical parameters, particularly equations. The algorithm of work is as follows:

Insert is chosen from the list of tasks → Equation → two parameters are set from the drop-down menu:

- a) → the type of brackets (Brackets)
- b) → the type of matrix.

The examples offered are generally applicable to the remaining courses of study students at the University of Mining and Geology, regardless of the foreign languages taught or the training levels of language. The example sentences for seminars / exercises / homework assignments / control are connected with the **issue of "The Language of Mathematics"** which is obligatory on the curriculum for the module in English for Special Purposes (ESP) offered to students in all engineering courses of studies who do foreign languages at the University of Mining and Geology "St. Ivan Rilski".

**The assignment.** Using the Google classroom platform, the following task is assigned to students for homework together with a table of explanations:

*Exercise №1 (forward translation, from English into Bulgarian):*

Translate the following sentences into Bulgarian for the needs of the Bulgarian audience*:		
№	English	Bulgarian
1.	The outside diameter of the pipe is 6 inches.	
2.	The length of the pipeline is 100 yards.	
3.	The distance between Sofia and Athens overland is 490 miles.	
4.	The size of room 135A is as follows: L 20 ft , W 15 ft, H 12 ft.	
5.	The wall thickness in room 301A is half a foot.	

*Exercise №2 (back translation, from Bulgarian into English):*

Translate the following sentences into English for the needs of the British/American audience*:		
№	Bulgarian	English
1.	Хеликоптерната площадка е с размери 20x25 м.	
2.	Той е 1,70 м. висок.	
3.	Дебелината на стената на тръбата е малко над 1 см., а вътрешният диаметър е 12,5 см.	
4.	Морското дъно е на 500 м. дълбочина.	
5.	Платформата е с площ 450 м <sup>2</sup> .	

\*i.e. give variants in the imperial and in the metric systems; for the sake of facility, convert with approximation using the following conversion guidelines:

1 inch	=	2.54 cm	≈ 2.5 cm
1 foot	=	30.48 cm	≈ 31 cm ≈ 1/3 m, i.e. 1 m is approximately equal to 3 ft
1 yard	=	3 feet = 0.9144 m	≈ 1 m
1 mile	=	1.609 km	≈ 1.5 km

An example of translation with variants:  
 Участъкът е 10 м. дълъг = The section is 10 m long.  
 = The section is about 30 feet long.

To perform the task, it is of paramount importance to offer students methodical assistance in the form of:

- a table with units of measurement or links to this type of table (we list here only a fragment of the links available:

[https://www.google.com/search?q=convert+imperial+measurements+into+metric&rlz=1C1AOHY\\_enBG709BG711&oq=convert+imperial+into+metric&aqs=chrome.2.69i57j0l5.17992j0j7&sourceid=chrome&ie=UTF-8](https://www.google.com/search?q=convert+imperial+measurements+into+metric&rlz=1C1AOHY_enBG709BG711&oq=convert+imperial+into+metric&aqs=chrome.2.69i57j0l5.17992j0j7&sourceid=chrome&ie=UTF-8)

<https://www.metric-conversions.org/measurement-conversions.htm>

<https://www.calculator.net/conversion-calculator.html>

<https://www.mathsisfun.com/metric-imperial-conversion-charts.html>)

- examples of converting measurement units from the imperial and from the metric (SI) systems;

- the communicative value of the task – such measurement units should be added in the written communication with English-speaking colleagues / contacts / subordinates or employees that are used by the audience reading the translated sentences and that make the mathematical discourse more comprehensible; the acquiring, practicing, and future automation of the skill for quick conversion with approximation would make the oral discourse quick/effective.;

- the objective of the activity – that it is not an end in itself, nor is it in arithmetic with the help of Google translator; but that it is for converting feet into the approximate centimeters, inches into the approximate centimeters, yards into approximate meters, miles into the approximate kilometers. Or vice versa: from meters into the approximate feet/or in case students are better-versed in the imperial system into feet and inches, from centimeters into the approximate inches, and so on;

- the expected results – thinking about how to make use of the possibilities offered by the higher versions of Word 10 and the embedded tools, the sentences in the target language should be produced with variants using matrices wherewith the measurement units of the imperial and the metric (SI) systems will be visualised.

Only then can students proceed to the implementation of the tasks stage by stage.

**The stage of the initial (tabular) implementation of the assignment.** Just as we had expected, most of the students did the exercises following the general pattern of "read and directly translate in the table enclosed". This was most often achieved with the help of Google translator which, very mischievously, mind you, offers such brilliantly pucky variants as:

5.	The wall thickness in room 301A is half a foot.	Дебелината на стената в стая 301A е половин <b>крак</b> .
----	---	---

or as the following variant which diligently employs keyboard tools for listing variants (we have in mind the forward slash) that are absolutely inappropriate for our terminological purposes:

1.	The outside diameter of the pipe is 6 inches	Външният диаметър на лупата/тръбата е 6 инча.
----	--	---

Thus, students have totally ignored the subtasks for converting and giving variants in matrices. Some have even “conscientiously” provided translation variants with four digits (!) after the decimal point. Of course, the discussion that ensued has allowed them to reconsider the notion of approximation and work with the other measuring system.

At this stage, the correct implementation of the task for translation and conversion with approximation only in a tabular form would look like this (the variants are separated with forward slashes and are given in bold in order to make them more visible):

*Exercise №1 (forward translation, from English into Bulgarian):*

Translate the following sentences into Bulgarian for the needs of the Bulgarian audience*:		
№	English	Bulgarian
1.	The outside diameter of the pipe is 6 inches.	Външният диаметър на тръбата е <b>6 инча/около 20 см.</b>
2.	The length of the pipeline is 100 yards.	Дължината на тръбопровода е <b>100 ярда/около 100 м./малко под 100 м./ 91,50 м.</b>
3.	The distance between Sofia and Athens overland is 490 miles.	Разстоянието между София и Атина по суша е <b>490 мили/около 740 км./790 км.</b>
4.	The size of room 135A is as follows: L 20 ft, W 15 ft, H 12 ft.	Размерите на зала 135А са както следва: дължина <b>20 фута/около 7 м.</b> , ширина <b>15 фута/5 м.</b> и височина <b>12 фута/4 м.</b>
5.	The wall thickness in room 301A is half a foot.	Дебелината на стените в зала 301А е <b>половин фут/15 см.</b>

*Exercise №2 (back translation, from Bulgarian into English):*

Translate the following sentences into English for the needs of the British/American audience*:		
№	Bulgarian	English
1	Хеликоптерната площадка е с размери 20x25 м.	The heliport is <b>20 by 25 m/ about 7 ft by 8 ft.</b>
2	Той е 1,70 м. висок.	He is <b>1.70 m/5 foot 7 inches/ 5 ft 7 in tall.</b>
3	Дебелината на стената на тръбата е малко над 1 см., а вътрешният диаметър е 12,5 см.	The wall thickness of the pipe is <b>slightly over 1 cm/ half an inch and its/the bore is 12.5 cm/5 inches</b>
4	Морското дъно е на 500 м. дълбочина.	The sea bed is at a depth of <b>500 m/1500 ft/ a third of a mile.</b> or: The sea bed is <b>500 m/1500 ft deep.</b>
5	Платформата е с площ 450 м <sup>2</sup> .	The area of the platform is <b>450 square metres/about 400 square feet/4050 sq ft.</b> or: The platform has an area of <b>450 square metres/about 400 square feet/4050 sq ft.</b>

Here it is obligatory to pay attention to the following peculiarity when giving variants with brackets/slashes as in the translations presented in the table above: sometimes it is confusing because the variants of a word and of a separate

phrase may be located in different parts of the sentence. This can be avoided by giving the variants with matrix from the Equation tools. By inserting a matrix with variants, the work is diligent and it is clearly seen where the variants of whichever word/phrase are in the sentence.

**The stage of the subsequent (matrix) implementation of the task.** In translation work, giving variants of words or phrases on the whiteboard is a frequent activity in class. The lecturer usually writes them down between two vertical lines. Variants of translated words/phrases given between vertical lines are also suggested by the lecturer when they hand out from translations of texts from homework or from five-minute flash tests. It is precisely the graphical presentation of such vertical lines that is the ultimate goal of our task. Similar activities are performed with a computer as those when writing mathematical equations with a computer, i.e. the appropriate keys are pressed and the relevant symbol from the menu is chosen. The menu is for mathematical equations in the package of Word 10 and above (**Word 10** → **task bar** → **Tools** → **Equation tools**). In our case, the chosen symbol is the matrix. In the matrix, instead of inserting figures, we insert both figures and words/phrases which are synonymous in the translated sentence. The program itself arranges them one below the other. That's why we have included this class exercise as a word processing activity: this is not a mere translation, but a better shaped visual presentation of the output translation product with a slight tinkering with the equation menu.

In order to fulfil the task correctly, the students who have not read the preparatory material yet (at least the excerpt from the article cited above, if not the whole article), have to do that at last. Following the steps listed in the algorithm leads to attempts for giving variants after the method required.

The first students' attempts invariably contain lots of mistakes of the following type (the examples are from Exercise № 2 on back translation):

➤ *lexical* - as in

2. He is  $\left. \begin{array}{l} \text{1.70m.} \\ \text{|||about|||} \\ \text{near} \end{array} \right\} 5.60 \text{ ft.} \left. \right\} \text{tall.}$

where the adjective “near” has been used instead of the adverb “nearly”;

➤ *grammar* – as in

4. The seabed's depth is  $\left. \begin{array}{l} \text{500m.} \\ \text{|||about 1640 ft.} \end{array} \right\}.$

where possessive case for animate nouns has been used instead of the “of-phrase” for possession of objects, as in “the depth of the seabed”;

➤ *conceptual* – as in

5. The platform area is  $\left. \begin{array}{l} \text{450 m}^2. \\ \text{|||about 4844 ft}^2. \end{array} \right\} \text{long.}$

where the term “long” has been used and the student hasn't taken into consideration that area is not long but is measured in square meters, square feet, etc.;

➤ *syntactic* – as in

3. The thickness of the pipe wall is just over

$\left. \begin{array}{l} \text{1cm.} \\ \text{|||0.03 foot|||} \\ \text{and the inside diameter is} \\ \text{12.5cm.} \\ \text{|||about 0.41 ft.} \end{array} \right\}$

where the student has graphically presented the variants as one matrix with two sub-matrices. Yet, the correct syntactic order should have been in the form of two matrices with variants of the following type: the main sentence is "The wall thickness of the pipe is just over.... (the first set of variants must be inserted here) and the bore, or inside diameter is.....(the second set of variants is inserted here)".

**The stage of the task implementation analysis.** When analysing the work at this stage, it is obligatory to give instructions regarding the correct syntactic order of the sentences with the variants. Only those words / phrases / parts of sentences are placed within the matrix that are synonymous, and the sentence goes along the main line. Here is an example of such an explanation:

**Външният диаметър на тръбата е .....**  
and after this part of the sentence, the matrix from the Equations toolbox is placed and the variants are inserted below each other, like this:

6 инча	
15 см.	
около	
приблизително	15 см.

The example above is of a sentence from the homework assignment on translation from Bulgarian into English. The variants of the matrix and the sub-matrix are coloured to make the explanation clearer. The matrix comprises four variants. It is given with a pair of single vertical lines. Two of the variants are in a sub-matrix because they are parts of a similar construction and have a common part; this sub-matrix is placed within the basic one and is represented by a pair of double vertical lines.

Another mandatory explanation to give to students when working with the sets of variants is that they cannot be used in Google classroom, since they are not visualised there; instead, they can be implemented in a Word file. Therefore, the elements in the example above are not displayed in the homework submitted in Google classroom, but are clearly visible in the files sent by ordinary e-mail.

In order to assimilate the comments and consolidate the corrections made, the students can be given additional tasks, in the form of instructions, on the insertion of variants (the examples below are extracted from comments on the implementation of Exercise № 1 in submitted homework assignment on forward translation, from English into Bulgarian):

**In sentence № 2**  
Дължината на тръбопровода е

100 ярда	
91,5 м.	
около	
приблизително	91 см.

below "91 cm", you can even add the variant "1m." to the matrix (as part of the "приблизително 1м./approximately 1 meter" variant), because the word "около/приблизително/approximately" saves from accurate calculations or from annoying calculations

with 2 characters after the decimal point; in this case, another sub-matrix within double lines is introduced immediately after the one with "около/about; приблизително/approximately";

**In sentence № 3**  
Разстоянието между София и Атина по суша е

490 мили	
788,4 км.	
около	
приблизително	788 км.

below "788 км", you can add "790 км" - again due to the life-saving "приблизително/approximately" and again inserted by means of an extra sub-matrix for the numbers.

**The stage of the final implementation of the task.** We offer the visualisation of the correct implementation of the exercises in order to present multiple variants in a digital form:

**Exercise №1 (forward translation, from English into Bulgarian):**  
Translate the following sentences into Bulgarian for the needs of the Bulgarian audience\*:

№	English	Bulgarian
1.	The outside diameter of the pipe is 6 inches.	Външният диаметър на тръбата е   около  6 инча     20 см  .
2.	The length of the pipeline is 100 yards.	Дължината на тръбопровода е   около  100 ярда     100 м   малко под   100 м     100 ярда     91,50 м
3.	The distance between Sofia and Athens overland is 490 miles.	Разстоянието между София и Атина по суша е   около  490 мили     790 км     740 км     490 мили     740 км.     790 км.
4.	The size of room 135A is as follows: L 20 ft , W 15 ft, H 12 ft.	Размерите на зала 135А са както следва: дължина   около  20 фута     7 м  , ширина   15 фута     5 м   и височина   12 фута     4 м.
5.	The wall thickness in room 301A is half a foot.	Дебелината на стените в зала 301А е   половин фут     15 см.  .

**Exercise №2 (back translation, from Bulgarian into English):**  
Translate the following sentences into English for the needs of the British/American audience\*:

№	Bulgarian	English
1	Хеликоптерната площадка е с размери 20x25 м.	The heliport is   about  7ft by 8ft     20 by 25 m  .

2	Той е 1,70 м. висок.	He is <b>1.70 m</b> tall. <b>5 foot 7 inches</b> <b>5 ft 7 in</b>
3	Дебелината на стената на тръбата е малко над 1 см., а вътрешният диаметър е 12,5 см.	The wall thickness of the pipe is <b>slightly over 1 cm</b> and <b>its</b> bore is <b>the</b> <b>12.5 cm</b> <b>5 inches</b> .
4	Морското дъно е на 500 м. дълбочина.	The sea bed is at a depth of <b>500 m</b> <b>1500 ft</b> <b>a third of a mile</b> . Or: The sea bed is <b>500 m</b> <b>1500 ft</b> deep.
5	Платформата е с площ 450 м <sup>2</sup> .	The area of the platform is <b>450 square metres</b> <b>about 400 square feet</b> <b>4050 sq ft.</b> Or: The platform has an area of <b>450 square metres</b> <b>about 400 square feet</b> <b>4050 sq ft.</b>

## Results accomplished

Following the implementation of the activities on the tasks assigned, we have established the achievement of the following results:

- Implementation of assignments on forward and back translation, requiring independent work with a general English dictionary and a dictionary of terms;
- Expanding students' knowledge and skills related to the production of terms and to the translation stylistics;
- Introducing students to the two systems of measuring units (the imperial and the metric/SI systems);
- Providing opportunities for concurrent work with both systems;
- Introducing students to the opportunities for applying the systems of the units of measurement in their communication with English-speaking colleagues;
- Acquisition of skills on the part of students to convert units of measurement from one system into the other;
- Improving these skills in order to quickly convert with approximation and skillfully handle both systems simultaneously;
- Creating conditions for a fast and efficient oral discourse;
- Introducing students to the features and functional capacities of the word processing program Microsoft® Word 10;
- Improved skills when working with the tools embedded in the Word 10 application;
- Applying the program for the purposes of the visualisation of a text with variants;
- Improving students' computer skills;
- Optimising the process of foreign language teaching at the University of Mining and Geology "St. Ivan Rilski".

## Conclusion

In this article, the authors' team share the experience that they have gained during the practical educational in the module in English for special purposes (ESP) in the period of distance learning. The objectives of the activities offered in the class work have been fulfilled. The focus in the implementation of tasks was on the work with forward and back translation, on the production of terms, on word processing with the functional opportunities of the word processing program Microsoft® Word 10, and on giving variants of the units of measurement from the imperial and the metric (SI) systems. Students' knowledge has been broadened and their skills in working with terms have increased.

The authors' team expresses their hope that, from the educational point of view, the students have been satisfied with our mutual work in view of its contribution to their future occupational development and the increase in their competitiveness.

## References

- Purvanova, M., I. Drunkov, L. Meshekov. 2016. A Computer Approach to the Issue of Multiple Variants in Foreign Language Teaching. - *Annual of the University of Mining and Geology "St. Ivan Rilski"*, 59, Part 4, 132-137 (in Bulgarian with English abstract).
- Purvanova, M., M. Hristova, V. Angelova, M. Papazova, Ts. Velichkova. 2011. Interaktivni metodi za podpomagane na chuzhdoezikovoto obuchenie v MGU "Sv. Ivan Rilski" – *Proceedings of the Department of Human Sciences, University of Mining and Geology "St. Ivan Rilski"*, XI, 65-83.
- Purvanova, M., M. Hristova, V. Panichkova, Ts. Vukadinova, E. Balacheva, E. Davcheva. 2017. Enhancing Students' Skills to Work with Texts in FLT for Special Purposes at the University of Mining and Geology "St. Ivan Rilski" - *Journal of Mining and Geological Sciences*, 60, Part 4, 62-67.
- Purvanova, M., V. Panichkova, M. Papazova, M. Hristova. 2014. Razrabotvane, aprobirane i izpolzване na novi uchebni materialy pri obuchenieto po specializiran chuzhd ezik v MGU "Sv. Ivan Rilski" - *Annual of the University of Mining and Geology "St. Ivan Rilski"*, 57, Part 4, 97-103 (in Bulgarian with English abstract).
- <https://www.calculator.net/conversion-calculator.html>
- [https://www.google.com/search?q=convert+imperial+measurements+into+metric&rlz=1C1A0HY\\_enBG709BG711&oq=convert+imperial+into+metric&aqs=chrome.2.69i57j0l5.17992j0j7&sourceid=chrome&ie=UTF-8](https://www.google.com/search?q=convert+imperial+measurements+into+metric&rlz=1C1A0HY_enBG709BG711&oq=convert+imperial+into+metric&aqs=chrome.2.69i57j0l5.17992j0j7&sourceid=chrome&ie=UTF-8)
- <https://www.mathsisfun.com/metric-imperial-conversion-charts.html>
- <https://www.metric-conversions.org/measurement-conversions.html>
- <http://www.mgu.bg/new/main.php?menu=3&submenu=10>
- <http://www.mgu.bg/new/main.php?menu=5&submenu=15&session=16>
- <https://www.microsoft.com>

## POSSIBILITIES AND RESOLUTIONS OF MONGOLIAN ENERGY SECTOR

**Siilegmaa Sereenen**

*University of Mining and Geology "St. Ivan Rilski", 1700 Sofia; ssilegmaa@must.edu.mn*

**ABSTRACT.** Mongolia is the part of the earth; therefore, earth's problem is Mongolian problem. In one hand, for the energy and gas sector, the main reason of utilization gas for the energy is of course environmental protection or reduction of air pollution. In other hand, energy manages the economy of every country. If the country has the energy resource, it can be decided any kind of method. Then, there are some air pollution problems, energy and economy dependence and also, the mineral resource. Thus with increase of coal mine capacity, emission of methane to atmosphere will increase. Greenhouse gas emission of Mongolia was estimated at 20 million tons in 2016. If the current development trend will be kept, greenhouse gas emission may reach 50 million tons by 2030. From the other hand, Mongolia has promised in Paris to reduce greenhouse gas emission by 14 percent by 2030. Mongolia is dependent country from energy, especially from petroleum products. This actual problem influences to Mongolian economics. There are many ways to become independent country. Here in: to build the oil refinery; to produce petroleum product from coal; to extract and refine the CBM and CMM at Tavan tolgoi coal mining (transform to LNG and CNG).

**Keywords:** coal, independence, pipeline, LNG, CNG

### ВЪЗМОЖНОСТИ И РЕЗОЛЮЦИИ НА МОНГОЛСКАТА ЕНЕРГЕТИКА

**Сийлегмаа Серееен**

*Минно-геоложки университет „Св. Иван Рилски“, 1700 София*

**РЕЗЮМЕ.** Монголия е частта на земята; следователно, земният проблем е монголски проблем. От една страна, за енергийния и газовия сектор основната причина за използването на газ за енергията е, разбира се, опазването на околната среда или намаляването на замърсяването на въздуха. От друга страна, енергията управлява икономиката на всяка страна. Ако страната разполага с енергийния ресурс, може да се реши какъвто и да е метод. Тогава има някои проблеми със замърсяването на въздуха, енергийната и икономическата зависимост, а също и минералния ресурс. По този начин с увеличаване на капацитета на въглищните мини, емисиите на метан в атмосферата ще се увеличат. Емисиите на парникови газове от Монголия бяха оценени на 20 милиона тона през 2016 г. Ако сегашната тенденция на развитие ще се запази, емисиите на парникови газове могат да достигнат 50 милиона тона до 2030 г. От друга страна, Монголия обеща в Париж да намали емисиите на парникови газове с 14 процента до 2030 година. Монголия е зависима страна от енергията, особено от петролните продукти. Този действителен проблем влияе на монголската икономика. Има много начини да стане независима държава. Тук в: за изграждане на рафинерия за петрол; за производство на нефтен продукт от въглища; за извличане и рафиниране на CBM и CMM при добива на въглища Tavan tolgoi (трансформация в LNG и CNG)

**Ключови думи:** въглища, независимост, тръбопровод, ВПГ, СПГ

### Introduction

Mongolia is a Central Asian country neighbouring with the Russian Federation and the People's Republic of China. The country has a total territory of 1 565 600 km<sup>2</sup>. Mongolia has a sharply continental climate, with long, cold and dry winters and brief, mild, and relatively wet summers. Mongolia is divided into 21 aimags (provinces), and further into 331 soums (counties). Ulaanbaatar is the national capital; approximately 1,3 million people live in Ulaanbaatar. The Darkhan and Erdenet is the second and third largest cities with population of 70 000- 85 000 people. According to statistics of 2020, the population of Mongolia is 3 363 510. This is an increase by 1.6 percent or 640,3 thousand person since 2006. Since the collapse of the Soviet Union and COMECON in 1990 (withdraw of Soviet assistance was equivalent to the loss of 30 percent of GDP), Mongolia has faced with restructuring and transforming its previously centrally planned economy into one that is market-based and private sector driven. This result is published by Janarbaatar Jamsran (2018). Mongolia has implemented a series of economic reforms since 1990, aiming at stabilization of the economic performance and restructuring the economy

into a market based system. Before 1921, the main energy resource for heating homes was the animal waste in Mongolia. At first, Chinese people used the coal for heating homes and households in Mongolia around 1900. The first power and thermal plant was built in Ulaanbaatar city, in 1923. Following, the electricity transmitting lines were been constructed whole areas in Mongolia. Cities and towns were constructed all over the Mongolia and new power and thermal plants were been built. Now, there are 7 power and thermal plants in Mongolia. Of course, coal is still the main resource of heating for homes, apartments, public places and factories. At the same time, the first vehicles were imported to Mongolia and it was the establishment of Mongolian oil and gas sector. But, Soviet Union Government had been responsible the petroleum products export issues until 1941. In 1941, the government of Mongolian People's Republic made a decision and they established the petroleum products importing department and bought the all petroleum products storage depots and gas stations from Soviet Union. In other hand, the 78<sup>th</sup> anniversary of Mongolian oil and gas sector will be celebrated this year. In 1949, the "Mongol Neft Trans" was established and the crude oil and natural gas exploration were performed in Dornod and

Dornogobi provinces. The Zuunbayan and Tsagaan Els oil fields were discovered during above mentioned exploration and the first oil refinery were built in 1954. Unfortunately, the little explosion was occurred in the oil refinery in 1969 and also oil rate was reduced, new exploration plans were not implemented until 1990; at last the oil refinery was closed.

The collapse of the Soviet Union in 1989 had far-reaching impacts for Mongolia, politically, economically and socially. A parliamentary democracy was put in place, the development of upstream petroleum operation recommenced, and the Petroleum Law of Mongolia and related regulations were put into effect in 1991. The government initiated the "Petroleum Program" classifying prospective petroleum areas into contract blocks and releasing them for international bidding.

In 1993, the first Production Sharing Contract (PSC) was signed with SOCO from the USA and the first exploration well of 3,000 meters depth was drilled a year later. In 1997, well 19-3 on Block XIX was recorded as the country's first free flowing oil well. Soon after, oil was exported from Mongolia by trucks to China to be refined.

The second biggest oil refinery is been built in Mongolia nowadays. Also, some companies are trying to produce petroleum products from coal. Everyone knows that coal is the main energy resource which is located in the earth.

The petroleum product producing process from coal depends on the world market price of per barrel crude oil. Right now, the world market price of per barrel crude oil is not encouraging the coal processing and its product utilization activity. If I rank the above mentioned ways, I will put the CBM at the first and the CNG or LNG at the second. Because, utilization of natural gas is the basic method reducing air pollution. Natural gas can be produced from crude oil, coal and CBM or biomass, easily. In additional, the Mongolian coal reserve is calculated 175 billion tonnages and there are 15 coal basins, over 300 coal fields in Mongolia. Mongolia is ranked at the 15<sup>th</sup> country by coal reserve in the world. Some CBM occurrences have just defined in Mongolia. The pilot factory was built last year in Tavan Tolgoi coal mining site. Therefore, we have to study the CBM and its utilization possibility and other special, important problems. The data are published by Tseveenjav (2019), as well as by Zoljargal et al. (2019).

There is no natural gas deposit discovered in Mongolia. But large coal deposits contain methane gas in pores of coal, from where it is released to atmosphere during coal mining. It had been considered as economically unfeasible, however thanks to modern technology it is now being developed in many countries as profitable business.

Obviously there is large potential of coal mine methane in Mongolia as a country with vast coal resources. If we can use coal mine methane, it is the purist and cheapest fuel for electricity generation, for the transportation vehicle and for households. If not, just a greenhouse gas emission silently released to the atmosphere.

If we can use coal mine methane, it is the purist and cheapest fuel or electricity generation, for the transportation vehicle and for households. If not, just a greenhouse gas emission silently released to the atmosphere.

## The overview of Mongolian energy and gas sector

In 2019, Mongolia's electricity production has reached a volume of 6,624.8 million kWh, an increase of 8.8% compared to the previous year's production. 93% of total electricity was produced by thermal power plants, 6% by solar and wind, 1% by hydro power sources, and 0.06% by diesel generators. Total heat energy production has been reached a volume of 9,425.1 thousand Gcal, an increase of 5% or 448.5 thousand Gcal, compared to the previous year.

During the year, 1,683.6 million kWh of electricity has been imported making an increase of 161.2 million kWh or 10.6% compared to the previous year.

The majority of heating and electricity energy is being generated by coal fired thermal power plant and the remained small amount is from hydro, wind, solar and diesel stations. Also, we got electricity from Russia, which takes 20 percents of our electricity supply.

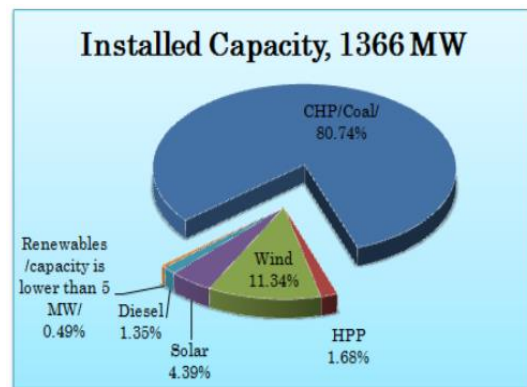


Fig. 1. Energy generation types

Likewise, the demand for refined oil products has been met 100% by imports. Consumption has been increasing nearly every year until it dropped slightly in 2014 and 2015 reflecting the country's economic downturn during these years. It is now back on upward trend, with the highest ever import of ca. 1.5 million tonnes petroleum products in 2019. Further increase is expected in the long-term.

More than 90% of the imported oil products come from Russia and the remainder from countries such as China, Republic of Korea and others.

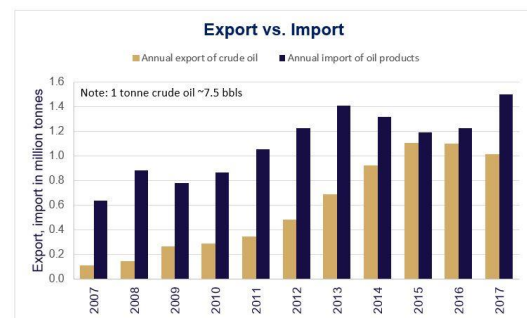


Fig. 2. Mongolian crude oil export and oil products import

To reduce its dependence on imports, the Government of Mongolia is seeking to build the country's own refinery, supported by a 1 Billion USD soft credit line from India. In June

2018, the Ministry of Mining and Heavy Industry reported that the final detailed feasibility study which was completed by “Engineers India Ltd” had been received. The refinery with an initial capacity of 1.5 million tonnes p.a. would be built in Altanshiree Soum near Sainshand City in Umnugobi province.

## Mongolian potential resources and reserves of energy and gas

### Coal resources

Mongolia has about 173.5 billion tonnes of coal, distributed among 15 basins and 3 fields. We have both thermal and coking coal deposits and their economic value and infrastructural surroundings are significantly varied. Estimated reserves of coal by A+B+C1 classification were 37.4 billion tonnes.

These reserves were estimated at an average depth of 300m, with most of it concentrated in the South Gobi and Choir-Nyalga basins in the central economic region. About 57.6% of the estimated reserves consist of hard coal and is mainly distributed in the West, Central and Khangai regions. Over 60% of explored reserves of hard coal is in the Tavan Tolgoi, Ukhaa Khudag, Baruun Naran and Naryn Sukhait deposits. The rest of the hard coal is in the basins of Kharkhiraa, Mongol Altai, South Khangai, Ongi River and South Gobi. Brown coal with high moisture and low calorific values makes for about 41% of the total estimated reserves and is mostly distributed in East and Central regions.

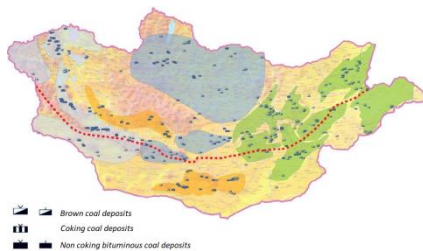


Fig. 3. Distribution of coal resources in Mongolia

### CBM

Coal mine study was started by Storm Cat Energy in 2004, when they drilled 11 boreholes in Noyon basin in South Gobi and concluded that 18.7 to 37.4 billion cubic meters of methane can be found at Naryn Sukhait coal deposit.

In 2012, a team of experts of Mongolian Nature and Environment Consortium and Raven Ridge Resources Incorporated from the US with support of the US EPA conducted studies on coal mine methane at three open pit mines of Baganuur, Tavan Tolgoi and Naryn Sukhait. They conducted gas analysis on core samples taken from Baganuur and Naryn Sukhait mines and prepared pre-feasibility study report for utilization of methane gas.

In 2014, Erdenes Tavan Tolgoi and Kogas of Korea signed MOU to start coal bed methane study at Tavan Tolgoi. Elgen LLC, a domestic drilling company cooperated with Kogas for drilling prospecting boreholes to depth of 700-900 meters and constructed pilot plant for extraction and purification of coal bed methane. Following those achievements, state owned Erdenes Methane LLC was created for further development of methane gas resources at Tavan Tolgoi. It is being considered

that Tavan Tolgoi coal deposit might contain around 40 million tons or 60 billion cubic meters of methane gas.

Over 300 coal deposits were discovered in Mongolia across major coal 15 basins. The country’s geological resources of coal are estimated at 175 billions tons. This clearly shows a huge potential for development of coal mine methane. The data are published by ADB (2018)

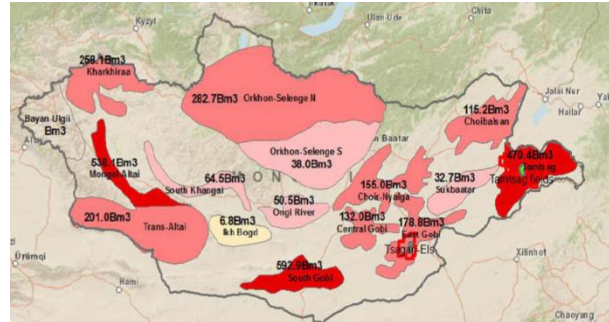


Fig. 4. Potential resources of methane gas in coal bearing basins of Mongolia



Fig. 5. Pilot plant of extraction and purification of methane gas at Tavan Tolgoi

### Petroleum

Petroleum exploration and production in Mongolia are performed solely under PSCs signed over each petroleum block between the investor and Government of Mongolia. There is no national oil company (NOC) in Mongolia.

As of 2019, there are a total of 32 petroleum blocks and Mongolia has concluded PSCs with 22 domestic and foreign companies on 27 blocks so far. Three of these blocks have advanced to production, one was cancelled and one relinquished, while the others are still being explored.

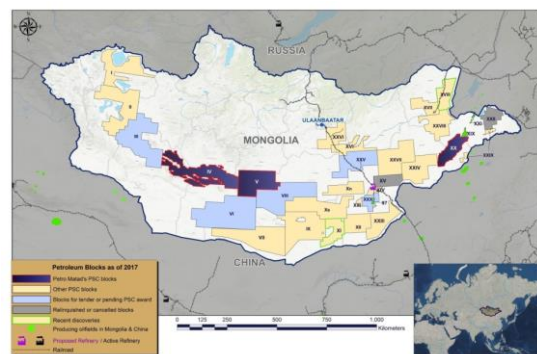
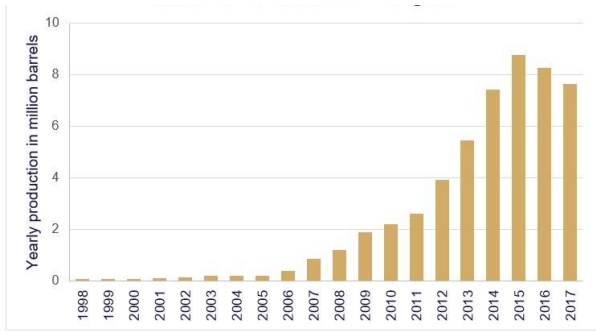


Fig. 6. Petroleum blocks in Mongolia

**Exploration, Production, Recent Discoveries**

After the resumption of upstream petroleum activities in the early 1990s, circa 51 million barrels of oil have cumulatively been produced in Mongolia between 1996 and 2017.



**Fig. 7. Crude oil production in Mongolia**

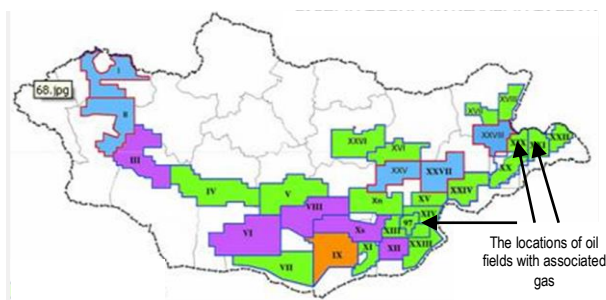
Mongolia's oil production steadily increased until 2015, reaching a daily production of ca. 24,000 barrels of oil. However, it has shown slight decreases in 2016 and 2017. More than 90% of the country's annual production has been solely from Blocks XIX and XXI in Tamsag basin in eastern Mongolia in recent years.

From 1993 to 2016, total 33,494 line km 2D seismic, 6,274 km<sup>2</sup> 3D seismic, gravity survey covering 272,890 km<sup>2</sup> area (incl. 11,000 km<sup>2</sup> FTG), 11,000 km<sup>2</sup> HRAM and 77,630 km<sup>2</sup> magnetic survey were conducted, and more than 1,500 wells have been drilled. Investments totaling 3.45 billion USD were made in petroleum exploration and exploitation in Mongolia by PSC contractors during the same period. Only about 70 of those 1,500 wells were drilled outside the three blocks that have advanced to production stage.

In addition to the three producing blocks, oil discoveries have been reported in two other blocks, namely Blocks XI and XVIII.

The (proved) ultimate recovery (proved reserves plus cumulative production) for the 3 producing PSC blocks was estimated at total 43 million tonnes (ca. 320 million barrels) of oil. The estimates were officially accepted by the state committee in 2011 and 2012, and no update has been reported since then.

**Associated gas reserve in Mongolia**



**Toson Uul –XIX**  
 Proven reserve – 6.98 trillion cubic meters  
 Probable reserve – 0.33 trillion cubic meters  
 Possible reserve – 2.98 trillion cubic meters  
 Proven reserve for developing – 0.77 trillion cubic meters

**Fig. 8. Associated gas reserve in Mongolia**

**Renewable energy**

Renewable energy accounted for more than 3% of the domestically produced energy used in Mongolia. The Mongolia's hydroelectric plants produce 28.3 MW, making the largest contribution to the country's renewable energy". Policy target: 20-25% of electricity provided by renewable energies by 2020

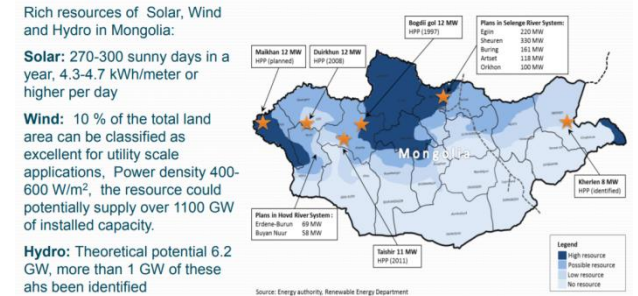


**Fig. 9. Renewable**

**Geothermal exploration and energy utilization in Mongolia**

The existence of numerous hot springs in Mongolia's Hangai province is indicative for large geothermal energy resources, which are remnants of the region's volcanic geological history. Previous studies have shown that a combined, geothermal heat and power plant could provide cheap and clean energy for the province center Tsetserleg. With this project we will introduce the missing geophysical component of the so far conducted geothermal exploration program in the Hangai. We will establish scientific methods to image the geothermal reservoir near Tsetserleg, which feeds the hot springs in Tsenkher and Shivert. The result will be of great importance for promoting the construction of geothermal power plant.

This project is a collaboration between ETH Zurich and the Mongolian Academy of Sciences. It is funded by the Swiss Programme for Research on Global Issues for Development (r4d programme) – a joint funding initiative by the Swiss Agency for Development and Cooperation (SDC) and the Swiss National Science Foundation (SNSF).

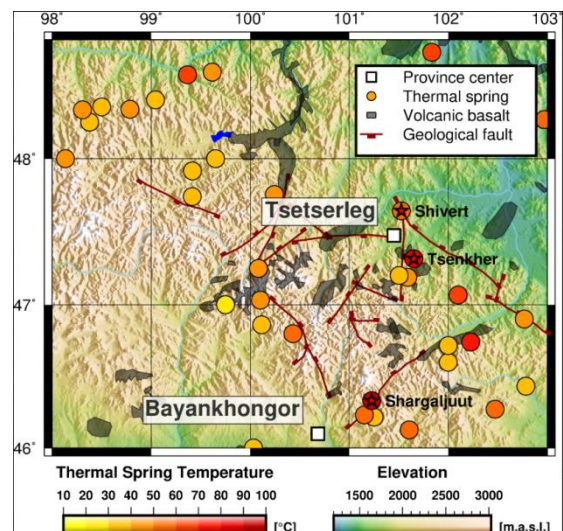


**Fig. 10. Geothermal energy study in Arkhangai province, Mongolia**

## Biogas

The main resource of biogas is the animal waste in Mongolia. There are 2 small plants in Mongolia near the cow farm. These plants were built by South Korean Government support. Unfortunately, these two plants are not producing biogas now. Because many Mongolians are nomadic people (nomadic herding still the same as before) and they do not have sufficient information about biogas and green house gas, also biogas trucks and cars. Although, animal waste will be the main resource of biogas in Mongolia.

The number of livestock animals in Mongolia reached 66.46 million, a record high since the nomadic country began a livestock animal census in 1918, a senior expert of the National Statistics Office said Thursday.

A census conducted between Dec. 7-17 showed the number of livestock animals in 2018 increased by 244,700, or 0.4 percent, from the previous year, Erdene-Ochir Myagmarkhand announced at a press conference.

According to the preliminary result of the nationwide census, sheep accounted for 46.0 percent of all livestock, goats accounted for 40.8 percent, cattle accounted for 6.6 percent, horses accounted for 5.9 percent and camels accounted for 0.7 percent.

Among the country's 21 provinces, the northernmost Khuvsgul has the largest number of livestock with 5.7 million, followed by Uvurkhangai and Arkhangai in the central provinces, with about 5.5 million respectively.

There are 230,800 herder households with livestock animals, up 0.8 percent from last year.

The promotion of animal husbandry is seen as the most reachable solution to diversify the landlocked country's mining-dependent economy. Currently, mineral products account for over 90 percent of its total exports. (Dugerjav, 2018, Narantsetseg et al., 2019, 2017a, 2016b, Gatumur and Oyuntugs, 2017, 2018, 2019)

## Conclusion

The first reasonable issue of this study is air pollution. Therefore, as before mentioned, air pollution is at the crisis level in Ulaanbaatar city, Mongolia, especially during the winter time. It can be seen that PM<sub>2.5</sub> is 4 to 4.5 times higher than permissible level of standard. In Mongolia, the main pollutant is the ger district (where people live in the Mongolian national habitat "ger" or private houses)-s in Ulaanbaatar city and other urban centers. Of course, because coal is used for heating homes and producing electricity (over 95 percent) in Mongolia. Using coal for heating and electricity producing has enough low KEП (in Mongolia, it is 44.12%). There are many experiences for reducing air pollution, the most optimal and successful version is natural gas and renewable energy.

The second reason is the energy or economy independent of Mongolia. Petroleum products are imported from Russia (up to 95%), China (to 3%) and other countries, although, electricity is imported from Russia during overloaded hours (evening hours), recently the LNG import has begun.

The third, energy sector's structure and activities are not clear, especially gas sector's laws, regulations, codes and standards are few and weak. Of course, there are some

policies in energy and gas sectors, although implementation and controlling issues are not as well as it can be.

The fourth, however, there are many kinds of energy resources in Mongolia, such as coal, crude oil (associated gas), animal feedstock, wind, solar, geothermal, CBM and etc. The proven reserve of coal was estimated over 37.1 billion tonnages in 2016, and anthracite occurred over 30 percent in the coal basins, resulting in some CBM researches and studies being processed in Mongolia, since 2000. For crude oil, the proven reserve of associated gas was calculated, although not enough high (proven reserve for developing – 0.77 trillion cubic meters). The (proved) ultimate recovery (proved reserves plus cumulative production) for the 3 producing PSC blocks were estimated at total 43 million tons (ca. 320 million barrels) of oil. The estimates were officially accepted by the state committee in 2011 and 2012, and no update has been reported since then. The next potential energy resource can be biogas, because the number of livestock animals in Mongolia reached 66.46 million, but mainly traditional nomadic herder life is dominated in Mongolia.

For the renewable, for example, solar, wind, hydro and geothermal; some projects are implementing.

As the above data, it can be seen that coal and CBM are the main future energy resources for Mongolia.

In 2012, a team of experts of Mongolian Nature and Environment Consortium and Raven Ridge Resources Incorporated from the US with support of the US EPA conducted studies on coal mine methane at three open pit mines of Baganuur, Tavan Tolgoi and Naryn Sukhait. They conducted gas analysis on core samples taken from Baganuur and Naryn Sukhait mines and prepared pre-feasibility study report for utilization of methane gas.

In 2014, Erdenes Tavan Tolgoi and Kogas of Korea signed MOU to start coal bed methane study at Tavan Tolgoi. Elgen LLC, a domestic drilling company cooperated with Kogas for drilling prospecting boreholes to depth of 700-900 meters and constructed pilot plant for extraction and purification of coal bed methane. Following those achievements, state owned Erdenes Methane LLC was created for further development of methane gas resources at Tavan Tolgoi. It is being considered that Tavan Tolgoi coal deposit might contain around 40 million tons or 60 billion cubic meters of methane gas.

Over 300 coal deposits were discovered in Mongolia across major coal 15 basins. The country's geological resources of coal are estimated at 175 billion tons. This clearly shows a huge potential for development of coal mine methane.

Mongolian Nature and Environment Consortium guesses that methane resources of Mongolia can be estimated at 3 trillion cubic meters in total. About 63.9 percent of all methane resources are concentrated in bituminous coal deposits, while brown coal and anthracite contain less methane.

These numbers are simply calculated through multiplying coal resources by typical content of methane gas in similar type of coal based on reference data from international and domestic studies. It should be noted that an extensive geological exploration shall be done in order to convert those suggestions to real reserves.

Overall, the future main resource can be the CBM (LNG, CNG or NG), therefore, researches and studies will connect with this future research.

**Acknowledgements.** Special thanks to Mongolian Energy and Oil sector's scientists and researchers and Governmental organizations.

## References

- Asian Development Bank. 2018. *Updating Energy Sector Development Plan*. Ulaanbaatar, 35 p. (in English)
- Dugerjav L. 2018. Summarizing study in the Energy Sector . *Proceeding of Oil and Gas Conference, 19, Part 1, 213-229*. (in Mongolian)
- Gantumur S. 2019. The geothermal energy study in Arkhangai province. *Proceeding of Oil and Gas Conference, 19, Part 1, 179\*186*. (in Mongolian)
- Janarbaatar J. 2018. The Ministry of Energy. – *Energy sector of Mongolia, Country report*. Ulaanbaatar, 20 p. (in English)
- Narantsetseg et al., 2019. Unconventional Oil and Gas reserves and future usages. *Proceeding of Oil and Gas Conference, Part 1, 109-126*. (in Mongolian)
- Oyuntugs M. 2018. Economical profit for using the renewable energy. *Proceeding of Oil and Gas Conference, 18, Part 1, 89-96*. (in Mongolian)
- Tseveenjav J. 2019. Mongolian Oil and Gas sector's actual problems and Deciding methods. *Proceeding of Oil and Gas Conference, 20, Part 1, 16-29*. (in Mongolian)
- Zoljargal J. 2018. *Possibility and Development in Energy Sector of Mongolia. Natural gas and Crude oil*. Ulaanbaatar, 312 p. (in Mongolian and English)

## CHALLENGES IN THE BLACKBOARD PLATFORM USAGE AT KNOWLEDGE VERIFICATION IN MASTER TRAINING

**Sevdalin I. Spassov<sup>1</sup>, Georgi M. Marinov<sup>2</sup>**

<sup>1</sup> "G. S. Rakovski" National Defence College, 1504 Sofia; s.spasov@rmdc.bg

<sup>2</sup> "G. S. Rakovski" National Defence College, 1504 Sofia

**ABSTRACT.** A study have been made of the options for creating and conducting tests in the BlackBoard platform for testing the knowledge of masters at the "G. S. Rakovski" National Defence College. Various possibilities for creating and conducting tests have been tested. The tests are adapted to the limitations of the communication speed of and to the system requirements in the tests conduction process. The possibility for stable operation of the BlackBoard platform has been tested. Some limitations in the operation of the platform have been identified during its loading by many users and recommendations have been given for improving its work.

**Key words:** distance learning, Blackboard, tests

### ПРЕДИЗВИКАТЕЛСТВА В ИЗПОЛЗВАНЕ НА ПЛАТФОРМАТА BLACKBOARD ЗА ПРОВЕРКА НА ЗНАНИЯТА ПРИ ОБУЧЕНИЕ НА МАГИСТРИ

**Севдалин И. Спасов, Георги М. Маринов**

Военна академия „Г. С. Раковски“, 1504 София

**РЕЗЮМЕ.** Направено е изследване на възможностите за създаване и провеждане на тестове в платформата BlackBoard за проверка знанията на магистри във Военна академия „Г. С. Раковски“. Проверени са различни възможности за създаване на тестове и тяхното провеждане. Тестовите са адаптирани към ограничения в скоростта на комуникация и към системни изисквания в процеса на провеждане на тестовите. Експериментирано е създаването на типови фалове с няколко различни видове въпроси и тяхното автоматично зареждане в създаваните тестове. Проверена е възможността за устойчива работа на платформата BlackBoard при провеждане на едновременно тестово изпитване на много обучаеми. Констатирани са някои ограничения в работата на платформата при нейното натоварване от много потребители и са дадени препоръки за подобряване на работата с нея.

**Ключови думи:** дистанционно обучение, платформа Blackboard, тестове

### Introduction

The study aims to identify some major challenges at the usage of the Blackboard Learn 9.1 distance learning platform (hereinafter the platform, the system) to test the master program students knowledge in the process of their training and to propose approaches to improve performance. The following tasks have been solved to achieve this goal: clarifying the possibilities of the platform for teaching and control of learning materials, analysis of identified imperfections and proposing possible approaches and solutions to improve work with it. The results of the analyzes can be used by teachers and administrators who use the distance learning platform Blackboard Learn 9.1 to teach and control the acquisition of learning material in the process of teaching bachelors and masters. The proposed approaches and solutions to improve the usage of the distance learning platform may be important with their usefulness in overcoming some of its limitations and imperfections.

Only the platform's possibilities for teaching and control of the studied material's assimilation have been analyzed for study's purposes. This stems from the aim of the study, which is to analyze the main challenges in using the Blackboard Learn 9.1 platform to test the master degree students' knowledge in the process of their training to outline

approaches and solutions to improve work with it. The capabilities of the learning control platform depend not only on its main characteristics, but also on its ability to teach it.

The hypothesis of the research is by revealing the main reasons for the imperfections in the use of the platform for testing the students' knowledge, the main approaches and solutions for improving the work with it could be found.

The methods of analysis, data processing and comparison have been mainly used at the research of the Blackboard Learn 9.1 platform capabilities for teaching and control of study material learning.

### Blackboard Learn 9.1 platform teaching capabilities

In order to explore the main challenges in using the distance learning platform, the question must be answered: what are the main factors influencing the assimilation and control of the learning material?

The first main factor is Blackboard Learn 9.1 platform teaching capabilities. The web-based system "Blackboard Learn" 9.1 fully complies with the requirements for online learning and administration of the learning process, allowing students to access electronic textbooks, lectures,

presentations, electronic self-preparation tests, exams and additional information about their student's status.

One of the important elements of any information system is the control of access to it. Each user can access the web-based system "Blackboard Learn" 9.1, after checking his unique username and password. This is a standard approach to controlling access to civilian information systems, while military communication and information systems require reliable identification procedures (Aleksandrova, K., 2010).

E-textbooks are created by teacher (s), and they can be written and oriented depending on the audience for which they are intended (according to the specialty of the students). The content of textbooks and lectures can be both textual and supplemented with charts, pictures, video and audio files.

The creation and conduct of qualification courses is one of the good features of the web-based system "Blackboard Learn". For example, only in the field of security and defense logistics, 3 electronic courses for targeted qualification for distance learning have been created and tested, developed by a team at the Logistics Department of the Command and Staff Faculty, in which students are enrolled and trained (Marinov, G., 2015), as follows:

- at the course "Healthy and safe working conditions" - 76 students;
- at the course "Systems for planning and management of logistics in NATO and the European Union" - 81 students;
- at the course "Information systems supporting the management of security and defense logistics of the country" - 23 students.

A total of 180 students have been tested and evaluated so far, through tests conducted after each lecture and certification tests at the end of each course in the electronic platform "Blackboard Learn".

The system has the opportunity to give additional literature to students by publishing it in the form of files. This is done by selecting "Upload files" from the menu "Content collection" and from the menu "Uploading" a window opens (Fig. 1), from which you can choose whether to upload a single file or multiple files. The default is to upload a single file. Then click on "Select file" to open the window (Fig. 1), where you can select the file you want to upload.

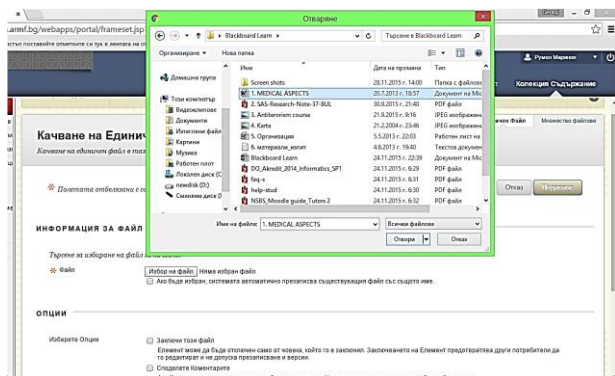


Fig. 1. Selection of a file to upload

Additional training literature can be provided to learners by posting links to various sources on the Internet such as Wiki, specialized sites and others. Using chat with learners is another opportunity to support the teaching of learning material. Through it, in a text mode of communication, various questions from the taught material can be clarified, different

questions of the learners can be answered, etc. This form of communication with students is a good feedback for the teacher, but there is one significant drawback - it does not offer audio and video connection and cannot make "live" contact with students. This lack of a live connection negatively affects the learning process and therefore other applications that have the potential for this type of connection must be found and used.

## Blackboard Learn 9.1 platform's testing capabilities

Master knowledge testing is carried out in each discipline studied or in each qualification course after the introduction of the platform in 2014. It was used for the students' knowledge control during the pandemic by COVID- 19 too.

### Blackboard Learn 9.1 platform capabilities for creation of various students' knowledge control forms

The Blackboard Learn 9.1 platform has great capabilities for learning control of teaching material. Its main capabilities are for creating and using tests, but it also offers other forms of control such as checking essays, term papers, and checking other students' written work (Blackboard Inc., 2010).

### Tests creation possibilities

The analysis here is made mainly of the possibilities for creating, conducting and reporting test results. In the platform there is an opportunity for each teacher to choose whether students to test their knowledge at the end of each lesson and / or to test their knowledge through self-preparation tests. The self-preparation tests can be generated by each student at will, as he asks the number of questions from each topic that he wants to get in the test in a given subject. For this purpose, the lecturer needs to introduce in advance the bank of questions with different degrees of complexity and in different thematic areas of the subject he teaches. This gives students a good opportunity to test their knowledge and also creates interest in working with the system.

Every teacher has rich opportunities to create tests. Access to the menu for their creation is very convenient: the teacher enters his account and in the menu "Disciplines" selects the submenu "Exams / Tests" and in the opened window of this submenu in the top bar selects the drop-down menu "Creation and assessment" and finally "Test" (Fig. 2).

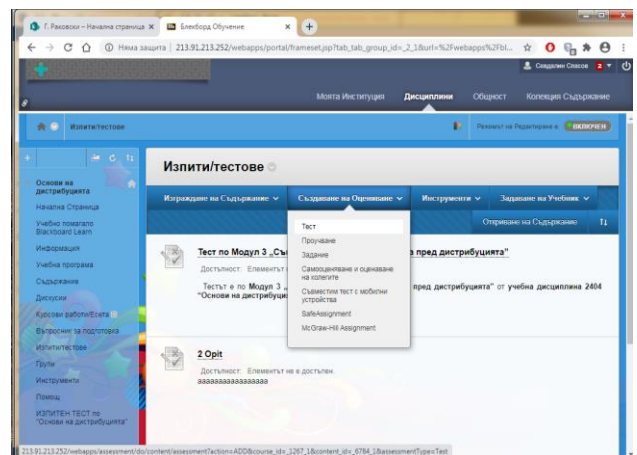


Fig. 2. Access to the tests creation and edition menu

Several interesting options can be seen in the "Exams / Tests" submenu / "Create and evaluate" drop-down menu. These are the options for creating a Study, Assignment, Mobile devices compatible test and others. This is a demonstration of the rich possibilities of the system for creating and using various students' knowledge control forms.

The platform has the feature that first only the name and options of the test are set, and then the created test is entered in order to create the test questions: manually or to be entered automatically.

One big advantage of the platform is that there can be created very large variety of test questions. For example, they can create test questions of the following types: True / False, Hotspot, One Correct Answer, Multiple Correct Answers, Essay, Or / or, Short Answer, Cup of Short Questions, Likert Scale, File Answer, Arrange answers, Filling in a few blanks, Filling in the blanks, Shuffle sentence, Matching, Numeric answer, Finding questions and others (Fig. 3).

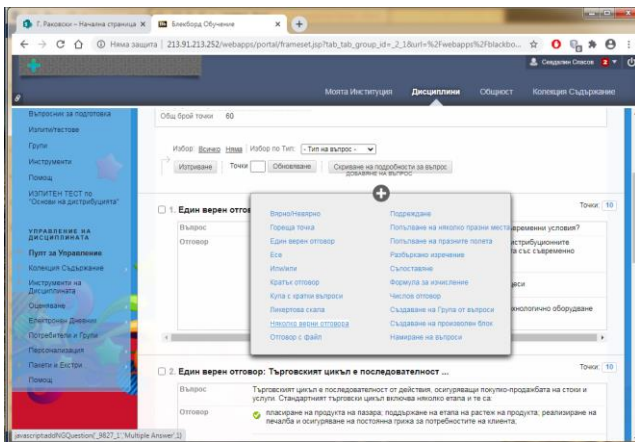


Fig. 3. Test question types

The teacher has this rich arsenal of question types, which allows him to create an optimal test to check the knowledge of students.

Another very significant advantage of the Blackboard Learn 9.1 platform is that it offers the test developer the ability to upload a test as a ready-to-use file. This feature has several requirements for this file: to be of text type (\*.txt), to have formatting of all questions, to format in a unique way the answers for each type of test and a number of other requirements for formatting the elements of the file. This requires the test file to be created according to its formatting specifications or to be formatted after it has already been created. These formatting requirements for file elements create some inconvenience to the test creator. However, this feature significantly reduces the time and complexity of creating the test when developing tests with a large number of questions, which greatly facilitates its creator. This is also true for tests with 10 or more questions, which means that this method is effective for creating almost all tests.

### Conducting and reporting test results possibilities

The teacher has good opportunities for conducting tests. A number of options are set when creating and editing the test, such as: the time during which the test will be active, the total time to solve it and how many attempts students have to solve it. In the instructions to the students there is an opportunity to specify other conditions for conducting the test, such as what

types of questions it contains, whether the test will be terminated automatically after the expiration of the time for its solution and others.

The system offers a set of options for displaying the questions on the screen in front of the learners before the test, as well as displaying the results for their feedback (Fig. 4).

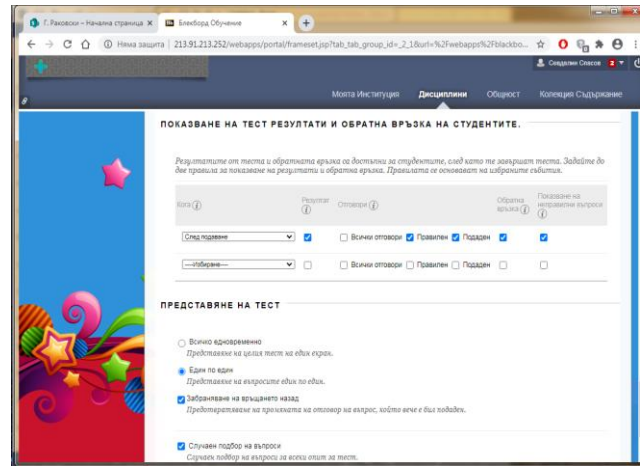


Fig. 4. Test's options screen

The system offers an opportunity to monitor the process of solving the test by the students during the test. It can also be seen whether a trainee has logged in to their account, whether they have started solving the test and whether they have completed it. A number of parameters can be observed, such as the time from the beginning of solving the test, as well as the time remaining until its end. These options for controlling the test process are very convenient, especially in cases where the test is interrupted for various reasons. This is most often due to technical reasons: for example, disconnection from the Internet or overloading the system's servers. This allows system administrators to respond, such as reconnecting or restarting servers.

For example, during the COVID-19 pandemic, when testing the learning material through tests, many classrooms had to work in the system at the same time. In some cases, there were interruptions in the testing due to technical reasons. They were mainly due to interruption of the internet connection of some students or overloading of the system's servers. Cases of congestion on the platform's servers are important for the analysis of its capabilities. During the examination session for the summer semester of the academic year 2019-2020 at the "G. S. Rakovski" National Defence College, the "Blackboard Learn 9.1" platform was actively used for testing the students in the master's specialties through tests. As many study groups entered the system and took the tests at the same time, in some cases there were breakdowns and interruptions in its work.

A statistical analysis of the interruptions in the operation of the system has been made on the basis of the collected limited amount of data. It should be clarified that this analysis does not take into account the status and quality of the Internet connection, but only the number of users working simultaneously in the system. Table 1 gives data on them, where the first row shows the crash numbers, the second row shows the number of users working simultaneously in the system (x), and the third row shows the average number of users for this sample of 11 reports.

Table 1 System's crashes statistic data

№	1	2	3	4	5	6	7	8	9	10	11
x	354	238	169	241	198	314	174	157	226	187	279
$\bar{x}$	230,64	230,64	230,64	230,64	230,64	230,64	230,64	230,64	230,64	230,64	230,64

The data in Table 1 show that a system failure occurred in a different number of users working simultaneously in the system, but their average number in which it occurred was equal to 230 people. Of course, this result is influenced not only by the number of users working in the system at the same time, but also by the status and quality of the Internet connection.

In order to get an idea of how much the data varies around the arithmetic mean ("x upper slash"), the standard deviation "s" has been calculated according to expression (1):

$$s = \sqrt{\frac{\sum_{i=1}^N (x - \bar{x})^2}{N - 1}} \quad (1)$$

where N - number of values in the sample;

x – number of concurrent users at the time of system outage.

The number of values of the sequence N in the denominator of expression (1) is reduced by one, because the sample is small (N ≤ 30).

The value of the standard deviation is obtained equal to s = 20.02 at this case. This is a relatively large value, as the deviation of the data in the series is a not low.

## Conclusion

The Blackboard Learn 9.1 platform has very good capabilities to represent learning material by allowing learners to access e-textbooks, lectures, presentations, and additional information about their condition. Students can be provided with additional literature for preparation by publishing links to various sources on the Internet such as Wiki, specialized sites and others.

The Blackboard Learn 9.1 platform has great capabilities to test knowledge of the students. Its main capabilities are creating and using tests, but it also offers other forms of control such as essays checking, term papers and checking other written work of students.

Nevertheless the above mentioned advantages, there are some challenges to test knowledge of the magister program students using the Blackboard Learn 9.1 platform. They can be summarized as follows:

- Lack of live visual and audio communication between students and teachers, especially at the time they have to enter the system together and communicate with each other;

- There are interruptions in the process of solving the tests for technical reasons: mainly due to interruption of the Internet connection or overload of the system's servers;

- Lack of constant control over the learners - distance learning requires strict discipline and its result depends on the abilities and consciousness of the learner;

- Need for a sufficient number of practical classes for students to work with the system.

The web-based system "Blackboard Learn" 9.1, fully complies with the requirements for learning in the Internet environment and administration of the learning process, giving students access to electronic textbooks, lectures, presentations, electronic tests for self-preparation, exams and additional information about their condition.

There are two main disadvantages of the system: lack of visual and audio communication in real time between students and teachers and interruption of the test due to overload of the system's servers. To overcome them, the following suggestions can be made:

- To use the Teams application from Office 365 for visual and audio communication between students and teachers in combination with BLACKBOARD LEARN 9.1 in teaching and to test knowledge of the learners;

- Use hot backup on both the Blackboard Learn 9.1 database server and the application server to avoid overloading the platform when many users log in at the same time. In addition, the lack of constant control over the learners and the need for a sufficient number of practical classes for students to work with the system can be overcome by motivating the learners and by administrative measures so that the learning process goes smoothly.

Experience from the Blackboard Learn 9.1 platform usage shows it has the potential for further use, especially by expanding its capabilities and by combining it with other systems that complement or improve its features.

## References

- Aleksandrova, K., 2010, Comparative analysis of modern tools and technologies for individual identification, International Scientific Conference "Hemus – 2010", 10 pages, (in Bulgarian).
- Blackboard Inc., 2010, Blackboard Learn 9.1 Advanced Integration and Data Management Guide, Blackboard Inc., 149 pages.
- Marinov, G., 2015. Blackboard Learn 9.1 User Manual for the students at „Rakovski“ National Defence College, RNDC, 68 pages, ISBN 978-954-9348-78-1, (in Bulgarian).

## STUDY OF STUDENTS' ATTITUDES IN APPLYING INNOVATIVE FORMS OF TRAINING IN PHYSICAL EDUCATION AND SPORTS AT THE UNIVERSITY OF MINING AND GEOLOGY "St. IVAN RILSKI"

Ivanka Stavreva<sup>1</sup>, Yordan Ivanov<sup>1</sup>, Vanya Tsoleva<sup>1</sup>, Spas Stavrev<sup>2</sup>, Nadezhda Kostova<sup>3</sup>, Evgeni Yordanov<sup>1</sup>, Milena Purvanova<sup>1</sup>

<sup>1</sup> University of Mining and Geology "St. Ivan Rilski", 1700 Sofia; vania.stavreva@abv.bg

<sup>2</sup> University of National and World Economy, 1700 Sofia; stavrevspas@hotmail.com

<sup>3</sup> National Sports Academy, 1700 Sofia; sugareva\_n@abv.bg

**ABSTRACT.** The current study was conducted with first- and second-year students from all courses of study at the University of Mining and Geology "St. Ivan Rilski"-Sofia who are offered the course unit in *Physical Education and Sports*. The aim of the study is to establish the attitude of students in applying new, contemporary forms of training in physical education and sports that are imposed, on the one hand, by the global pandemic of the corona virus disease (Covid-19), but also by the need for physical activity of students in a crisis situation throughout the world. Applying the survey method, results have been obtained of the sportological attitude of students and their stand on modern digital tools and methods of teaching through the distance form of communication and the use of electronic sources for gaining knowledge, including the level of their foreign language education. The obtained results are processed by applying mathematical and statistical tools. Following a thorough analysis, conclusions have been drawn regarding the level of sportological attitudes of students, their opinion on the innovative forms of education and their place in future classes in physical education and sports at the University of Mining and Geology "St. Ivan Rilski" as a successful pattern of education in higher schools in Bulgaria.

**Keywords:** physical education and sports, sportological analysis, models, innovation, electronic education

### ИЗСЛЕДВАНЕ НАГЛАСИТЕ НА СТУДЕНТИТЕ ПРИ ПРИЛАГАНЕ НА ИНОВАТИВНИ ФОРМИ НА ОБУЧЕНИЕ ПО ФИЗИЧЕСКО ВЪЗПИТАНИЕ И СПОРТ В МГУ „СВ. ИВАН РИЛСКИ“

Ivanka Stavreva<sup>1</sup>, Yordan Ivanov<sup>1</sup>, Vanya Tsoleva<sup>1</sup>, Spas Stavrev<sup>2</sup>, Nadezhda Kostova<sup>3</sup>, Evgeni Yordanov<sup>1</sup>, Milena Purvanova<sup>1</sup>

<sup>1</sup> Минно-геоложки университет „Св. Иван Рилски“, 1700 София

<sup>2</sup> Университет за национално и световно стопанство, 1700 София

<sup>3</sup> Национална спортна академия, 1700 София

**РЕЗЮМЕ.** Настоящото изследване е проведено със студенти от първи и втори курс от всички специалности в МГУ „Св. Иван Рилски“ - София, изучаващи дисциплината „Физическо възпитание и спорт“. Целта на проучването е да установи нагласата на студентите при прилагане на нови, съвременни форми на обучение по физическо възпитание и спорт, наложени от една страна от световната пандемия от Covid-19, но и от необходимостта от физическа активност на студентите в създадалата се кризисна за света ситуация. Чрез приложения анкетен метод са получени резултати за спортологичните нагласи на студентите и отношението им към съвременни дигитални средства и методи на преподаване, чрез дистанционната форма на комуникация и използване на електронни източници за обогатяване на знанията, в т.ч. и нивото на чуждозиковата им подготовка. Получените резултати са обработени чрез математико-статистически инструментариум. След задълбочен анализ са направени изводи относно нивото на спортологичните нагласи на студентите, отношението към иновативните форми на обучение и тяхното място в бъдещите занимания по физическото възпитание и спорт в МГУ "Св. Иван Рилски" като успешен модел на обучение във висшите училища в България.

**Ключови думи:** физическо възпитание и спорт, спортологичен анализ, модели, иновации, електронно обучение

### Introduction

In our daily contacts and conversations, the expression that sport is a social phenomenon is often used. This is a well-known fact which has been confirmed in full force in recent months. Forced by the Covid-19 pandemic, governments all over the world have severely restricted free movement and physical activity. The ban on the use of stadiums, gyms, fitness centres, swimming pools, tennis courts and many other sports facilities has brought about immobilisation and in many cases nervous breakdown. All those measures have resulted in the awareness of the need and significance of physical activity and

sports. The issue has largely turned into social and institutional.

Along with the outbreak of the pandemic, the issue of prolonging educational activities from the academic year 2019/2020 until the end of the epidemic has come to the fore. On the instructions of the Ministry of Health and of the established National Crisis Headquarters, all universities closed. In an address to the personnel at the University of Mining and Geology "St. I. Rilski", the Rector Prof. Dr. Eng. Ivaylo Koprev appealed for a transition to distance learning up until the removal of the extraordinary measures (www.mgu.bg).

Despite the specific character of its activities, the Department of Physical Education and Sports has been among the first to respond to this challenge adequately and in a professional manner. Presentations were made for every individual sport on pre-assigned topics. Video materials were offered for self-study, as well as exercises for motor activity at home. As an additional incentive for physical activity, several challenges were addressed to the students to respond to and perform. All of the above were uploaded in the Google Forms platform, so that each student could have access to the materials and be prepared for the forthcoming final test in the sport for which they had registered. The social network on the Facebook page of the department has also been extensively used for further information. At the end of the academic year, students were examined by taking a test.

### Aims of the study

The crisis situation which we were faced with at the beginning of this year has required establishing students' attitudes towards distance learning (DO) and the effect of the electronic form of teaching in view of storage and enhancement of the training process in the course unit of *Physical Education and Sports*.

The aim of our research is to explore students' opinion and attitude to innovative forms of education, to examine their stand, and to make analyses of the future work of the Department of Physical Education and Sports at the University of Mining and Geology "St. Ivan Rilski, given the extraordinary epidemiological circumstances throughout the world and in Bulgaria.

### Purpose

To study the attitudes of students regarding their need for sports, a survey has been conducted with target groups who participated in distance learning. In developing the questionnaire, we have resorted to the experience of Y. Ivanov and B. Tsolov (2003), Y. Ivanov et al. (2005), V. Tsoleva and Y. Ivanov (2013), M. Parvanova et al. (2014), P. Yusein and M. Purvanova (2018). With the aim of adapting the course unit in *Physical Education and Sports* to the profesiograms of students and their future occupational and applied activities, the questionnaire includes major key and priority issues that determine the contemporary trends in the attitude of students to their classes in physical education and sports activities. The main part of the current study is to establish the attitudes of students towards distance and e-learning in a crisis situation and their preferences for choosing a foreign language in relation to their sports awareness.

### Research tasks

The tasks we have assigned are as follows:

1. To conduct a comprehensive survey with students in order to determine the benefits of physical education and sports;
2. To establish the attitude of the respondents to distance learning, the contemporary means and methods of communication in the training in physical education, sports knowledge, and the effect of using a foreign language to obtain additional information on the type of sport chosen;
3. To analyse and summarise the results obtained and to give recommendations for future work with students in their classes in physical education.

### Significance

The implementation of the tasks set will allow us to give an accurate assessment of the success in employing new models and in applying innovative approaches in the training in physical education and sports at the university. This will enhance the learning process in higher schools with regard to the educational component and the students' motivational basis.

### Research methods

The research contingent were 98 university students of both sexes; 75 (76.5%) of those were male students and 23 (23.5%) were female students. The average age of all respondents was 21.3 years. In terms of gender, the average age of men was 21.1 years, and 22.4 years of women. The survey was conducted anonymously, whereby we aimed at greater freedom and objectivity of the respondents. The participants in the survey were 72 first-year students and 26 second-year students from the 3 faculties at the University of Mining and Geology: the Faculty of Mining Technology (MTF), the Faculty of Mining and Electromechanics (MEMF), and the Faculty of Geo-Exploration (GPF). They are distributed by number and by course of studies in the respective faculties as follows:

- **FACULTY OF MINING TECHNOLOGY**

The overall number of surveyed students from the faculty is **34** distributed in 5 courses of studies as follows:

- *Mine Surveying and Geodesy* - 15 students;
- *Management of Resources and Production Systems* - 8 students;
- *Development of Minerals* - 6 студента;
- *Underground Construction* - 4 students;
- *Mineral Processing and Recycling* - 1 student;

- **FACULTY OF MINING AND ELECTROMECHANICS**

The total number of surveyed students from the faculty is **47** distributed in 5 courses of studies as follows:

- *Computer Technologies in Engineering* - 36 students;
- *Electrical Power Engineering and Electrical Equipment* - 5 students;
- *Gassy, Combustion, and Purifying Equipment and Technologies* - 4 students;
- *Automation, Information, and Controlling Equipment* - 1 student;
- *Complex Mechanisation and Computer Design in Mechanical Engineering* - 1 student;

- **FACULTY OF GEO-EXPLORATION**

The overall number of surveyed students from the faculty is **17** distributed in 5 courses of studies as follows:

- *Ecology and Environmental Protection* - 7 students;
- *Biotechnology* - 3 students;
- *Drilling, Extraction, and Transport of Oil and Gas* - 3 We surveyed the students' sports attitudes with questions about their attitude to physical education and sports, the need to study the discipline "Physical Education and Sports", as well as whether they play sports in their spare time. students;
- *Geology and Exploration of Mineral and Energy Resources* - 2 students;
- *Hydrogeology and Engineering Geology* - 2 students.

## Result analysis

The survey was conducted immediately after the end of the academic year and after the removal of the restrictive measures by the government. The aim was to ensure that the acquired knowledge and the impressions gained would guarantee the clear, correct and timely completion of the surveys. The overall number of questions was 11, but we are going to analyse 8 of them. The 3 remaining questions will be the object of a separate research.

The questions included are indicative of the research innovativeness which also lies in its interdisciplinary nature. So far, the Department of Physical Education and Sports has not affiliated to other non-sport university departments.

All of the 98 students surveyed study a foreign language and are distributed into the following proportions: 72 students (74%) study in English, 11 students (11%) study Russian, 10 students (10%) are engaged in Spanish, and 5 people (5%) study German. Figure 1 shows the percentage of students in terms of the foreign language studied.

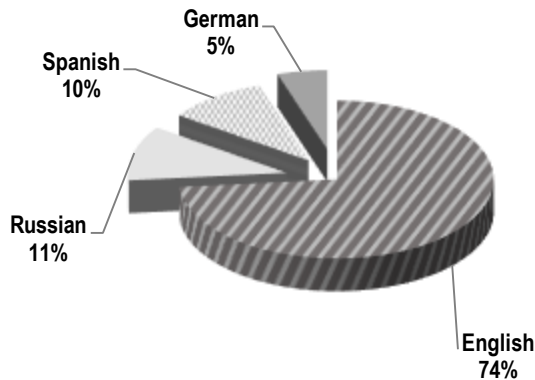


Fig. 1. Distribution of students in terms of foreign language studied (in percentage)

The students' sportological attitudes were surveyed by means of questions concerning their attitude to classes in physical education and sports, the need to study the course unit in *Physical Education and Sports*, as well as whether they play sports in their spare time.

Fig. 2 presents the answers to the question about students' attitude to PE and sports activities. 91% of the surveyed students are positive and 8% of the contingent are indifferent, which we consider might change with the necessary talks about the benefits of sports. Only 1 student has a negative attitude, which, statistically, is no cause of concern.

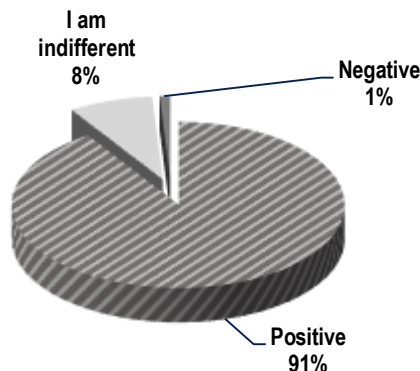


Fig. 2. What is your attitude to classes in *Physical Education and Sports*?

The numerical expression of the answers to the question about the need to study the course unit of *Physical Education and Sports* at the higher school is presented in Fig.3. 82% of the students gave a positive answer and 18% supplied a negative one. At the beginning of each class, the practice of delivering micro-lectures has already been established whereby further explanation is supplied regarding the benefits of PE and sports for students' health, physical ability (Ivanov, 2003), and above all its professional and applied orientation for their future occupational fulfilment in the vocational field. We believe that such explanations will contribute to the broadening of students' sports knowledge and are a powerful motive for developing positive attitudes towards physical education. Besides, the scientific team has carried out research in this direction: see V. Tsoleva and Y. Ivanov (2013), Y. Ivanov et al. (2016) and I. Stavreva (2019). Their research has proved the significance and established the occupational and applied effectiveness of physical education and sports for students at the University of Mining and Geology "St. Ivan Rilski".

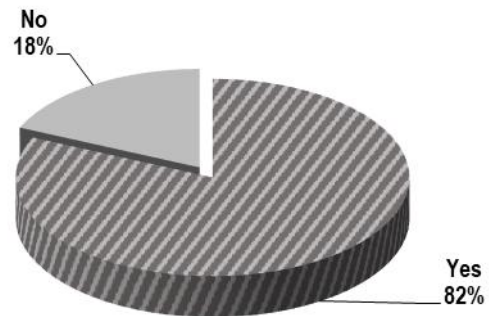


Fig. 3. Do you consider that it is necessary to offer the course of studies in *Physical Education and Sports* at the higher school?

Part of the survey was focused on how students perceived the organisation of the educational process in physical education and sports. When asked about their preferences for the organisation of the process under normal conditions, 49% (48 students) favoured classes conducted in general sports groups. The second largest group, 37% of the respondents (36 students), voiced their desire for classes in groups by the type of sport chosen. Only 14% of all wanted to join teams by type of sport, i.e. to be trained in sports improvement groups (see Fig. 4). Establishing the types of sport of an applied nature has been the topic of a research work by I. Stavreva (2019) which aimed at facilitating the occupational development of future engineers at our university.

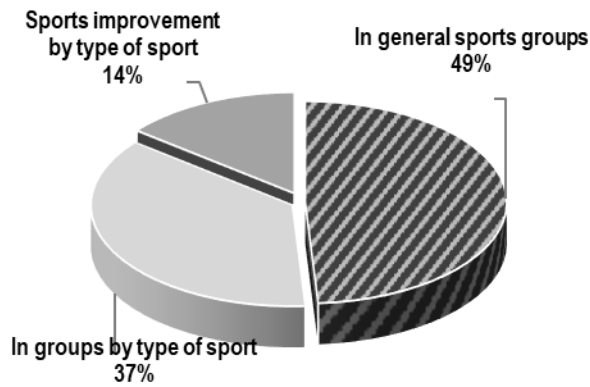


Fig. 4. What are your preferences for the form of organisation of the educational process in *Physical Education and Sports*?

For the first time ever, classes in the course of the semester have been conducted in an emergency crisis situation. This has led to the inclusion of a question about the opinion of students on the organisation of distance learning. The results are presented in fig. 5. 46% of the surveyed group have answered that they positively accept the distance form of education. This is almost half of the respondents (45 people). The rest are divided as follows: 22% have certain reservations, whereas the assessment of 32% is negative and they have stated that they do not accept this form of training. To us, these are logical answers, given the nature of the activities themselves and the lack of accompanying emotion and communication when conducting them under normal conditions.

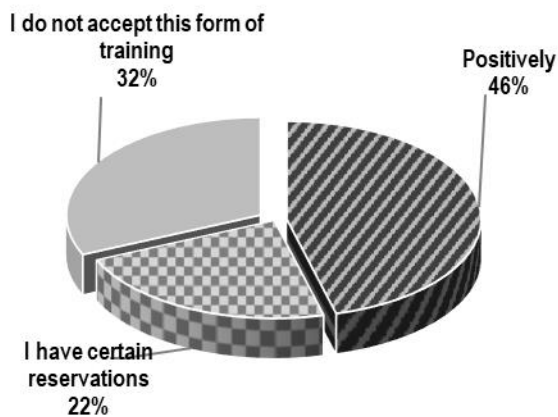


Fig. 5. How do you accept distance learning in a crisis situation?

In the fifth question from the survey, we asked the students whether they would choose the same sport in the next academic year. The majority have stated their willingness to go in for the same type of sport. A few have claimed that they would switch to another, more dynamic or more interesting, sport. Three students from the total panel have voiced their desire for new sports which are not on the curriculum of the department, such as *kickboxing, tennis and folk dances* (rather like extra-mural activities).

Logically, the next question we asked concerned students' sports activities outside the classroom, in their free time. This issue is also extremely important. Through it, we establish whether we have achieved one of the functions of physical education in higher school, namely for students to acquire the

habits and to create the need to continue physical activity and sports after the educational process is over. 67% of the respondents who go in for some sport in their free time have given a positive answer. 30% play some sport from time to time, and only 3% (which amounts to 3 students out of all respondents) do not go in for sports (Fig. 6). We are specifically interested in the group of students who answered this question with "sometimes" or "no" in view of a future study related to their arguments for restraining from or non-practicing of any sports.

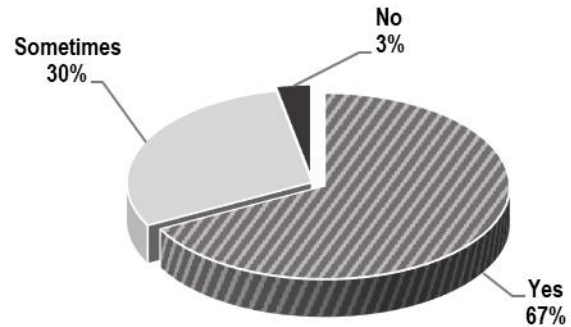


Fig. 6. Do you play sports in your free time?

It has been of a particular interest to collect data on the study of foreign languages and to what extent students have employed them to gather up-to-date information about sports in the course of the distance learning. The results in fig. 7 show that 35% of the students believe that the use of a foreign language has considerably facilitated the process of their acquisition of information about sports. 43% of the participants in the survey have answered that their knowledge of a foreign language has helped them gather information on certain sports topics. The remaining 22% have relied only on sources in their mother tongue during distance learning in physical education. To sum up the answers, in the emergency situation, all respondents have sought for sports information which is a testimony to their extraordinary interest and serious approach to the course unit in *Physical Education*.

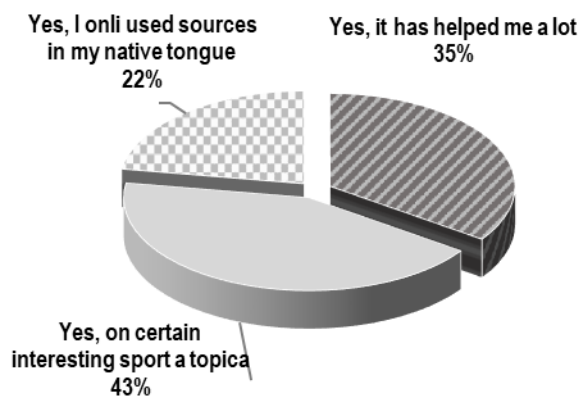


Fig. 7. Have you been facilitated by your knowledge of a foreign language in obtaining up-to-date information about sports during the distance learning?

In conclusion, we aimed to summarise the opinion of the tested contingent on the approach applied to the education

during the pandemic. 48% of the respondents have answered giving a positive assessment, 25% of the students have certain reservations, and 27% do not approve of the approach (Fig. 8). We believe that as this first attempt in this direction has achieved a lot in the name of the course unit and of the students themselves. All the more that this has been the first research with an emphasis on the importance and benefits of foreign language proficiency for the training in *Physical Education and Sports* to be carried out so far.

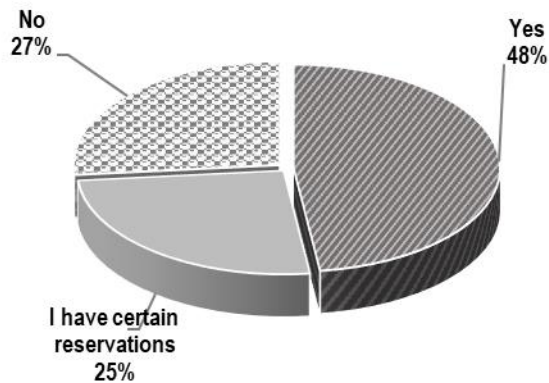


Fig. 8. Did you like our approach during the pandemic?

The research will help improve the educational pattern. It gives an idea of students' sportological attitudes and indicates the degree of readiness to accept innovations in the system of training in the course unit in *Physical Education and Sports*. Last but not least, it introduces the educational body to a successful model of work which has been established in the newly created epidemiological conditions of this year.

## Conclusion

- Students' positive opinion of the course unit in *Physical Education* and their positive attitude to the distance form of learning in the emergency environment have been established;
- Students' preferences for the type of sport and for the possible inclusion of new sports at the University of Mining and Geology "St. Ivan Rilski" have been revealed;
- The excellent work has been attested by the acquisition of habits and the creation of a need for physical activity in students. Those are proved by the 67% of the students going in for sports on a regular basis and a further 30% doing it sometimes in their spare time;
- Students' interest in the course unit in *Physical Education* has been confirmed by their search for alternative sources of information in foreign languages.

## References

- Bachvarov, M., Y. Ivanov, B. Tsolov. 2005. Sportologiya na obrazovatelната компонента на fizicheskoto vazpitanie. – *Sport i nauka*, 5-6, 126-132 (in Bulgarian).
- Ivanov, Y. 2003. Nov podhod za povishavane efektivnostta na protsesa po fizicheskoto vazpitanie v usloviyata na visshite uchilishta. – *Sport i nauka*, 2, 65-71 (in Bulgarian).
- Ivanov, Y., B. Tsolov, V. Borisova (Tsolova). 2005. Three Major Problems before the Physical Education Process and Sport at the Higher Academic Establishments in Bulgaria. – *Annual of the University of Mining and Geology "St. Ivan Rilski"*, 48, Part 4, 103-105 (in Bulgarian with English abstract).
- Ivanov, Y., V. Tsolova, G. Ignatov. 2016. Adaptatsiya na fizicheskoto vazpitanie na studentite kam ekstremalnite situatsii na badeshtata im profesiya. Adaptatsiya na fizicheskoto vazpitanie il sporta na studentite kam iziskvaniyata na savremennoto obshtestvo. – *Sbornik nauchni dokladi ot yubileina konferentsiya po sluchai 60 godini katedra FV i sport –organizirano sportno dvizhenie v MGU i 80 godini ot rozhdenieto na prof. dn Mihail Bachvarov. Zona Art PRINT EOOD, NSA PRESS, IDK pri NSA, Sofia*, 19-30 (in Bulgarian).
- Purvanova, M., V. Panichkova, M. Papazova, M. Hristova. 2014. Development, Approbation, and Application of New Educational Materials in Foreign Language Teaching for Special Purposes at the University of Mining and Geology "St. Ivan Rilski" – *Annual of the University of Mining and Geology "St. Ivan Rilski"*, 57, Part 4, 97–103 (in Bulgarian with English abstract).
- Stavreva, I. 2019. *Profesionalno-prilozhna efektivnost na fizicheskoto vazpitanie i sport v MGU "Sv. Ivan Rilski"*. Diss, VTU "Sv. sv. Kiril I Metodiy", Veliko Tarnovo, 174.
- Tsolova, V., Y. Ivanov. 2013. *Fizicheskoto vazpitanie vav visshite uchilishta – nov metodichen podhod*. Pechat BPS, Sofia, 107 (in Bulgarian).
- Yusein, P., M. Purvanova. 2018. Difficulties in Teaching English for Special Purposes to Engineers as a Foreign Language – *Journal of Mining and Geological Sciences*, 61, Part IV. "St. Ivan Rilski", Sofia, 54-59.  
<http://mgu.bg/new/main.php?submenu=200&id=833/30.03.2020>.  
<http://mgu.bg/new/main.php?submenu=200&id=836/12.05.2020>.

## COMMITTED EMPLOYEES - INNOVATIVE COMPETITIVE ADVANTAGE OF MINING COMPANIES

**Boryana Trifonova**

*University of Mining and Geology "St. Ivan Rilski", 1700 Sofia; E-mail: boryana\_trifonova@abv.bg*

**ABSTRACT.** The awareness of the need for committed employees is the first step toward effective motivation of human resources in an organization. The work of committed employees is of higher quality, they work with passion, initiative and their goals are identical with the common goals. These are the people thanks to whom development is achieved, new practices are introduced, and they are a source of innovations. Under the conditions of the current crisis, it would be difficult for companies to cope in the global competitive environment, if they are not oriented to talent retention and investment in the commitment of their human resources. The purpose of the present report is to prove the essential role of employee commitment as an innovative competitive advantage in the conditions of a crisis. Showing good practices for the commitment of human resources, applicable in the mineral resources sector, provide guidance for the companies in that industry on how to succeed in this unsafe situation. Truly, the success of a company is due to the inspired people working for it.

**Keywords:** committed employees, innovations, competition, mining companies

### АНГАЖИРАНИТЕ СЛУЖИТЕЛИ – ИНОВАТИВНО КОНКУРЕНТНО ПРЕДИМСТВО НА МИННИТЕ КОМПАНИИ

**Боряна Трифонова**

*Минно-геоложки университет „Св. Иван Рилски“, 1700 София*

**РЕЗЮМЕ.** Осъзнаването на необходимостта от ангажирани служители е първата стъпка към ефективното мотивиране на човешките ресурси в една организация. Ангажираните служители работят по-качествено и със страст, инициативни са и техните цели съвпадат с общите цели. Това са хората, благодарение на които се постига развитие, въвеждат се нови практики и са източник на иновации. В условията на настоящата криза, компаниите които не са ориентирани към задържане на таланта и инвестиране в човешки ресурси в посока тяхната ангажираност, трудно биха се справили в глобалната конкурентна среда. Целта на настоящият доклад е да изведе водещото значение на ангажираността на служителите като иновативно конкурентно предимство в условията на криза. Посочването на добри практики за ангажираност на човешките ресурси, приложими в минерално-суровинния сектор, дава насоки на компаниите от този бранш за успех в тази несигурна обстановка. Именно, успехът на една компания се дължи на вдъхновените хора, работещи за нея.

**Ключови думи:** ангажирани служители, иновации, конкуренция, минни компании

## Introduction

The awareness of the need for committed employees is the first step toward effective motivation of human resources in an organization. The work of committed employees is of higher quality, they work with passion, initiative and their goals are identical with the common goals. These are the people thanks to whom development is achieved, new practices are introduced, and they are a source of innovations. Under the conditions of the current crisis, it would be difficult for companies to cope in the global competitive environment, if they are not oriented to talent retention and investment in the commitment of their human resources.

The purpose of the present report is to prove the essential role of employee commitment as an innovative competitive advantage under the conditions of a crisis. As a result of the single conducted national study of employee commitment in the information technology sector, five basic factors were established for achieving commitment. (Audit Advice Associates, 2015) The examples for the use of these factors for human resources management in mining Companies have been popularized in company and industry periodicals.

Showing good practices for the commitment of human resources which are applicable in the minerals and raw materials sector provides guidance for the companies in that industry to succeed in this unsafe situation.

### 1. Basic factors for achieving commitment

The main challenge and responsibility of company management is to increase employee commitment as a guarantee for success when getting out of the current crisis. Commitment is a state that can be achieved as a result of the impact of diverse interdependent factors in combination with age, cultural and regional characteristics. The following five can be enumerated as factors for achieving commitment: leadership, recognition, providing opportunities, knowledge management and communication. (The single study of 18 commitment factors was used, conducted in Bulgaria in 2015, Audit Advice Associates, 2015) The enumerated factors impact employees in different ways. They can improve the work environment and social relations when they are tied to the goals and guidelines for company development.

• **Leadership** - the management of the company is inseparably linked to people's work. Leadership is intrinsic to the behavior of the leader, consolidating the efforts and capabilities of employees for the achievement of the organization's goals. It includes the distinctive qualities of the person accomplishing the impact over the team. In order to be a leader, a person needs to stand out with high social status and with impact on the behavior of others. But leadership should not be associated with the personal qualities and motivation of the leader only. More important is the established relationship system of the team, including the initiative shown and the responsibility taken by the leader for the team's actions. From this point of view, companies need to analyze the preparedness of individual employees to be leaders and offer them the respective training for their development in this direction.

• **Recognition** - this is an act of respect and an award for the long-term efforts of each member of the team. Recognition is most often achieved through compensation and bonuses, but only if there is a fair and transparent system for performance evaluation in force. Most often these stimuli are insufficient to achieve the desired employee commitment. In addition to them, it is necessary to express respect, gratitude and praise for work well done. In this manner, deep and lasting sense of ownership and belonging are created in the employee with respect to the organization that recognized his contribution.

• **Providing opportunities** - assistance for the career growth of individual employees involves creating clear rules for climbing the hierarchy and respect for efforts. As a result of encouragement and initiative and self-organizing, responsibility, innovativeness and continuity are achieved in the work of the team. This is a possibility for organizations to achieve long-term success, relying on the deployed managerial and organizing potential of their employees.

• **Knowledge management** - in the modern technologically changing world the manner in which organizations manage knowledge both at the individual and at the group level is of crucial importance for their competitiveness. Knowledge management is a modern approach for collecting, entering, processing, sharing and analyzing the information existing within, and outside of, the organization. This factor is of the highest importance for employee commitment, due to the fact that today we witness very fast obsolescence of personnel knowledge and skills. The organization must be ready to invest in the training of its employees, but also to inspire them to obtain new knowledge and skills to apply them at work. Committed employees who realize that knowledge is capital and a competitive advantage can assist their organizations not only in their survival in times of crisis, but also in their future evolution.

• **Communication** - the connecting process, important for the management of any organization. With the help of communication, the behavior of human resources is modified in the name of the changes implemented and goals achieved. Communication is a bilateral process and employee feedback to management is of significant importance for the effectiveness of the organization. As a result of more frequent conversations with employees, interpersonal conflicts and problems can be detected on time. Open, timely and honest communication which builds trust in management and

managerial decisions is of crucial importance for employee commitment.

The impartiality of the analysis of factors for the achievement of commitment requires to underscore that their use in human resources management is different. Despite its innovativeness, their combination and application cannot be taken as a cure-all for any problems related to this key process for business organizations. The increasing employee commitment is a possibility for development based on innovative latest practices. When employees are bound to the goals and guidelines for development, they help to establish a good work atmosphere, especially under the conditions of a need for continuous changes at all levels. It is a fact that in the current economic conditions the growth and evolution of a company are directly related to innovations, therefore, employee commitment is a suitable method for the purpose. (Galabova, B., B. Trifonova. 2018).

## 2. Good practices in the companies in the minerals and raw materials sector

In the contemporary Bulgarian practice different examples are found for applying employee commitment factors. They are present in many enterprises of the minerals and raw materials industry where significant results have been achieved. Different combinations of factors are possible related to their adaptation to the conditions in the company itself and the specific needs and goals. The advantages of their adequate and timely implementation lead to visible and measurable effects.

Achieving commitment in the companies of the minerals and raw materials sector represents an innovative solution for systematic discovery and exploitation of the possibilities and opportunities internal to the company. The following are good practices for retaining key employees used by the companies in this industry: trainings and development programs, involvement in interesting and challenging projects, praise, recognition of possibilities and career growth, as well as social benefits. In leading mining companies, examples can be shown of the implementation of diverse initiatives from the ones listed:

### • Training and career development

Employees in leading mining companies periodically participate in specialized trainings embedded in the companies' programs for training activity. Companies have at their disposal their own professional training centers which organize the trainings which in the current crisis are remote. In addition to them, trainings and workshops are organized for the acquisition of new knowledge and skills and to improve employee qualification. They are delivered in partnership with the largest technical universities in the country. These trainings contribute for good results when achieving company goals, for improving work quality and productivity.

The possibilities for career growth offered by companies are highly valued by employees. A good practice in these companies is when those who have proven to be good at their job raise in the hierarchy. This happens after direct monitoring on the part of management, systematic recording of achieved high results with developed internal training programs for the training and development of leadership skills. The possibilities

for growth in the hierarchy motivate employees to such a degree that they invest efforts and resources in order to preserve this trend and strive to climb the career ladder. In addition, external coaching specialists are hired for the professional development of managers.

• **Providing possibilities and inclusion in Project**

The projects which Bulgarian Network develops, especially "I am proud of my parents' work" and "Profession bazaar", provide direct benefits for mining companies and show how much mining production has changed in the last years and are in keeping with our transparency with respect to society, employees and media. (News, Mining and Geology journal. 2020) Thanks to them, new technologies, automation, investments in environmental preservation in the minerals and raw materials sectors are popularized. By involving employees in the projects, the sense is created that the work performed is exciting, challenging and interesting. In practice, when implementing the projects, the management of each company direct their efforts towards redesigning jobs and work places which gives satisfaction to the personnel.

The following are projects directed towards the people working in the industry and with guaranteed benefits for society and regions: "Business achievements for social entrepreneurship" and "Employment for unemployed young women in regions with heavy industry". They are directed toward business skill training and providing opportunities to develop entrepreneurship and involve women in the active economic life. (Project of Industrial Cluster Srednogie, 2020) The commitment of employees and their inclusion in company goals is also related to company activities for the preservation of national traditions and of the Bulgarian heritage. A related project of mining companies is "Bulgarian school", thanks to which a private school and a kindergarten are operating which preserve the Bulgarian Revival traditions. The "Biodiversity monitoring plan" takes the endangered protected plant and animal species, observes them, draws a plan for their preservation and includes the recultivation of areas where the activity has already finished. Under the project for "Preservation of the cultural heritage", archaeological explorations and excavations were carried out in the regions with mining activities, so as to preserve the Bulgarian heritage for future generations. (Dundee Precious Metals, 2012)

Today, business has a continuously increasing importance for the sustainability of society. The lessons from the crisis which we should follow are that society requires a much higher level of commitment, solidarity, and responsibility. It is necessary to increase employee commitment to overcome difficulties, including observing corporate culture. Ethical firms will be the most attractive ones in the future, not only as employers, but also as business partners. (News, Mining and Geology journal. 2020)

• **Effective communication, praise, appreciation**

This factor has a strong impact on the results of the individual activity of employees. When a person finishes work, he expects recognition for his merits. Expects to be noticed and appreciated. The lack of appreciation by the boss causes the worker to feel that, since he was not noticed and appreciated for work, this will not happen. In mining companies where a large part of work positions are related to specific knowledge, skills and competence and other positions also

with a health risk, managers aim to evaluate workers fairly and decrease the level of de-motivation.

Commitment reflects the feelings and behavior of employees caused by their ties and relations with the company. With time, mining companies have created a reward system (for example "Best in the profession") and this causes employees to strongly wish to prove themselves, which explains the very high degree of commitment. To some degree, this factor creates a competitive atmosphere with the purpose each employee to give the best he can and, as a result of this, apart from material incentives, a sense of one's importance and value will be generated.

• **Leadership**

It is good leadership of a company when the goal is to inspire and inflame the entire personnel. To build trust in management, managerial staff demonstrates before the personnel with confidence that it knows where the company is going, that it has developed good plans for the future and, on its part, it is capable of fulfilling them. Something positive in leading mining companies is the endeavor to master behavioral skills for holding conversations and negotiations, for making individual and group decisions. Examples of targeted improvement of firm culture in the industry exist since 1996 already. Programs for the stimulation of creative activity and encouragement of good work and new relevant ideas and proposals are developed and constantly updated. (Tsotsorkov, L. 1996)

The initiative "Let use work together" targets building the desired firm culture, aiming to deploy employee commitment and unused potential. (Bulgarian Chamber of Mining and Geology /BCMG/, 2019) This project applies the theory of systemic leadership, including the creation of a work environment in which teams willingly give the best they can. Employees from all levels in the company participate in the initiative with the goal to feel more responsible with respect to the commitments they make and the behavior they display. Specific training is conducted by means of adapted materials revised for the needs of the personnel. A cartoon film was created which includes illustrative situations from the real work environment, seen from the point of view of systemic leadership models. Employees of the company with different main professions are in the role of trainers. This helps to create an environment of trust, openness, understanding and reciprocity between the participants and facilitates perception.

• **Social benefits**

Social benefits are a sign of social status for employees of mining companies. Taking them away would not only lead to a very high degree of de-motivation, but also to a sense of offense, lowering of the social status. The majority of employees in mining companies believe that respect for employee rights, fair salaries and safe work conditions are most frequently found on the part of a "responsible" employer. (Petrova, V. 2016)

Leading mining companies develop their social policy to a very high level. With time, they upgrade this policy trying to satisfy most needs of separate individuals and of the group as a whole (the entire personnel). Examples of social benefits are: the dining facilities, a medical facility to provide emergency aid in the case of incidents, providing parking lots for the personal cars of employees and for managers. In addition, employees are provided with: cards with 20% discount for SPA services,

shopping coupons for specific store chains, possibilities to improve qualifications, participation in different workshops, additional pension and health insurance. The main purpose of the social policy of the company is not only personnel retention, but also getting their loyalty. In turn, employees get opportunities to satisfy their immaterial and material needs, to feel social, not just workers.

It is possible to point at a number of examples for express responsibility of leading mining companies for the human resources working there. The stress is placed on applying a policy for preserving the health of all workers. In addition to the provided safety measures for mechanical devices and machines, the installation of safety railing and barriers, letting in only after and alcohol test, weekly safety meetings, trainings for healthy and safe work conditions and for work with biological agents, annual preventive medical checks are provided for all hired employees.

The management of mining companies strive to retain their key employees which is also reflected in the implementation of an intelligent system for quality management, environmental protection and work health and safety. It allows the instructions and rules for safe work to be subject of continuous control, periodic audits and ongoing evaluation of the possibilities for improvement. The following are examples of good practices in relation to the integrated system, implemented and applied at the corporate level: (Serous 7) seven activities and operations evaluated with highest risk, (Take 5) five steps for the safety of each work place, company Work Conditions Committee, manager visits for safety, safe barometer, Safety Day and a health campaign to quit smoking. (Bulgarian Chamber of Mining and Geology /BCMG/, 2019)

The high economic performance is related to significant capital investments in modern technologies and to investments in upskilling of employees (Galabova, Nestorov, 2019). The continuous improvement of work health and safety conditions and of the unfavorable impact on the environment after mining and extraction activities is the foundation of the sustainable development of mining companies. It is the main priority of the management of mining companies. It helps to build a sense of belonging in employees. This sense makes people identify with the organization and strengthens commitment even more.

## Conclusion

The impartiality of the analysis of factors for the achievement of commitment requires to underscore that their use in human resources management is different. Despite its innovativeness, their combination and application cannot be taken as a cure-all for any and all problems related to this key process for business organizations. Achieving commitment in the enterprises of the minerals and raw materials sector represents an innovative solution for the systematic discovery and

exploitation of the conditions and possibilities internal to the firm. Good practices for the retention of key employees used in enterprises from this industry are the following: trainings and development programs, inclusion in interesting and challenging projects, praise, recognition of possibilities and career growth, as well as social benefits.

The goal of mining companies is to create competitive advantage by supporting their strong technical and commercial performance with expert management of social processes. This includes building a work environment in which teams willingly give their best. And this, on its part, unlocks the potential of employees, encourages their creativity, leads to increased productivity and better business performance. It is necessary to deploy the internal process of organizational development which, by means of a system of qualifying and stimulus measures, will lead to improvement of the management of human resources in these companies.

## References

- Audit Advice Associates, 2015, Osnovni faktori za angajiranostta na slujitelite v ikt, [https://computerworld.bg/it\\_liders/2015/10/23/3464164\\_osnovni\\_faktori\\_za\\_angajiranostta\\_na\\_slujitelite\\_v\\_ikt/](https://computerworld.bg/it_liders/2015/10/23/3464164_osnovni_faktori_za_angajiranostta_na_slujitelite_v_ikt/) (in Bulgarian).
- Bulgarian Chamber of Mining and Geology/BCMG/, 2019, Annual reports the mineral raw material industry in Bulgaria, 63p.
- Dundee Precious Metals, 2012, Sustainability report of "Dundee Precious Metals" JSC, 56p.
- Galabova, B., N. Nestorov. 2019, Role of the mining industry in the Bulgarian economy, Mining and Geology journal, number.5, p.18-24. (in Bulgarian with English abstract).
- Galabova, B., B. Trifonova. 2018, Innovative practices in the management of the mining company, Journal of mining and geological sciences, Vol. 61, Part IV, Humanitarian Sciences and Economics, p.25-28.
- News, 2020, Bulgarska sesia na svetoven forum "Recover better, recover stronger, recover together", Mining and Geology journal, number.4-5, p.4-5 (in Bulgarian).
- Petrova, V. 2016, The impact of corporate social responsibility on employees in the mining industry, Annual of the UMG "St. Ivan Rilski", Vol. 59, Part IV, Humanitarian Sciences and Economics, p.40-42 (in Bulgarian with English abstract).
- Project of Industrial Cluster Srednogorie, 2020, <http://www.srednogorie.eu>
- Tsotsorkov, L.1996, Osnovi na firmenata kultura v MOK Asarel-Medet AD Panagyurishte, Sofia, 315p. (in Bulgarian).

## THE NEW GENERATION OF MANAGERS IN A GLOBAL ASPECT

**Tsvetina Ts. Tsakova**

*University of Forestry, Sofia, 10 Kliment Ohridski Blvd.*

**ABSTRACT.** The traditional industrial management is described in detail in the novel *Shirley* by the English writer Charlotte Bronte. She lives and works during the Victorian Age (1837-1901) when England reaches the peak of its economic development. Today the digitalization and robotization of the economy as well as the global connection and interdependence define the change in the style of the business management. The routine in industrial management yields to sophisticated approaches. The multinational companies create a new generation of managers with an innovative mentality. The modern CEO (Chief Executive Officer) should combine in a creative way the social policy and the sustainable development of the corporation.

**Keywords:** generation, global, digitalization, industrial management, innovation

### НОВАТА ГЕНЕРАЦИЯ МЕНИДЖЪРИ В ГЛОБАЛЕН АСПЕКТ

**Цветина Ц. Цакоева**

*Лесотехнически университет, София, бул. „Климент Охридски“ 10*

**РЕЗЮМЕ.** Традиционният индустриален мениджмънт е описан детайлно в романа „Шърли“ на английската писателка Шарлот Бронте. Тя живее и твори през Викторианската епоха (1837-1901), когато Англия достига върха на своето могъщество в икономическото си развитие. Днес дигитализацията и роботизацията на икономиката, както и глобалната свързаност и взаимозависимост предопределят промяна в стила на управление на бизнеса. Рутината в индустриалния мениджмънт отстъпва на иновационни подходи. Мултинационалните компании създават нова генерация мениджъри с новаторски менталитет. Съвременният CEO (Chief Executive Officer) трябва творчески да съчетава социалната политика и устойчивото развитие на корпорацията.

**Ключови думи:** генерация, глобален, дигитализация, индустриален мениджмънт, иновация

Our century is characterized by the so called digital revolution. The artificial intellect is applied in all economic branches and human activities. A network society is established which is tightly connected with the global knowledge-based economy.

The digital 21<sup>st</sup> century is a century of interaction. The human intellect builds and programs the artificial intellect. The high technology machine-building in the industrially developed countries is dependent on the mass production of details in the countries from Eastern Europe and Asia. The different industrial activities form a circle economy and other analogous business and social connections and interactions.

The modern information society imposes changes in the methods of scientific research. The literary scholars go out of the box of their scientific activity and participate in academic debates, connected with the current social-economic life, e.g. with the actual business reality. The aim of the research is to reveal the possibilities for the adaptation of the industrial management to the challenges of the tendencies of the development of the global economy.

The study is made on the basis of several scientific subjects, and in the context of distant historical periods. The modern innovative interdisciplinary (multidisciplinary) approach forms a network of experts in the humanitarian, social and economic scientific fields. Through their discussion a convergence of the different concepts and a basis for a comprehensive and complex research is established.

The traditional style of management of business is described in detail in the English writer Charlotte Bronte's novel *Shirley*. The author lives and works during the Victorian Age (1837-1901) when England is in a period of an economic boom.

The discourse in the novel describes in a non-consecutive chronology the events connected with the introduction of high technology machines in the textile mills in Yorkshire, England in the period of The Industrial Revolution.

The main heroine is the sole heiress to an estate and a textile mill. Traditionally in the patriarchal society only the sons inherit and manage the family companies. Shirley manages the inherited estate with an animal farm attached to it very successfully when hardly out of age, owing to her personal abilities – intellect, courage, independence, self-confidence. Robert Moore is appointed manager to the textile mill.

The active Shirley is at the farm or at Robert Moore's office from morning till night. In the evening, instead of embroidering as is traditional for the Victorian women, the main heroine reads till late. Every day she reads the newspapers. The young business lady is not interested in the secular gossip in the daily papers, yet she never misses the editorials. She follows both the financial and Stock Exchange information, as well as the foreign news in the newspapers.

The Victorian business lady manages wisely and with her own style. She prefers the office to the aristocratic balls. Shirley is serious and does not play the coquette when she discusses the production problems at the factory with Robert Moore. On

his part, the manager of her textile company also behaves in a businesslike manner with the new owner. Today the big companies have an ethical code with which they form and regulate the relations and moral values of their employees, e.g. of their team.

Shirley personally controls the work at her estate by not behaving proudly, e.g. as a mistress of the house in the real sense of the word. She often follows the incomes and outcomes by writing everything in a ledger. Once, during a weekly balance check, she finds out a fraud in the housekeeper's accounts. Instead of a scandal, the tolerant lady lectures Mrs Gill on thrift.

The idea that there is no demeaning labour is featured in the novel. The mistress of the estate works together with her subordinates in emergencies. The generous and noble Shirley ensures provisions and medical bandages, not only to the soldiers who defend her factory, but also to the wounded rebels.

The virtuous Shirley is not greedy. She establishes a charity fund with her own start-up capital and for this aim she invests half of the profit of her estate. The main heroine organizes the collection of the financial means for the fund and their just distribution with the help of the single women like Miss Ainley. The business lady aids with the collected money the unemployed poor whose percentage is very high during *The Industrial Revolution*. Today, this humanitarian activity is very popular, and different forms of charity are used.

The main heroine's public activity should also be mentioned, in order to construct the whole image of the Victorian business lady. The communicative Shirley meets and wins the trust of one of the most influential men – The Reverend Helstone and Mister Yorke soon after she arrives at the parish. The business lady discusses the actual social and political information with them.

The innovative thesis in the context of patriarchal society that gender is not a decisive factor in the choice of a career, e.g. that there are no female and male professions is proven in the description of Shirley's social status as a business lady.

Charlotte Bronte looks ahead in the future through the literary image of Shirley in the eponymous novel. The Victorian owner's and employer's methods of management, ethical code, charity and public activity are identical to the ones of the modern business lady.

In comparison to the introduction of highly productive machines in the industry during the Victorian Age, the present industrial revolution is accompanied by digitalization. It influences the global knowledge-based economy strongly. The industrial management accepts the challenges of the world tendencies and changes itself. The new generation of managers combines the social policy with the intellectual economic growth.

The choice of the topic concerning the new generation of managers is not random – it corresponds to the actual gender imbalance in the company management. According to a number of researches the European business is still dominated by men.

The reasons for the gender imbalance in the corporate management are the following:

1. A lack of a national policy, legislation and motivation measures concerning the equality of the genders.
2. Measures about the combination of the family and the professional life of the employees are not applied.
3. The inherited patriarchal stereotypes from the past concerning the woman's role in the family and labour. The double "burden" of both professional and family

life limits the possibilities for women for a business leadership.

4. The non-transparent practices concerning appointments and nominations in the boards of the companies spread in many countries around the world. The directors are usually chosen through personal acquaintance and contacts, e.g. through the so-called "friendship circle networks", and not through publicly announced interviews.
5. Last, but not least, the business leadership is still considered a man's model of success. The employees should be always available, and if possible they should be mobile at all times. The interruption of the career development, due to motherhood and other family reasons could also influence negatively the chances of women to have manager's positions in the corporate business (MLSP, 2015, p.37).

The dynamics of the digital revolution changes the actual business environment quickly. The modern digital society and the negative demographic growth in the European countries create a deficiency of highly qualified technical staff. Ludolf von Wartenberg, president of the biggest association of employers in Germany gives a characteristic of the problem connected with the loss of jobs in most Western industrialized countries:

*The creation of jobs is not an aim in itself. We have to realize that we could participate in the international competition only with new products. Because of the open markets, we would rarely have mass production in Germany. A bigger growth could only be achieved with innovations. And the economic growth ensures jobs. That is why we should return on the frontline of the technical progress (Wissema, 2006, p.25).*

The multinational companies adapt to the global knowledge-based economy. The corporate business invests in intangible assets such as Research and Development-R&D. The aim of the investments is to exchange knowledge with other companies, to sell know-how, and to support *technostarters* – entrepreneurs who establish a new company on the basis of knowledge and technologies.

The technological paradigm for an interaction between the corporate business and science is the established incubator by *Philips Electronics* (a building in which the entrepreneurs develop their start-ups) in their high technological campus in the city of Eindhoven, The Netherlands (Wissema, 2006, p.22).

The establishment of a start-up for some entrepreneurs, and its sale in a few years is the short cut for climbing up of the hierarchical ladder to top management positions. The company owners prefer hiring entrepreneurs who have proven themselves on the market and know the management very well, instead of diligent business administrators. They may be very good analyzers, but they have become CEOs (Chief Executive Officers) by chance.

During the first decades of the XXI century the big international companies create a new generation of managers with an innovative mentality. Their credo is that the careers should be combined with the personal lives of the employees. The corporate business invests not only in the professional development, but also in the workability of the employees (fitness halls, kindergartens, flexible working hours for the parents of young children, etc.). The aim of the employers is to attract highly qualified staff, disregarding their gender.

During the last few years the multinational companies with offices in our country competed for the prize "Most wanted employer". In 2019 the award went to one of the biggest world IT companies with more than 10 000 employees- Hewlett Packard Enterprise (HPE). The executive director of HPE Global Delivery Bulgaria Centre Mario Garbeshkov tells:

*During the past year HPE managed to achieve and confirm the desired stable financial results. At the same time the company adheres to its strategic aims to transfer its portfolio to more high technological decisions and complex software services... We invested in key partnerships and united with smaller but leading companies in some market niches...We also invested in our employees, in their development and benefits as a part of the family of a leading technological leader...In the last years the abilities and the companies in Bulgaria grow with a dynamic tempo and innovative practices, which conditions the big competition in the IT sphere. What distinguishes HPE are the values and the atmosphere in which we work.*

*The employees are what makes a company successful...This year we announced our Work that fits your life programme behind which is the so called Wellness Friday. Every second Friday from the month the employees have 3 hours free time at the end of the work day...6 months 100 % paid leave for the regular gross salary for mothers and fathers (Capital, 2020, p.29).*

Therefore, the modern manager must know and apply creatively the formula for a successful combination of the social policy and the sustainable development of the company.

The mass digitalization of the economy and the global connectedness change not only management, but also marketing abruptly, especially the model "software as a service". The global IT market is huge and expands quickly. Old and new multinational software companies which create strong products participate in it. The successful competitive formula of the small software companies is mainly fast decisions and the focus on a particular service.

Kate Fitzgerald, president and director of incomes in the cloud *Leanplum*, with an office in Sofia, tells about the competitive advantages of the small software company for mobile marketing:

*We developed something that we call ICP (Ideal customer Profile). We often work with dynamic companies, which are established after 2000, because usually these are the companies that create mobile applications...The marketing and the finding of clients are very different...We should reach the clients before anyone else does, and not expect them to come*

*to us. We should add to this that the clients are much better informed...*

*The big companies have much bigger budgets for trading teams. But our plus is that we can take faster decisions....This speed is of critical importance...I think that the biggest challenge in front of each smaller company is to be focused...We focus on the mobile Internet (Capital, 2020, p.71-73).*

It should be noted that the digital competence has huge importance for the industrial management. But in the era of interaction we shouldn't ignore the humanitarian skills – of creativity, communicativeness and adaptability. The machines do not replace but help the person in the process of digitalization.

The modern digital systems create big possibilities but robots lack ethics, emotionality and critical thinking, respectively the taking of the right decision. That is why, it could be figuratively put, that the person is the mentor of the robot.

In conclusion, it should be underlined that the global economy, based on knowledge and innovations, changes the rules of industrial management drastically. The successful CEO who controls the investments through the distribution of the capital in the interest of the owners, remains in the past. The routine in the management yields to innovative approaches. The modern CEO should decide a complex task because the multinational companies invest more in intangible assets – research and development (R&D). Therefore, the CEO should distribute the capital in such a way, so as to manage the company in the long term interest of its owners.

## References

- Bronte, Charlotte. *Shirley*. Wordsworth Editions Limited, 1993.
- Висема, Ханс. *Техностартерите и университетите трето поколение*. София, 2006.
- Гърбешков, Марио. *Служителите са това, което прави една компания успешна*. Сп. Капитал, 20 декември-9 януари. София, 2020.
- Министерство на труда и социалната политика (МТСП) и Център за икономическо развитие. *Равенство на жените и мъжете при вземане на решения в икономиката*. София, 2015.
- Tsakova, Tsvetina. *The Construction of Feminine Identity in Charlotte Bronte's Novels* (PhD thesis). Sofia, 2019.
- Фидджералд, Кейт. *Предимствата да си по-бърз от големите*. Сп. Капитал, 10-16 януари, София, 2020.



[www.asarel.com](http://www.asarel.com)

*От природата за хората,  
от хората за природата*



**АСАРЕЛ МЕДЕТ-АД**  
КОМПАНИЯ С ЕВРОПЕЙСКО ЛИЦЕ,  
БЪЛГАРСКО СЪРЦЕ И СИЛЕН  
ПАНАГЮРСКИ ДУХ



## Аурубис България

Ние сме част от водеща международна група за производство на мед и най-големият преработвател на мед в света.

Компанията ни е на първо място в металургичната индустрия в страната и водещ производител на мед в Югоизточна Европа.

Ние сме втората по големина компания в България като размер на годишните приходи.

Инвестирали сме над 1.2 милиарда лева в модернизация на производството и опазване на околната среда.



# БАЛУЗЗ

БЪЛГАРСКА АСОЦИАЦИЯ ЗА ПРОИЗВОДСТВО И УПОТРЕБА НА ВЗРИВНИ ВЕЩЕСТВА

## БЪЛГАРСКА АСОЦИАЦИЯ ЗА ПРОИЗВОДСТВО И УПОТРЕБА НА ВЗРИВНИ ВЕЩЕСТВА

### ЗА НАС

През 2010 година в гр. Варна беше основа неправителствената организация Сдружение на производители на взривни вещества в България с основна цел подпомагане, насърчаване и защита интересите на своите членове, производители на взривни вещества.

В края на 2019 г., на свое Извънредно Общо събрание, Сдружението направи промени в своят устав и наименование с цел разширяване обхвата на дейността, така че да се даде възможност членове да бъдат и юридически лица, чиято дейност е свързана само с употребата на взривни вещества.

През януари 2020 г. е извършена пререгистрация в Агенцията по вписване на Сдружението с новото наименование - "Българска асоциация за производство и употреба на взривни вещества".

От 2019 г. Сдружението е член на **Европейската Федерация на взривните инженери.**

### ЦЕЛИ

Асоциацията има за цел да подпомага развитието в областта на производството и употребата на взривни вещества и свободната конкуренция в Република България

### КОЙ МОЖЕ ДА БЪДЕ ЧЛЕН

Членове на Асоциацията, могат да бъдат:

1. физически и юридически лица, регистрирани по Търговския закон, производители, вносители и официални дистрибутори и извършващи дейности, свързани с употребата на взривни вещества.
2. институции и организации, занимаващи се с образователна, научна и изследователска дейност, пряко свързана с производството и употребата на взривни вещества.

### УЧРЕДИТЕЛИ И ЧЛЕНОВЕ НА АСОЦИАЦИЯТА:

**ЕСКАНА ИНВЕСТ 96 АД** 

 **ВИА 2000 ООД**®

 **НИКАК** ООД

**МАХАМ**

**ОРИКА МЕД БЪЛГАРИЯ**



### КОНТАКТИ

<https://baepb.com>

e-mail: [info@baepb.com](mailto:info@baepb.com)

Елена Филипова - Председател

e-mail: [filipova@baepb.com](mailto:filipova@baepb.com)

Мая Ненкова – Секретар

e-mail: [nenkova@baepb.com](mailto:nenkova@baepb.com)



## Съвременното лице на българския рудодобив

[dundeeprecious.com](http://dundeeprecious.com)



*Sustainable development  
- quality life standard*

*Устойчиво развитие  
- стандарт за качествен живот*

**45 ГОДИНИ  
ЕЛАЦИТЕ-МЕД**



**21 ГОДИНИ В ГРУПА  
ГЕОТЕХМИН**

**УПРАВЛЕНИЕ**

с. Мирково 2086, Тел: (02) 923 77 21,  
e-mail: [office@ellatzite-med.com](mailto:office@ellatzite-med.com)

**HEAD OFFICE**

2086 Mirkovo, Bulgaria, Tel: (+3592) 923 77 21,  
e-mail: [office@ellatzite-med.com](mailto:office@ellatzite-med.com)

**РУДОДОБИВЕН КОМПЛЕКС**

гр. Етрополе 2180, Тел: (02) 923 76 72,  
e-mail: [mine.complex@ellatzite-med.com](mailto:mine.complex@ellatzite-med.com)

**MINE COMPLEX**

2180 Etropole, Bulgaria, Tel: (+3592) 923 76 72,  
e-mail: [mine.complex@ellatzite-med.com](mailto:mine.complex@ellatzite-med.com)

**ОБОГАТИТЕЛЕН КОМПЛЕКС**

с. Мирково 2086, Тел: (02) 923 77 29,  
e-mail: [flotation.complex@ellatzite-med.com](mailto:flotation.complex@ellatzite-med.com)

**FLOTATION COMPLEX**

2086 Mirkovo, Bulgaria, Tel: (+3592) 923 77 29,  
e-mail: [flotation.complex@ellatzite-med.com](mailto:flotation.complex@ellatzite-med.com)



# ЕСКАНА



КОНТАКТИ : 9010 гр. Варна  
ул. "Арх. Петко Момилев" №26  
Централа: 052 303127  
Факс: 052 303475  
e-mail: office@eskana.com

STARO ORYANOVO QUARRY

Natural sands quarry

"ЕСКАНА" АД е акционерно дружество с предмет на дейност добив и търговия с инертни материали. Компанията е основен производител на сертифицирани трошенокаменни фракции и естествени пясъци във варненска област и наследник на бившето държавно предприятие „Инертни материали“ гр.Варна, създадено през тридесетте години на миналия век. Дружеството е водещо в българската минна индустрия, активен член на БАПИМ. Представител е на модерния бизнес в България, с изразена гражданска позиция и отговорно отношение към околната среда и социалните проблеми в регионите, на чиито територии е разположено. Приоритет на ръководството на "ЕСКАНА" АД е непрекъснато повишаване качеството на работа, качество на продуктите, коректно обслужване, грижа за околната среда, здравето и безопасността при работа. За осъществяване на тази политика в компанията е внедрена и се поддържа интегрирана система за управление, съответстваща на международните стандарти ISO 9001:2015, ISO 14001:2015, OHSAS 18001:2007, HACCP като неразделна част от цялостното управление на фирма Ескана АД и на всички свързани дъщерни дружества.

## Предлагани продукти и услуги:

- |                                 |                               |
|---------------------------------|-------------------------------|
| § Трошенокаменни фракции        | § Проектиране                 |
| § Естествени пясъци             | § Баластри                    |
| § Микронизиран калциев карбонат | § Скалнооблицовъчни материали |
| § PVC & AL дограма и фасади     | § Строителство                |
| § Геологопроучвателни дейности  | § Геодезия и маркшайдерство   |

[www.eskana.com](http://www.eskana.com)



# ЕСКАНА ИНВЕСТ 96 АД



## ОСНОВНИ ДЕЙНОСТИ:

- Производство опаковани взривни вещества “ЕСКАНФО” и “Хидромайт 1100”.
- Мобилно производство на насипни взривни вещества
  - За открити рудници и кариери – “Хидромайт 70”, “Хидромайт 70 AL”, “Хидромайт 100” и “ЕСКАНФО”;
  - За тунели и подземни рудници – “Хидромайт 100”



- Превоз на опасни товари по шосе EXII, EXIII, MEMU



- Търговия и съхранение на взривни материали
- Охранителна дейност
- Пробивно-взривни работи

## КОНТАКТИ:

<https://www.eskanainvest96.com>



## Геологопроучвателни и минни проекти

*С грижа за  
природата  
създаваме нови  
възможности  
за хората*



1680 София, бул. България 102, тел.: 02 808 25 10  
e-mail: euromax@asarel-investment.com

Геострой АД е сред водещите строителни компании в България. Дружеството е със сериозен опит и дългогодишна история в изпълнението на разнообразни и мащабни проекти. Геострой предоставя на клиентите си широк спектър от качествени услуги благодарение на разнородните си компетенции и потенциал.

Геострой е вписано в Централния професионален регистър на строителя за извършване на всички категории строителни дейности от I до V група.

В сферата на минната индустрия дружеството успешно изпълнява:

- Изкоп, натоварване и транспорт на минни маси
- Поддръжка и ремонт на руднични пътища
- Тунелно и минно строителство
- Геодезически услуги



## **15 YEARS** **GHOSTROY AD**

Geostroy AD is among the leading construction companies in Bulgaria. The company boasts considerable experience and a long list of successfully completed large-scale projects. Thanks to its competencies and potential, Geostroy provides a wide range of good quality services to its clients.

Geostroy is listed in the Central Register of Professional Builders at the Bulgarian Construction Chamber for executing construction works in all site categories from groups 1 to 5.

In the mining industry, the company has been successfully performing:

- Excavation, loading and haulage of mined materials
- Maintenance and repair of mine haulage roads
- Tunnelling and mining construction
- Mine surveying services

[WWW.GEOSTROY.COM](http://WWW.GEOSTROY.COM)  
[OFFICE@GEOSTROY.COM](mailto:OFFICE@GEOSTROY.COM)

# 30 GEOTECHMIN ГЕОТЕХМИН

[www.geotechmin.com](http://www.geotechmin.com)



*Small steps.  
Big traces.*



A PARTNER YOU  
CAN RELY ON

**GT**  
**15 YEARS**

+359 2 930 70 63

office@geotrading.bg

www.geotrading.bg



Каолин  
Kaolin



Фелдшпат  
Feldspar



Доломит  
Dolomite



Варовик  
Limestone



Кварцов  
пясък  
Silica sand



Шамот  
Chamotte



ЧАСТ ОТ КВАРЦВЕРКЕ ГРУП

# ПЕ-ВА КОМЕРС

Повече от *25 години*  
доказано  
добри партньори

 гр. Казанлък

Индустриална зона ЮГ

office@pe-va-comers.com



peva\_comers@abv.bg

 0887 611 632



peva-comers.com

- проектиране на взривни работи
- извършване на взривни работи
- сондажни услуги



# Пи Би Екс Консултинг ЕООД

...предлага



... в областта на минното дело и добива на инертни материали, както и при разработката и безопасното производство, качествен контрол и използване на продукти и технологии за промишлени взривни вещества и средства за взривяване.

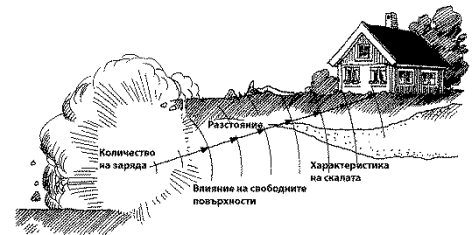


Благодарение на широката ни мрежа от контакти сред водещи специалисти в минното дело от целия свят, някои от които – признати експерти в бранша, ние можем да помогнем за намиране на творчески решения на въпроси и проблеми, свързани с използването на взривната енергия – за мирни цели по безопасен начин, в точното количество, време и място.



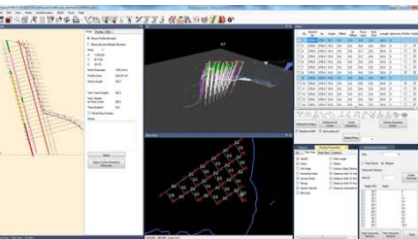
## КОНСУЛТАНТСКИ УСЛУГИ

В областта на химията, технологията, материалознанието, производството и използването на експлозивите, например: Оптимизация на съществуващи линии и производствени процеси за взривни вещества и средства за взривяване; Изпитвания и методи за изпитване на различни параметри на ВВ и СВ; Оценка на риска и измерване на нежеланите въздействия от взривните работи и други...



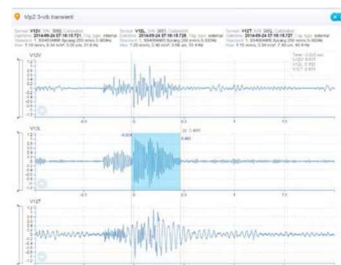
## ПРОДУКТИ И АКСЕСОАРИ В ПОМОЩ НА ВЗРИВНИКА

Quarry Manager™ - Софтуерни решения на български език за управление на ПВР и на останалите дейности от минния цикъл; IGNIUS - Система за дистанционно иницииране на неелектрически взривни мрежи и много други...



Thanks to our broad contact network among leading mining experts around the world, we could help in providing creative and balanced solutions and answers to questions related to use the right amount of blasting energy, in the right place and time – for safe peaceful applications. We offer:

CONSULTING SERVICES, PRODUCTS AND ACCESSORIES IN THE BLASTER'S AID



...offers



... in the field of Mining and Quarry & Construction industries, developing, technology, quality control and safe manufacturing and use of Civil Explosives and Initiation Systems.



www.thrace-resources.com  
**ТРЕЙС РИСОРСИЗ ЕООД**

част от групата компании на Асарел-Мегем АД от 2012 г.

## **Създаваме нови възможности!**

Модерна, социалноотговорна компания, която развива нови геологопроучвателни и минни проекти, като прилага най-добрите управленски и производствени практики с грижа за хората, природата и обществото.

## **Проект „Брезник“**

Добив и обогатяване на **златосъдържащи руди** от находище „Милин камък“ край гр. Брезник.

Прогнозните начални инвестиции за реализацията на проекта са **над 120 млн. лв.**







**UNIVERSITY OF  
MINING AND GEOLOGY  
"ST. IVAN RILSKI"**

[www.mgu.bg](http://www.mgu.bg)